Characterisation of Condensin Subunits in *Drosophila melanogaster*

Ellada Savvidou

Matriculation number 0129605

A thesis submitted to the University of Edinburgh in conformity with the requirements of examination for a PhD

2005

This thesis is gratefully dedicated to my
husband Christos and my parents Kyriacos and Xenia
for their love and support

Acknowledgements

First of all I would like to thank my supervisor Margarete Heck for her support and guidance during this work. Also, I am grateful to past and present members of the lab, Sharron Vass, Neville Cobbe, Brian McHugh, Bin Yu and Marie-Luise Lupart for their tremendous help and encouragement. Also I would like to thank Bill Earnshaw and Andreas Merdes and members of their labs for helpful advice at group meetings.

Also I am deeply grateful to Sir Ken Murray and The Darwin Trust for giving me the opportunity to study at Edinburgh University and for supporting me financially during my studies.

I would like to thank to two very good friends, Sophia Papadia and Georgia Vedra, for always being at my side, understanding and supporting me in all the difficulties I had and also for being fun to be around.

I would like to thank my parents, Kyriacos and Xenia and my brothers and sisters for their love, support and encouragement, not only during my studies, but also at every step in my life.

Last but not least I would like to thank my husband Christos for his love and extreme patience during the last two years. I know that he suffered silently most of this time and that he had to overcome many difficulties alone. I hope that in the future I will be able to make it up to him.

Finally, I know that without God s love and mercy none of this would be accomplished.

Abstract

The precise mechanism of chromosome condensation and decondensation remains a mystery, despite progress over the last 20 years aimed at identifying components essential to the compaction of the genome during mitosis. A multiprotein complex, condensin, is considered to play a crucial role in this process along with having been shown to be essential for proper chromosome segregation during mitosis. This complex, conserved from yeast to humans, has been best characterised in *Xenopus* egg extracts and yeast. It consists of two SMC (Structural Maintenance of Chromosomes) proteins, SMC2 and SMC4, forming a heterodimer, and three non-SMC proteins, CAP-D2, CAP-G and CAP-H.

In this study, I analysed the localization and role of the CAP-D2 non-SMC condensin subunit and its effects on the stability of the condensin complex. I demonstrated that a condensin complex exists in *Drosophila* embryos, containing CAP-D2, the anticipated SMC2 and SMC4 proteins, and the CAP-H/Barren and CAP-G (non-SMC) subunits. CAP-D2 is a nuclear protein throughout the cell cycle, increasing in level during S phase, present on chromosome axes in mitosis, and still present on chromosomes as they start to decondense late in mitosis. The consequences of CAP-D2 loss after dsRNA-mediated interference were analysed, and it was discovered that the protein is essential for chromosome arm and centromere resolution. The loss of CAP-D2 after RNAi had additional downstream consequences on the stability of CAP-H, the localization of DNA topoisomerase II and other condensin subunits, chromosome segregation, and the dynamics of chromosome passenger and metaphase checkpoint proteins. Furthermore, even after interfering with two components important for chromosome architecture (DNA topoisomerase II and condensin), chromosomes were still able to compact, paving the way for the identification of further components or activities required for this essential process.

Analysis of an SMC2 mutation showed severe chromosome abnormalities similar to those observed after CAP-D2 depletion. Chromosome organisation was compromised, sister chromatid resolution was lost and chromosomes failed to segregate properly during anaphase. Nevertheless, overall chromosome compaction was normal in the majority of mitotic cells, suggesting that the entire condensin complex is primarily required for resolution of sister chromatids and establishment of mitotic chromosome architecture rather than chromosome compaction in *Drosophila*. In addition levels of the other condensin subunits and other chromosomal proteins were greatly affected in this mutant.

A condensin II complex has been recently identified in vertebrate cell, consisting of the two SMC subunits: SMC2 and SMC4, and three non-SMC subunits, CAP-D3, CAP-H2 and CAP-G2. Sequence analysis suggests the existence in *Drosophila* of CAP-D3 and CAP-H2, but not CAP-G2. An examination of the *Drosophila* CAP-D3 condensin II subunit has been performed and preliminary results suggest a role of this protein and likely of the entire condensin II complex in male meiosis.

Table of Contents

Abbreviations

A. thaliana	*Arabidopsis thaliana*
BrdU	Bromodeoxyuridine
BSA	Bovine Serum Albumin
C. elegans	*Caenorhabditis elegans*
C-terminus	Carboxyl terminus
CID	Centromere Identifier
CLAP	Chymostatin, Leupeptin, Antipain, Pepstatin A
D. melanogaster	*Drosophila melanogaster*
DAPI	4', 6-diamidino-2-phenylindole
Df	Deficiency of chromosomal region
DTT	Dithiothreitol
dsRNA	Double stranded RNA
dsRNAi	Double stranded RNA-mediated interference
EBR	Ephrussi Beadle Ringer s Solution
E. coli	*Escherichia coli*
ECL	Enhanced Chemiluminescence
EDTA	Ethylenediaminetetraacetic acid
EM	Electron Microscopy
EMS	Ethylmethane Sulfonate
EST	Expressed Sequence Tag
FBS	Fetal Bovine Serum
GFP	Green Fluorescent Protein
H. sapiens	*Homo sapiens*
HEAT	Huntingtin, Elongation factor 3, A-subunit of protein phosphatase A, TOR
HEPES	N-(2-hydroxyethyl)piperazine-N'-(2-ethanesulfonic acid)
hr or hrs	hour or hours, respectively
HRP	Horseradish peroxidase

IPTG	Isopropyl-β-D-thiogalactopyranoside
LB	Luria-Bertrani broth
MAR	Matrix Attachment Region
N-terminus	Amino terminus
OD	Optical density
ORF	Open Reading Frame
PAGE	Polyacrylamide Gel Electrophoresis
PBS	Phosphate Buffered Saline
PCR	Polymerase Chain Reaction
P~H3	Phosphorylated histone H3
PMSF	Phenylmethyl Sulfonyl Fluoride
PFA	Paraformaldehyde
RT-PCR	Reverse Transcriptase - Polymerase Chain Reaction
SAR	Scaffold Attachment Region
SDS	Sodium Dodecyl Sulfate
SMC	Structural Maintenance of Chromosomes
S. cerevisiae	*Saccharomyces cerevisiae*
S. pombe	*Schizosaccharomyces pombe*
TAE	Tris acetate buffer with EDTA
TBE	Tris borate buffer with EDTA
TE	Tris buffer with EDTA
topoisomerase II	Topo II or topo II
UAS	Upstream Activating Sequence
UTR	Untranslated Region
UV	Ultraviolet
X. laevis	*Xenopus laevis*

CHAPTER 1
INTRODUCTION

Cell division and in general the regulation of the cell cycle constitute fundamental procedures for the continuation of life. Understanding the cell cycle is important for the resolution of defects that cause human diseases such as cancer and genetic abnormalities. The architecture and function of the mitotic chromosomes determines among others, the success of mitosis and the generation of two new healthy cells. The establishment of cohesion between the two sister chromatids during DNA replication and the proper condensation of the chromosomes at the onset of mitosis outline some of the most important events for the successful completion of cell division. These two things assure firstly that the two sister chromatids will remain attached to each other until the metaphase to anaphase transition in order to resist the tension applied by the spindle and secondly that they will compact to form a mitotic chromosome. Interactions between the mitotic chromosomes and the mitotic spindle result in the separation of sister chromatids and their migration to the opposite poles during anaphase. Thus, mitotic chromosome dynamics are attractive for research. In this thesis, I have attempted to analyse the contribution of different condensin components to chromosome dynamics in the fruit fly *Drosophila melanogaster.*

1.1. Overview of the Cell Cycle

A cell goes through the cell cycle in order to give rise to two daughter cells which are identical to the parent cell. The cell cycle is divided into four phases: S phase (DNA synthetic phase), in which the DNA is replicated, mitosis (M phase), which upon its completion gives rise to two daughter cells, and the two gap phases (G1: the interval between the end of mitosis and DNA replication [S phase], and G2: the interval between DNA replication and the entry into mitosis). S phase and the two gap phases

are referred to as interphase. Each of these phases is important for the correct progression of the cell cycle.

G1 phase.

During G1 phase in metazoans, the cell makes the decision whether to proceed into another cell cycle or to remain in a non-dividing state either permanently (differentiation) or temporarily. Kinases play crucial roles for the passage from this point through the cell cycle, but also for other checkpoints during the cell cycle and appear to be necessary in all eukaryotes. The cell cycle regulatory kinases are activated after their association with a subunit called cyclin. Thus, they are termed cyclin dependent kinases (CDKs) and their regulation depends on different cyclins (Morgan, 1997; Murray, 2004; Doree and Hunt, 2002). Cyclins are a diverse group of proteins with a highly conserved "cyclin box". They owe their name to their observed cyclic accumulation and destruction during the cell cycle. The Cdk4/6-cyclin D complex along with other molecules is the major regulator for the passage from the restriction point (the point after which the cell cycle will proceed even if proliferating signals are withdrawn) to the onset of S phase (Donjerkovic and Scott, 2000; Ekholm and Reed, 2000). Cdk2-cyclin E is responsible for a second wave of phosphorylations that culminates in the transcription of genes that are essential for the initiation of DNA replication (Donjerkovic and Scott, 2000; Lee and Yang, 2003).

S phase

Genetic information in the form of DNA has to be inherited from the parent to the two daughter cells intact and accurately. DNA replication is responsible for the accuracy that occurs during the synthetic phase (S phase). Replication begins at certain sites of the chromosomal DNA termed Origins of Replication. Eukaryotes initiate replication at many origins distributed along the chromosomes in contrast to prokaryotes that have a single origin of replication. In budding yeast (*Saccharomyces cerevisiae*), replication begins within Autonomously Replicating Sequences (ARS) and a pre-replication complex assembles at every replication origin before the onset of S phase (Toone et al.,

1997). One of the members of this pre-replication complex is the ORC complex (origin of recognition complex), which consists of six proteins and probably is implicated in the initiation of DNA replication. Recent studies have shown that preferred origins of DNA replication exist and a pre-replication complex is assembled in mammalian cells as well, but these origins are much more complexed (Gerbi et al., 2002). The initiation of DNA replication, in mammals, seems to be triggered by a combination of protein kinases, including Cdk2-cyclin E and Cdk2-cyclin A kinases, as well as a specialised kinase Cdc7p-Dbf4p (Reed, 1997; Sclafani, 2000).

Experiments have shown that there is a very distinctive pattern of DNA synthesis occurring at different times of S phase. Euchromatin replicates early on throughout the nucleus, while later replicating regions appear concentrated around the nucleoli and other areas of more condensed chromatin. Towards the end of S phase, replication is concentrated in heterochromatic areas. Besides DNA replication, two other important events occur during S phase. The first is the establishment of cohesion between the two replicated sister chromatids (Nasmyth, 2001) and the second event is the duplication of the centrosome (microtubule organising centre), which requires phosphorylation by the Cdk2-cyclin E or Cdk2-cyclin A kinases (Tarapore et al., 2002; Winey, 1999; Meraldi, 1999 et al.).

G2 phase

G2 represents the interval between the end of S phase and the beginning of mitotic prophase. During this phase, and in particular at the G2/M transition, dramatic morphological and physiological changes occur. Responsible for these changes are different inhibitory or stimulatory protein kinases and phosphatases among which are the Cdk2-cyclin A kinase, the Cdk1-cyclin B kinase and the family of Cdc25 phosphatases (Smits and Medema, 2001; Jackman and Pines, 1997; Nilsson and Hoffmann, 2000). In late S and G2 phases, activation of the Cdc25B phosphatase activates the Cdk2-cyclin A kinase, which regulates several events at the G2/M transition such as chromosome condensation and microtubule behaviour (Goldstone et al., 2001; Pollard and Earnshaw, 2002). At this point of the cycle, the separated centrosomes are transformed into spindle

poles, initiating microtubule organisation and formation of the spindle over the surface of the nucleus (Pollard and Earnshaw, 2002).

Cdk1-cyclin B, the major mitotic kinase, also seems to have a significant role at the G2/M transition. Cyclin B is newly synthesised at the latest stage of S and at the beginning of G2 phases and is associated with the Cdk1 kinase (Smits and Medema, 2001). Cdk1 kinase is present at a constant level throughout the cell cycle and is distributed diffusely throughout the cell. The Cdk1-cyclin B heterodimer is exported from and imported into the nucleus, spending most of the time in the cytoplasm associated with microtubules. This enzyme accumulates into the nucleus later on, after the phosphorylation of cyclin B by a kinase. Before that, a phosphatase called Cdc25C is activated probably by a member of another family of kinases called the Polo family (Myer et al., 2005). This activation results in the accumulation of Cdc25C into the nucleus. Then the Cdc25C activates the Cdk1-cyclin B kinase, which acts on the nuclear lamina and causes nuclear envelope breakdown at the onset of prometaphase (Smits and Medema, 2001).

DNA damage checkpoints

DNA damage checkpoint is the mechanism that detects damaged DNA and generates a signal that arrests cells in the G1 phase of the cell cycle, slows down S phase (DNA synthesis), arrests cells in the G2 phase, and increase the transcription of genes encoding proteins that participate in DNA replication and repair (Elledge, 1996). These physiological responses, that facilitate DNA repair processes, are thought to be induced by both prokaryotes and eukaryotes. The position of arrest within the cell cycle varies depending upon the phase in which the damage is sensed. The delay/arrest of cell cycle progression that provides time for DNA repair or, when the damage is beyond the repair, may permanently prevent cell proliferation by cellular senescence, is mediated by a network of signalling pathways referred to as cell cycle checkpoints (Lukas et al., 2004).

Mitosis

Mitosis results in the formation of two daughter cells from a single cell. Mitotic events are subdivided into six phases: prophase, prometaphase, metaphase, anaphase, telophase and cytokinesis (Figure 1.1).

Prophase

Prophase is the first stage of mitosis and is characterised by various nuclear and cytoplasmic changes. At the onset of prophase, chromosomes condense starting from isolated patches of chromatin at the nuclear periphery and they become visible as two distinct sister chromatids closely paired along their entire length. As chromosomes condense, proteins of the kinetochore multiprotein complex move from the cytoplasm into the nucleus and associate with the kinetochores. A kinetochore is a button like structure on the centromeric heterochromatin, which directs chromosomal movements during mitosis (Pollard and Earnshaw, 2002).

At this point of the cell cycle, histone H1 is phosphorylated by Cdk1-cyclin B *in vivo* (Swank et al., 1997) and histone H3 by Aurora B kinase (Adams et al., 2001). It is thought that the unfolding of the local chromatin due to histone phosphorylation may permit binding of different factors such as the condensin complex (Hirano, 2002). Also topoisomerase II, an enzyme that can change DNA topology by passing one double helix strand through another and which locates at centromeres and along mitotic chromosome arms, seems to be connected to chromosome condensation at the onset of prophase (Wang, 2002). Dramatic changes occur in the cytoplasm during prophase. Most of the cytoskeleton reorganises but especially so the microtubule network. The extented microtubule network that covers the whole cytoplasm during interphase is converted into two dense radial arrays, called asters, of short dynamic microtubules around each centrosome. γ-tubulin (a minor tubulin isoform) ring complexes (γ-TURC) in the pericentriolar material nucleate the microtubules so that each aster acts as a microtubule organising centre (MTOC). Most of the actin and intermediate filaments disassemble (including the nuclear lamina), the Golgi apparatus and the endoplasmic reticulum

fragment, endocytosis and exocytosis are greatly decreased and protein synthesis stops by the action of Cdk1-cyclin B (Pollard and Earnshaw, 2002).

Prometaphase

Prometaphase is mainly characterised by nuclear envelope disassembly and interactions between microtubules and kinetochores in order to align the chromosomes in a group midway between the poles. Every mitotic chromosome has two opposite kinetochores, one on each sister chromatid, which are attached to opposite spindle poles. This bipolar orientation is important for giving a balance of opposing forces, that together with the action of kinesins (a family of motor proteins distributed along the chromosome arms), results in a movement of the chromosomes to a point midway between the spindle poles. During prometaphase the assembly of the mitotic spindle that starts from prophase with the separation of the asters, is completed. At this point, cyclin A is degraded (Pollard and Earnshaw, 2002).

Metaphase

Metaphase is a very short period of the cell cycle. At this phase all chromosomes are properly attached to microtubules from opposite poles and they are situated midway between the two spindle poles. Once the chromosomes are properly aligned in the middle of the spindle, they form a structure called the metaphase plate (Pollard and Earnshaw, 2002). The proper alignment of chromosomes and the achievement of bipolar orientation is critical for the accuracy of segregation of replicated chromosomes. For this reason, entry into anaphase is delayed by the metaphase checkpoint or spindle assembly checkpoint. This checkpoint involves protein kinases and other factors that are associated with kinetochores during prophase or prometaphase and dissociate from kinetochores after these are stably attached to the spindle (Rieder and Maiato, 2004; Musacchio and Hardwick, 2002). One of these kinases is BubR1 which locates at the outer plate of the kinetochore and it appears to interact with CENP-E, the giant kinesin protein that associates with chromosomes during nuclear envelope breakdown (Maiato et al., 2004; Mao et al., 2003; Tanudji et al., 2004). Interactions between these proteins

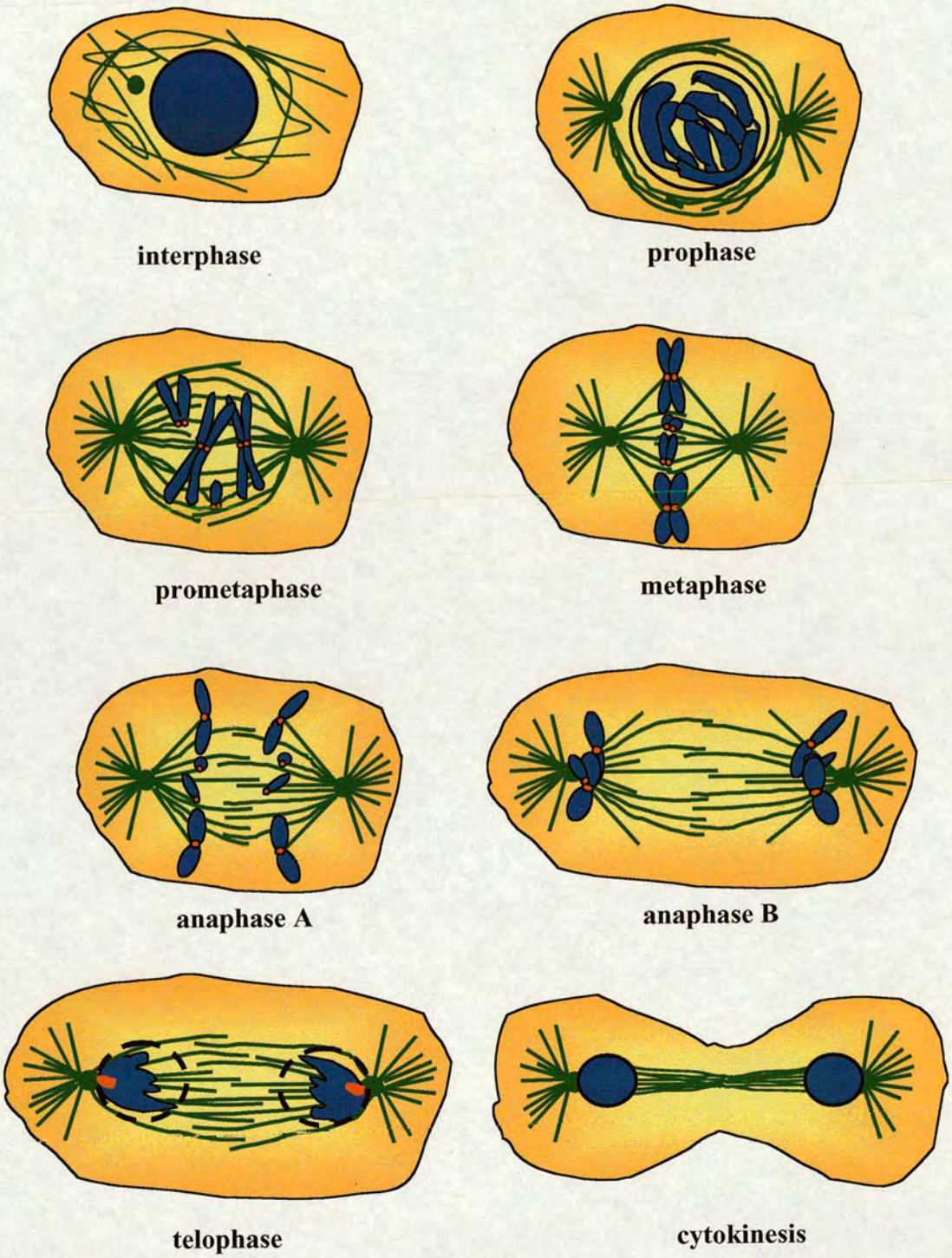

Figure 1.1. Overview of the phases of mitosis in a typical metazoan cell. Spindle and astral microtubules are shown in green, chromosomes and kinetochores are shown in dark blue and red respectively and the nuclear envelope is shown in black.

along with other factors satisfy the metaphase checkpoint (Cleveland et al., 2003; Musacchio and Hardwick, 2002).

Anaphase

During the critical stage of anaphase, sister chromatids move to opposite spindle poles (anaphase A) and the poles move apart (anaphase B). The entry into anaphase is triggered by a drop in Cdk1 activity and is completed by APC/C-directed cleavage of proteins including securin and cyclin B by proteosomes (Irniger, 2002). The shortening of the microtubules that are attached to kinetochores (kinetochore microtubules) and the involvement of motor proteins that are present on the chromosomes contribute to chromosome movement during anaphase A. In anaphase B, spindle poles separate from one another. Due to this, the spindle is elongated and the interpolar microtubules (microtubules that connect the two spindle poles) are reorganised into a highly organised central spindle between the separating chromatids (Pollard and Earnshaw, 2002).

Telophase

During telophase the nuclear envelope reassembles around the segregated chromosomes. Other dramatic changes at this point prepare the cell for the ensuing division of the cell (Pollard and Earnshaw, 2002).

Cytokinesis

Cytokinesis is the process that divides the mother cell into two daughter cells. In animal cells, a contractile ring is formed by actin filaments and separates the daughter cells from one another. The central spindle appears to play a critical role in early and late cytokinesis. It contains kinesins and components called chromosomal passengers, which seem to be essential for the completion of cytokinesis (Pollard and Earnshaw, 2002).

1.2. Chromosome condensation

Chromosomal DNA, if stretched end to end, measures about 2 metres in any one cell of the human body and therefore must be highly folded to fit into a nucleus of only 10 μm diameter. DNA has to condense even further prior to cell division in order to form the

highly compact metaphase chromosome comprising two distinct sister chromatids, capable of withstanding anaphase segregation (Heck, 1997; McHugh and Heck, 2003; Swedlow and Hirano, 2003). Several levels of packing enable DNA to achieve this packaging and a number of structural proteins are involved. The simplest level of packing involves the winding of DNA around octamers of core histones in a structure called the nucleosome. This shortens DNA about 7-fold relative to naked DNA (Kornberg, 1974; Olins et al., 1976; Richmond et al., 1984). The folding of regularly spaced nucleosomes forms a shorter, thicker filament, called the 30 nm chromatin fibre, in which the DNA is about 40-fold more compact than when naked (Widom and Klug, 1985; Williams et al, 1986; Woodcock and Dimitrov, 2001; Woodcock et al., 1984). The most highly condensed and least understood stage takes place prior to chromosome segregation when the DNA in metaphase chromosomes of higher eukaryotic cells is compacted nearly 10,000-fold in length (Li et al., 1998). The way that chromatin organizes into this higher-order structure of mitotic chromosomes is not well understood and the different models that have been proposed remain controversial (Belmont, 2002; Swedlow and Hirano, 2003).

1.2.1. First level of compaction: the nucleosome

Interphase nucleosomal chromatin under low salt conditions appears (by electron microscopy) as "beads on a string" with a diameter of about 10 nm. This packaging results when 166 bp of DNA winds around an octamer of core histones in a left-handed superhelix following a helical path along the surface of the octamer (Figure 1.2). The histone octamer consists of an $[H3]_2$:$[H4]_2$ tetramer, flanked on either side by an H2A:H2B heterodimer. Each core histone has a compact domain of 70 to 80 amino acid residues and a flexible N-terminal tail of approximately 30 amino acids outside the nucleosome (Pollard and Earnshaw, 2002). These N-terminal tails allow the nucleosomes to pack into a 30 nm fibre, while specific modifications of the tails are crucial for modulation of chromatin structure (Figure 1.2). This fibre has been variously modelled as either a solenoidal coiling, random or organized folding of the nucleosomal fibre — its actual structure remains undetermined. Fragility of the 30 nm fibre during

preparation is likely responsible for the inability to unambiguously ascertain its architecture (Pollard and Earnshaw, 2002; Woodcock and Dimitrov, 2001).

Histone H1, or other linker histones, binds to a variable amount of "linker" DNA that extends between adjacent nucleosomes (Pollard and Earnshaw, 2002). The N-terminal tails of the histones are also important for extra-nucleosomal interactions. The variants of linker histone differ from the core histones in that the globular central domain is flanked by unstructured basic domains at both the N- and C-termini. Histone H1 resides at the side of the nucleosome where DNA enters and exits the nucleosome. The master cell cycle regulatory kinase, CDK1 (cdc2:cyclinB), phosphorylates serine and threonine residues on the histone H1 tails *in vivo* during mitosis (Swank et al., 1997). Hyperphosphorylation of histone H1 was originally thought to be important for mitotic chromosome condensation (Bradbury, 1992) but recent studies show that phosphorylation is not required for this process (Guo et al., 1995; Ohsumi et al., 1993; Roth and Allis, 1992; Shen et al., 1995).

Mitosis-specific phosphorylation of histone H3 at serine-10 (by Aurora B kinase) coincides with the initiation of chromosome condensation, suggesting that phosphorylation of histone H3 drives chromosome compaction (Hendzel et al., 1997). However, the effects of histone H3 phosphorylation on chromosome condensation appear to be variable between several studies (Swedlow and Hirano, 2003), and it seems unlikely to be required for this process. Moreover, the N-terminal tails of histones may also be acetylated or methylated, resulting in an epigenetic "histone code" important for gene expression or assembly of heterochromatin (Cosgrove et al., 2004; Turner, 2002).

1.2.2. Above and beyond the nucleososme- mitotic chromosome condensation

The mechanism for packaging the 30 nm fibre into the highly compact, characteristc rod-shaped mitotic chromosomes remains a fundamental question for modern cell biologists (Belmont, 2002; Swedlow and Hirano, 2003). The shortening of DNA by roughly 10,000-fold is essential for the proper physical separation of sister chromatids to opposite poles, e.g. in order to avoid cleavage of the genome by an ingressing cleavage furrow. In addition, chromosomes must be properly aligned via their kinetochores to

ensure that one of each chromatid pair ends up in each new daughter cell. However, early approaches utilizing electron microscopy to examine isolated native mitotic chromosomes only served to confirm that the DNA is indeed very densely packed within chromosomes.

Several approaches have been utilized in an attempt to expose the factors underlying higher order chromosome structure. One classical view, based on the appearance of DNA in sperm (Inoué and Sato, 1964), suggests that folding or helical coiling of the 30 nm fibre into increasingly larger structures gives rise to a condensed chromosome (Figure 1.2.A) (Belmont et al., 1987; Sedat and Manuelidis, 1978). Recently a higher order folding has been tested by stably integrating tandem arrays of bacterial *lac* operator sequences into human cells that express GFP fused to the *lac* repressor. This strategy generates a marked chromatin locus that can be specifically visualised by fluorescence or electron microscopy (Belmont and Bruce, 1994; Swedlow and Hirano, 2003). In this study, the analysis of chromosome decondensation between telophase and early G1 indicated one or more levels of compaction between the 30 nm chromatin fibre and an ~100-130 nm chromonema fibre, which itself folded into telophase chromosomes (Figure 1.2.A) (Belmont and Bruce, 1994). Furthermore, ultrustructural analysis of two different transgene insertion sites , both spanning less than the full chromatin width, provided strong support for hierarchical models of chromosome architecture (Strukov et al., 2003). Specifically, 250 nm diameter folding subunit was visualised directly within fully condensed metaphase chromosomes. Nevertheless, further experiments using this strategy will prove if folded domains self assemble into progressively larger structures.

On the other hand, some of the first hints about large scale chromatin folding were obtained after depleting core histones from highly purified mitotic chromosomes (either with a high salt concentration or polyanions which compete with histones by charge) under conditions that maintain residual non-histone proteins. Long extended loops of DNA (about 15-100 kb) surrounded a protein core that retained the general size and shape of a native chromosome (Paulson and Laemmli, 1977). These striking images led to a model known as the "radial loop model" in which the folding of the chromatin

fibre into loops was mediated by proteins of an insoluble chromosome "scaffold" that was essential for the final size and shape of a chromosome (Figure 1.2.B) (Marsden and Laemmli, 1979). In the presence of 2M NaCl, the scaffold and DNA halo were stable, suggesting that the scaffold may hold DNA loops in a compact conformation (Laemmli et al., 1978). In the same study, when nucleases were used to isolate the scaffold without its associated DNA halo, it was suggested that the structural integrity of the scaffold was independent of DNA. In another approach, scaffolds were able to contract and expand in a reversible way in response to alterations in ionic strength (Earnshaw and Laemmli, 1983), suggesting that similar conformational changes of native chromosomes may result from salt induced changes in scaffold structure. Furthermore, scaffolds were found to be fibrous in nature and to retain differentiated regions that appear to derive from the kinetochores and chromatid axes (Earnshaw and Laemmli, 1983). These observations, in conjunction with experimental data proposing that ordering of chromatin is similar throughout the cell cycle, let to a hypothetical model suggesting that the increased compaction during mitosis (particularly during metaphase) is probably a consequence of transitions of the scaffold structure from a dispersed interphase network to a contracted mitotic conformation (Belmont, 2002; Earnshaw and Laemmli, 1983).

However, the organisation of the 30 nm fibre into the 15-100 kb loops is not enough to account for the compaction of the genome in mitotic chromosomes. A model in which regular helical coiling of the loops in metaphase chromosomes (Boy de la Tour and Laemmli, 1988; Maeshima and Laemmli, 2003; Rattner and Lin, 1985) results in paired sister chromatids of opposite helical handedness (mirror symmetry) (Boy de la Tour and Laemmli, 1988), may also contribute to higher order packaging (Figure 1.2.B). This model was a variation of the basic radial model.

Nevertheless, with such severe extraction methods, the scaffold was considered by many to be an artefact, a result of inappropriate protein interactions created during preparation of this fraction (Belmont, 2002; McHugh and Heck, 2003). For this reason, a detailed biochemical and functional analysis of the scaffold components was required to resolve the controversy. Evidence for chromatin loops existing in native chromosomes, derived from examination of lampbrush chromosomes, where

chromosome loop domains were easily observed. Lampbrush chromosomes are found in oocytes of amphibia and other organisms and their chromatin loops are sites of intense transcriptional activity, required to produce the stockpiles of components needed for cell division during early development of the fertilised egg (Pollard and Earnshaw, 2002). The loops are particularly visible because each DNA loop is coated with many RNA transcripts together with proteins that package them.

Further support for the concept of a mitotic chromosome scaffold came from the identification of *cis*-acting DNA sequences interacting with the proteinaceous component. Using low salt conditions, which extract most of the histone and non-histone proteins but preserve the specific interactions of the DNA loops and the scaffold, specific DNA attachment sites were mapped. These sequences identified were called scaffold attachment regions (SARs) (Hart and Laemmli, 1998; Mirkovitch et al., 1987; Mirkovitch et al., 1984). SAR sequences were identified in both nuclear (nuclear matrix, interphase nuclei) and mitotic scaffolds (Mirkovitch et al., 1987). DNA sequences that associate preferentially with nuclear matrix are defined as MARs (matrix attachment regions). SARs/MARs are AT-rich DNA sequences and the DNA between two SAR sequences separated by up to 100 kb of DNA, would form a chromatin loop (Hart and Laemmli, 1998; Saitoh and Laemmli, 1994). Using AT-specific fluorochrome dyes, SARs were visualised as a queue along the longitudinal axis of the chromosome that alternately followed a fairly linear or tightly coiled path (Saitoh and Laemmli, 1994). This alternating folding pattern was proposed as a link between chromosome structure and the banding patterns observed on mitotic chromosomes with several dyes. In the Q bands (AT-rich), the AT queue is tightly coiled or folded while the R bands (GC-rich) contain a more central (unfolded) AT queue. A number of proteins such as Topoisomerase II (a protein of the chromosome scaffold), histone H1 and HMG-I/Y were shown to bind SARs highly selectively (Adachi et al., 1989; Izaurralde et al., 1989; Zhao et al, 1993). However, when labelled chromosome regions with altered SAR sequences were engineered, using the lac operator/repressor system, no defect was observed in chromosome organisation (Strukov et al, 2003). In the same study, when

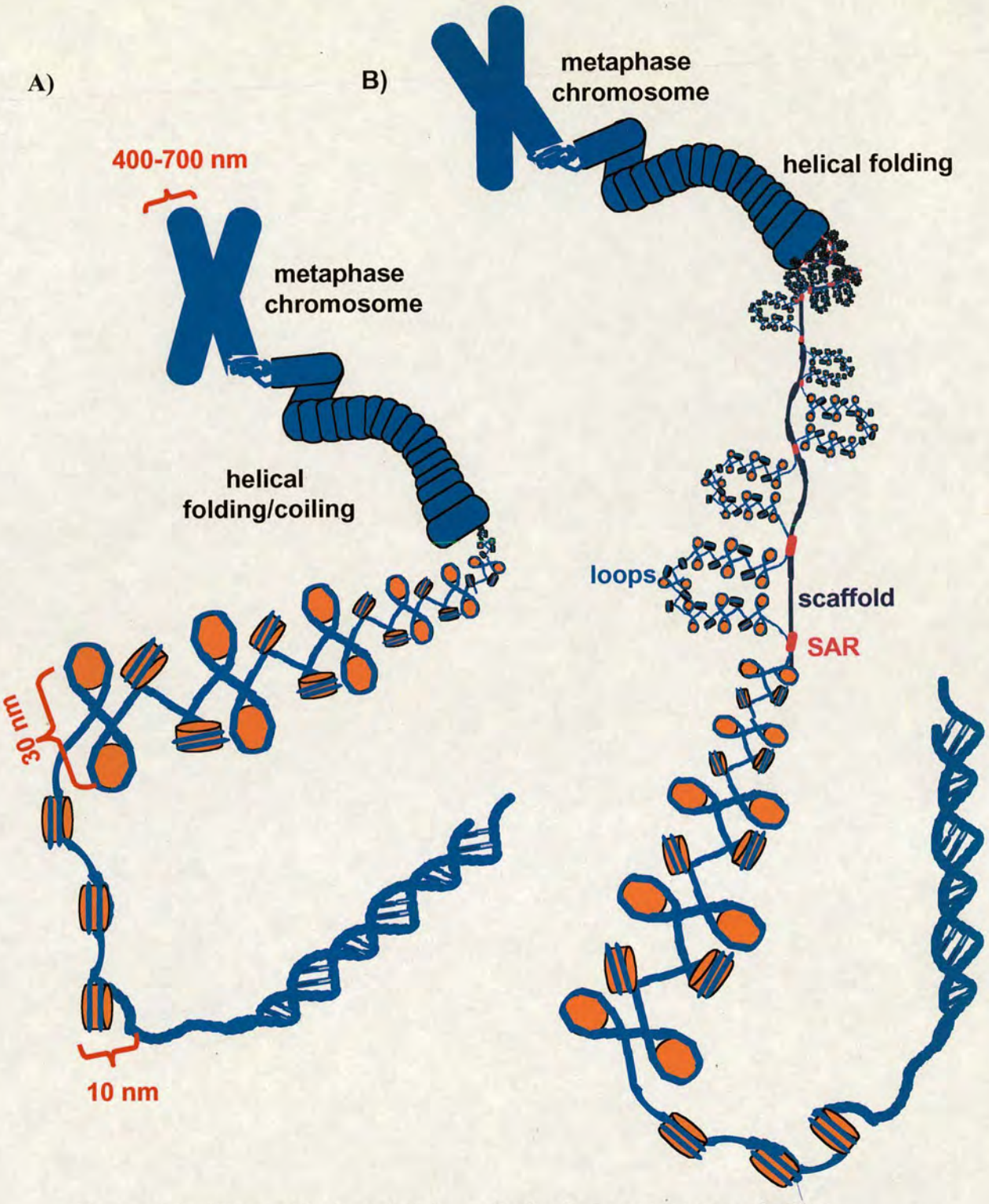

Figure 1.2. Hierarchical models for mitotic chromosome organisation.

The first level of compaction involves the winding of DNA around octamers of core histones in a structure called the nucleosome, resulting in a 10 nm fiber which provides a 6-7 fold linear compaction of DNA. The folding of regularly spaced nucleosomes forms a shorter, thicker filament, called the 30 nm chromatin fiber, in which the DNA is about 40-fold more compact than when naked. **A.** The chromonema fiber model proposes that folding and/or coiling of the chromatin fiber would create higher-order domains that could fold into progressively larger structures (400-700 nm), possibly based on protein:protein or protein:DNA interactions between neighbouring chromatin fibers (Belmont and Bruce, 1994). **B.** The radial loop domain model proposes that the chromatin fiber folds into loops, mediated by proteins in the chromosome scaffold and *cis*-acting SAR sequences (Hart and Laemmli, 1998), while regular helical coiling of the loops results in the formation of metaphase chromosomes (400-700 nm).

ultrustructural analysis of two different transgene insertion sites, both spanning less than the full chromatin width, clearly contradicted predictions of the radial loop model while provided strong support for hierarchical models of chromosome architecture. Specifically, 250 nm diameter folding subunit was visualised directly within fully condensed metaphase chromosomes.

To test the role of SARs in chromatin condensation, artificial proteins (MATH proteins) which bind to these regions (but have no other obvious direct effect on condensation) were constructed (Strick and Laemmli, 1995). MATH proteins had multiple tandem copies of the AT hook, a 14 residue sequence from HMGI-Y proteins with high affinity for the minor groove of extensive poly dT stretches of DNA. These proteins might compete with true condensation factors for binding sites and therefore disrupt the condensation process. The MATH proteins were demonstrated to specifically bind SARs in chromatin and chromosomes while MATH20 (a protein containing 20 hooks) disrupted the normal events of mitotic chromosome assembly when added to *Xenopus laevis* egg extracts. However, titration of SARs with MATH20 blocked only shape determination of chromatids, rather than chromatin condensation *per se*. When MATH20 was added after formation of chromatids, the latter collapsed and they reshaped by an active mitotic process into spherical chromatin balls, suggesting the requirement of SARs in the shape maintenance of chromosomes (Strick and Laemmli, 1995). However, the significance of these experiments for chromosome condensation *in vivo* has been questioned (Koshland and Strunnikov, 1996). The abnormal chromosome morphology could be a consequence of the binding of true condensation factors to non-SAR regions of the chromatin. Thus, condensation could still proceed but the final chromosome structure would be defective. Moreover, as similar morphological defects have been reported in cells deficient in topoisomerase IIα (also a factor in chromosome condensation and segregation), it appears that the competitive binding of MATH20 to SARs may genuinely reflect the importance of these *cis*-acting sequences for chromosome assembly (Grue et al., 1998; Hirano and Mitchison, 1993).

Since *cis*-acting sequences are significant for mitotic chromosome architecture, it might be expected that the location of specific sequences within the mitotic chromosome

would be defined. Using fluorescence *in situ* hybridazitation to extracted metaphase chromosomes, it was shown that specific human DNA sequences occupy distinctive positions with respect to the axial region of chromosomes and that the DNA is organised into loops emanating from this region (Bickmore and Oghene, 1996). However, experiments with the GFP-*lac* repressor chromatin marker or FISH on extracted chromosome halos, suggested that chromosome architecture is fairly dynamic and that most sequences do not localise within a certain region of the chromosome. It appears that the position of a sequence at a particular time is depended on the cell cycle state and transcriptional activity (Swedlow and Hirano, 2003). Furthermore, the axial localisation of several sequences marked with the GFP-*lac* repressor system was only observed during metaphase but not during prophase or prometaphase, suggesting that a major structural transition occurs at late stages of condensation, between prophase and metaphase. This structural transition is consistent with all chromosome models involving coiling/uncoiling of an underlying chromatid, including coiled-radial loop and coiled-chromonema models (Dietzel and Belmont, 2001).

An alternative approach to chromosome structural analysis, monitored changes in chromosome elasticity and deformability by using micromechanical force measurements. Firstly, measurements of both longitudinal deformability and bending rigidity were performed on *in vitro* assembled chromosomes in *Xenopus* egg extract by using specially designed micropipettes (Houchmandzadeh and Dimitrov, 1999). The relationship between the values of these two parameters was found to be most consistent with models in which mitotic chromosomes are composed of thin rigid cores of protein surrounded by a soft envelope, as predicted by the scaffold hypothesis. Similarly, several other studies revealed that when chromosomes were stretched under controlled conditions allowing force measurements, mitotic chromosomes could be stretched five times their native length without permanent elongation (Houchmandzadeh et al., 1997; Nicklas, 1983; Poirier et al., 2000). The remarkably elasticity of chromosomes could suggest that the mechanical integrity of mitotic chromosomes is maintained by a proteinaceous axial core. However, recent experiments by Poirier and Marko by using micromechanical force measurement during nuclease digestion seem to rule out the

possibility that mitotic chromosome structure is based on a mechanically contiguous proteinaceous scaffold (Poirier and Marko, 2002). In this study, as DNA cuts are introduced within a mitotic chromosome by either micrococcal nuclease or frequently cutting restriction enzymes, first chromosome elasticity is lost and then the chromosome is completely dissolved. These data suggest that the mechanical integrity of chromosomes is largely dependent on DNA (chromatin network) and is maintained by cross-links between chromatin fibres. The frequency of these cross-links is estimated to be about every 15 kb (Poirier and Marko, 2002). Nonetheless, measures of chromosome stiffness by different groups have varied widely making it difficult to build a definitive model of chromosome architecture (Marshall et al., 2001; Swedlow and Hirano, 2003).

Undoubtedly, it could be possible that both the chromosome scaffold and DNA, contribute to the structural integrity of chromosomes. Bearing in mind that the question of whether the native scaffold is stabilised through protein-protein interactions is unresolved (Gasser et al., 1986), it could be suggested that the proteins of the scaffold are not contiguously connected through the chromosome and that DNA itself links the scaffold together (Poirier and Marko, 2002).

1.3. Biochemical analysis of the chromosome scaffold and the components of mitotic chromosomes

Biochemical analysis of scaffolds, isolated from extracted mitotic chromosomes, revealed two major components Sc1 and Sc2 (Sc1 at 170 kDa and Sc2 at 135 kDa) and a number of smaller, less abundant proteins (Lewis and Laemmli, 1982; Gassmann et al., 2004). The identification of Sc1 as DNA topoisomerase II (Earnshaw et al., 1985; Gasser et al., 1986) and Sc2 as an SMC protein (a subunit of the condensin complex) (Saitoh et al., 1994), provided the first evidences that proteins involved in mitotic chromosome dynamics were components of the scaffold fraction. In addition to this, characterization of chromosomes remodelled from sperm chromatin in *Xenopus* egg extracts, resulted in the identification of several protein components binding to these *in vitro* assembled structures. The mitotic chromosome fraction contained histones and linker histones, topoisomerase IIα, chromokinesin, the chromatin remodeling ATPase

ISWI, and a complex subsequently named condensin (Hirano et al., 1997; Hirano and Mitchison, 1994; MacCallum, 2002; Vernos et al., 1995). These studies demonstrated that mitotic chromosomes are rich in ATPases, which are likely important to induce conformational changes of chromosomes and to support microtubule-dependent movement of chromosomes (Swedlow and Hirano, 2003).

1.3.1. The role of topoisomerase II during mitosis

Topoisomerase II is an ATP-dependent enzyme that can alter DNA topology by passing one double-strand helix through another via a transient double-strand break, an activity necessary for the resolution of catenated sister DNA strands (Wang, 2002).
While yeast and *Drosophila* have a single topoisomerase II gene, there are two distinct isoforms in higher eukaryotes, topoisomerase IIα (170 kDa) and topoisomerase IIβ (180 kDa) that are encoded by different genes. Topoisomerase IIα and IIβ have identical catalytic activities *in vitro* but different localisation patterns *in vivo* (Porter and Farr, 2004a; Swedlow and Hirano, 2003). Nearly all the topoisomerase IIα is concentrated in mitotic chromosomes and is preferentially expressed in proliferating cells, increasing in S, peaking in G2/M and diminishing in G1 phase (Heck et al., 1988). By contrast, immunolabeling studies have suggested that topoisomerase IIβ is diffusely nucleoplasmic in interphase and mitosis (Chaly et al, 1996; Meyer et al., 1997), with its levels not changing significantly throughout the cell cycle. However recent studies have concluded that a minor but significant fraction of IIβ is associated with mitotic chromatin (Christensen et al., 2002; Null et al., 2002). Nevertheless, it seems that while topoisomerase IIα is essential for mitosis, topoisomerase IIβ is dispensable and its main function and whether it has an accessory role in mitotic chromosome structure remains unresolved. Furthermore, more complexity arises from the discovery that both topoisomerase genes give rise to splice variants, in conjunction with the uncertainty over whether topoisomerase II protein, which has a dimerisation domain, exists as homo- and/or heterodimers (Porter and Farr, 2004a).

Localisation studies in different species revealed disparate results for the distribution of topoisomerase II on mitotic chromosomes. In higher eukaryotes this

enzyme showed an axial distribution through the core of hypotonically swollen chromosome arms (Earnshaw and Heck, 1985; Gasser et al., 1986; Maeshima and Laemmli, 2003; Saitoh and Laemmli, 1994), and/or an apparent concentration at the centromeres (Cobb et al., 1999; Maeshima and Laemmli, 2003; Taagepera et al., 1993). Laemmli and colleagues (Laemmli et al., 1978) proposed that closure of chromatin loops was one function of the mitotic chromosome scaffold. Thus, the axial contribution of topoisomerase II may reflect the localisation of the protein at the base of chromosome loops. Indeed, localisation of topoisomerase II at the axial region of swollen chicken chromosomes and the aggregation of a subset of chromosomal DNA after addition of anti-topoisomerase II antibodies to swollen chromosomes, suggested that the protein is localised in numerous separate "islets" on a small subset of chromosomal sequences (Earnshaw and Heck, 1985). Furthermore, topoisomerase II was shown to bind AT-rich SARs highly selectively and to associate with the mitotic chromosome scaffold (Adachi et al., 1989; Hart and Laemmli, 1998), while examination of meiotic chicken chromosomes showed mainly an axial distribution with some association with centromeres and synaptonemal complexes (Moens and Earnshaw, 1989). However, this distribution of topoisomerase II predicts that mitotic chromosome condensation should require stoichiometric levels of the enzyme, a certain quantity of topoisomerase II for the association of each chromosome loop to the scaffold. That was confirmed, when, after immunodepletion of topoisomerase II in an *in vitro* chromosome assembly system, the endogenous levels of the protein were required in order to restore the complete condensation activity (Adachi et al., 1991).

Nonetheless, examination of the role of topoisomerase II in mitotic chromosome assembly and organisation *in vitro*, using *Xenopus* egg extract, suggested that while topoisomerase II activity was required for chromosome assembly and organisation, it did not appear to play a scaffolding role in the structural maintenance of chromosomes (Hirano and Mitchison, 1993). In the same study, analysis of the localisation of topoisomerase II revealed that the protein was not restricted to the chromosome axis but was uniformly distributed throughout the condensed chromosomes. Similarly, studies examining histone depleted HeLa chromosomes (Boy de la Tour and Laemmli, 1988)

and *in vivo* studies in *Drosophila* revealed the protein to have a more uniform distribution on chromosomes (Buchenau et al., 1993; Swedlow et al., 1993).

The different localisation patterns of topoisomerase II on mitotic chromosomes may reflect differences in the fixation and preparation conditions used in several of these studies, species-specific differences in the chromosomal distribution of topoisomerase II, or even differential specificity of the different topoisomerase II antibodies used in these studies, that may detect distinct subsets at different chromosomal locations (Warburton and Earnshaw, 1997). Studies focusing on cell cycle distribution of topoisomerase II, in diverse mammalian cell lines representing both eutherians and metatherians (human, mouse, rat, Chinese hamster, rat kangaroo, wallaby and Indian muntjac), revealed that the staining pattern of this enzyme changes as cells progress through mitosis (Rattner et al., 1996; Sumner, 1996). Particularly, staining by indirect immunofluorescence using antibodies against topoisomerase IIα showed a punctuate staining of variable intensity in interphase, in all species examined. In prophase, as chromosomes start to condense, topoisomerase IIα was distributed on individual chromosomes and the levels of the protein appeared highest. In metaphase the intensity of topoisomerase IIα was found to be highest at the centromeres in all species examined, while the axial pattern along the arms was still present. During anaphase, the centromeric topoisomerase II intensity decreased to a level similar to that on the chromosome arms.

The centromeric accumulation of topoisomerase II observed from prometaphase until early anaphase (Christensen et al., 2002; Gorbsky, 1994; Maeshima and Laemmli, 2003; Null et al., 2002; Rattner et al., 1996; Sumner, 1996; Taagepera et al., 1993) and during prophase of meiosis I (Cobb et al., 1999; Moens and Earnshaw, 1989) suggests that this protein may have a specific function at centromeres. Indeed, inhibition of topoisomerase II activity using the ICRF-193 drug inhibitor, prevented the accumulation of topoisomerase II at the centromeres and disrupted the compaction of centromeric heterochromatin beneath the kinetochore and kinetochore structure (Rattner et al., 1996). Similarly, when DNA damage was caused in human cells undergoing mitosis using an inhibitor of topoisomerase IIα, defects in kinetochore attatchment and function were observed which in turn led to activation of the Mad-2 based spindle assembly checkpoint

(Mikhailov et al., 2002). The presence of topoisomerase II at the centromeres has also been related to centromeric cohesion as a function of the scaffold, in contrast to its role in separating entangled sister chromatids. This is supported by the observation that chromatids separate in the centromere region but not along their arms when cells entering anaphase are treated with topoisomerase II inhibitors (Downes et al., 1991; Gorbsky, 1994). Moreover, conjugation of topoisomerase II with the small ubiquitin-related modifier (SUMO), specifically affects the separation of sister centromeres but not the catalytic activity of the enzyme (Bachant et al., 2002), suggesting that a specific subpopulation of topoisomerase II functions at centromeres.

Furthermore, post-translational modifications of topoisomerase II such as phosphorylation have been associated with the mitotic activity of this protein. Phosphorylation of topoisomerase II has been demonstrated *in vitro* by various kinases (Porter and Farr, 2004a) and its phosphorylation increases during the S and G2/M phases (Estey et al, 1987). Both topoisomerase IIα and IIβ are phosphorylated (Ishida et al., 1996; Ishida et al., 2001; Kimura et al., 1996; Wells et al., 1995; Wells and Hickson, 1995). Since topoisomerase IIα plays an essential role in cell proliferation, many studies tried to analyse how its activity and localisation are affected by phosphorylation. Using antibodies against various phospho-oligopeptides of topoisomerase IIα, it was revealed that while phosphorylation of topoisomerase IIα at threonine 1342 occurs *in vivo* throughout the cell cycle (Ishida et al., 1996), phosphorylation at serine 1212 occurs only during mitosis (Ishida et al., 2001). Moreover, phosphorylated topoisomerase IIα at serine 1212 re-localises from chromosome arms to the centromeres and this movement is blocked by an inhibitor of topoisomerase II activity.

However, the idea of an immobilised topoisomerase II as a part of a static structural scaffold has been questioned and *in vivo* studies of fluorescently labelled topoisomerase II in human cells and *Drosophila* have revealed a dynamic behaviour of the protein during mitosis (Christensen et al., 2002; Swedlow et al., 1993; Tavormina et al., 2002). When rhodamine-labeled topoisomerase II was injected into *Drosophila* embryos, it was demonstrated that this enzyme was uniformly present throughout chromosomes, reaching its maximum at prometaphase and minimum at telophase

(Swedlow et al., 1993). In the same study, it was noted that two pools of the protein leave the chromosome, one following prophase and the other following anaphase, suggesting that there may be different forms of the enzyme with different functions or localisations.

In human cells, GFP-tagged topoisomerase IIα was reported to localise along the axial regions and centromeres of metaphase chromosomes (Tavormina et al., 2002). During anaphase, the centromeric pools of the protein were diminished while the cytoplasmic population was increased. Furthermore, fluorescence recovery after photobleaching (FRAP) revealed that topoisomerase IIα was extremely mobile and that the whole chromosomal population was in equilibrium with a large cytoplasmic pool. However, the catalytic activity of the enzyme was essential for the rapid dynamic exchange between chromosomal and cytoplasmic populations, since recovery after photobleaching was blocked by treatment of cells with drugs that trap topoisomerase IIα on DNA as a "closed clamp". Taking in account that the recovery after photobleaching was less than 100%, it could be suggested that a subpopulation of the chromosome and kinetochore associated topoisomerase IIα was more stably associated. A similar study of GFP-tagged topoisomerase IIα and IIβ resulted in very similar results for the IIα isoform (Christensen et al., 2002). During interphase the two isoforms accumulated in nucleoli, while in mitosis only topoisomerase IIα was chromosome-associated to high level. FRAP experiments revealed that the entire complement of both isoforms was completely mobile and free to exchange between nuclear subcompartments in interphase. During mitosis, topoisomerase IIα was also completely mobile and it showed a uniform distribution on the chromosomes in contrast to the axial localisation reported previously by Tavormina et al (Tavormina et al., 2002). However, it was also demonstrated in this study that a minor fraction of topoisomerase IIβ associates with chromosomes during mitosis, suggesting that both isoforms could play a role in mitotic chromosome architecture and chromosome segregation. Taken together, these data support the idea of a dynamic behaviour of topoisomerase II during the cell cycle and that this protein is not an immobile component of the scaffold.

Whether topoisomerase II is a "scaffold" component, does not rule out its role in mitotic chromosome dynamics along with other proteins important for chromosome assembly. Topoisomerase II activity is required for the resolution of the catenated strands of DNA so that each chromatid of a pair becomes an individual unit, facilitating successful separation during anaphase (Gimenez-Abian et al., 2000). Indeed, mutations in topoisomerase II in both *Saccharomyces cerevisiae* and *Schizosaccharomyces pombe* were lethal in mitosis, with sister chromatids failing to segregate properly (DiNardo et al., 1984; Holm et al., 1985; Uemura and Yanagida, 1984). Further analysis in *S. pombe* revealed that topoisomerase II was also required for the final stages of chromosome condensation, possibly in collaboration with the condensin complex (Uemura et al., 1987). However, the role of topoisomerase II in the process of chromosome condensation has been controversial since disruption of its function in different organisms resulted in different chromosome morphologies (Swedlow and Hirano, 2003; Warburton and Earnshaw, 1997). In contrast to *S. pombe*, in *S. cerevisiae*, establishment and maintenance of chromosome condensation (although very difficult to see in this organism) is independent of topoisomerase II activity (Lavoie et al., 2002). In *Xenopus* egg extracts, inhibitors of topoisomerase II (Hirano and Mitchison, 1991; Newport and Spann, 1987) or immunodepletion of topoisomerase II (Adachi et al., 1991; Wood and Earnshaw, 1990) prevented complete condensation of chromosomes.

In mammalian cells, matters are complicated by the proposed existence of a temporary G2 topoisomerase II-dependent checkpoint that regulates entry into mitosis. When the checkpoint is evaded, cells that attempt mitotic chromosome condensation produce highly elongated and imperfectly condensed chromosomal structures (Downes et al., 1991). Interestingly, in another study of the formation of mitotic chromosomes during checkpoint override after G2 arrest with topoisomerase II inhibitors, it was demonstrated that topoisomerase II-dependent decatenation was not required to remodel chromatin into a condensed chromosome with two axial cores (Andreassen et al., 1997). Likewise, extraction of topoisomerase II from condensed chromosomes did not affect chromosome morphology, but was required for the establishment of chromosome assembly and condensation (Hirano and Mitchison, 1993), suggesting that the role of

topoisomerase II in achieving full condensation was enzymatic, not structural. Recently, analysis of a conditional topoisomerase II mutation in mammalian cells revealed that topoisomerase IIα plays a largely redundant role in chromosome condensation, but an essential catalytic role in chromosome segregation (Carpenter and Porter, 2004).

In *Drosophila*, inhibition of topoisomerase II by injection of antibodies or enzyme inhibitors to blastoderm embryos, interfered with the condensation of chromatin and its proper arrangement into a metaphase plate (Buchenau et al., 1993). Furthermore, depletion of topoisomerase II by RNAi in *Drosophila* resulted in a 2.5-fold decrease in the level of chromatin compaction but overall chromosome condensation occurred without topoisomerase II (Chang et al., 2003). In the same study, chromosome morphology was abnormal and one or more chromosome arms frequently stretched out from the metaphase plate, suggesting an unexpected role for topo II in chromosome arm congression. Finally the decatanation activity of topoisomerase II allows the formation of cytologically distinguishable pairs of apposed sister chromatids, a process known as sister chromatid resolution (Gimenez-Abian et al., 1995; Losada et al., 2002), and the complete separation of sister chromatids in anaphase (Holm et al., 1985; Shamu and Murray, 1992; Uemura and Yanagida, 1984). The most prominent defects observed after disruption of the topoisomerase II activity are defects in chromatid segregation and the formation of chromosome bridges during anaphase (Swedlow and Hirano, 2003).

The distribution of topoisomerase II and its contribution to the hypothetical chromosome scaffold remains controversial. It is possible that a subpopulation of topoisomerase II associates with SAR regions during mitosis, while other pools associate with other sequences which have a role distinct from that of the scaffold (Swedlow and Hirano, 2003). It should also be noted that topoisomerase II can function as an ATP-dependent protein clamp (Wang, 2002) and the enzyme might be immobilized on DNA or chromosomes when its ATPase cycle is inactive. Furthermore the role of topoisomerase II activity in chromosome condensation remains unclear. Two different proposals have emerged, one supporting that topoisomerase II is essential for complete chromosome condensation (Adachi et al., 1991; Newport and Spann, 1987; Uemura et al., 1987; Wood and Earnshaw, 1990), while the other suggests that although

the enzyme is required for the establishment of condensation, it is unnecessary for maintenance of the condensed state (Hirano and Mitchison, 1993). The definitive role of topoisomerase II in chromosome assembly during mitosis remains to be determined but will likely be dependent on other factors such as development or genome organisation. However, it is obvious that topoisomerase II alone can not bring together chromosome organisation suggesting that other factors are also implicated in this process.

1.3.2. The SMC family

ScII, the second abundant component of the chromosome scaffold to be identified is a member of the SMC family of proteins (Saitoh et al., 1994). Originally discovered in *S. cerevisiae* (Larionov et al., 1985; Strunnikov et al., 1993), the SMCs (Stability of Minichromosomes, later Structural Maintenance of Chromosomes) are known to be present in species from mycoplasma to mammals, constituting a family of highly conserved and ubiquitous proteins, called the SMC family (Cobbe and Heck, 2000; Cobbe and Heck, 2004; Hirano, 1999). All members are large polypeptides with a molecular mass of 110-170 kDa and they share a similar structural organisation (Cobbe and Heck, 2000; Strunnikov and Jessberger, 1999). Secondary structure analysis predicts the proteins to have two extended coiled-coil domains of 250-400 residues, which are separated by a central globular hinge region of about 150 amino acid residues (Figure 1.3.A). The N- and C- termini at the end of the coiled-coil domains are highly conserved among SMC proteins (Strunnikov and Jessberger, 1999). The N-terminal domain contains an ATP binding motif (a putative Walker A box) (Saitoh et al., 1994) and it has been shown to bind an ATP analogue (Akhmedov et al., 1998). The C-terminal domain contains a "DA" box resembling a Walker B motif (ATP hydrolysis signal) (Saitoh et al., 1994; Walker et al., 1982) and it has been shown to bind DNA, with preference for AT-rich sequences such as SARs and MARs (Akhmedov et al., 1998; Graumann et al., 1998). Originally Saitoh *et al.* (1994) suggested a model for the molecular architecture of SMC proteins, proposing the formation of a functional ATPase domain by uniting the "DA" box with the ATP-binding motif A. Indeed, crystallographic studies confirmed that a functional ATPase pocket is jointly formed by

the close contact of the N- and C- terminal regions (Löwe et al., 2001), while directed mutagenesis showed that both motifs contribute to ATP binding and hydrolysis (Hirano et al., 2001). Since SMC proteins generally form dimers (Hirano et al., 1997; Melby et al., 1998), initially it was thought, that dimer formation is mediated by antiparallel arrangement of the coiled-coil domains of two SMC proteins, producing a symmetrical molecule with both the N- and C- termini at each end (Melby et al., 1998). Furthermore, it was believed that the central hinge was flexible and allowed opening and closing of the two arms (Hirano et al., 2001). However, recent studies have indicated that the coiled-coil regions of an individual SMC fold back onto each other in an intra-molecular manner and that dimerisation is mediated by hinge-hinge interactions of the self-folded monomers (Figure 1.3.B) (Haering et al., 2002; Hirano and Hirano, 2002). Most of the molecular architecture studies of SMCs have been performed with bacterial SMCs, but the conserved structure between eukaryotic and prokaryotic SMC proteins strongly suggests that they all share similar structural organisation.

Most bacteria and archaeal species contain a single *smc* gene, suggesting that bacteria and archaeal SMC proteins are likely to function as homodimers (Hirano, 1999; Hirano, 2002). The Gram-positive bacteria have an SMC protein with a domain structure similar to the eukaryotic SMCs (Melby et al., 1998). A subclass of Gram-negative bacteria, including *E. coli*, lack SMC proteins but they contain a *muKB* gene that encodes for a protein with structural and functional similarities to SMCs (Hiraga, 2000). The only difference is that the MuKB protein does not have the "DA" box at the C-terminus (Graumann et al., 1998). The MukB protein has features of a myosin-like motor protein and is involved in chromosome condensation and/or movement (Hiraga, 1992; Hu et al., 1996; Niki et al., 1991; Wake and Errington, 1995). *mukE* and *mukF* which are in an operon with *mukB*, are also required for efficient chromosome partitioning and their products are thought to interact with MukB (Yamanaka et al., 1996).

Most of the functional studies on SMC genes focused on the corresponding gene from *Bacillus subtilis*, *bsSMC*. Genetic studies of this protein suggested that BsSMC protein is essential for chromosome condensation and partitioning (Britton et al., 1998;

Moriya et al., 1998). Immunolocalisation studies revealed that the protein is associated with the chromosome but is also present in discrete foci near the poles of the cell (Graumann et al., 1998; Volkov et al., 2003). The redistribution of BsSMC protein within the cell, depending on the growth phase and the stage of the cell cycle, suggests a dynamic movement of the protein and a functional contribution to chromosome condensation and segregation. Recently, it has been proposed that chromosome segregation in *B. subtilis* takes place in at least two steps : an SMC-independent step in which origins of replication move apart and a subsequent SMC-dependent step in which newly duplicated chromosomes condense and segregate (Graumann, 2000). Therefore, it seems that BsSMC is not a required component of the mitotic motor that initially drives origins apart after their duplication but is needed to maintain the conserved arrangement of the daughter chromosomes and for their faithful segregation (Graumann, 2000; Weitao et al., 2000). Initially, biochemical studies using direct franctionation of *B. subtilis* protein extract indicated that no other proteins interact with the BsSMC protein or if a complex exists, the subunits bind to the BsSMC either transiently or with low affinity (Hirano and Hirano, 1998). However, recent studies have shown that the BsSMC protein interacts *in vivo* with two highly conserved prokaryotic proteins, ScpA and ScpB (Mascarenhas et al., 2002; Soppa et al., 2002), which bind to the SMC head domains (Volkov et al., 2003). SMC colocalises with its interacting partners, ScpA and ScpB, and the specific localisation of SMC depends on both Scp proteins suggesting that all three proteins may be complexed together (Volkov et al., 2003). Furthermore, in the same study, purified SMCs showed non-specific binding to double-stranded DNA (independent of Scp proteins or ATP), which were retained on DNA after binding to closed circular DNA but not to linear DNA. Hirano and Hirano (1998), showed that the BsSMC preferentially bound to single-stranded DNA (ssDNA) and that it has a DNA-stimulated ATPase activity much greater with ssDNA than with double-stranded DNA (Hirano and Hirano, 1998). Moreover, BsSMC formed large nucleoprotein aggregates in an ATP-dependent and ssDNA-specific manner, possibly forming a primitive type of chromosome condensation that occurs during segregation of bacterial chromosomes. Interestingly, mutations in the hinge domain disturbed dimerisation of BsSMCs and

reduced the ability to interact with DNA (Hirano and Hirano, 2002), suggesting that the major DNA-binding activity does not reside in the ATPase catalytic domains at the ends of a dimmer, but instead at the hinge regions. In contrast, in another study the SMC head domains and hinge region did not show strong DNA binding activity, suggesting that the coiled-coil regions in SMC mediate an association with DNA in a ring-like structure (Volkov et al., 2003). A model emerging from this study proposes that an SMC complex forms condensation centres that actively affect global chromosome compaction from a defined position on the bacterial nucleoid.

Eukaryotic SMCs comprise at least six distinct subfamilies (SMC1-SMC6), which are organised in three pairs of heterodimers. According to this pairing, eukaryotic SMCs are classified in the following subgroups: SMC1 and SMC3, SMC2 and SMC4, and SMC5 and SMC6. These heterodimers are further associated with other non-SMC subunits to form functional multiprotein complexes. SMCs have been shown to be implicated in different functions according to their associating subunits. The SMC1/SMC3 heterodimer is part of the cohesin complex, responsible for sister chromatid cohesion, (Guacci et al., 1997; Losada et al., 2002; Michaelis et al., 1997; Tóth et al., 1999) and is also involved in recombination as part of the RC-1 complex (Jessberger et al., 1996). The SMC2/SMC4 heterodimer is suggested to have a role in mediating mitotic chromosome condensation, as part of the condensin complex (Hirano and Mitchison, 1994; Sutani and Yanagida, 1997; Sutani et al., 1999). A form of this complex also participates in dosage compensation in *Caenorhabditis elegans* (Chuang et al., 1994; Lieb et al., 1998; Lieb et al., 1996). Finally, the SMC5 and SMC6 proteins are part of a complex which is involved in DNA repair (Fousteri and Lehmann, 2000; Fujioka et al., 2002; Harvey et al., 2004).

The ability of particular eukaryotic SMC molecules to associate as heterodimers is suggested by their coimmunoprecipitation in roughly equimolar amounts (Darwiche et al., 1999; Hirano and Mitchison, 1994; Lieb et al., 1998; Losada et al., 1998; Schmiesing et al., 1998; Sutani et al., 1999). The potential for eukaryotic SMCs to form homodimers has been demonstrated only when individual proteins were highly overexpressed, possibly having titrated out the natural SMC partner (Strunnikov et al.,

1995). Moreover, it seems that homodimers are not functional as their *in vitro* activity depends on the combined presence of both subunits (Kimura and Hirano, 1997; Kimura et al., 1999; Schmiesing et al., 1998; Sutani and Yanagida, 1997). In addition, mutation of only one SMC partner produces defects *in vivo* (Chuang et al., 1994; Lieb et al., 1998; Michaelis et al., 1997; Saka et al., 1994; Steffensen et al., 2001; Strunnikov et al., 1995; Strunnikov et al., 1993). The hypothesis that more than two SMC proteins may participate in one complex is precluded, first by considering the overall mass of isolated SMC-containing complexes and the known mass of their other components (Hirano et al., 1997; Hirano and Mitchison, 1994; Losada et al., 1998; Sutani and Yanagida, 1997; Sutani et al., 1999) and secondly by unsuccessful attempts to detect complexes containing more than two SMC proteins (Haering et al., 2002).

1.4. The condensin complex and mitotic chromosome condensation

Mitotic chromosome condensation consists of a process in which interphase chromatin is 1) compacted, and 2) resolved into two distinct rod-shaped sister chromatids. Recent studies have contributed to the unraveling of this process. Initially, mutations in two proteins, Cut3p and Cut14p in *S. pombe*, were found to exhibit defects in chromosome condensation and to display a 'cut' phenotype in which septation occurs in the absence of normal nuclear division (Saka et al., 1994). Subsequently, a five subunit "condensin" complex was identified biochemically in *Xenopus* (Hirano et al., 1997; Hirano and Mitchison, 1994) and subsequently found in *Schizosaccharomyces pombe* (Sutani et al., 1999), *Saccharomyces cerevisiae* (Freeman et al., 2000), *Homo sapiens* (Kimura et al, 2001; Schmiesing et al., 2000) *Caenorhabditis elegans* (Chuang et al., 1994; Hagstrom et al., 2002; Lieb et al., 1998; Lieb et al., 1996) and *Drosophila melanogaster* (Bhat et al., 1996; Savvidou et al., In Press; Steffensen et al, 2001). This complex was termed "condensin" and consisted of two SMC proteins (CAP-E/SMC2/Cut14 and CAP-C/SMC4/Cut3) and three non-SMC subunits (CAP-D2/Ycs4/Cnd1, CAP-G/Ycs5/Cnd3, and CAP-H/Brn1/Cnd2) (Figure 1.3.B). Most subunits have been identified in all eukaryotes examined to date (Cobbe and Heck, 2000). Genetic studies in yeast and *Drosophila* have shown that each of the condensin subunits is essential and is required

A)

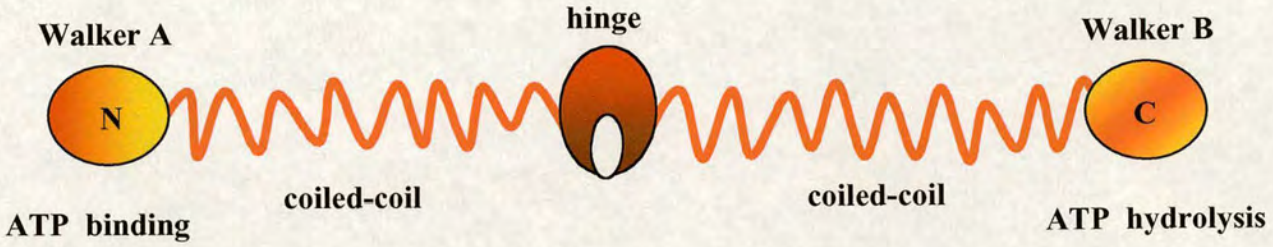

B)

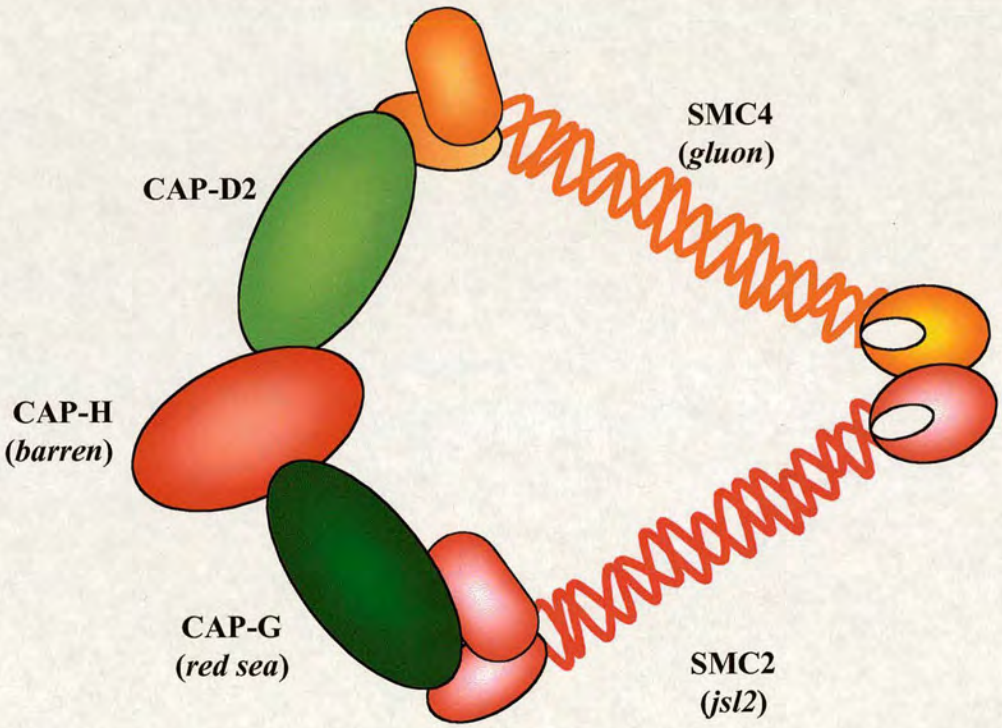

Figure 1.3. A. Secondary structure of SMC proteins. SMCs have two extended coiled-coil domains which are separated by a central hinge. The N- and C- termini at the end of the coiled-coil domains are highly conserved among SMC proteins. The N-terminal domain contains an ATP binding motif (a putative Walker A box), while the C-terminal domain contains a 'DA' box resembling a Walker B motif (ATP hydrolysis motif).
B. Representation of the condensin complex, showing the SMC2/SMC4 heterodimer and three regulatory non-SMC proteins, named after their *Xenopus* orthologues. The names of available *Drosophila* mutants for each of the proteins are shown in parentheses. The depicted position of the non-SMC subunits is random, since no specific data exist for the way that these proteins interact with each other and with the SMC subunits.

for proper condensation and/or segregation of mitotic chromosomes (Losada and Hirano, 2001). Where chromosomes are clearly visible, the main phenotype observed in the condensin mutants is a severe defect in chromosome segregation during anaphase. The failure to segregate leads to the formation of so-called anaphase bridges, a phenotype also observed in topoisomerase II mutants supporting the idea that topoisomerase II is important for mitotic chromosome assembly (Hirano, 2002). Recently, a second condensin complex, called condensin II, was identified in vertebrates (Ono et al., 2003). This complex shares the same two SMC subunits as the original complex, now named condensin I, but appears to contain different non-SMC subunits (named CAP-D3, CAP-G2, and CAP-H2).

CAP-D2/CAP-D3 and CAP-G/CAP-G2 non-SMC subunits, share a structural motif called the HEAT repeats (Neuwald and Hirano, 2000; Ono et al., 2003). The HEAT (Huntingtin, Elongation factor 3, A-subunit of protein phosphatase A, TOR) repeats are tandem repeats of an α-helical structural unit that create a protein-recognition interface with an extended solenoidal shape and on which other proteins can assemble (Andrade et al., 2001). It is possible that HEAT repeats could serve as a scaffold that would be involved in condensin complex assembly, condensin-condensin interactions or interactions between condensin and chromatin components such as histones, as well as other chromosomal proteins involved in chromosome assembly. In addition to CAP-D2/CAP-D3 and CAP-G/CAP-G2, a number of other proteins have been found to contain HEAT repeats. These proteins have other functions such as nuclear transport (importin β), transcriptional control (TAF-172/Mot1) and chromatid cohesion (Scc2/Mis4 and Pds5/BimD/Spo76). Recently, Barren/CAP-H has been classified into a new superfamily of eukaryotic and prokaryotic proteins, called kleisin (Schleiffer et al., 2003). This family also includes ScpA, Scc1 (mitotic cohesin complex) and Rec8 (meiotic cohesin complex). The N- and C-terminal domains of the kleisin proteins are conserved and they define the members of this family.

The subcellular localisation of the condensin subunits during the cell cycle seems to vary among different organisms, suggesting that condensin function may be regulated by multiple mechanisms. In *X. laevis*, *D. melanogaster*, *S. pombe and H. sapiens* the

condensin subunits associate with chromatin at early stages of chromosome condensation and dissociate at the exit of mitosis, as chromosomes decondense (Bhat et al., 1996; Cabello et al., 2001; Cubizolles et al., 1998; Hirano and Mitchison, 1994; Schmiesing et al., 2000; Sutani et al., 1999). While several studies support the idea that the condensin complex is required from prophase onward (Cabello et al., 2001; Dej et al., 2004; Hagstrom et al., 2002; Hudson et al., 2003; Kaitna et al., 2002), recent localisation studies on human cells showed that condensin I associates with chromosomes in prometaphase and only low levels are present on chromosomes in prophase (Maeshima and Laemmli, 2003). This suggests that the formation of prophase chromatids may occur independently of condensin I or with interphase levels of chromatin-bound condensin. Alternatively, it could be possible that an early stage of condensation within the prophase nucleus is mediated by condensin II, which is predominantly nuclear throughout interphase and is loaded onto chromosomes during prophase, while condensin I associates with chromosomes only after envelope break down (Ono et al., 2004; Hirano, 2005). However, during interphase the localisation of the condensin I complex tends to differ among different organisms. In chicken, the ScII protein homologue of SMC2/XCAP-E, appears to be nuclear during interphase but leaks out of the nucleus during nuclear preparation (Saitoh et al., 1994). In human cells the majority of the condensin I complex localises in the cytoplasm during interphase while some remains as foci in the interphase nucleus (Ball et al., 2002; Cabello et al., 2001; Schmiesing et al., 1998; Schmiesing et al., 2000). The subcellular distribution of the entire complex in human cells may be regulated in a cell cycle-dependent manner. The major fraction of *Drosophila* SMC4 and Barren (CAP-H) is cytoplasmic, while a minor fraction is associated with chromatin in telophase and interphase (Steffensen et al., 2001). In contrast *Drosophila* CAP-D2 appears to be nuclear throughout interphase (Savvidou et al., In Press). In *Xenopus*, all five members of the condensin appear to be nuclear during interphase (Hirano et al., 1997) and to associate with the granular compartment of the nucleolus (Uzbekov et al., 2003), suggesting sequestration to this structure or a role in the organisation of the nucleolus and/or ribosome biogenesis. In *Xenopus*, the phosphorylation of the non-SMC subunits may be required for the mitosis-

specific association of the condensin complex with chromatin (Hirano et al., 1997). However this phosphorylation does not seem to be sufficient for the association of condensin with chromatin, suggesting that other factors are involved in this process. In *S. pombe*, all five condensin subunits are cytoplasmic during interphase and accumulate in the nucleus during mitosis (fungal mitosis occurs within a nucleus) (Sutani et al., 1999), suggesting that condensin activity is regulated by shuttling in and out of the nucleus. A possible explanation is that the condensin complex might be active throughout the cell cycle and that the nuclear localisation of the complex has to be regulated. Furthermore, it has been shown that the nuclear import of the complex depends on phosphorylation of the Cut3 (SMC4) subunit and this phosphorylation is likely to be performed by Cdc2 kinase. In *S. cerevisiae*, the condensin complex localises to the nucleus and associates with chromatin throughout the cell cycle (Bhalla et al., 2002; Freeman et al., 2000; Ouspenski et al., 2000), but specifically concentrates at the rDNA region during G2/M phase (Freeman et al., 2000). It has been suggested that the complex may be implicated in suppressing inter-repeat rDNA recombination and believed to be required for silencing at the silent mating loci (Bhalla et al., 2002).

Studies of condensin function have resulted in conflicting hypotheses as to the role of this complex. In *Xenopus*, when condensin was depleted from mitotic extracts before or after condensation, unreplicated chromatin failed to assemble into individual chromatids or became completely disorganised, suggesting that the complex was required for both assembly and maintenance of mitotic chromosomes (Hirano et al., 1997; Hirano and Mitchison, 1994). *In vivo* analysis of the chromosome condensation process was initially performed on mutants in *S. pombe* (Saka et al., 1994; Sutani et al., 1999) and later on in *S. cerevisiae* (Lavoie et al., 2000; Ouspenski et al., 2000; Strunnikov et al., 1995) and *Drosophila* (Bhat et al., 1996). Mutants in Cut3 and Cut14 genes (SMC4 and SMC2, respectively) of *S. pombe* exhibited chromosome condensation defects and displayed a 'cut' phenotype where septation (cell division) occurred with incompletely separated chromosomes (Saka et al., 1994). Fluorescence *in situ* hybridization in these mutants demonstrated that the length of mitotic chromosome arms increased while the centromeric DNA could separate and move to the opposite poles

normally. Similar segregation defects were observed in *S. cerevisiae* in SMC2/4 and Brn1p (CAP-H) mutants (Bhalla et al., 2002; Freeman et al., 2000; Lavoie et al., 2000; Ouspenski et al., 2000; Strunnikov et al., 1995). Fluorescent *in situ* hybridisation analysis showed that condensation was defective, suggesting that the segregation defect was a consequence of insufficient condensation. In *S. pombe* and *S. cerevisiae*, studies have shown that all members of the condensin complex are required for proper chromosome condensation and segregation (Lavoie et al., 2002; Ouspenski et al., 2000; Strunnikov et al., 1995; Sutani et al., 1999).

In contrast, genetic studies in *D. melanogaster* (in SMC4, Barren and CAP-G mutants) and *C. elegans* showed that resolution between the sister chromatids rather than condensation of the chromosomes was compromised when the condensin complex was disrupted (Bhat et al., 1996; Dej et al., 2004; Hagstrom et al., 2002; Steffensen et al., 2001). In both organisms, a high degree of compaction relative to interphase was accomplished and a bipolar metaphase plate formed. However, severe chromosome segregation defects and chromosome breakage were observed in anaphase and telophase. DmSMC4 and DmCAP-D2 RNAi in *Drosophila* cultured cells confirmed the requirement of these proteins for chromosome organisation and segregation (Coelho et al., 2003; Savvidou et al., In Press). A common phenotype of the absence of condensin subunits in most organisms is the formation of chromosome bridges due to incomplete resolution and ensuing failure of sister chromatids to separate completely during anaphase (Hagstrom and Meyer, 2003). Particular insight was gleaned when the robustness of chromosome architecture was assessed after SMC2 knock-out in DT40 cells — while chromosomes still reached normal levels of condensation, clear defects in association of other non-histone chromosomal proteins was observed (Hudson et al., 2003), resulting in compromised structural integrity.

Recently, depletion of human condensin I by RNAi produced swollen, unresolved chromosomes (Ono et al., 2003; Watrin and Legagneux, 2005), while depletion of condensin II resulted in curly, irregularly-shaped chromosomes (Ono et al., 2003; Ono et al., 2004). Furthermore, the centromere/kinetochore regions were structurally disorganised from the

depletion of either condensin I or II subunits suggesting a specific role for both complexes in centromere organisation (Ono et al., 2004).

1.4.1. Biochemical and real-time activities of condensin complex

Even though the way that the condensin complex accomplishes condensation (if it does) is far from understood, much of the current knowledge of condensin comes from the characterisation of the complex from *Xenopus* egg extract. Condensin was first identified using an *in vitro* chromosome assembly process in which demembranated sperm nuclei were added to a *Xenopus* egg extract (Hirano et al., 1997; Hirano and Mitchison, 1994). The complex was termed 13S according to its sucrose sedimentation coefficient. The 13S holocomplex is composed of two subcomplexes: an 8S core subcomplex consisting of the two SMCs (XCAP-C and XCAP-E) and an 11S regulatory subcomplex consisting of the three non-SMC subunits (XCAP-D2, XCAP-G and XCAP-H) (Hirano et al., 1997; Kimura and Hirano, 2000). The 13S condensin complex, in contrast to topoisomerase II, has been shown to be required for both the establishment and maintenance of chromosome condensation (Hirano et al., 1997; Hirano and Mitchison, 1993; Hirano and Mitchison, 1994). Each of the condensin subunits is essential and required for proper organisation and segregation of mitotic chromosomes, but exactly how the complex contributes to these processes is still unclear.

Purified 13S and 8S complexes have been shown to bind DNA *in vitro* but only the 13S complex can be recruited onto chromatin (Kimura and Hirano, 2000). The 13S condensin complex displays a DNA-stimulated ATPase activity and reconfigures DNA in an ATP-dependent manner (Hirano et al., 2001; Kimura and Hirano, 1997; Kimura and Hirano, 2000). It introduces positive supercoils into relaxed circular DNA in the presence of topoisomerase I and it converts nicked circular DNA into positively knotted forms in the presence of topoisomerase II *in vitro* (Kimura et al., 1999). The predominant products in this assay are positive 3-noded knots, suggesting that condensin has the ability not only to induce positive supercoiling of DNA but also to orient the introduced supercoils into a solenoidal form.

Recent observations of the condensin complex by electron spectroscopic imaging, suggest that a single condensin complex organises two oriented supercoils in its bound region by hydrolysing ATP (Bazett-Jones et al., 2002). In this way, it induces a superhelical tension that propagates into the protein-free region of DNA. The binding of condensin to DNA seems to be ATP-dependent and condensin-condensin interactions may not be essential for the supercoiling reaction. A model based on these observations proposes that a single condensin complex introduces two positive supercoils by a trapping mechanism (Haering et al., 2002) and forms a topological link between the condensin "clamp" and the trapped DNA strands. If a free translocation of the DNA strands is allowed without disrupting the topological link, a positive loop of DNA would be created that is constrained by the clamp. An array of positive loops directed by the concerted action of condensin might then contribute to mitotic chromosome organisation (Figure 1.4.A) (Swedlow and Hirano, 2003). Another model called, the superhelical tension model, predicts that local positive supercoiling driven by condensin introduces compensatory superhelical tension into the neighbouring region of DNA, which in turn acts as a driving force for the compaction of a chromatin fibre (Figure 1.4.B) (Kimura and Hirano, 1997). Despite the fact that there is no evidence for the occurrence of such a superhelical tension in metaphase chromosomes, several other models of chromosome organisation predict successive coiling of chromatin fibres (Belmont and Bruce, 1994), which should also result in superhelical tension.

Neither 8S nor the 11S subcomplexes could bind to chromatin and induce supercoiling activity in the *Xenopus in vitro* chromosome assembly assay. However, even though both SMC subunits share ATP binding domains, SMC heterodimers showed a weak ATPase activity which was not stimulated by DNA (Kimura and Hirano, 2000). The 8S subcomplex also failed to change DNA conformation in the topoisomerase-based supercoiling assays. In *S. cerevisiae*, the DNA-bound species became resistant to salt extraction at high SMC2/SMC4:DNA ratios (Stray and Lindsley, 2003). However, the reaction remained reversible, as the subcomplex had the ability to bind competitor DNA. Furthermore, in the presence of ATP, high molar ratios of *S. cerevisiae* SMC2/SMC4 subcomplex promoted a geometric change in circular DNA that

could be trapped as knots by topoisomerase II but not as supercoils by topoisomerase I. Similarly, the SMC2/SMC4 subcomplex of *S. pombe* also formed large protein/DNA complexes, but failed to exhibit ATPase activity (Yoshimura et al., 2002). Taken together, these data suggest that the non-SMC subcomplex plays an important regulatory role in ATPase activity and chromatin binding of the 13S holocomplex. Indeed, the three non-SMC subunits, CAP-D2, CAP-G and CAP-H have been shown to bind to one (or both) of the catalytic ends of the SMC heterodimer (Anderson et al., 2002; Yoshimura et al., 2002). They have been proposed to have dual roles in the regulation of condensin function: one is to activate the SMC ATPases to perform ATP-dependent supercoiling activity, and the other is to allow the holocomplex to associate with chromatin in a mitosis-specific manner (Kimura and Hirano, 2000).

Even though the above biochemical and spectroscopic data show that structural changes are induced by addition of condensin to naked DNA templates, many essential questions of how condensin actually mediates chromosome assembly still remain unanswered. Does condensin drive chromosome assembly directly or does it help to set up a structure that loads other critical assembly factors (Porter et al., 2004b)? Two groups using either magnetic field or optical trap methods, acting on beads attached to the end of DNA have tried to analyse condensin activity on single DNA molecules (Case et al., 2004; Strick et al., 2004). These studies showed that both vertebrate and bacterial condensins drive DNA compaction in a stepwise, ATP-dependent fashion with a surprising level of cooperativity. The measurement of individual compaction steps revealed approximately 60 nm step sizes and these values are in agreement with the results obtained by spectroscopic imaging (Bazett-Jones et al., 2002). MukBEF required nucleotide binding for activity and it could compact DNA in the presence of either ATP or a non-hydrolyzable form of ATP (Case et al., 2004). In contrast *Xenopus* condensin required ATP for stable DNA binding but required nucleotide hydrolysis for DNA compaction. ATP binding by the *Bacillus subtilis* condensin complex was necessary for the closure of the two arms of the condensin complex (Hirano and Hirano, 2004). Taken together, these results suggest that condensin binds DNA in an open form, but it can compact DNA only in its closed state which is induced, at least partly, by ATP binding.

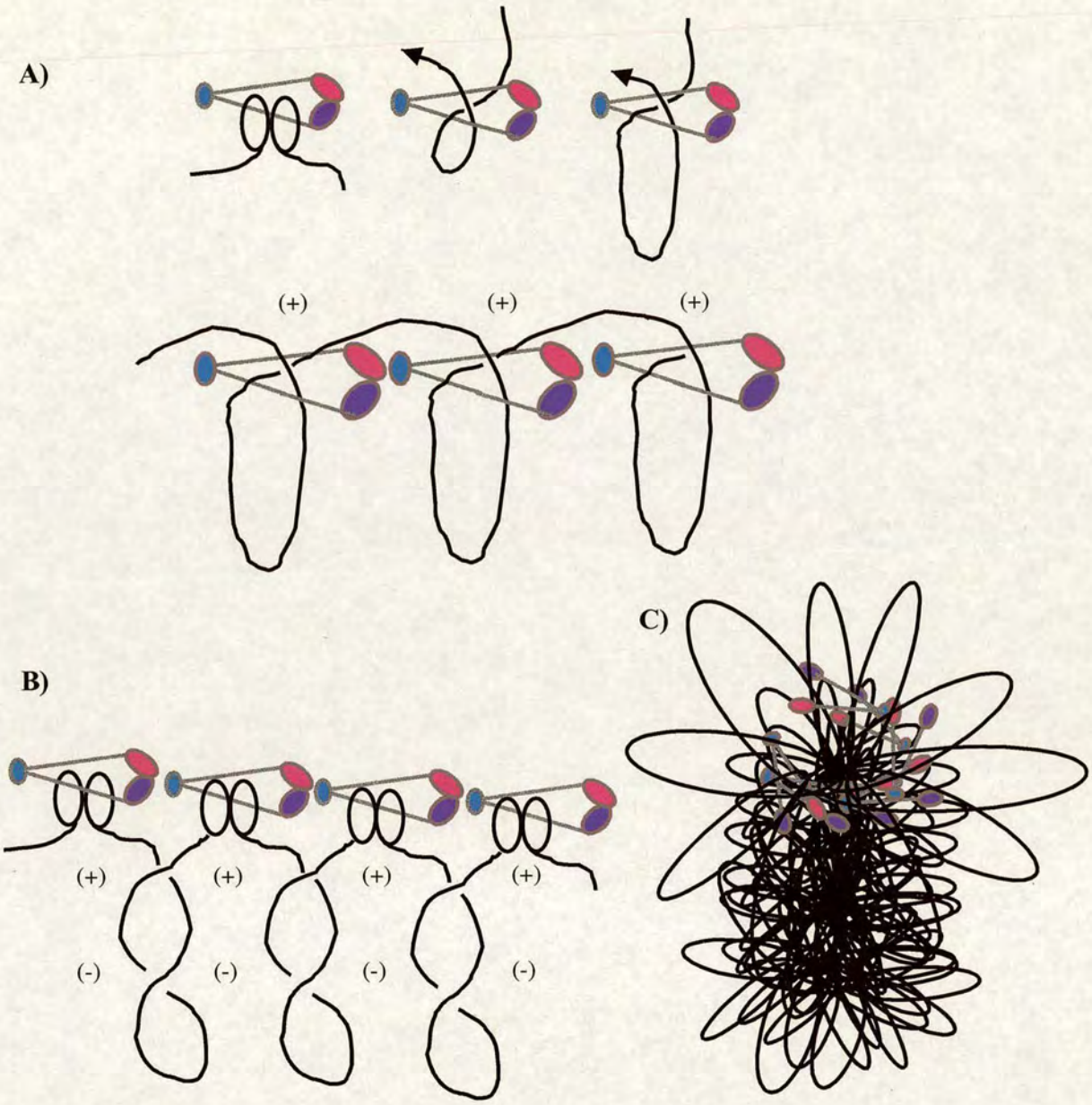

Figure 1.4. Hypothetical models for the mechanical contribution of condensin to chromosome organization.
A. In this model condensin traps two positive supercoils, thereby forming a topological link between the protein "clamp" and the trapped DNA strands. If a free translocation of the DNA strands is allowed without disrupting the topological link, a positive loop of DNA would be created. An array of positive loops directed by the conserted action of condensin might contribute to chromatin compaction.
B. Superhelical helical tension model. In this model, local positive supercoiling activity driven by condensin introduces a compensatory, negative superhelical tension into the neighbouring region of DNA. This tension may in turn act as a driving force for the compaction of a chromatin fiber.
C. A speculative model for condensin assembly that incorporates the highly ordered and cooperative condensin-condensin and condensin-DNA interactions. Adapted from Swedlow and Hirano (2003).

From both studies (Case et al., 2004; Strick et al., 2004), it seems that a high degree of cooperativity of binding between individual condensin molecules is important for condensin activity. In conclusion, it can be suggested that condensin complexes can organise themselves onto a DNA template in a highly ordered fashion, probably involving intramolecular interactions between condensin components (Figure 1.4.C). These condensin-condensin interactions could form a contiguous structural island and other proteins such as DNA topoisomerase II, chromatin remodelling factors or chromokinesin could collaborate with condensin in these specific sites in order to organise higher order chromosome structure (Porter et al., 2004b).

But how does condensin bind DNA? Interestingly, a recent biochemical study showed that that the SMC head domains and hinge region do not have strong DNA binding activity, suggesting that the coiled-coil regions in SMCs mediate an association with DNA and they may bind to DNA as a ring-like structure (Volkov et al., 2003). Similarly, cohesin, a related SMC-containing complex, has been proposed to trap double-stranded DNA between the two arms of the SMC1-SMC3 heterodimer (Gruber et al., 2003; Haering et al., 2002; Haering and Nasmyth, 2003). In this model the non-SMC subcomplex acts as a clamp, which controls the capture and release of the substrate DNA by the SMC dimer. Another study, using atomic force microscopy suggests that condensin could form a DNA loop by folding two distantly located DNA segments (Yoshimura et al., 2002). Thus, dynamic trapping of two DNA segments within the two-armed structure may be the fundamental mechanism of action that is shared by all SMC proteins, including condensin and cohesin (Haering et al., 2002). The catalytic domain of SMC proteins is similar to that of ABC (ATP binding cassette) transporters (Löwe et al., 2001; Saitoh et al., 1994). These transporters comprise a large family of membrane-bound ATPases actively transporting small molecules across a cellular membrane. Furthermore, the geometry of protein structure between the ATPase domain of SMCs and ABC proteins is very similar (Locher et al., 2002). Therefore, it has been proposed that ATP binding and hydrolysis allows the closing/opening of the two coiled-coil arms, similar to the association/dissociation of the two catalytic domains of the ABC transporters (Hirano et al., 2001).

1.4.2. Regulation of condensin through phosphorylation

In *Xenopus* the supercoiling activity of 13S condensin has been shown to require mitosis specific phosphorylation of the three non-SMC subunits by Cdc2 (Cdk1-Cyclin B), the major mitotic kinase (Hirano et al., 1997; Kimura et al., 1998). XCAP-D2 is phosphorylated at its C-terminus probably directly by Cdc2, while XCAP-H is phosphorylated most likely by Cdc2 but also by other kinases (Kimura et al., 1998). This hyperphosphorylation of the 11S subcomplex has been proposed to activate the ATPase activity of the SMC heterodimer and to allow the 13S holocomplex to associate with chromatin in a mitosis specific manner (Kimura and Hirano, 2000). In human cells, condensin is phosphorylated throughout the cell cycle but mitosis-specific phosphorylation of the three non-SMC subunits at specific sites by the Cdc2 kinase, has been shown to be responsible for chromosomal targeting of condensin (Kimura et al., 2001; Takemoto et al., 2003). Furthermore, the supercoiling activity of human condensin increased dramatically after phosphorylation. In *S. pombe*, phosphorylation of Cut3/SMC4 at threonine-19 by Cdc2 is necessary for the translocation of the condensin complex from the cytoplasm into the nucleus (Sutani et al., 1999) but not for its supercoiling activity. This phosphorylation site is not conserved in human condensin, suggesting that the regulation of chromatin targeting may be species-specific.

1.4.3. Targeting of the condensin complex to chromosomes

Even though mitosis-specific phosphorylation of condensin subunits has been shown in *Xenopus* and human cells to be required for the association of condensin complex with chromosomes, it seems that this phosphorylation is not sufficient for this loading and that other mitotically activated factors are involved (Kimura and Hirano, 2000).

A non-histone candidate for such a receptor is AKAP95, an A-kinase (cAMP-dependent protein kinase) anchoring protein of 95 kDa, which in human cells it has been shown to function as a targeting protein for the condensin complex (Collas et al., 1999; Steen et al., 2000). AKAP95 is localised in the nuclear matrix during interphase, relocalises to chromatin upon mitosis and targets condensin after nuclear envelope break down in mitotic HeLa cells. Immunodepletion experiments in human cell mitotic

extracts showed that AKAP95 is required for the recruitment of condensin independently of the anchoring and activity of the PKA (Collas et al., 1999). In AKAP95 depleted extracts, the amount of recruited condensin complex and the extent of chromosome condensation was proportional to the concentration of recombinant AKAP95 that was added back to the rescue experiments (Steen et al., 2000). A model emerging from these observations, proposes that the AKAP95 would act as a structural platform for the loading of condensin. Furthermore two-hyprid and GST-pull down experiments showed that AKAP95 and CAP-H ineract directly (Eide et al., 2002). However, this does not preclude the existence of additional factors that contribute to the loading of condensin onto chromatin. Interestingly, during the first mitosis in mouse embryos only maternal chromosomes require AKAP95 for condensin recruitment while parental chromosomes recruit condensin in an AKAP95-independent manner (Bomar et al., 2002), suggesting that different mechanisms exist depending on the structure and/or biochemical composition of chromatin.

Recently, it has been shown that the C-terminus of the human condensin subunit CNAP1/CAP-D2 possesses a mitotic chromosome-targeting domain that does not require the other condensin components (Ball et al., 2002). The same region also contains a functional bipartite nuclear localisation signal. A mutated CNAP1/CAP-D2 missing the C-terminal chromosome-targeting domain was able to form a complete condensin complex but failed to associate with mitotic chromosomes, suggesting that CNAP1/CAPD2 is responsible for the recruitment of the human condensin complex onto chromosomes. This targeting is thought to be mediated by direct interactions with histones H1 and H3 *in vitro*. The H3 interaction appears to be mediated through the histone tail, and a subfragment containing the targeting domain of CNAP1/CAP-D2 was found to interact with histone H3 *in vivo*. However, these results are contradictory to the observation that in *Xenopus* the 11S non-SMC subcomplex was unable to bind chromatin by itself (Kimura and Hirano, 2000). Several explanations have emerged to reconcile these observations such as that the other two non-SMC subunits repress the targeting function of CNAP1/CAPD2 and this repression is finally released with the formation of the condensin holocomplex. Alternatively, stable association of

CNAP1/CAPD2 with chromatin may require additional factors which may be missing in the *Xenopus in vitro* system, or that there may be species-specific differences between human and *Xenopus* systems (Ball et al., 2002).

1.4.4. Other factors involved in condensin loading and chromosome condensation: role for histone H3 phosphorylation.

The phosphorylation of histone H3 at the onset of mitosis has been proposed to play a role in condensin recruitment and chromosome condensation. Histone H3 is phosphorylated on serine 10 in the N-terminal tail during late G2/early prophase (Hendzel et al., 1997), an event that coincides with the initiation of chromosome condensation. Aurora B has been proposed to be the physiological kinase that phosphorylates histone H3 during mitosis (Giet and Glover, 2001; Hsu et al., 2000; Speliotes et al., 2000) and this kinase is a member of the chromosomal passenger complex along with INCENP, Survivin, Borealin, and TD-60 (Adams et al., 2001a; Gassmann et al., 2004; Sampath et al., 2004). Chromosome passengers localise to centromeres at prometaphase and metaphase, associate with the central spindle at the onset of anaphase and finally localise to the midbody in cytokinesis. Both INCENP and Survivin are required for the correct targeting of Aurora B in mitosis.

A model that connects the phosphorylation of histone H3 and chromosome condensation proposes that the modification of the histone may send a signal to initiate chromosome condensation and this phosphorylation could function as a receptor for the recruitment of proteins such as the condensin complex (Hirano, 2002). Histone H3 mutations in *Tetrahymena thermophila* have shown abnormal chromosome condensation and extensive chromosome loss (Lanlal et al., 1999), while phosphorylation of H3 has been shown to be required for proper chromosome condensation and segregation (Wei et al., 1999). In mammalian cells, analysis of histone H3 phosphorylation during mitosis revealed that phosphorylation is necessary for the initiation, but not maintenance, of chromosome condensation in these cells (Van Hooser et al., 1998). When Aurora B was depleted by RNAi in *Drosophila*, Barren/CAP-H was not properly targeted to chromosomes (Giet and Glover, 2001). Similarly in *C. elegans*, depletion of Aurora B

prevented the association of SMC4 with mitotic chromosomes (Hagstrom et al., 2002). However, CNAP1/CAPD2 was shown to bind histone H3 *in vitro*, regardless of the H3 phosphorylation state (Ball et al., 2002). Moreover, other studies suggest that neither the recruiting of the condensin complex, nor chromosome condensation are affected when phosphorylation of histone H3 is reduced by depletion of Aurora B in *Xenopus* egg extracts (MacCallum et al., 2002). In the same organism, the condensin complex can interact with "tail-less" nucleosomes (de La Barre et al., 2000), while artificial induction of H3 phosphorylation is not sufficient to recruit condensin to chromosomes (Murnion et al., 2001). Nevertheless, studies with intact or tail-less histones in *Xenopus* showed that the flexible tails of histones are important for chromosome assembly, each one with differing efficiency, while nucleosomes are necessary for recruiting chromosome assembly factors different from topoisomerase II and condensin (de La Barre et al., 2000). Furthermore, the N-terminus of H2B was shown to be essential for chromosome condensation in *Xenopus* but not that of histone H3 or its phosphorylation (de la Barre, 2001). In *S. cerevisiae* phosphorylation of histone H3 on serine 10 is dispensable for cell cycle progression (Hsu et al., 2000). In plants, H3 phosphorylation occurs in late prophase on already quite compact chromosomes and is restricted to the pericentromeric heterochromatin (Kaszas and Cande, 2000).

Whether phosphorylation of H3 on serine 10 is essential for chromosome dynamics remains controversial. However, speculative models tried to explain the relationship between histone H3 phosphorylation and chromosome dynamics. One of these models implicates Aurora B in regulating the cohesin complex (holds sister chromatids together). Polo-like kinase regulates the dissociation of cohesin from chromatin that occurs at the onset of mitosis in vertebrate cells (Sumara et al., 2002). Another study showed that Aurora B kinase cooperates with polo-like kinase to facilitate the dissociation of cohesin in *Xenopus* egg extract (Losada et al., 2002). Depletion of the two kinases blocked cohesin release and compromised the resolution of sister chromatids, while rod-shaped chromosomes with a normal level of compaction were still assembled. Aurora B, unlike polo-like kinase, can not phosphorylate cohesin subunits *in vitro*. One possible scenario is that phosphorylation of histone H3 by Aurora B directly

contributes to the resolution of sister chromatids, possibly by enchancing the structural flexibility of the chromatin fibres or by increasing the electrostatic repulsion between the two chromatids (Swedlow and Hirano, 2003). This model could explain several previous observations. First, the resolution of chromatids occurs along with phosphorylation of histone H3 and chromosome compaction during prophase. Second, in *S cerevisiae* whereas H3 phosphorylation is dispensable, neither prophase release of cohesin nor sister chromatid resolution is prominent in this organism (Hsu et al., 2000). Third, Aurora B is required for the release of arm cohesion during meiosis I in *C. elegans* (Kaitna et al., 2002; Rogers et al., 2002) implicating that this function of Aurora B may be utilised in both mitosis and meiosis.

Nevertheless, a completely different model, called 'the ready production label', proposes that cells use the phosphorylation of histone H3 to mark the chromosomes when they are ready to progress through anaphase and telophase (de la Barre et al., 2001). This model was based on the observation that in all experimental systems described, including plants, chromosomes were heavily phosphorylated at metaphase and dephosphorylated upon exit of mitosis. Thus H3 phosphorylation could be viewed as a type of 'ready production label', and this label would have to be attached to histone H3 once the chromosomes had passed through the various checkpoints and have reached metaphase. Consistent with this model, is the observation that the main defects associated with deficiencies of H3 phosphorylation occurred after metaphase (Hans and Dimitrov, 2001). However, future work is necessary to clarify the exact role of H3 phosphorylation in mitotic chromosome dynamics.

Finally in addition to the phosphorylation on Ser10, it has been shown that histone H3 is also phosphorylated on serine 28 probably by Aurora B (Goto et al., 1999; Goto et al., 2002) and on threonine 11 (Preuss, 2003) in a mitosis-specific manner. However, it is unclear whether these modifications are causally linked. While the role of these phosphorylations in chromosome dynamics remains to be determined, it seems that in *Xenopus* the phosphorylation at serine 28 is not essential for chromosome condensation (de la Barre et al., 2001).

1.4.5. Condensin complex and interphase

Beside their essential contribution to mitotic chromosome dynamics the condensin subunits appear to play important roles at non-mitotic stages of the cell cycle as well. In *C. elegans*, transcription from each of the X chromosomes is reduced two-fold in hermaphrodites (XX) of this organism, to match the level of X-linked gene expression in males (XO), a process that is known as dosage compensation. Among the proteins that are implicated in this pathway are MIX-1, DPY-27, DPY-26 and DPY-28 (Meyer, 2000). The discovery that DPY-27 is an SMC4 variant provided the first hint that SMC proteins may be involved in this process (Chuang et al., 1994; Chuang et al., 1996). Subsequently, MIX-1 was identified as an SMC2 homologue required for both mitotic chromosome behaviour and dosage compensation (Lieb et al., 1998). The restricted localisation of MIX-1 on the X chromosome was dependent on DPY-27. Like condensin, the dosage compensation complex consists of a MIX-1/DPY-27 (SMC2/4) heterodimer and at least two non-SMC subunits, DPY-26 and DPY-28 (Hagstrom and Meyer, 2003; Lieb et al., 1996). In contrast, the conventional condensin complex in *C. elegans* consists of MIX-1, SMC4 (Hagstrom et al., 2002) and a non-SMC subunit, HCP-6 (Stear and Roth, 2002), that belongs to the condensin II-specific subunits (Ono et al., 2003). It has been suggested that the two complexes are functioning in a similar way by altering the higher-order structure of chromosomes, one to regulate gene expression and the other to act on chromosome condensation.

Another example of a role for the condensin complex in transcriptional control comes from the study of the Bithorax (BX-C) complex in *Drosophila*. Genes of this genomic region are maintained epigenetically active or repressed throughout development by a balance of Trithorax-group and Polycomb-group proteins. These proteins bind to *cis*-acting sequences named polycomb-responsive elements (PRE). It has been shown that Barren/CAP-H and topoisomerase II cooperate with the Polycomb-group proteins to maintain the silent state of gene expression (Lupo et al., 2001). Furthermore, in a *Barren* mutant, PRE-induced gene silencing was shown to be impaired. Whether the conventional condensin complex or a variant thereof is involved in this process is not known.

Ycs4/CAP-D2 and SMC4 but not SMC2 appear to be required for transcriptional silencing at the mating-type loci in *S. cerevisiae* (Bhalla et al., 2002). This suggests that, as in the case of dosage compensation in *C. elegans*, a specialised variant of the canonical condensin complex may be involved in this process. Similarly, Cnd2/CAP-H was recently shown to be required for the activity of Cds1/Chk2 (a G2 checkpoint kinase) in *S. pombe* (Aono et al., 2002). Although all the other condensin components in *S. pombe* were also required for full Cds1 activity, the SMC2/Cut14 and SMC4/Cut3 proteins did not seem to be necessary for viability in the presence of hydroxyurea during S phase, suggesting that this non-mitotic function may be supported by unique subsets of condensin components.

1.4.6. Interphase chromosome functions and mitotic chromosome condensation

Several perturbations of interphase chromatin function seem to affect the formation of chromosomes in the subsequent mitosis. In *Drosophila*, mutants affecting ORC2, a component of the Origin Recognition Complex, disrupted the normal pattern of chromosomal replication in S phase and produced irregularly-condensed mitotic chromosomes (Loupart et al., 2000). The abnormally-late replicating regions of euchromatin exhibited the greatest problems in mitotic condensation. Interestingly, another study of ORC2, ORC3, and ORC5 showed that the mitotic chromosomes were shorter and thicker than wild type (Pflumm and Botchan, 2001). Also, it was observed that mutations in other replication factors such as MCM10, MCM4 and PCNA displayed a similar phenotype as the ORC mutants, suggesting that this phenotype is not a specific consequence of ORC disruption, but rather that it correlates with abnormal replication (Christensen et al., 2003; Pflumm and Botchan, 2001). These observations led to a model that links DNA replication and mitotic chromosome condensation, where the density of functional replication origins determines the size of DNA loops and thereby modulates the shape of mitotic chromosomes. However, mutations in RFC4, a subunit of the replication factor C complex, caused aberrant checkpoint control in response to inhibition of DNA replication or damage to chromosomes (Krause et al., 2001). This mutant also displayed striking defects in mitotic chromosome cohesion and

condensation which are believe to be due to inhibition of multiple RFC complexes important for replication, DNA structure checkpoint and cohesin. It could however be possible, that the mitotic phenotypes observed in the mutants described above, are a result of indirect effects of the perturbation of cell cycle progression (though phenotypes not seen with chemical inhibitors).

1.5. Respective roles for the condensin complex and topoisomerase II in chromosome dynamics

Condensin mutants in several organisms (Bhalla et al., 2002; Hagstrom et al., 2002; Saka et al., 1994; Steffensen et al., 2001; Strunnikov et al., 1995; Sutani et al., 1999) display very similar phenotypes to those of topoisomerase II (DiNardo et al., 1984; Holm et al., 1985; Uemura et al., 1987) with obvious effects on chromosome condensation (compaction and resolution) and segregation. As previously mentioned, localisation studies revealed that topoisomerase II is axially distributed in the chromosome arms with some concentration at the centromeres, a distribution that is also observed for condensin subunits (Maeshima and Laemmli, 2003; Steffensen et al., 2001). The localisation pattern and the phenotype after the depletion of either the condensin complex or Topo II suggest that these two components of the chromosome scaffold may collaborate to bring about chromosome compaction and organisation. However, the two components are sequentially loaded onto chromosomes, suggesting that chromosome assembly is taking place in two steps (Maeshima and Laemmli, 2003). Topoisomerase II is loaded onto chromatid axis during prophase whereas condensin is loaded only during prometaphase. Double staining for topoisomerase II and condensin generated a "barber pole" appearance and the two components alternate along the solenoidal axis. Nevertheless, topoisomerase II was mislocalised on SMC2-depleted chromosomes in chicken DT40 cells and CAP-D2-depleted cells in *Drosophila*, suggesting that condensin is required for the recruitment of topoisomerase II along chromatid axes and at centromeres (Hudson et al., 2003; Savvidou et al, In Press). Furthermore, immunodepletion and immunoblocking experiments in *Xenopus* indicate that both topoisomerase II and the condensin complex are required for chromosome

condensation. However, whereas topoisomerase II is only required for the establishment of chromosome condensation in this organism (Hirano and Mitchison, 1993), the condensin complex is required for both establishment and maintenance of chromosome structure (Hirano and Mitchison, 1994). Biochemical and localisation studies in *Drosophila* showed that CAP-H/Barren associated with topoisomerase II throughout mitosis, while SMC4 appeared to be responsible for the axial localisation of topoisomerase II on the chromosomes and for its decatenation activity (Bhat et al., 1996; Coelho et al., 2003). However, in *S. pombe*, the localisation but not the activity of Topo II was affected in condensin mutants (Bhalla et al., 2002), while Topo II localization to well-defined axial structures in *Xenopus* was independent of condensin (Cuvier and Hirano, 2003). Given that chromosomes experience different constraints depending on the cell, organism, or time in development, it is perhaps not surprising that a 'unified' hypothesis regarding these two components has not emerged.

1.6. Condensin complex II

Recently, a second condensin complex, called condensin II, was identified in vertebrates (Ono et al., 2003; Yeong et al., 2003). This complex shares the same two SMC subunits as the original condensin complex, now named condensin I, but appears to contain different non-SMC subunits (named CAP-D3, CAP-G2, and CAP-H2). The condensin complex II was originally identified in human cells and *Xenopus* but all of the three non-SMC subunits were found in *Arabidopsis thaliana*, suggesting that condensin II is widespread among the eukaryotic kingdoms. The *D. melanogaster* genome lacks a sequence encoding CAP-G2 whereas none of the condensin II-specific non-SMC genes are present in *S. pombe* or *S. cerevisiae*. Intriquingly, the genome of *C. elegans* encodes for the three condensin II-specific subunits but none of the condensin I specific subunits. The CAP-D3 and CAP-G2 proteins contain HEAT repeats (Ono et al., 2003), while CAP-H2 corresponds to kleisin-β (Schleiffer et al., 2003).

The two complexes appear to alternate along the axis of metaphase chromatids but show a unique distribution at the centromere/kinetochore region (Ono et al., 2004). Depletion of these complexes in *Xenopus* and HeLa cells produced distinct defects in

chromosome morphology, suggesting that the complexes may contribute differently to mitotic chromosome architecture (Ono et al., 2003). Depletion of either of the SMC subunits resulted in fuzzy, cloud-like chromosomes in which no sister chromatids could be distinguished. Depletion of condensin I produced swollen chromosomes, while depletion of condensin II resulted in curly, irregularly-shaped chromosomes. Furthermore, the centromere/kinetochore regions were structurally disorganised from the depletion of either condensin I or II subunits suggesting a specific role for both complexes in centromere organisation (Ono et al., 2004). Similarly, another study in mammalian cells showed that the two complexes associate sequentially with chromosomes: condensin II is predominantly nuclear during interphase and associates with chromatin in prophase, in contrast to condensin I which is cytoplasmic and thus can interact with chromosomes only after envelope breakdown (Hirota et al., 2004). In this study, RNAi analysis revealed distinct functions for the two complexes in mitotic chromosome assembly. Condensin II is required for chromosome condensation in early prophase, whereas condensin I is required for the complete dissociation of cohesin from chromosome arms, for chromosome shortening and for normal timing of progression through prometaphase and metaphase. Further analysis of these two complexes in mammalian cells and in other organisms will hopefully elucidate their distinct contributions to mitotic chromosome architecture.

1.7. Conclusions

How do chromatin fibres fold and organise into mitotic chromosomes? The precise mechanism of chromosome organisation remains a mystery, despite progress over the last 25 years aimed at identifying components essential to the compaction of the genome during mitosis. Modern experimental approaches are now providing novel insights into the old questions and raise exciting sets of new questions. Indeed, recent studies of condensin have resolved the old controversy by showing that non-histone proteins in addition to histones play an essential role in mitotic chromosome structure. However, it seems that condensin is only one piece of a complicated puzzle and the interplay of condensin with other factors is far from completely understood. Depending on the exact

interacting partners, several condensin variants exist with roles in both mitotic and non-mitotic functions. It could be suggested that these diverse functions are fulfilled by similar mechanisms involving chromatin remodelling and local distortions of DNA. Nevertheless, contributing data suggest that the proposed actions of condensins and topoisomerase II alone are not sufficient for mitotic chromosome assembly, paving the way for the identification of further components or activities required for this essential process. These may include proteins involved in DNA replication (Christensen et al., 2003; Dej et al., 2004; Loupart et al., 2000; Pflumm and Botchan, 2001) or diverse factors such as kinases (Yu et al., 2004) and proteases (McHugh et al., 2004), demonstrating that much remains to be learnt about the full requirements for chromosome condensation.

1.8. The cohesin complex and sister chromatid cohesion

Sister chromatid cohesion is established between the two replicated sister chromatids during S phase by an evolutionarily conserved protein complex called cohesin. The cohesin complex consists of a heterodimer of SMC1 and SMC3 and two additional non-SMC subunits called Scc1/Mcd1/Rad21 and Scc3/SA (Losada and Hirano, 2001). Vertebrate cells have two isoforms of SA: SA1 and SA2. In meiosis, there is a meiosis-specific cohesin subunit homologous to Scc1, known as Rec8 (Buonomo et al., 2000). The cohesin complex was first identified in *Xenopus* and then in *S. cerevisiae*, *S. pombe*, *Drosophila* and humans (Losada et al., 2000; Sumara et al., 2000; Tomonaga et al., 2000; Tóth et al., 1999; Vass et al., 2003; Warren et al., 2000a). Mutations in cohesin subunits cause precocious sister chromatid separation (Guacci et al., 1994; Michaelis et al., 1997; Tóth et al., 1999), while mutations that prevent cohesin from being removed inhibit chromosome separation (Hauf et al., 2001; Rogers et al., 2002; Uhlmann et al., 1999).

In most organisms, cohesin associates with chromosomes during G1 but it is only during S phase that it gets tightly associated and generates cohesion between sister DNAs as they emerge from replication forks (Riedel et al., 2004). The role of cohesin during G1, is, however, not understood. Sister chromatid cohesion is maintained until

the metaphase to anaphase transition when chromatids separate to opposite poles. While in yeast cohesin dissociates from chromosomes at the beginning of anaphase (Guacci et al., 1997; Michaelis et al., 1997), in vertebrates and flies most of the cohesin complex (~95%) dissociates from chromosomes in prophase and only a small amount of cohesin can be detected at centromeric regions (Losada and Hirano, 2001). Cohesin is also essential for meiosis and its chromosomal location clearly parallels the differential cohesion events of meiosis I and II. During meiosis I, in which homologues pair, cohesin localises all along the arms. It is released along the arms when homologues segregate at the end of meiosis I, but remains at the centromeres until the end of meiosis II to keep the sister chromatids paired until their segregation (Hagstrom and Meyer, 2003).

The dissolution of cohesion is triggered by the Anaphase Promoting Complex (APC/C). In *S. cerevisiae* the APC/C is activated and targets a protein called securin (Pds1) for degradation by ubiquitin-dependent proteolysis. The result of this degradation is the activation of securin's binding partner, a conserved enzyme referred to as separase (Esp1). Its cysteine protease activity specifically cleaves Scc1/Mcd1 at two sites and sister chromatids are separated (Ciosk et al., 1998; Uhlmann et al., 1999; Uhlmann et al., 2000). In addition, phosphorylation of Scc1 by the Polo/cdc5 kinase enhances the cleavage reaction (Hirano, 2002). A similar mechanism occurs in *S. pombe* (Tomonaga et al., 2000). In contrast, dissolution of cohesion in higher eukaryotes occurs in two steps: a separase independent (or APC independent) step in prophase for dissolution of arm cohesion and a separase dependent step in anaphase for dissolution of centromeric cohesion (cleavage of the Scc1/Rad21 subunits). Recent studies in *Xenopus* propose that Polo-like kinase regulates the dissociation of cohesin from chromosome arms in prophase (Sumara et al., 2002). The nature of the molecular difference between arm and centromeric cohesion was not known until recently. MEI-S332 in *Drosophila* (Kerrebrock et al., 1995; LeBlanc et al., 1999; Moore et al., 1998) and Sgo1 (Shugoshin) in yeast (Katis et al., 2004; Kitajima et al., 2004; Marston and Amon., 2004; Rabitsch et al., 2004) have been shown to protect centromeric cohesion during meiosis I. Similarly, it has been shown recently that Sgo1 is essential to prevent

premature sister centromere separation in mitosis (Salic et al., 2004), suggesting that this protein protects centromeric cohesin from cleavage during prophase. The difference in cohesin dissociation between lower and higher eukaryotes may have to do with the higher degree of condensation in higher eukaryotic chromosomes that takes place during prophase.

Chromatin immunoprecipitation assays in *S. cerevisiae* have shown that cohesin has a preference for AT-rich sequences and is associated with specific regions near centromeres and along chromosome arms (Hirano, 2002). The association of cohesin with centromeres seems to require functional kinetochore proteins, suggesting that cohesin binding may be regulated in a different way to centromeres and chromosome arms. It has been shown in *S. pombe* that Swi6, a counterpart of heterochromatin protein HP1, enhances recruitment of cohesin to centromeres (Bernard et al., 2001). In *S. cerevisiae*, the HEAT protein Scc2 forms a complex with Scc4 and this complex is necessary for the stable association of cohesin with chromosomes during S phase but is not necessary for maintaining cohesion during G2 and M phases (Ciosk et al., 2000; Tóth et al., 1999). The homolog of Scc2 in *S.pombe*, Mis4, appears to play a similar role (Tomonaga et al., 2000). The Eco1p/Ctf7p protein in *S. cerevisiae* is necessary for the establishment of cohesion during S phase but not for its maintenance (Tóth et al., 1999). Eco1p has also been shown to interact genetically with PCNA (Pol30p), a known replication protein, and with Ctf18, subunit of cohesin-loading replication factor C (Skibbens et al., 1999) confirming the link between DNA replication and sister chromatid cohesion. Additional evidence for this is provided from studies in budding yeast, where DNA polymerase Polσ interacts with Trf4, a protein involved in cohesion (Hirano, 2002). Pds5, a HEAT-repeat containing protein which associates weakly with cohesin, has been shown to be required for the protection of cohesin during G2 phase (Hartman et al., 2000; Panizza et al., 2000; Tanaka et al., 2001). Finally recent studies suggest that chromatin-remodelling complexes might also have a role in sister chromatid cohesion, either in the recruitment of cohesin to particular sequences along the arms or in the establishment of cohesion during DNA replication (Riedel et al, 2004).

An important clue to how cohesin associates with replicated and unreplicated chromatin and holds DNAs together, is the recent discovery that cohesin forms a large tripartite ring structure within which DNA strands might be entrapped (Gruber et al., 2003; Haering et al., 2002). The SMC1 and SMC3 subunits dimerise by interacting at the hinge domain, forming a V-shaped heterodimer, as previously described for SMC subunits. It has been shown that the N-terminal end of Scc1 binds to SMC3, while its C-terminus binds to SMC1 (Haering et al., 2002). Thus, the Scc1 subunit of cohesin has been proposed to close a ring by connecting the two heads at the ends of the SMC1/SMC3 heterodimer, the arms of which comprise 50 nm-long coiled-coils. The diameter of the ring of close to 50 nm would be large enough to hold two sister DNA strands even when wrapped around histones (Uhlmann, 2004). Consequently, if sister DNAs were trapped within the same ring, it would explain how proteolytic cleavage of Scc1 by separase liberates DNA from a ring, thereby destroying the connection between sister chromatids and triggering their disjunction at the metaphase to anaphase transition (Riedel et al., 2004). Nevertheless, if cohesin indeed traps DNA within the ring, how does the DNA gets inside? It was suggested that ATP hydrolysis by cohesin might be coupled to the active transport of DNA into the ring (Uhlmann, 2003). Experiments have shown that ATP hydrolysis is indeed required for DNA binding by cohesin (Arumugam et al., 2003; Weitzer et al., 2003), possibly by weakening the interaction between the SMC1 and SMC3 heads and thus opening a gap by which the DNA can enter. Furthermore, it was shown that SMC ATPase heads by themselves cannot bind to DNA but they only promote DNA binding when connected to a closed ring (Weitzer et al., 2003). DNA transport into the ring by the ATPase heads would explain both the requirement for ATP hydrolysis as well as an intact cohesin ring for DNA binding. However, there are still many questions that need to be addressed and this model still remains controversial.

It has to be mentioned that for each organism or different cell cycles, a different mechanism may exist that ensures the correct balance between cohesion and condensation. Concerning the potential contribution of cohesin to chromosome condensation, experiments in *S. cerevisiae* suggest that cohesin is required not only for

the initiation of condensation, but also for the maintenance of a condensed state (Losada and Hirano, 2001). Also, the Trf4 and Pds5 proteins in *S. cerevisiae* and Mis4 protein in *S. pombe* were found to be involved in both cohesion and condensation. However, this observation does not seem to be hold in metazoans. So any structural or functional link between cohesion and condensation, remains to be determined.

1.9. Why Drosophila melanogaster?

The fruit fly *Drosophila melanogaster* has been selected as a model organism for the study of the biological function of individual condensin subunits. It offers numerous advantages as an experimental organism that provide an excellent system for the analysis of chromosome dynamics.

Generally there is a high level of conservation of genes, pathways and cellular processes between *Drosophila* and other higher metazoa. *Drosophila* has proliferating tissues such as larval neuroblasts and imaginal discs, that display a conventional cell cycle consisting of G1, S, G2 and M phases. Furthermore, the fundamental cell cycle machinery (including cyclins and their cyclin-dependent kinases) is highly conserved. *Drosophila* is a good candidate for this particular study since its well-defined cytology and simple karyotype of only four pairs of chromosomes (of which three are relatively large) simplify the analysis of chromosome dynamics. *Drosophila* allows the study of proteins not only at the cellular level, but also during different developmental stages. Syncytial embryos provide a way to study synchronised rapid nuclear divisions. Later stages, such as larvae are useful for providing tissues rich in mitotic activity, such as third instar larval neuroblasts and imaginal discs. The *Drosophila* system also provides established protocols for the study of meiosis in germ-line tissues. Spermatogenesis offers an excellent system for genetic analysis of both the regulation of cellular differentiation and the structural basis of cellular and subcellular morphogenesis, while oogenesis is an excellent biological system for studying developmental programming. In addition, many cell lines are available, mainly from *Drosophila* embryonic tissues, which facilitate the study of several processes at the level of single cells.

However, the most powerful tool that makes *Drosophila* such an attractive model organism is its genetics. The advantages of *Drosophila* in genetic analysis include its short generation time and ease of culture. Furthermore, several types of mutations in *Drosophila*, especially those caused by transposon insertions, are very useful for the study of the biological function of the gene disrupted. The advantage of transposons (generally the P-element) versus chemically-induced mutations is that the flanking sequences of the disrupted gene can be identified by inverse-PCR and thus rapid identification of the affected gene can be obtained. P-elements can also be used for ectopic expression of a given sequence under the control of a wide range promoters allowing either temporally controlled expression (by heat-shock promoters) or tissue-specific expression (UAS/GAL4). Recessive lethal mutations can be maintained for several generations in *Drosophila*, thanks to the use of balancer chromosomes which have multiple inversions that effectively suppress recombination.

The mapping and characterisation of new genes is greatly facilitated by many large collections of existing characterised mutations and deficiency stocks (in which a section of a chromosome is deleted). In addition, extensive libraries of partial or full cDNAs as well as the availability of a complete and annotated euchromatic genome sequence (by the *Berkeley Drosophila Genome Project, BDGP*) ensure that molecular understanding of a gene can be achieved rapidly.

Finally the potential of combining genetic and molecular approaches to questions of gene expression, cell biology, development and neurobiology attract more and more scientists to work with *Drosophila*. In addition, of the close to 2000 disease genes identified in humans, roughly 75% have clear homologues in *Drosophila melanogaster*.

1.9.1. The life cycle of Drosophila melanogaster

The fly develops from the embryonic stage, through three larval stages (1^{st}, 2^{nd} and 3^{rd} instars) and a pupal stage, into adult stage within approximately 9-10 days (Figure 1.5). Starting from the egg, fertilisation is followed by 13 rapid and synchronous cycles of nuclear divisions consisting of S and M phase, known as the syncytial divisions. These are completed within two hours. There after, cell membranes form around the nuclei to

form the cellular blastoderm. It is important to note that the syncytial cycles of the embryo are driven entirely by maternal deposition of mRNA and protein, while later cycles depend on zygotic contribution and what may be left of the maternal complement. After cellularisation, synchronisation of mitosis is lost and morphogenesis is initiated. Approximately 24 hours after fertilisation, the first instar larvae hatch. The first instar larva eats its way through food and then undergoes ecdysis (molting) 24 hours after hatching. The second instar larva similarly eats and grows for a day before it also undergoes ecdysis. The third instar larva eats for two days and the larva then emerges from the food medium and wanders on the vial wall until it pupates. Pupation lasts for about four days and terminates with eclosion, in which the adult fly emerges from the pupal case. Most of the growth in the three larval stages is caused by an increase in cell size with endoreduplication of the genome, rather that diploid cell proliferation, known as polyploidization. However, there are exceptions to this, such as brains and imaginal discs that will transform into adult structures during the ensuing pupal stage. These tissues continue to proliferate by a conventional mitotic cell cycle. Polyploidization results in structures such as the polytene chromosomes of the salivary glands of third instar larvae, in which replicated chromatids lie alongside each other with a characteristic banding pattern, reflecting differential packaging and transcriptional activity at various regions. These structures are very useful for analysing chromosome architecture in *Drosophila.*

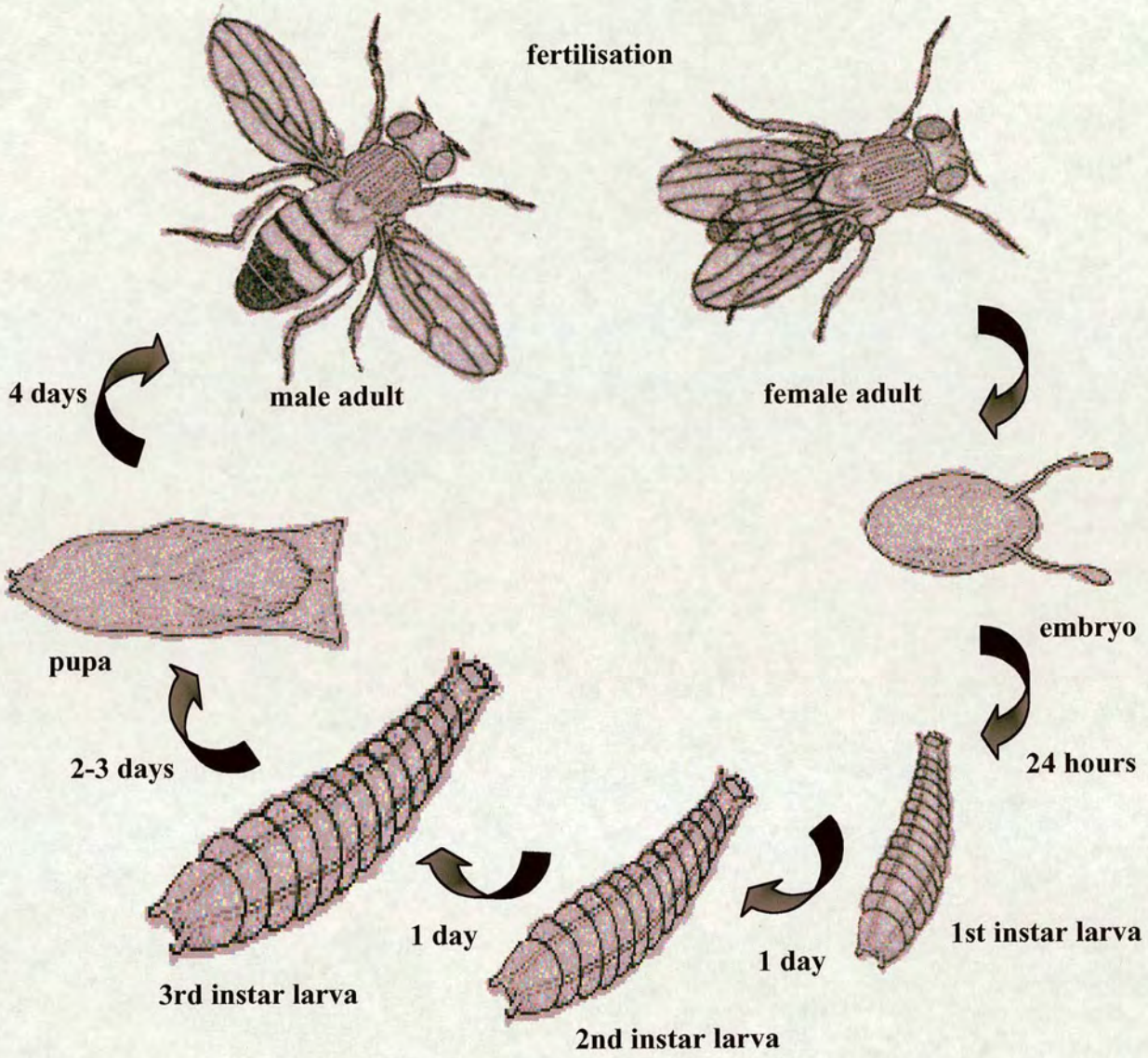

Figure 1.5. The life cycle of *Drosophila melanogaster* . The fly develops from the embryonic stage, through three larval stages (1st, 2nd and 3rd instars) and a pupal stage, into adult stage within approximately 9-10 days at 25°C.

1.10. Background of the Drosophila condensin complex

The *Drosophila* Barren (CAP-H homologue) was first identified as a gene product required for sister chromatid segregation in *Drosophila* (Bhat et al., 1996). Mitotic defects in *barr* embryos resulted in a loss of peripheral and central nervous system (PNS and CNS respectively). In this mutant, centromeres moved apart at the metaphase to anaphase transition and Cyclin B was degraded, but sister chromatids failed to segregate properly. This phenotype was reminiscent of the one observed in topoisomerase II mutants and it was shown that Barren associates with topoisomerase II throughout mitosis and alters the activity of topoisomerase II.

Mutations affecting the *Drosophila SMC4* gene known as *gluon* were first identified through a screen of P-element mutations affecting embryonic peripheral nervous system development in *Drosophila melanogaster* (Kania et al., 1995). Further analysis of this mutant revealed that SMC4 is required for chromosome segregation during different developmental stages (Steffensen et al., 2001). However, it was shown that the SMC4 subunit was required for sister chromatid resolution rather than compaction along the longitudinal axis. Recently, depletion of SMC4 by RNAi showed that topoisomerase II-dependent DNA decatanation activity *in vitro* was significantly reduced in the absence of SMC4 (Coelho et al., 2003).

Mutations affecting the CAP-G non-SMC condensin subunit in *Drosophila*, displayed abnormal chromosome resolution and segregation (Dej et al., 2004). In this study the requirement of dCAP-G for condensation during prophase and prometaphase was illustrated, suggesting that an alternative mechanism ensures that chromosomes are condensed prior to metaphase. In addition, a role for dCAP-G in interphase in regulating heterochromatic gene expression was revealed.

An EMS mutagenesis screen that took place in Dr. Jeff Sekelsky's lab at the University of North Carolina, generated seven lethal lines which possibly were affecting the *SMC2* gene in *Drosophila*. These lines were sent to our lab in order to be analysed. Initial characterisation of these lines by Hannah Townley, an honours student in the lab, revealed that one of these lines was a potential *SMC2* mutation. Further characterisation of this mutant was performed by me.

Initially, as a means of identifying condensin subunits in *Drosophila melanogaster*, available protein sequences of identified subunits in *Xenopus* were used as query sequences in TBLASTN searches of the *Drosophila* EST database (BDGP). This search resulted in the identification of DmSMC2, DmSMC4, DmCAP-D2 and DmCAP-G. EST clones for each subunit were analysed further and antibodies were raised against these subunits. This work was done by Dr Margarete Heck and Soren Steffensen, a collaborator from Claudio Sunkel's laboratory in Portugal (Table 1). Antibodies against DmCAP-H/Barren were generated and described by Bhat *et al.* (1996). In this work further characterisation of the condensin subunits was performed using these antibodies. However, the main aim of this project was the characterisation of the CAP-D2 subunit and its potential role in chromosome condensation.

Gene name	Mutants	Chromosome arm	Polytene location	Antibodies	Protein size	CG number
SMC2	*JSL2*	2R	51D1-2	R782	1179 aa (134 kDa)	10212
SMC4	*gluon*	2L	36A12-14	R688	1409 aa (160 kDa)	11397
CAP-D2	_	3R	99B7	R797	1381 aa (158 kDa)	1911
CAP-H/ Barren	*barren*	2L	38B1-2	anti-Barren	736 aa (83 kDa)	10726
CAP-G	*red sea*	2R	49E6-F8	attempted	1008 aa (116 kDa)	17054

Table 1. General information of the *Drosophila* condensin subunits, including available mutants and antibodies that were used successfully in immonofluorescence or immunoblotting analysis. Antibodies generated against the CAP-G subunit did not give any specific signal either by immunofluorescence or by immunoblotting. CG number represents the identification number in Flybase.

1.11. Aims of the project

When I started this project, most of the existing data for the contribution of the condensin complex to chromosome dynamics derived from yeast genetic studies and *Xenopus* biochemical data. Bearing in mind that each organism has differences in cytology and that yeast is a unicellular organism and *Xenopus* is multicellular (but not genetically tractable), it would be important to study chromosome condensation in a different organism. The fruit fly *Drosophila melanogaster* appears to be a good candidate for this study. As already mentioned previously, its well-defined cytology and the simple karyotype simplify the analysis of chromosome dynamics. *Drosophila* also allows the study of proteins during different developmental stages, while several types of mutations in *Drosophila* and especially those caused by transposon insertions are useful for the study of the function of the disrupted genes. In this study, I have attempted to analyse the role of different condensin subunits in chromosome dynamics. An advantage for this study was the fact that antibodies against all the subunits of the condensin complex were available as well as antibodies against other chromosomal proteins. Thereby, the subcellular distribution of proteins of the condensin complex could be examined, but also the behaviour of the rest of these subunits could be assessed in the absence of one or another component of the condensin complex. The main focus of this study was the analysis of the *Drosophila* CAP-D2 non-SMC condensin subunit. At the same time, analysis of an *SMC2* mutant was performed. Finally, following the identification of a condensin complex II in vertebrate cells, I initiated the study of CAP-D3, one of the non-SMC subunits of this complex in *Drosophila*.

CHAPTER 2

MATERIALS AND METHODS

2.1 MATERIALS

2.1.1. Drosophila melanogaster stocks

Fly stock	Information
CaS (CantonS)	*Drosophila* wild type stock
B# 3365	*Df(2L)cl7, pr[1] cn[1]/CyO* Deficiency uncovering the *CAP-D3* gene with breakpoints at 25D7;26A7. Obtained from Bloomington Stock Centre.
B# 6624	*w[1118]; st[1] e[1] l(3)3450-M[H1]/TM6B, Tb[1]* Deficiency uncovering the *CAP-D3* gene with breakpoints at 25D2-4;25F2-4. Obtained from Bloomington Stock Centre.
B# 25	*Df(2L)cl-h1/CyO, amos[Roi-1]* Deficiency uncovering the *CAP-D3* gene with breakpoints at 25D4;25F12. Obtained from Bloomington Stock Centre.
B# 4187	*al, dp, b, pr, cn, c, px, sp/CyO* Second chromosome multiple marker used for the recombination of *JSL2/CyO-GFP* line.
B# 4347	*al, dp, b, pr, Bl, cn, c, px, sp/CyO* Second chromosome multiple marker used for the recombination of *JSL2/CyO-GFP* line.
B# 1150	*w1/Dp(1;Y)y+; Df(2R)knSA3, Tp(1;2)TE21F22A/CyO* Deficiency uncovering the *SMC2* gene with breakpoints at 51B05-11;51D07-E02, 03C;03C;21F-22A08. Obtained from Bloomington Stock Centre.

B# 13964	*y1; P{SUPor-P}CG7277KG03584/CyO; ry506* P-element insertion in *CG7277* gene. The insertion point is at 025-E06 chromosome region of the 2nd chromosome. Obtained from Bloomington Stock Centre.
B# 2386	*Df(2L)DS6, b[1] pr[1] cn[1]/CyO* Deficiency uncovering the cluster of histone H3 genes with breakpoints at 38F05;39E07-F01. Obtained from Bloomington Stock Centre.
Bc, Gla/CyO-GFP	Stock used for balancing the 2nd chromosome over the *CyO-GFP* balancer.
P{EP}2415/CyO *EP(2)2415* synonym	P-element insertion in *CG14016* gene. Obtained from Bloomington Stock Centre (Berkeley Drosophila Genome Project)
15026/4D	*P{EPgy2}/CyO* *CAP-D3* mutation. P-element insertion in the *CAP-D3* gene. Obtained from Bloomington Stock Centre (Berkeley Drosophila Genome Project).
glu^{17C}	$gluon^{17C}$*/Kr-GFP* Mutation affecting the *SMC4* locus. Sequenced by Neville Cobbe
$barr^{L305}$	$barr^{L305}$*/Kr-GFP* Null mutation of *barren* gene. Obtained from Hugo Bellen.
JSL2/SM6a	*y,w / y+Y; cn, JSL2, bw, sp /SM6a* Mutation affecting the *SMC2* gene. Obtained from Jeff Sekelsky.
JSL2/CyO-GFP	*y,w / y+Y; cn, JSL2, bw, sp /CyO-GFP* Mutation affecting the *SMC2* gene. Obtained from Jeff Sekelsky.
JSL2/CyO-GFP	*b, pr, cn, JSL2, sp/CyO-GFP* Mutation affecting the SMC2 gene. Recombinant line 58 obtained after recombination of the 2nd chromosome of the *JSL2/CyO-GFP* line.

2.1.2. Bacterial Strains

Escherichia coli XL1 Blue (New England Biolabs)

F' proAB lacI^{q}lacZΔM15 TN10(Tet^r)/recA1 endA1 gyrA96(Nal^r) thil hsdR17($r_k^- m_k^+$) supE44 relA1 lac

Escherichia coli BL-21 (New England Biolabs)

F- ompT hsdSB (rB-mB-) gal dcm(DE3)

Escherichia coli ER2566 (New England Biolabs)

F-λ-fhuA2 [lon] ompT lacZ:: T7 gene1 gal sulA11 D(mcrC-mrr)114::IS10 R(mcr-73::miniTn10-TetS)2 R(zgb-210::Tn10) (TetS) endA1 [dcm]

Escherichia coli M15[pREP4] (Qiagen)

Derived from *E. coli* K12

phenotype: *Nal^S, Str^S, Rif^S, Thi$^-$, Lac$^-$, Ara$^+$, Gal$^+$, Mtl$^-$, F$^-$, RecA$^+$, Uvr$^+$, Lon$^+$*

2.1.3. Commonly used solutions

BSA

Bovine serum albumin, 30% stock solution (Sigma).

CLAP

1 mg/ml chymostatin, 1 mg/lm leupeptin, 1 mg/ml antipain, 1 mg/ml pepstatin A (Sigma) in DMSO.

Coomassie Blue stain

0.5% Coomassie Blue in methanol.

Coomassie Blue stain diluent

35% methanol, 14% acetic acid.

Coomassie Blue fast destain

35% methanol, 10% acetic acid.

Coomassie Blue slow destain

10% methanol, 7% acetic acid.

Cytoskeletal Buffer (1X)

137 mM NaCl, 5 mM KCl, 1.1 mM $NaHPO_4$, 0.4 mM KH_2PO_4, 2 mM $MgCl_2$, 2 mM EGTA, 5 mM PIPES, 5.5 mM Glucose, pH 6.1 with HCl.

DAPI

4',6-diamidino-2-phenylindole (Sigma), stock solution of 1 mg/ml in water, kept at 4°C or -20°C.

DTT

1 M Dithiothreitol (Fisher) in ddH_2O.

Dulbecco's PBS (10X stock solution)

1.37 M NaCl, 26.8 mM KCl, 14.7 mM KH_2PO_4, 64.6 mM Na_2HPO_4, pH 7.4 (filter sterilized).

EBR (Ephrussi Beadle Ringer's Solution) (10X stock solution)

1.30 M NaCl, 47 mM KCl, 19 mM $CaCl_2$, 100 mM HEPES, pH6.9 (filter sterilized).

EBR lysis buffer

1X EBR, 10 mM EDTA, 10 mM DTT, 1:100 dilution of CLAP, PMSF and trasylol protease inhibitors.

IPTG (stock solution)

500mM Isopropyl-β-D-thiogalactopyranoside in ddH_2O.

Laemmli gel buffer for stacking gel (Upper Buffer)

0.5 M trizma base, pH 6.8 with HCl.

Laemmli gel buffer for resolving gel (Lower Buffer)

1.5 M trizma base, pH 8.8 with HCl.

Laemmli gel running buffer (10X stock solution)

25 mM trizma base, 192 mM glycine, 1% SDS.

LB (Luria-Bertrani broth)

1% Bacto-tryptone, 0.5% Bacto-yeast extract, 1% NaCl, pH 7.4.

MOPS SDS Running Buffer (20X stock solution)

1 M 3-(N-morpholino) propane sulphonic acid, 1 M Tris base, 2% SDS, 20.5 mM EDTA, pH 7.7.

Mowiol

14% Mowiol, 28% glycerol in PBS.

PBSTx

1X PBS with 0.1% TritonX-100.

PBSTw

PBS with 0.1% Tween-20.

PFA

16% paraformaldehyde ampules from TAAB.

SOB

2% Bacto-tryptone, 0.5% Bacto-yeast extract, 8.6 mM NaCl, 50 mM $MgCl_2$, 2.5 mM KCl, pH 7.4.

SOC

SOB with 20 mM Glucose.

Stripping Solution

100 mM β-mercaptoethanol, 2% SDS, 62.5 mM Tris, pH 6.7.

TBS (Tris-buffered saline) (1X)

137 mM NaCl, 20 mM Tris base, pH 7.6 with HCl.

TAE (1X)

40 mM Tris-acetate, 1 mM EDTA, pH 8.0.

TBE (1X)

45 mM Tris-borate, 1 mM EDTA, pH 8.0.

TE (1X)

10 mM Tris-HCl, 1 mM EDTA, pH 7.6.

Towbin buffer (protein transfer solution)

25 mM Tris (Sigma 7-9), 20% methanol, 250 mM Glycine Sigma-Aldrich, 0.1% SDS.

5X loading dye for DNA agarose gels

17.5% Ficoll 400, 100 mM EDTA, pH 8.0, 2.5% SDS, 0.25% Bromophenol blue, 0.25% Xylene cyanol FF.

3X loading dye for protein gels

6% SDS, 150 mM Upper Buffer (0.5 M trizma-base, pH6.8), 30% Glycerol, 0.03% bromophenol blue, 6 mM EDTA.

2.2 METHODS

2.2.1. Preparation of electrocompetent cells

2 ml overnight culture of appropriate bacterium (BL21 or XL-1 Blue) was grown with shaking at 37 °C in SOB medium. 0.5 ml of the overnight culture was diluted into each of two 2 litre flasks containing 500 ml SOB. The larger cultures were grown with shaking at 37°C to an optical density OD_{600} of 0.8 (about four hours). The flasks were chilled in ice for about 15-30 minutes. All subsequent steps were performed on ice (it is important the bacterial cells remain cold, otherwise their competence is affected).

The bacterial cells were harvested by centrifuging in sterile, chilled bottles for 15 minutes at 2500 rpm in a Beckman JLA 10.500 rotor at 4°C. The supernatant was removed and the cell pellet for each culture was resuspended in 500 ml ice-cold 10% glycerol in distilled sterile water. The resuspended culture was centrifuged again at 2500 rpm for 15 minutes at 4°C and the supernatant was removed. Each pellet was resuspended in 4.5 ml 10% glycerol and aliquots of 200 µl were snap-frozen in liquid nitrogen and stored at -80°C.

2.2.2. Electroporation

Electroporations were performed in appropriate cuvettes (0.2 cm, Invitrogen) by using a BioRad electroporator. Tubes of competent cells (aliquots of 200 µl) were thawed on ice. At the same time, an appropriate amount of 1.5 ml Eppendorf tubes and 0.2 cm disposable cuvettes were placed on ice to cool at 4°C. 80 µl of competent cells were

added to the 1.5 ml tubes and an appropriate amount of DNA (1-2 μl) was added as well and mixed. Cuvettes were tapped so that the sample went to the bottom and then electroporated at the following conditions: resistance set at 200 Ohms, capacitance set at 25 μ FD and volts set at 2.5 kV. After the electroporation, 1 ml of SOC medium was immediately added to each cuvette. The mixture was then transferred to 1.5 ml eppendorf tubes and incubated at 37°C for 30-60 minutes. Dilutions of the cultures were plated out on agar plates containing the appropriate antibiotic.

2.2.3. Genomic DNA extraction

20 flies or larvae (second or third instar) were frozen down in 1.5 ml tubes in -70°C for 5 minutes (or at -20°C for longer) and then homogenised in 300 μl of Solution A (0.1mM Tris-HCl, pH 9.0, 0.1mM EDTA, pH 8.0, 0.1% SDS) by using a Polytron (Kinematica). The homogenised mixture was incubated at 70°C for 30 minutes and then 42 μl of 8 M potassium acetate were added. The mix was centrifuged twice at 13,000 rpm, 4°C for 15 minutes each, to obtain a clear supernatant. 150 μl of isopropanol was added to the supernatant and the DNA was precipitated for 1 hour at –70°C. The DNA was then pelleted at 13,000 rpm for 15 minutes at 4°C and washed with 70% ethanol (500 μl) for 15 min at 13,000 rpm. The pellet was air dried and the genomic DNA was resuspended in 100 μl of TE and then extracted once with equal volume of phenol:chloroform:isoamyl alcohol (PCI, 25:24:1) at 13,000 rpm for 5 minutes and once more with chloroform (13,000 rpm, 5 minutes) to remove any remaining phenol. The genomic DNA was then precipitated with 1/10 of the volume in sodium acetate and 2.5 volumes of ethanol for at least 1 hour at -70°C, centrifuged at 13,000 rpm for 15 minutes at 4°C, washed in 70% ethanol as described above and resuspended in a final volume of 30 μl TE. Genomic DNA was kept at 4°C.

For the extraction of genomic DNA from a single larva, exactly the same procedure was followed with an adjustment to the volumes of Solution A (100 μl), 8M potassium acetate (14μl), isopropanol (50μl) and final TE (10μl).

2.2.4. Plasmid DNA extraction

For small scale plasmid DNA isolation, 3 ml *E. coli* (XL1-Blue, DH5) culture was grown overnight at 37°C with shaking, 2 ml of which were used for plasmid DNA extraction and the remainder was used for making frozen glycerol stocks (700 µl of culture and 300 µl of glycerol). All small scale plasmid DNA extractions (mini-preps) were performed using the UltraClean™ Plasmid Miniprep Kit from MoBio, according to manufacturer's instructions. Larger scale extractions of up to 50 ml were performed using either the UltraClean™ Midiprep columns from MoBio or the Qiagen MidiPrep Kit, according to manufacturer's instructions.

2.2.5. Restriction digestion of DNA plasmids

Restriction digestion of DNA plasmids was performed in 1.5 ml Eppendorf tubes as follows:

DNA (plasmid preps)	1-2 µl
New England Biolabs enzyme(s) (20,000 u/ml)	1 µl
Bovine serum albumin (10 mg/ml)	0.2 µl
New England Biolabs 10X buffer	1 µl
Sterile deionised water	up to 20 µl

Unless otherwise indicated, the 10X reaction buffer provided with the enzyme was used. Digestions were normally performed at 37°C for 3-4 hours. The size of the cloned insert was estimated by running an aliquot of the plasmid digest on a 1% agarose gel in TBE.

2.2.6. Agarose gel electrophoresis

Unless stated in the text, agarose gels were usually prepared in a concentration of 1 % SeaKem LE Agarose (BioWhittaker Molecular Applications) containing 0.3 µg/ml of ethidium bromide. Gels were electrophoresed in electrophoresis tanks (Owl Scientific Plastics) in 1X TBE buffer. Different gel sizes were used according to the number of

samples and/or the degree of separation required. Gel size: mini (50 mls, run at 70-80 V), midi (100 ml, run at 100 V) and maxi (300 ml, run at 150 V).

2.2.7. Purification of DNA from agarose gels

Electrophoresis was performed in low-melt agarose gels (MacroSieve low melting temperature agarose for separation of molecules <1 kb, Flowgen) containing 0.3 µg/ml ethidium bromide. 1X TBE buffer was used and the desired bands were excised under UV irradiation using a razor blade and placed into 1.5 ml Eppendorf tubes. DNA was purified from agarose gel by using the Perfectprep Gel Cleanup Kit (Eppendorf). Samples were weighed and the appropriate volume of Binding Buffer was added. The gel was incubated for 5 to 10 minutes at 50°C and finally DNA was isolated by following the manufacturer's instructions (Perfectprep Gel Cleanup procedure).

2.2.8. Amplification of genomic or plasmid DNA by PCR

Most PCR reactions were performed by using the *Pfu* DNA polymerase (with proofreading activity, Promega). The following basic protocol for a typical 50 µl reaction was used and the optimal Mg^{2+} concentration for each primer pair had to be determined:

Pfu DNA polymerase buffer with $MgSO_4$ (10X)	5 µl
dNTPs (1.25 mM each)	4 µl
primer mix (2 µM each)	12.5 µl
$MgSO_4$ (25 mM)	0-4 µl
Pfu DNA polymerase (2-3 u/µl)	0.5 µl
DNA template (50-200 ng)	variable
Sterile deionised water	up to 50 µl

PCR reactions were performed in a Biometra Personal Cycler or a Biometra Gradient Cycler according to the following protocol:

Initial Denaturation	95°C	2 minutes	
Denaturation	95°C	30 seconds	x 35 cycles
Annealing	50-58°C	30 seconds	
Extension	75°C	2-5 minutes	
Final extension	75°C	10 minutes	
Hold	4°C		

Amplifications of large PCR targets (bigger than 1 kb) were usually performed using *Herculase* hotstart DNA polymerase (Stratagene) using the following protocol for a typical 50 µl reaction:

10X *Herculase* buffer	5 µl
dNTPs (1.25 mM each)	4 µl
primer mix (2µM each)	12.5 µl
Herculase (5 u/µl)	0.25 µl
DNA template (50-200 ng)	variable
Sterile deionised water	up to 50 µl

PCR reactions were performed in a Biometra Personal Cycler or a Biometra Gradient Cycler according to the following protocol:

Initial Denaturation	94°C	2 minutes	
Denaturation	96°C	30 seconds	x 30 cycles
Annealing	50-58°C	30 seconds	
Extension	72°C	2-5 minutes	
Final extension	72°C	10 minutes	
Hold	4°C		

2.2.9. Purification of DNA from PCR reactions

DNA products from PCR reactions were usually purified by using the UltraClean™ PCR Clean-up™ Kit (MoBio Laboratories). This method was preferred when only a single PCR product was amplified in a reaction. The entire PCR reaction was used and 5 volumes of the SpinBind reagent were added. The DNA was finally purified using the Spin Filter columns by following the manufacturer's instructions and the DNA was eluted in 25 µl of elution buffer.

2.2.10. Sequencing of DNA samples from plasmids or purified PCR products

(a) Sequencing reactions were performed using 250-500 ng of template DNA in conjunction with 3.2 pmol of the appropriate primer and 8 µl of either dRhodamine or Big Dye terminator cycle sequencing kit (Perkin Elmer/Applied Biosystems), in a total reaction volume of 20 µl. The reactions were performed in a Biometra Personal Cycler according to the following protocol:

Ramp	96°C		
Denaturation	96°C	30 seconds	x 25 cycles
Annealing	50°C	15 seconds	
Extension	60°C	4 minutes	
Hold	4°C		

The completed sequencing reactions were precipitated as follows:
2 µl (1/10 of the volume) of 3M sodium acetate (pH 5.3) and 50 µl (2.5 of the volume) ethanol were added to each sequencing tube. The tubes were mixed by vortexing, placed on ice for 15 minutes, then spun at 13,000 rpm in a benchtop microfuge at 4°C for 30 minutes. The pellets were washed with 250 µl of 70% ethanol and spun at 13,000 rpm for 10 minutes at room temperature. The supernatant was removed and the pellets were air dried completely by placing the tubes in a 37 °C block with the lids open for 5-

10 minutes. The dried samples were then taken to the ICMB sequencing facility for loading onto an ABI prism sequencer.

(b) A slightly different protocol had to be followed the last year since the protocol of the sequencing kit changed. Sequencing reactions were performed using 250-500 ng of template DNA in conjunction with 3.2 pmol of the appropriate primer and 4 µl of Big Dye terminator cycle sequencing kit version 3.1 (Perkin Elmer, Applied Biosystems), in a total reaction volume of 20 µl. The reactions were performed in a Biometra Personal Cycler according to the following protocol:

95°C	5 minutes	
96°C	30 seconds	x 25 cycles
55°C	15 seconds	
60°C	4 minutes	
Hold	15°C	

The reactions were then transferred to 1.5 ml tubes and taken to the ICMB sequencing facility for loading onto an ABI prism sequencer.

2.2.11. RNA extraction from larval tissues and whole or partial flies

Total RNA from third instar larvae, brains, testes, ovaries, heads, carcasses and whole flies was prepared by using the RNeasy RNA extraction kit (Qiagen). Flies or tissues were disrupted and homogenised in appropriate volume of Buffer RLT (Lysis buffer) containing 10 µl/ml β-Mercaptoethanol using a motorised pestle. Total RNA was then purified by using the RNeasy columns according to manufacturer's instructions (RNeasy Mini Protocol for Isolation of Total RNA from Animal Tissues). RNA was finally eluted in 25 µl of RNAase-free dH_2O and stored at -20°C.

2.2.12. DNase treatment of total RNA

Total RNA was treated with DNAse I, Amplification Grade (Invitrogen) prior to reverse transcription as follows:

DNAase I, Amp Grade 1u/µl	1µl
10X DNaseI Reaction Buffer	1µl
total RNA	1µg
DEPC-treated Water	up to10 µl

The reaction mixture was incubated for 15 minutes at room temperature and the DNAse I was inactivated by the addition of 1 µl of 25 mM EDTA solution. The reaction was heated at 65°C for 10 minutes and the RNA was ready to be used in reverse transcription, prior to amplification.

2.2.13. RT-PCR from total RNA

RT-PCR was performed on total RNA (DNase-treated) isolated from third instar larvae, brains, testes, ovaries, heads, carcasses and whole flies by using two different approaches. In the first one, the Sensiscript Reverse Transcriptase from Qiagen was used for first strand cDNA synthesis using low amounts of RNA (< 50 ng)
The reaction was performed as follows:

10X Buffer RT	2µl
dNTPs (5 mM each dNTP)	2µl
Oligo-dT primer (10 µM)	2 µl
RNase inhibitor (10 units/µl)	1 µl
Sensiscript Reverse Transcriptase	1 µl
RNase-free water	up to 20 µl
Template RNA (< 50 ng)	variable

The reaction was incubated at 37 °C for 1 hour and a small aliquot was used as template for PCR amplification with the standard PCR reaction, as described previously. The products were then visualised by electrophoreses on a 1% agarose gel.

In the second method the Access RT-PCR system (Promega) was used. In this procedure, cDNA synthesis and PCR amplification were taking place in the same tube (one step reaction). Specific primers to the gene of interest were used for the PCR amplification. The reaction was performed as follows:

Nuclease-free water	up to 50 µl
AMV/*Tfl* 5X Reaction Buffer	10 µl
dNTP mix (10 mM each dNTP)	1 µl
primer mix 50 pmol	25 µl
25mM $MgSO_4$	2 µl

The reagents were mixed by pipetting and the remaining components were added as follows:

AMV reverse transcriptase (5u/µl)	1 µl
Tfl DNA Polymerase (5u/µl)	1 µl

The components were vortexed gently and the reactions were initiated by adding RNA template:

RNA template	2-2.5 µl

The reactions were performed in a Biometra Personal Cycler or a Biometra Gradient Cycler according to the following protocol:

1. First strand DNA synthesis

reverse transcription	48°C	45 minutes
AMV/RT inactivation/ RNA/cDNA/primer denaturation	94°C	2 minutes

2. Second strand synthesis and PCR amplification:

denaturation	94°C	30 seconds	x 40 cycles
annealing	60°C	1 minute	
extension	68°C	2 minutes	
final extension	68°C	7 minutes	
hold	4°C		

10 µl of each reaction was analysed by agarose gel electrophoresis (1% agarose).

2.2.14. Maintenance of Drosophila stocks

Flies were cultured in bottles or vials containing "Dundee" maize medium (14 litres water, 150g agar, 1100g glucose, 620g brewer's yeast, 1000g maize meal, 80g dried yeast, 38g nipagin (p-hydroxy benzoic acid methyl ester), 380 ml absolute alcohol, 45 ml propionic acid). To fatten flies prior to embryo collection or larval dissection, yeast paste (dried yeast diluted with water) was placed into the vial. Yeast paste was also added to mutant fly stocks that were sick or difficult to maintain. Flies were usually kept at 25°C with tipping into a new vial once a week, or at 18°C with tipping into a new vial once every three weeks. Crosses were performed at room temperature using virgin female flies, collected as soon as possible after eclosion.

2.2.15. Determination of hatching frequencies

Male and female flies of the desired genotype were kept together for two days in vials of medium supplemented with yeast paste to allow the females to fatten. The fattened flies were then placed in 800 ml collection cages placed over red wine concentrate agar plates (25% red wine concentrate, 2.25% Difco Bacto agar, 2.5% sucrose, 0.15% Nipagin pH6.5) with yeast paste. The flies were left to mate for 6 hours and the eggs laid were collected and arranged in 10 rows of 20 on red wine agar plates. The collection plates were then kept in a humidified incubator at 25°C for 30 hours (wild type embryonic development usually requires 24 hours at 25°C) and the number of embryos that did not

hatch after this time were counted. The same procedure was followed with wild type flies, in order to estimate the number of embryos that were dying due to embryo manipulation.

2.2.16. Lethality test of JSL2 homozygous animals

In order to determine if the larvae homozygous for the *JSL2* mutation were dying at second or third instar stage or if they were able to pupate, a lethality test was performed. Male and female flies of the desired genotype were kept together in vials of yeast-glucose-agar medium supplemented with yeast paste. Second or third instar larvae homozygous for the mutation were collected under an epifluorescence microscope and placed on red wine agar plates. The collection plates were then kept in a humidified incubator at 25°C for 2-3 days (wild type larva development usually requires 2-3 days at 25°C). The number of larvae that fail to pupate or to eclose into flies was counted. As a control, wild type larvae were treated in the same way and numbers were determined.

2.2.17. Concanavalin A-treated coverslips

Coverslips (22x22 mm/1.5 thick) were washed twice in deionised water for 15 minutes each time and then incubated in 0.5 M HCl for 30 minutes. The coverslips were washed twice in deionised water for 15 minutes each time and then placed in 100% ethanol for 30 minutes. Excess ethanol was drained off and each coverslip was dipped in Concanavalin A solution (0.5 mg/ml in dH_2O), coated completely and drained of excess Con A solution. The coverslips were placed to dry on clean blotting paper and were sterilised for 1 hour by UV irradiation prior to use.

2.2.18. Poly-L-lysine treated slides

Microscope slides (76 x 26 x 1.0/1.2 mm thick, twin frosted one end, ground edges, Berliner Glass KG) were washed overnight in dH_2O containing Decon (diluted 1:5 with dH_2O). The slides were rinsed with dH_2O, washed with 95% ethanol for 2-3 hours and rinsed again with dH_2O. The slides were then placed in poly-L-lysine solution (0.1%

w/v in water, Sigma-Aldrich) for at least 45 minutes, rinsed with dH_2O and left to dry overnight in a 65°C incubator.

2.2.19. Cell Culture

Drosophila embryonic S2 cells were maintained in serum free Schneider's Insect Medium (Sigma) supplemented with 10% Insect qualified Fetal Bovine Serum (FBS, Gibco). Cells were grown at 27°C in a humidified atmosphere (*Hera* Cell, Heareus) and were maintained by passaging the culture once a week (cells were usually diluted 1:30 for maintaining the stock and 1:10 for use in RNAi or immunofluoresence).

2.2.20. Double stranded RNA interference

RNAi was performed in *Drosophila* S2 cells as previously described (Clemens et al., 2000; Vass et al., 2003). Template DNA was prepared by PCR as described in Chapter 2. The PCR primers were fused to T7 RNA polymerase promoter and the PCR product obtained was used as template for RNA synthesis using the Megascript T7 kit (Ambion) according to the manufacturer's instructions and as follows:

2 µl of 10X Reaction buffer
2 µl of ATP, CTP, GTP, UTP
2 µl of enzyme mix
1 µg of template DNA
up to 20 µl with nuclease-free dH_2O

The reaction was incubated at 37°C for 4 hours followed by precipitation of the RNA with 3 M sodium acetate, pH 5.3 (1/10 th of the volume) and 100% ethanol (2.5 volumes). The reactions were placed on ice for 15 minutes, centrifuged at 13,000 rpm for 30 minutes at 4°C, washed with 250 µl of 70 % ethanol at 13,000 rpm for 10 minutes at room temperature and air dried at 37°C for 5-10 minutes. The pellets were resuspended in 30 µl of nuclease-free dH_2O. To prepare dsRNA, the resuspended

pellets were heated to 65°C for 30 minutes and then placed in a 65°C water bath and allowed to cool slowly to room temperature. The concentration of dsRNA was obtained by determining the OD at 260 nm and the calculation that an OD_{260} of 1= 45 μg/ml of dsRNA. An aliquot of the dsRNA was electrophoresed on a 1% agarose gel and it was finally stored at - 20°C until required.

Particularly, two fragments from the 5' end of CAP-D2 (forward primer at 251-270 bp of ORF and reverse primer at 873-892 bp of ORF) were fused to T7 RNA polymerase promoter and were used as PCR primers. The Drosophila EST clone LD40412 was used as a template for the PCR reaction. The PCR product obtained (~642bp) was used as template for dsRNA synthesis. A random human intronic sequence was used to generate control dsRNA, which was synthesized in the same way. Topo II dsRNA was obtained as described previously (Chang et al., 2003). For the CAP-D3 dsRNA, the EST clone RE18364 was used as a template for the PCR reactions. Two PCR products were obtained from two different regions of the ORF. The first one was obtained with a primer pair that included the start codon (r1 ~ 639 bp) and the second one with a primer pair further inside the message (r2 ~ 723 bp). The two products were used in two independent experiments.

For the RNAi experiment, $1x10^6$ cells/ml were diluted in serum free Schneider's Insect Medium. 25 μg/ml of dsRNA was added to the cells (30 μg/ml for the CAP-D3 RNAi). 1ml of these cells was placed into each well of a 6-well (35mm) plate and incubated for 60 to 90 min at room temperature. After the incubation 2mls of Schneider's Medium supplemented with 10% FBS was added to each well. The cells were placed in the 27°C humidified incubator and samples were processed for immunoblotting or for immunofluorescence at designated time points. In the double dsRNAi experiment, the two different dsRNAs were added to the cells at the same time and the procedure followed was the same as described above.

For some experiments, cells were grown on sterilized Concanavalin A treated coverslips in a 35mm 6-well plate (Rogers, 2002), but only for the last 24 hours before being processed for immunofluorescence. The cell culture was usually dilute (1:5) before cells were allowed to grow on Concanavalin A-coverslips.

In some cases, S2 cells (RNAi treated or control) were exposed to 30 μM colchicine for 7 hours, 67 hours after the RNAi treatment. Cells were then processed for immunoblotting or immunofluorescence.

2.2.21. Preparation of Cell Extracts

Cells were counted under the microscope with a hematocytometer, centrifuged at 2,000 rpm for 2 min and washed with 0.5 ml of PBS (phosphate-buffered saline: 137 mM NaCl, 2.7 mM KCl, 6.46 mM Na_2HPO_4, 1.47 mM KH_2PO_4 pH 7.4). The pellet was resuspended at a specific concentration in PBS and warm (at 65°C) sample buffer [3X sample buffer: 2% SDS, 10% Glycerol, 0.01% Bromophenol Blue, 2 mM EDTA, 50 mM trizma base pH 6.8] with 10 mM DTT (1/10 of final volume) was added. The cells were lysed by sonication and the extract was boiled at 100°C for 5 to 10 min. The volume of PBS and sample buffer was calculated so that the final cell concentration was $5x10^4$cells/μl.

2.2.22. Preparation of Embryo Extracts

To identify embryos homozygous for $barr^{L305}$ and glu^{17C} the mutant chromosomes were balanced over *CyO, P {w^{+mc}=GAL4-Kr.C}DC3, P{w^{+mc}=UAS-GFP.S65T}DC7* as described (Casso et al., 2000). One hour collections of embryos were aged for 12 hours, dechorionated with 50% bleach for 1 min and then sorted under a fluorescence dissecting microscope. Homozygous embryos (*Kr-GFP* negative) were homogenised with a motorised pestle in EBR lysis buffer [EBR (13 mM NaCl, 0.47 mM KCl, 0.19 mM $CaCl_2$, 1 mM HEPES pH 6.9), 10 mM EDTA, 10 mM DTT, 1:100 dilution of CLAP, PMSF and trasylol] and warm (at 65°C) 3X Sample buffer with 100 mM DTT was added immediately. The embryo extract was boiled at 100°C for 10 min. Usually 100 embryos were homogenised in 50 μl of EBR lysis buffer and 25 μl of warm 3X Sample buffer with DTT was added. Samples were kept at - 20°C. For preparation of extract from wild type embryos the procedure was exactly the same as described above except that no sorting under the microscope was necessary.

2.2.23. Preparation of larval extracts

30 second or third instar larvae were collected from vials and washed three times with 1X EBR solution in a dissecting dish using a transfer pipette. Larvae were then transferred to a 2 ml Eppendorf tube and excess EBR was removed with a yellow tip. The larvae were homogenised by Polytron homogeniser (Kinematica, AG) for approximately 30 seconds in 300 µl EBR lysis buffer and 150 µl warm (at 65°C) 3X Sample buffer with 100 mM DTT was added immediately. The extract was boiled at 100°C for 10 min. The sample was then centrifuged for 2 minutes at 13,000 rpm in a benchtop microfuge (Heraeus Instruments 'Biofuge 13') and the supernatant was removed to a fresh tube and kept at -20°C. 15µl of this preparation is equivalent to one larva. The same procedure was followed for extract preparation from flies.

2.2.24. Preparation of larval brain extracts, pupal or adult testes and ovary extracts

Male and female flies of the desired genotype were kept together in vials of yeast-glucose agar medium supplemented with yeast paste, and they were left to mate. Second or third instar larvae were collected from vials and they were dissected under a dissecting microscope. 10-20 brains were homogenised with a motorised pestle in 50 µl EBR lysis buffer [EBR (13 mM NaCl, 0.47 mM KCl, 0.19 mM $CaCl_2$, 1 mM HEPES pH 6.9), 10 mM EDTA, 10 mM DTT, 1:100 dilution of CLAP, PMSF and trasylol] and 25 µl of warm (at 65°C) 3X Sample buffer with 100 mM DTT was added immediately. The brain extract was boiled at 100°C for 10 min. Samples were kept at -20°C. The same procedure was followed for extracts from testes or ovaries. Usually 20 testes or ovaries, dissected from late pupae or adult flies, were used for this purpose.

2.2.25. SDS-PAGE of proteins

Two different types of gels and gel apparatus were used for electrophoresis of protein samples: Hoefer Scientific Instruments 'Vertical Slab Gel Unit' for large gels and Novex Mini Cell (Xcell SureLock, Invitrogen) for small pre-cast gels (Invitrogen). The Novex small pre-cast (ready-made) gels were used according to manufacturer's instructions and

electrophoreses was performed in 1X MOPS SDS Running Buffer (20X stock: 1 M MOPS free acid, 1 M Tris-base, 69.3 mM SDS, 20.5 mM EDTA dH_2O up to 500 ml) at 200 V. In this section, only the preparation of the larger SDS-PAGE gels will be described:

Two glass plates (16 cm x 18 cm) were washed with dH_2O, Decon (diluted 1:5 in dH_2O) again with dH_2O and finally rinsed with 70% ethanol and wiped dry with a paper towel. The glass plates were placed one on top of the other but separated with 2 spacers (0.75 mm or 1.5 mm), one at either end. The plates were clamped together and the bottom end was sealed with parafilm. The clamped plates were placed on the gel apparatus and the resolving (lower) acrylamide gel was poured in between the glass plates from the top first, followed by the stacking (upper) gel. The amount of solutions used are summarised in the following table according to different acrylamide percentages:

Resolving (Lower) Gel

Recipes for 1-1.5 mm thick gel (bold text) or 1-0.75 mm thick gel. The lower buffer consists of 1.5 M trizma-base, pH 8.8. Acrylamide refers to a stock of 30% acrylamide: 0.8% Bis-acrylamide (Severn Biotech Ltd). AMPS is a 10% stock of Ammonium Persulphate (Sigma).

	7.5%		10%		12.5%	
lower buffer	**10 ml**	5 ml	**10 ml**	5 ml	**10 ml**	5 ml
acrylamide	**10 ml**	5 ml	**13.3 ml**	6.65 ml	**18.3 ml**	9.17 ml
20% SDS	**200 µl**	100 µl	**200 µl**	100 µl	**200 µl**	100 µl
0.5 M EDTA	**80 µl**	40µl	**80 µl**	40 µl	**80 µl**	40 µl
dH_2O	**19.72 ml**	9.86 ml	**16.42 µl**	8.21µl	**11.39 µl**	5.69µl
10% AMPS	**400 µl**	200 µl	**400µl**	200 µl	**400µl**	200 µl
TEMED	**40 µl**	20 µl	**40µl**	20 µl	**40µl**	20 µl

After pouring the resolving gel, butanol saturated with 0.25X lower buffer was layered over the top in order to create a sharp interface between resolving and stacking gels.

Resolving gels were allowed to polymerise for 20-30 minutes at room temperature. The butanol layer was poured off, washed with dH_2O and the stacking gel was poured on top.

Stacking (Upper) gel

The Upper buffer consists of 0.5 M trizma-base, pH 6.8. All stacking gels were made up in 10 ml containing:

Upper buffer	2.5 ml
Acrylamide	1.33 ml
20% SDS	50 µl
0.5 M EDTA	20 µl
UREA to 8 M	4.8 g
dH_2O	up to 10 ml
10% AMPS	100 µl
TEMED	10 µl

A plastic comb was placed on top of the stacking gel to form the wells and the gel was allowed to polymerise for 15 minutes at room temperature. The polymerised gel slab was then fixed in position in the buffer tank and 1X Running buffer (25 mM trizma-base, 192 mM glycine, 1% SDS) was poured into the upper and lower chambers. Protein samples containing 1X Sample buffer and 100 mM DTT were boiled for 5 minutes and then loaded into the wells using a Hamilton syringe. 30 µl of a molecular weight marker (SeeBlue Plus 2, Invitrogen) were loaded in the first well. Gels were run at 50-60 V overnight or at 15 mA during the day.

For the RNAi experiment, $5x10^5$ cells were loaded per lane while for the analysis of embryos, 5 embryos were loaded per lane for both the wild type (*Canton S*) and mutant material. For extracts from other tissues the amount of tissue loaded is indicated in the text.

2.2.26. Coomassie staining of gels

To observe protein bands, gels were stained with Coomassie Blue (0.5% Coomassie Blue in methanol) diluted 1:5 in Stain diluent solution (35% methanol, 14% acetic acid in dH_2O) for 1 hour (or overnight) at room temperature. The gel was then destained with Fast Destain solution (35% methanol, 10% acetic acid in dH_2O) for 1 hour at room temperature and destained further with Slow Destain solution (10% methanol, 7% acetic acid in dH_2O) for 1 hour (or overnight) at room temperature. The gel was then placed between two cellophanes (IDEA Scientific company) which were clamped together using a plastic square box making sure that no bubbles were present. The gel was placed in a fan incubator (BioRad) to dry for three hours.

2.2.27. Transfer of SDS-PAGE gels onto nitrocellulose

After electrophoresis, the separated proteins were transferred to Protran nitrocellulose membrane (Schleicher and Schuell) by electroblotting, in preparation for probing with antibodies. 4 litres of Towbin Buffer were prepared (per litre: 800 ml dH_2O, 3.025 g Sigma 7-9 Tris, 14.425 g Sigma-Aldrich glycine, 200 ml methanol. Of these 4 litres, 250 ml were decanted for soaking the Protran membrane and 18.5 ml 20% SDS were then added to give a final concentration of 0.1% SDS). The blot was then assembled in the transfer cassette, in the following order:

(-pole)- sponge- Whatman blotting paper- gel- nitrocellulose- Whatman blotting paper- sponge- (+pole). The cassette containing the gel and nitrocellulose were placed in the transfer tank (BioRad Trans-Blot) and the transfer was performed at 55 volts for 3.5 hours at 4°C. After transfer, the membrane was rinsed with dH_2O and stained with Ponceau-S (0.2% Ponceau-S in 3% trichloroacetic acid) for five minutes at room temperature with shaking. The membrane was rinsed with dH_2O and the position of the molecular weight markers and the resolving/stacking interface were marked on the filter with a pencil. The membrane was stored at 4°C or washed once with PBS/Tw (PBS with 0.1% Tween 20) and used immediately for immunoblotting.

2.2.28. Immunoblotting

Protein extracts were separated by SDS-PAGE and transferred onto nitrocellulose membranes in a Trans-Blot apparatus as described previously. Membranes were blocked in PBS+0.1% Tween 20 (PBSTw) and 5% semi-skimmed milk (less than 0.1% fat) for 1hr at RT (or overnight at 4°C) and then incubated for 1-1.5 hours (or overnight at 4°C) with the primary antibody in PBSTw. After washing three times for 5, 15 and 10 min with PBSTw, the membranes were incubated in a horseradish peroxidase-linked (HRP) secondary antibody for 1 hr in PBSTw at room temperature. Finally the membranes were washed as above in PBSTw and immunocomplexes were detected by enhanced chemiluminescence (ECL, Amersham Biosciences). The nitrocellulose was then exposed to Kodak XAR-5 film for autoradiography for 30 seconds, 60 seconds and 5 minutes. Films were developed using a Konica SRX-101A developer and additional longer or shorter exposures were performed if necessary.

2.2.29. Stripping of blotted nitrocellulose membrane

Nitrocellulose membranes that were already used for immunoblotting were stripped of the primary antibodies in order to be used for further immunoblotting with different primary antibodies. The membrane was washed twice in PBSTw for 15 minutes each time and incubated in a Stripping Solution (100 mM β-mercaptoethanol, 2% SDS, 62.5 mM Tris, pH 6.7) for 30 minutes at 65°C. The membrane was then rinsed several times with PBSTw and washed twice for 10 minutes each time and then for 1-2 hours at room temperature (or overnight at 4°C) with PBSTw. The membrane was ready to be used for another immunoblotting.

2.2.30. Phosphorimager Analysis

Samples were processed as described for immunoblotting but instead of using an HRP secondary, a Cy5 conjugated secondary antibody (Jackson ImmunoResearch Laboratories) was used in a dilution of 1:200. The intensity of the signal was measured by using the STORM 860 scanning phosphorimager and calculated using the ImageQuant program (Amersham). The intensity was finally normalised by using α-

tubulin as a loading control. Values were corrected by subtracting the background of the corresponding lane from each band.

2.2.31. Generation of Antigens and Antibodies

Polyhistidine (6His)-tagged fragments of DmSMC2 and DmCAP-D2 were produced using the residues 24-309 and 951-1162 respectively, by cloning a BamH1-HindIII fragment of the cDNA into a pQE30 (QIA*express* system, Qiagen) expression vector. The constructs were expressed in *E. coli* M15[pREP4] cells (Qiagen) and the proteins were purified on Ni-agarose columns (Qiagen) and subjected to SDS-PAGE. Individual protein bands were excised from the gel, ground under LN_2, and injected into rabbits (Scottish Antibody Production Unit, Pentlands Science Park). This work has been performed by Soren Steffensen and Dr Margarete Heck and it is described in detail in Steffensen *et al* (2001). The same procedure was followed for the generation of Topo II antibody, in which residues 1079-1333 were used and a BamH1-HindIII fragment of the genomic DNA was cloned into a pET23a (Novagen) expression vector. The construct was transformed into *E.coli* BL21 cells (Novagen) and the protein was purified as described above (this part was performed by Soren Steffensen). Individual gel bands were excised from the gel, ground under LN_2, and injected into guinea pigs and rats (Scottish Antibody Production Unit, Pentlands Science Park). For CAP-D3 antibody, a peptide corresponding to the terminal 15 amino acids of the protein (residues 1253-1267, CDMLVTELIFQPPDW) was synthesised and injected into rabbits (Genosphere).

2.2.32. 6xHis-tagged protein expression in E. coli

Different types of cells for expression were used (BL21, ER 2566 cells and M15), depending on the expression vector. For BL21 and ER2566, the same procedure was followed for protein expression and is described below:

BL21 or ER2566 cells were transformed with the desired expression construct as described previously. 3 ml of medium containing the 50 μg/ml ampicillin was inoculated with a single colony from the transformed cells and grown overnight at 37°C. The following morning, a 100 ml LB medium containing 50 μg /ml ampicillin was

inoculated with 100-200 µl of the overnight culture and then grown at 37°C for about 4 hours until an OD_{600} of 0.8 was obtained. 1 ml of the uninduced culture was kept at 4°C for further processing, while 0.5 mM IPTG (stock of 500 mM) was added to the 100 ml culture to induce expression of the recombinant protein. The cells were induced for 2-3 hours at 37°C. 1 ml of the induced culture was kept at 4°C for further processing. The induced 100 ml culture was pelleted by spinning at 4,000 rpm for 15 minutes at 4°C (Beckman JLA 10.500 rotor). The pellet from the whole culture was resuspended in 10 ml of TEN (1x TE, 0.1 mM NaCl) and transferred to a 50 ml Falcon tube. The culture was centrifuged again at 4,000 rpm for 15 minutes at 4°C in a benchtop centrifuge. The supernatant was then discarded and the pellet were completely drained by inverting the tube on a paper towel. Pellets were frozen at - 80°C until required.

The 1 ml uninduced and induced cultures that were kept at 4°C were centrifuged at 4,000 rpm for 5 minutes at 4°C in a benchtop microfuge, washed with 1 ml of TEN and spun again at 4,000 rpm for 5 minutes at 4°C. The pellet was resuspended in 60µl of 1X TE and 30µl sample buffer containing DTT (2 µl) was added immediately. The mixture was boiled at 100°C for 5 minutes, then sonicated (approximately 1 second bursts for about 1 minute) and stored at -20°C. 10 µl of the uninduced and induced samples were analysed on SDS-PAGE gel and stained with Coomassie blue as described previously in order to see if the recombinant protein was induced. To increase expression, different IPTG concentrations (0.2 mM – 1 mM) and induction temperatures (40°C, 25°C, 18°C) were attempted.

M15[pREP4] cells (Qiagen) were ideal for the expression of recombinant proteins encoded by pQE vectors. These cells contained multiple copies of the low-copy pREP4 (kanamycin resistant), which express the *l*ac repressor protein (encoded by the *l*ac I gene) which binds to the operator sequences and tightly regulates recombinant protein expression. The transformation of these cells and the expression of the protein were performed according to the manufacturer's instructions (The QIAexpressionist, Qiagen).

2.2.33. 6xHis-tagged protein purification using Ni-NTA beads (batch purification)

Frozen pellets of bacteria containing induced recombinant protein were thawed on ice for 10-20 minutes, with occasional vortexing. The pellets were weighed and 20 ml of Lysis Buffer (8M urea, 5 mM immidazole, pH 8.0) per gram of pellet were used to lyse the cells for 1 hour at room temperature with moderate shaking. After lysis, the viscous solution was spun at 10,000 rpm for 20-30 minutes to pellet the cellular debris. The supernatant or 'cleared lysate' was collected and 100µl were kept for SDS-PAGE analysis. Ni-NTA beads (Qiagen) were added to the cleared lysate (1 ml of beads per 6-7 ml of cleared lysate), and incubated for 1 hour at room temperature with shaking. The beads were pelleted at 2000 rpm for 5 minutes using a benchtop centrifuge and another 100 µl aliquot of the flow through was taken. The remaining flow through was discarded and the beads were washed 3 times with Wash Buffer (8 M urea, 5 mM immidazole, pH 6.3) with shaking. The first two washes were performed with 10 ml Wash Buffer each and after the second wash the beads were spun down in a benchtop centrifuge at 2,000 rpm for 5 minutes and an aliquot of 100 µl was kept. The third wash was performed with 5 ml of Wash Buffer and the beads were poured into a BioRad chromatography column and spun at 2,000 rpm for 5 minutes. A 100 µl aliquot was taken from the third wash and rest was discarded. Bound proteins were eluted off the beads by adding 0.5 ml of Elution Buffer (either 8 urea, 5 mM immidazole, pH 4.5 OR 8 M urea, 500 mM immidazole, pH 6.3) and spinning this through the BioRad column for 5 minutes at 2000 rpm directly into 1.5 ml eppendorf tube. This was repeated for 5-6 times and the elution fractions were stored at –20 °C. The beads were kept at 4°C for regeneration or were stripped of remaining bound protein by boiling in sample buffer. 10 µl of uninduced, induced cleared lysate and flow-through, 30 µl of each wash and 50 µl of each elution fraction was analysed by SDS-PAGE.

In some cases the BugBuster kit (His-Bind Purification kit, Novagen) for protein purification was used according to the manufacturer's instructions. Usually proteins were in inclusion bodies and thus an extra step for purification of inclusion bodies was performed according to the manufacturer's instructions.

2.2.34. Preparation of antigen for injection

Protein samples were electrophoresed on a large SDS-PAGE gel with one preparative well for sample and run overnight as described previously. The gel was rinsed 3 times, 10 minutes each, with dH_2O and stained with Aqueous Coomassie Blue (0.1% Coomassie Brilliant Blue R in 1X Laemmli Running Buffer without SDS [25 mM trizma base, 192 mM glycine]) for 1 hour at room temperature with shaking. The gel was then destained for 3 times, 10 minutes each, with 1X Laemmli Running buffer until the band of interest was clearly visible. The desired band was excised using a fresh cover slip and ground to fine powder using a pre-chilled ceramic mortar and pestle (Philip Harris) and a small amount of liquid nitrogen. The ground protein was placed in a centrifuge tube using a small piece of weighing paper and it was stored at – 80°C or sent on dry ice to Scottish Antibody Production Unit (SAPU) for injections.

2.2.35. Affinity purification of antibodies

All subsequent steps were performed at 4°C. AffiGel® 10/15 Gel beads (BioRad) were used. AffiGel-10 is best for binding proteins near or below their isoelectric point, while AffiGel-15 is better for binding proteins near or above their isoelectric point. The following conditions refer to a mixture of the AffiGel-10 and AffiGel-15 for better yield of protein binding.

Binding of antigen to AffiGel column:

0.5 ml of each affigel-10 and affigel-15 beads were mixed and washed twice, with 10 ml of cold sterilised dH_2O each time. The beads were centrifuged in between the washes for 2 minutes at 3,500 rpm at 4°C and they were finally diluted in 1 ml cold 100 mM MOPS, pH 7.5. 0.5 ml of the antigen (recombinant protein) was added to the beads and the mixture was incubated at 4°C for 6-7 hours with rotation. After the incubation, the mixture was centrifuged at 3,500 rpm at 4°C for 2 minutes and a sample was taken from the supernatant, while the rest was discarded. The beads were incubated with 1 ml of 1 M Ethanolamine-HCl, pH 8.0 for 1 hour at 4°C with rotation (for blocking any free binding sites on the resin) and then transferred to a BioRad column. The beads were

washed with each of the solutions that were going to be used later in the affinity purification to ensure that any material that would be eluted/removed by them would not do so during the purification. Thus the column was washed subsequently with:

5 ml of TBS (20 mM tris pH 7.5, 150 mM NaCl)
5 ml 20 mM tris pH 7.5, 500 mM NaCl
5 ml of glycine (100 mM glycine, pH 2.5)
5 ml of 50 mM tris, pH 8.8
5 ml ethanolamine (100 mM ethanolamine, pH 8.0)
2 x 5 ml TBS

The column was allowed to drain in between the washes. Finally the column was used immediately for affinity purification of the antibody or it was stored in TBS at 4°C until required. The efficiency of antigen binding to the beads was tested by comparing protein samples that were not applied to the AffiGel column and protein samples after incubation with AffiGel beads. The samples were analysed side by side on an SDS-PAGE gel and stained with Coomassie blue as described previously.

Affinity purification

Usually 1 ml of the immune serum was used for the purification and it was heated at 56°C for 30 minutes to inactivate complement. The serum was placed on ice to cool and it then was centrifuged at 13,000 rpm for 2 minutes to remove debris and the supernatant was transferred into a fresh eppendorf tube. The serum was diluted 1:5 in TBS solution and applied to the column with the bound antigen. The serum was collected and re-applied to the column for 5 times and finally was collected and stored at 4°C. The column was then washed subsequently with 5 ml of TBS twice and with 5 ml of 20 mM Tris pH 7.5, 500 mM NaCl twice. The antibody was eluted off the column using 0.5 ml of 100 mM glycine, pH 2.5. The elution step was repeated 10 times and each elution fraction was collected into an eppendorf tube containing 42 µl of 1 M Tris-Cl, pH 7.5 and 50 µl of 5 mg/ml BSA (for neutralisation). The column was finally washed with 10

ml of TBS and stored in TBS at 4°C. The elution samples were stored at 4°C and they were tested, along with other samples kept during the affinity purification procedure, by immunoblotting against cell extract or against the recombinant protein (antigen) that was used for the affinity purification. Elution samples were usually used at 1:10 dilution for immunoblotting analysis.

2.2.36. Identification of the Condensin Complex: Immunoprecipitation using protein A-sepharose

Extract preparation: 0-5 hr *Drosophila* embryos were homogenised in one volume of buffer A (15 mM NaCl, 60 mM KCl, 2 mM EDTA, 0.34 M sucrose, 15 mM Hepes pH 7.9) and complete protease inhibitors (Roche) using a loose pestle. The homogenate was centrifuged for 5 minutes at 5000 x g at 4°C in a benchtop centrifuge. The middle layer was collected, aliquoted and flash frozen in liquid nitrogen. Dimethyl pimelimidate cross-linking of CAP-D2 antibody to protein A-sepharose was performed according to Harlow and Lane (Harlow and Lane, 1999). For immunoprecipitation from crude extracts, antibody beads were incubated with the extract for 1 hr at 4°C. The beads were washed 10 times with 20 volumes of PBS, and then eluted and washed with PBS containing 250 and 500 mM NaCl. Protein interactions that were resistant to 500 mM NaCl were eluted using 2% SDS in PBS.

2.2.37. Immunoprecipitations using the Dynabeds® M-280 Sheep anti-Rabbit IgG

Immunoprecipitations were also performed by using magnetic beads with affinity purified Sheep anti-Rabbit IgG covalently bound to the surface (Dynabeds® M-280 Sheep anti-Rabbit IgG, *DYNAL* Biotech). Extract preparation: 0-5 hr embryos were homogenised in one volume of PBS containing 0.2% Triton-X 100 and complete protease inhibitors (Sigma) using a motorised pestle. The homogenate was centrifuged through a mesh for 5 minutes at 5000 x g at 4°C in a benchtop centrifuge. The extract was collected, aliquoted, flash frozen in LN_2 and kept at -80°C.

The immunoprecipitation procedure was performed according to the manufacturer's instructions. 1-2 x 10^8 (6-7 x 10^8 beads/ml) beads were transferred in an 1.5 ml

Eppendorf tube and washed three times with the washing buffer (1X PBS) using a magnet. The antibody (usually diluted 1:2 or 1:3 in 1X PBS buffer) was added to the washed beads and incubated overnight at 4°C with slow tilt rotation mixing. The antibody was then removed and the beads were washed three times with the washing buffer. Crosslinking of the antibody with the beads was achieved by using Dimethyl pimelimidate dihydrochloride (DMP). Initially the beads were washed twice with 1 ml each time of 0.2 M triethanolamine, pH 8.2 and then 1 ml of 20 mM of DMP (diluted in 0.2 M triethanolamine) was added to the beads. The mixture was incubated for 30 minutes at 20°C with rotational mixing and the reaction was stopped with the addition of 1 ml of 50 mM Tris, pH 7.5 and incubated for 15 minutes with rotational mixing. The crosslinked beads were washed three times with 1 ml each time of PBS/BSA (1X PBS and 0.2% BSA) and ~300-600 µl of embryo extract were added and the mixture was incubated for 1-1.5 hours at 4°C with rotation. The embryo extract was then removed and the beads were washed three times with 1 ml washing buffer each time. The beads were eluted and washed with PBS containing 250 and 500 mM NaCl (diluted in 1X PBS and containing 0.05% Triton-X 100). Protein interactions that were resistant to 500 mM NaCl were eluted using 2% SDS in PBS. Finally the beads were boiled in 1X Sample buffer for 10 minutes and samples were analysed by SDS-PAGE.

2.2.38. Preparing samples for Mass Spectrometry

Protein samples from immunoprecipitations (washes and elutions) were electrophoresed on a large SDS-PAGE gel and run overnight to resolve the proteins. Immediately after the dye front left the gel, electrophoresis was terminated. The gel was disassembled and rinsed twice, for 10 minutes each, with sterilised deionised water. The gel was then stained overnight with the GelCode® Blue Stain Reagent (PIERCE) at room temperature and it was destained twice with sterilised deionised water for 2-3 hours until individual bands could be observed. If the signal was weak, the staining with the GelCode reagent was repeated once more overnight at room temperature. After destaining, the gel was photographed and individual bands were excised from the gel either with clean coverslips or with a clean razor blade that was washed with ethanol

before cutting a new band. The bands were placed in 1.5 ml eppendorf tubes and they were taken to the ICMB Mass Spectrometry Facility for further analysis. Samples from pre-immune serum were electrophoresed as well and protein bands were excised and sent for mass spectrometry analysis.

2.2.39. Immunofluorescence of Drosophila Cultured Cells

$2x10^5$ cells diluted in 1X EBR were centrifuged onto poly-L-lysine-coated slides (500 µl of cells) for 2 min at 2000 rpm in a cytospin column (Cytospin 3, *SHANDON*). The cells were immediately fixed for 4 min in 4% PFA in PBS at RT, washed for 5 min in PBS+0.1% Triton-X (PBSTx) and permeabilised in PBS +0.5% Tx for 5 min. After the permeabilisation, cells were blocked for 1 hr at RT in 5% Bovine Serum Albumin (BSA, Sigma). Cells were washed in PBSTx for 5 min and incubated for 1 hr in the primary antibody in PBSTx+0.5% BSA. After three 5 min washes in PBSTx, cells were incubated in the secondary antibody (conjugated fluorochromes, Molecular Probes or Jackson ImmunoResearch Laboratories) in PBSTx+0.5% BSA and in 1µg/ml DAPI for DNA staining. Cells were washed four times, 5 min each, in PBSTx and coverslips were mounted onto the slides with Mowiol (Calbiochem) and viewed under the fluorescent microscope. For some antibodies (DSA1, Drad21/Scc1, SMC2, SMC4, guinea pig topo II and CAP-D3), 0.5% Triton-X was included in the fixative and the incubation in this solution was done for 10 min. A permeabilisation step was performed as well as described above.

For hypotonic treatment, cells were diluted in 0.25X EBR at a concentration of $2x10^5$ for 1-2 min at RT and then centrifuged onto poly-L-lysine slides and processed as described above. Cells that were grown on Concanavalin A-coated coverslips for 24hr in a 6-well (35mm) plate were then fixed and processed as described above. For immunofluorescence using INCENP antibody, the fixation step was performed in 4% PFA diluted in Cytoskeletal Buffer (137 mM NaCl, 5 mM KCl, 1.1 mM $NaHPO_4$, 0.4 mM KH_2PO_4, 2 mM $MgCl_2$, 2 mM EGTA, 5 mM PIPES, 5.5 mM Glucose, pH 6.1 with HCl) instead of PBS for 4 minutes and the subsequent steps were the same as described

above. The Cytoskeletal Buffer was recommended for preservation of microtubules during immunofluorescence.

2.2.40. BrdU Incorporation in Drosophila Cultured Cells

Cells growing in flasks were incubated for 30 min in medium containing 6 μg/ml BrdU (bromodeoxyuridine). $2x10^5$ cells were centrifuged onto poly-L-lysine slides and processed as described for immunofluorescence except that DAPI was omitted. The primary antibody in this case was anti-CAP-D2 and the secondary was Alexa 594 goat anti-rabbit conjugate. After the anti-CAP-D2 immunofluorescence was complete, the cells were post-fixed immediately in 4% PFA in PBS for 1 hr at RT, washed for 5 min in PBSTx and then incubated for 15 min in freshly prepared 2N HCl. After a 5 min wash in PBSTx, cells were blocked for 30 min in PBS+5% BSA and washed for 5 min in PBSTx and then incubated with the rat anti-BrdU antibody (1:2 dilution) in PBSTx+0.5% BSA at 4°C for 16 hrs. After three 5 min washes, the cells were incubated with Alexa 488 goat anti-rat conjugate (1:500 dilution) in PBSTx+0.5% BSA for 1 hr at RT. 1 μg/ml DAPI was added during the last incubation. Finally cells were washed four times for 5 min each with PBSTx and coverslips were mounted onto the slides with Mowiol.

2.2.41. Antibody staining of larval brains

Third instar larvae were collected from vials and washed in EBR in a dissecting dish to remove excess food. Individual larvae were transferred to a new well containing EBR and brains were dissected under a dissecting microscope. 4-5 brains were processed on one slide and thus dissected brains were placed into a new well containing EBR until ready, but never for more than 10 minutes. The brains were hypotonically swollen for 3 minutes in 0.25X EBR and fixed for 5 minutes in 4% paraformaldehyde (TAAB), 5% acetic acid, 0.1% Triton-X 100 in 0.16X EBR by placing them in a drop on a siliconised coverslip. A poly-L-lysine slide was inverted onto the coverslip and the brains were squashed during the fix repeatedly by pressing very hard on the slide. The slide was dipped in LN_2 and the coverslip was breathed on to warm and flicked off with a razor

blade. The slide was placed immediately into a Coplin jar containing PBS for 2 minutes and it was then permeabilised for 3 times 10 minutes each in PBSTx (1X PBS + 0.1% Triton-X 100). Blocking was performed in 3% BSA in PBS for 1 hour at room temperature. After blocking, the slide was washed for 5 minutes in PBSTx and then incubated overnight at 4°C in the primary antibody diluted in PBS + 0.3 % BSA. The slide was washed 6 times for 5 minutes each in PBSTx and the appropriate secondary antibody diluted in 3% BSA in PBS was applied for 1-2 hours at room temperature. The slide was then washed 6 times, 5 minutes each, in PBSTx. The brains were also stained with DAPI (0.1 μg/ml) that was included in the secondary antibody. Slides were finally drained and mounted in Mowiol, allowing 30 minutes for the Mowiol to set and examined under the fluorescence microscope.

2.2.42. Bonaccorsi et al fixation of larval brains

This protocol has been adapted from Bonaccorsi *et al* (2000) and is recommended for analysis of mitotic spindles in *Drosophila* neuroblasts.

Brains were dissected from second or third instar larvae in EBR as described above and fixed in 4% paraformaldehyde (PFA) in PBS for 30 minutes at room temperature in a dissecting dish. Following this, the brains were transferred to a new well containing 45% acetic acid (in dH_2O) for 3 minutes, then transferred to a drop (10-15 μl) of 60% acetic acid on a siliconised coverslip and squashed gently onto a poly-L-ysine slide. The slide was flash-frozen in liquid nitrogen and the coverslip was removed. The slide was placed in a coplin jar with 100% ethanol at - 20°C for 10 minutes. The brains were then permeabilised in PBSTx for 10 minutes at room temperature, washed twice in PBS, 5 minutes each, and then blocked in 1X PBS + 3% BSA. Primary and secondary antibody incubations, washes and DAPI staining were performed as described above.

2.2.43. DAPI staining of larval brains

Brains were dissected from second or third instar larvae in EBR as described above and fixed twice in 45% acetic acid, 1.5 minutes each, in a dissecting dish. The brains were

then transferred to a drop of 45% acetic acid (5 µl per drop) on a siliconised coverslip and a poly-L-lysine slide was inverted on top of the coverslip (total fixation should not exceed 3 minutes). The brains were squashed by pressing on the inverted slide (placed between folded Kim-wipe paper) and flash-frozen by dipping in liquid nitrogen. The coverslip was breathed on to warm and flicked off with a razor blade and immersed immediately in a Coplin jar containing PBS for 5 minutes to wash off acetic acid. The slide was transferred to a jar containing 0.1 µg/ml DAPI in PBSTx for 10 minutes and then washed 3 times, 5 minutes each, with PBSTx. Slides were finally drained and mounted in Mowiol, allowing 30 minutes for the Mowiol to set and examined under the fluorescence microscope.

2.2.44. Embryo collection and preparation for immunofluorescence

Flies of the appropriate stock were transferred to a collection cage and left to lay eggs on a red wine concentrate-agar dish with a dollop of thick yeast paste in the centre. The cage was left undisturbed for the desired laying period and the red wine agar dish was then exchanged for a fresh one in order to obtain subsequent embryo collections. Embryos were rinsed with water and brushed from the agar plate using a large paintbrush and transferred into a microsieve with a plastic pipette. The embryos were rinsed with water into the microsieve to remove yeast and then dechorionated in a freshly diluted 50% hypochlorite bleach solution (diluted with dH_2O) for 1-2 minutes. As soon as chorion fragments were observed floating on the sieve, the embryos were rinsed with water and then subsequently with EBR. Dechorionated embryos were transferred into a small glass vial, using heptane (heptane covered half the tube). The embryos were then fixed in equal volumes of heptane (to permeabilize the vitelline membrane) and 40% EM grade formaldehyde (Electron Microscopy Sciences, PA) with extremely gentle agitation for 3-5 minutes, ensuring that the embryos were spread in a monolayer at the interface between the two phases. The lower formaldehyde phase was then removed carefully using a glass Pasteur pipette and replaced with an equal volume of methanol (BDH ultrapure) to remove the vitelline membrane. The vial was shaken vigorously, vortexed for 15 seconds and then left to stand upright for one minute. The

devitellinised embryos which had sedimented to the bottom of the vial were removed using a glass Pasteur pipette and transferred into a 1.5 ml Eppendorf tube. The embryos were washed 5 times with fresh methanol and mixing in between to remove any remaining formaldehyde or heptane. Fixed embryos were stored in methanol at 4°C or -20°C until required for immunofluorescent labelling. Several fixation protocols were tested and the most successful staining for CAP-D2 was obtained when a permeabilisation step (2% Triton X in PBS) was performed after the fixation for 10-15 minutes.

2.2.45. Antibody staining of Drosophila embryos

Fixed embryos were rehydrated by performing five minute washes in a series of methanol solutions as follows:

100% methanol
90% methanol/10% PBS
75% methanol/25% PBSTx (1X PBS + 0.05% Triton-X 100)
50% methanol/50% PBSTx
25% methanol/75% PBSTx
100% PBSTx

All subsequent washes and incubations were performed using a rotating wheel. The embryos were blocked in 10% BSA in PBSTx (PBS + 0.2% Triton-X 100) for 1.5 hours at room temperature and then washed in PBSTx two times for 15 minutes each. Embryos were then incubated in primary antibody overnight at 4°C (CAP-D2 antibody 1:10,000 diluted in PBSTx + 0.5% BSA). Embryos were washed four times, 15 minutes each, with PBSTx and incubated for 2 hours at room temperature in the desired secondary antibody at a dilution of 1:1,000 in PBSTx + 0.5% BSA. The secondary antibody dilution also contained 0.1 μg/ml DAPI, for DNA labelling. After the incubation, embryos were washed 4 times, 15 minutes each, with PBSTx, transferred on

a glass slide and mounted with 90% glycerol in PBS. Finally, a coverslip was placed over the sample and the edges were sealed with nail varnish.

2.2.46. DAPI staining of Drosophila testes

Pupal testes were dissected in EBR solution in a dissecting dish. Testes were then fixed in 4% PFA in PBS for 15-20 minutes, permeabilised in 0.1% Triton-X 100 in PBS for 5 minutes, stained with 0.1 μg/ml DAPI in PBS for 15 minutes and washed in PBSTx (PBS + 0.1 % Triton-X 100) for 5 minutes. Testes were then transferred to a microscope slide, a coverslip was placed on top and the testes were squashed by pressing on the coverslip. Excess liquid was removed by a Kim Wipe paper tissue. The preparation was observed under a fluorescence microscope.

2.2.47. Preparation of live testes squashes

Testes from pupae or adults were dissected in EBR under a dissecting microscope. The testes were transferred on a clean slide and a coverslip (22 x 22 mm) was placed carefully on top without pressing. A very mild squashing was obtained by removing excessive buffer from the edges of the coverslip with a piece of blotting paper. Preparations were then analysed under phase-contrast optics usually with the 40X objective. Sperm motility assay was performed in the same way. Sperm were pulled out of the seminal vesicle before the coverslip was placed on top and if the sperm were motile, sinusoidal movement was observed. In general, excessive exposure to ether or CO_2 should be avoided since sperm movement is sensitive to these reagents.

2.2.48. Antibody injection in Drosophila embryos

Embryo preparation:

A 45 minute collection of wild type embryos expressing H2A-GFP was used for the CAP-D2 antibody injection. The embryos were collected in a sieve as described previously and they were dechorionated with 50% bleach in dH_2O for 1-2 minutes. The sieve was rinsed thoroughly with water and dried with a paper towel. The embryos were transferred to an agar slice and lined up under a light microscope with their anterior ends

to the right. Usually 20-30 embryos were lined up per agar slice and were then picked up using a coverslip with one side coated in heptane glue. The embryos stuck to the sticky surface and the coverslip was placed in a box containing silica gel for approximately 10 minutes to desiccate the embryos. After desiccation, the embryos were covered with halocarbon oil, series 700 (Halocarbon Products Company) and the coverslip was attached to a metal slide with some heptane glue.

Antibody preparation and injection:

10 µl of the CAP-D2 antibody was dialysed using 0.025 µm filters (MILLIPORE) against 3 litres of Injection buffer (10X buffer: 0.1 M NaPi [NaH_2PO_4 + Na_2HPO_4], 0.5 M KCl). The antibody that was obtained (usually 30-40 µl) was concentrated using the Biomax 5K concentrator columns (MILLIPORE). The antibody was tested by immunoblotting and stored at 4°C or used immediately for injections. Pre-immune serum was dialysed in the same way.

For the injections, a femtotip needle (Eppendorf) was loaded with approximately 2 µl of the dialysed CAP-D2 antibody, pre-immune serum or injection buffer using a microloader pipette tip (Eppendorf). Bubbles were avoided by loading the sample at the base of the needle. The needle was fixed to the injecting apparatus that was next to the Olympus Delta-Vision microscope (Applied Precision). The slide with the embryos was placed on the Delta-Vision microscope stage and the tip of the needle was focused so as to be at the same level with the prepared embryos. Only syncytial embryos that were undergoing mitotic divisions were injected. Immediately after injection, individual embryos were observed under the 40x objective using blue light and images were captured every 10 seconds (for 10 minutes in total) using the Delta-Vision microscope SoftwoRx programme. Finally at the end of the captures, a movie was created.

2.2.49. Microscopy

All preparations were examined with an Olympus Provis microscope, equipped with epifluorescence optics. Images were captured with an Orca II CCD camera (Hamamatsu) and Smart-Capture 2 software (Digital Scientific). All images were

processed with Adobe Photoshop software. For examining the localisation and the presence of several proteins on the chromosomes in the RNAi experiment, all images were obtained with the same camera settings and the same exposure time was maintained between the controls and the CAP-D2 RNAi experiment.

2.2.50. Antibodies

The primary antibodies were used for immunofluorescence as follows:

- α-tubulin (mouse monoclonal antibody B5-1-2 used at 1:500, Sigma),
- γ-tubulin (mouse monoclonal T 6557 used at 1:50, Sigma),
- P~H3 (mouse monoclonal used at 1:500, 9706L, New England Biolabs),
- BrdU (rat antibody used at 1:2, Harlan Sera Lab),
- CID (chicken polyclonal used at 1:200, (Blower and Karpen, 2001)),
- Topo II (rabbit polyclonal used at 1:500, and guinea pig polyclonal used at 1:500),
- Barren (rabbit polyclonal used at 1:500 (Bhat et al., 1996)),
- SMC2 (rabbit polyclonal used at 1;500),
- SMC4 (rabbit and sheep polyclonals used at 1:500 (Steffensen et al., 2001),
- Drad21/SCC1 (rabbit polyclonal used at 1:500 (Warren et al., 2000b)),
- DSA1 (rabbit polyclonal used at 1:500 (Valdeolmillos, 2004)),
- BubR1 (rabbit polyclonal used at 1:1000),
- Bub3 (rabbit polyclonal used at 1:500),
- sheep Cyclin B (used at 1:500),
- INCENP (rabbit polyclonal used at 1:500, (Adams et al., 2001b)),
- CAP-D2 (rabbit polyclonal used at 1:1000 for immunofluorescence and 1:10,000 for immunoblotting),
- CAP-D3 (rabbit polyclonal used at 1:200 for immunofluorescence and 1:500 for immunoblotting),
- PCNA (rabbit polyclonal used at 1:500),
- ASH1 (affinity purified rabbit polyclonal used at 1:500),

- ORC-2 (rabbit polyclonal used at 1:2000),
- ORC-3 (mouse polyclonal used at 1:10,000),
- CP-190 (rabbit polyclonal used at 1:500),
- CNN (mouse polyclonal used at 1:500),
- HP1 (mouse polyclonal used at 1:250),
- Prod (rabbit polyclonal used at 1:500),
- ZW10 (rabbit polyclonal used at 1:500),
- BEAF-32 (rabbit polyclonal used at 1:1000),
- Histone H3 (rabbit polyclonal used at 1:5000),
- Tis-2 (affinity purified rabbit polyclonal used at 1:10).

All fluorescently conjugated secondary antibodies (Molecular Probes, Jackson ImmunoResearch Laboratories) and Horseradish Reroxidase (HRP) conjugated antibodies (Amersham Biosciences) were used according to the manufacturer's instructions.

2.3. TABLES OF EST CLONES AND OLIGONUCLEOTIDES (PRIMERS)

EST name	Length	Source	Vector	Host cells	Restriction sites	Antibiotic resistance
LD40412 (AI520293)	Full length cDNA	embryo	pOT2	XL-1 blue	EcoR1-XhoI	chloramphenicol 12.5μg/mg
LD10348 (AA816786)	5' prime	embryo	pBluescript SK	SOLR	EcoR1-XhoI	ampicillin 200 μg/mg
LD41419 (AI515757)	5' prime	embryo	pOT2	XL-1 blue	EcoR1-XhoI	chloramphenicol 12.5μl/mg
LD08652 (AA264983)	3' prime	embryo	pBluescript SK	SOLR	EcoR1-XhoI	ampicillin 200 μg/mg
LD19049 (AA539797)	5' prime	embryo	pBluescript SK	SOLR	EcoR1-XhoI	ampicillin 200 μg/mg
LD17278 (AA539174)	5' prime	embryo	pBluescript SK	SOLR	EcoR1-XhoI	ampicillin 200 μg/mg

Table I. CAP-D2 EST clones (ResGen, Invitrogen Corboration).

EST name	Length	Source	Vector	Host cells	Restriction sites	Antibiotic resistance
RE18364 (BI213051)	full length cDNA	embryo	pFlc-1	XL-1 blue	XhoI-BamH1	ampicillin 200 μg/mg
AT11671 (BF497492)	full length cDNA	adult testes	pOTB7	XL-1 blue	EcoR1-XhoI	ampicillin 200 μg/mg

Table II. CAP-D3 EST clones (*Drosophila* Gene Collection).

Primer name	Primer direction	Primer sequence
T7 primer	forward	5'- AATACGACTCACTATAGG -3'
T3 primer	reverse	5'- AATTAACCCTCACTAAAGG -3'
M13 forward primer	forward	5'- TGTAAAACGACGGCCAGT -3'
M13 reverse primer	reverse	5'- CAGGAAACAGCTATGAC -3'
PM001 primer	reverse	5'- CGTTAGAACGCGGCTACAAT -3'

Table III. Primers used for sequencing of inserts in several constructs.

Vector	Sequencing primers of inserts
pBluescript and pOTB7	M13 forward and M13 reverse
pOT2	T7 forward and PM001reverse
pFLC-1	T7 forward and T3 reverse

Table IV. Primer pairs used for sequencing of inserts in different vectors.

Primer name	Start position on coding sequence	Primer direction	Primer sequence T7 sequence TTAATACGACTCACTATAGGG was added at the 5' end.
CAP-D2 R1F	251	forward	5'- TTGACCTGCTCTACCTGACC -3'
CAP-D2 R1R	873	reverse	5'- CCGAAGAGTCAGAACTGTCC -3'

Table V. Primers used to deplete CAP-D2 by RNAi.

Primer name	Primer direction	Primer sequence T7 sequence TTAATACGACTCACTATAGGG was added at the 5' end
Control F	forward	5' GGGATCATCTGCAAGGAGCTC 3'
Control R	reverse	5' TCACAACGACCCTTTGAAGTG 3'

Table VI. Primers used to amplify a product from a human intron that was used as control in the RNAi experiments.

Primer name	Start position on genomic sequence	Primer direction	Primer sequence
SMC2-pF	19	forward	5' CGGATCCACTAGGTTCCGTACT 3'
SMC2-pR1	554	reverse	5' GAAAAGAACGCCAGGAATTAAA 3'
SMC2-tF	4235	forward	5' TTGTACATTTTGGATGAGGTGGA 3'
SMC2-tR	4906	reverse	5' GACTGCTTCAAAAGCTCACCAT 3'

Table VII. Primers used to sequence *DmSMC2*.

Primer name	Start position on coding sequence	Primer direction	Primer sequence
SMC2-1	375	forward	5' GAAGGTGCAAGACTTCTTCTGCTC 3'
SMC2-2	919	forward	5' CGGGCACTAGAAGCTACCGCTA 3'
SMC2-3	2,922	reverse	5' GAGAGTGCGTTCCATTTTGTCC 3'
SMC2-4	3,219	forward	5' TGGCATATGGAAGGAGAGTCTCG 3'
SMC2-5	1,398	forward	5' AAGTCTCGATTACGAGGGCGGTC 3'
SMC2-6	2,568	reverse	5' GCGGCACTGGAGCTATTTACT 3'
SMC2-7	1,905	forward	5' ACAAATCAGCTACGACCCCC 3'
SMC2-8	2,706	forward	5' TTCTTCACCTCCAGCTCAATCTCC 3'
SMC2-9	387	reverse	5' GCTGGATGGAGCAGAAGAAG 3'
SMC2-10	2,041	reverse	5' CTCCCTGTACTCCTTTTCTATTTG 3'
SMC2-11	2,070	forward	5' CTCTGAGATAGCCCAAGTG 3'
SMC2-12	2,322	forward	5' CGAGGCGAAGTTGGCAGATG 3'
SMC2-13	2,395	forward	5' ACCAAGCAAAGGGCGGAGAAATC 3'
SMC2-14	2,818	forward	5' CCGGAGGAGAAGAACTGC 3'
SMC2-15	3,016	forward	5' GTGGCGATGGACAAGGAG 3'
SMC2-16	3,140	forward	5' TACCGGGTGCTGAAGCGAAACTC 3'
SMC2-17	814	reverse	5' GTTTTCAATGCTCTCGACCTCTGC 3'
SMC2-18	1,285	reverse	5' CTCACCCTCACGCTGTTTCAATAC 3'
SMC2-19	1,620	reverse	5' AACTTCCGCCGGCTGTCTGG 3'
SMC2-20	2,047	reverse	5' GTCGATCTCCCTGTACTCCTTTTC 3'
SMC2-21	738	reverse	5' CATTAGCCTCCACCGTCTTG 3'
SMC2-22	387	reverse	5' GCTGGATGGAGCAGAAGAAG 3'
SMC2-23	2,392	reverse	5' CTCCGCCCTTTGCTTGGTCAC 3'
SMC2-24	2,777	reverse	5' CTCAAGGGCTTCCATCCGTTTCT 3'
SMC2-25	3,057	reverse	5' ATCCTGCTCTTCTTCGTCCATC 3'
SMC2-26	3,417	reverse	5' ACCATCCTTGAGAGACACAATC 3'
SMC2-27	49	forward	5' CGCACGGAGATAGAAGGATTC 3'
SMC2-28	319	forward	5' GTGGTTGTCGGAGGCAAG 3'
SMC2-29	528	reverse	5' TTGGTGGCATCTCGCTTG 3'
SMC2-30	700	forward	5' CACATCTCCGCCAAGTATCTC 3'
SMC2-31	738	forward	5' CAAGACGGTGGAGGCTAATG 3'
SMC2-32	795	reverse	5' GAGGTTCTTGGCGTGAGTG 3'
SMC2-33	1,923	forward	5' CCGTATTAATTGTCGTTCTGTG 3'
SMC2-34	2,172	reverse	5' CCTGTTCTCGCACATGGTT 3'
SMC2-35	2,287	reverse	5' CTTGCGAGGTCTTCTGCTT 3'
SMC2-36	2,813	forward	5' GGATTCCGGAGGAGAAGAAC 3'
SMC2-37	2,854	forward	5' CGGTACGATTACAGCAAGGAG 3'
SMC2-38	3,052	reverse	5' GCTCTTCTTCGTCCATCTTCAC 3'
SMC2-39	1,001	forward	5' CATCCAAAAACATTGAGGATGA 3''
SMC2-40	1,588	reverse	5' GTGAAAGACATGCAAAACTCCA 3'
SMC2-41	1,232	forward	5' AGGCACAGACCACCATTAAGAC 3'
SMC2-42	1,994	reverse	5' CTGCTCCTAAAGGTGCTAACGT 3'
SMC2-43	2,209	reverse	5' CAACAGAATCAGGCTGAAATTG 3'

Table VIII. Primers used to sequence *DmSMC2*.

Name of primer pair	Primer pair
A1	Pf+9
A2	PF+pR1
A3	27+9
A4	27+29
A5	1+17
A6	30+18
A7	31+18
A8	31+19
A9	2+18
A10	2+20
A11	2+10
A12	5+34
A13	41+26
A14	41+3
A15	41+25
A16	41+24
A17	7+10
A18	39+42
A19	39+3
A20	39+25
A21	39+24
A22	39+43
A23	11+35
A24	12+6
A25	11+23
A26	13+3
A27	13+24
A28	11+6
A29	36+26
A30	37+25
A31	8+38
A32	8+25
A33	4+26
A34	4+tR
A35	tF+tR
A36	36+tR
A37	7+34
A38	33+34
A39	5+19
A40	37+38
A41	33+23
A42	36+3
A43	13+38

Table IX. Primer pairs that were used to amplify the *Dm*SMC2 gene.

Primer name	Start position on P-element sequence	Primer direction	Primer sequence
EPgy2F1	9418	forward	5' GACATGCACTGCGCTCAAACTA 3'
EPgy2F2	9378	forward	5' CGATCACTTCCCGCTTACAC 3'
EPgy2F3	9132	forward	5' TGGCAGCCTGGACATTATCT 3'
EPgy2R1	2041	reverse	5' TGACTTACATTTATCGTGGCAA 3'
EPgy2R2	2202	reverse	5' GCATCTCATTAATATTCGCGA 3'
EPgy2R3	2544	reverse	5' AACTGCTCCATATCCCGGGCTACT 3'
P-stop R	12	reverse	5' CATGATGAAATAACATAA 3'
EP-R1	393	reverse	5' GAACCAGAAAAGATAAAAGAAGGC 3'
EP-R2	519	reverse	5' TGAAAATAAGAGCTTGAGGGAAAA 3'
EP-F1	9875	forward	5' TGACTCTGCGACGTATTTATCTTA 3'
EP-F2	10758	forward	5' TCACTCAGACTCAATACGACACTC 3'
EPRT-F1	491	forward	5' TGTGCGTTAGGTCCTGTTCATTGT 3'
EPRT-R1	1134	reverse	5' CGATTTTTGATGTAAGGTATGCA 3'
EPRT-F2	1658	forward	5' GAAGCCGCCAAAGAGCAGGAATG 3'
EPRT-R2	2282	reverse	5' ACTAAGAAGGGTGTGGTTTCAGGC 3'
EPRT-F3	4247	forward	5' TTTCACACTTTCCCCTGCTTACCC 3'
EPRT-R3	4918	reverse	5' TCTCAAGCGACCAGGCGATCTCA 3'
EPRT-F4	6705	forward	5' CCAGCGGGGAACAGTGACGAATAA 3'
EPRT-R4	7230	reverse	5' TCAGTGTTCGGGTAATCAGGTGGC 3'
EPRT-F5	9249	forward	5' CAGCATTTTCCGTTTTGTGTTAT 3'
EPRT-R5	9875	reverse	5' TGATCTGCGACGTATTTATCTTA 3'

Table X. Primers designed to amplify regions of the P-element *P{EPgy2}* that is inserted in the *CAP-D3* gene.

Primer name	Start position on genomic sequence	Primer direction	Primer sequence
CAP-D3F1	7923	forward	5' GGAGTTGTGATTGATGGCGGATAC 3'
CAP-D3F2	7785	forward	5' CACGTCGCTGGCAAAGTTATC 3'
CAP-D3F3	7010	forward	5' CGAGCTTGAAACCGGCGTATGC 3'
CAP-D3R1	9945	reverse	5' GCTACCGATGCCTGGGGATTG 3'
CAP-D3R2	10489	reverse	5' ACTGGATGATTGTGATAGCCGGTC 3'
CAP-D3R3	11206	reverse	5' TGCTCTTCATCATGCGCCG 3'
CAPD3F1	159	forward	5' CAGCAGCGGGCGGAGAA 3'
CAPD3F2	439	forward	5' STATGCAGCTAGCCCTCAAT 3'
CAPD3R1	995	reverse	5' CTTTTACATTGAGTGCGTGGTG 3'
CAPD3R2	3038	reverse	5' TGACCAGGCTATTTTGAGGGGC 3'
CAPD3R3	9353	reverse	5' CAACAAGCAGAGGAAGAGGGCGAAA 3'
CAPD3 NP F	8709	forward	5' TACATTGAGTGCGTGGTGTCCAAAT 3'
CAPD3 NP R	9001	reverse	5' GCCACGAGGTGTCCGACGTGC 3'
Primer name	**Start position on coding sequence**	**Primer direction**	**Primer sequence**
tetF	115	forward	5' CAGCAGCGGGCGGAGAAGT 3'
tetR	863	reverse	5' GTGGAGCGATGCAAAGTGGGG 3'
3'ORF F	3190	forward	5' CCCGACGCCCTGATTGTGGTT 3'
3' ORF R	3714	reverse	5' GACCACGCCGACTGCCTCCCGT 3'

Table XI. Primers designed to amplify regions of the *CAP-D3* gene.

Primer name	Start position on coding sequence	Primer direction	Primer sequence T7 sequence TTAATACGACTCACTATAGGG was added at the 5' end
D3RF1	1	forward	5' ATGTCGGATTTCCATCGTAT 3'
D3RR1	639	reverse	5' CGACAGGATCATTCGTTGTCT 3'
D3RF2	1418	forward	5' ACGAGCTGCGTTTCGAGAAGC 3'
D3RR2	2141	reverse	5' CGCTGCAGCTGATCACTGGCT 3'

Table XII. Primers used to deplete CAP-D3 by RNAi.

Primer name	Start position on cDNA sequence	Primer direction	Primer sequence
31648F1	41	forward	5' ACAAACAAGTGCTAAAATAAATGA 3'
31648F2	173	forward	5' CGCCCTCAAAACTCAGTCCATAAG 3'
31648R1	674	reverse	5' GAGGTGGACATGCCCGT 3'
31648R2	798	reverse	5' ACTTCCCCAGCTATGCAAAACCTC 3'
7277F1	35	forward	5' TGAAATTTCGGAAGATGTTGGG 3'
7277F2	198	forward	5' TATAATCATCGGAGGCGGCGGACT 3'
7277R1	1544	reverse	5' TTGTGAGCGGAATAAAGTC 3'
7277R2	1382	reverse	5' GTTCAGTCCGGTGGTCTTGCT 3'
31915F1	205	forward	5' CATTTTGGTGTGCATTTCAGGAC 3'
31915F2	450	forward	5' ACGAATTTAAGCCGGAGGAGCAGAG 3'
31915R1	2009	reverse	5' TCTACCGAACAAAAACCATGC 3'
31915R2	2228	reverse	5' AAGATAACACAAGTAGTAGTAATC 3'
14016F1	1	forward	5' ATGCCATCGCCCAAGAAA 3'
14016F2	137	forward	5' TGGCCATCTGCACCAAGTT 3'
14016R1	690	reverse	5' GGAGAAAATATGCGAGTACAGC 3'
14016R2	594	reverse	5' CATGCTCATCCAAGGCCACG 3'
14015F1	49	forward	5' CGCTTGCGAAAATGCTGCTAAAAA 3'
14015F2	288	forward	5' CAGCGGGAGAACGGAGTGATT 3'
14015R1	1986	reverse	5' ACACCAAAGGAAATTATCTATG 3'
14015R2	1724	reverse	5' CGCACTTCATTCCAATTACATAAG 3'

Table XIII. Primers used to sequence the five genes that are located within the *CAP-D3* gene.

Name of primer pair	Primers
S1	CAP-D3F1 + EPgy2R1
S2	CAP-D3F1 + EPgy2R2
S3	CAP-D3F1 + EPgy2R3
S4	CAP-D3F3 + EPgy2R1
S5	CAP-D3R2 + EPgy2F1
S6	CAP-D3R2 + EPgy2F2
S7	CAP-D3R2 + EPgy2F3
31648	31648F1 + 31648R1
7277	7277F1 + 7277R1
31915	31915F1 + 31915R1
14016	14016F2 + 14016R2
14015	14015F1 + 14015R1
D5'	tetF + tetR
D3'	3'ORF F + 3'ORF R
r1	D3RF1 + D3RR1
r2	D3RF2 + D3RR2
P1	EPRT-F1 + EPRT-R1
P2	EPRT-F2 + EPRT-R2
P3	EPRT-F3 + EPRT-R3
P4	EPRT-F4 + EPRT-R4
P5	EPRT-F5 + EPRT-R5
P6	EPRT-F4 + EPRT-R5
F1a	CAPD3 NP F + EP-R1
F1b	CAPD3 NP F + EP-R2
F2	EP-F2 + CAPD3 NP R
F3	CAPD3 NP F + EPRT-R1
F4	EPRT-F1 + CAPD3 NP R
W1	CAPD3 NP F + CAPD3 NP R

Table XIV. Primer pairs used to amplify regions of the *CAP-D3* gene and the P-element for several purposes as indicated in Chapter 6.

CHAPTER 3

CHARACTERISATION OF THE *DROSOPHILA* CAP-D2 CONDENSIN SUBUNIT

3.1. Introduction

The main focus of this study is the characterisation of the biological function of condensin subunits and particularly of the CAP-D2 non-SMC subunit. An antibody against this protein was raised by Margarete Heck in collaboration with Claudio Sunkel's laboratory in Portugal, but it was not characterised further. Before attempting to unravel the functional contribution of this protein to chromosome assembly and organisation, further analysis of its subcellular distribution during the cell cycle was necessary. Thereby, general characterisation of the CAP-D2 condensin subunit was performed using the CAP-D2 antibody and this work will be described in this chapter.

3.2. Characterisation of the CAP-D2 condensin subunit

3.2.1. The Drosophila CAP-D2 gene

The *CAP-D2* gene (CG1911) is located on the right arm of the third chromosome of *Drosophila melanogaster* in 99B7 (nucleotides: 25430764-25555351) (Figure 3.1 A). A 4281 bp cDNA encodes a protein of 1381 amino acid residues (M_r 158 kDa, pI 5.67). The gene consists of 5 small introns and 6 exons (Figure 3.1 B). Searching the PROSITE protein motif library, some putative motifs were detected on CAP-D2 protein such as N-glycosylation sites, cAMP- and cGMP- dependent protein kinase C phosphorylation sites, caseine kinase II phosphorylation sites, tyrosine kinase phosphorylation sites, a bipartite nuclear targeting sequence (1347-1363 aa, Figure 3.1 B) and several other sites. A SMART search gave a coiled-coil region (intimately associated regions of long alpha helices) by using the method of Lupas *et al* (Lupas et al., 1991) and several regions with low residue complexity by using Wootton's and Federhen's method. These sites could be useful for indicating putative molecular functions of CAP-D2 protein. Neuwald and Hirano (Neuwald and Hirano, 2000) found that *Xenopus* CAP-D2 protein contains HEAT repeats (tandemly arranged bihelical structures that appear to function as flexible joints

A)

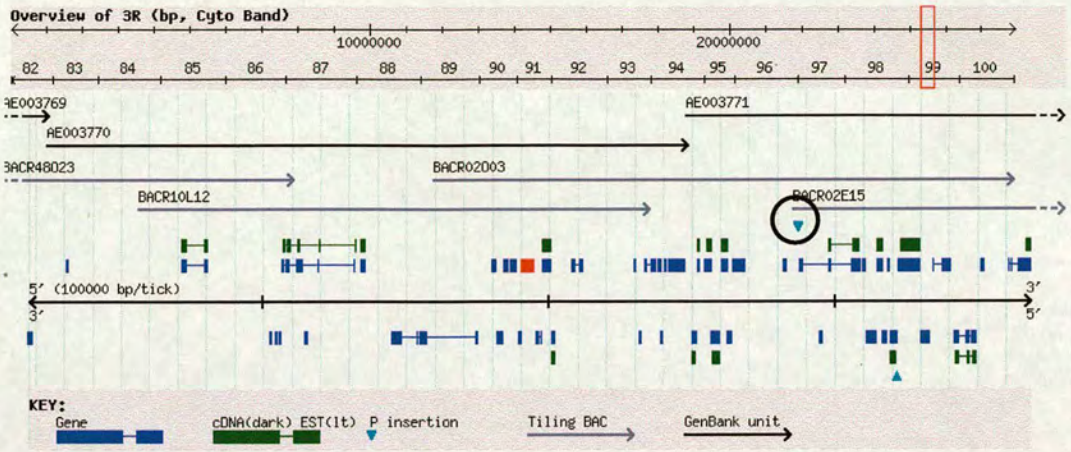

B)

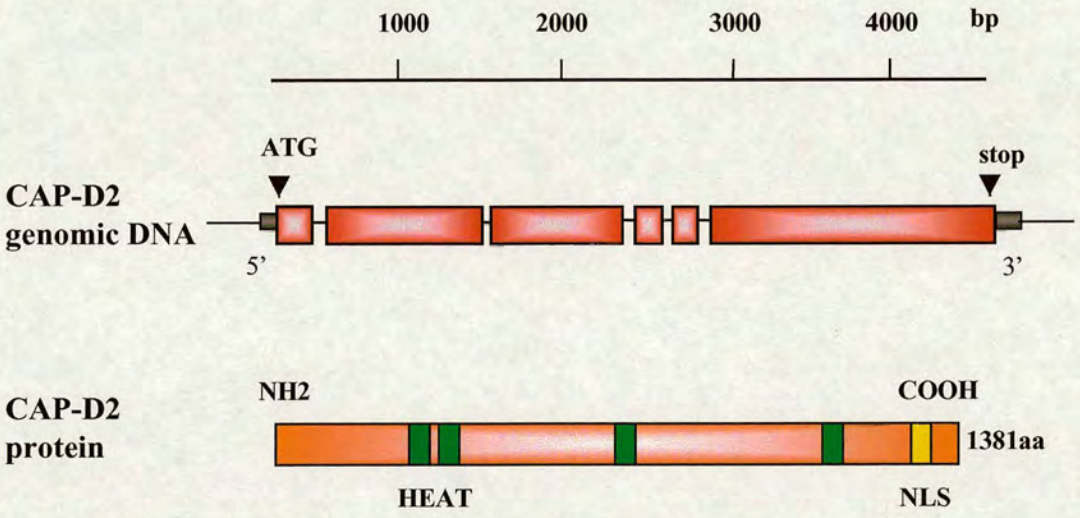

Figure 3.1. A. Overview of the right arm of the third chromosome. The CAP-D2 gene (red square) is located in 99B7 chromosome locus (nucleotides: 25430764-25555351). A P-element has been reported recently, which locates about 100,000 bp away from the CAP-D2 gene (indicated by an arrowhead). The map was adapted from Flybase.
B. The CAP-D2 gene consists of 5 small introns and 6 exons. A 4281 bp cDNA encodes a protein of 1381 amino acid residues. The four HEAT repeats (green boxes, 362-398aa, 402-438aa, 652-688aa and 1050-1068aa) and the nuclear bipartite signal (yellow box, 1347-1363aa) are indicated on the protein sequence.

that can wrap around target substrates and act as scaffolding on which other molecular components may assemble) by using iterative search and Gibbs sampling alignment procedures. A simple search was attempted for DmCAP-D2, which resulted in the finding of four HEAT repeats and seven ARM repeats (Armadillo repeats) (Figure 3.1 B). ARM and HEAT repeats are considered to be evolutionarily related and to share a common phylogenetic origin even though they have diverged significantly (Andrade et al., 2001). However, there is no experimental evidence for the function of these repeats.

Antibodies that recognise individual subunits of the condensin complex are necessary for the localisation and characterisation of this complex during the cell cycle. As already mentioned, polyclonal antibodies against SMC2, SMC4, Barren (CAP-H homologue), CAP-G and CAP-D2 were available. The SMC4, SMC2 and CAP-G antibodies were already characterised by Soren Steffensen (Steffensen, 2001; Steffensen et al., 2001) and Neville Cobbe (Cobbe, 2003), while the Barren antibody was characterised by Bhat *et al* (Bhat et al., 1996). My work includes the characterisation of the CAP-D2 antibody. The antibody was raised against the C-terminal 211 aa of the CAP-D2 protein (951-1162 aa) (Figure 3.2 A). This fragment was cloned into a pQE30 vector and tagged with 6 histidine residues in the N-terminus to enable purification by Ni-affinity chromatography (QIA*express*, Qiagen). The protein fragment, with a molecular weight of approximately 26 kDa, was expressed in a QIAexpress system and excised from SDS-PAGE gel. This purified fragment was then used to immunise two rabbits (R797 and R796) each producing 3 bleeds after three injections. As mentioned previously, the generation of the antibody was done by Dr M. Heck and S. Steffensen, however the characterisation of the antibody by Western immunoblotting and indirect immunofluorescence was performed by me.

3.2.2. Immunoblotting with the CAP-D2 antibody

Optimisation of the western blotting conditions for this antibody was necessary. For this purpose, *Drosophila* cultured cell (S2 or Dmel2 cells) extract was analysed by immunoblotting with the CAP-D2 antibody. Different blocking agents, antibody dilutions and incubation conditions were attempted with the best results obtained when

the membrane was blocked with 5% milk and incubated with the CAP-D2 antibody in a dilution of 1:10,000. All incubations were performed for 1 hour at room temperature in PBS-Tween solution. All three bleeds of the CAP-D2 immunised sera were tested and a prominent band of about 137 kDa was detected. Pre-immune serum of the rabbit that was immunised against the CAP-D2 protein was available and used as a control in the western blot in different dilutions. None of the pre-immune dilutions could detect the 137 kDa band indicating that the CAP-D2 antibody specifically detects this protein (Figure 3.2 B). The difference between the predicted (158 kDa) and the detected 137 kDa band of CAP-D2 protein could be due to the electrophoresis conditions, to the precision of the molecular weight marker or to post-translational modifications. The results that are shown in Figure 3.2(B) are from one of the two rabbits (R797) that were immunised against the CAP-D2 protein. The serum of the second rabbit (R796) could detect the 137 kDa band, but the signal was fainter (data not shown). Finally the CAP-D2 antibody could detect the protein from as few as of 4×10^4 cells (Figure 3.2 D).

3.2.3. Protein Expression and Purification of CAP-D2

In order to confirm that the antibody was specifically detecting the CAP-D2 protein, immunoblot analysis was performed against the protein fragment that was used to generate the antibody. The protein fragment was expressed in bacteria by using the IPTG inducible QIA*express* system (using the pQE30 vector), which is repressed without induction. The expressed fragment was recovered in inclusion bodies (insoluble aggregates containing the protein), that were solubilised under denaturing conditions and purified by Ni-affinity chromatography through its 6-His tag (QIA*express*, Qiagen). An expression level of ~ 0.4 g/L of the protein was obtained. Different combinations of IPTG concentrations and induction periods were attempted in order to increase the yield, unfortunately with no success. The quantitation of the protein was performed by comparing amounts of the CAP-D2 protein with specific amounts of purified BSA protein (0.1-50 µg/µl) on an SDS-PAGE gel after staining with Coomasie blue. Immunoblot analysis against the purified CAP-D2 protein and against cell extract from the induced and uninduced cultures revealed a prominent band at the predicted size

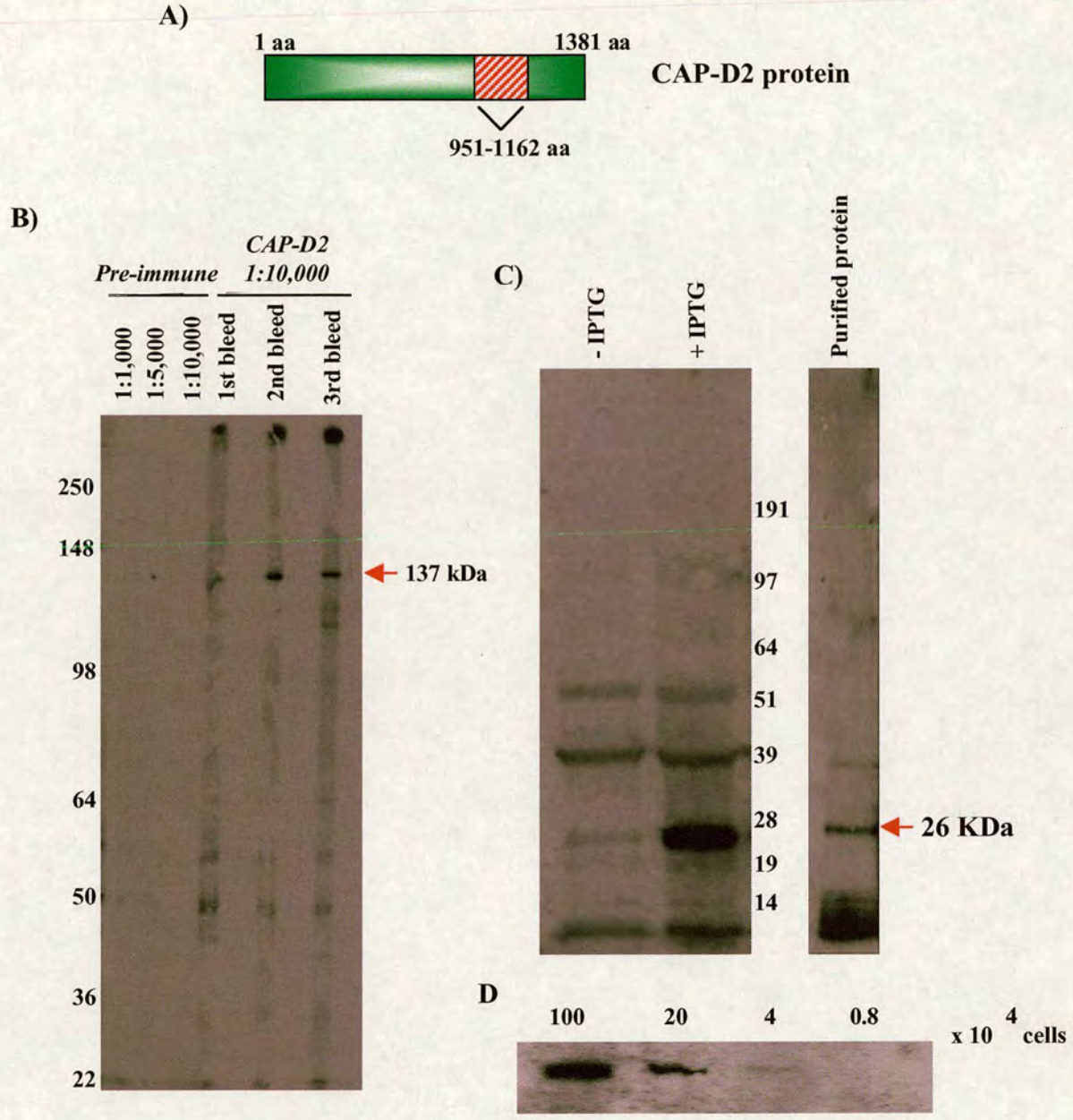

Figure 3.2. A. Schematic representation of the CAP-D2 protein region that was used for the generation of the CAP-D2 antibody. 951 to 1162 amino acid residues were used (indicated by red diagonal lines).

B. Immunoblot analysis of Dmel2 cell extract (8.5x 10^6 cells/gel) by using three different serum bleeds immunised against CAP-D2 protein fraction, in 1:10,000 dilution. The serum recognises a prominent band of 137 kDa which corresponds to CAP-D2 protein. Available preimmune serum from the same animal was tested in different dilutions (1:1000, 1:5000, 1:10000) but no band of the expected size was detected.

C. Western blot analysis against the purified CAP-D2 protein and against cell extract from the induced (+IPTG) and uninduced (-IPTG) cultures by using the CAP-D2 antibody. A prominent band of about the estimated size (~ 26 Kda) was detected in the induced culture and in the purified protein fraction. This band was almost undetectable in the uninduced culture.

D. Titration of the number of S2 cells, in which the CAP-D2 antibody can detect the CAP-D2 protein. The antibody could detect the protein from as few as of $4x10^4$ of cells, in a dilution of 1:10,000 .

(~ 26 kDa) in both the induced and purified protein fractions (Figure 3.2 C). This suggested that the antibody could detect the protein specifically but further characterisation was still necessary (i.e. immunofluorescence). From the immunoblot it was evident that the protein was expressed after induction with IPTG but the purification yield was low suggesting that a different purification protocol should be used. One possibility is to use β-mercaptoethanol in the Denaturing buffer, thereby reducing disulfide bonds. The existence of disulfide bonds between the polypeptide chains might be the cause of the formation of inclusion bodies. The expression and purification of the fusion protein could also be useful for affinity purifying the CAP-D2 antibody but higher yield of the protein purification should be obtained first. Nevertheless, affinity purification of the antibody was not necessary for analysis by immunoblotting or immunofluorescence (see 3.2.4) since the background staining caused by the antibody was very low.

3.2.4. Immunolocalisation of CAP-D2

The subcellular localisation of the CAP-D2 protein during the cell cycle could be very important for understanding the protein's function. This was analysed by indirect immunofluoresence. The most successful chromosomal staining was obtained in cultured cells that had been centrifuged onto poly-L-lysine slides (cytospin), thereby adhering and flattening the cells and making the chromosomal epitopes more accessible. To examine the localisation of CAP-D2 during mitosis, S2 cultured cells (*Drosophila* embryonic cells) were cytospun onto poly-L-lysine slides and stained for CAP-D2, phosphorylated histone 3 (P~H3) and DNA. In prophase, during early stages of chromosome condensation, the CAP-D2 protein accumulated in the condensing chromatin. In prometaphase, the protein showed a localisation along the condensed chromosome arms, with more intense labeling of the centromeric regions (Figure 3.3 A). That was confirmed by using CID (centromere identifier) as a marker. CID is the *Drosophila* homolog of CENP-A, a variant of histone H3, which localises exclusively to centromeres and plays a key role in assembling the kinetochore during mitosis (Henikoff, 2000). The

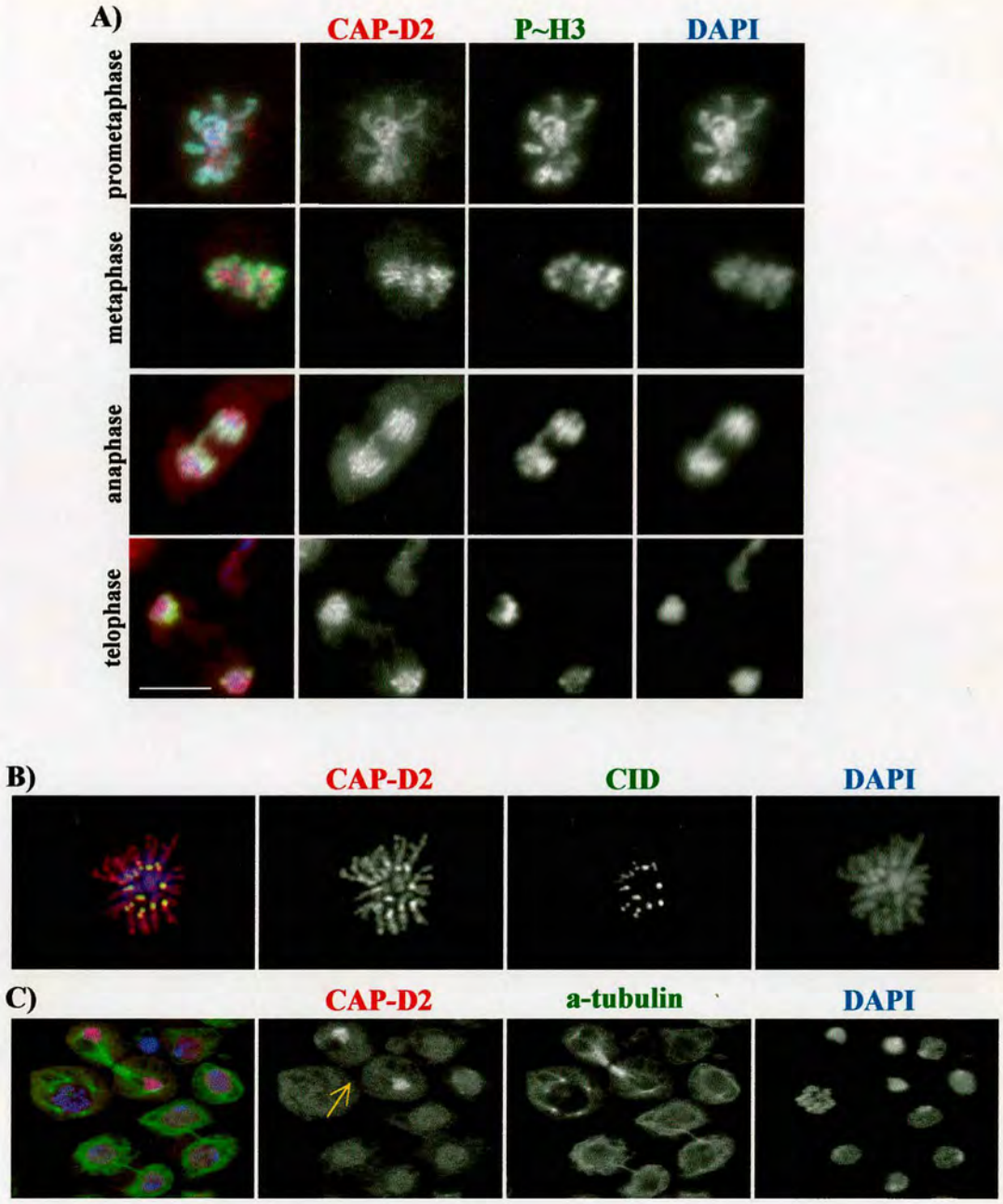

Figure 3.3. Characterisation of CAP-D2 during mitosis.
A. CAP-D2 localises to a central axis in chromatids and shows accumulation at the centromeres from prometaphase until telophase. P~H3 was used as a mitotic marker. During late anaphase and telophase, where chromosomes decondense, CAP-D2 still associates with chromosomes. CAP-D2 (red), P~H3 (green), and DNA (blue).
B. Accumulation of CAP-D2 at centromeres during metaphase. CID was used as a centromere marker. CAP-D2 (red), CID (green), and DNA (blue).
C. CAP-D2 is still strong in the daughter nuclei of a cell undergoing cytokinesis (arrow). CAP-D2 (red), α-tubulin (green), and DNA (blue).
The scale bar represents 10μm.

accumulation of CAP-D2 at centromeres can be clearly observed in both the merged and CAP-D2 image of a cell stained with CID and CAP-D2 (Figure 3.3 B). In metaphase and early anaphase when chromosomes are fully condensed, the labeling was more intense throughout the core of the chromatids. During telophase CAP-D2 protein was still tightly associated to chromosomes, even as chromosomes start to decondense (Figure 3.3 A). The nuclear staining for CAP-D2 protein was still intense during late telophase but it was decreased during cytokinesis. The two phases could be partially distinguished by using an antibody against α-tubulin, since α-tubulin is present at the midbody (Figure 3.3 C). During cytokinesis the midbody is thinner than in telophase so these two phases can be partially distinguished. These results suggest that CAP-D2 associates with chromosomes in prophase, distributes axially on the chromosome arms with enrichment at the centromeres during prometaphase, is present throughout anaphase and telophase and even remains tightly associated with chromosomes as they start to decondense.

Immunofluorescence revealed that CAP-D2 is mainly nuclear and present at different levels during interphase. Therefore several markers were utilized to further characterise the levels of the protein during interphase (Figure 3.4). An antibody to γ-tubulin, a centrosomal component, was used to denote cells that were in G1 phase, prior to centrosome duplication. G1 cells (single centrosome) showed the level of CAP-D2 in the cytoplasm to be almost as high as in the nucleus (Figure 3.4 A, top). Cells with 2 centrosomes (in S or G2 phase) (Loupart et al., 2000) had much higher levels of nuclear CAP-D2 (Figure 3.4 A, bottom). For the discrimination of S phase, BrdU, a thymidine analog was used. BrdU (Bromo-deoxyuridine) is incorporated into DNA in place of dTTP during DNA replication (S phase). Cells positive for BrdU showed nuclear staining of CAP-D2 (Figure 3.4 B). While the intensity of the CAP-D2 signal varied among BrdU positive cells (compare 3.4 B, top and bottom), analysis of replication patterns with 2 thymidine analogues (Chloro-deoxyuridine and Iodo-deoxyuridine) (Manders et al., 1992) demonstrated that the nuclear level of CAP-D2 increased as cells progressed through S phase (demonstrated by Dr M-L Loupart, data not shown). Cyclin B was used to identify cells that were in late G2/early prophase. Cyclin B forms a

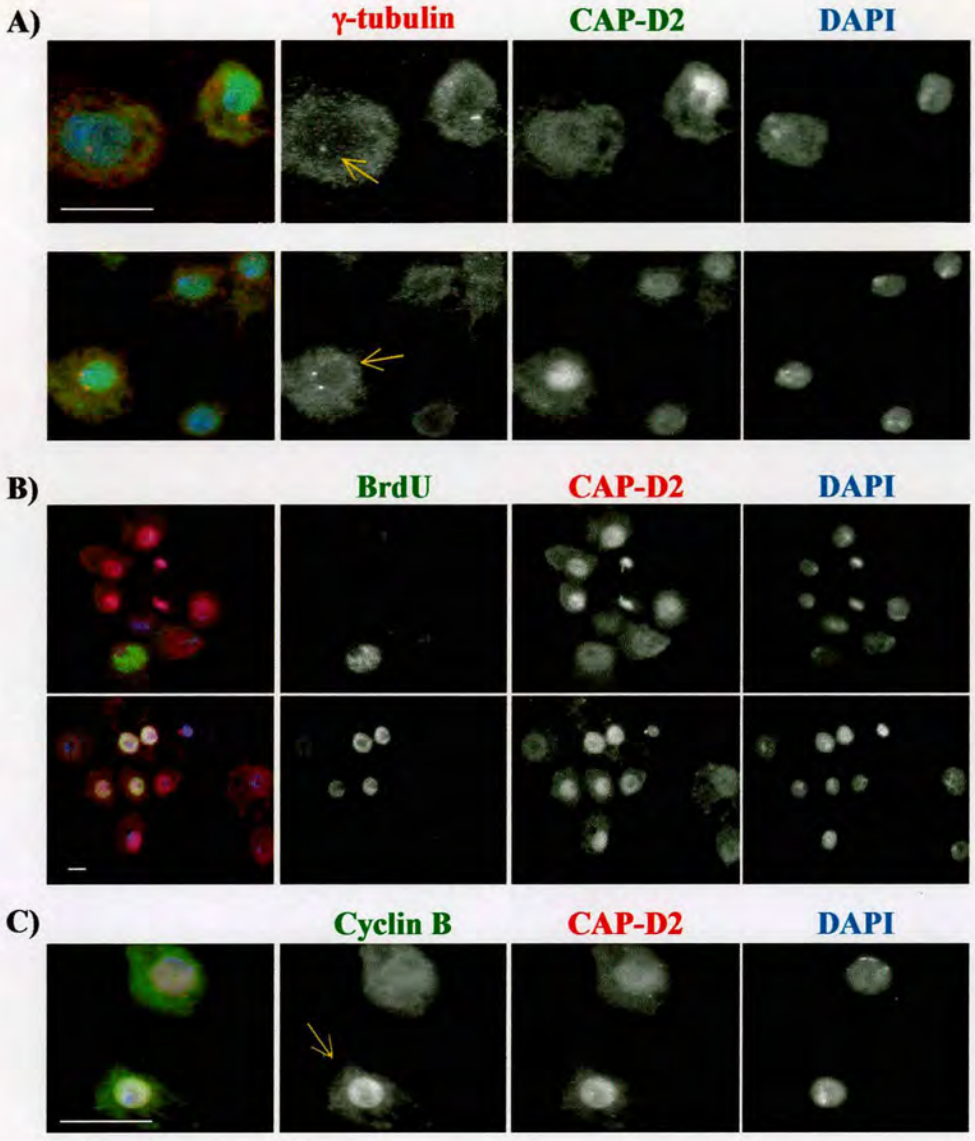

Figure 3.4. CAP-D2 localisation during interphase.
S2 cultured cells were cytospun onto poly-L-lysine slides, then fixed and stained with various antibodies as described.
A. CAP-D2 localises in the nucleus during interphase. G1 cells (using γ-tubulin as a marker) show nuclear staining for CAP-D2 with a diffuse cytoplasmic staining. Cells in G1 phase (single centrosome, arrow in upper panel) have less nuclear CAP-D2 than cells with two centrosomes (cells in S or G2 phase, arrow in lower panel). γ-tubulin (red), CAP-D2 (green), and DNA (blue).
B. S phase cells (detected after BrdU incorporation) show strong nuclear staining for CAP-D2, but at differing levels. BrdU (green), CAP-D2 (red), and DNA (blue).
C. Cells in late G2/early prophase (arrow) show an intense staining for CAP-D2. Cyclin B (nuclear during late G2/early prophase) was used as a marker for this stage. Cyclin B (green), CAP-D2 (red), and DNA (blue).
The scale bar represents 10μm.

complex with Cdk1 kinase, which considers to be one of the major mitotic kinases. This protein complex moves from the cytoplasm into the nucleus at late G2/early prophase, associates with condensed chromosomes during prophase and prometaphase and subsequently associates with the mitotic spindle during metaphase (Huang and Raff, 1999; Raff et al., 2002). Cells that had nuclear Cyclin B showed an intense nuclear staining for CAP-D2 (Figure 3.4 C). Taken together, these results suggest that *Drosophila* CAP-D2 is nuclear during interphase, with low levels in G1 that increase during S and are highest in late G2/early prophase. Bearing in mind that the major fraction of *Drosophila* SMC4 and Barren is mainly cytoplasmic during telophase and interphase (Steffensen et al., 2001), it could be suggested that CAP-D2 is responsible for a function other than mitotic chromosome condensation during interphase or may be sequestered away from SMCs to regulate activity of the condensin complex.

3.2.5. Localisation of CAP-D2 in third instar larval brains and early Drosophila embryos

As described above for S2 cells, CAP-D2 associates with chromosomes in prophase, distributes axially on the chromosome arms during prometaphase, is present throughout anaphase and telophase and even remains tightly associated with chromosomes as they start to decondense. To observe if a similar localisation occurs *in vivo*, third instar larval brains and syncytial embryos were stained for CAP-D2 and P~H3. The CAP-D2 antibody did not work very well in either the larval brains or the syncytial embryos and thus different conditions needed to be tested in order to obtain good staining. Even with different conditions, the quality of the results was not as good as in tissue culture cells.

In third instar larval brains, CAP-D2 localised on condensed chromosomes during prometaphase and metaphase and even remained tightly associated on chromosomes as they decondensed during anaphase and telophase. The protein was still present on chromatin during late telophase and cytokinesis (Figure 3.5 A). Interphase cells showed mainly nuclear staining of CAP-D2 with some protein localised in the cytoplasm (Figure 3.5 B). In early syncytial embryos, CAP-D2 showed a slightly different pattern of

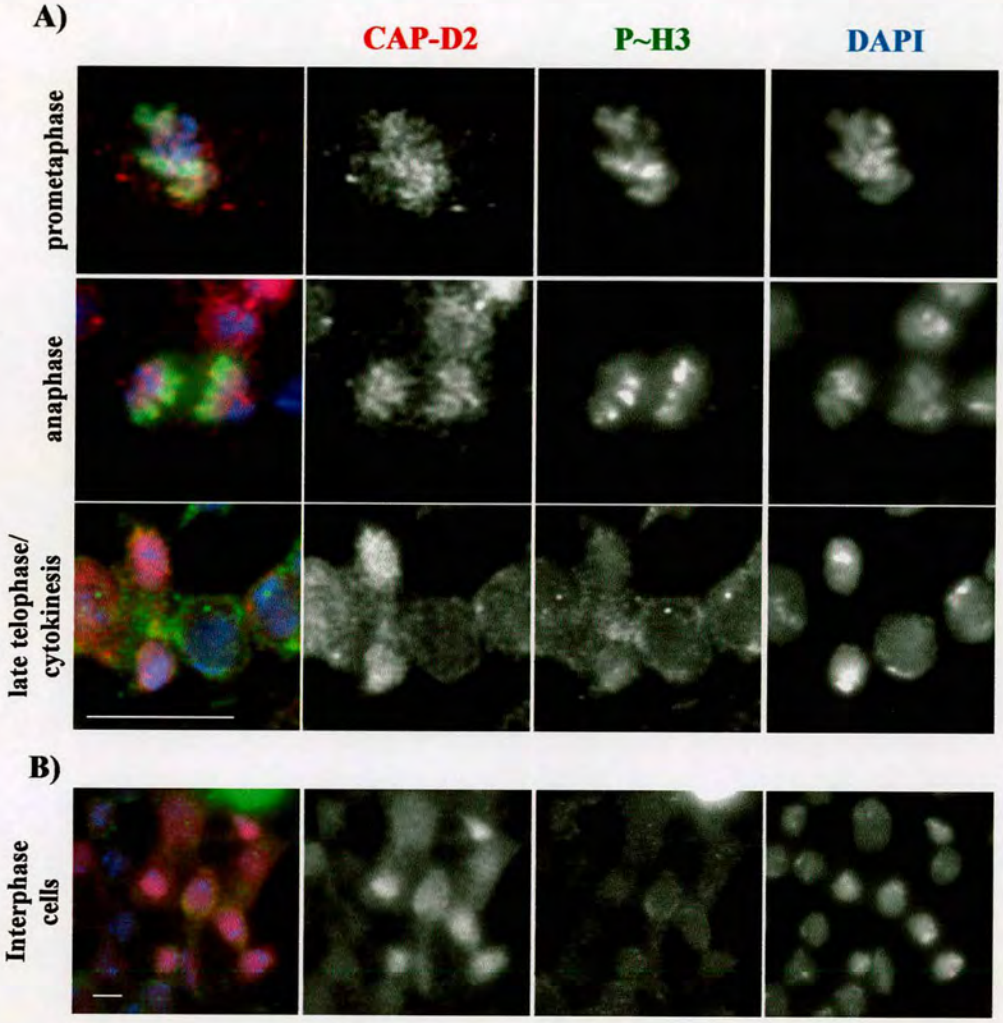

Figure 3.5. CAP-D2 localisation in third instar larval brains.
Brain squashes were performed according to "Antibody staining of larval brains" protocol and stained for CAP-D2 (red), P~H3 (green) and DAPI (blue).
A. CAP-D2 localised along the chromatids during prometaphase and remained tightly associated with chromosomes as they decondense during anaphase and late telophase/cytokinesis.
B. Interphase cells showed mainly nuclear staining of CAP-D2, while some protein localises in the cytoplasm.
The scale bar represents 10μm.

localisation. In very early embryogenesis (syncytial embryo), CAP-D2 was dispersed in the nucleus and not restricted to chromosomes during mitosis. This pattern of localisation was more obvious during prophase/prometaphase (Figure 3.6 A). The abundance of CAP-D2 in the nucleus during this stage could be a consequence of the maternal contribution to early embryos or possibly CAP-D2 is required for another function beyond the condensin complex during this developmental stage. In later stages of embryogenesis, CAP-D2 was mainly restricted on condensed chromosomes from prometaphase to metaphase and remained tightly associated with chromosomes as they began to decondense during anaphase (Figure 3.6 B). Finally CAP-D2 was found to dissociate from chromosomes during late telophase. No signal could be detected on chromosomes with the pre-immune serum (Figure 3.6 C). Taking these results into consideration, it seems that CAP-D2 has similar localisation patterns both *in vivo* and *in vitro*, with the exception of early stages of embryogenesis. Beyond this exception, the protein associates with chromosomes in early stages of mitosis and even remains tightly associated with chromosomes as they decondense during anaphase and telophase.

3.2.6. Developmental expression of CAP-D2

To determine the developmental expression pattern of CAP-D2 an immunoblot analysis was performed against total extracts from syncytial embryos (0-4 hours after egg deposition), cellularised embryos (4-24 hours after egg deposition), first-, second- and third instar larvae, early and late pupae, male and female adults, by using the CAP-D2 antibody. This analysis showed that CAP-D2 is present throughout development with high amounts of protein in embryos and female adults (Figure 3.7 A, the amount of protein loaded in female flies lane is 2-3 fold less compared to the rest, according to α-tubulin loading control. Thus, the amount of CAP-D2 protein should be considered to be at least 2-3 fold more from what is shown). This distribution is consistent with the level of cell proliferation in these tissues: embryos are mitotically active while female flies are meiotically active and contain a stockpile of proteins in their eggs used in early stages of embryogenesis. Thus CAP-D2 is needed in high amounts in tissues that are mitotically or meiotically active.

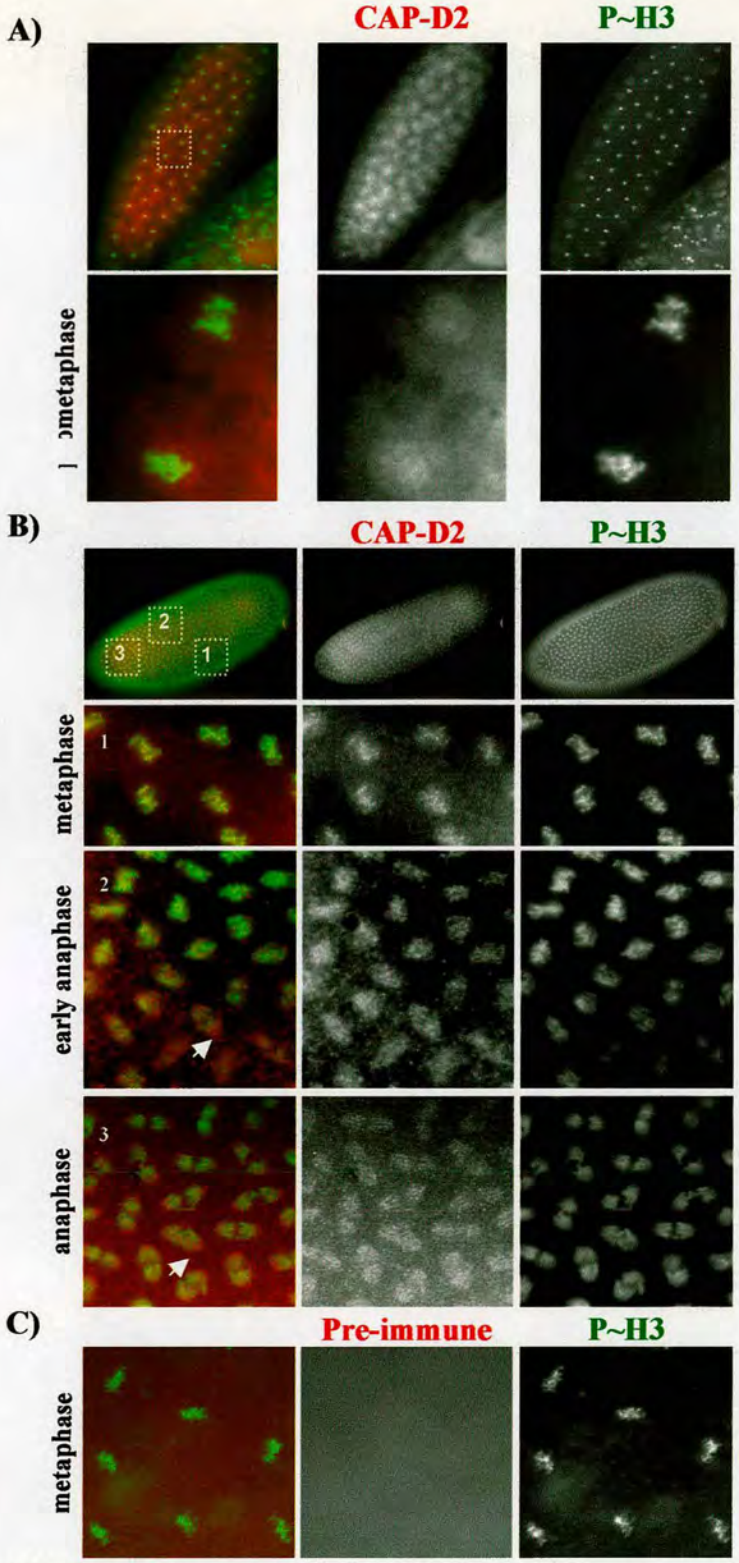

Figure 3.6. CAP-D2 localisation in syncytial *Drosophila* embryos. Embryos were prepared as described in materials and methods and stained for CAP-D2 (red) and P~H3 (green). **A.** Early stage syncytial embryo. CAP-D2 was dispersed in the nucleus and was not restricted onto chromosomes during mitosis. This pattern of localisation was more obvious during prophase/prometaphase. The bottom panel is a higher magnification (100x) of an area from the top panel (40x) indicated by a box. **B.** Late stage syncytial embryo. CAP-D2 was mainly restricted on condensed chromosomes from prometaphase to metaphase and even remained tightly associated with chromosomes as they start to decondense during anaphase (arrow). The three bottom panels are higher magnifications (100x) of different areas from the top panel (40x) indicated by a box and a number. **C.** The pre-immune serum could not detect any specific signal on syncytial embryos.

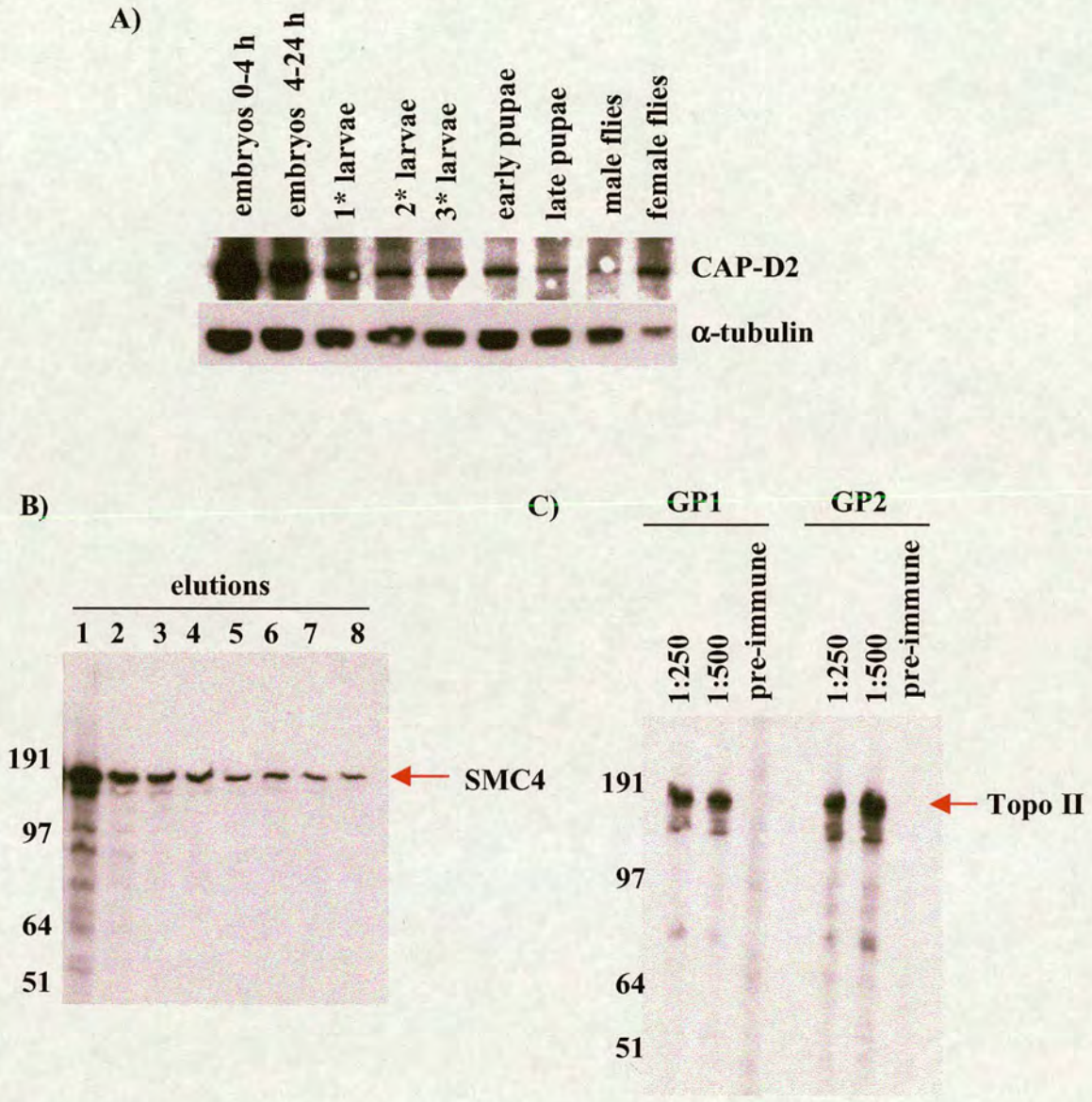

Figure 3.7. A. Immunoblot analysis against protein extracts from different *Drosophila* developmental stages by using the CAP-D2 antibody. CAP-D2 is present throughout development with high amounts of protein in embryos and female adults. α-tubulin was used as a loading control.

B. Immunoblot analysis against S2 cell extract ($125x10^5$ cell/gel) by using the elution fractions (8 sequential elutions performed with 100 mM glycine pH 2.5) of the affinity purified SMC4 antibody . All the elution fractions (1-8) were recognising a band of the right size (160 kDa), which corresponds to the SMC4 protein. The background bands could possibly be degradation products of SMC4 protein.

C. Immunoblot analysis of S2 cell extract ($5x\ 10^5$ cells/lane) by using two different Topoisomerase II antibodies raised in guinea pig (GP1 and GP2). Two different dilutions were used (1:250 and 1:500) and both antibodies recognised a prominent band of the right size (170 kDa), which corresponds to Topoisomerase II. Available pre-immune serum from the two guinea pigs was tested in a dilution of 1:250 but no band of the expected size was detected.

3.3. Co-immunolocalisation of CAP-D2 and SMC4

Drosophila SMC4 and Barren have been shown to associate with chromosomes during prophase and to dissociate during anaphase as chromosomes start to decondense. Also the major fraction of these proteins is mainly cytoplasmic during telophase and interphase (Steffensen et al., 2001). This localisation is different from what has been described above for CAP-D2. In order to assess if that is the case, co-immunolocalisation studies were performed with the CAP-D2 (raised in rabbit) and SMC4 (raised in sheep) antibodies. The co-localisation of Barren or SMC2 with CAP-D2 was not possible since all antibodies were raised in rabbits. To observe the localisation of these proteins during mitosis, S2 tissue culture cells were cytospun onto poly-L-lysine slides, extracted during fixation and stained for CAP-D2, SMC4 and DAPI. The two condensin subunits were found to co-localise to the chromosome axes during prometaphase and metaphase. Nevertheless, some parts of the chromosomes were more strongly labelled with CAP-D2 i.e. centromeres, while SMC4 was less restricted to the chromosomes axes compared to CAP-D2. During anaphase, as chromosomes decondensed, SMC4 dissociated from chromosomes with a fainter signal near the centromeric regions and quite high at the end of chromosome arms. In contrast CAP-D2 was still present throughout the chromatids (Figure 3.8 A). The differences in the localisation between the two proteins could be due to the quality of the antibodies, since both of them are members of the same complex and they are expected to dissociate from chromosomes at the same time. Nevertheless, the distinct timing of dissociation of the different condensin subunits could be due to a CAP-D2 function performed beyond that required of condensin, or to regulate activity of condensin complex. Evidence for this comes from human cells where it has been shown that the C terminal-end of CAP-D2 possesses a mitotic chromosome-targeting domain that does not require the other condensin subunits (Ball et al., 2002). It is possible that a similar regulation occurs in *Drosophila* and that CAP-D2 binds independently of the other subunits to chromosomes.

To observe the co-localisation of these two subunits during interphase two different approaches were followed. In the first approach S2 cells were treated as described above, while in the second S2 cells were cytospun onto poly-L-lysine slides,

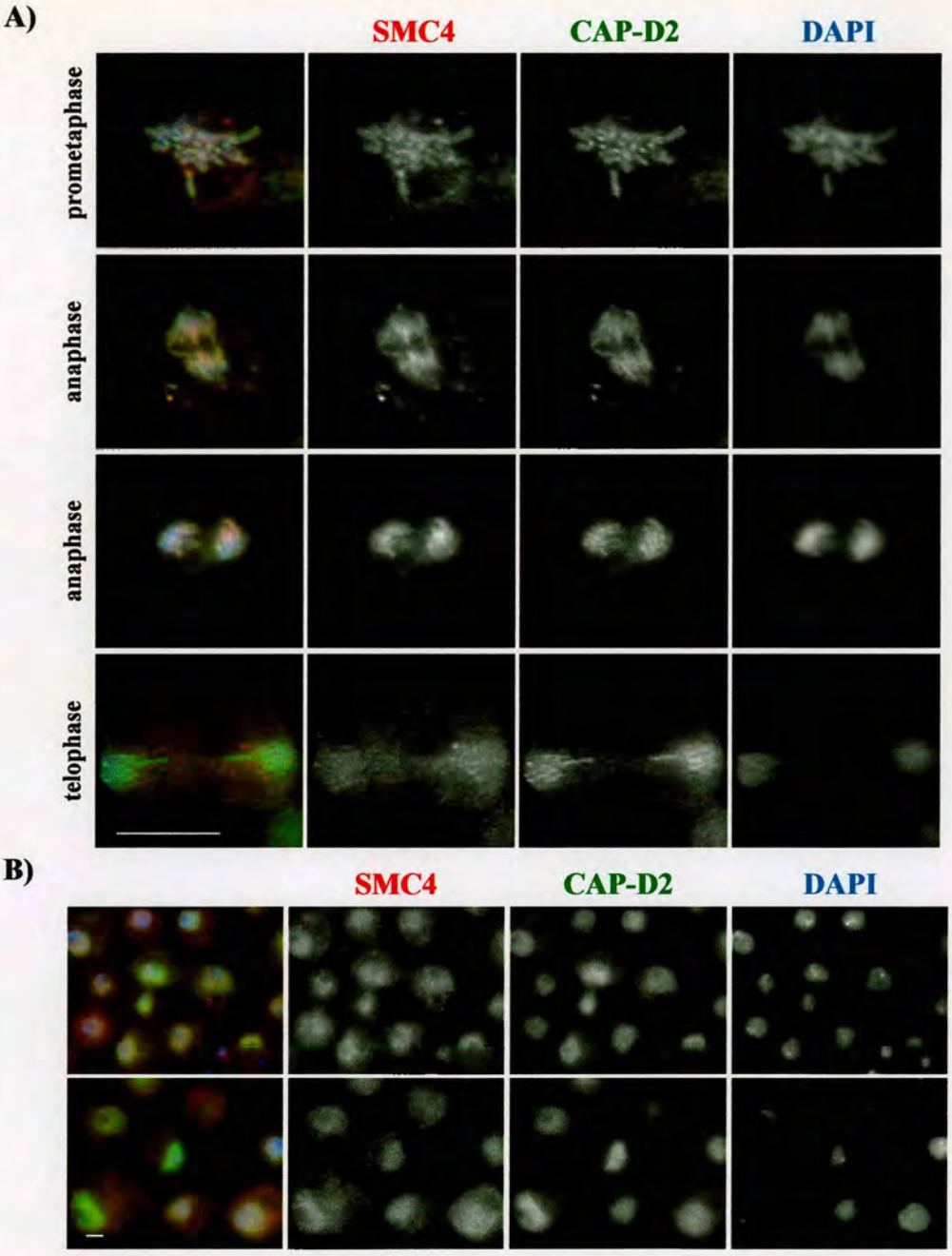

Figure 3.8. A. Co-immunolocalisation of CAP-D2 and SMC4 during mitosis. Cells were cytospun onto poly-L-lysine slides, extracted during fixation and stained for CAP-D2 (green), SMC4 (red) and DAPI (blue). The two proteins co-localise at the chromosome axes during prometaphase. SMC4 comes off the chromosomes as they start to decondense during anaphase, while CAP-D2 persists throughout the length of the chromosomes. In telophase SMC4 is diffuse in the cytoplasm and the nucleus, while CAP-D2 is still tightly associated to chromosomes. The scale bar is 10 μm. **B.** Co-immunolocalisation of CAP-D2 and SMC4 during interphase. Cells were cytospun onto poly-L-lysine slides, fixed and permeabilised and stained for CAP-D2 (green), SMC4 (red) and DAPI (blue). The two proteins localise mainly in the nucleus. The nuclear levels of CAP-D2 appear higher compared to SMC4, while SMC4 signal is more disperse in the cytoplasm and the nucleus. The scale bar is 10 μm

fixed and then permeabilised in order to maintain the cytoplasmic structure that is lost when cells are extracted during fixation. By both approaches it appeared that SMC4 was mainly nuclear with a high cytoplasmic staining and co-localised with CAP-D2. The only observable difference, was that nuclear levels of CAP-D2 were higher compared to SMC4, while SMC4 signal was more disperse in the cytoplasm and the nucleus (Figure 3.8 B). As already mentioned, it was previously shown that SMC4 is mainly cytoplasmic during interphase (Steffensen et al., 2001). The two different results could be due to the fact that the antibody used in Steffensen et al (Steffensen et al., 2001) was affinity purified. In this case the affinity purified antibody was presumably recognising only specific epitopes, while the non-affinity purified antibody (used in this study), could bind to additional unspecific epitopes. An attempt to affinity purify the antibody was successful by immunoblotting (Figure 3.7 B) but failed by immunofluorescence and thus this issue was not clarified.

3.4. Characterisation of a DNA topoisomerase II (Topo II) antibody and co-immunolocalisation with CAP-D2

Localisation studies revealed that topoisomerase II (Topo II), a major protein of the chromosome scaffold, is distributed axially in the chromosome arms with some concentration at the centromeres, in a manner similar to condensin subunits (Maeshima and Laemmli, 2003; Steffensen et al., 2001). Colocalization and biochemical studies in *Drosophila* indicated that Barren associates and alters the activity of topoisomerase II throughout mitosis (Bhat et al., 1996), while cell extracts from DmSMC4 dsRNA-treated cells show significantly reduced topoisomerase II-dependent DNA decatenation activity *in vitro* (Coelho et al., 2003). Furthermore, yeast mutations in Topo II exhibit segregation defects similar to those observed in condensin mutations (Holm et al., 1985). For this reason, colocalisation and functional (see Chapter 4) studies between Topoisomerase II and CAP-D2 could be informative for the elucidation of the interrelation of these proteins.

In order to be able to perform colocalisation studies between topoisomerase II and CAP-D2, antibodies recognising these proteins that were raised in different animals were

necessary. In collaboration with Soren Steffensen, we were able to raise an antibody against topoisomerase II in guinea pig. Two animals were injected with the topoisomerase II protein [guinea pig 1 (GP1) and guinea pig 2 (GP2)]. Immunoblot analyis against cell extract with the immunised sera revealed that the antibodies could detect specifically a prominent band of the estimated size (~170 kDa) in a dilution of 1:500. This band corresponds to topoisomerase II and was not detected with the pre-immune sera (Figure 3.7 C).

To examine the localisation of topoisomerase II with these antibodies and its colocalisation with CAP-D2, cells were cytospun onto poly-L-lysine slides and stained for topoisomerase II, CAP-D2 and DAPI. The two proteins colocalised at the chromosome axes in prometaphase, metaphase and anaphase and remained tightly associated with chromatin until late telophase (Figure 3.9 A). When metaphase chromosome spreads were performed, after cells were arrested in metaphase with colchicine, individual chromosomes could be observed. From this preparation it was obvious that CAP-D2 and topoisomerase II colocalised along the chromosomes but topoisomerase II was less restricted to the chromosome axes and was less abundant at the centromeres compared to CAP-D2 (Figure 3.9 B). The colocalisation of the two proteins at the chromosome axes may suggest that they collaborate to organize mitotic chromosomes. However, their distinct localisation at the centromeres combined with the fact that topoisomerase II is not strictly restricted to the chromosome axes, may suggest that the two proteins also have distinct roles.

3.5. Biochemical identification of a condensin complex in Drosophila- Immunoprecipitations with the CAP-D2 antibody

Even though a five member condensin complex has been shown to exist in other organisms (Freeman et al., 2000; Hirano et al., 1997; Kimura, 2001; Sutani et al., 1999), no biochemical data exist to support this in *Drosophila*. For this reason, immunoprecipitations with the *Drosophila* CAP-D2 antibody were performed by Sue Cotterill (St. George's University in London), using 0-5 hour embryo extracts. Bound proteins were eluted sequentially with 0.5 M NaCl and 2% SDS in PBS. I analysed the

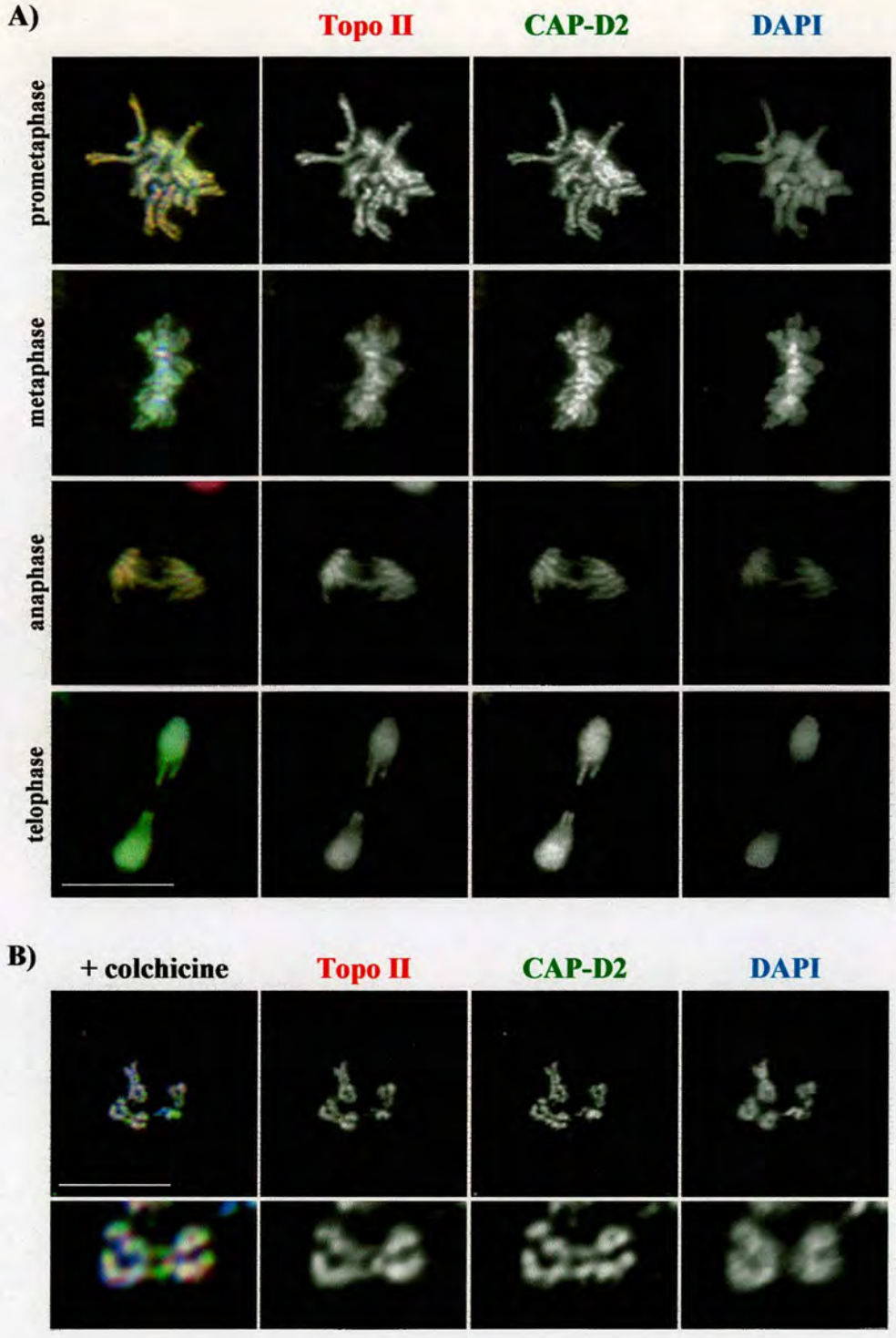

Figure 3.9. Co-immunolocalisation of CAP-D2 and Topoisomerase II. S2 cells were cytospun onto poly-L-lysine slides, extracted during fixation and stained for CAP-D2 (green), Topo II (red) and DAPI (blue).

A. The two proteins colocalised at the chromosome axes in prometaphase, metaphase and anaphase and remained tightly associated to chromatin until late telophase. The scale bar represents 10μm.

B. Metaphase chromosome spreads after cells were treated with colchicine. An individual chromosome is shown in the bottom panel in a higher magnification. The two proteins colocalise partially. Note that Topo II is less restricted to the chromosome axes and is less abundant at the centromeres compared to CAP-D2. The scale bar represents 10μm.

fractions by immunoblotting with SMC2, SMC4, CAP-D2, and CAP-H/Barren antibodies. All four proteins were present suggesting that they participate in the same complex. SMC2 and SMC4 proteins were eluted with both NaCl and SDS solutions, while CAP-D2 and CAP-H were only eluted with the SDS (Figure 3.10). This result suggests two possibilities. First, the CAP-D2 and CAP-H non-SMC subunits may be more tightly associated with each other than they are with the SMC subunits of the condensin complex (a similar observation was made for the cohesin complex (Vass et al., 2003)). Second, the SMCs eluting with NaCl may be participating in another complex, such as the condensin II complex (Ono et al., 2003). As the antibody generated to the CAP-G protein was not working by immunoblotting, the presence of this protein in the complex could not be assessed by immunoblotting.

Additional evidence for a condensin complex came from mass spectrometric analysis This was performed firstly, to confirm that CAP-G protein was a member of the condensin complex, since it could not be identified by immunoblotting, and secondly, to find novel proteins that interact with CAP-D2. The different samples were electrophoresed onto an SDS-PAGE gel and bands were isolated from both the pre-immune and CAP-D2 fractions (Figure 3.10). After these bands were analysed by mass spectrometry all five condensin subunits, including CAP-G, were specifically identified in the CAP-D2 fractions. In addition, some other proteins were identified as possible interactors with CAP-D2. One such protein was ASH1, a Drosophila trithorax group protein, required for methylation of lysine 4 residues on histone H3. Methylation of lysine 4 is believed to activate transcription by relaxing chromatin (Beisel et al., 2002), a process that could also involve members of the condensin complex (PEV analysis, Neville Cobbe, personal communication). To confirm this interaction, the elution fractions were analysed by immunoblotting with an antibody against ASH1 protein. Unfortunately, no band could be detected in the CAP-D2 elution fractions suggesting that no interaction exists between the two proteins. The rest of the proteins that were identified as possible interactors of CAP-D2 were considered contaminants (such as heat-shock proteins, etc). For this reason a different approach was followed in order to

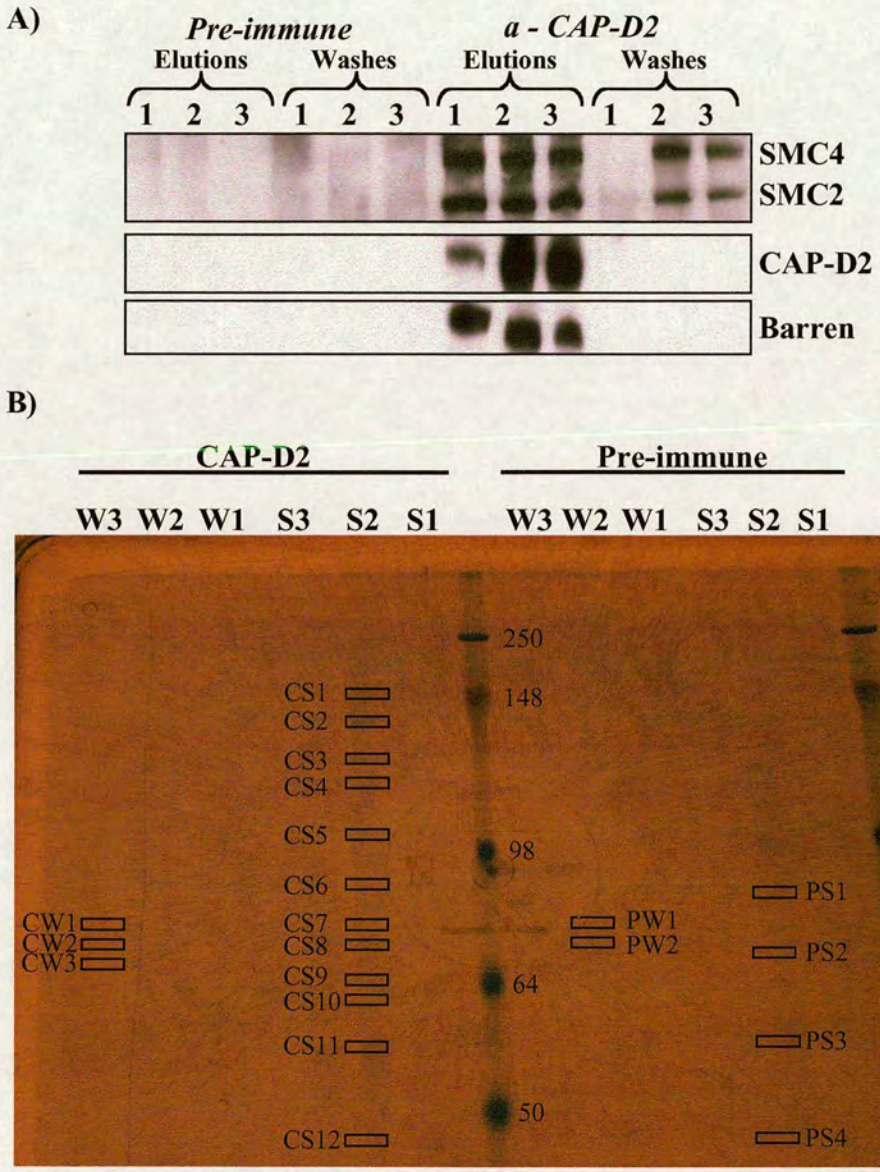

Figure 3.10. Identification of a condensin complex in 0-5 hr embryo extracts following immunoprecipitation with an antibody recognizing *Drosophila* CAP-D2. Three 0.5M NaCl washes and three 2% SDS elutions are shown for preimmune and immune precipitations.

A. The samples were analysed by immunoblotting with SMC2, SMC4 and CAP-H/Barren antibodies. A fraction of SMC2 and SMC4 eluted already in the washes, but more so with the elutions, while CAP-H/Barren appeared more tightly bound to one another as they only eluted with 2% SDS.

B. The immunoprecipitation samples were electrophoresed on a 7.5% poly-acrylamide gel and stained with *BlueCode* Coomasie. Bands, indicated by boxes, from both the pre-immune and CAP-D2 fractions were isolated and sent for mass spectrometry. CAP-G was identified in the CS8 band, CAP-D2 in CS2, Barren in CS7 and SMC2 in CS3. SMC4 was identified in another preparation.

identify novel interactors of CAP-D2 protein. The immunoprecipitation fractions were analysed by immunoblotting, by using antibodies against known proteins that are involved in the cell cycle and chromatin organization. Such proteins were INCENP (chromosomal passenger), PCNA (DNA replication), Tis2 (a centromeric protein currently being characterized in the lab), ORC-2 and-3 (origin recognition complex), CP190 (centrosomal protein), centrosomin (CNN), HP1 (heterochromatin protein), Bub3 (mitotic checkpoint protein), BubR1 (mitotic checkpoint protein), Cyclin B, Prod (PROliferation Disrupter, heterochromatin binding), CID (centromere identifier), ZW10 (mitotic spindle checkpoint), BEAF-32 (DNA binding) and topoisomerase II. Unfortunately, none of these proteins was found by immunoblotting to interact with CAP-D2 immunoprecipitations.

In order to identify novel proteins that interact with CAP-D2, immunoprecipitations were repeated by following another procedure (as my supervision of honours student). Immunoprecipitations were performed by using magnetic Dynabeads thereby avoiding undesirable contaminants that may precipitate with the Sepharose beads during centrifugation. 0-4 hour embryo extracts were used and bound proteins were eluted sequentially with 0.25 M NaCl, 0.5 M NaCl and 2% SDS in PBS. In order to confirm that the immunoprecipitations were successful, an immunoblot analysis was performed on the eluates with CAP-D2, SMC2, SMC4 and Barren antibodies. All four proteins were present in the CAP-D2 fractions, suggesting that the immunoprecipitations were successful (Figure 3.11 A).

In the next step, the different eluates were electrophoresed onto an SDS gel and bands were excised from both the pre-immune and CAP-D2 fractions (Figure 3.11 B and C). These bands were analysed by mass spectrometry and several proteins were identified as possible interactors with the CAP-D2 protein. For each band, a list of 25 putative interactors was obtained after blasting the resulting peptides against the *Drosophila* database. Each resulting protein had a MOWSE score, a number that indicates how likely the identified protein is to be "real". The function of these proteins was found by using the *Drosophila* Genome Database (www.flybase.net). Proteins that were absent from the pre-immune fractions were selected and finally categorized into

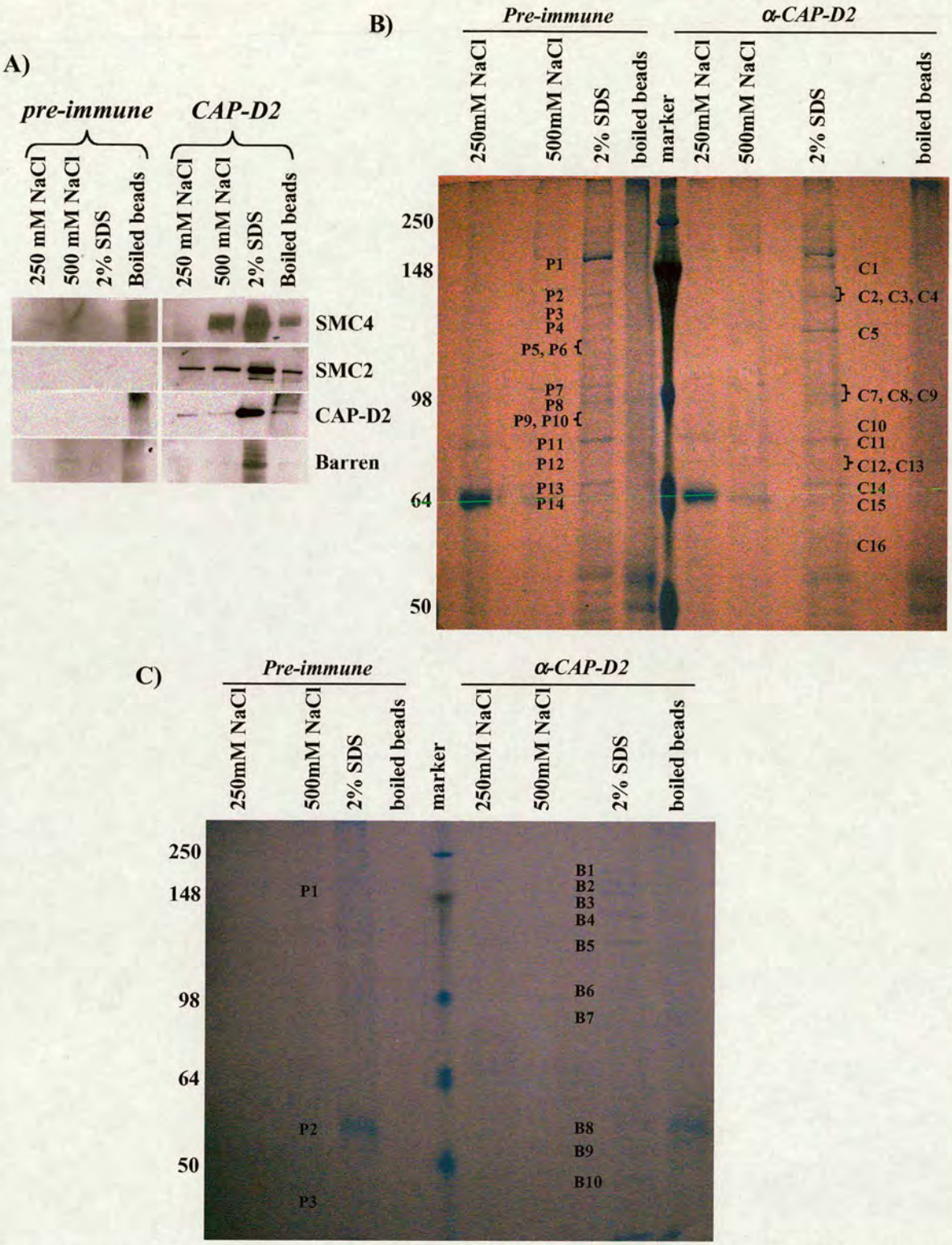

Figure 3.11. Identification of possible CAP-D2 interactors in 0-4 hr embryo extracts following immunoprecipitation with an antibody recognizing *Drosophila* CAP-D2. 0.25M NaCl, 0.5M NaCl washes, 2% SDS elution and elution after boiling the beads in 1X sample buffer are shown for preimmune and immune precipitations.

A. The samples were analysed by immunoblotting with SMC2, SMC4 and CAP-H/Barren antibodies. All four proteins were present at the elution fractions of immune precipitation.

B and C. The immunoprecipitation samples were electrophoresed on a 7.5% poly-acrylamide gel and stained with *BlueCode* Coomassie. Bands, indicated by numbers, from both the pre-immune and CAP-D2 fractions were isolated and sent for mass spectrometry. (B) and (C) represent two independent immunoprecipitation experiments.

different groups by using several criteria. The first group contained proteins that were involved in the cell cycle, in mitosis and in cell communication (Table 1) due to the putative role of CAP-D2 in interphase as well as mitosis. Proteins that were involved in cell communication were also selected since CAP-D2 was found to interact with proteins that are involved in cell communication (CG13502 and CG13131) in a *Drosophila* protein-protein interaction database (www.jhubiomed.org/perl/flynet.pl). These interactions were detected experimentally or mapped cross-species from *Saccharomyces cerevisiae* orthologs. The second group contained the four first proteins that had the highest MOWSE score from each band whose function did not fall into the first group (Table 2).

The immunoprecipitation procedure was performed twice (Figure 3.11 B and C) and the two sets of results were compared in order to find proteins that were present in both experiments. These proteins are highlighted in red and likely represent true interactors since they were identified in two independent experiments. However, all 25 proteins that were identified for each band and that were neither present in the pre-immune nor in the two categories mentioned above, could be still true interactors of the CAP-D2 protein. Nevertheless, the possibility for this is low since their MOWSE score was quite low.

The interactions between these proteins and CAP-D2 are preliminary and further experimental data are necessary to show which of these proteins truly interact with CAP-D2. This screen could be a start for a new project.

Protein Name	Band Name	MOWSE Score	Molecular weight/kDa	Molecular Function	Biological process
CG15824	B1	1.6e+006	227.587	Unknown	Putatively involved in cell comunication
CG11371	B4	1.34e+05	110.582	Unknown	Putatively involved in cell comunication
CG31510	B4	9.88e+04	129.29	Putatively involved in cell communication	Unknown
CG9277	B9	1.39e+12	50.148	Structural constituent of cytoskeleton ; GTP-binding; tubulin binding.	Cell motility; chromosome segregation; cytoskeleton organisation and biogenesis; intracellular protein transport; microtubule based process; mitosis
CG5270	B1	1.05e+004	253.676	Putative actin binding	Putatively involved in cell cycle
CG16742	B1	9.73e+003	160.899	Putative actin binding	Unknown
CG30132	B8	4.4e+004	78.312	DNA topoisomerase (ATP hydrolysing activity)	Early meiotic recombination module assembly; late meiotic recombination module assembly; meiotic recombination.
CG1618	B8	1.61e+04	82.556	ATPase activity	Intracellular protein tranport; mitosis
CG9356	B8	1.3Ee+04	49.990	Putative chromatin binding	Putatively involved in cell cycle
CG11248	B8	8044	96.073	Structural constituent of cytoskeleton; microtubule binding	Cell cycle; intracellular protein transport; mitosis; protein tergeting
CG2512	B9	1.14e+11	49.891	GTP-binding; structural constituent of cytoskeleton; tubulin binding	Cell motility; chromosome segregation; intracellular protein transport; mitosis
CG1913	B9	1.149e+11	49.909	GTP-binding; structural constituent of cytoskeleton; tubulin binding	Cell motility; chromosome segregation; cytoskeleton organisation and biogenesis; intracellular protein transport; mitosis
CG16940	B6	426	116.842	Exoribonuclease II activity; nucleic acid binding	RNA catabolism; mitosis

Table 3.1. Possible CAP-D2 interactors that are involved in cell communication, cell cycle and mitosis.

Protein Name	Band Name	MOWSE Score	Molecular weight/kDa	Molecular Function	Biological process
CG6349	B1	2.72e+004	169.9	Alpha DNA polymerase activity, nucleic acid binding; 3 -5 exodeoxy-ribonuclease activity	Involved in DNA strand elongation;DNA recombination
CG13930	B3	1.459e+04	77.626	Motor activity; putatively involved in microtubule —based movement which is a component of the microtubule associated complex	Unknown
CG6743	B4 B5	1.008e+05 5094	97.383	Transporter activity	Protein targeting
CG3836	B5	3.297e+04	112.874	RNA polymerase II transcription factor activity	Oocyte cell fate determination; protein localisation
CG32940 (aka Pif)	B5 C8	1.514e+04 1.49e+05	149.069	Unkown	Unkown
CG1571	B7 B8	8208 2.15e+04	75.816	Motor activity; Structural constituent of cytoskeleton; ATPase activity coupled	Microtubule based movement
CG15695	B8	5.79e+04	83.096	Unknown	Unknown
CG14870	C9	1.009e+05	26.866	Unknown	Unknown
CG18102 (aka Dynamin, Shibire)	C10	3.736e+05	93.760	Actin binding; microtubule binding; Microtubule motor activity; structural constituent of cytoskeleton; GTPase activity; small GTPase activity; dynamin GTPase activity	Defence response; intracellular protein transport
CG13127	C9	5.693e+04	52.372	Unknown	Unknown

Table 3.2. Possible CAP-D2 interactors that their MOWSE score was in the top four for each band that was sent for mass spectrometry.

CHAPTER 4

FUNCTIONAL ANALYSIS OF CAP-D2

4.1. Introduction

The condensin complex is known to be involved in chromosome condensation and segregation. However, exact roles for individual proteins within the complex remain to be determined. Mutations are useful tools for the elucidation of roles of proteins and thus a search was carried out in the Gadfly database in order to find a putative *CAP-D2* mutation. Unfortunately no mutations that disrupt the *CAP-D2* gene were identified. A P-element insertion located approximately 100,000 bp downstream of the *CAP-D2* gene (Figure 3.1) and a deficiency (deletion of a whole chromosomal region [Df (3R) Dr-rv1, loc: 2538400-25500982)] that uncovers the region between 99B6-11), were identified. The deficiency also uncovers the *bub3* gene (locus 99B7) located next to the *CAP-D2* gene (CAP-D2 is located at the 3' UTR of *bub3* gene). Bub3 is involved in the mitotic checkpoint and thus interpretation of the analysis of a deficiency uncovering both *CAP-D2* and *bub3* genes would be very difficult and complicated, therefore no attempt to study this deficiency was undertaken. As for the P element insertion, P hopping could have been attempted however due to its large distance from the region, the possibility to get the P-element in the *CAP-D2* gene was low. Thus, P hopping was not attempted either.

As no *CAP-D2* mutations were available, double stranded RNA mediated interference (dsRNAi) on S2 cells was used to elucidate the role of CAP-D2. This method, originally pioneered in *C. elegans*, has been widely used in different organisms including *Drosophila* (Sharp, 2001).

4.2. CAP-D2 dsRNA-mediated interference (RNAi) in Drosophila cultured cells results in abnormal chromosome morphology and behaviour

In order to perform double stranded RNA mediated interference on CAP-D2, several *Drosophila* EST clones showing homology with the CAP-D2 gene were obtained and sequenced to confirm they contained the CAP-D2 cDNA (Chapter 2, Table I). The EST clone LD40412, contained the 5' end of the CAP-D2 cDNA and was used as a template for the PCR reaction to produce a 642 bp fragment of CAP-D2 dsRNA as described in Chapter 2 (Figure 4.1). S2 cultured cells were incubated with the dsRNA and samples were collected subsequently at 24 hr time points. Two negative controls were performed at the same time: cells that were incubated with dsRNA synthesized from a human intron (C) and cells with no dsRNA (-). Protein extracts from each time point were analysed by immunoblotting (Figure 4.2 A). A decrease in CAP-D2 levels was already apparent at 48 hrs and the protein was greatly depleted by 72 hrs and nearly undetectable by 96 hrs (the final depletion was estimated to be ~94% based on quantitation of known cell numbers, Figure 3.2 D). The levels of the protein were unaffected in control cells, and chromosomes appeared normal through mitosis (Figure 4.2 A and B). Immunofluorescence of the CAP-D2 RNAi cells confirmed that these cells had no CAP-D2 on their chromosomes. 48 hrs after the RNAi treatment, CAP-D2 signal was decreased (data not shown) and by 72 hrs no CAP-D2 protein could be detected on the chromosomes of cells exhibiting abnormal chromosome morphology (Figure 4.2 C). However these cells appeared to have some cytoplasmic staining which was also present in control cells and was therefore considered to be background staining. The cytoplasm was maintained in this preparation since the cells were fixed and then permeabilised.

After counting the number of viable cells it was apparent that CAP-D2 RNAi cells grew more slowly than control cells. Cell number reached a plateau 72 hrs after treatment, and it did not change significantly afterwards (Figure 4.3 A).
Different time points were assessed for mitotic index and the distribution of mitotic phases. The percentage of cells positive for histone H3 phosphorylated on Serine 10 (P~H3), indicative for mitotic cells, was increased 2-3 fold in the CAP-D2 RNAi

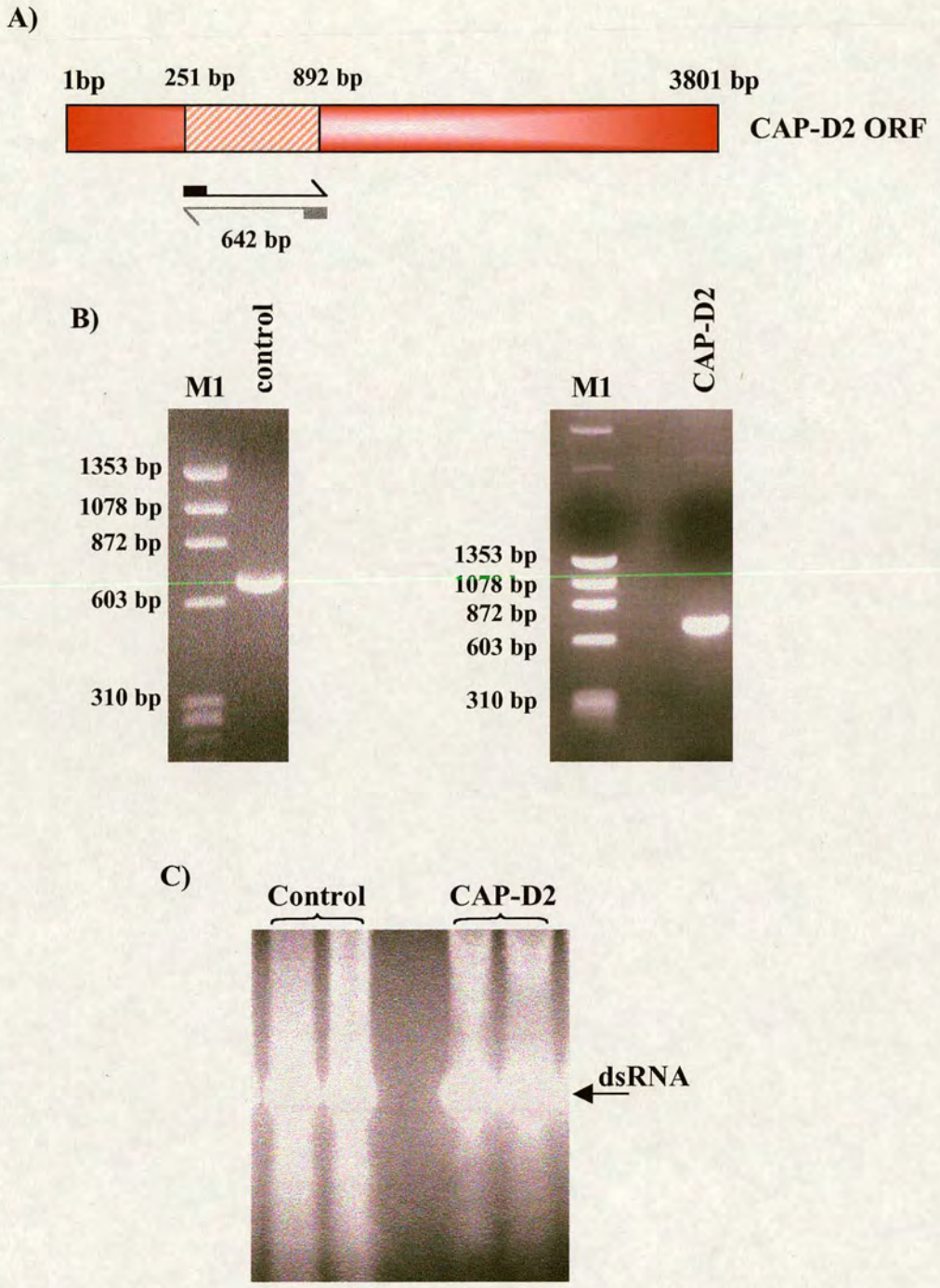

Figure 4.1 .

A. Diagram showing the position of the primer pair that was used to amplify a 642 bp product for CAP-D2 dsRNA (red diagonal lines). The sequence of these primers is shown in Table V.

B. PCR products after amplification of a region of a human intron (control) and a region of the 5' prime end of CAP-D2 cDNA. M1 is ϕX174 phage digested with HaeIII molecular weight marker.

C. Control and CAP-D2 dsRNA products. The PCR products shown in (B) were used as a template for the dsRNA synthesis of control and CAP-D2, respectively.

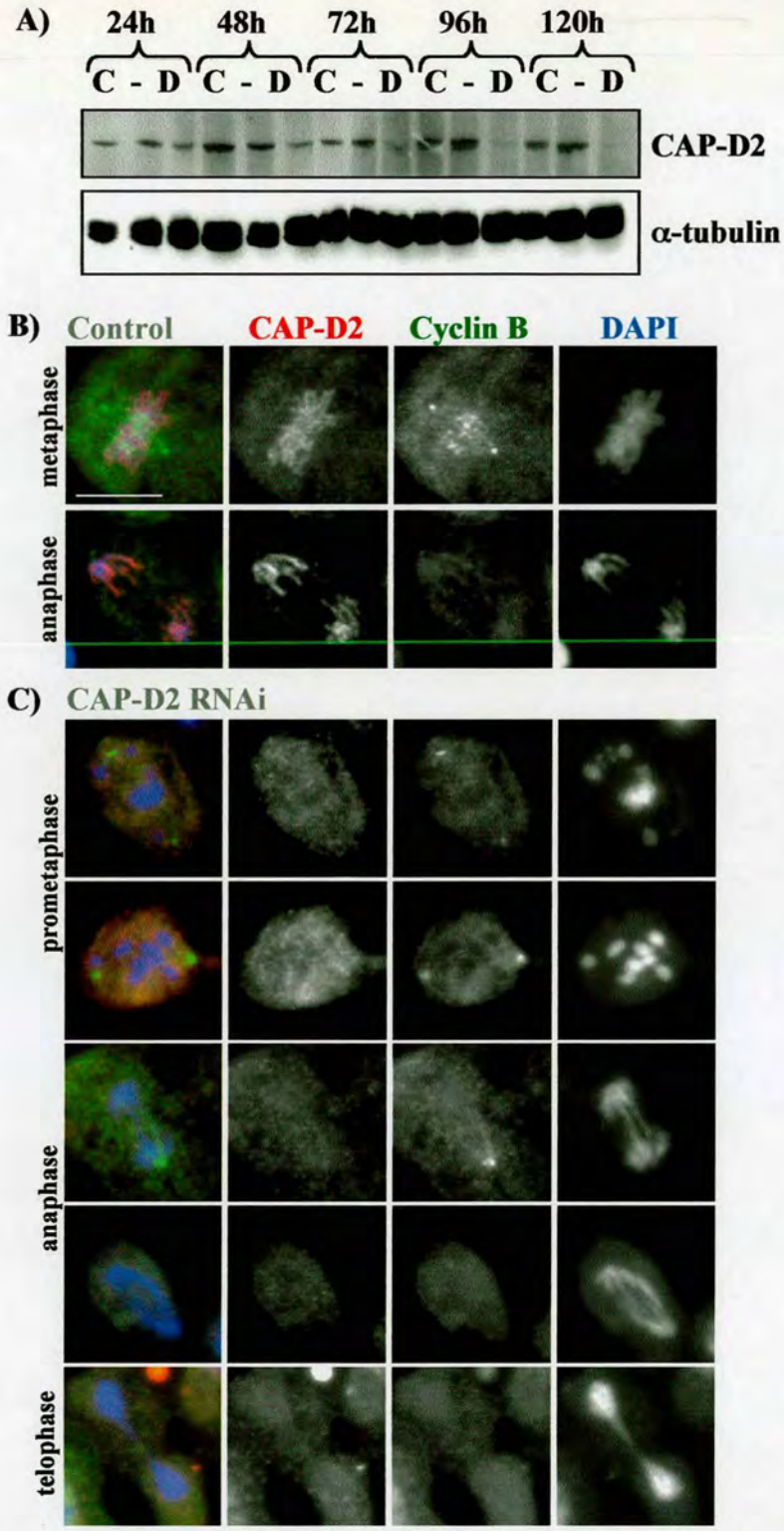

Figure 4.2. CAP-D2 dsRNA-interference in *Drosophila* S2 cells results in abnormal chromosome morphology and segregation.

A. Immunoblot showing the depletion of CAP-D2 after treatment with dsRNA. $5x10^5$ cells were loaded per lane. CAP-D2 levels start to decrease as early as 48 hours and the protein becomes undetectable at 96 and 120 hours. α-tubulin was used as a loading control. Key: C (control dsRNA), - (no dsRNA), D (CAP-D2 dsRNA). **B and C**. Immunofluorescence analysis of control and CAP-D2 RNAi cells. Cells were cytospun 72 hours after treatment onto poly-L-lysine slides and stained for CAP-D2 (red), Cyclin B (green), and DNA (blue). **C.** CAP-D2 depleted cells have no CAP-D2 on condensed chromosomes and exhibit an abnormal chromosome morphology. Cells also show severe segregation defects and unequal daughter nuclei. The scale bar represents 10μm.

between 36 and 72 hours (6.7% of RNAi treated cells versus 2.2% of control cells, at 48 hours) (Figure 4.3 B). At 24 hrs, 25% of the mitotic cells were abnormal while approximately 97% of mitotic cells displayed abnormal chromosome morphology between 48 hrs and 72 hrs (only 4-11% of control mitotic cells appeared abnormal) (Figure 4.3 C). Therefore, most of the phenotypic analysis was carried out 65 or 72 hrs after treatment with dsRNA. Analysis by immunofluorescence showed dramatic chromosome defects after treatment with CAP-D2 dsRNA including failures in chromatid resolution, chromosome alignment, and segregation. Chromosomes were not properly aligned on the metaphase plate and they appeared fuzzy with ill-defined sister chromatids. In anaphase, chromosomes failed to resolve and segregate properly to the two poles with chromosome bridges forming between the two daughter nuclei (Figure 4.2 C).

A consequence of the abnormal chromosome morphology was that the mitotic stage of the CAP-D2 depleted cells could not be easily determined. Particularly, it was not trivial to distinguish if cells were in prometaphase or anaphase. Thus the stage of the mitotic cells could only be distinguished after staining for mitotic proteins that are degraded naturally during anaphase, such as Cyclin B and members of the cohesin complex. Initially cells were stained for Cyclin B, a cofactor for the mitotic CDC2 kinase that moves from the cytoplasm into the nucleus in late G2/early prophase, associates with condensed chromosomes during prophase and prometaphase, and subsequently associates with mitotic spindle and spindle poles during metaphase and finally is degraded during anaphase (Huang, 1999; Raff, 2002). It was obvious that the majority of CAP-D2 depleted cells were positive for Cyclin B as they had Cyclin B on the spindle and spindle poles (Figure 4.2 C, top two), and were therefore considered to be in prometaphase with unaligned chromosomes. Cells were grouped into the different phases of mitosis by using P~H3/α-tubulin/Cyclin B triple staining (Figure 4.4 A). Between 36 hours and 72 hours, 67-88% of RNAi mitotic cells were in prometaphase compared to only 19-51% of control cells, suggesting a pronounced prometaphase delay (Figure 4.4 B). The anaphase index for the same period was very low: only 4% of mitotic cells were in anaphase

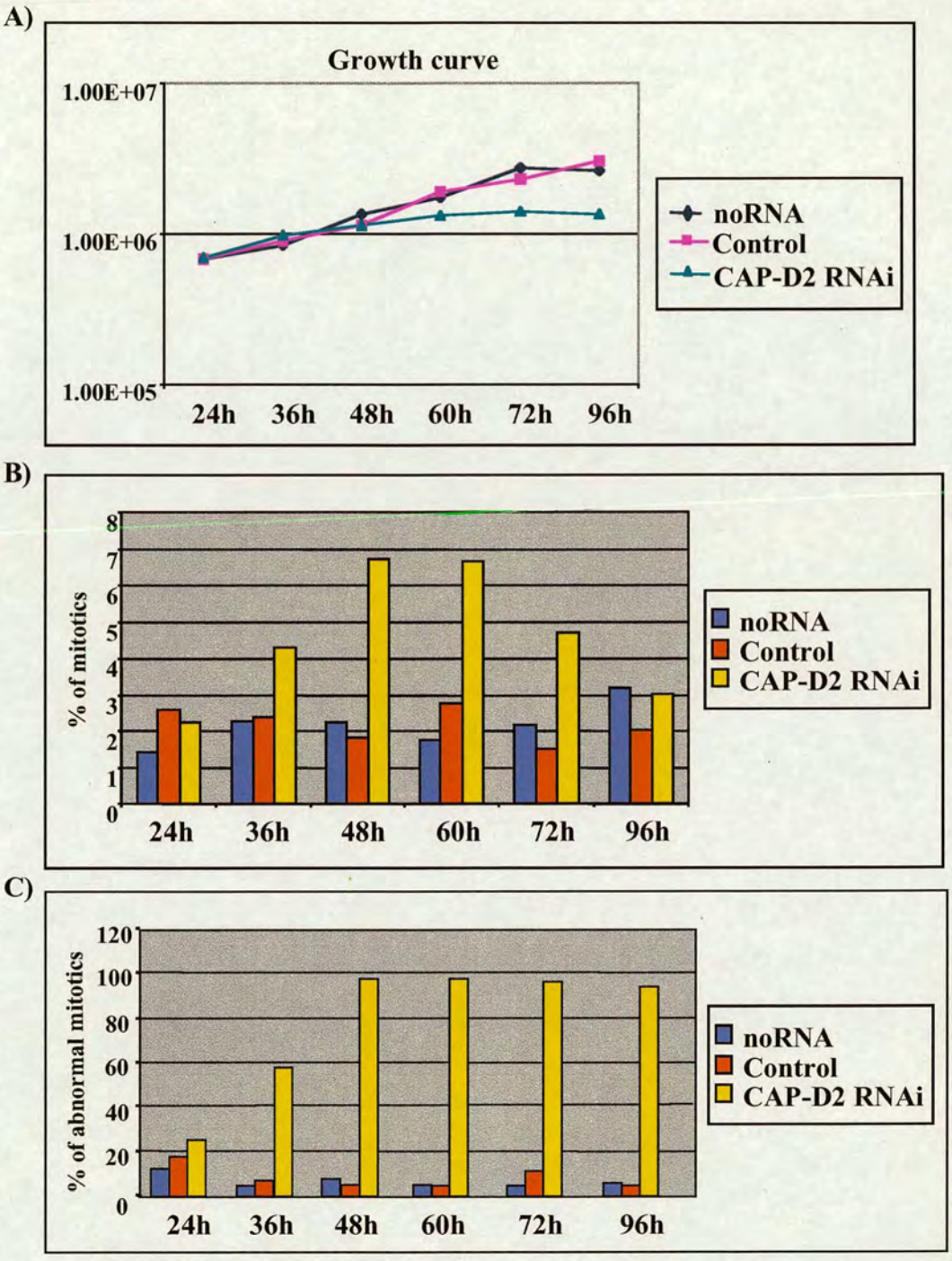

Figure 4.3.

A. Growth curve showing the number of cells at different time points after dsRNAi treatment. CAP-D2 RNAi cells grew more slowly than control cells. Cell number reached a plateau 72 hrs after treatment, and cell number did not change significantly after that time.

B. Graph showing the percentage of mitotic cells in control and CAP-D2 RNAi cells. The percentage of mitotic cells was increased 2-3 fold in the CAP-D2 RNAi between 36 and 72 hours.

C. Graph showing the percentage of abnormal mitotic cells in control and CAP-D2 RNAi cells. The majority of cells are abnormal, 48 hours after dsRNAi treatment.

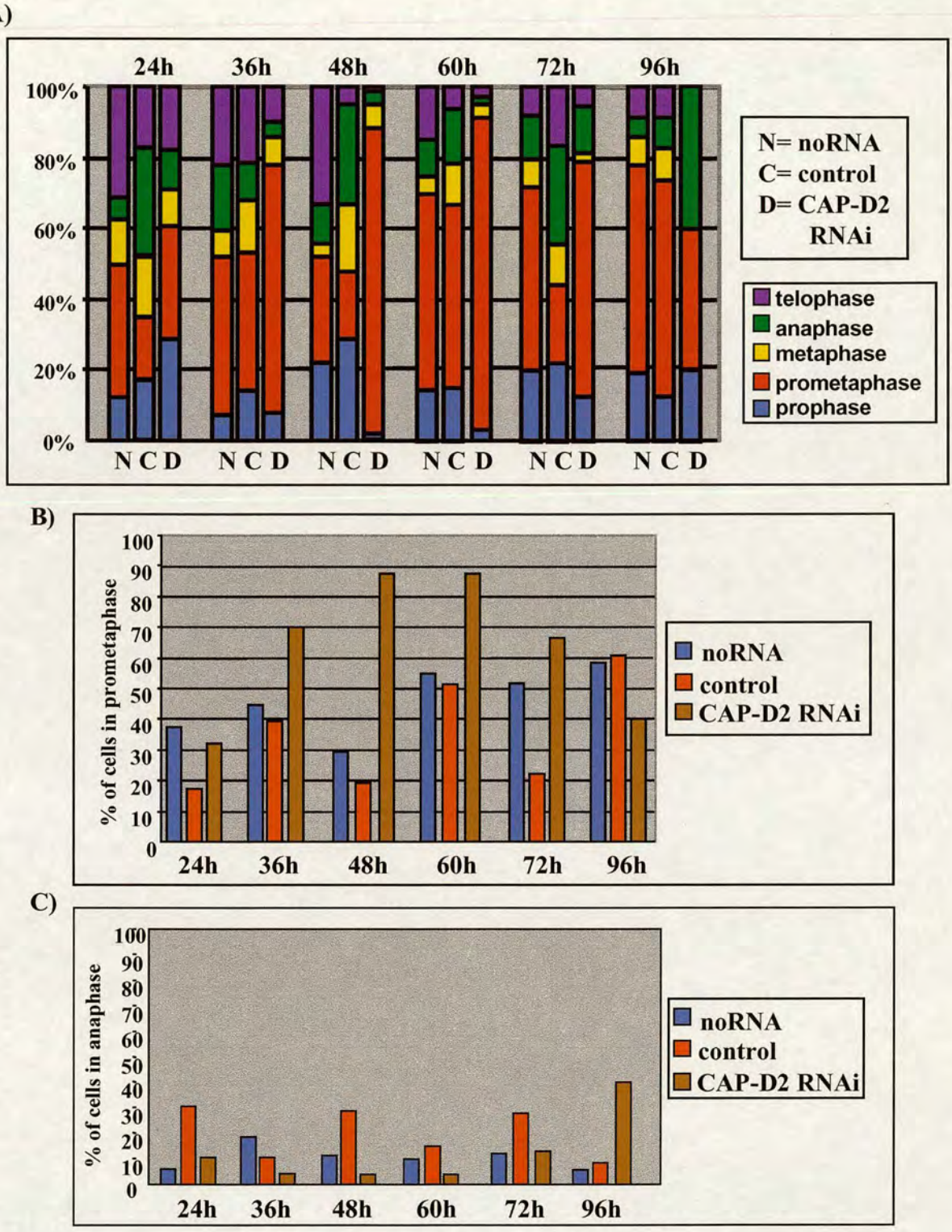

Figure 4.4.

A. Graph showing the distribution of mitotic cells in the different mitotic phases after staining with Cyclin B/P~H3/α-tubulin, in control and CAP-D2 depleted cells.

B. Graph showing the percentage of prometaphase cells after staining with Cyclin B/P~H3/α-tubulin, in control and CAP-D2 RNAi cells. There was a pronounced prometaphase delay between 36 and 72 hours in the CAP-D2 depleted cells. 67-88% of mitotic cells were in prometaphase during this period compared to only 19-51% of control cells.

C. Graph showing the percentage of anaphase cells after staining with Cyclin B/P~H3/α-tubulin, in control and CAP-D2 RNAi cells. The anaphase index between 36 and 72 hours was very low in the CAP-D2 depleted cells. Only 4% of mitotic cells were in anaphase compared to 10-30% of control cells.

compared to 10-30% of control cells (Figure 4.4 C). The rest of the mitotic cells were distributed in the other mitotic phases without any noticeable delay (Figure 4.4 A).

However, it was observed in control cells, that Cyclin B was not degraded from spindle poles in a minority of anaphase cells, as it normally is (Figure 4.2 B, bottom). In order to exclude any overinterpretation of the results by using Cyclin B, the stage of the mitotic cells (prometaphase or anaphase) was also estimated after staining for DSA1, a subunit of the cohesin complex. DSA1 localises along the condensed chromosomes during prometaphase, with more intense labelling in the centromeric regions and a fainter labelling between sister chromatid arms. In metaphase, it is highly concentrated at centromeres and persists there until sister chromatids separate at the onset of anaphase (no DSA1 can be detected on chromosomes). DSA1 also stains the spindle poles and the spindle microtubules. During anaphase, the spindle poles are the most intensely stained structures (Valdeolmillos et al., 2004). The protein levels of DSA1 appeared unaffected in the CAP-D2 RNAi cells (Figure 4.5 A). Cells were categorised in the different phases of mitosis by using DSA1/CID double staining (Figure 4.5 B and C and 4.6 A). At 48 hours, the majority of cells were positive for DSA1 and were therefore considered to be in prometaphase with unaligned chromosomes (67% of mitotic RNAi cells compared to 35% of control cells), suggesting a pronounced prometaphase delay (Figure 4.5 C1 and 4.6 B). The anaphase index for the same period was very similar to control cells (17% of mitotic RNAi cells compared to 20% of control cells) (Figure 4.6 B). At 72 hours, the prometaphase index of the RNAi cells was not significantly higher compared to control cells (66% of RNAi mitotic cells compared to 63% of control cells), while the anaphase index was higher in the RNAi cells (23% in the RNAi cells compared to 16% of control cells) (Figure 4.6 B). These results are similar to those found after Cyclin B staining. However, the peak in prometaphase index appeared to be different in the DSA1 and Cyclin B experiments: when stained for DSA1 the prometaphase index was slightly higher, but very similar to control cells at 72 hours, while in the Cyclin B staining the reduction of the prometaphase index happened sometime after 72 hours. One possibility is that this event could be dependent upon the particular stage of the culture when subjected to RNAi at 0 time. Another difference

Figure 4.5. A. Immunoblotting showing that the levels of DSA1 were not affected 72 hours after CAP-D2 RNAi treatment. - (no dsRNA), C (control dsRNA), D (CAP-D2 dsRNA). α-tubulin was used as a loading control. **B and C.** Centromere resolution is disrupted in the CAP-D2 depleted cells. Control (B) and CAP-D2 depleted (C) cells were cytospun onto poly-L-lysine slides 72 hours after dsRNAi treatment, fixed and stained for DSA1 (green), CID (red) and DNA (blue). The majority of prometaphase/metaphase cells had normal CID staining between sister chromatids (C1 and higher magnification), while a small percentage showed CID slightly stretched (C2 and higher magnification). Cells in anaphase showed severe centromere stretching on chromosomes (C3, C4 and C5 and higher magnification). The DSA1 staining indicates the mitotic phase of the cells. The white boxes indicate the region from where the higher magnifications were taken. The scale bar represents 10μm.

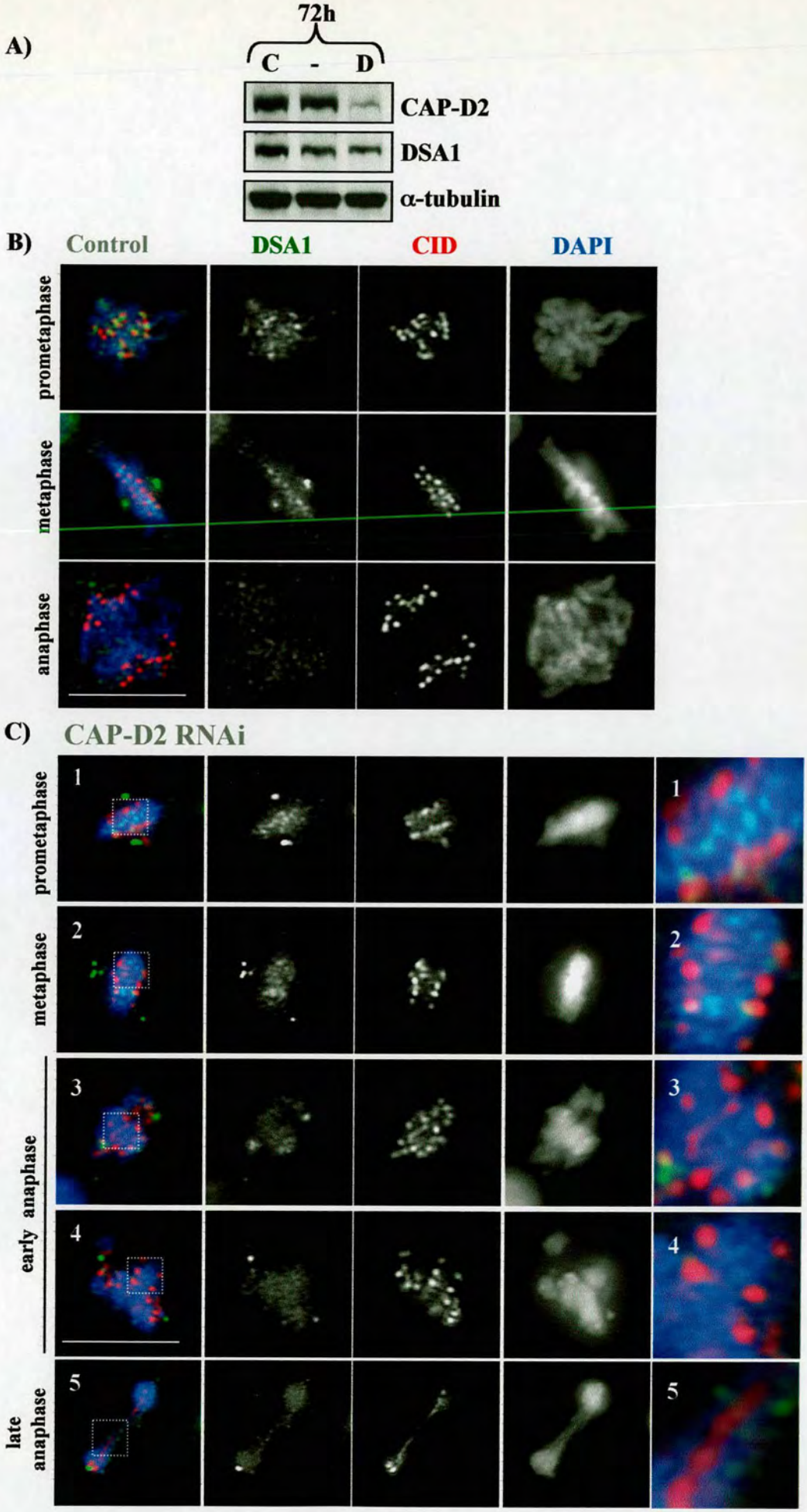
A)
72h
C
-
D
CAP-D2
DSA1
α-tubulin
B)
Control
DSA1
CID
DAPI
prometaphase
metaphase
anaphase
C)
CAP-D2 RNAi
prometaphase
metaphase
early anaphase
late anaphase
1
2
3
4
5

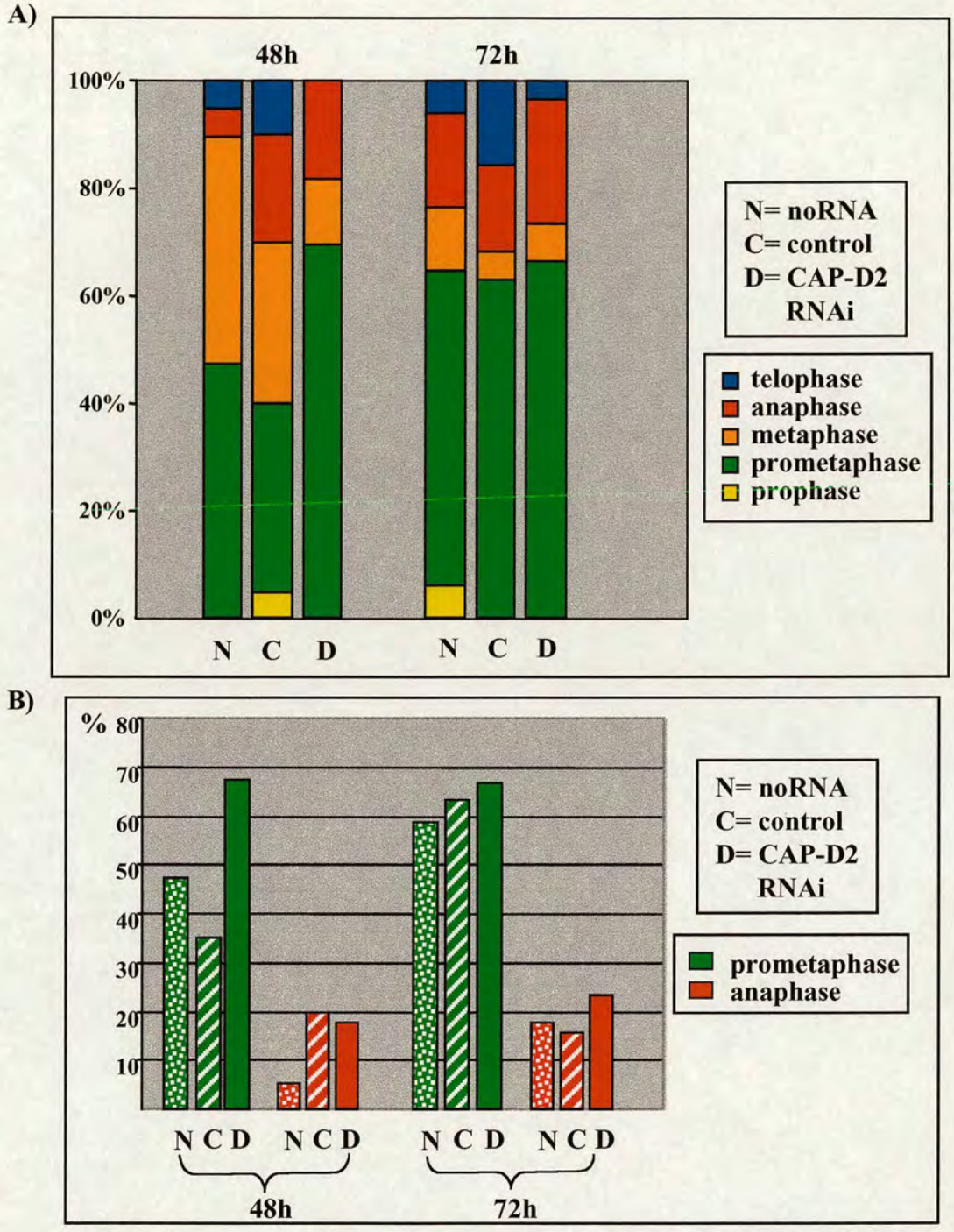

Figure 4.6.

A. Graph showing the distribution of mitotic cells in the different mitotic phases after staining with DSA1/CID at 48 and 72 hours, in control and CAP-D2 depleted cells.

B. Graph showing the percentage of prometaphase and anaphase cells at 48 and 72 hours after staining with DSA1/CID, in control and CAP-D2 depleted cells. Cells are delayed in prometaphase at 48h (67% of mitotic RNAi cells compared to 35% of control) but they finally progress into anaphase, 72 hours after CAP-D2 depletion (23% of RNAi mitotic cells compared to 16% of control).

A)

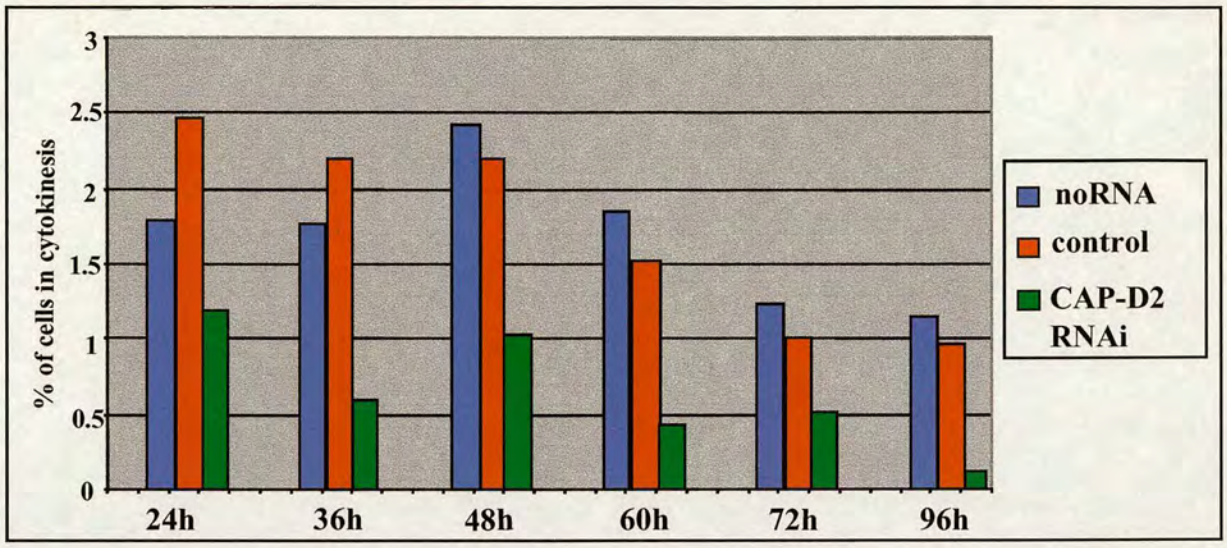

B)

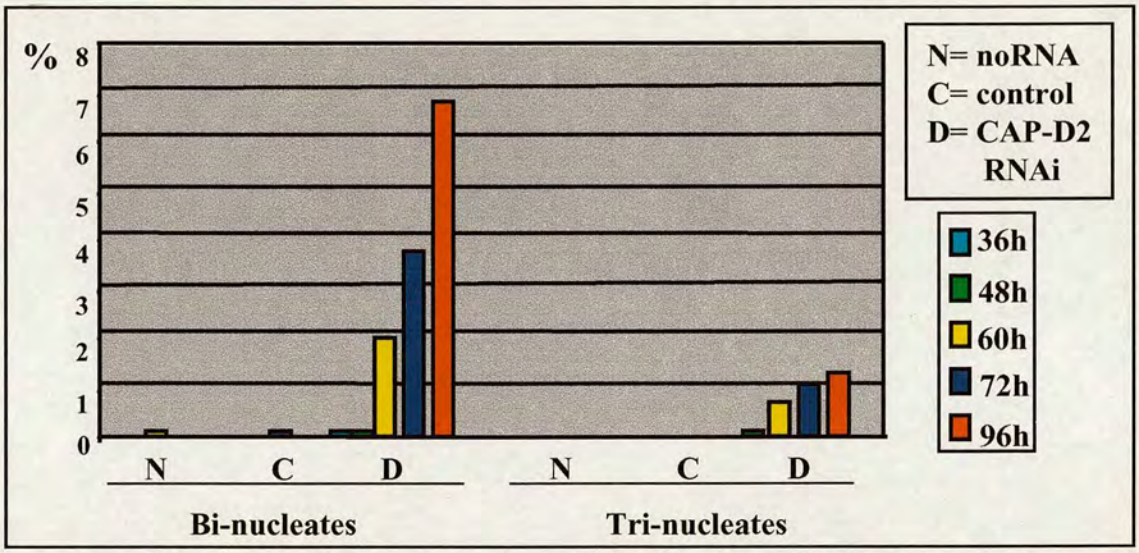

Figure 4.7

A. Graph showing the percentage of cells in cytokinesis in control and CAP-D2 depleted cells. The percentage of cells in cytokinesis is very low in the CAP-D2 depleted cells at all time points.

B. Graph showing the percentage of bi- and tri- nucleate cells in control and CAP-D2 depleted cells. The percentage of bi- and tri- nucleate cells increases by time in the CAP-D2 depleted cells while is almost undetectable in control cells.

between stainings was the anaphase index which was estimated to be higher at both 48 and 72 hours after staining for DSA1 compared to Cyclin B staining. However, this is consistent with the observation that Cyclin B persists on the spindle poles of some cells that entered anaphase. The mitotic phase of the cells that were in anaphase, with Cyclin B still present on the spindle poles, could be easily distinguished in control cells from their overall chromosome morphology. In the RNAi treated cells however, cells positive for Cyclin B were considered to be in prometaphase, since their chromosome morphology was compromised and subsequently no conclusion could be made for their mitotic stage. It is possible that some of these cells were in anaphase.

Nevertheless, it was obvious from both approaches that CAP-D2 RNAi cells were delayed in prometaphase before progressing into anaphase, albeit with evident failures in segregation that resulted in chromosome bridges forming bi-nucleate or even tri-nucleate cells (Figure 4.2 C, 4.9 B4 and 4.7 B). Frequently, daughter nuclei of unequal size were also observed, suggesting that chromosomes had not been equally distributed to the two poles during anaphase. Intriguingly, chromosomes were compacted relative to an interphase state in the CAP-D2 RNAi cells, though the resulting chromosomes appeared fuzzy, unresolved and hypercondensed. The hypercondensation is possibly a result of prometaphase delay.

4.3. Chromosome and centromere resolution are compromised after CAP-D2 depletion

In order to confirm that chromatid resolution was defective, cells were treated with a hypotonic buffer that results in better chromosome spreading and improved observation of individual chromatids. The control cells appeared to have normal chromosome resolution and individual chromatid arms could be easily distinguished (Figure 4.8 A). In hypotonically treated CAP-D2 RNAi cells, individual chromatids were not visible and chromosomes appeared as balls of chromatin distinct from one another, albeit with usual levels of phospho-histone H3 (Figure 4.8 B).

Immunolabeling for CID showed that centromeres were often stretched in the CAP-D2 RNAi cells (Figure 4.5 C and 4.9 B), while in control cells, centromeres were

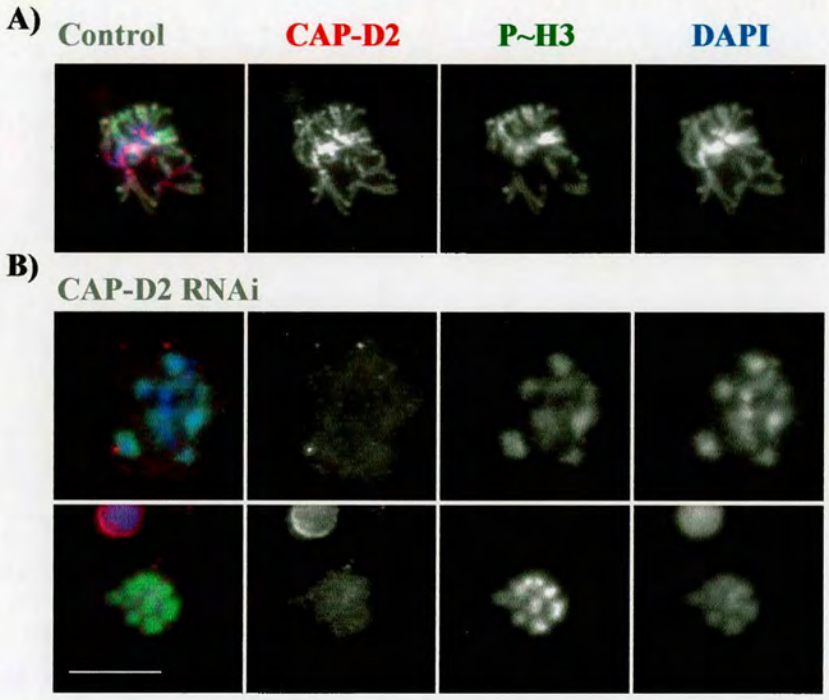

Figure 4.8. Chromosome resolution is compromised after CAP-D2 depletion. A and B. Hypotonic treatment of control (A) and CAP-D2 depleted (B) cells 65 hours after dsRNA treatment shows that chromatid resolution is defective in the CAP-D2 depleted cells. Cells were hypotonically treated, centrifuged onto poly-L-lysine slides, fixed and stained for CAP-D2 (red), P~H3 (green) and DNA (blue). Note that individual chromatids are not readily apparent after depletion of CAP-D2. The scale bar represents 10μm.

always distinct double dots in metaphase or cleanly separated from one another during anaphase (Figure 4.5 B and 4.9 A). The CID stretching was more obvious on chromosomes that were aligned on the metaphase plate and on chromosomes that were undergoing anaphase (Figure 4.9 B1 and B3, and higher magnification), while distinct double CID spots were only detected on individual unaligned chromosomes (Figure 4.9 B2, and higher magnification). Also, daughter nuclei connected with chromosome bridges still had centromeres extending between them (Figure 4.5 C5 and 4.9 B4, and higher magnification). In order to quantify these results, cells were stained for CID and DSA1 and categorised into different groups. 95% of the cells that displayed CID stretching between sister centromeres had no DSA1 on their chromosomes and were thus considered to be in anaphase (Figure 4.5 C3, 4.5 C4 and 4.5 C5, and higher magnification). 60% of these anaphase figures were in early anaphase, as concluded from the short distance between the centromeres of sister chromatids (Figure 4.5 C3 and 4.5 C4, and higher magnification). The remaining 5% of cells that displayed CID stretching were positive for DSA1 and thus were considered to be in prometaphase/metaphase (Figure 4.5 C2, and higher magnification), dependent upon chromosome alignment on the metaphase plate. The CID stretching in these cells was not as extreme as in anaphase cells. The rest of the prometaphase/metaphase cells had no obvious CID stretching between their sister chromatids (Figure 4.5 C1, and higher magnification). This suggests that tension applied upon bipolar alignment accentuates the defect in resolution, and therefore in anaphase, the most extreme stretching of CID stained regions was detected (Figure 4.5 C5, and higher magnification). These results suggest that CAP-D2, and likely the entire condensin complex, is primarily required for resolution of sister chromatids (of arms and centromeres) and in the establishment of mitotic chromosome architecture rather than chromosome compaction in *Drosophila*.

4.4. Topoisomerase II localisation is affected in the CAP-D2 depleted cells

DNA topoisomerase II (Topo II) has long been implicated in chromosome structure and dynamics, since its discovery as a chromosome 'scaffold' protein, and its

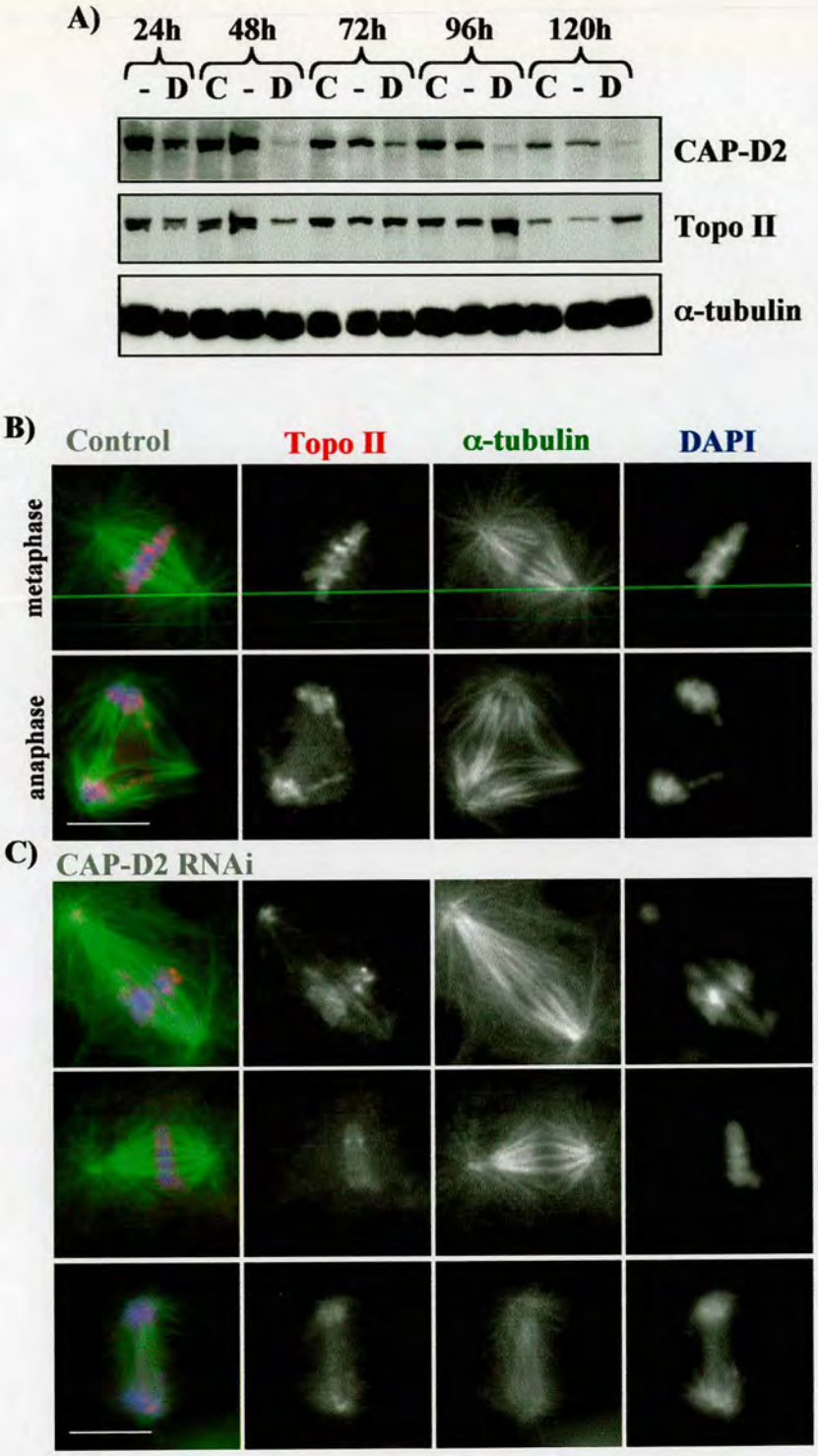

Figure 4.10. Effect on DNA topoisomerase II in CAP-D2 depleted cells. **A.** Immunoblotting of control and CAP-D2 depleted extracts with an antibody to Topo II shows that depletion of CAP-D2 does not affect the level of Topo II. α-tubulin was used as a loading control. C (control dsRNA), - (no RNA), D (CAP-D2 dsRNA). **B and C.** Immunolocalization of Topo II in control (B) and CAP-D2 depleted (C) cells after 65 hours of RNAi treatment. Cells were grown on Concanavalin A treated coverslips for the last 24 hrs, fixed and stained for Topo II (red), α-tubulin (green) and DNA (blue). In the CAP-D2 depleted cells, Topo II localises to chromatin but any axial localisation is lost. Also the protein is slightly less and diffuse. The scale bar represents 10μm

localization at the base of chromatin loops (Earnshaw et al., 1985; Earnshaw and Heck, 1985)(Gasser et al., 1986). Biochemical and localisation studies in *Drosophila* showed that CAP-H/Barren associated with Topo II throughout mitosis, while SMC4 appeared to be responsible for the axial localisation of Topo II on the chromosomes and for its decatenation activity (Bhat et al., 1996; Coelho et al., 2003). However, in *S. pombe*, the localisation but not the activity of Topo II was affected in condensin mutations, while Topo II localization to well-defined axial structures in *Xenopus* was independent of condensin (Bhalla et al., 2002; Cuvier and Hirano, 2003). Furthermore, in this study (Chapter 3), it has been shown that CAP-D2 and Topo II colocalise partially along the chromosomes axes during mitosis. For these reasons I decided to investigate whether the stability and localisation of Topo II were affected in the CAP-D2 depleted cells. By immunoblotting, the level of Topo II appeared to be unaffected (Figure 4.10 A). However, the localisation of Topo II was altered in the CAP-D2 depleted cells. Cells grown on Concanavalin A coverslips were stained for Topo II and α-tubulin. In control cells, Topo II associated with chromosomes in an axial pattern (Figure 4.10 B). In the CAP-D2 depleted cells, Topo II still localized to chromatin, even though chromosome morphology was abnormal (Figure 4.10 C). However, distribution was not restricted to an axial core and the protein was slightly less and more diffuse compared to control cells. This suggests that Topo II localisation is dependent upon CAP-D2.

4.5. CAP-H/Barren is unstable in cells depleted of CAP-D2

As CAP-D2 is one subunit of a complex, it is possible that associated proteins may be affected by its depletion. For this reason, the stability and localisation of the other subunits of the complex were analysed upon depletion of CAP-D2. Immunoblotting of RNAi cell extracts for CAP-H/Barren, revealed that the levels of this protein were affected by the depletion of CAP-D2 (Figure 4.11 A). CAP-H/Barren may be more tightly associated with CAP-D2 compared to the SMC subunits, as suggested in the immunoprecipitations presented in Chapter 3. As no sequence similarity exists between the two proteins, the depletion by RNAi should be specifically directed only against

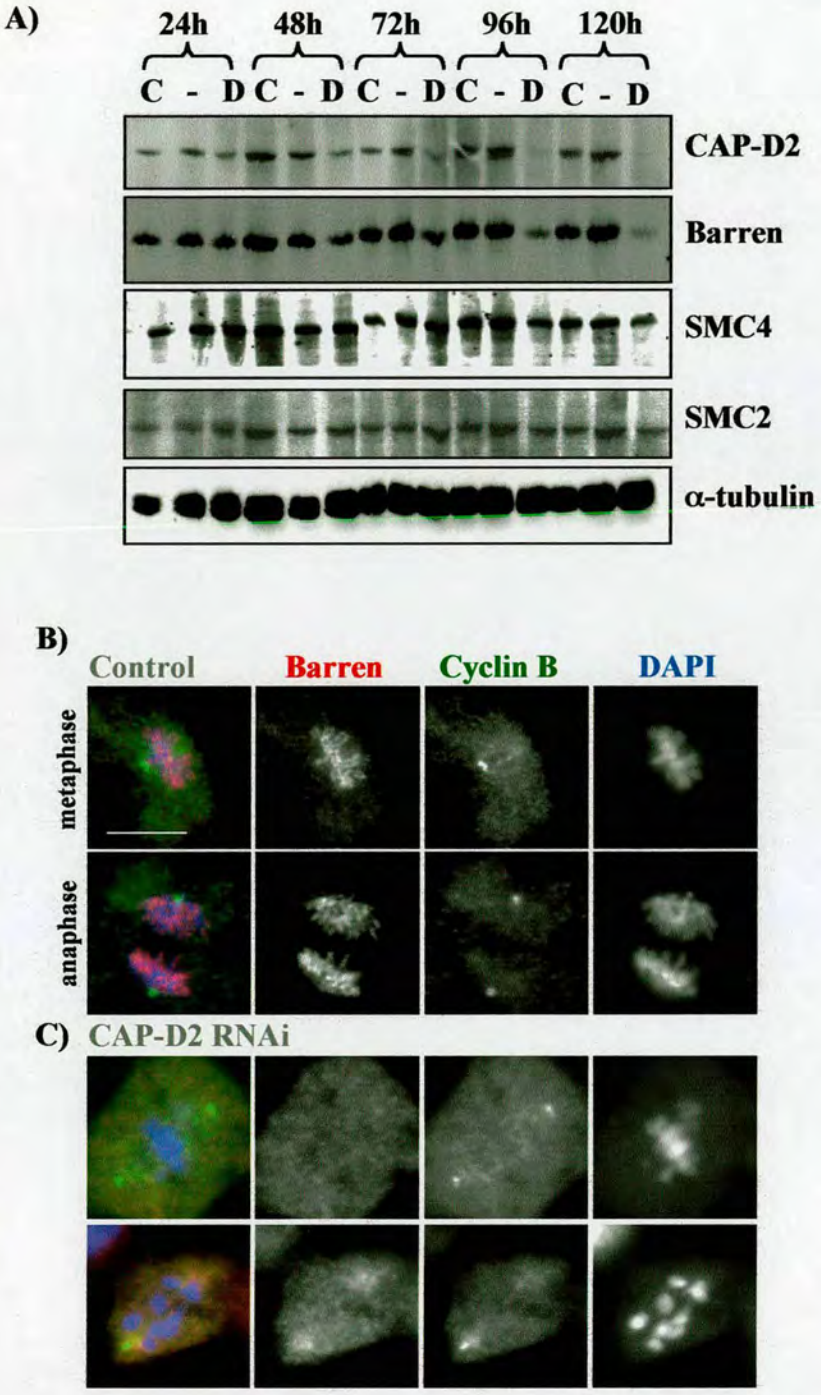

Figure 4.11. Effect on condensin subunits.
A. Immunoblotting of control and CAP-D2 depleted extracts with Barren, SMC4 and SMC2 antibodies demonstrates that Barren levels are reduced while SMC4 and SMC2 levels appear largely unaffected after loss of CAP-D2. α-tubulin was used as a loading control. Key: C (control dsRNA), - (no RNA), D (CAP-D2 dsRNA). **B and C.** Cells from both control (B) and CAP-D2 RNAi (C) experiments were cytospun onto poly-L-lysine slides 72 hours after treatment and stained for Barren (red), Cyclin B (green) and DNA (blue). Barren is absent from mitotic chromosomes and it appears to localise diffusely in the cytoplasm after CAP-D2 RNAi. The scale bar represents 10μm.

CAP-D2. In contrast, when the same analysis of SMC2 and SMC4 was done, no substantial change was observed in their protein levels (Figure 4.11 A).

4.6. Immunolocalisation of Barren, SMC4 and SMC2 in CAP-D2 depleted cells

Although the levels of CAP-H, SMC2 and SMC4 were not similarly affected, it was possible that localisation could still be influenced after the depletion of CAP-D2. To examine this, cells were cytospun onto poly-L-lysine slides after dsRNA treatment and immunofluorescence for CAP-H, SMC4 and SMC2 was performed. In control cells, CAP-H associated with chromosomes and localised to sister chromatid cores (Figure 4.11 B). In the CAP-D2 depleted cells, CAP-H protein appeared to localise diffusely in the cytoplasm and no CAP-H could be detected on the chromosomes (Figure 4.11 C).

To examine the localisation of the SMC4 subunit, double staining with CAP-D2 (rabbit) and SMC4 (sheep) antibodies was performed 65 hrs after dsRNA treatment. It was thus possible to observe the localisation of SMC4 in cells that were clearly negative for CAP-D2. Cells were extracted during fixation and thus no cytoplasmic staining was observed for CAP-D2. In both control and CAP-D2 depleted cells, SMC4 was localised on the chromosomes (Figure 4.12 A), even though chromosome morphology was abnormal in the CAP-D2 depleted cells (Figure 4.12 B). However, distribution was not restricted to an axial core in the CAP-D2 depleted cells, presumably because of the abnormal chromosome organisation. In approximately 40% of the abnormal cells, the SMC4 signal was more severely reduced (Figure 4.12 B1 and B4) than in other CAP-D2 depleted cells (Figure 4.12 B2 and B3), which may reflect an uneven RNAi efficiency across the cell population.

SMC2 stability and localisation was also examined. As for SMC4, the levels of SMC2 appeared largely unaffected as CAP-D2 was depleted (Figure 4.11 A). Because both CAP-D2 and SMC2 antibodies were raised in rabbits, double immunolabeling was not possible. Therefore, cells were double-labelled for SMC2 and topoisomerase II (using the guinea pig antibody), as a marker for the chromosome scaffold . In control cells, both SMC2 and topoisomerase II associated with chromosomes in a striking axial pattern (Figure 4.13 A). After CAP-D2 depletion, SMC2 localized to chromatin masses,

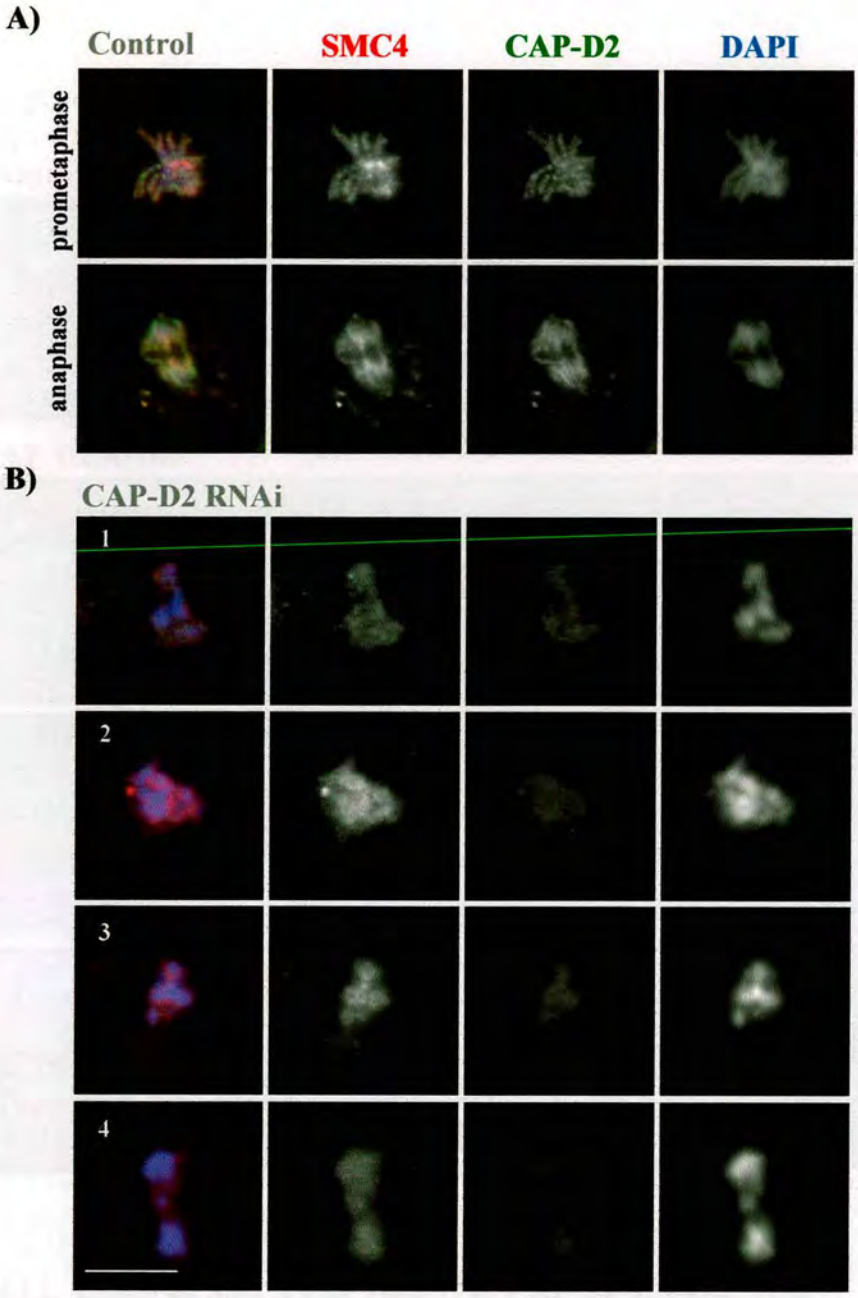

Figure 4.12. Control (A) and CAP-D2 RNAi (B) cells were cytospun onto poly-L-lysine slides 65 hours after treatment, extracted during fixation, and stained for SMC4 (red), CAP-D2 (green) and DNA (blue). While cells have varying levels of SMC4 on chromatin (compare B1 and B4 with B2 and B3), any axial localisation of SMC4 is lost in the CAP-D2 depleted cells. The scale bar is 10 μm.

albeit in an unrestricted manner reflecting aberrant chromosome organisation, similar to SMC4 behaviour. Approximately half of these cells (~43%) had what appeared to be reduced levels of SMC2 (Figure 4.13 B1) while 47% had higher levels of SMC2 (Figure 4.13 B2). Cells with reduced levels of SMC2 also had decreased levels of topoisomerase II, suggesting that these cells may be overall more severely affected. The remaining 10% had SMC2 localise diffusely on chromosomes and mitotic spindle (Figure 4.13 B3). In these cells, Topo II was also slightly diffuse but not to the same extent as SMC2. Taken together, these results suggest that the axial localisation of SMC4, SMC2, and Topoisomerase II is dependent on proper chromosome resolution which requires CAP-D2, and CAP-H/Barren (as it is also depleted).

4.7. Cohesin dissociates normally from chromosomes at the onset of anaphase in CAP-D2 depleted cells

It is possible that chromosome bridges formed during anaphase in CAP-D2 depleted cells are a consequence of an abnormal dissociation of cohesin during anaphase. However, as described above for DSA1, both its levels and its localisation were similar to those observed for control cells (Figure 4.5). DSA1 dissociated from chromosomes at the onset of anaphase as normal. Similarly, when the stability and localisation of Drad21/Scc1, another subunit of the cohesin complex was assessed, no difference was observed between control and RNAi treated cells (Figure 4.14). The Drad21/Scc1 subunit had a similar localisation pattern as that described for DSA1. From these observations it can be concluded that the dissociation of cohesin from chromosomes during anaphase is not dependent on CAP-D2.

4.8. Compromise in mitotic coordination after loss of condensin function:

4.8.1. Effect on chromosome passengers

The chromosome is not an isolated entity, but rather must be considered in the context of the rest of the cell. INCENP is a member of the chromosomal passenger complex along with Aurora B kinase, Survivin, Borealin, and TD-60 (Adams et al., 2001a; Gassmann et al., 2004; Sampath et al., 2004). Chromosome passengers localise to centromeres at

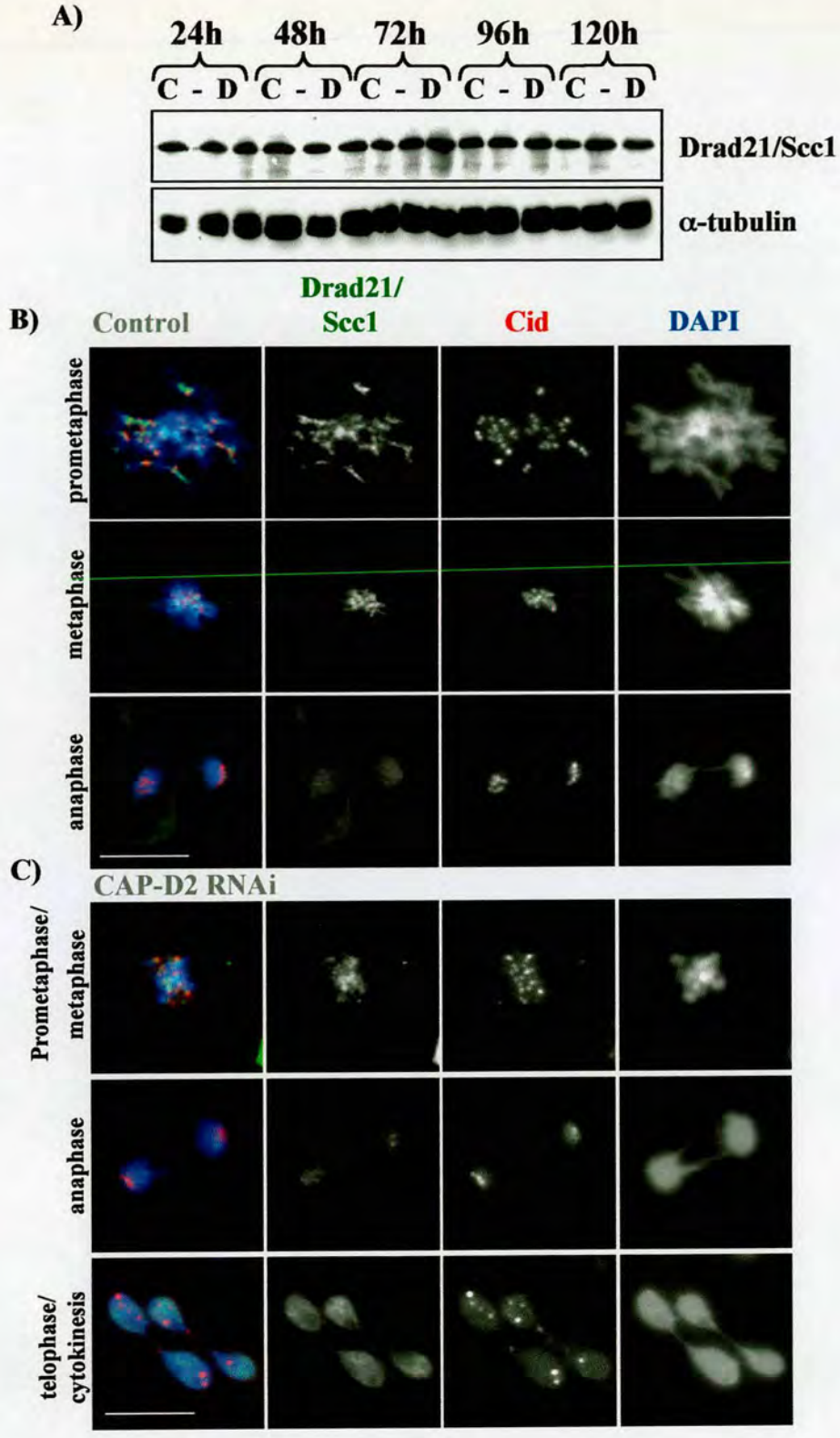

Figure 4.14. Cohesin dissociates normally from chromosomes at the onset of anaphase **A.** Immunoblotting showing that the levels of Drad21/Scc1 were not affected after CAP-D2 RNAi treatment. - (no dsRNA), C (control dsRNA), D (CAP-D2 dsRNA). α-tubulin was used as a loading control. **B and C.** Dad21 dissociates normally from chromosomes at the onset of anaphase in the CAP-D2 depleted cells. Control (B) and CAP-D2 depleted (C) cells were cytospun onto poly-L-lysine slides 72 hours after dsRNAi treatment, fixed and stained for Drad21/Scc1 (green), CID (red) and DNA (blue). Drad21is present at the centromeres during prometaphase/metaphase and it dissociates during anaphase in both control (B) and CAP-D2 (C) depleted cells. The scale bar represents 10μm.

prometaphase and metaphase, associate with the central spindle at the onset of anaphase and finally localise to the midbody in cytokinesis. INCENP is required for the correct targeting of Aurora B at all times in mitosis and Aurora B has been shown to phosphorylate histone H3 during mitosis, an event that coincides with the initiation of chromosome condensation.

The stability and localisation of INCENP was examined to assess whether chromosome passenger dynamics were affected when condensin function was compromised. While immunoblotting for INCENP revealed that protein level was unaffected in CAP-D2 dsRNA treated cells (Figure 4.15 A), the localisation of this protein was clearly affected (Figure 4.15 C). Cells grown on Concanavalin A-coverslips were stained for INCENP and α-tubulin. In CAP-D2 RNAi prometaphase cells, INCENP localized to chromatin but occupied a more extensive area compared to the restricted centromeric localisation in control cells (compare Figure 4.15 B with 4.15 C1). This may be a result of the stretched centromeric regions in CAP-D2 depleted cells, as shown by CID staining. In 60% of anaphase cells (generally 'early' anaphases), INCENP was abnormally present on chromatin and dispersed throughout the spindle, with failure to concentrate on the spindle midzone (compare Figure 4.15 B with 4.15 C2). The remaining 40% of the anaphase cells (generally 'later' anaphases) showed the expected association of INCENP with the central spindle even though these cells had severe segregation problems (Figure 4.15 C3). In 50% of cells undergoing cytokinesis, INCENP was unexpectedly still on chromatin as well as localised to the midbody (Figure 4.15 C4). In the remaining dividing cells, INCENP localised to the midbody, albeit in a more dispersed fashion (Figure 4.15 C5). From these observations, it can be concluded that proper chromosome resolution and segregation is requisite for the appropriate timing of passenger transfer. However, by the end of mitosis, the majority of INCENP localizes appropriately with the midbody.

Figure 4.15. INCENP exhibits temporal mislocalization in cells depleted of CAP-D2.

A. Immunoblotting of control and CAP-D2 depleted extracts with the INCENP antibody at 72 and 96 hours showed that the protein level has not been affected by the depletion of CAP-D2. α-tubulin was used as a loading control. - (no dsRNA), C (control dsRNA), D (CAP-D2 dsRNA).

B and C. Immunolocalisation of INCENP in control (B) and CAP-D2 depleted (C) cells 65 hours after dsRNA treatment. Cells were grown on Concanavalin A coverslips for the last 24 hrs, fixed and stained for INCENP (red), α-tubulin (green), and DNA (blue). In comparison to control prometaphase cells, INCENP occupies a more extensive area on prometaphase chromosomes (C1) after CAP-D2 depletion. In anaphase, INCENP is dispersed throughout the spindle and on the chromosomes (C2), or associates with the central spindle normally (C3). In cytokinesis, INCENP can be found abnormally on the chromosomes as well as the midbody (C4), or just at the midbody as expected (C5). The scale bar represents 10μm

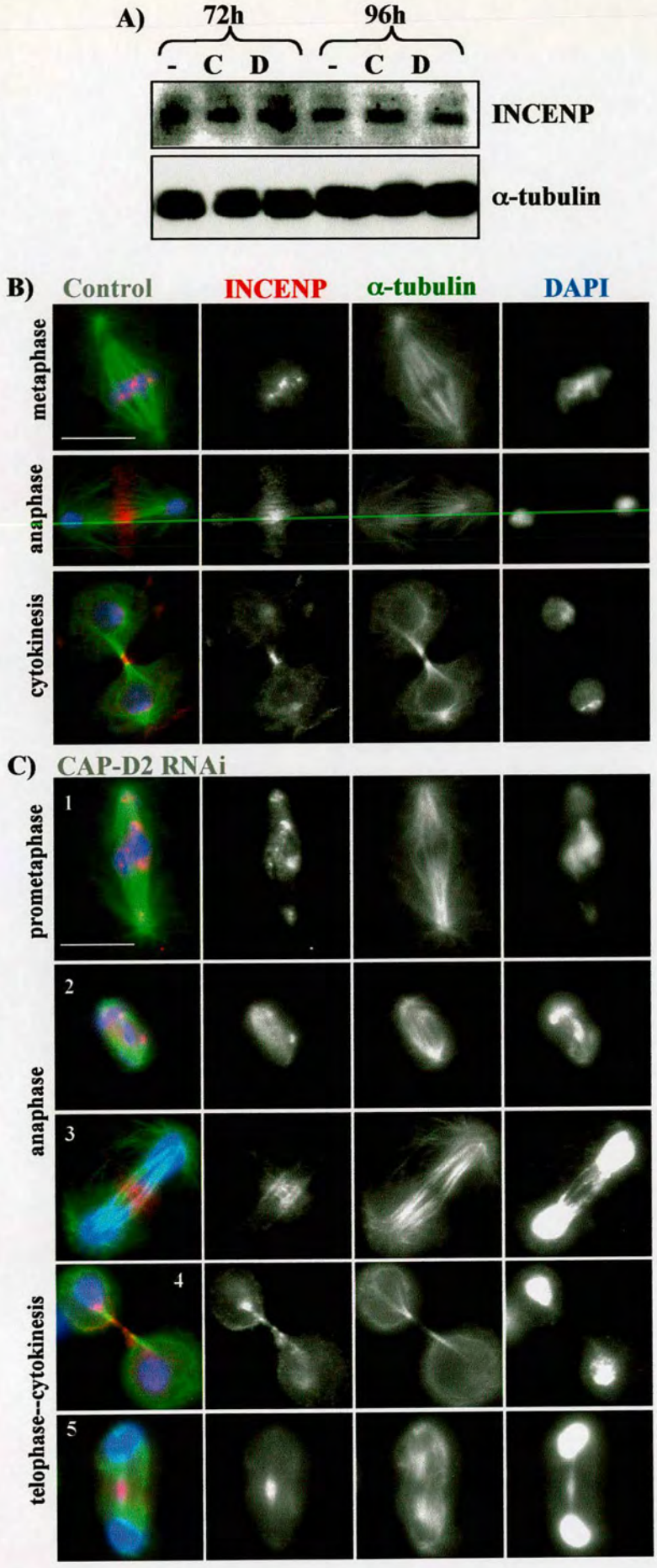
A)
72h
96h
- C D - C D
INCENP
α-tubulin
B)
Control
INCENP
α-tubulin
DAPI
metaphase
anaphase
cytokinesis
C)
CAP-D2 RNAi
prometaphase
anaphase
telophase--cytokinesis
1
2
3
4
5

4.8.2. Metaphase checkpoint

BubR1 is a metaphase checkpoint protein kinase that 'senses' the completion of chromosome alignment at the metaphase plate. It associates with kinetochores during prophase and dissociates from kinetochores that have made stable attachments to the spindle (Chen et al., 2002; Jablonski et al., 1998; Taylor et al., 2001). To examine the status of the metaphase checkpoint in CAP-D2 depleted cells, cells grown on Concanavalin A coverslips were analysed for BubR1 and α-tubulin 65 hours after dsRNA treatment. In control cells, BubR1 associated with chromosomes that were not yet aligned to the metaphase plate while BubR1 signal was greatly reduced in chromosomes that had satisfied the metaphase checkpoint by achieving alignment on the metaphase plate (Figure 4.16 A, upper). As expected during anaphase, BubR1 was undetectable at kinetochores (Figure 4.16 A, middle). Chromosomes in prometaphase/metaphase RNAi cells were normal with regard to appearance of BubR1 staining (Figure 4.16 B, upper two). However, there was still detectable BubR1 on anaphase and telophase chromosomes in CAP-D2 RNAi cells (Figure 4.16 B, lower two). Though these cells had proceeded into anaphase, paradoxically they behaved as though the checkpoint was still operative, exhibiting evident BubR1 localization. These cells apparently were not satisfied for the metaphase checkpoint but they nevertheless proceeded into anaphase. It is also possible that cells never entered metaphase and that they proceeded from prometaphase directly into anaphase with unaligned chromosomes never progressing onto the metaphase plate. This could explain the fact that spindle poles have an intense BubR1 signal (Figure 4.16 B, arrows). Also this possibility is consistent with what was observed after staining for DSA1/CID. CAP-D2 depleted cells in early anaphase (negative for DSA1) had unaligned chromosomes with two CID spots, which failed to bi-orient properly on the metaphase plate and individual chromatids never separated during anaphase (Figure 4.5 C3 and C4). However, it could be possible that BubR1 epitopes were more accessible to the antibody, since the chromatin was not organised properly, and thus a BubR1 signal is still detected on chromosomes. As observed for CID, the BubR1 signal was also stretched along chromatin, suggesting that

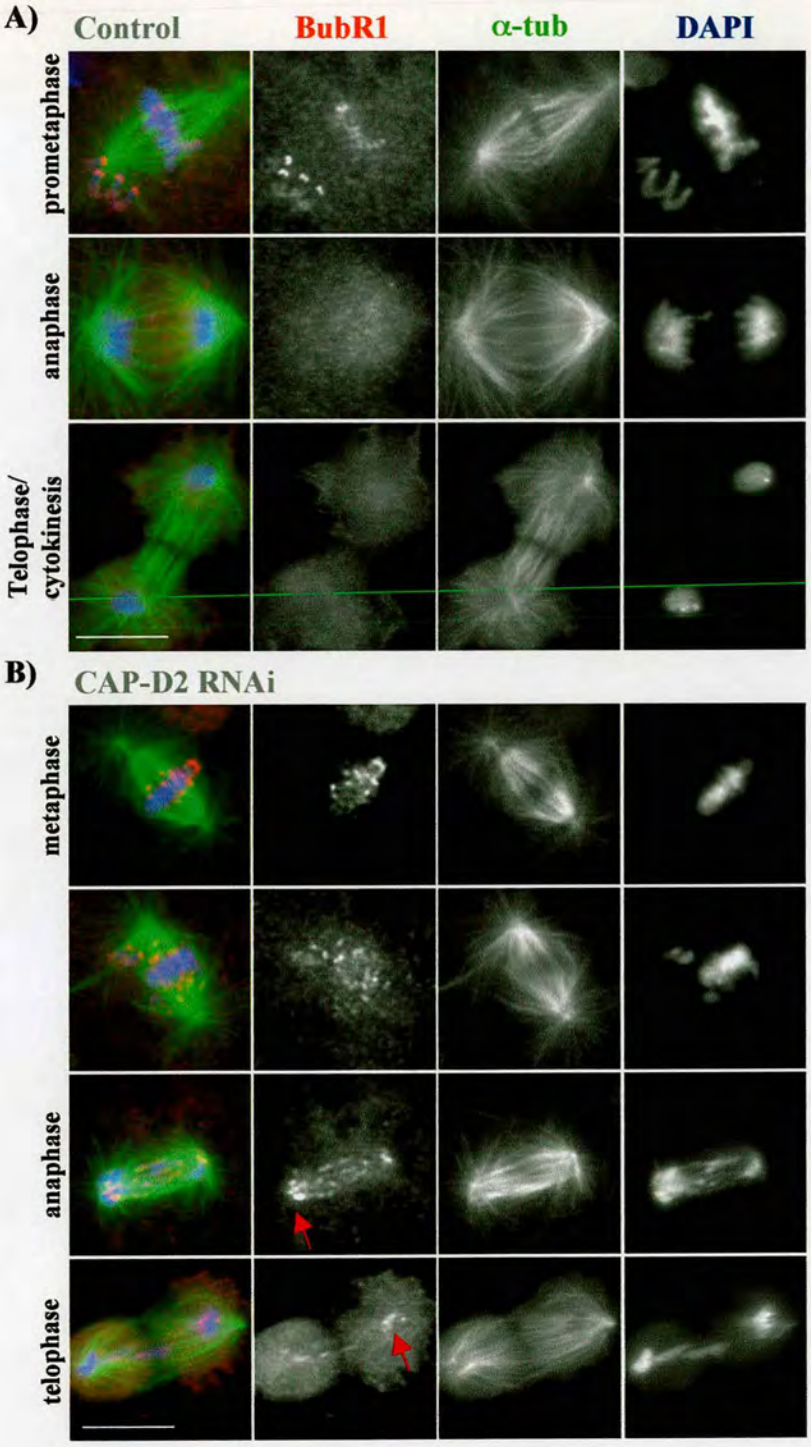

Figure 4.16. Aberrant behaviour of BubR1, a metaphase checkpoint protein, after CAP-D2 depletion.

Control (A) and CAP-D2 depleted (B) cells were processed 65 hours after dsRNAi treatment, grown on Concanavalin A coverslips for the last 24 hrs, fixed and stained for BubR1 (red), α-tubulin (green), and DNA (blue). CAP-D2 depleted cells that are in anaphase or telophase (arrows), as determined from chromosome morphology and from comparison with cells that were stained with Cyclin B or DSA1, have BubR1 on their centromeres, while it is undetectable on centromeres of aligned and separated chromosomes in wild type cells. The scale bar is 10 μm.

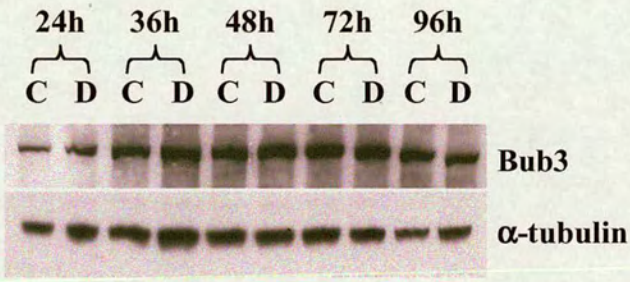

Figure 4.17. Bub3 levels are unaffected in the CAP-D2 depleted cells
Immunoblot analysis of control (C) and CAP-D2 (D) depleted cells with the Bub3 antibody. Bub3 protein levels are unaffected in the CAP-D2 depleted cells. C (control dsRNA), D (CAP-D2 dsRNA).

defective centromere resolution may have had additional consequences on the localization of at least one metaphase checkpoint component. Intriguingly, aberrant metaphase checkpoint behaviour after the depletion of CAP-D2 may be causal to the observed prometaphase delay.

As already mentioned previously, the *CAP-D2* gene is located in the 3' UTR of the *bub3* gene. Despite the fact that depletion by RNAi should be specifically directed only against CAP-D2, I decided to check that Bub3 protein levels were not affected after CAP-D2 depletion. Immunoblot analysis of control and CAP-D2 depleted cells revealed that the levels of Bub3 were unaffected (Figure 4.17). Thus the checkpoint defects described above were not a consequence of indirect depletion of Bub3.

4.9. Depletion of both CAP-D2 and Topo II results in chromosome morphology no more severe than that observed in cells depleted for CAP-D2 alone

Since the resolution of sister chromatids was compromised in CAP-D2 depleted cells and Topo II is important for decatenating DNA strands, it seems likely that the condensin complex and Topo II collaborate to organise mitotic chromosomes. Furthermore, the phenotype observed in this study when CAP-D2 was depleted by RNAi, was very similar to the phenotype obtained after depletion of Topo II (Chang et al., 2003) (Figure 4.18 C and D). In order to determine if these proteins have similar or distinct roles in organising mitotic chromosomes, CAP-D2/Topo II double RNAi was performed. Immunoblotting showed that both proteins were greatly depleted 72 hours after treatment (Figure 4.18 A). Immunofluorescence analysis at 96 hours revealed that cells depleted for both proteins (Figure 4.19 B) exhibited an abnormal chromosome morphology and behaviour no more severe than in either of the single depletions (Figure 4.18 C and D). Surprisingly, the ability of chromosomes to compact appeared as it did in either single RNAi (compare Figure 4.18 C and D with 4.19 B). In addition, chromosomes in the double RNAi failed to resolve, and formed bridges during anaphase (Figure 4.19 B). Chromosome congression defects, observed previously after Topo II depletion (Chang et al., 2003) were also noted (Figure 4.18 D, top two and 4.19 B, top).

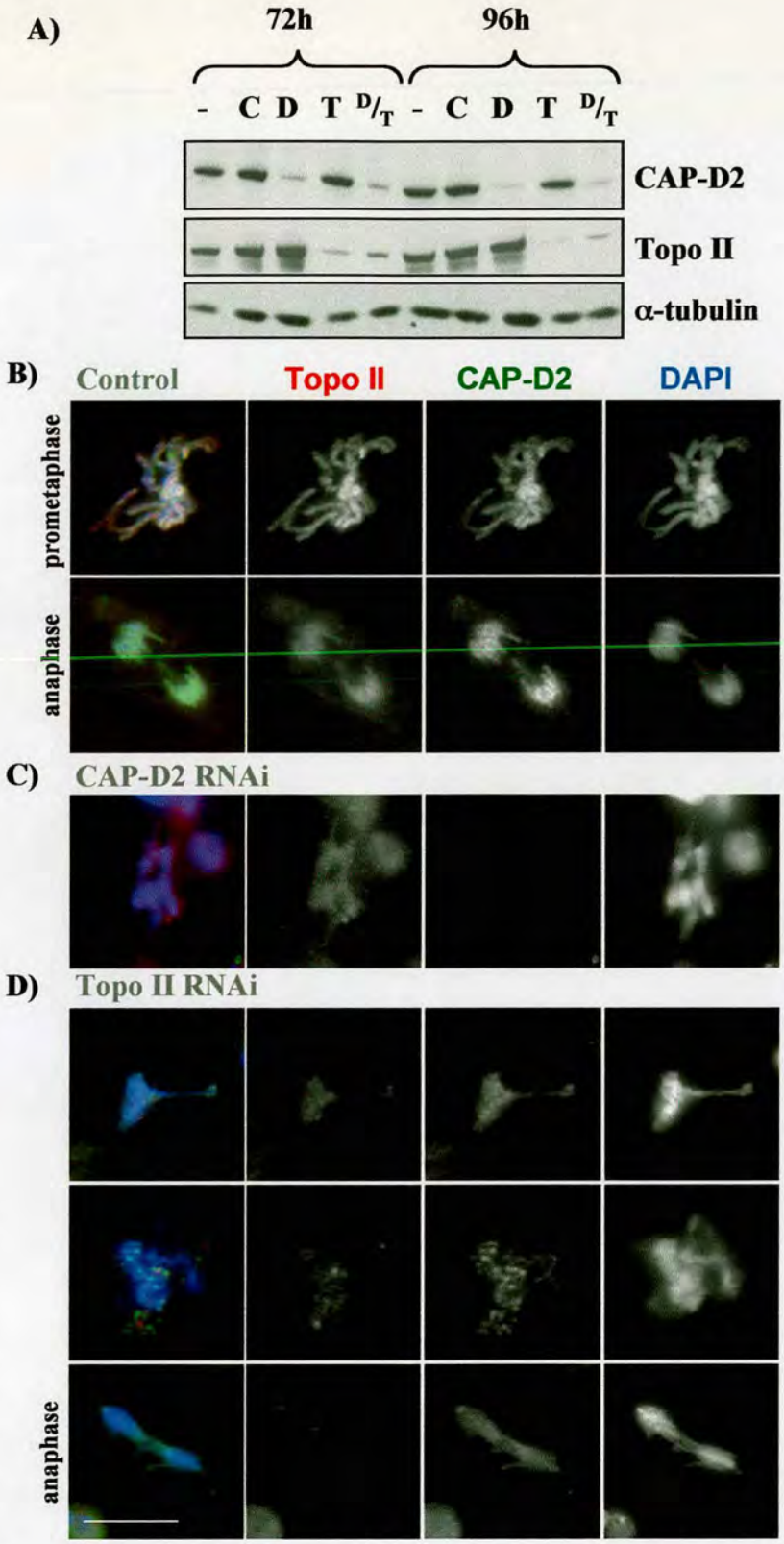

Figure 4.18. Depletion of CAP-D2 and DNA topoisomerase II results in a similar phenotype. **A.** The depletion of CAP-D2 and Topo II after treatment with two dsRNAs was assessed at 72 and 96 hours by immunoblot analysis. Both proteins were depleted with similar kinetics and they are almost undetectable by 96 hrs. α-tubulin was used as a loading control. - (no dsRNA), C (control dsRNA), D (CAP-D2 dsRNA), T (Topo II dsRNA), $^{D}/_{T}$ (CAP-D2/Topo II dsRNA). **B, C and D**. Analysis of the chromosome morphology in control (B) CAP-D2 (C) and Topo II (D) depleted cells. Cells were cytospun onto poly-L-lysine slides, extracted during fixation and stained for Topo II (red), CAP-D2 (green), and DNA (blue), 96 hours after the dsRNA treatment. Chromosome morphology was abnormal and remarkably similar between the two experiments. Note the chromosome congression defect after Topo II depletion. The scale bar is 10 μm.

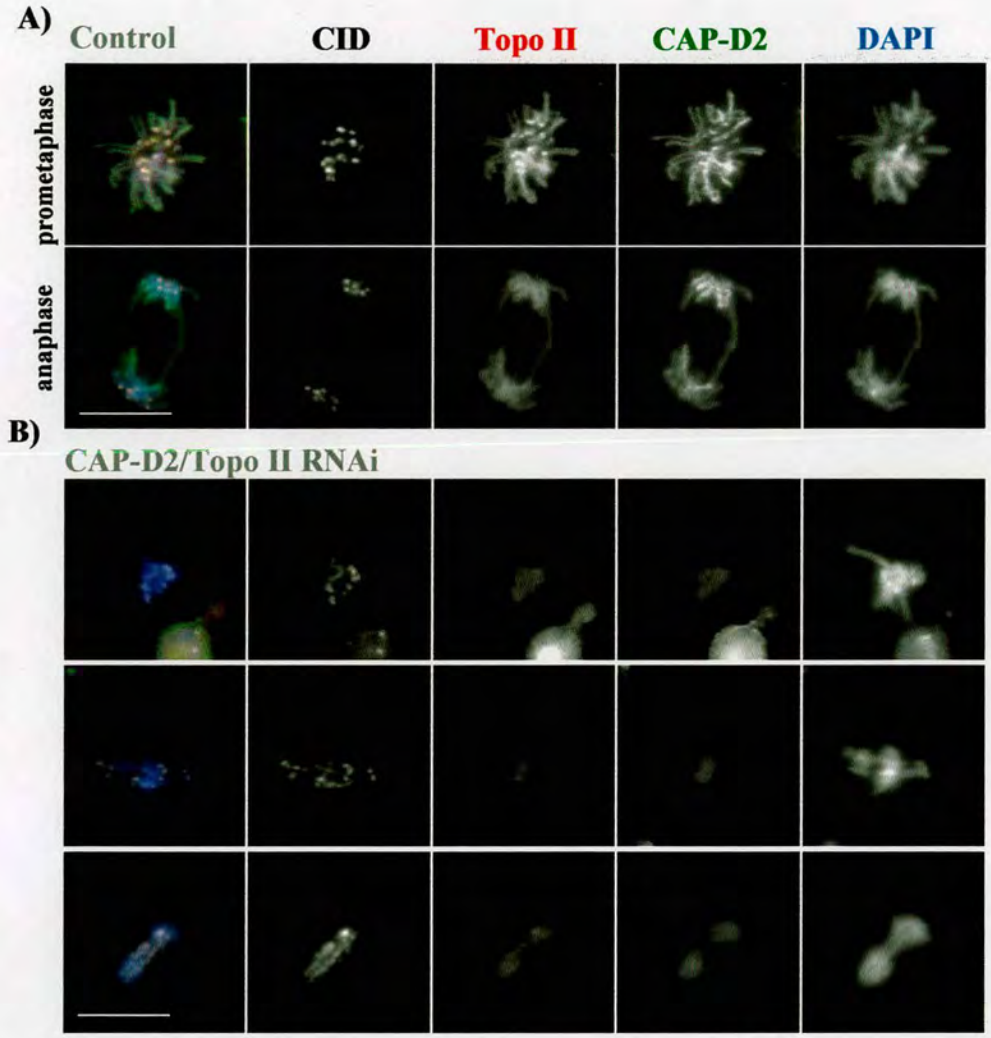

Figure 4.19. Analysis of the chromosome morphology in control (A) and CAP-D2/Topo II doubly-depleted (B) cells. Cells were cytospun onto poly-L-lysine slides, extracted during fixation and stained for Topo II (red), CAP-D2 (green), CID (white) and DNA (blue), 96 hours after the dsRNA treatment. Chromosome morphology was abnormal and remarkably similar to that observed after single CAP-D2 and Topo II RNAi. Centromeres were stretched along the chromatin in anaphase as observed after CAP-D2 depletion alone. The scale bar is 10 μm.

A)

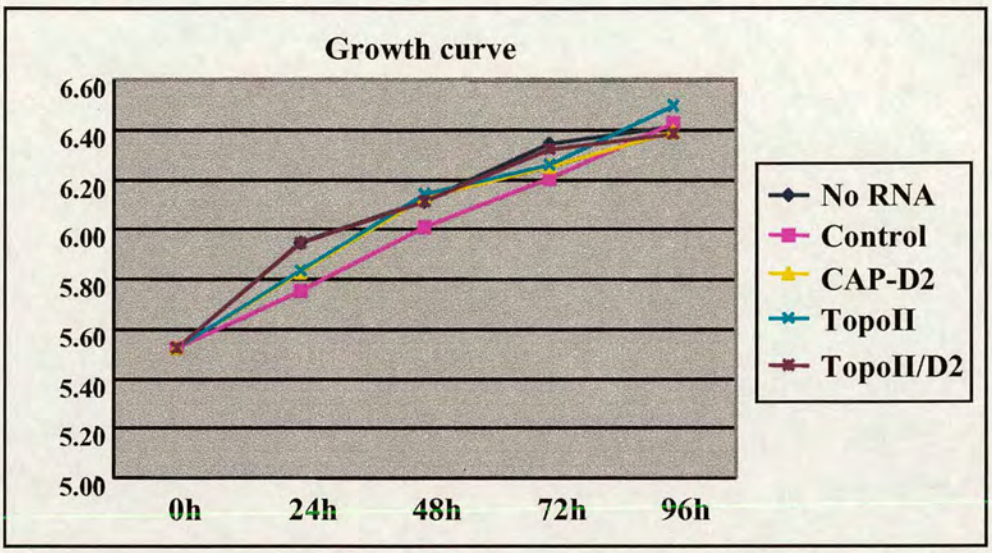

B)

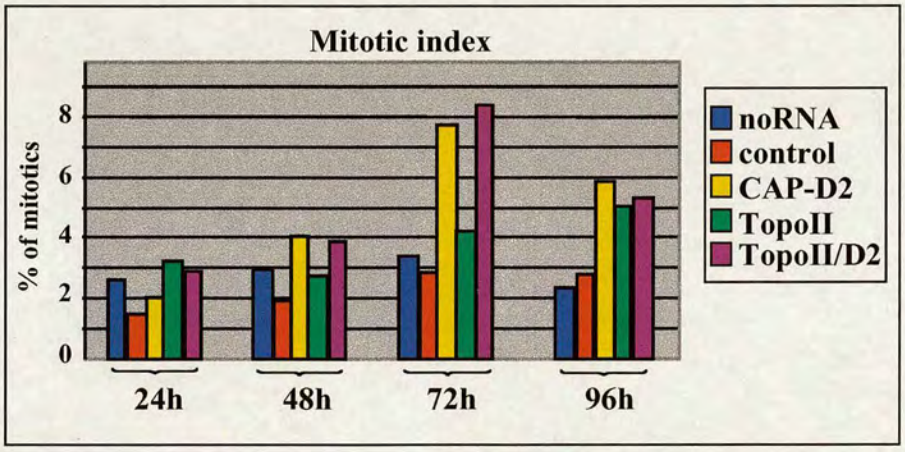

Figure 4.20.

A. Growth curve showing the number of cells at different time points after CAP-D2 and Topo II single depletions and CAP-D2/Topo II double depletion. Cells grow with similar kinetics in controls and single and double depletions.

B. Graph showing the percentage of mitotic cells in control and RNAi cells. The percentage of mitotic cells was increased 2-3 fold in the CAP-D2 RNAi single depletion and CAP-D2/Topo II double depletion at 72 and 96 hours. The mitotic index was mainly increased at 96 hours in the single Topo II depletion.

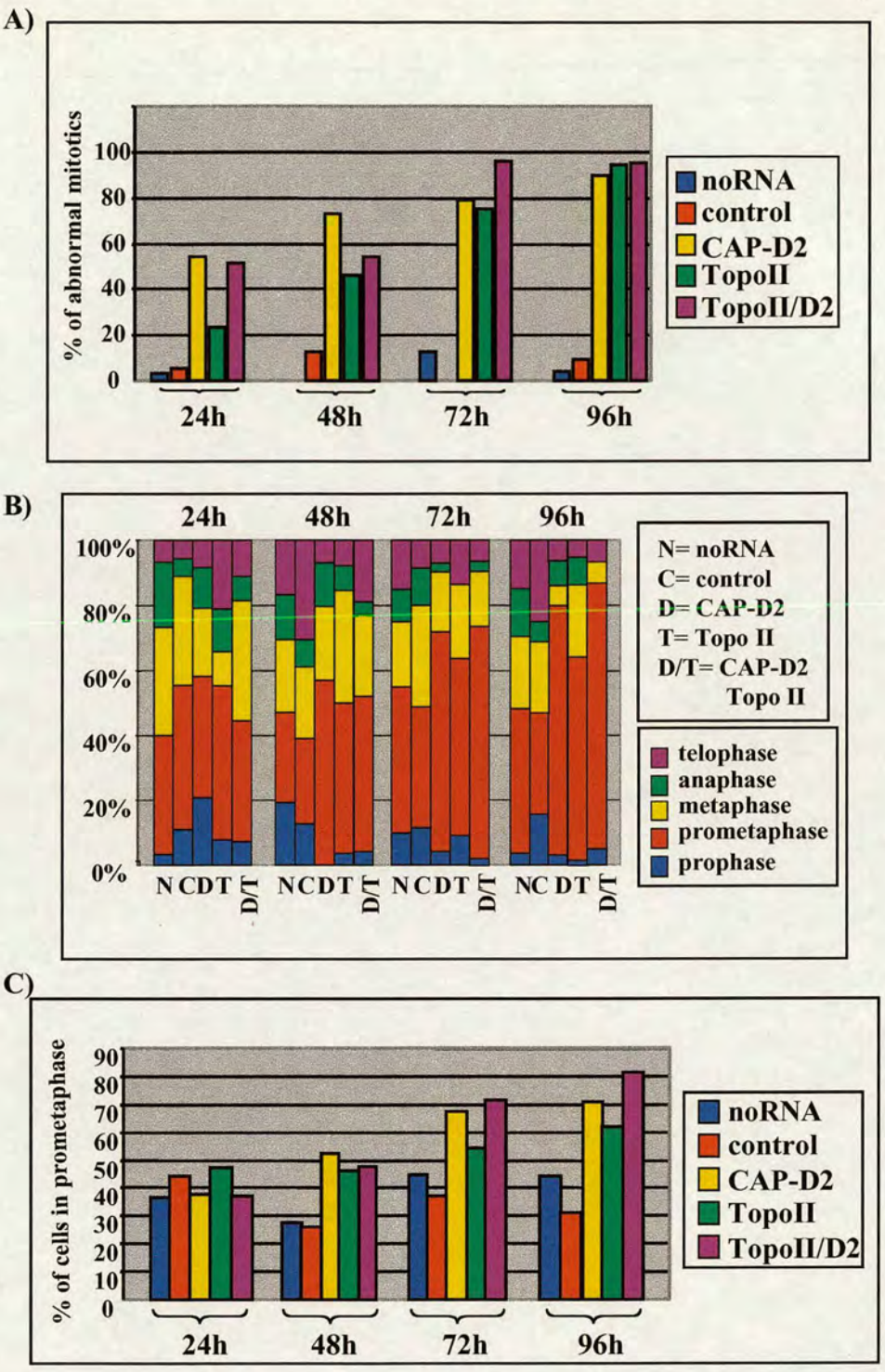

Figure 4.21.

A. Graph showing the percentage of abnormal mitotic cells in control, CAP-D2 and Topo II RNAi single depletions and CAP-D2/Topo II double depletions. The majority of cells are abnormal, 72 hours after dsRNAi treatment in both single and double depletion.

B. Graph showing the distribution of mitotic cells in the different mitotic phases after staining with Cyclin B/P~H3/α-tubulin, in control and RNAi cells

C. Graph showing the percentage of prometaphase cells after staining with Cyclin B/P~H3/α-tubulin, in control and RNAi cells. There was a pronounced prometaphase delay between 48 and 96 hours in the CAP-D2 depleted and CAP-D2/Topo II depleted cells. In the Topo II depleted cells there was a prometaphase delay but not as significant as in the CAP-D2 single and the double experiment.

A)

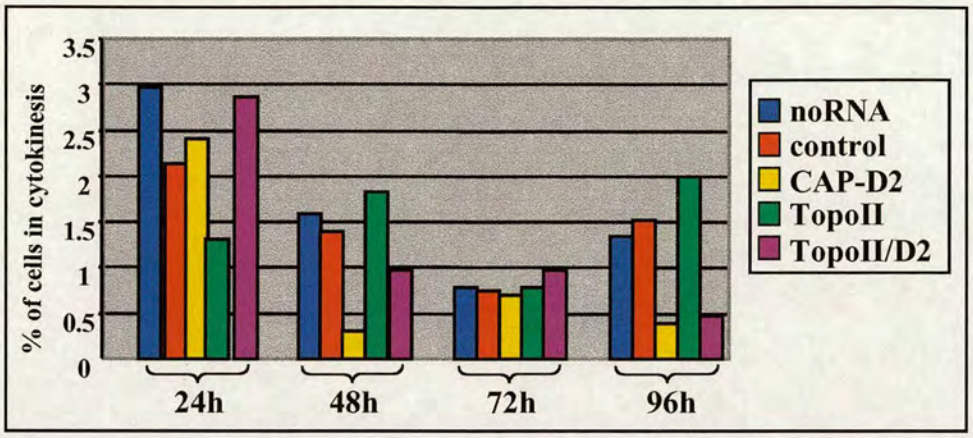

B)

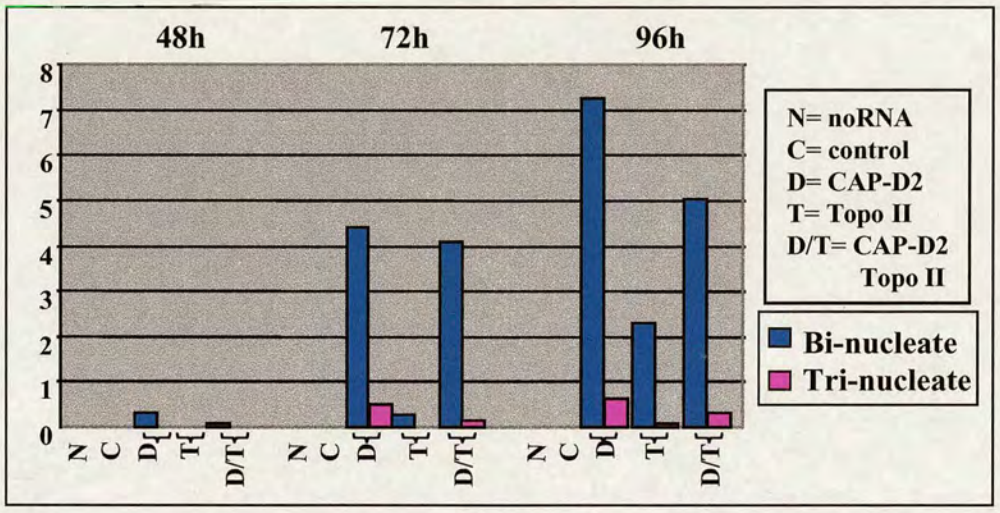

Figure 4.22

A. Graph showing the percentage of cells in cytokinesis in control, CAP-D2 and Topo II RNAi single depletions and CAP-D2/Topo II double depletion.

The percentage of cells in cytokinesis is very low in the CAP-D2 single and CAP-D2/Topo II double depletions 48 hours after dsRNAi. The percentage in the Topo II single depletion is very similar to the controls.

B. Graph showing the percentage of bi- and tri- nucleate cells in control and RNAi cells. The percentage of bi- and tri- nucleate cells increases by time in both the single and double depletions.

After counting the number of viable cells it was obvious that RNAi cells grew with similar kinetics as control cells (Figure 4.20 A). Different time points were assessed for mitotic index and the distribution of mitotic phases. The percentage of cells positive for histone H3 phosphorylated on Serine 10 (P~H3) was increased 2-3 fold in the double RNAi compare to the single CAP-D2 RNAi between 72 and 96 hours (7.7% versus 3.1% at 72 hours) (Figure 4.20 B). In the Topo II single depletion the mitotic index was similar to controls at 72 hours but was slightly higher at 96 hours (4.6% versus 2.5%). The number of abnormal mitotic cells was similar between the single and double depletions and increased over time (Figure 4.21 A). Cells were categorised into the different phases of mitosis by using P~H3/α-tubulin/Cyclin B triple staining (Figure 4.21 B). There was a pronounced prometaphase delay between 48 hours and 96 hours in the CAP-D2 single and the CAP-D2/Topo II double depletions (about 2-fold increase), while no significant prometaphase delay could be seen in the Topo II single depletion (Figure 4.21 C). Finally bi- and tri- nucleate cells were observed in equal levels in both the double and single depletions (Figure 4.22 B).

In order to better assess the different phenotypes of the single and double depletions, metaphase chromosome spreads were performed after cells were treated with colchicine. RNAi treated and control cells were cytospun onto poly-L-lysine slides and stained for CAP-D2, TopoII and DNA. The control cells displayed the typical X-shaped structure and sister chromatids were properly resolved. Both CAP-D2 and Topo II localised axially along the length of the chromosomes and the two proteins partially co-localised. (Figure 4.23 A1, A2 and 4.23 B, control). In both Topo II and CAP-D2 single depletions and in the TopoII/CAP-D2 double depletion chromosome morphology was very abnormal. The structural integrity of these chromosomes was compromised with chromatin appearing torn and stretched. No axial staining could be observed in either experiment (Figure 4.23 A3, A4 and A5). However Topo II levels were not significantly affected in the CAP-D2 RNAi, as previously mentioned (Figure 4.23 A3). Similarly, levels of CAP-D2 were not affected in the Topo II depleted cells (Figure 4.23 A4), which is consistent with previous observations for Barren localisation (Chang et al., 2003). When individual chromosomes were observed it was apparent that sister

Figure 4.23. Depletion of CAP-D2 and DNA Topoisomerase II in colchicine treated S2 cells

A and B. Metaphase chromosome spreads of control, Topo II depleted cells, CAP-D2 depleted cells and CAP-D2/Topo II doubly-depleted cells, after cells were treated with colchicine. Cells were cytospun onto poly-L-lysine slides, extracted during fixation and stained for Topo II (red), CAP-D2 (green) and DNA (blue), 74 hours after dsRNA treatment. **A.** Control cells displayed the typical X-shaped structure and sister chromatids could be easily distinguished. Both CAP-D2 and TopoII localised axially along the length of the chromosomes and the two proteins were partially colocalised (A1, A2 and B, Control). In Topo II (A3) and CAP-D2 (A4) single depletions and in the CAP-D2/Topo II double depletion (A5) no sister chromatid resolution could be observed and chromosomes appeared fuzzy. The scale bar is 10 μm.

B. Individual chromosomes observed in chromosome spreads. The phenotype was similar between the two single (CAP-D2 RNAi and Topo II RNAi) and the double (CAP-D2/Topo II RNAi) experiments. Chromosomes appeared unresolved and fuzzy.

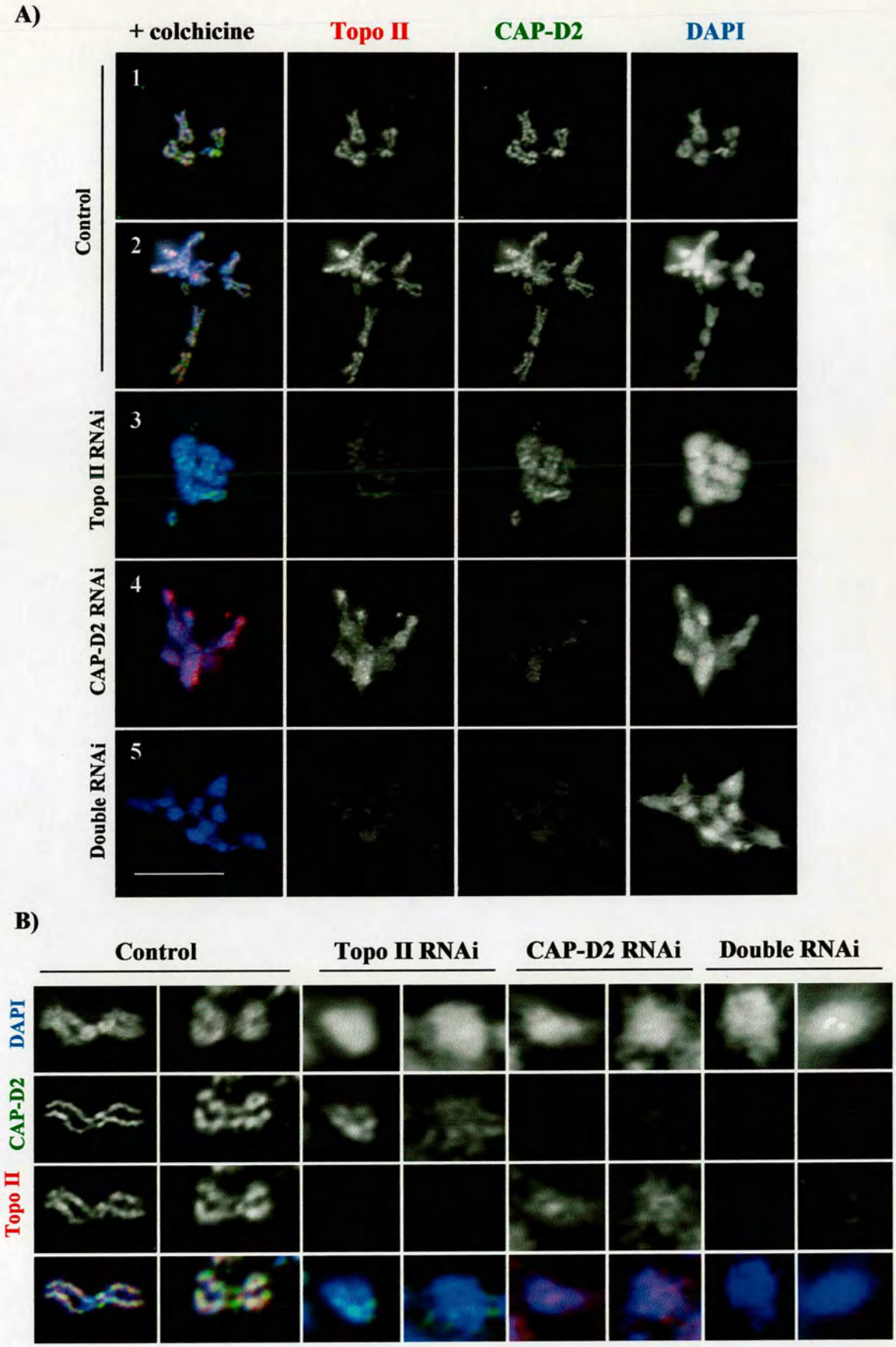
A)
+ colchicine
Topo II
CAP-D2
DAPI
Control
Topo II RNAi
CAP-D2 RNAi
Double RNAi
1
2
3
4
5
B)
Control
Topo II RNAi
CAP-D2 RNAi
Double RNAi
DAPI
CAP-D2
Topo II

chromatids were not resolved and chromosomes appeared fuzzy and diffuse (Figure 4.23 B). The phenotype was similar between the single and double depletion experiments as chromosomes appeared well compacted but unresolved. Since no difference in phenotype was observed at this level between the CAP-D2, Topo II and CAP-D2/Topo II doubly depleted cells, it appears most likely that Topo II and the condensin complex participate in the same pathway to resolve sister chromatids. It is therefore suggested that additional, as yet unidentified, factors are required for to bring about appropriate chromosome compaction during mitosis.

4.10. Reciprocal dependence on stability: CAP-D2 is unstable in a barren mutant

Depletion of the CAP-D2 protein by dsRNAi affected the stability of the CAP-H/Barren protein. To test if reciprocal stability was true (i.e. the levels of CAP-D2 protein were affected by the absence of CAP-H/Barren), a *barren* mutant, $barr^{L305}$, was examined. $barr^{L305}$ is a null mutation which causes lethality late in embryogenesis (Bhat et al., 1996). Analysis by immunoblotting of embryonic extract from *barr* homozygous embryos (~12-13 hours old) showed that when the level of Barren was decreased, CAP-D2 was greatly reduced as well (Figure 4.24 A). Quantitation of protein levels using phosphorimaging revealed that Barren was decreased 8-fold compared to wild type embryos while the level of CAP-D2 was 6-fold lower. The fact that both proteins were decreased to nearly the same extent strongly suggests that the two proteins are tightly associated with each other and that they very likely depend on each other for stability. The residual Barren protein on the blot was a maternal contribution to the embryos. When the same membrane was reprobed with antibodies to SMC2 and SMC4 subunits, it was obvious that their levels were also reduced but not to the same extent (Figure 4.24 A). Quantitative analysis showed that SMC2 was reduced 4-fold and SMC4 3.5-fold, consistent with participation of some of the two SMC proteins in a second complex. It is possible, of course, that some of the remaining SMC proteins are maternal components that are quite stable (see $gluon^{17C}$ mutant). Quantitations were repeated twice in two independent experiments. The presence and stability of Scc1/Drad21, a member of the

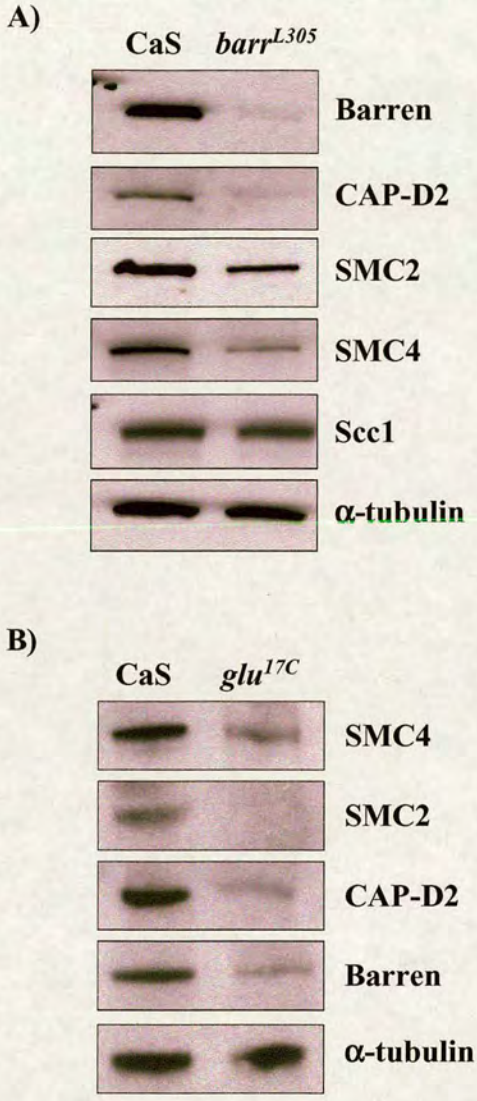

Figure 4.24. Instability of additional condensin subunits after mutation of only one in *Drosophila*. **A.** CAP-D2 is unstable when Barren is absent in a *barr*^{L305} mutant. Immunoblot of embryonic extract from 12-13hours wild type (Canton S) and *barr*^{L305} homozygous embryos shows that Barren is almost undetectable in homozygous mutant embryos. The remaining protein is the maternal contribution to the embryos. The membrane was probed for Barren, CAP-D2, SMC2, SMC4 and Scc1 and the decrease in protein level was calculated using phosphorimaging. 5 embryos were loaded per lane. Barren levels decreased 8-fold, CAP-D2 levels decreased 6-fold and SMC2 and SMC4 levels decreased 4-fold and 3.5-fold respectively. α-tubulin was used as a loading control. **B.** Stability of other condensin subunits in an SMC4 (*gluon*^{17C}) mutation. Immunoblot of embryonic extract from 12-13 hours wild type (Canton S) and *gluon*^{17C} homozygous embryos with the SMC4, SMC2, CAP-D2 and Barren antibodies. The levels of the four proteins were calculated using phosphorimaging. 5 embryos were loaded per lane. SMC4 shows a 5.9-fold decrease in protein levels, SMC2 shows a 5.6-fold decrease , while Barren and CAP-D2 show a 4.7-fold decrease. α-tubulin was used as a loading control.

cohesin complex (Vass et al., 2003), was analyzed as well. This protein appeared to be unaffected, as was the level of α-tubulin, by mutation of CAP-H/Barren (Figure 4.24 A).

The stability of the condensin subunits was also examined in an SMC4 mutant, *gluon*^{17C}. This is an embryonic lethal null mutation for SMC4, that removes approximately 31 kb including the SMC4 gene (accession AJ543652). Analysis by quantitative immunoblotting of *gluon*^{17C} embryonic extract (~12-13 hours old) showed that the SMC4 protein was decreased 5.9-fold compared to wild type embryos (Figure 4.24 B). The existence of residual protein suggested that the maternal component was possibly quite stable, or that the remaining protein may be required later in development for another function. When the levels of the rest of the subunits were assessed, it was observed that the SMC2 subunit was decreased to the same extent as SMC4 (5.6 fold), while CAP-D2 and CAP-H/Barren were reduced 4.7-fold (Figure 4.24 B). These results revealed that in the absence of one of the condensin subunits in *Drosophila*, the abundance and stability of the rest were affected. Furthermore, the strength of the interactions between the four examined members of the condensin complex appears to vary as the non-SMC subunits, CAP-D2 and CAP-H/Barren, show similar tight dependencies on one another for stability in the animal and in cultured cells.

4.11. In vivo analysis of CAP-D2 function

The functional analysis of CAP-D2 described above was carried out in tissue culture cells. It would be interesting to assess the CAP-D2 function in an in vivo system. For this reason I attempted to inject syncytial *Drosophila* embryos that were expressing H2A-GFP with the CAP-D2 antibody. Therefore, it was able to observe the phenotype caused in the absence of CAP-D2 and also to calculate the time of the delay in each mitotic phase. For this reason the CAP-D2 antibody was dialysed in a specific buffer as described in Chapter 2 and it was injected into embryos. Unfortunately, no phenotype was observed. At the same time the buffer alone was injected as a control. Even though the antibody was concentrated before the injections, it is possible that it was not concentrated enough in order to cause loss of CAP-D2 function. Nevertheless, no further attempts were carried out with this analysis.

CHAPTER 5

Characterisation of *JSL2* - an *SMC2* mutation

5.1. Introduction

An EMS mutagenesis screen that took place in Dr. Jeff Sekelsky's lab at the University of North Carolina, generated seven lethal lines named *JSL-2*,-6,-10,-11,-12,-13,-14. His lab was interested in the Ercc1 (excision repair endonuclease) protein, which maps close to the *SMC2* locus (CG10212), a subunit of the condensin complex. The seven lines were not disrupting the *ercc1* gene, thus they were sent to our lab in order to be analysed as potential *SMC2* mutations. An honours student in the lab in 2001, Hannah Townley, crossed each line to the others in order to characterise which of these lines were allelic. *JSL-6* and —10 were allelic and *JSL-10* and -11 as well. Also she found that *JSL- 6*, 10, 13, 14 were embryonic lethal and *JSL-2*, 11, and 12 were larval lethal. By analysing the larval lethal lines by immunoblotting with an antibody against SMC2, she found that only the *JSL2* line lacked the 136 kDa band that was present in the wild type and corresponded to the SMC2 protein. Also a smaller protein of about 57 kDA was present in the mutant extracts, but it was absent from the wild type. Homozygous mutant larvae could reach the point of third instar before dying. The mutation was carried over the *CyO-GFP* balancer and homozygous larvae could be easily selected under the fluorescence microscope. The next step was to sequence the mutation in order to confirm that the mutation was affecting the *SMC2* gene. My contribution to this project involves the sequencing of the mutation and its further characterisation.

5.2. Sequencing of the JSL2 mutation

The *SMC2* gene maps to the right arm of the second chromosome in the 51C5 region. A 4456 bp cDNA encodes a protein of 1179 amino acids (M_r=136 kDa). The gene consists of six introns and seven exons (Figure 5.1 A). In order to sequence the *JSL2* mutation, primers were designed to cover the whole gene including 500bp upstream and downstream of the *SMC2* gene (Figure 5.2) (Table VII and VIII. Primers SMC2-1 to -36 were designed by Neville Cobbe, a PhD student in the lab before I arrived).

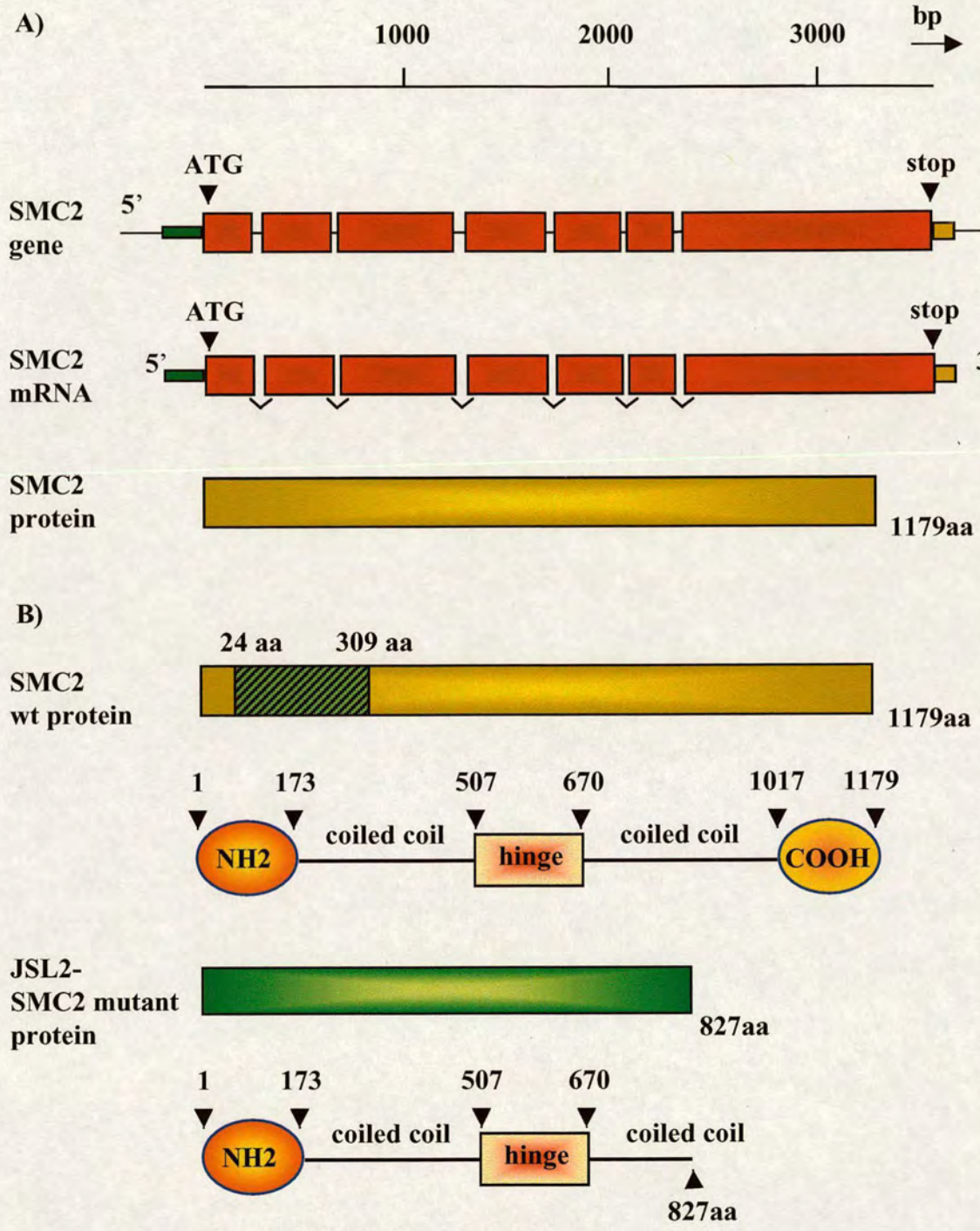

Figure 5.1. A. Representation of the *DmSMC2* gene. The gene consists of 6 introns and 7 exons. A 4456 bp cDNA encodes for a protein of 1180 amino acid residues. **B.** Sequencing of *JSL2*, an *SMC2* mutation, revealed that cytidine was substituted by thymidine at the position 2482 of the coding sequence, causing a stop codon in the place of glutamine and the production of a truncated protein of 827 amino acid residues. The truncated protein lacks the carboxyl globular domain and a part of the coiled coil sequence, which are necessary for the function of the SMC2 protein. Amino acids 24-309 (green box with diagonal lines on wild type SMC2 protein) represent the protein region that was used for the generation of the SMC2 antibody.

Genomic DNA was extracted from homozygous second instar *JSL2* larvae. The size of the homozygous *JSL2* larvae was almost one third of the wild type and that made the work difficult. The reason that second instar larvae were selected was that the *JSL2* homozygous flies were dying as second instar larvae instead of third instar, a year after the mutation arrived in the lab, probably because additional mutations were introduced into the stock during its maintenance. The gene was amplified by PCR by using different combinations of primers (Table IX, Figure 5.4 and 5.5). The PCR products covered the whole gene and were usually overlapping in order to confirm the sequencing results (Figure 5.2). PFU, a proof reading polymerase (3'→5' exonuclease activity, Promega), was used for PCR amplification in order to minimise any mistakes introduced by the enzyme. As a control, the wild type *SMC2* gene was amplified from wild type *CaS* third instar larval DNA using the same primer-pairs (Figure 5.3). The PCR products were then sequenced and the results were analysed by the *Lasergene* Navigator EditSeq alignment program. In the mutant sequence, a base was substituted (cytidine to thymidine) in the position 2482 of the coding sequence. This caused the change of the codon that encodes for the amino acid Glutamine (Q) to a stop codon (CAG codon to TAG codon) which should result in the synthesis of a truncated protein of about 827 amino acid residues (predicted M_r ~94 kDa). The truncated protein lacks the carboxyl globular domain and a part of the coiled-coil sequence, which presumably are necessary for the function of the SMC2 protein (Figure 5.1 B). In an immunoblot analysis, a band of about 52 kDa was recognised in the extract from homozygous mutant larvae, which was absent from the wild type (Figure 5.8). The size of this band was smaller than the estimated size. This could be due to the fact that the truncated protein is not stable and it gets degraded or that it runs anomalously on gels.

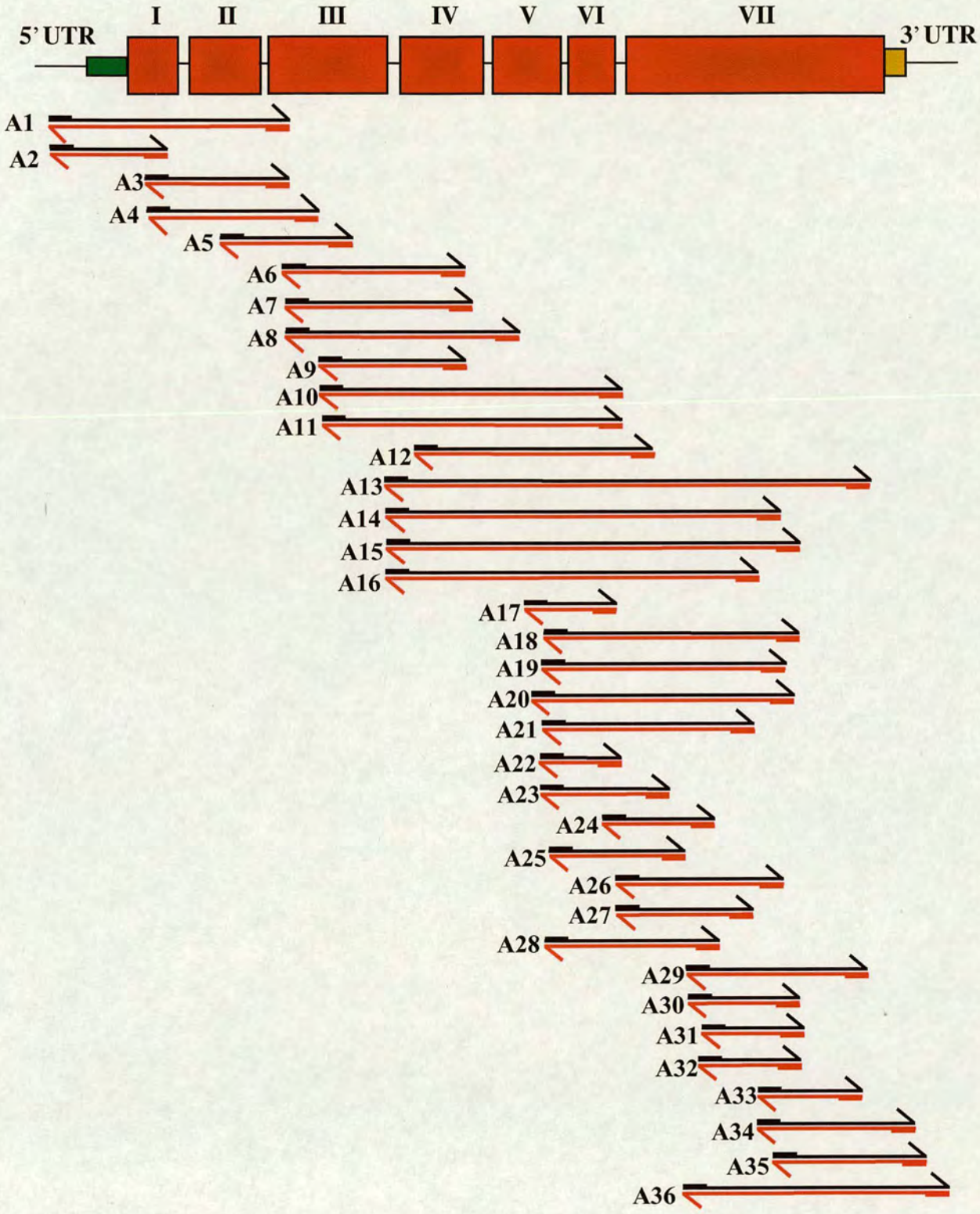

Figure 5.2. Strategy used for the amplification of *SMC2* gene. Primer pairs A1-36 are shown. The position of the primer pairs is shown relative to the *SMC2* gene regions. The numbers I-VII correspond to the seven exons of the *SMC2* gene. The 5' and 3'UTR's of the *SMC2* gene are shown as well. The primers used are summarised in Tables VII, VIII and IX.

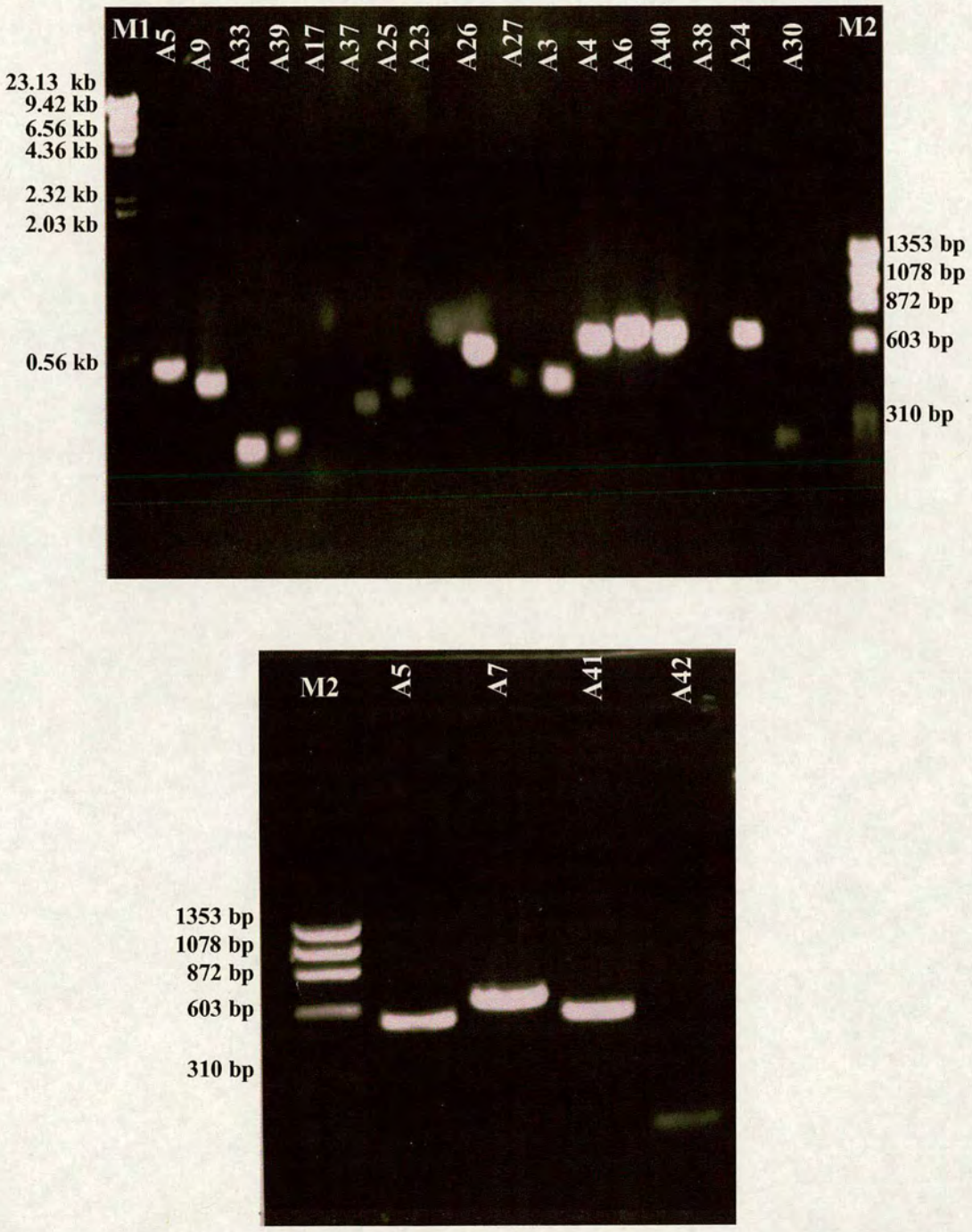

Figure 5.3 . PCR products after amplification of the *SMC2* gene from wild type *CaS* third instar larval genomic DNA. The primer pairs that were used to amplify each product are shown (A1-43). M1 and M2 are the λ phage digested with HindII and ϕX174 phage digested with HaeIII, molecular weight markers respectively.

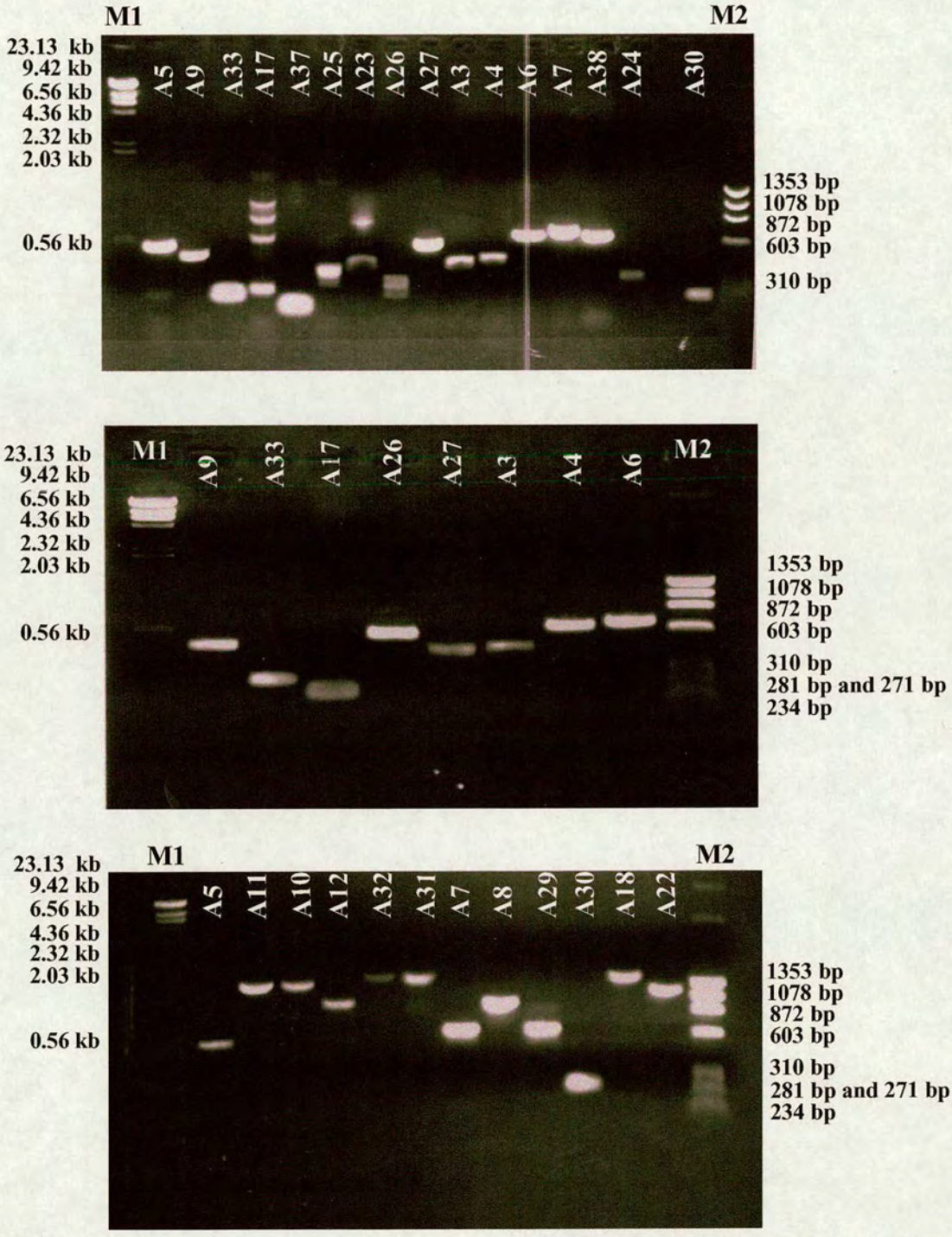

Figure 5.4 . PCR products after amplification of the *SMC2* gene from genomic DNA of *JSL2* homozygous second instar larvae. The primer pairs that were used to amplify each product are shown (A1-43). M1 and M2 are the λ phage digested with HindII and ϕX174 phage digested with HaeIII, molecular weight markers respectively.

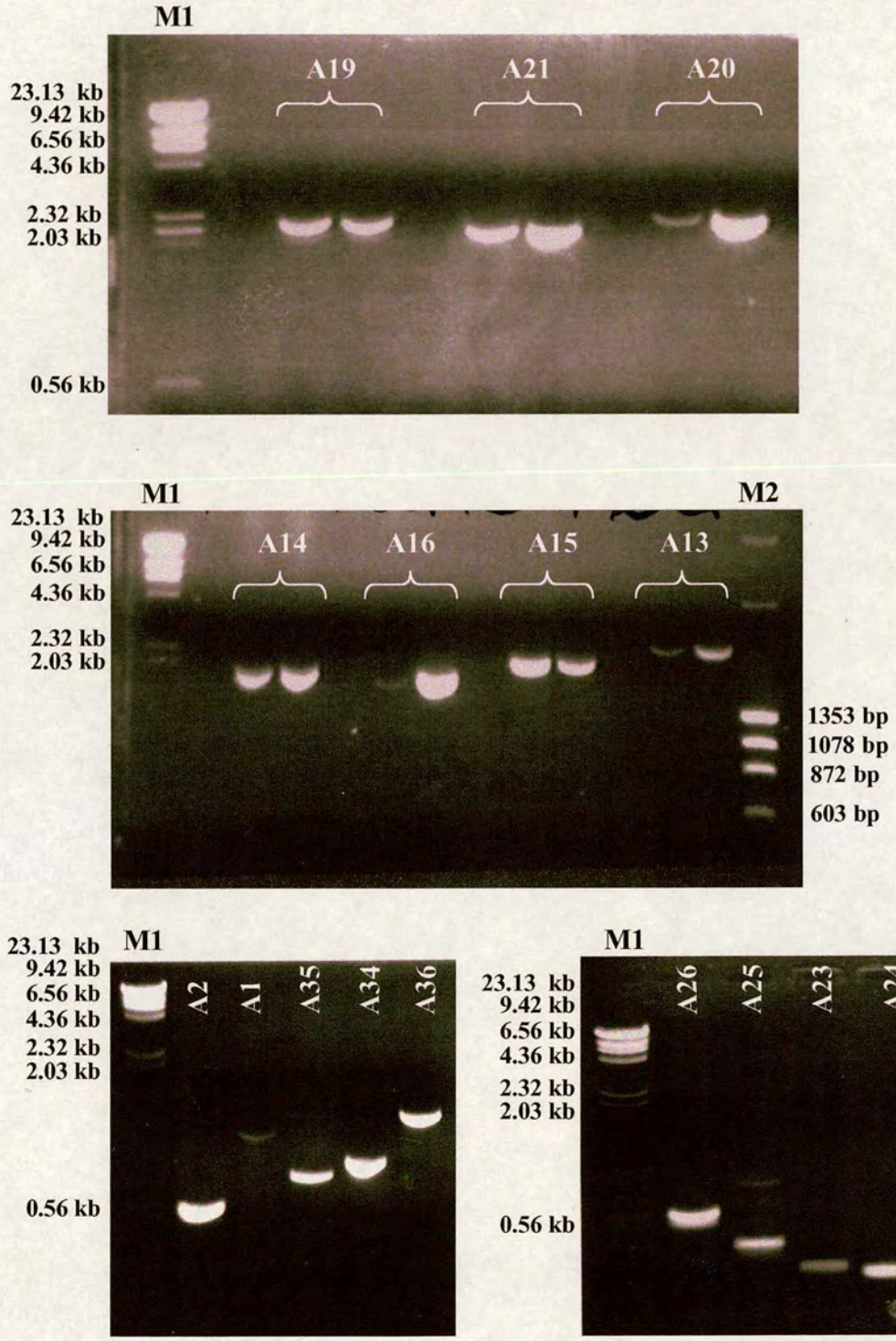

Figure 5.5 . PCR products after amplification of the *SMC2* gene from homozygous for the *JSL2* mutation second instar larval genomic DNA. The primer pairs that were used to amplify each product are shown (A1-43). M1 and M2 are the λ phage digested with HindII and ϕX174 phage digested with HaeIII, molecular weight markers respectively.

5.3. Genetic recombination of the JSL2 mutation

The homozygous *JSL2* flies were originally dying as third instar larvae, but a year after as second instar larvae, suggesting that possible modifiers or mutations were introduced into the stock during its maintenance. An additional mutation could cause several problems and could complicate the interpretation of the results during the characterisation of the *JSL2* mutant. Furthermore, due to smaller size, it is very difficult to dissect tissues, such as brains, from second instar larvae. Thus, a genetic recombination was necessary in order to clean the stock of any additional mutations beyond the *JSL2* mutation.

As mentioned above the *SMC2* gene is located on the second chromosome. There was a possibility that the additional mutation was in one of the other chromosomes and not on the second. Since the third chromosome is bigger than the second, and the fourth chromosome does not carry many genes it was possible that the background mutation was on the third chromosome. In this case genetic recombination of the second chromosome would not be necessary. In order to test this possibility, virgin females from the *JSL2* mutation were crossed with males from the *Bc, Gla/CyO-GFP* stock as follows:

$$\frac{JSL2}{CyO\text{ - }GFP} \times \frac{Bc,\ Gla}{CyO\text{ - }GFP}$$

$$\downarrow$$

$$\frac{JSL2}{CyO\text{ - }GFP} \quad \frac{Bc,\ Gla}{CyO\text{ - }GFP} \quad \frac{Bc,\ Gla}{JSL2} \quad \frac{CyO\text{ - }GFP}{CyO\text{ - }GFP}$$

where *Gla* is a marker on the second chromosome, which gives a dark, smaller and smoother eye phenotype and *CyO* is a balancer chromosome which precludes recombination of the second chromosome and it carries the dominant marker *Curly* (*Cy*) which gives curly wings, and a recessive lethal mutation causing embryonic lethality.

Virgin female *JSL2/CyO-GFP* progeny were selected and crossed again with male *Bc, Gla/CyO-GFP*. This cross was repeated three times and finally *JSL2/CyO-GFP* progeny were selected and the stock was expanded. The *JSL2/CyO-GFP* progeny were distinguished as they had normal eyes (absence of *Bc, Gla*). The *CyO-GFP/CyO-GFP* progeny do not make it to adults. By following this procedure all chromosomes except for the second could swap or even recombine with their homologs between the *JSL2/CyO-GFP* and *Bc, Gla/CyO-GFP* stocks and thus the *JSL2/CyO-GFP* could be cleaned up from the background mutation. Recombination events though would mostly happen between the homologs of the third chromosome since recombination does not occur on the fourth chromosome and the X or Y chromosomes.

In order to test if the additional mutation was lost after chromosomes were 'cleaned up' as described above, *JSL2/CyO-GFP* progeny were crossed between them. Homozygous progeny for the *JSL2* mutation (*JSL2/JSL2*) were selected under a fluorescence microscope as they were negative for GFP. After a lethality test was performed on these progeny, it was obvious that the homozygotes for the *JSL2* mutation were still dying at second instar larvae and no improvement was observed on their size. This result suggested that the additional mutation was probably on the second chromosome and thus genetic recombination of this chromosome was necessary.

5.4. Genetic recombination of the second chromosome of the JSL2 line

For the genetic recombination of the second chromosome two stocks with multiple markers on the second chromosome were used. The first one was the *4187/CyO* (*al, dp, b, pr, cn, c, px, sp/CyO*) and the second was the *4347/CyO* (*al, dp, b, pr, Bl, cn, c, px, sp/CyO*). The *SMC2* gene is mapped at the 51C5 chromosome locus and is located between the *cinnabar* (*cn*) and *curved* (*c*) markers (Figure.5.6). The original *JSL2* line had the *cn* (*cinnabar*), *br* (*brown*) and *sp* (*speck*) markers on the second chromosome as well.

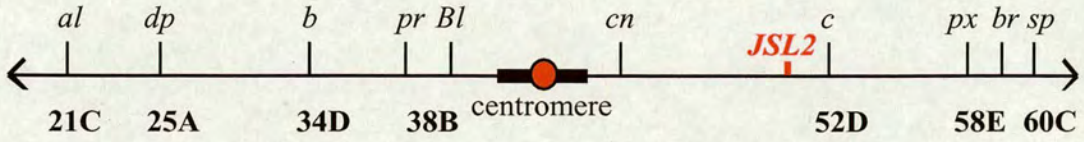

Figure 5.6. Map of the second chromosome

Initially the following cross was performed:

$$\frac{cn,\ JSL2,\ sp}{CyO\text{-}GFP} \times \frac{4187}{CyO}$$

$$\downarrow$$

$$\frac{cn,\ JSL2,\ sp}{CyO} \quad \frac{4187}{CyO\text{-}GFP} \quad \frac{cn,\ JSL2,\ sp}{4187} \quad \frac{CyO\text{-}GFP}{CyO}$$

The *cn, JSL2, sp/4187* virgin females were selected. These flies were easily distinguished as they had straight wings (absence of *CyO* marker). The selection of female flies was necessary at this point since meiotic recombination occurs only in females. At the second step of the recombination *cn, JSL2, sp/4187* virgin females were crossed to male *4347/CyO* as follows:

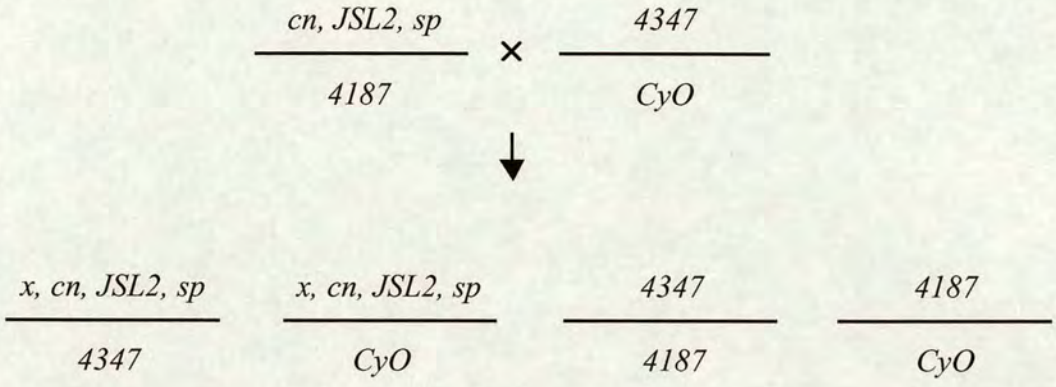

x=any markers that were introduced on the chromosome that contains the *JSL2* mutation after recombination took place in the oocytes of the *cn, JSL2, sp/4187* female flies.

From this cross male *x, cn, JSL2, sp/4347* flies were selected. These flies were distinguished as they had straight wings. Most of the *4347/4187* flies that also had straight wings were dying before they eclosed into flies. Some escapers were easily distinguished as they had all the markers present and they were very sick. Male *x, cn, JSL2, sp/4347* flies were selected as recombination does not occur in male flies and thus a stock from recombinant flies could be maintained.

Since the *SMC2* gene (and thus the *JSL2* mutation) is located between *cinnabar* and *curved* markers, it was desirable for this region not to be recombined so that the mutation would not be lost. For this reason *x, cn, JSL2, sp/4347* flies that did not have *cinnabar* and *curved* present should be selected. The fact that *cinnabar* was already present on the second chromosome of the *JSL2* line could not permit the selection of flies that did not have the region around *cinnabar* recombined. Thus, only *x, cn, JSL2, sp/4347* flies that did not have *curved* could be selected as possible carriers of the *JSL2* mutation. The phenotype of these flies could be *al* or *dp* or *b* or *pr* or *cn,* or *px* or *sp* or any combination of these markers depending on how many recombination events took place. The desired line would be the one with the most markers present, since that would be an indication that most of the second chromosome was recombined. Fly lines, with

several combinations of these markers were obtained that lacked *curved* and these flies were then crossed to *Bc, Gla/CyO-GFP* as follows:

$$\frac{x1,\ cn,\ JSL2,\ sp}{4347} \times \frac{Bc,\ Gla}{CyO\text{-}GFP}$$

$$\downarrow$$

$$\frac{x1,\ cn,\ JSL2,\ sp}{CyO\text{-}GFP} \qquad \frac{x1,\ cn,\ JSL2,\ sp}{Bc,\ Gla} \qquad \frac{Bc,\ Gla}{4347} \qquad \frac{4347}{CyO\text{-}GFP}$$

where *x1*= any markers, except from *curved* (c), that were introduced on the chromosome that contains the *JSL2* mutation, after recombination took place.

This cross was necessary in order to obtain a stock that had the recombined chromosome over a balancer. The *x1, cn, JSL2, sp/CyO-GFP* progeny were selected and crossed between them in order to obtain a stock. These flies were easily distinguished as they had normal eyes. The *4347/CyO-GFP* also had normal eyes but the dominant *Bl* marker on the 4347 chromosome could distinguish these flies from the desirable *x1, cn, JSL2, sp/CyO-GFP* progeny. To test which of the recombinant lines retained the *JSL2* mutation a complementation test was performed between the *x1, cn, JSL2, sp/CyO-GFP* flies and the original *cn, JSL2, sp/CyO-GFP* stock as follows:

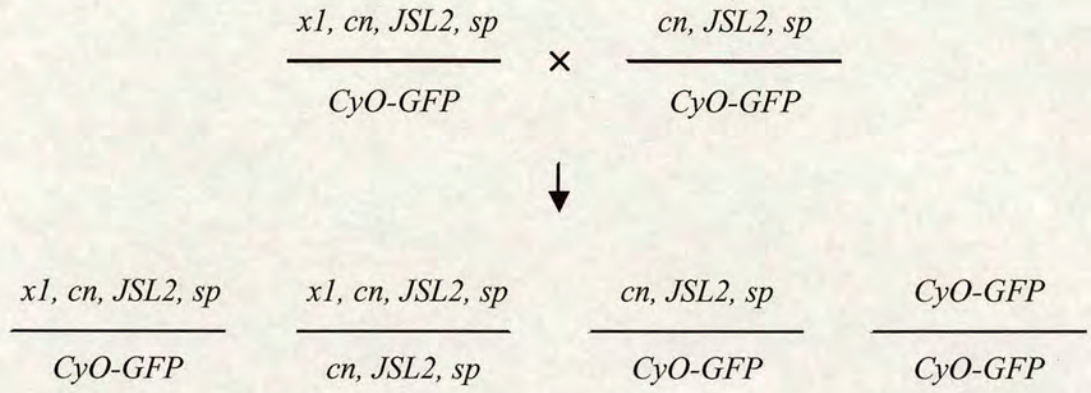

If the *x1, cn, JSL2, sp/cn, JSL2, sp* progeny were viable and flies emerged it meant that the *JSL2* mutation was lost from the recombined chromosome since the homozygotes for the *JSL2* mutation are expected to die as third instar larvae. The *x1 ,cn, JSL2, sp/cn, JSL2, sp* flies were distinguished by their straight wings. After a complementation test was performed with the recombined lines, a line with the *JSL2* mutation was obtained (line 58). This *JSL2* allele, *b, pr, cn, JSL2, sp/CyO-GFP*, had a significant part of the second chromosome recombined since most of the markers were present. The line was expanded and used for further characterisation of the mutant.

5.5. Lethality test and hatching frequency of the recombinant JSL2 allele

The main reason that the recombination was performed was to clean the *JSL2/CyO-GFP* stock of any additional mutations and to improve the health of the homozygous individuals. To test if this succeeded, recombinant *b, pr, cn, JSL2, sp/CyO-GFP* flies were crossed inter se and a lethality test was performed on the homozygous progeny. The progeny homozygous for *JSL2* were selected under a fluorescence microscope as being negative for GFP. It was obvious that these progeny were dying at early pupae. A more detailed characterisation of the lethal phase revealed that 90.4% were dying as early pupae while 9.6% were dying as third instar larvae, compared to 100% of *CaS* flies that pupated and eclosed into flies. The third instar homozygous larvae were clearly bigger and healthier compared to the second instar homozygous larvae before the

recombination. Their size though was slightly smaller compared to wild type *CaS* third instar larvae.

Another hypothesis to test was if any homozygotes for the *JSL2* mutation were dying during embryogenesis. To test this, a hatching frequency was performed with the progeny when *b, pr, cn, JSL2, sp/CyO-GFP* flies were crossed with each other. 30% of embryos were dying before they hatched into larvae. The expected ratio for embryonic lethality was 25%, which corresponds to the *CyO-GFP/CyO-GFP* progeny. The resulting ratio was slightly higher than expected (about 5%) but this is probably due to the way that the embryos were handled during the experiment. That was confirmed when the hatching frequency was tested in wild type *CaS* progeny. The resulting ratio was 7% of embryonic lethality while the expected ratio was 0%. Similarly the embryonic lethality in the control (*CaS*) was probably due to the way that the embryos were handled.

5.6. Sequencing of the recombinant JSL2 allele

In order to confirm that the mutation was present in the recombinant *JSL2* allele, the region of the *SMC2* gene that contained the *JSL2* mutation was sequenced. Genomic DNA from single *JSL2* homozygous larvae was used as a template for the PCR reactions. The primer pairs A26, A27 and A43 were used to amplify the region around the mutation and the resulting PCR products were sequenced (Figure 5.7). A base substitution (cytidine to thymidine) was observed at the position 2482 of the coding sequence, a mutation that was identical with the one in the original *JSL2/CyO-GFP* stock (CAG → TAG, premature stop codon). This suggests that the recombinant *JSL2/CyO-GFP* allele was an *SMC2* mutant which could be further characterised. Originally 20 homozygous larvae (GFP negative) were used for genomic DNA isolation. When the above procedure was followed and the PCR products were sequenced the results revealed that there was a mixture of mutant and wild type genomic DNA. This suggests that probably some heterozygous flies (*JSL2/CyO-GFP*) may not express GFP and thus they were selected as mutant homozygotes or that the selection of the homozygotes was not carefully done.

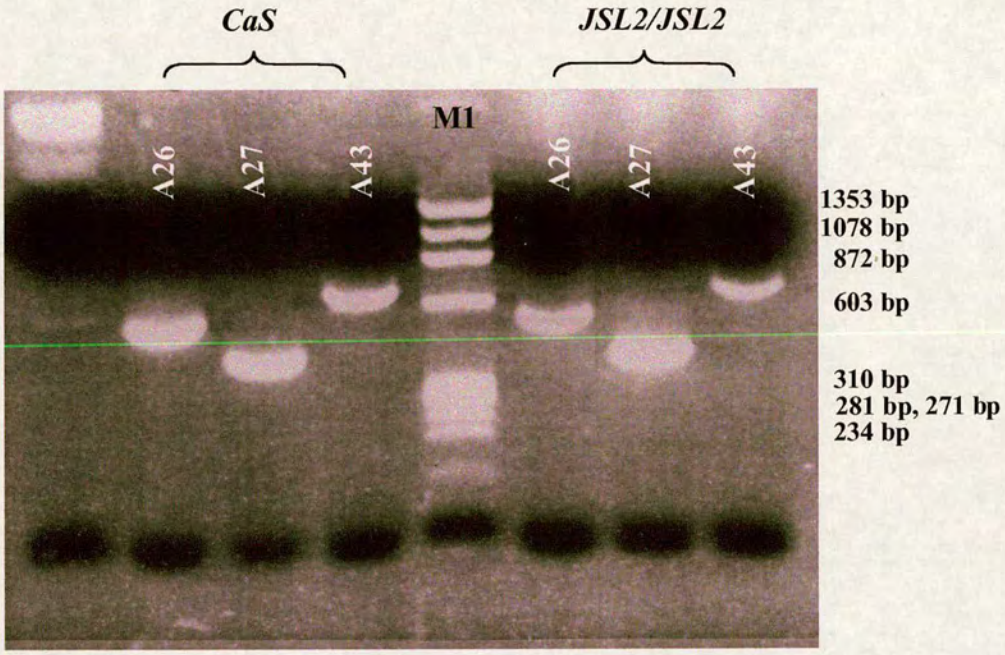

Figure 5.7. PCR products after amplification of the region of the *SMC2* gene that contained the *JSL2* mutation. Genomic DNA from single homozygous third instar larvae from the recombinant *JSL2* allele was used. Primer pairs A26, A27 and A43 were used for the amplification. M2 is the ϕX174 phage digested with HaeIII, molecular weight marker.

For this reason single larvae were used for genomic DNA isolation and further sequencing of the mutation.

5.7. Phenotypic and biochemical characterisation of larval JSL2 mutants

The existence of the *JSL2* mutation allows the *in vivo* study of the function of the protein. In this mutation, the homozygous animals die as early pupae allowing the phenotypic and biochemical characterisation of larval tissues that are rich in mitotic activity. Such tissues are third instar larval brains which can be used in order to assess the role of SMC2 firstly in chromosome morphology and architecture (phenotypic characterisation) and secondly in the stability of the condensin complex and of other mitotic proteins (biochemical characterisation).

5.7.1. Biochemical characterisation

The sequencing of the *JSL2* mutation revealed that a premature stop codon causes the production of a truncated protein of 827 aa. To confirm that and also to show that the full length SMC2 protein was absent from the homozygous *JSL2* animals, an immunoblot analysis was performed. Third instar brain extracts from wild type (*CaS*), heterozygous (*JSL2/CyO-GFP*) and homozygous (*JSL2/JSL2*) larvae were probed with the SMC2 antibody. The antibody was generated against the N-terminal region of the SMC2 protein (amino acids 24-309) (Figure 5.1 B). In the homozygous extract, it was obvious that the full length SMC2 protein was absent, while a smaller protein of about 52 kDa was present (Figure 5.8 A, arrow). The smaller protein probably corresponds to the truncated protein of which the size is estimated to be around 94 kDa. The difference between the size of the 52 kDa band and the predicted size could be due to the fact that the truncated protein is not stable and it gets degraded or that the conformation of the truncated protein is such that allows the protein to run faster. Furthermore in the heterozygous lane, a similarly sized band appeared to be present (absent from the wild type), strongly suggesting that this band corresponds to the truncated protein.

In the absence of SMC2 it was reasonable to test if the stability of the rest of the condensin components and of other proteins that are involved in chromosome dynamics

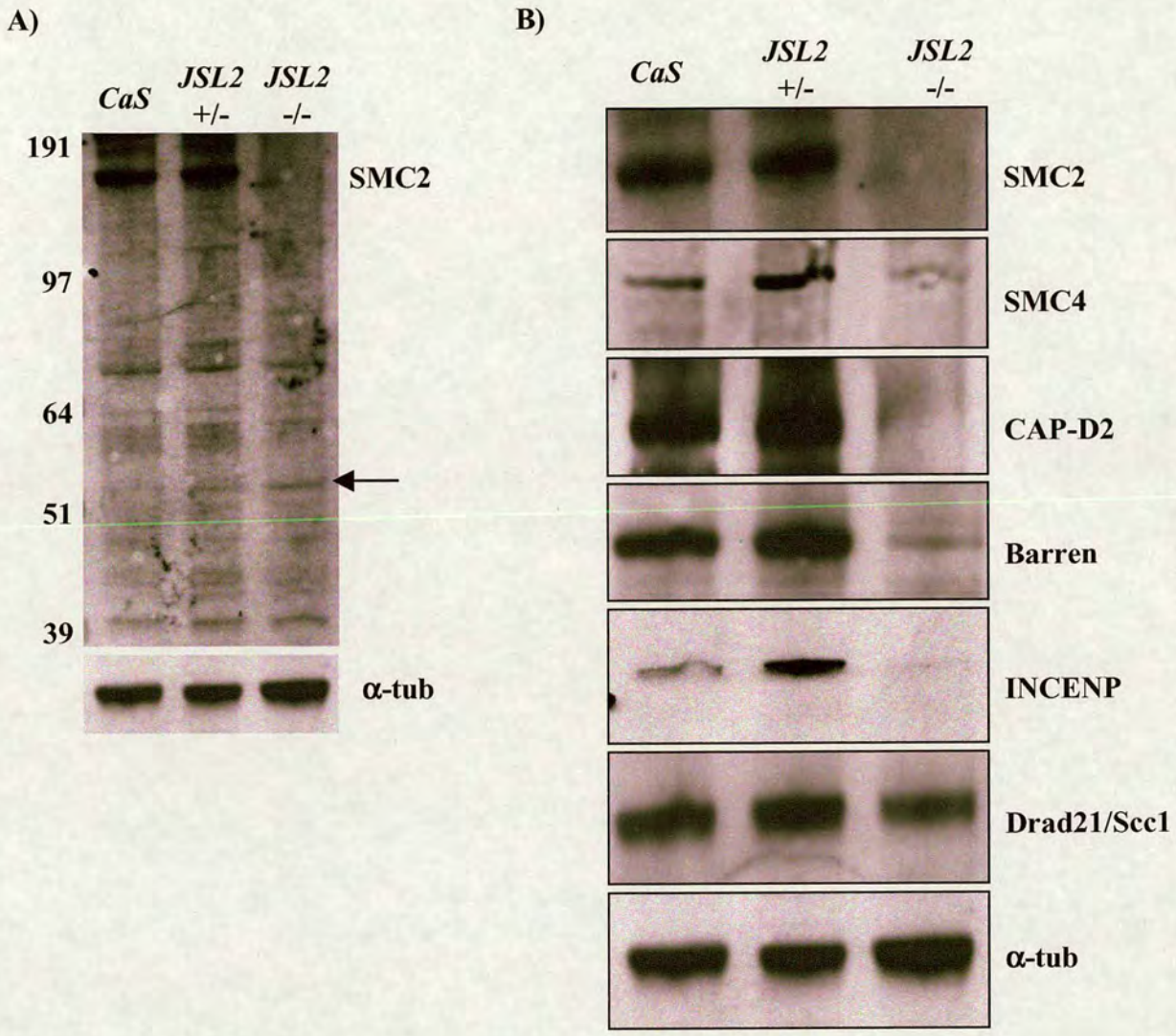

Figure 5.8. A. Immunoblot analysis of wild type *CaS*, heterozygous *JSL2/CyO-GFP* (*JSL2* +/-) and homozygous *JSL2/JSL2* (*JSL2* -/-) third instar larval brains by using the SMC2 antibody. The full length SMC2 protein (136kDa) is absent from homozygous brain extracts. A truncated protein of approximately 52 kDa is present in the homozygous and heterozygous brain extracts while it is absent from the wild type (black arrow). Approximately two third instar larval brains were loaded from the wild type and heterozygous brain extracts and four brains from the homozygous brain extracts. α-tubulin was used as a loading control.

B. Immunoblot analysis of third instar larval brain extracts of wild type *CaS*, heterozygous *JSL2/CyO-GFP* (*JSL2* +/-) and homozygous *JSL2/JSL2* (*JSL2* -/-) larvae. By using antibodies against condensin subunits it was obvious that the protein levels of CAP-D2, Barren and SMC4 were greatly reduced in the absence of SMC2 in the homozygous brain extracts. Quantitation with the phosphorimager revealed that SMC4 was reduced 6.5-fold, CAP-D2 8.2-fold and Barren 14-fold compared to wild type *CaS* brain extracts. INCENP levels were also greatly reduced in the absence of SMC2 protein while Drad21/Scc1 levels appeared unaffected. Approximately two third instar larval brains were loaded from the wild type and heterozygous brain extracts and four brains from the homozygous brain extracts. α-tubulin was used as a loading control.

(Figure 5.8 B). Quantitation of protein levels using phosphorimaging revealed that SMC4 was decreased 6.5-fold, CAP-D2 8.2-fold and Barren 14-fold compared to wild type brain extracts, suggesting that the stability of these proteins is greatly affected by the absence of SMC2.

In order to investigate if the stability of chromosomal passengers was affected by the absence of SMC2, an antibody against INCENP was used. As already mentioned in a previous chapter, INCENP is required for the correct targeting of Aurora B at all times in mitosis and Aurora B has been shown to phosphorylate histone H3 during mitosis, an event that coincides with the initiation of chromosome condensation (Adams et al., 2001b). When immunoblotting of larval brain extracts was performed with the INCENP antibody, it was obvious that the protein levels were greatly reduced in the homozygotes compared to wild type and heterozygous extracts (Figure 5.8 B). This result was surprising, bearing in mind that INCENP levels were not affected when condensin function was compromised after depletion of CAP-D2 (Chapter 4.8.1).

In *Drosophila*, most of the cohesin complex dissociates from chromosomes in prophase and only a small amount remains associated at centromeric regions (Warren et al., 2000b). To assess if the cohesin complex is affected by the absence of SMC2, an antibody against the Drad21/Scc1 cohesin component was used. Analysis by immunoblotting showed that no significant change was observed in the protein levels (Figure 5.8 B) suggesting that probably cohesin and condensin complexes are not interacting directly. Also to ensure that wild type, heterozygous and homozygous extracts were equally loaded, α-tubulin was used as a loading control.

5.7.2. Phenotypic characterisation of the JSL2 mutant

The phenotypic characterisation of the *JSL2* mutant was very important in order to understand the role of the SMC2 protein in chromosome organisation. The overall size of the homozygous brains was smaller than both the heterozygous and wild type brains (Figure 5.9), suggesting that proliferation was affected. When third instar larval brains from heterozygous (control) and homozygous larvae were squashed and stained for phosphorylated H3, α-tubulin and DNA (by following the "Bonaccorsi" protocol

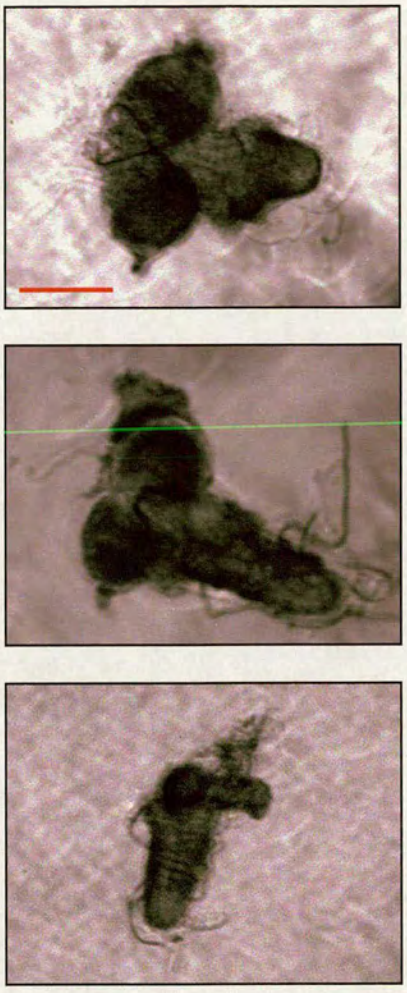

Figure 5.9. Wild type *CaS*, heterozygous *JSL2/CyO-GFP* and homozygous *JSL2/JSL2* whole third instar larval brains. The homozygous brain is almost half the size compared to wild type and is certainly smaller compared to heterozygous brains. Scale bar is 20μm.

(Bonaccorsi et al., 2000)), the first major defect observed in the homozygous mutant brains, was the overall lack of mitotic cells. Indeed, when the mitotic index was determined, based on chromosome morphology, it was obvious that the percentage of mitotic cells was significantly lower compared to the control (0.26% in the mutant versus 1.62% in the control) (Figure 5.10 A). That was also confirmed, when an immunoblot analysis against third instar larval brains using an antibody against the phosphorylated histone H3 was performed. This analysis showed that the level of phosphorylated histone H3 was greatly reduced in the homozygous brain extract while it was normal in the heterozygous and wild type brain extracts (Figure 5.10 B). Both of these approaches strongly suggest that the mitotic index is greatly reduced in the *JSL2* mutant. This observation could explain the unexpected reduction of INCENP levels and the fact that the levels of all the condensin subunits were more severely affected compared to the *gluon*^{17C} mutant, which is a null for SMC4.

As an additional control, an immunoblot analysis using an antibody against histone H3 was performed. The levels of this protein should be unaffected by the absence of SMC2. However, after the experiment was performed it was obvious that the level of histone H3 was also reduced in the homozygous brain extract (Figure 5.10 C). A small reduction was observed in the heterozygous extract. As already mentioned previously, the reduction of mitotic proteins in the homozygous brain extracts was perhaps not suprising since the mitotic index was significantly low. The reduction of histone H3 was unexpected, since this protein is not a mitotic protein and its levels should not be affected by the absence of SMC2. For this reason, I decided to look if there was an additional mutation in the *JSL2* line that affects the histone *H3* gene. For this reason, a deficiency *2386/CyO* (*Df(2L)DS6, b[1] pr[1] cn[1]/CyO*) that uncovers the cluster of histone *H3* genes on the second chromosome was used to do a complementation test with the *JSL2/CyO-GFP* line.

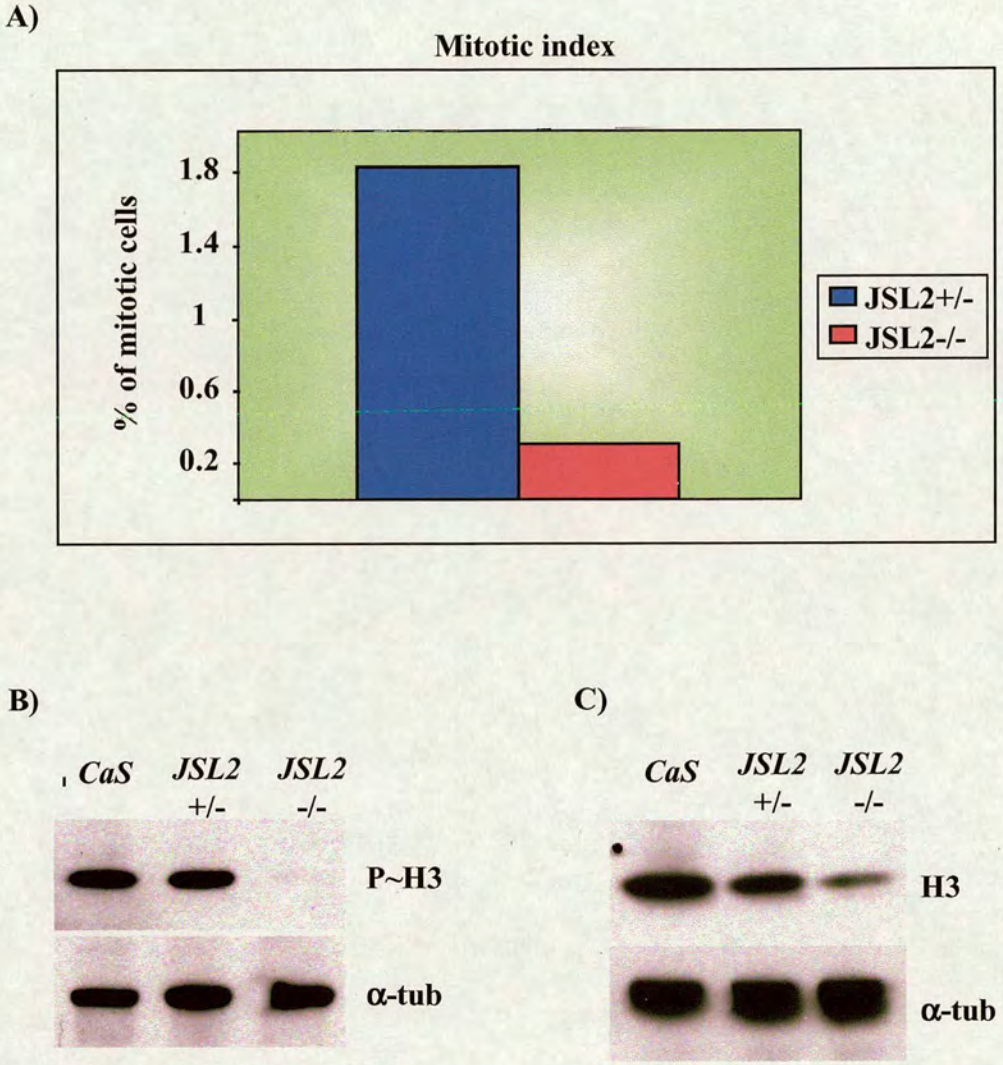

Figure 5.10. A. Histogram showing the mitotic index in control (*JSL2* +/-) and homozygous *JSL2/JSL2* (*JSL2* -/-) third instar larval brains. The percentage of mitotic cells is significantly lower in the homozygous brains compared to control brains. 20 brains were scored for each sample.
B and C. Immunoblot analysis of wild type *CaS*, heterozygous *JSL2/CyO-GFP* (*JSL2* +/-) and homozygous *JSL2/JSL2* (*JSL2* -/-) third instar larval brains, using antibodies against phosphorylated histone H3 (P~H3) and histone H3. The level of P~H3 is greatly reduced in the homozygous mutant extracts compared to wilt type and heterozygous extracts (B). The level of histone H3 is also reduced in the homozygous brain extract compared to wild type. Suprisingly a slight reduction is also observed in the heterozygous extract (C). α-tubulin was used as a loading control.

The following cross was performed:

$$\frac{JSL2}{CyO - GFP} \times \frac{2386}{CyO}$$

$$\downarrow$$

	$\frac{JSL2}{CyO}$	$\frac{2386}{CyO - GFP}$	$\frac{2386}{JSL2}$	$\frac{CyO}{CyO - GFP}$
expected ratio	33%	33%	33%	die
observed ratio	40%	40%	20%	die

If the *2386/JSL2* progeny are viable and flies emerge, it means that the *JSL2* line does not have a lethal mutation in the *H3* genes. This is because progeny homozygous for histone *H3* mutations would be expected to die early in development since histone *H3* is an essential gene. *2386/JSL2* flies were distinguished by their straight wings. From this cross, 20% of the viable progeny were *2386/JSL2*. The expected ratio that corresponds to these progeny if they are all equally viable is 33% since *CyO/CyO-GFP* progeny die during embryogenesis. The fact that the resulting ratio is lower than the expected (semi-lethal phenotype), could be because several genes are missing in the deficiency stock and in combination with the *JSL2* mutation could cause lethality before flies enclose. The 20% of viable *2386/JSL2* flies though suggests that most likely additional mutation exists in the *JSL2* line that affects the histone *H3* gene. The reason that histone H3 levels were reduced in the *JSL2* homozygous brain extract remains a mystery.

Analysis of the few mitotic cells that were present in the homozygous brains showed several defects in chromosome morphology (Figure 5.11 B and 5.12 B). Chromosomes appeared fuzzy with almost no sister chromatid resolution. Prometaphase and metaphase chromosomes appeared as unresolved chromatin masses with unaligned chromosomes (Figure 5.11 B). 12% of cells in prometaphase and metaphase displayed

defects in chromosome condensation (Figure 5.11 B (c)). These defects refer to mitotic chromosomes that contained regions of undercompacted chromatin connected by normally compacted chromatin (irregularly condensed chromosomes), a defect that was also observed in ORC mutants affecting the normal pattern of chromosomal replication (Loupart et al., 2000). Furthermore, cells in anaphase and telophase showed extensive chromatin bridges and had unequal nuclei probably as a result of defective chromosome segregation during mitosis (Figure 5.12 B). However, the stage of many mitotic cells (56%) could not be easily determined as the chromosome structure was so abnormal (Figure 5.13 A). On the other hand, control cells from heterozygous brains showed normal chromosome morphology and chromosomes were segregating normally during anaphase (Figure 5.11 A and 5.12 A).

As mentioned previously, INCENP through interaction with Aurora B, is involved in histone H3 phosphorylation during mitosis. Bearing in mind that INCENP levels were greatly reduced in the homozygous larval brain extracts, as well as the levels of phosphorylated H3, it was necessary to test if individual mutant mitotic cells had normal levels of phosphorylated histone H3. To assess that, the same exposure time for P~H3 was used to capture images of both control and mutant mitotic cells. In most of the mutant mitotic cells, the level of P~H3 appeared similar to the control cells and no significant change was observed. Interestingly though, 28% of mutant cells, which looked mitotic, as judged by their chromosome morphology, were negative for phosphorylated histone H3 (Figure 5.13 B (b) and (c)). Nevertheless it was not determined if these cells were definitely mitotic cells, interphase cells with abnormal morphology, or apoptotic. A way to test this, was to look for the presence of the mitotic spindle. Usually though, no mitotic spindle or any microtubule structure could be observed in these P~H3 negative cells, even though the protocol that was used for brain squashes was able to preserve microtubule organisation. This suggests that probably these cells are in interphase or that mitotic spindle organisation is defective in the mutant cells. Indeed mitotic spindles were not usually observed in 92% of mutant mitotic cells suggesting that mitotic spindle organisation was defective. In contrast to the mutant cells, in control cells a mitotic spindle could usually be observed (in 80% of mitotic

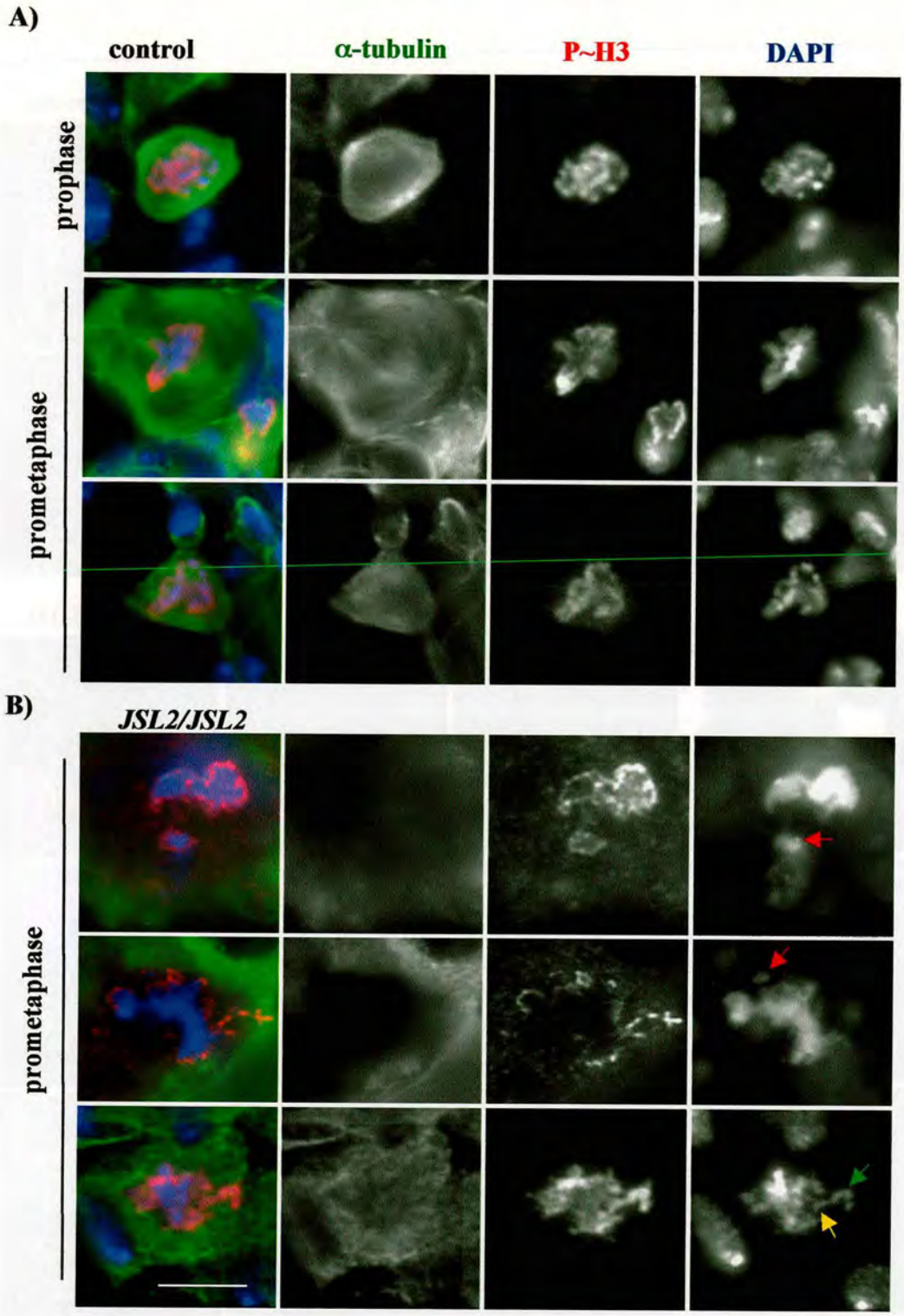

Figure 5.11. Control (A) and homozygous *JSL2/JSL2* (B) third instar larval neuroblasts. Brains were squashed and stained for P~H3 (red), α-tubulin (green) and DNA (DAPI, blue) according to the Bonaccorsi protocol. Prophase and prometaphase figures are shown in control panel (A). Individual chromatids can be easily observed (A) and chromosome organisation and compaction appears normal. Also a mitotic spindle can be easily observed in panel (A). In homozygous brains (B), prometaphase cells appeared as unresolved chromatin masses with unaligned chromosomes (red arrows). In some cells, chromosome condensation was irregular, since some parts of a chromosome appeared undercompacted (yellow arrow) compared to other regions within the same chromosome (green arrow). Also a well organised mitotic spindle could not be observed in these cells. Scale bar is 10μm.

cells). It is important to mention though, that P~H3 negative cells that looked like mitotic cells were present in the control brains but not in the same ratio as in mutant cells (2% in control brains versus 28% in mutant brains) (Figure 5.13 B (a)).

5.7.3. Quantification of mitotic phenotypes in third instar larval brains

No delay was observed in prometaphase/metaphase in mutant brains since the percentage of cells in these phases was lower (32%) compared to control (54%) (Figure 5.14 A). Also no anaphase figures could be observed in the mutant brains (compared to 16.6% in control) while the percentage of telophase cells was still lower (8%) compared to control (12.5%) (Figure 5.14 A). Furthermore the mitotic index was significantly lower in the mutant as mentioned above (0.26 versus 1.62 in the control). Taken together, these results suggest that progression through mitosis was not delayed in mutant larval brains. In contrast it seems that cells were not entering mitosis probably as a consequence of accumulated chromosome abnormalities or activation of the DNA structure checkpoint. Even though 56% of mitotics could not be categorised to any of the mitotic phases, due to the lack of particular chromosome morphology, the overall reduction of the mitotic index in the mutant indicates that the above conclusion is still valid. All telophase cells in the mutant had chromosome bridges. Also a high percentage of interphase cells were joined with chromosome bridges (bi-nucleate cells, 2.66% compare to 0.06% in control cells) (Figure 5.14 B). Chromosome bridges probably result from the lack of sister chromatid resolution affecting chromosome segregation. In general all mitotic cells were abnormal in the mutant (100% compared to 4% in the control) (Figure 5.14 C).

5.7.4. Phenotypic characterisation of second instar JSL2 mutant brains

As discussed above, the mitotic index was reduced in the *JSL2* homozygous third instar brains and the chromosome morphology was highly abnormal, two features that were making the characterisation of the mutant very difficult. In order to bypass these two disadvantages, second instar larval brain squashes were performed and stained for α-tubulin, P~H3 and DNA. In this way it was possible that in second instar larval brains,

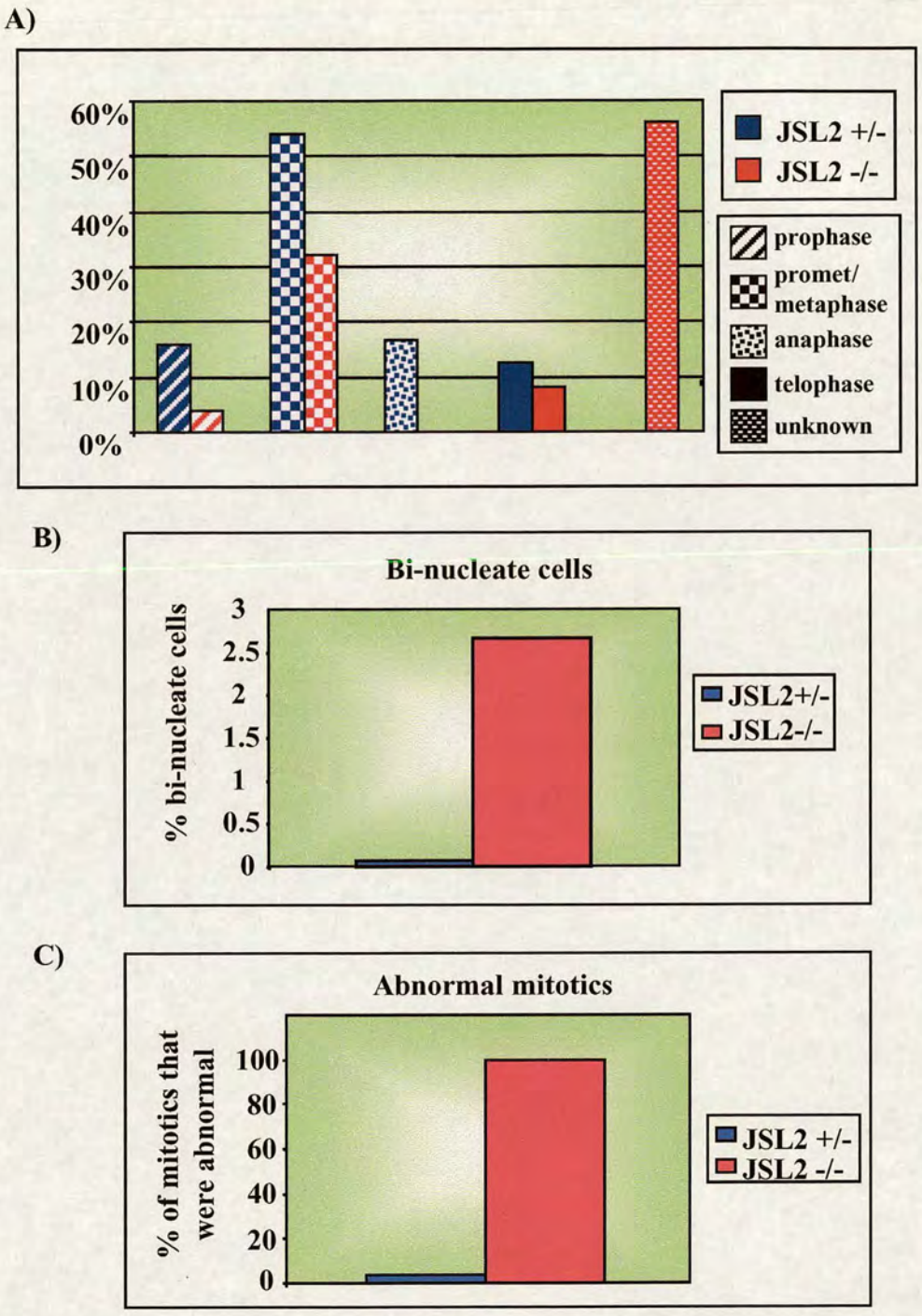

Figure 5.14. A. Graph showing the distribution of mitotic cells in the different mitotic phases in control (*JSL2* +/-) and homozygous (*JSL2* -/-) third instar larval brains. The mitotic stage of 56% of mutant mitotic neuroblasts could not be determined (unknown).

B. Histogram showing the percentage of bi-nucleate cells in control (*JSL2* +/-) and homozygous (*JSL2*-/-) third instar larval brains. The percentage of bi-nucleate cells is significantly higher in the homozygous larval brains compared to control larval brains. 20 brains were scored for each sample.

C. Histogram showing the percentage of abnormal mitotic cells in control (*JSL2* +/-) and homozygous (*JSL2*-/-) third instar larval brains. All mitotics are abnormal in the homozygous brains while only a small percentage is abnormal in control brains. 20 brains were scored for each sample.

chromosome morphology would be better and more mitotic cells may be present than in third instar larvae. Indeed, in homozygous second instar larval brains both the mitotic index and chromosome morphology were improved compared to third instar. The reason for that, was probably the fact that fewer chromosome defects had accumulated in second instar larvae than in third and thus more cells were still undergoing mitosis. Particularly, the mitotic index in homozygous second instar larval brains was almost double compared to third instar brains (0.4% in second instar compared to 0.26% of third instar), but still, it was significantly lower compared to the control (0.4% in the mutant versus 1.3% in the control) (Figure 5.15 A). The calculation of the mitotic index was based on chromosome morphology.

Chromosome morphology was not as severe as in third instar larvae but the defects observed were very similar. Chromosomes appeared fuzzy throughout mitosis. Prometaphase and metaphase chromosomes appeared as unresolved chromatin masses with unaligned chromosomes (Figure 5.15 C), while cells in anaphase and telophase showed extensive chromatin bridges (Figure 5.16 B). Ill-defined sister chromatids were observed and chromosome condensation was quite abnormal. Usually two (bi-nucleate) or even three (tri-nucleate) nuclei were joined with chromosome bridges, probably as a result of defective chromosome segregation and failed cytokinesis (Figure 5.16 B). In some cells though chromosome morphology was very abnormal and the stage of many mitotic cells could not be easily determined (29.2%) (Figure 5.17). On the other hand, chromosome morphology appeared normal in the heterozygous control (Figure 5.15 B, 5.16 A).

No significant delay was observed in the mitotic progression. The prometaphase/metaphase index was slightly higher in the mutant (56%) compared to control (45%) (Figure 5.18 A). Similarly to third instar brains, no anaphases were observed in the second instar mutant brains (in control 22% of mitotic cells were in anaphase) while the percentage of cells in telophase was similar between the mutant and the control (12.1% in mutant versus 13% in control) (Figure 5.18 A). All mitotic cells were abnormal in the mutant brains and all telophases had chromosome bridges. Furthermore a significant amount of interphase cells were joined with chromosome

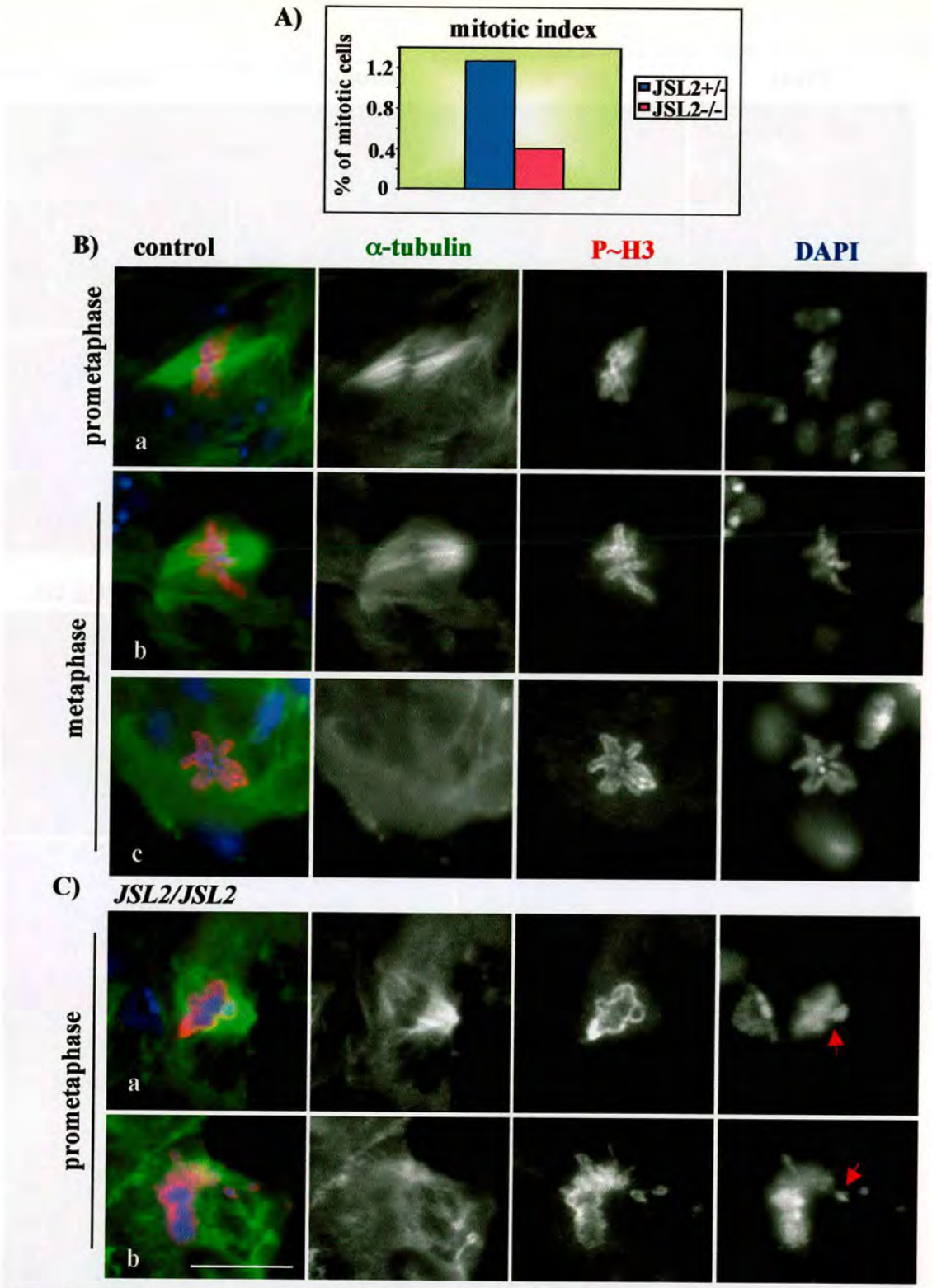

Figure 5.15. A. Histogram showing the mitotic index in control and homozygous *JSL2/JSL2* second instar larval brains. The percentage of mitotic cells is noticeably lower in the homozygous brains compared to control brains. 20 brains were scored for each sample. **B and C.** Brains were squashed and stained for P~H3 (red), α-tubulin (green) and DNA (DAPI, blue) according to the Bonaccorsi protocol. In control prometaphase and metaphase cells (B), chromosomes are properly condensed and organised with well defined chromosomes and sister chromatids (Bb and Bc). Mitotic spindle organisation appears normal (Ba and Bb). In homozygous *JSL2/JSL2* mutant cells (C), chromosomes are fuzzy and chromosome condensation appears quite abnormal. No well-defined chromatids could be observed. Chromosomes appeared as unresolved chromatid masses with unaligned chromosomes (red arrows). Mitotic spindle structure looks normal in C(a) but is disorganised in C(b). Scale bar is 10*μm*.

bridges (2.4% bi-nucleates versus 0.02% in control and 0.14% tri-nucleate versus 0% in control) (Figure 5.18 B).

5.7.5. Spindle morphology in second instar larval neuroblasts

A mitotic spindle was usually present in mutant cells, in contrast to third instar larvae. Its morphology though was usually abnormal compared to heterozygous controls (Figure 5.19 A). Usually monopolar spindles were observed and the overall structure of the spindle was defective. These abnormalities were categorised as follows: 17.7% of the mutant mitotic cells had normal mitotic spindle (Figure 5.15 C (a) and 5.19 B) while 46.34% had no spindle (28% of control cells had no mitotic spindle) (Figure 5.15 C (b) and 5.19 B). Of the rest of the mitotics, 6.7% had a partially disorganised spindle (Figure 5.19 A(a) and 5.19 B), 14.63% had microtubules growing from only one pole (monopolar spindles) (Figure 5.19 A(b) and 5.19 B), 4.87% had microtubules emanating from three different chromosome regions (tripolar spindles) (Figure 5.19 A(e) and 5.19 B) and 9.75% had microtubules emanating from chromosomes but they were not focused to a pole (Figure 5.19 A(c) and (d) and 5.19 B). As previously mentioned, these defects could be an indirect effect of accumulated chromosome abnormalities

5.8. Brief discussion

In conclusion, *JSL2* mutation is an *SMC2* mutation that causes lethality in early pupae. The fact that individuals homozygous for the *JSL2* mutation live up to this point is surprising, but is possible that the remaining truncated protein is functional in a way and it can partially rescue the loss of SMC2 protein. The overall morphology of brain cells is highly abnormal and chromosome organisation is definitely compromised. The main phenotype observed is the loss of sister chromatid resolution and the failure of chromosome segregation during anaphase, defects that were also observed after the depletion of other condensin subunits in *Drosophila* (Bhat et al., 1996; Coelho et al., 2003; Savvidou et al., In Press; Steffensen et al., 2001). Chromosome condensation is compromised and in some cases some parts of the chromosomes are less condensed than others (irregularly condensed chromosomes). A large number of mitotic cells could not

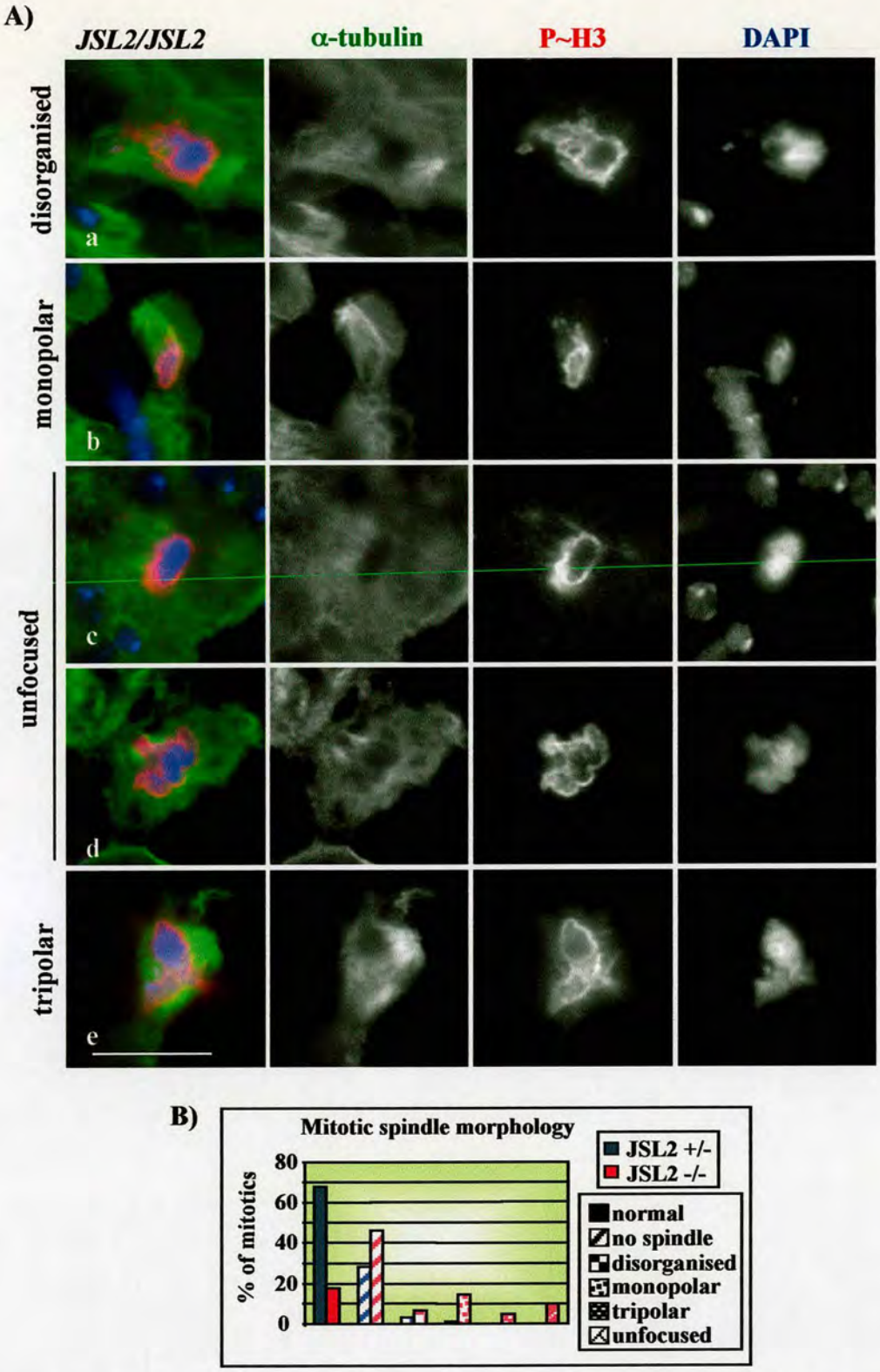

Figure 5.19. A. Homozygous *JSL2/JSL2* second instar larval neuroblasts. Brains were squashed and stained for P~H3 (red), α-tubulin (green) and DNA (DAPI, blue) according to the Bonaccorsi protocol. Several spindle abnormalities were observed in mitotic cells and cells were categorised according to their spindle defects. These groups contain cells with partially disorganised spindle (Aa), cells with a monopolar spindle (Ab), cells with a spindle that does not focus on a pole (Ac and Ad) and cells that their spindle looks like tripolar (Ae). Scale bar is 10*μm*.

B. Bar chart showing the percentage of mitotic cells, in control (*JSL2* +/-) and homozygous (*JSL2-/-)* second instar larval brains, that display a certain type of mitotic spindle abnormality as described in (A).

be categorised into definitive mitotic stages thus making the interpretation of the results difficult. Also the reduction in the levels of histone H3 is very difficult to interpret and no logical explanation could be found to explain it. The protein levels of the rest of the condensin subunits and INCENP are greatly reduced by the absence of SMC2. The reduction in INCENP levels is probably a consequence of the low mitotic index that is observed in *JSL2* mutant brains. Furthermore, mitotic spindle organisation is compromised in the mutant cells and only a small fraction of the mitotic population had normal spindles. The severity of the phenotype though, makes the characterisation of the mutant very difficult. Second instar larvae are very difficult to work with due to small size and the overall percentage of mitotic cells is very low. Thereby, it was not possible to get a lot of information from the characterisation of this mutant and thus, no further analysis was performed.

CHAPTER 6
CHARACTERISATION OF CAP-D3, A CONDENSIN II SUBUNIT

6.1. Introduction

The condensin complex plays an essential role in mitotic chromosome assembly and segregation from yeast to humans. Recently a second condensin complex (condensin complex II) has been identified in vertebrate cells. The two complexes, condensin I (the first identified condensin complex) and condensin II, share the same pair of the two SMC subunits, SMC2 and SMC4, but contain different sets of the non-SMC subunits, CAP-H2, CAP-G2 and CAP-D3 (Ono et al., 2003). It has been shown that the two complexes make distinct contributions to chromosome architecture and are differentially regulated during the cell cycle (Ono et al., 2004). Sequence analysis suggests the existence in *Drosophila* of CAP-D3 and CAP-H2, but not CAP-G2. A search in the database for any putative *Drosophila* mutations in CAP-H2 and CAP-D3 resulted in the identification of a *CAP-D3* mutation. Therefore, an examination of condensin II in *Drosophila*, was initiated.

6.1.1. Spermatogenesis in Drosophila

Analysis of the CAP-D3 mutation revealed mainly defects in spermatogenesis. Thereby, to be able to understand the phenotype caused from this mutation, a brief description of spermatogenesis will be given here.

Male meiosis occurs in the context of a complex developmental process, called spermatogenesis, that leads to the formation of 64 spermatids from each primary gonial cell (Figure 6.1). The *Drosophila* testis is a long tube with a straight apical and coiled basal end. Spermatogenesis begins in the germinal proliferation centre, an area located at the apical tip of the testes which is comprised of 5-9 germ-line stem cells (in adult flies) and 9-17 somatically derived, cyst progenitor cells, that flank the germ-line stem cells. The germ-line stem cells are arranged around a compact group of specialised

somatic cells known as the "hub". The asymmetric division of a stem cell generates a primary spermatogonium (gonial cell or goniablast) and another stem cell, which remains anchored at the apex of the testis. Concomitant with the formation of this primary gonial cell, the asymmetric division of two neighbouring cyst progenitor cells generates two cyst cells, which encyst the primary spermatogonium and its progeny until completion of spermatogenesis. The packet of the two cyst cells and the gonial cell is termed a cyst and is the basic unit of spermatogenic differentiation. Germ cells are displaced away from the tip as new cells form so that cysts of primary spermatocytes move down the testis and enter meiosis near the start of the coil.

The primary gonial cell undergoes four rounds of synchronous mitotic divisions, giving rise to a cyst of 16 primary spermatocytes. Cytokinesis is incomplete during these specialised divisions, leaving the cells connected by stable intercellular bridges called ring canals. These cells, after pre-meiotic DNA synthesis, enter a growth phase that lasts approximately 3.5 days, during which time the nuclear volume increases 25-fold. Nuclear growth is accompanied by extensive gene expression which results in the formation of the Y-chromosome lampbrush-like loops generated by several fertility factors.

At the end of the growth period, the Y-loops degenerate, and primary spermatocytes undergo meiosis I and meiosis II in metasynchrony, resulting in a cyst of 64 interconnected haploid spermatids. During the meiotic divisions, a very prominent spindle forms which is particularly amenable to cytological analysis. During the two meiotic divisions, the mitochondria in each spermatocyte line up along the pole-to-equator microtubules of the spindle and are separated equally to the daughter cells by cytokinesis. After telophase II, all the mitochondria in each early spermatid aggregate together and fuse into two giant mitochondria, which wrap around each other to form a phase dark, spherical structure termed the "Nebenkern" or mitochondria derivative. This stage is called the onion-stage, as in a cross section the concentric layers of mitochondrial membrane make this structure resemble an onion slice, and is used to describe early round haploid spermatids. Each of the 64 spermatids in an onion-stage cyst normally

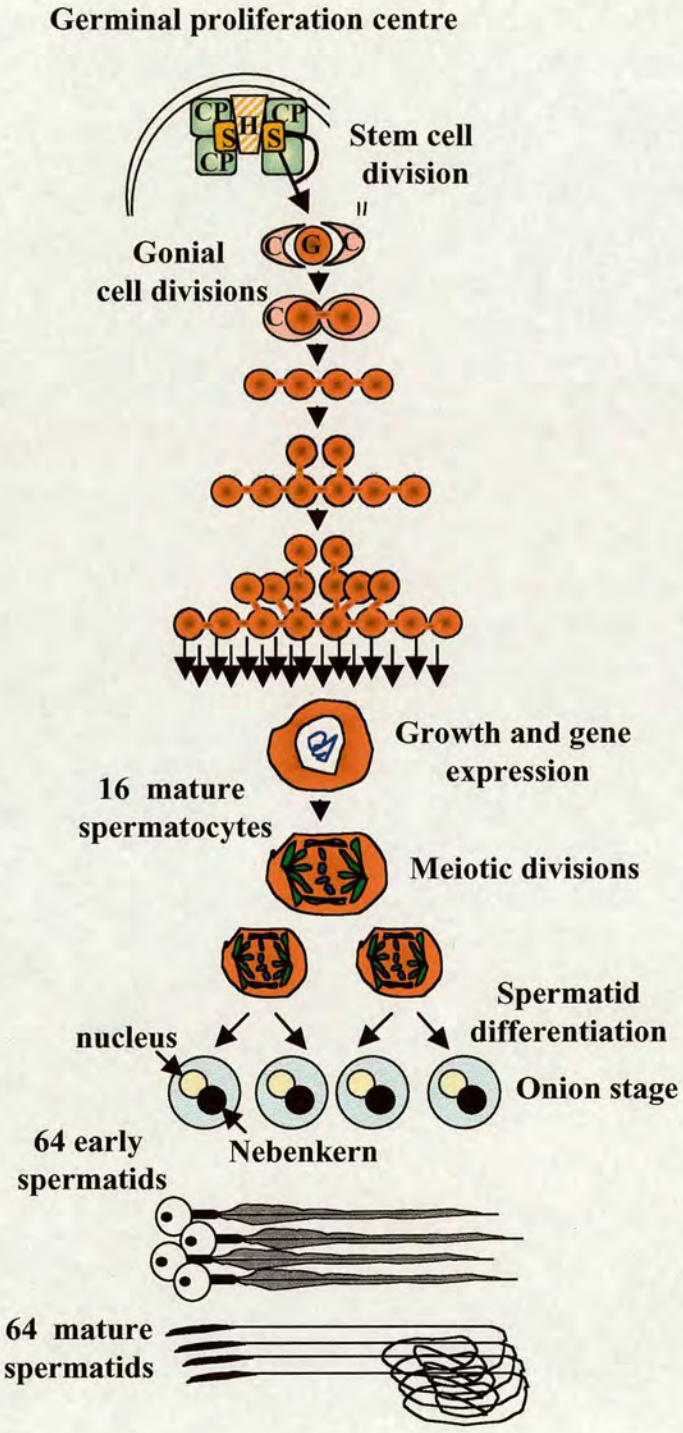

Figure 6.1. Spermatogenesis in *Drosophila melanogaster*. Male germ-line stem cells (S) lie next to the apical hub (H) at the tip of the testis. Each germ line stem cell is flanked by a pair of cyst progenitor cells (CP). When either a germ-stem cell or a cyst progenitor cell divides, the daughter that maintains contact with the hub retains stem cell character, whereas the daughter displaced away from the hub initiates differentiation-in the case of the germ line as a gonialblast (G), and in the case of the cyst progenitor as a cyst cell (C). Two cyst cells enclose the gonialblast and they never divide again, but enclose all progeny of the gonialblast throughout the remainder of spermatogenesis. The gonialblast and its spermatogonial daughter cells undergo four rounds of mitotic divisions with incomplete cytokinesis. The resulting 16 interconnected cells switch to the meiotic program and enter a period of growth and gene expression. For simplicity only one of the 16 primary spermatocytes in a cyst is shown. All 16 primary spermatocytes exit the cell growth stage and undergo two meiotic divisions resulting in a cyst of 64 interconnected, onion stage, haploid round spermatids. All the spermatids in an onion-stage cyst have the same-sized nucleus and mitochondrial derivative (Nebenkern). The haploid spermatids remain interconnected and proceed through the morphological change of spermiogenesis in synchrony. Finally, the fully elongated spermatids are individualised, coil to the base of the testis and are transferred to the seminal vesicle. The drawing has been adapted from Fuller (1998).

contains a single, phase-light, spherical nucleus paired with the phase dark, spherical Nebenkern. If all steps were normal in the preceding meiotic divisions, all the spermatid nuclei and Nebenkern in a cyst have a highly regular appearance and consistently exhibit similar sizes. This regular array of nuclei and Nebenkern allows easy identification of mutants that affect the meiotic divisions by examining onion-stage cysts with phase contrast light microscopy.

Spermiogenesis or spermatid differentiation in *Drosophila* proceeds by a dramatic series of morphological changes in which most, if not all, subcellular components are remodelled. Spermatids grow a long flagellum containing the axoneme, a complex microtubule-based organelle for motility. The wrapped layers of the mitochondrial derivative unfurl and mitochondria elongate along the flagellum. The ring canals are gathered to the elongating end of the flagellar bundle opposite the nuclei. The spermatid DNA becomes highly condensed and the nucleus is shaped along a microtubule scaffold. The mature spermadits are individualised by an actin-based structure called the "investment cone" and finally the sperm bundle coils to the base of the testis and is released into the seminal vesicle (Fuller, 1998).

The regular appearance of onion stage early spermatid cysts serves as a convenient diagnostic for identification of mutants that cause several different types of meiotic defects (Bate, 1993). Mutants that fail to undergo chromosome segregation and cytokinesis during meiosis commonly result in cysts with 16 onion-stage spermatids with 4N nuclei and large Nebenkern. Mutants that cause defects in spindle assembly and function often cause failure of cytokinesis as well as defects in chromosome segregation, resulting in onion-stage spermatid cysts with large or variable Nebenkern associated with variable numbers of differently sized nuclei. Mutants that cause defects in cytokinesis but not chromosome segregation should produce large Nebenkern associated with nuclei that are uniform and normal in size. Some mutations produce onion-stage spermatids that have Nebenkern but no nucleus visible by phase contrast optics, probably due to failure of chromatin to decondense at the end of meiotic divisions. Finally, some mutants produce onion-stage spermatids with normal sized

nuclei but no apparent Nebenkern, as a result of the loss of mitochondria between the gonial cell and mature primary spermatocyte stages (Bate, 1993).

6.2. The Drosophila CAP-D3 gene

The *CAP-D3* gene (CG31989) is located on the left arm of the second chromosome of *Drosophila melanogaster* in 25E5 (nucleotides: 5458120-5589325) (Figure 6.2 A). The *CAP-D3* gene is 11.2 kb long and it consists of 6 introns and 7 exons. A 5201 bp cDNA (3801bp coding sequence) encodes a protein of 1267 amino acid residues (M_r: 145 kDa, pI: 7.22) (Figure 6.2 B). The first intron of the gene is about 6 kb long and three other genes are located in it (Figure 6.3 A). These genes *CG31648*, *CG31915* and *CG7277*, are involved in cytochrome c oxidase biogenesis and complex assembly, in carbohydrate metabolism and in ubiquinone biosynthesis, respectively. There are an additional two genes, *CG14016* and *CG14015* in the 3' UTR of the *CAP-D3* gene (Figure 6.3 A). These genes are involved in nucleotide/nucleic acid metabolism and transcription regulation and in mannosidase activity, respectively. None of these genes overlaps with the others. The orientation of *CG7277*, *CG14016* and *CG14015* genes is from right to left which is opposite from the orientation of transcription of the *CAP-D3* gene (Figure 6.3 A). Finally there are two mutations that interrupt the *CG7277* and *CG14016* genes, which will be discussed later.

6.3. The CAP-D3 mutation

A search in the *Drosophila* database resulted in the identification of a *CAP-D3* mutation (*15026/4D*). This mutation is caused from a P-element insertion *P{EPgy2}* at the beginning of the third exon of the *CAP-D3* gene (1095 bp of ORF) (Figure 6.3 A). The P-element is 10,872 kb long and it contains two functional transgenes, the *mini-white* and the *intronless-yellow*, which can be used to follow the transposon (P-element) on the appropriate genetic background. The promoter of the P-element is at the 3' end of the P and the orientation is from left to right. This P-element also has a GAL4/UAS enhancer that allows the mis-expression of an adjacent gene downstream of the P-element promoter under the control of GAL4 (Bellen et al., 2004) (Figure 6.3 B).

A)

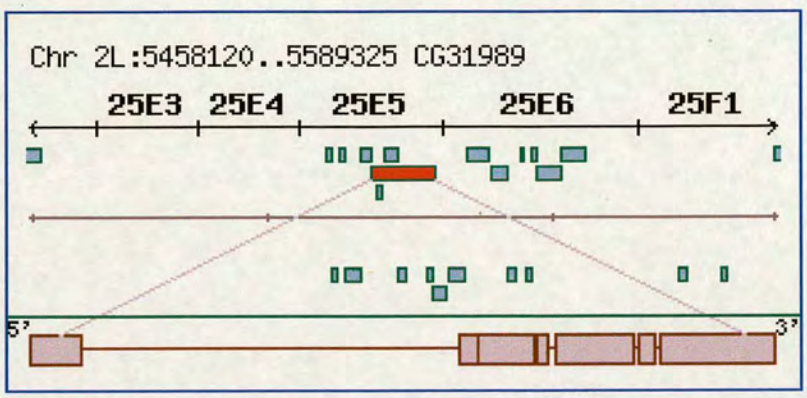

B)

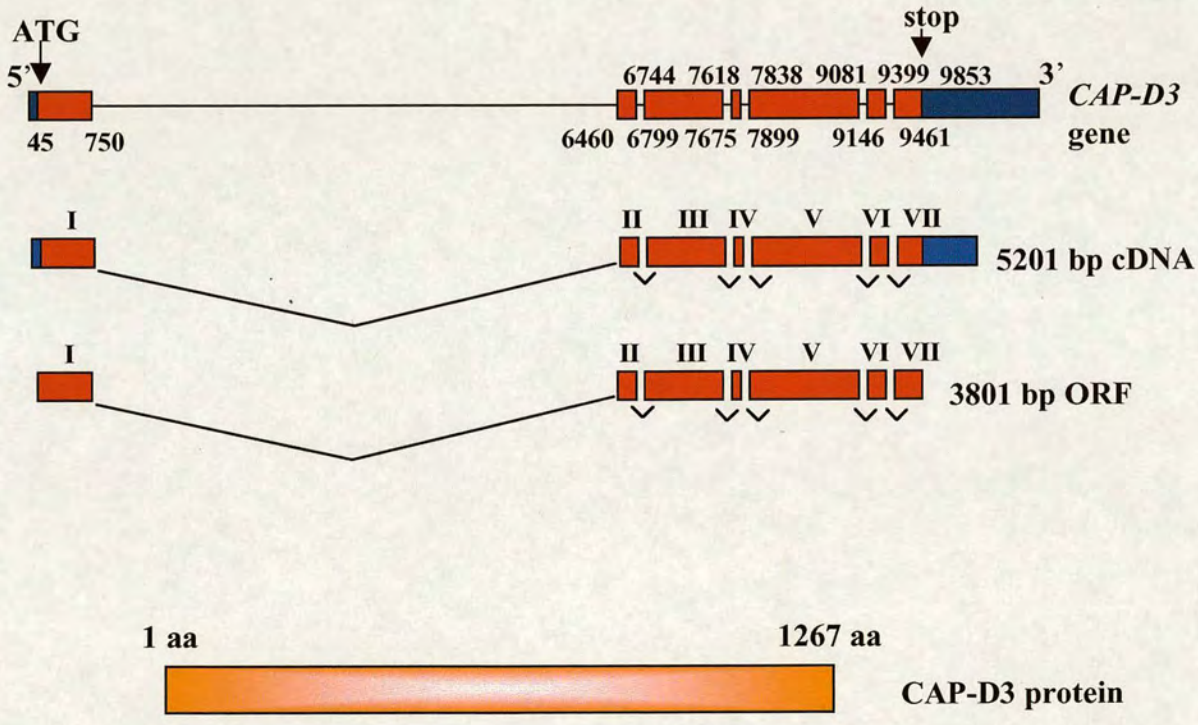

Figure 6.2. A. Overview of the left arm of the second chromosome. The *CAP-D3* gene (red square) is located in 25E5 chromosome locus (nucleotides: 5458120-5589325). The map was adapted from Flybase.
B. The *CAP-D3* gene is 11.2 kb long and it consists of 6 introns and 7 exons. A 5201 bp cDNA encodes a protein of 1267 amino acid residues. The numbers on the *CAP-D3* gene indicate the start and the end of the exons. Exons are indicated by I-VII numbers.

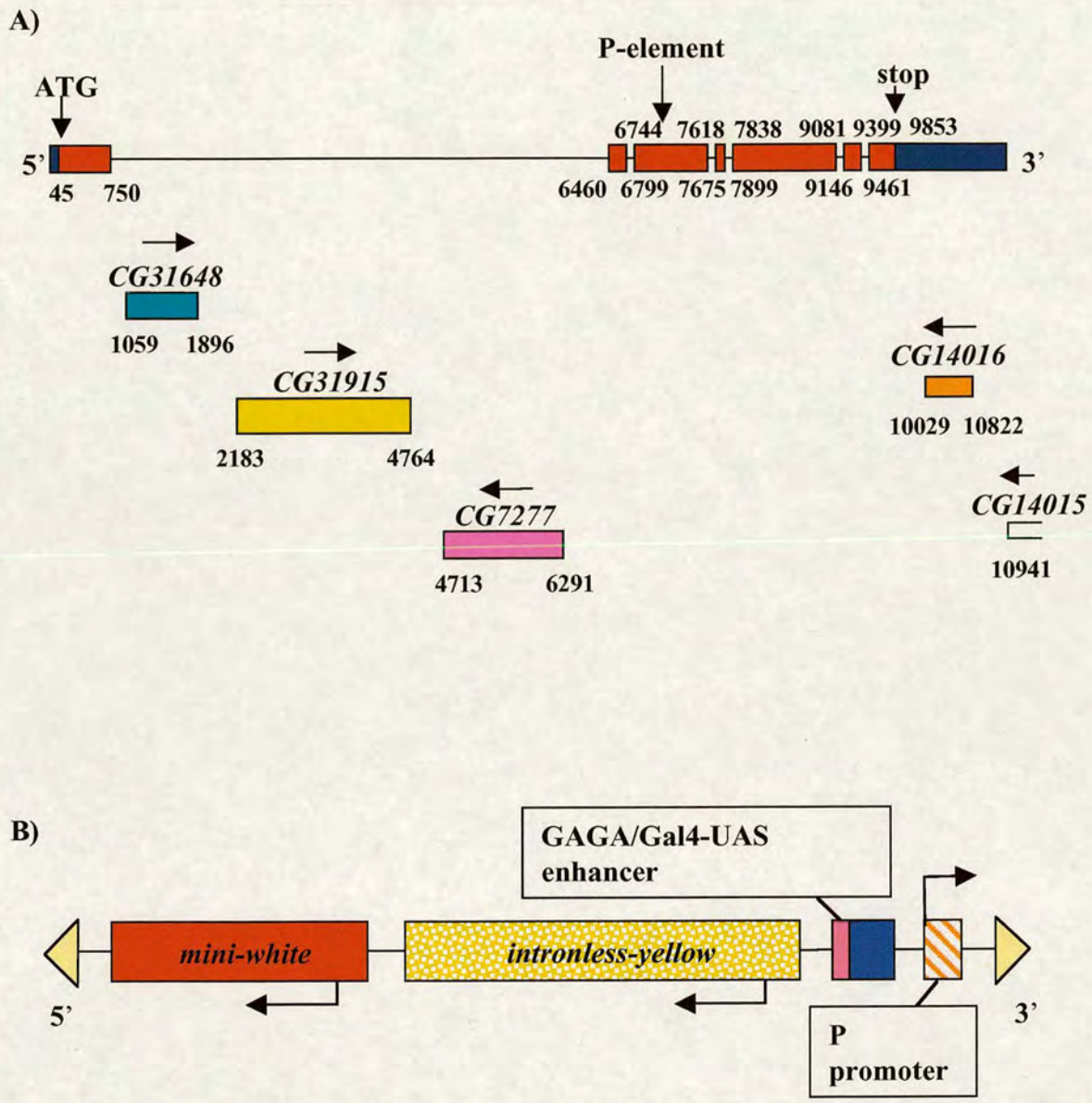

Figure 6.3. A. The first intron of the *CAP-D3* gene is about 6kb long and three other genes *CG31648*, *CG31915* and *CG7277* are located there. Two more genes, *CG14016* and *CG14015* are located in the 3' UTR of the *CAP-D3* gene. The orientation of *CG7277*, *CG14016* and *CG14015* genes is from right to left which is opposite to the transcription orientation of *CAP-D3* gene. A P-element, *P{EPgy2}*, insertion at the beginning of the third exon of the *CAP-D3* gene (1095 bp of ORF) interrupts the function of the gene, causing a mutation.
B. The P-element *P{EPgy2}* is 10,872 bp long and it contains two functional transgenes, the *mini-white* and the *intronless-yellow*, which can be used to follow the transposon (P-element) on the appropriate genetic background. The promoter of the P-element is at the 3' of the P and the orientation is from left to right. This P-element also has a GAL4/UAS enhancer that allows the mis-expression of an adjacent gene downstream of the P-element promoter under the control of ectopic GAL4 drivers.

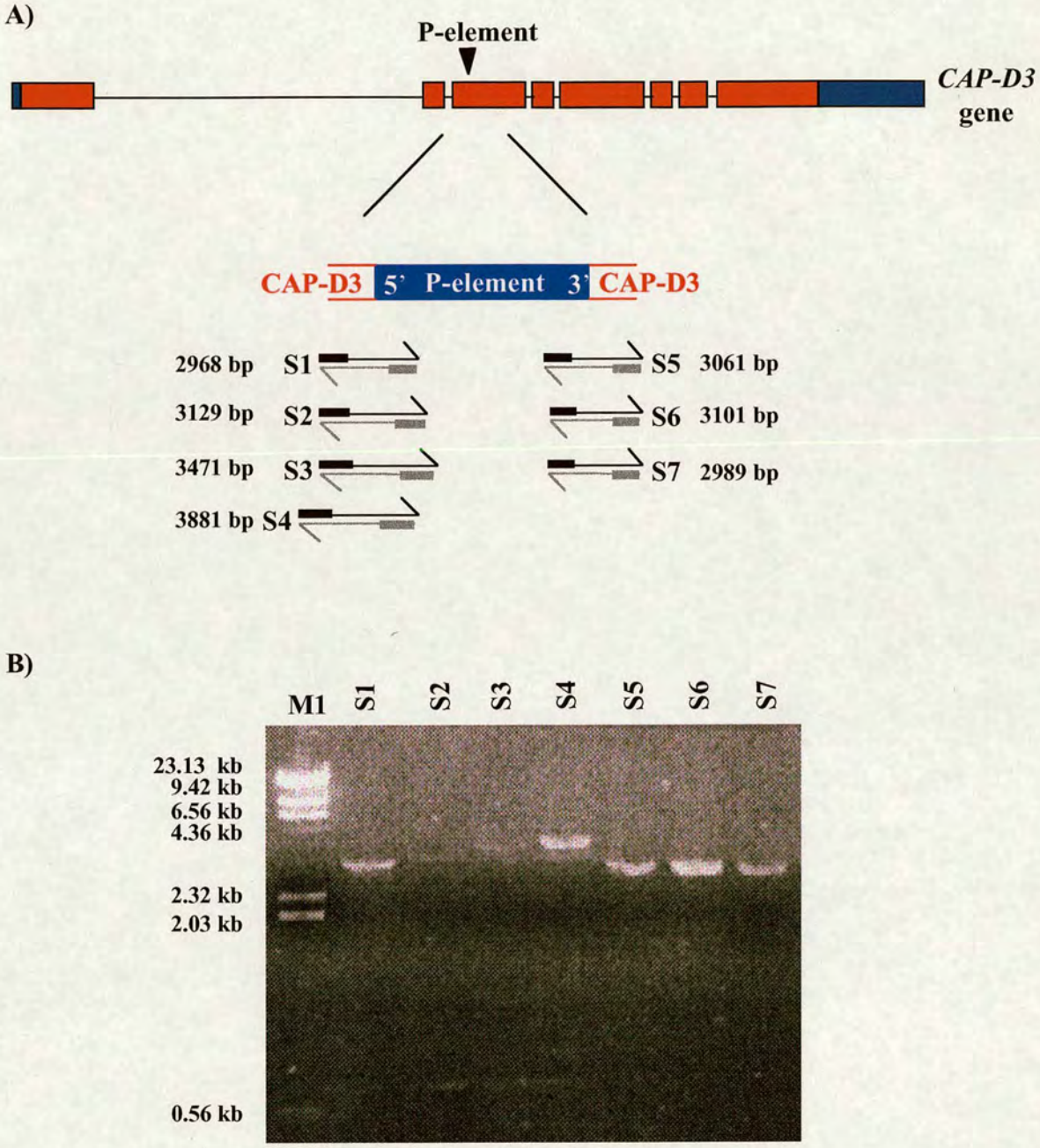

Figure 6.4. A. Strategy used to determine the exact position of P-element in the *CAP-D3* gene (5' and 3' flanking sequences of P-element). Primer pairs S1-7 were used (Table XIV). The position of the primer pairs is shown relative to the *CAP-D3* gene and the P-element. The exact position of the primers is summarised in Tables X and XI. The size of each PCR product is indicated next to each primer pair.

B. PCR products after amplification of the regions shown by the primer pairs in (A) (S1-S7). M1 molecular weight marker is the λ phage digested with HindII.

The exact position of the P-element insertion in the *CAP-D3* gene was reported in Flybase, however it was necessary to confirm it. Therefore, primer pairs at the 5' and 3' ends of the P-element and at the *CAP-D3* sequence flanking the P-element were designed (Figure 6.4 A). The region around the 5' and 3' of the P-element including CAP-D3 sequence was amplified by PCR and the reactions were sequenced (Figure 6.4 B). The P-element was indeed inserted at 1095 bp of the CAP-D3 ORF. Eight base pairs were duplicated at the insertion point as generally happens with P-element insertions (O'Hare, 1983). Thus, the last eight base pairs of the CAP-D3 sequence flanking the 5' end of the P-element were also present at the end of the 3' end of the P-element.

The *CAP-D3* mutation was carried over the *CyO* balancer. In order to test if homozygous flies were dying and in which developmental stage, heterozygous flies for the *CAP-D3* mutation were crossed inter se as follows:

$$\frac{P\{EPgy2\}}{CyO} \times \frac{P\{EPgy2\}}{CyO} \rightarrow \frac{P\{EPgy2\}}{CyO} \quad \frac{P\{EPgy2\}}{P\{EPgy2\}} \quad \frac{CyO}{CyO}$$

expected ratio	33%	67%	die
observed ratio	33%	67%	die

It was obvious that the homozygous progeny *P{EPgy2}/P{EPgy2}* were viable and healthy since flies with straight wings were present in the population in the expected ratio (33%). The *CyO/CyO* were dying in early embryogenesis. To test if the homozygous flies for the *CAP-D3* mutation were fertile, male and female homozygous flies for the mutation were crossed simultaneously to female and male wild type (*CaS*) flies respectively, as follows:

A. Check female fertility

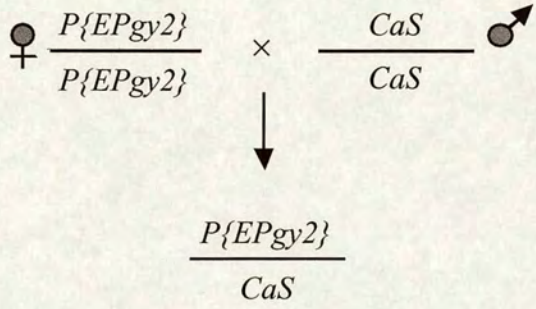

and

B. Check male fertility

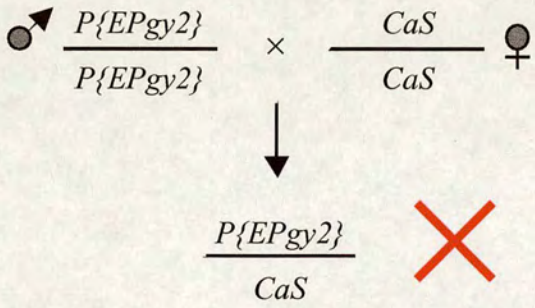

When male homozygous flies *P{EPgy2}/P{EPgy2}* were crossed with female wild type flies (B) no progeny eclosed (×), suggesting that male homozygous for the *CAP-D3* mutation were sterile. Therefore, it could be possible that CAP-D3 is involved in male meiosis. However, the fact that other genes are located in the *CAP-D3* gene it was possible that they were also affected by the P-element insertion. The disruption of these genes could be the causal of male sterility and for this reason several tests were performed in order to investigate this hypothesis (see 6.4).

6.4. The genes located in the CAP-D3 gene are not affected by the CAP-D3 mutation

Several tests were performed in order to investigate if the function of the 5 other genes that are located in the *CAP-D3* gene were affected by the P-element insertion in the *CAP-D3* mutation. Initially, RT-PCR was performed to test if the transcription of the genes was affected by the P-element insertion. mRNA from flies homozygous for the *CAP-D3* mutation was used to generate cDNA, while mRNA from wild type flies was used as a control. Primers were designed to cover the majority of the message RNA of each of the 5 genes and finally RT-PCR products of the expected size were obtained (Figure 6.5 A and 6.5 B). It was apparent that all five genes were normally transcribed in the *CAP-D3* homozygous flies and their levels were similar to wild type controls (Figure 6.5 B).

As mentioned previously, two P-element mutations interrupting the *CG7277* (*13964/CyO*) and *CG14016* (*EP(2)2415/CyO*) genes were available from the Bloomington Stock Centre. These mutations could be very useful for assessing if the interrupted genes (*CG7277* and *CG14016*) were affected by the P-element insertion in the *CAP-D3* mutant (demonstrated later on). When these fly lines were tested for the state of their homozygous flies, it was obvious that they were viable but the ratio was lower than expected, suggesting that they are semi lethal. This was concluded after heterozygous flies were crossed inter se independently for each line as follows:

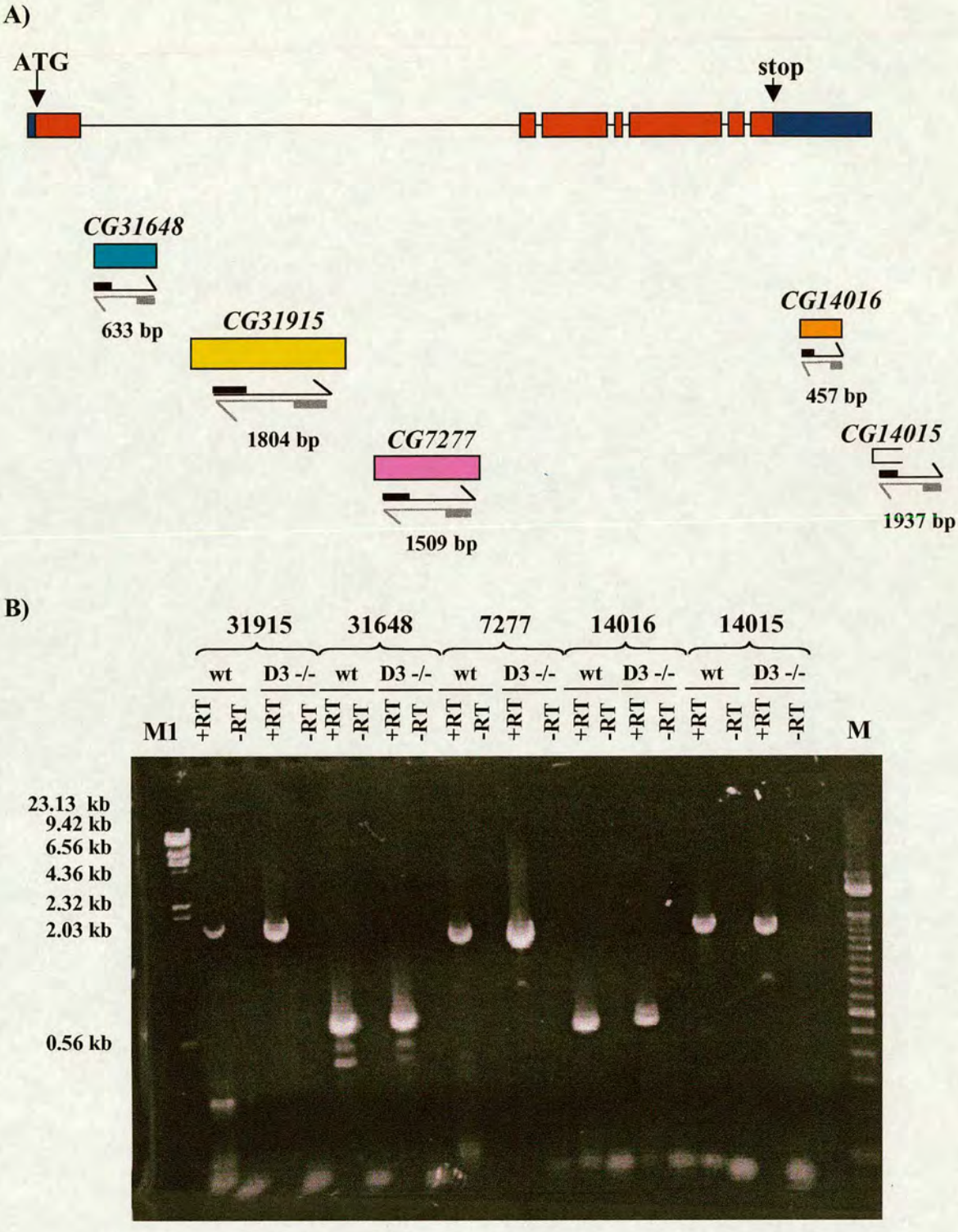

Figure 6.5. A. Strategy showing the amplification of the majority of the mRNA of each one of the 5 genes that locate in the *CAP-D3* gene (*CG31915*, *CG31648*, *CG7277*, *CG14016*, *CG14015*). The position of the primers is shown relative to the five genes and the *CAP-D3* gene. The exact position of the primers is summarised in Tables XIII and XIV. The size of each PCR product is indicated next to each primer pair.
B. RT-PCR products showing that the transcription levels of the five genes located in the *CAP-D3* gene are not affected by the P-element insertion. mRNA from wild type (wt) flies and flies homozygous for the *CAP-D3* mutation (D3 -/-) was used as template for the cDNA library. RT-PCR reactions without reverse transcriptase (-RT) were done as control. M1 is the λ phage digested with HindII molecular weight marker and M is the 1 kb DNA ladder.

A.

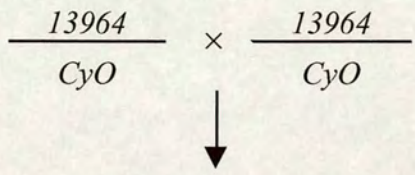

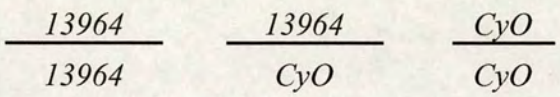

expected ratio	33%	67%	die
observed ratio	7%	93%	die

and

B.

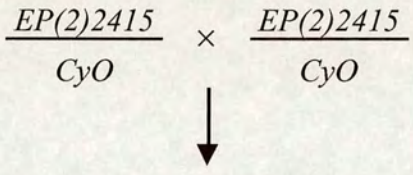

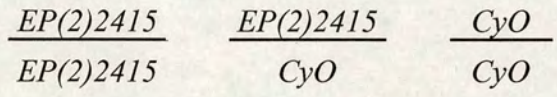

expected ratio	33%	67%	die
observed ratio	16%	84%	die

From the first cross (A), homozygous flies *13964/13964* were present in the population in a ratio of 7%, while the expected ratio was 33% since *CyO/CyO* progeny die during embryogenesis. Similarly, the *EP(2)2415/ EP(2)2415* homozygous flies (B) were present in 16% while the expected ratio was 33%. These results suggest that the homozygotes for these two mutations are semi-lethal. Furthermore, when the fertility of

the homozygous *13964/13964* and *EP(2)2415/ EP(2)2415* flies was tested as follows, it was obvious that they were both male sterile (×) (A2 and B2 respectively).

(A)

(1) check female fertility

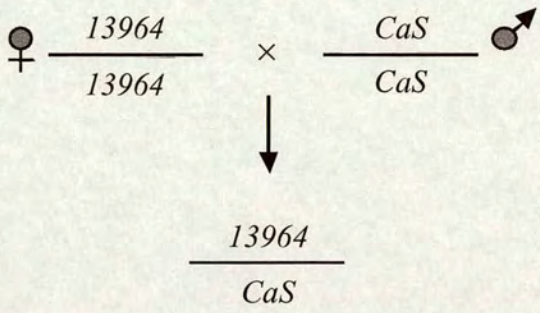

(2) check male fertility

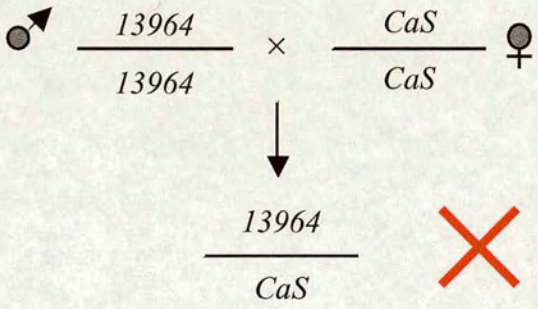

and

(B)

(1) check female fertility

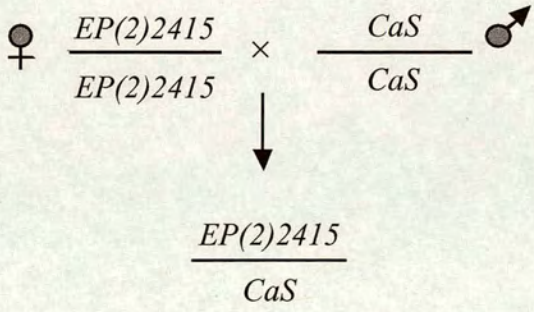

(2) check male fertility

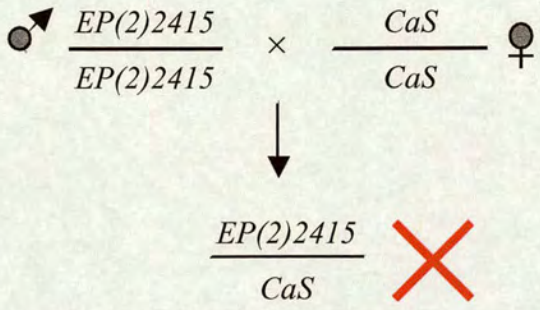

This could suggest that *CAP-D3* gene is affected in these two mutations since the P-element insertion in *CG7277* interrupts the first intron of the *CAP-D3* gene, while the mutation in *CG14016* interrupts the 3' UTR of the *CAP-D3* gene.

To test if the *CAP-D3* mutation was affecting the *CG7277* and *CG14016* genes, a complementation test was performed between the two mutations and the *CAP-D3* mutation as follows:

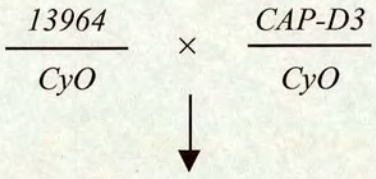

13964 / *CAP-D3*	*13964* / *CyO*	*CAP-D3* / *CyO*	*CyO* / *CyO*

expected ratio	33%	33%	33%	die
observed ratio	33%	33%	33%	die

and

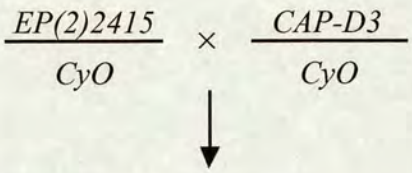

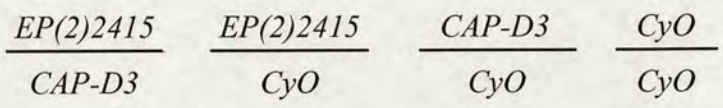

expected ratio	33%	33%	33%	die
observed ratio	31%	34%	34%	die

The trans-heterozygous flies for each case, *13964/CAP-D3* and *EP(2)2415/CAP-D3,* were easily distinguished as they had straight wings. The ratio of these flies was 33% for *13964/CAP-D3* and 31% for the *EP(2)2415/CAP-D3*, which was very close to the expected ratio of 33% in both cases, since *CyO/CyO* flies die during embryogenesis. Thus, it was obvious that the presence of *CAP-D3* gene (and subsequently the presence of the other genes) rescues the phenotype of the other two mutations, confirming that *CG7277* and *CG14016* genes are not affected in the *CAP-D3* mutation and thus they were able to rescue the phenotype of the *13964* and *EP(2)2415* mutations respectively. However, when the fertility of the trans-heterozygotes *13964/CAP-D3* and *EP(2)2415/CAP-D3* was assessed, it was apparent that they were both male sterile, suggesting that the P-element insertions in *CG7277* and *CG14016* genes may affect the *CAP-D3* gene or that these genes may also be important for fertility. Nevertheless, this observation has to be confirmed by RT-PCR from mRNA derived from *13964/13964* and *EP(2)2415/ EP(2)2415* homozygous flies. If the levels of CAP-D3 mRNA are affected in these mutations it means that the P-element insertions affect the *CAP-D3* gene.

Additional data that supports the idea that the other genes are not affected by the CAP-D3 P-element insertion came from *CAP-D3* mutant crosses to three deficiencies that uncover the *CAP-D3* region (deficiency *6624/CyO* [breakpoints: 25D2-4;25F2-4],

deficiency *25/CyO* [breakpoints: 25D4;25F1-2], and deficiency *3365/CyO* [breakpoints: 25D7;26A7]). Only the *3365/CyO* deficiency was molecularly mapped. The *CAP-D3* mutant was crossed to the deficiencies as follows:

a)

$$\frac{6624}{CyO} \times \frac{CAP\text{-}D3}{CyO} \downarrow$$

$$\frac{6624}{CAP\text{-}D3} \quad \frac{6624}{CyO} \quad \frac{CAP\text{-}D3}{CyO} \quad \frac{CyO}{CyO}$$

expected ratio	33%	33%	33%	die
observed ratio	29%	35%	35%	die

b)

$$\frac{3365}{CyO} \times \frac{CAP\text{-}D3}{CyO} \downarrow$$

$$\frac{3365}{CAP\text{-}D3} \quad \frac{3365}{CyO} \quad \frac{CAP\text{-}D3}{CyO} \quad \frac{CyO}{CyO}$$

expected ratio	33%	33%	33%	die
observed ratio	28%	36%	36%	die

c)

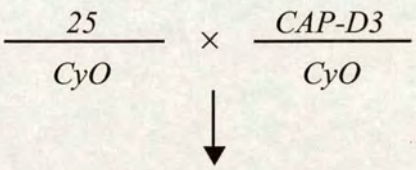

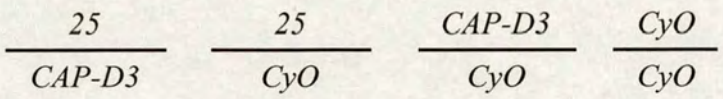

expected ratio	33%	33%	33%	die
observed ratio	32%	34%	34%	die

The *6624/CAP-D3*, *3365/CAP-D3* and *25/CAP-D3* progeny were all viable. The ratio for these progeny were 29%, 28% and 32% respectively, which were very close to the expected ratio of 33% since the *CyO/CyO* progeny die during embryogenesis. This suggests that the *CAP-D3* mutation was rescuing the loss of the neighbouring genes in the deficiency including the other genes located within the *CAP-D3* gene. Furthermore when a fertility test was performed on the *6624/CAP-D3*, *3365/CAP-D3* and *25/CAP-D3* progeny, it was apparent that the male progeny were sterile (×) (A2, B2 and C2), confirming that *CAP-D3* gene is probably involved in male meiosis.

(A)

(1) check female fertility

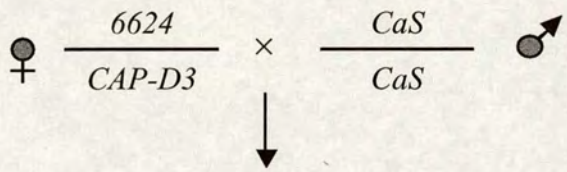

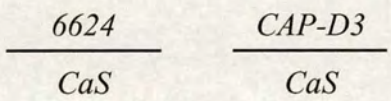

(2) check male fertility

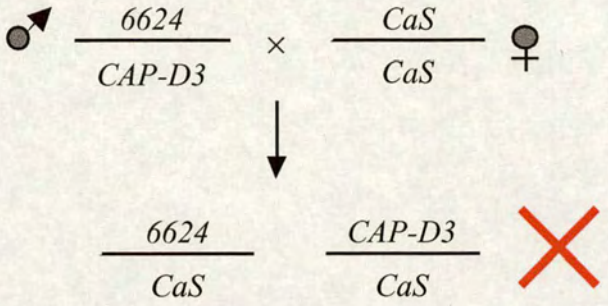

(B)

(1) check female fertility

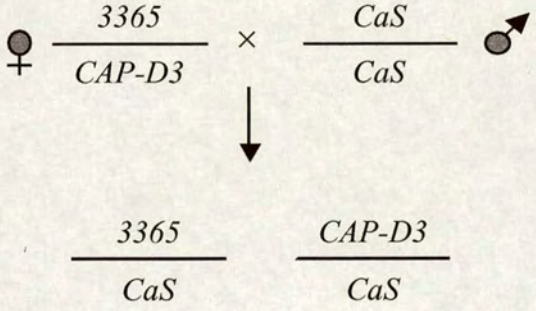

(2) check male fertility

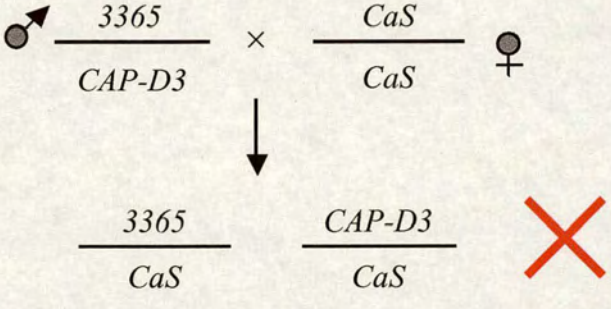

(C)

(1) check female fertility

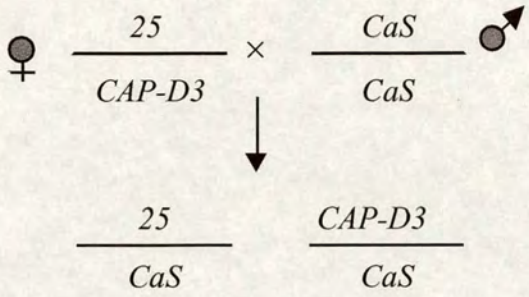

(2) check male fertility

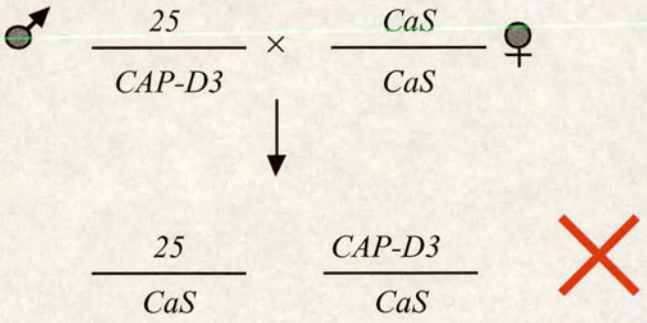

6.5. Developmental and tissue-specific expression of CAP-D3

Since the only observed defect in the *CAP-D3* mutation was male sterility, it was anticipated the *CAP-D3* gene would be expressed in testes. For this reason a search was carried out in Flybase to find any putative CAP-D3 EST clones. This search resulted in the finding of 5 ESTs, of which 4 derived from embryos and one from testes (Chapter 2.3, Table II). Two of the embryonic ESTs, RE18364 and RE74832, appear to contain full length cDNA (Figure 6.6 A). The testes EST, AT11671, was reported as full length, but it was missing the first 706 nucleotides of the CAP-D3 ORF, which corresponds to the first exon (706 bp), while it contained the 5' UTR of the cDNA (45 bp) (Figure 6.6 B). The testis clone could possibly be an alternatively spliced form that is necessary in testes. The predicted protein sequence for the testis clone was the same as the full length

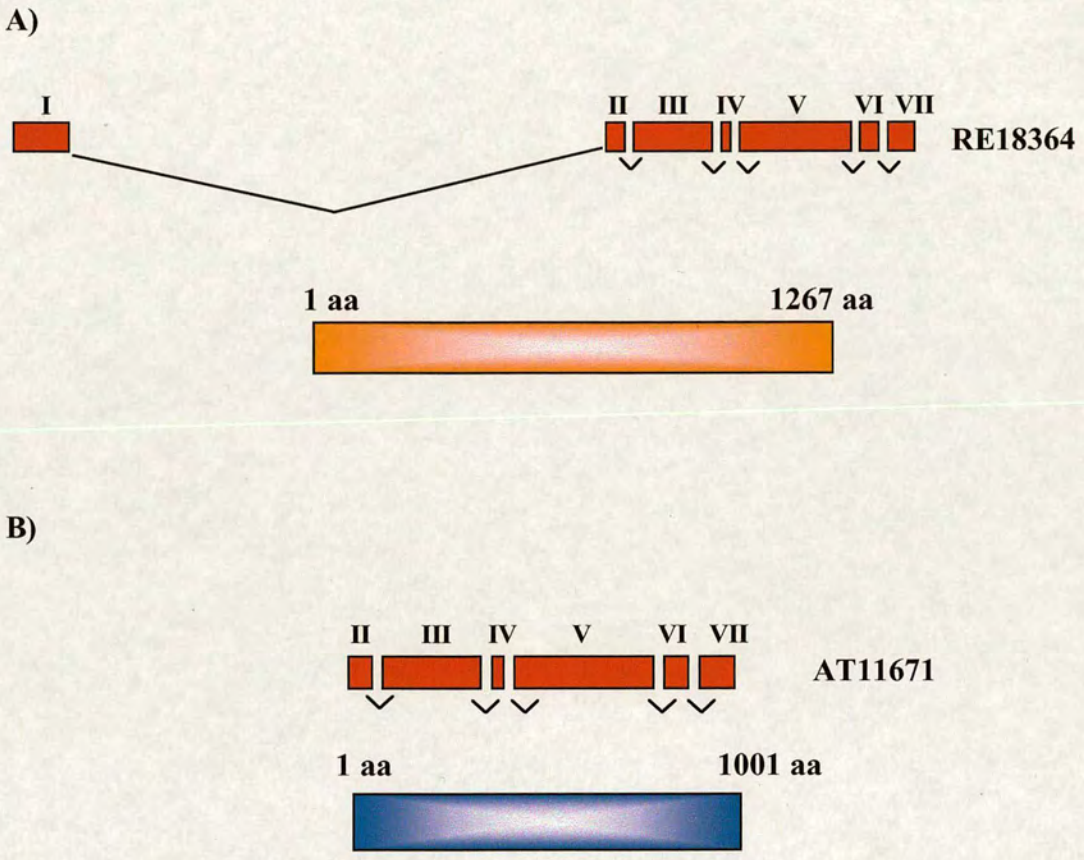

Figure 6.6. Alternatively possible spliced forms of the *CAP-D3* gene. The RE18364 EST from embryos contains the full length cDNA of the *CAP-D3* gene which encodes for the CAP-D3 protein of 1267 amino acids (A), while the AT11671 EST from testes is missing the first exon and it encodes for a protein of 1001 amino acids (B). Exons are marked with numbers I-VII.

CAP-D3 protein but it was missing the first 266 aa (Figure 6.6 B), suggesting that an alternative ATG start codon may exist at the beginning of the second exon. In order to confirm that these differences exist between the embryonic and testes ESTs, the RE18364 and AT11671 clones were obtained and sequenced. The embryonic clone contained the full length ORF and a part of the 5' and 3' UTR, while the testis clone was missing the first exon of the *CAP-D3* gene, which was in agreement with the Flybase data. Also the testis clone appeared to contained 30 bp from the first intron and 62 bp that did not match the *CAP-D3* genomic sequence. This 62 bp could be an artefact from the cloning, as it did not match any other genomic sequences after searching against sequences of different species. These results suggest that AT11671 EST clone could represent an alternatively spliced form of the *CAP-D3* gene that is required in testes or an artefactual chimera.

In order to test if alternatively spliced forms exist in testes and embryos, RT-PCR was performed from different fly tissues and developmental stages. For this purpose RNA was extracted from male and female brains, male and female 3rd instar larvae, adult testes and carcass (what was left from the male fly after testes were removed), adult ovaries and carcass (what was left from the female fly after ovaries were removed), testes from *CAP-D3* homozygous flies and carcass. Primers to cover the 5' and 3' of the CAP-D3 mRNA were designed (Figure 6.7 A). The primers for the 5' were designed to cover the majority of the first exon (that was absent from the EST clone found in testes), and a part of the second exon. The primers from the 3' were covering the last three exons of the message which were present in both the embryonic and testes EST clones. RT-PCR revealed a band of the expected size for both 5' and 3' of the mRNA in all tissues and developmental stages that were examined (Figure 6.7 B). In some tissues (*CAP-D3* carcass, female larvae, female brains and female carcass) the 5' of the mRNA was not present (Figure 6.7 B), but when the RT-PCR was repeated for these tissues, with higher amount of template, the expected product was obtained (Figure 6.8 B). These results suggest that the first exon is also transcribed in testes and it could be possible that two alternatively spliced forms exist in this tissue. The first form would include the first

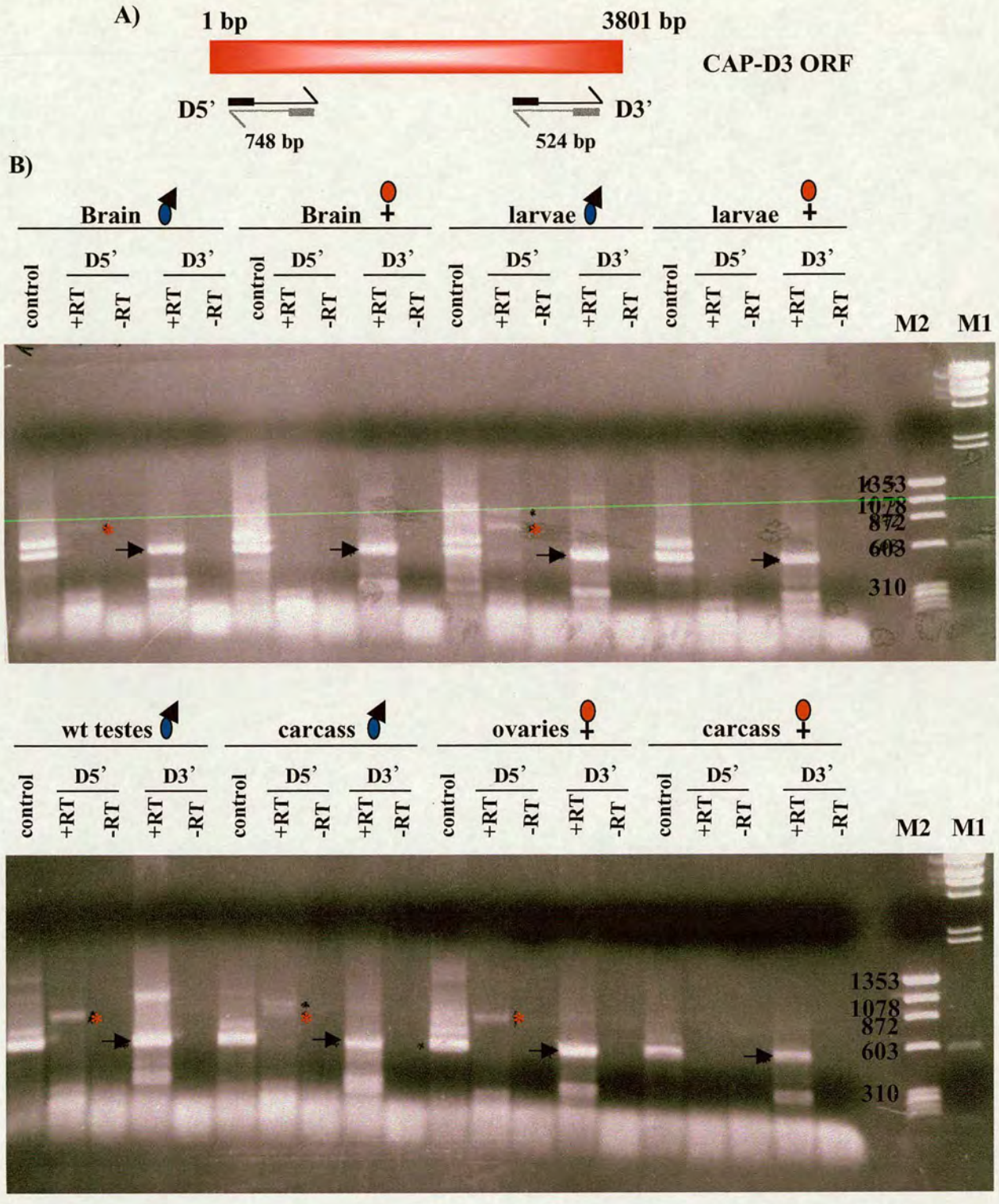

Figure 6.7. A. Diagram of the position of the primer pairs that were used to amplify the 5' (D5', 748 bp) and 3' (D3', 524bp) of the CAP-D3 ORF (Tables XI and XIV). The D5' product corresponds to the first two exons while the D3' product to the last three exons of the *CAP-D3* gene.

B. RT-PCR products after amplification of the 5' (D5', red asterisk) and 3' (D3', arrow) of the CAP-D3 ORF, in different tissues and developmental stages of *Drosophila melanogaster*. The 3' is present in all tissues and developmental stages while the 5' is present in brains, larvae, testes and carcass of male flies. Control primers were used to amplify a region of the *SMC2* gene (control). RT-PCR reactions without reverse transcriptase (-RT) were done as controls. M1 and M2 are molecular weight markers: λ phage digested with HindII and ϕX174 phage digested with HaeIII respectively. ♂=males, ♀ =females

A)

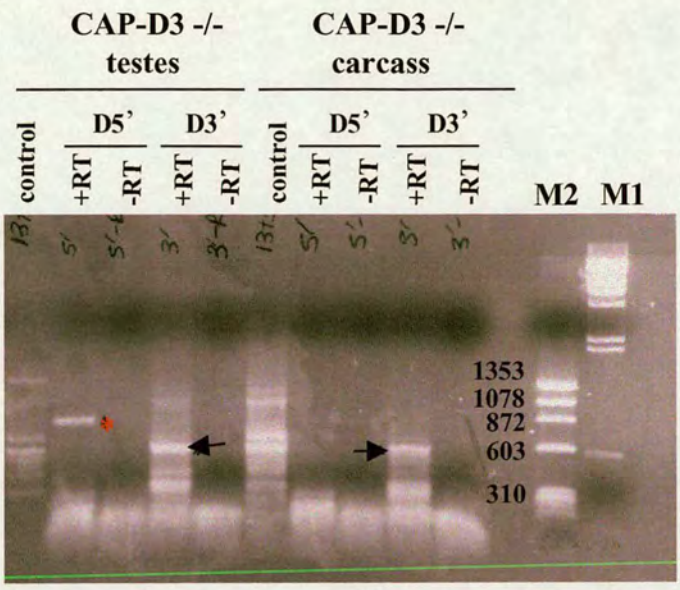

B)

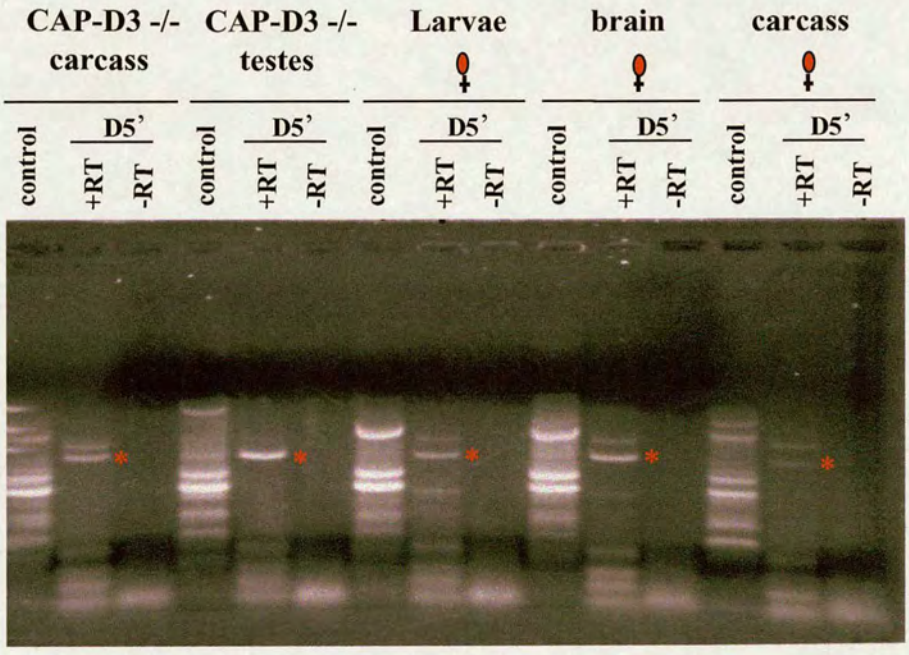

Figure 6.8. A. RT-PCR products after amplification of the 5' (D5', red asterisk) and 3' (D3', arrow) of the CAP-D3 ORF in the testes and male carcass of flies homozygous for the *CAP-D3* mutation. The 3' is present in both the testes and carcass, while the 5' is only present in the testes.

B. RT-PCR products after amplification of the 5' of the CAP-D3 ORF in tissues that the 5' failed to amplify by RT-PCR as shown in figure 6.6(B) and 6.7(A). The experiment was repeated with higher amount of template (cDNA) compared to figure 6.7(B) and 6.8(A). All tissues appear to include the 5' of the CAP-D3 ORF in the message RNA. Control primers were used to amplify a region of the *SMC2* gene (control). RT-PCR reactions without reverse transcriptase (-RT) were done as controls.

M1 and M2 are molecular weight markers: λ phage digested with HindII and ϕX174 phage digested with HaeIII respectively. ♂=males, ♀=females

exon while the second would not. However, further investigation is necessary in order to confirm if and which different forms of the CAP-D3 protein exist.

6.6. CAP-D3 antibody generation and characterisation

6.6.1. Antibody characterisation by immunoblotting

In order to analyse the role of condensin II in *Drosophila*, antibodies against the non-SMC subunits were necessary. Thus, peptide antibodies in two rabbits were generated against the 15 last amino acid residues of the C-terminus of CAP-D3 protein (Figure 6.9 A) (rabbits A2922 and A2923). Optimisation of immunoblotting conditions for these antibodies was necessary. For this purpose, extract from *Drosophila* cultured cells (S2 cells) was analysed by using the CAP-D3 antibodies (Figure 6.9 B). A prominent band of about 80 kDa was detected by both antibodies. Pre-immune sera of the rabbits that were immunised against the CAP-D3 peptide were used as a control in the immunoblotting. The pre-immune sera did not detect the 80 kDa band or any other band indicating that the CAP-D3 antibodies specifically detected this protein (Figure 6.9 B). The difference between the predicted (145 kDa) and the detected 80 kDa band of CAP-D3 protein could be because a different form exists in these cells or that the CAP-D3 protein is cleaved. Smaller products were also detected by the antibodies which probably represent degradation products of the CAP-D3 protein or unspecific proteins recognised by the antibody. A similar pattern of bands was detected by the two CAP-D3 antibodies but the signal from the A2922 serum was stronger and thus was considered to be better for immunoblotting analysis.

Since mutation of the *CAP-D3* gene results in male sterility, immunoblot analysis was performed against testis extract from wild type, heterozygous and homozygous flies by using the CAP-D3 antibody (A2922) (Figure 6.9 C). A prominent band of approximately the predicted size (~145 kDa) was present in all testes extracts. Smaller but less prominent bands were also present in these extracts. These bands could correspond to degradation products, alternatively spliced forms or post-translational modifications of the full length CAP-D3 protein. In the same analysis, carcass extract from wild type, heterozygous and homozygous flies was analysed and showed

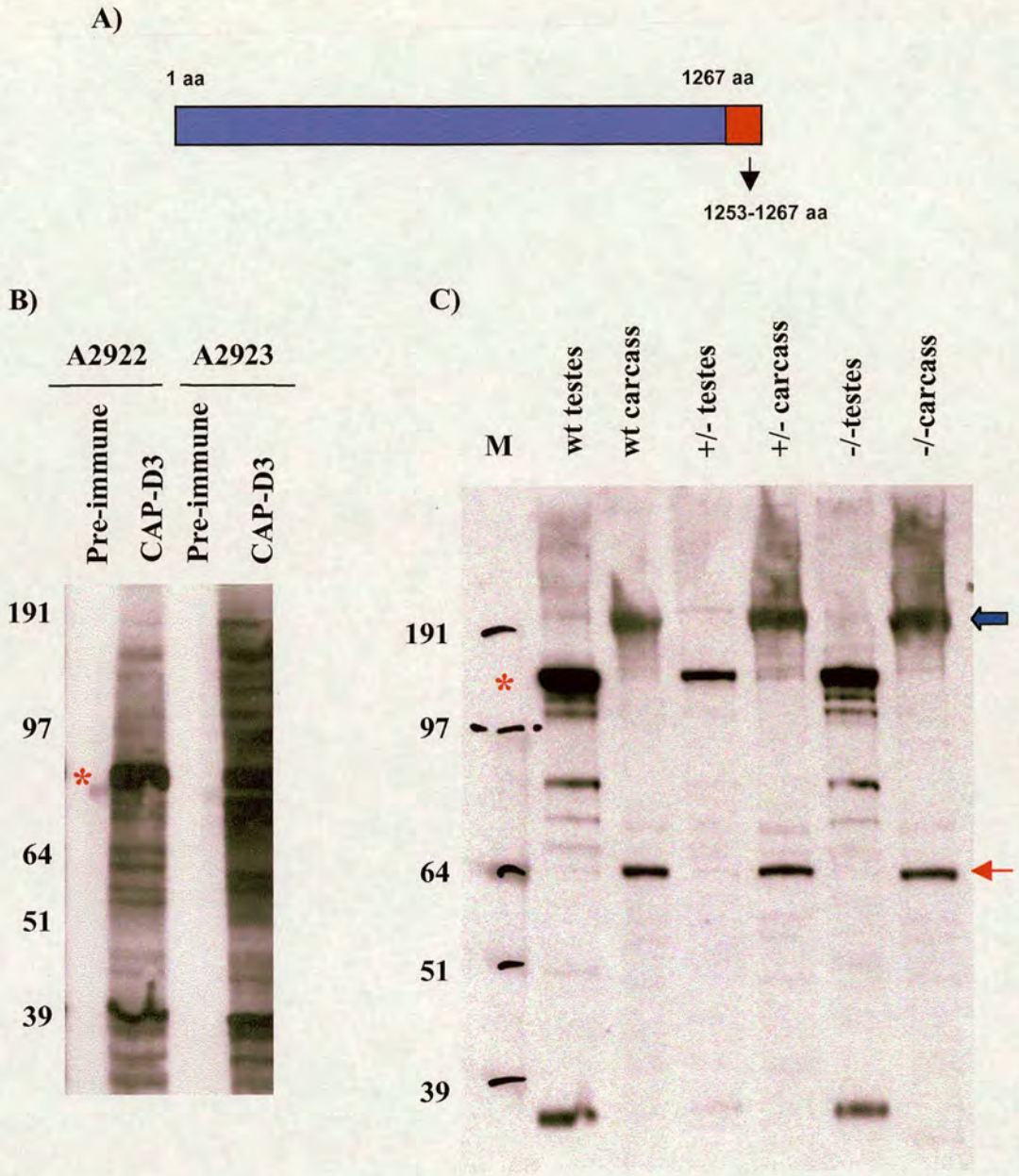

Figure 6.9. A. Schematic representation of the protein region that was used to generate the CAP-D3 peptide antibody. The 15 terminal amino acid residues were used (1253-1267).

B. Immunoblot analysis against cell extract (S2 cells, $5x10^5$ cells/lane) with the CAP-D3 antibodies revealed a prominent band of about 80 kDa (asterisk). The band was absent from the pre-immune lanes. Two CAP-D3 antibodies were used (A2922 and A2923) and a similar pattern of bands was detected by both. The A2922 gave stronger signal and thus was considered to be better for immunoblotting.

C. Immunoblot analysis against testes and male carcass extracts from wild type, heterozygous (+/-) and homozygous (-/-) flies. The A2922 antibody was used. Approximately four testes/lane were loaded, while an equivalent amount of protein from carcass extract was loaded (the protein extracts were compared by coomassie staining). The CAP-D3 antibody recognises a band of approximately the estimated size (145 kDa, asterisk) in all testes extracts including the homozygous mutant (-/-) lane. Smaller bands that are labelled in testes lanes are probably degradation products. In the carcass lane the ~145 kDa band is not detected, but a prominent band of ~191 kDa (block arrow) is recognised. Also a smaller band of ~64 kDa (arrow) is present as well. M is the SeeBlue Plus2 (Invitrogene) molecular weight marker.

prominent bands, of approximately 191 kDa and 64 kDa (Figure 6.9 C). These results strongly suggest that full length CAP-D3 protein is expressed in testes. However, it is very difficult to explain why the CAP-D3 protein is still present in homozygous flies. One possible explanation is that the P-element is not transcribed and only wild type full length CAP-D3 protein is produced. Another remote possibility is that part of the P-element is transcribed, which compensates for the upstream part of the *CAP-D3* gene that is not expressed and thus a protein of a size similar to the wild type protein is produced. Nevertheless, to be able to answer this question, further experiments would need to be performed (see 6.6.2).

To test if the full length CAP-D3 protein was present in tissues other than testes or in different developmental stages, a developmental and tissue-specific immunoblotting was performed. Extracts from male and female brains, male and female third instar larvae, testes, male head and male carcass (what was left from the fly after testes and head were removed), ovaries, female head and female carcass (what was left from the fly after ovaries and head were removed) were analysed by using the CAP-D3 antibody (Figure 6.10). Several banding patterns were revealed which were usually different for each extract and thus no conclusions could be easily made. A prominent band of approximately the predicted size for full length CAP-D3 protein (~145 kDa) was present in brain, testis and ovary extracts (Figure 6.10, asterisk). In the remaining extracts prominent bands of the predicted size were not recognised by the antibody. However, many bands were identified in all extracts suggesting that alternatively spliced forms might exist in different tissues and developmental stages. Some of these bands could be non-specific background proteins or degradation products of the CAP-D3 protein. Some of these products could correspond to post-translational modifications of the CAP-D3 protein. Nevertheless, it would be appropriate to affinity purify the CAP-D3 antibody in order to observe which bands are specifically detected by the CAP-D3 antibody.

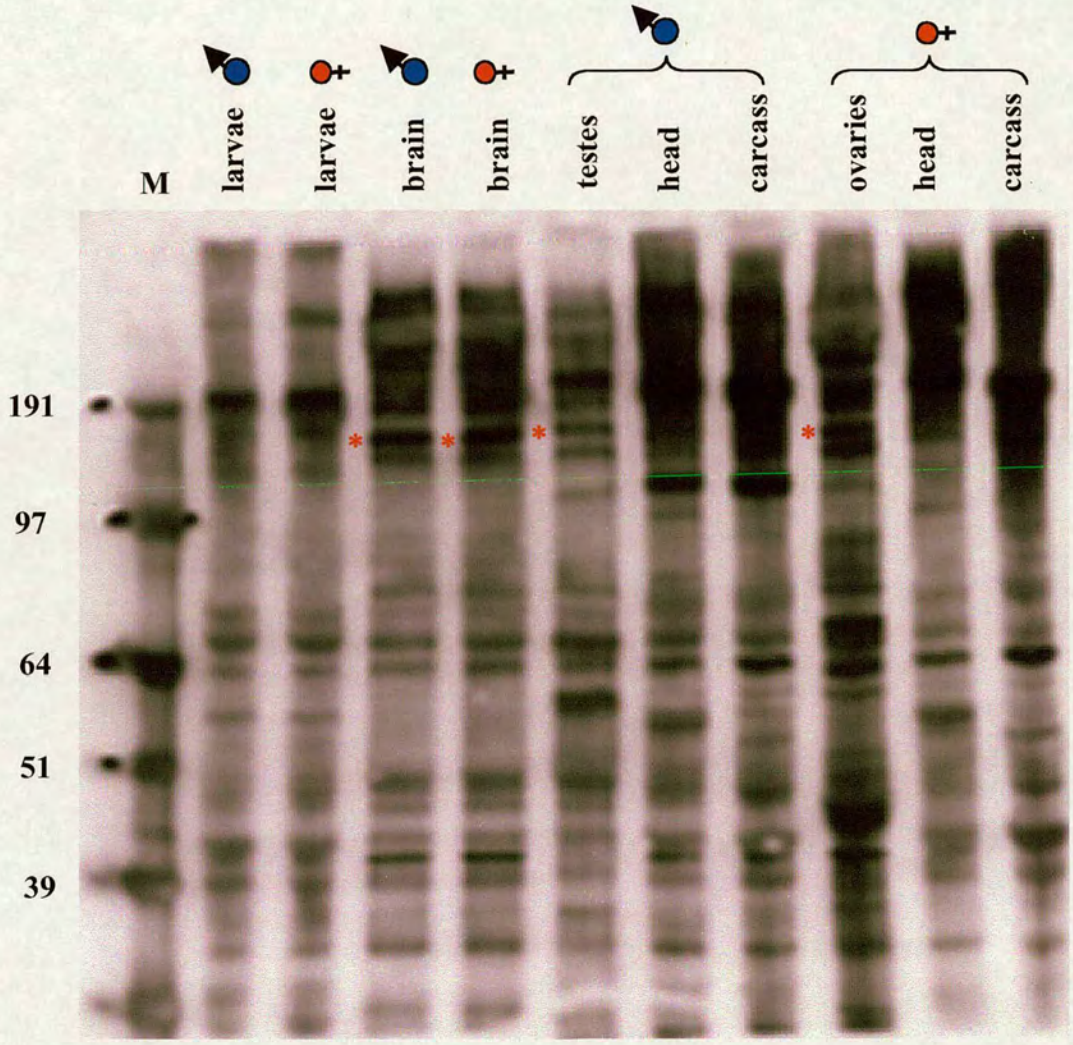

Figure 6.10. Developmental and tissue-specific immunoblot.
Immunoblot analysis against extracts from male and female brains, male and female third instar larvae, testes, male head and carcass, ovaries, female head and carcass were analysed by using the CAP-D3 antibody (A2922). A different banding pattern was revealed for each extract. A prominent band of approximately the estimated size for full length CAP-D3 (~145 kDa) is present in brain, testis and ovary extracts (asterisk). In the remaining extracts no prominent band of the predicted size is recognised by the antibody. However, many bands are identified in all extracts suggesting that alternatively spliced forms may exist in different tissues and developmental stages. M is the SeeBlue Plus2 (Invitrogene) molecular weight marker.

6.6.2. Transcription of the P-element in the CAP-D3 mutant

As previously mentioned, the CAP-D3 antibody recognises a band of the predicted size in both the wild type and *CAP-D3* homozygous mutant testes. One possibility is that the P-element is not transcribed along with the *CAP-D3* gene and thus a product of the predicted wild type size is produced. For this reason RT-PCR was performed in order to see if and how much of the P-element was transcribed along with the *CAP-D3* gene. As mentioned previously the P-element is 10,872 bp long and it contains two functional transgenes, the *mini-white* (*white*$^+$ gene missing the first intron) and the *intronless-yellow* (*yellow*$^+$ gene missing its intron), which can be used to follow the transposon on the appropriate genetic background (*white*$^+$ and *yellow*$^+$ are genes of the *Drosophila* genome and thus are also present in wild type flies). The orientation of these genes is from right to left which is opposite to the orientation of the *CAP-D3* gene. The promoter of the P-element is at the 3' end of the P-element and the orientation is from left to right. This P-element also has a GAL4/UAS enhancer. All the different regions of the P-element are linked between them with unspecific DNA sequences (Bellen, 2004; Geyer, 1992; Patton, 1992)(Figure 6.11 A).

For the RT-PCR reactions, primers along the P-element were designed (Figure 6.11) and mRNA from male flies homozygous for the *CAP-D3* mutation was used as a template for cDNA library. mRNA from male wild type flies was used as a control. At the same time, PCR reactions (as an additional control) were set up with genomic DNA as a template from wild type flies and flies homozygous for the *CAP-D3* mutation using the same primer pairs (Figure 6.12 B). The position of the primer pairs is indicated in Figure 6.11 while the presence or absence of the products as expected and as eventually obtained are shown in Figure 6.12(A). RT-PCR reactions with primer pairs 1, 3 and 5 were in agreement with what was expected (Figure 6.12 A and 6.12 B). In addition, when combinations between the fourth and fifth primer pairs (primer pair 6) were attempted, no RT-PCR products were amplified suggesting that this region was not transcribed. In this reaction, a product was expected from *CAP-D3* (-/-) genomic DNA with a size similar to wild type but it was not obtained.

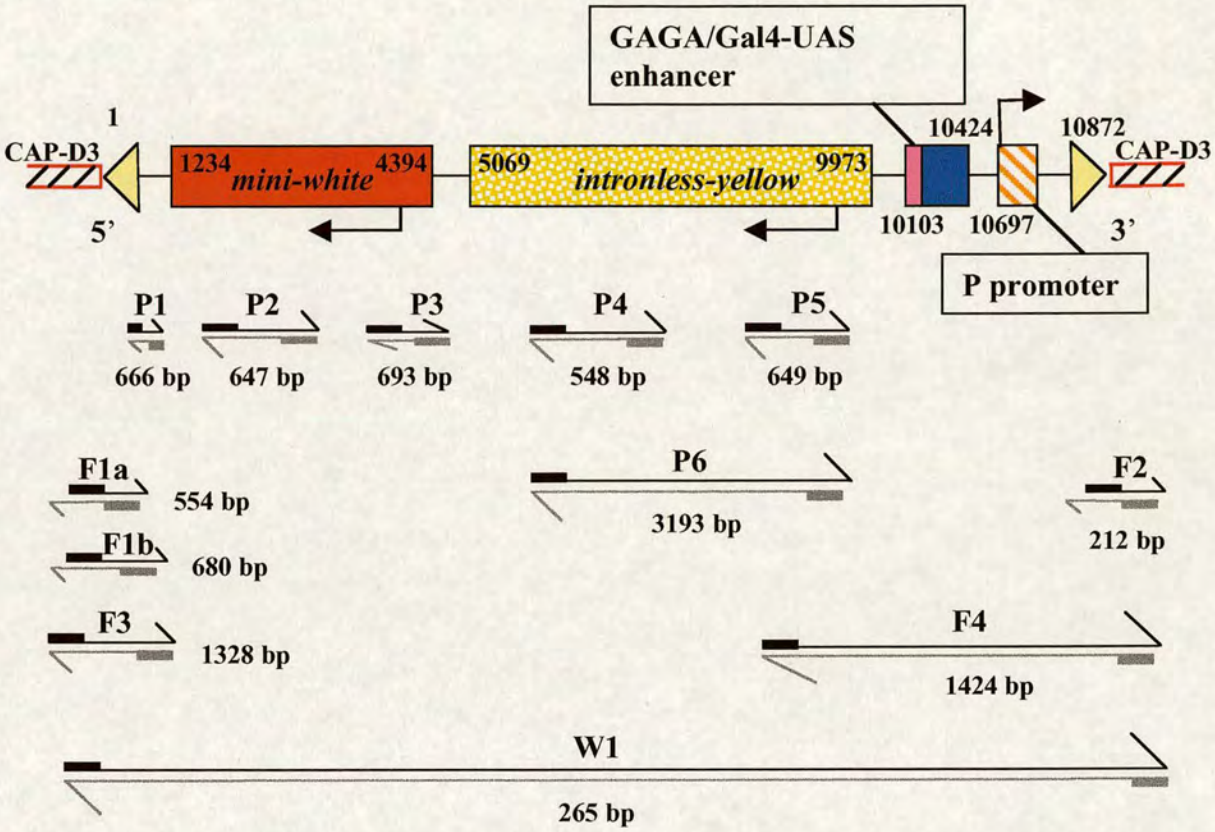

Figure 6.11. Diagram showing the position of several primer pairs relative to the different regions of the P-element *P{EPgy2}* and the *CAP-D3* flanking sequence. The primer pairs (P1-P6, F1-F4 and W1) were designed to investigate which parts of the P-element are transcribed and their exact position is summarised in tables X, XI and XIV. The numbers on the P-element indicate the start and end of the different parts of the P-element. The *white*$^+$ and *yellow*$^+$ genes are shown. The mRNA of the *yellow*$^+$ gene corresponds to the 5069-7106 bp of the P-element, while the rest of the indicated *yellow*$^+$ gene (7106-9973 bp) is 5' genomic sequence flanking the *yellow* $^+$ gene. The size of each PCR product is indicated on each primer pair.

A)

	Primer pair 1 P1		Primer pair 2 P2		Primer pair3 P3		Primer pair 4 P4		Primer pair 5 P5		Primer pair 6 P6	
	exp	obs	exp	obs	exp	obs	exp	obs	exp	obs	exp	obs
Wild type genomic DNA	×	×	√	√	×	×	√	√	√	√	√	√
CAP-D3 -/- Genomic DNA	√	√	√	√	√	√	√	√	√	√	√	×
Wild type RT-PCR	×	×	√	×	×	×	×	√	×	×	×	×
CAP-D3 -/- RT-PCR	×	×	√	√	×	×	×	√	×	×	×	×

B)

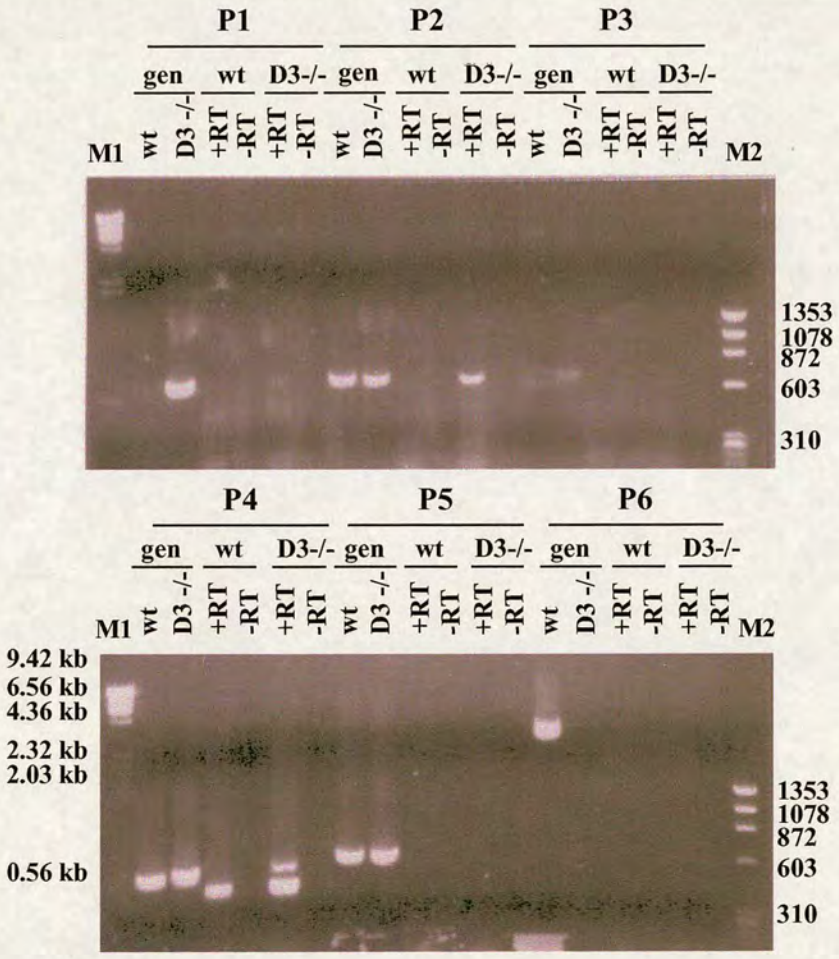

Figure 6.12. A. Table showing which products were expected (exp) to be amplified (√) or not (×) by RT-PCR and which products were amplified (obs) (√) or not (×) with the primer pairs P1-P6 (their position relative to P-element is shown in figure 6.11).
B. PCR (gen, genomic) and RT-PCR products amplified with the primer pairs P1-P6. Genomic DNA (gen) from wild type (wt) and *CAP-D3* homozygous mutant (D3 -/-) flies and cDNA from mRNA from wild type (wt) and *CAP-D3* homozygous mutant (D3 -/-) flies were used as a template. P1, P3 and P5 primer pairs amplified products as expected and are shown in 6.11(A). The products revealed from primer pairs P2, P4 and P6 disagree with the expected results. Reactions without reverse transcriptase were performed as controls (-RT). M1 and M2 are molecular weight markers: λ phage digested with HindII and ϕX174 phage digested with HaeIII respectively.

In primer pairs 2, 4 and 6 the results were unexpected, making the interpretation of the results very difficult. In primer pair 4, unexpected products were present in wild type and mutant *CAP-D3* RT-PCR reactions (Figure 6.12 B). In this case, no products were expected in either the wild type or the CAP-D3 since the reverse primer was located in the 5' flanking DNA of the *yellow* gene and thus no product should be amplified (*yellow* gene corresponds to 5069-7106 bp of P-element). The resulted products were smaller than expected, suggesting that they may be unspecific products. It could also be possible that a region of the 5' flanking DNA of the *yellow* gene is transcribed and thus these products were amplified. Furthermore, in the same reaction a bigger band was present in the *CAP-D3*(-/-) RT-PCR which was absent from the wild type. The presence of this band could not be explained either. Sequencing of these products would show if they are regions of the *yellow* gene or unspecific products. Primer pair 2 was amplifying a region of the *white* gene which is also present in wild type flies (Figure 6.12 A). This product though was not amplified in the RT-PCR reaction from wild type flies, while it was expected to be present (Figure 6.12 B). The reason for this was not clear.

The experiment was repeated three times with different PCR conditions and the results were reproducible. In conclusion, these results suggest that the *yellow* and *white* genes are transcribed independently of the *CAP-D3* gene but that the majority of the P-element is not transcribed along with the *CAP-D3* gene. This is supported by the observation that sequences linking different parts of the P-element are not transcribed (pair 1, pair 3 and pair 5). Furthermore, when RT-PCR was performed with primers that were covering the 5' and 3' ends of the P-element including the flanking*CAP-D3* region, it was obvious that these regions were transcribed (Figure 6.13 A). When the same was repeated with primers further inside the P-element (Figure 6.11), no products of the expected size were produced (Figure 6.13 B), suggesting that only a small part of the P-element (from the 5' and 3' ends) is transcribed. It also seems that the 5' of the *CAP-D3* gene (first, second and the start of the third exon) with a part of the 5' of the P-element are transcribed since an RT-PCR product of the expected size was obtained (Figure 6.8 A, 6.8 B and 6.13 A). Nevertheless, this message must not be part of the rest of the

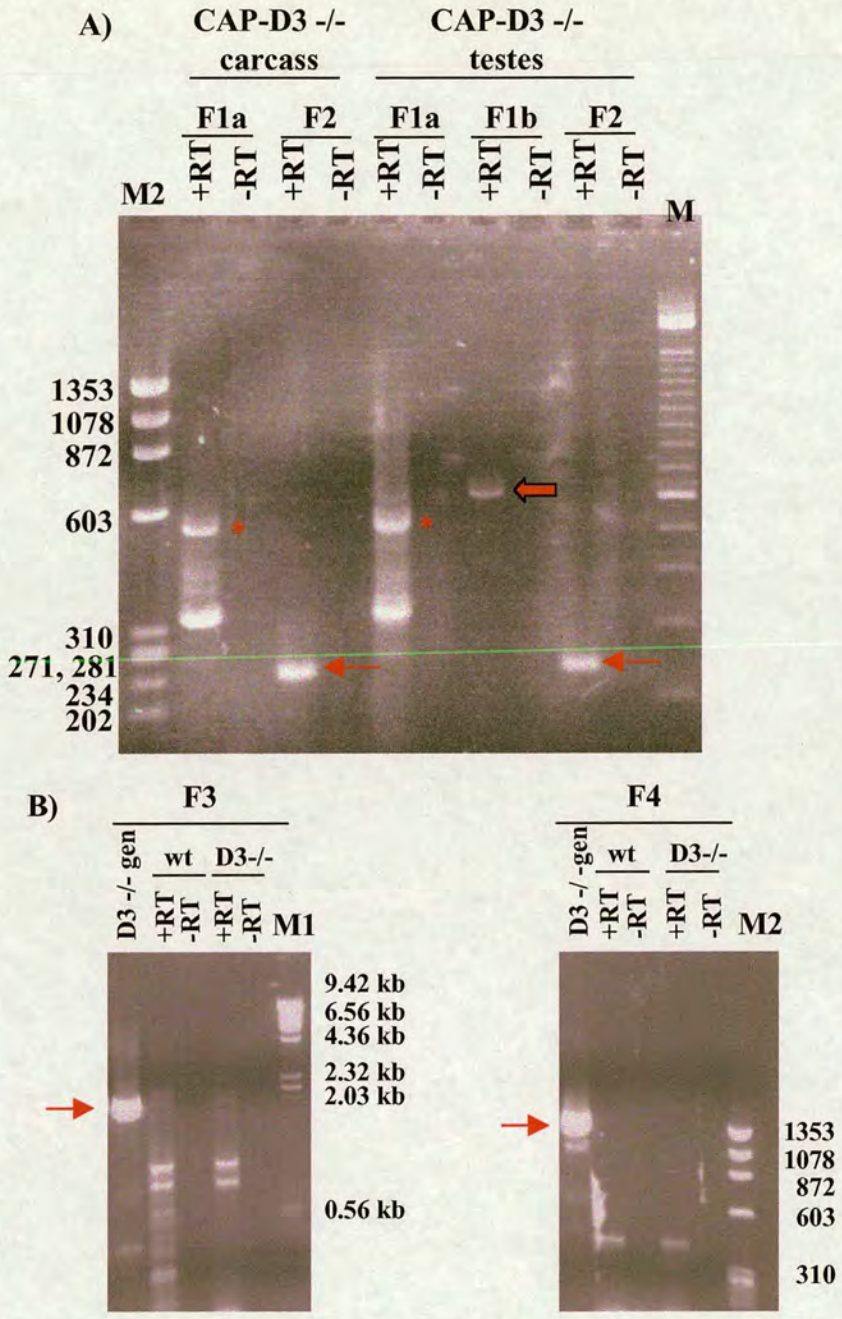

Figure 6.13. A. RT-PCR products amplified with the primer pairs F1a-F2. mRNA from testes and carcass of male flies homozygous for the *CAP-D3* (D3 -/-) mutation was used as a template for cDNA production. The position of the primers relative to the *CAP-D3* gene and the P-element is shown in figure 6.11. F1a and F1b primer pairs are amplifying a region between the 5' of the P-element and the *CAP-D3* gene (asterisk, F1a, 554 bp and block arrow, F1b, 680 bp) while the F2 primer pair is amplifying a region between the 3' of the P-element and the *CAP-D3* gene (F2, arrow, 220 bp). Reactions without reverse transcriptase were performed as controls (-RT). **B.** PCR (gen, genomic) and RT-PCR products amplified with the primer pairs F3 and F4. Genomic DNA (gen) from *CAP-D3* homozygous mutant (D3 -/-) flies and cDNA from mRNA from wild type (wt) and *CAP-D3* homozygous mutant (D3 -/-) flies were used as a template. The position of the primers is shown in Figure 6.11. No RT-PCR products of the expected size (arrows) were amplified. The bands that were amplified are probably unspecific products since they are also present in wild type lanes. Reactions without reverse transcriptase were performed as controls (-RT). M1 and M2 are molecular weight markers : λ phage digested with HindIII and ϕX174 phage digested with HaeIII respectively. M is the 1kb DNA ladder.

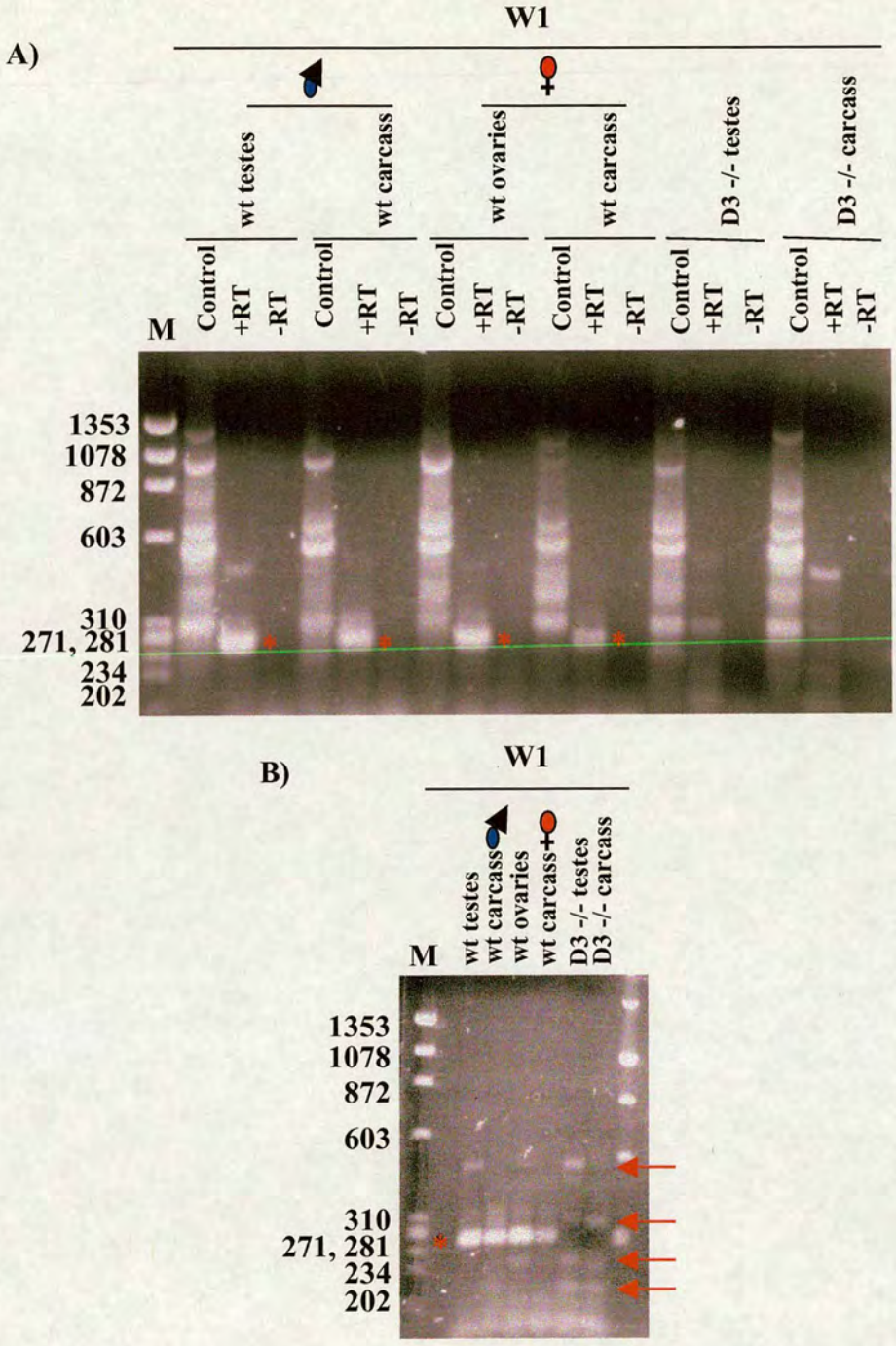

Figure 6.14 A. RT-PCR products amplified with the primer pair W1. mRNA from testes, ovaries and carcasses of wild type flies and flies homozygous for the *CAP-D3* (D3 -/-) mutation was used as a template for cDNA production. The primers are located on the CAP-D3 sequence flanking the P-element (Figure 6.11) and a product of ~257 bp is amplified in wild type tissues (asterisk). This product is absent from *CAP-D3* homozygous flies and no prominent band is amplified that would correspond to the part of the P-element that is transcribed. Reactions without reverse transcriptase were performed as controls (-RT). Control primers were used to amplify a region of the *SMC2* gene (control).

B. The same as in (A). All the reactions from (A) were loaded side by side to compare the products that were revealed from the reactions (only +RT). No product is amplified in testes and carcass homozygous for the *CAP-D3* mutation. Some bands that were revealed are also present in wild type tissues suggesting that they are unspecific products (arrows). ♂ = males, ♀ = females

M (molecular weight marker) is ϕX174 phage digested with HaeIII.

CAP-D3 message since no RT-PCR product was obtained with primers that were designed to cover the entire P-element message (primers were located on the CAP-D3 DNA sequence flanking the P-element) (Figure 6.11, 6.14 A and 6.14 B).

Unfortunately the antibody recognises only the C-terminus of the CAP-D3 ORF and thus it could not be determined if the N-terminus of the CAP-D3 is expressed as a separate stable protein or if the N-terminus is somehow linked to the rest of the CAP-D3 message. The best way to examine this is by Northern analysis. By this procedure it would also be possible to investigate if the CAP-D3 protein is indeed present in the mutant and if a part of the P-element is included in the CAP-D3 message by using probes from different parts of the CAP-D3 coding sequence and from the P-element. I did not attempt this due to lack of time.

6.6.3. CAP-D3 localisation in S2 tissue culture cells

Even though CAP-D3 is most probably involved in male meiosis, the existence of the embryonic ESTs and the observation that the antibody recognises a prominent band by immunoblotting S2 tissue culture cells, suggest that CAP-D3 may be more generally expressed. Therefore, the subcellular localisation of CAP-D3 was analysed by immunofluorescence in S2 tissue culture cells that were cytospun on poly-L-lysine slides (Figure 6.15). Immunolabeling revealed that the protein localised diffusely in the cytoplasm and the nucleus during interphase (Figure 6.15 A). During mitosis, CAP-D3 localised at the centromeres, partially overlapping with CID at prometaphase, metaphase and anaphase, while at telophase the signal was reduced and less restricted to the centromeres (Figure 6.15 B). The CAP-D3 was partially overlapping with CID since it was only localised in one side of CID (Figure 6.15 C). Both CAP-D3 antibodies were tested and both of them showed the same localisation. The A2923 antibody was slightly better since it gave a stronger signal and thus was considered to be better for immunofluorescence analysis. Nevertheless, since the *CAP-D3* mutant phenotype suggests a role for CAP-D3 in male meiosis, an extensive localisation study of CAP-D3 protein will be performed in the future in testes.

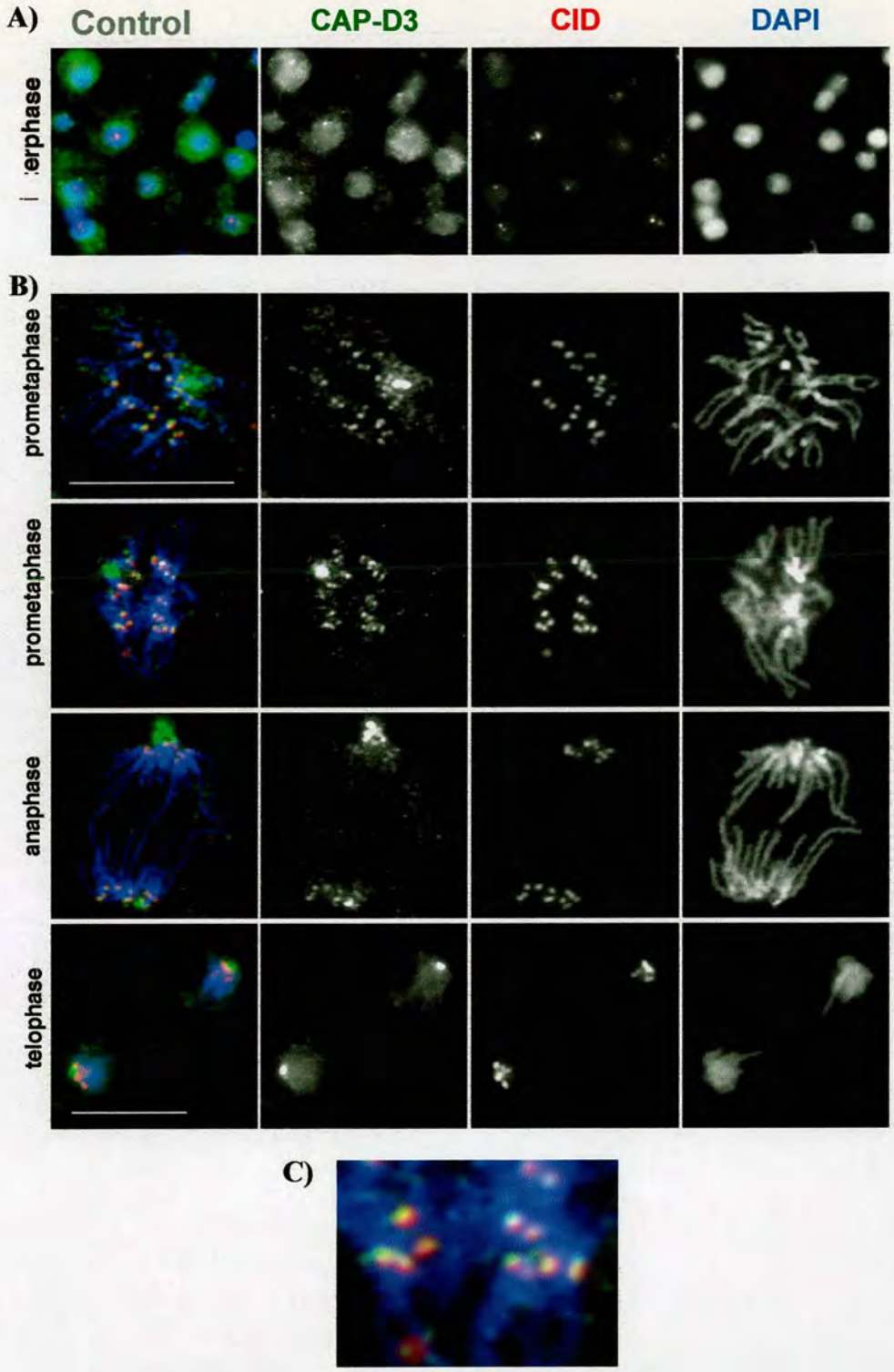

Figure 6.15. Immunolocalisation of CAP-D3 in S2 cells.
Cells were cytospun onto poly-L-lysine slides, extracted during fixation and stained for CAP-D3 (green, A2923), CID (red), and DNA (blue).
A. CAP-D3 is disperse in the cytoplasm and the nucleus during interphase.
B. CAP-D3 localises to the centromeres and partially overlaps with CID at prometaphase, metaphase and anaphase. The signal is slightly reduced during anaphase and is diffuse and less restricted to the centromeres at telophase. The antibody gives a non-specific centrosomal staining as well.
C. Higher magnification of a prometaphase cell showing that CAP-D3 is on one side of CID, since overlapping (yellow) and distinction (pure red, CID) of the two proteins can be observed.

6.7. CAP-D3 dsRNA mediated interference in Drosophila S2 cultured cells

To analyse the possible function of CAP-D3 on chromosome architecture and to investigate if CAP-D3 has a mitotic function, a double stranded RNA mediated interference on CAP-D3 was performed in S2 cells. For this reason the full length *Drosophila* EST clone RE18364 was used. Two different primer pairs were designed, the first was covering the majority of the first exon including the ATG (r1= 639bp) and the second was covering a part of the fifth exon (r2= 723 bp) (Figure 6.16 A). In this way, two different dsRNAs targeting different regions of the CAP-D3 mRNA were available, in order to target two any possible different splice forms (Figure 6.16 B). Also, even though depletion by RNAi should be specifically directed only against CAP-D3, the RNAi primers were carefully designed to be far away from the other genes located in the *CAP-D3* gene so that their function would not be disrupted. S2 cultured cells were incubated with the two different dsRNAs independently and samples were collected subsequently at 24 hr time points. Two negative controls were performed at the same time: cells that were incubated with dsRNA synthesized from a human intron (C) and cells with no dsRNA (-). Protein extracts from each time point were analysed by immunoblotting (Figure 6.16 C). No decrease in CAP-D3 levels was observed in the cells treated with CAP-D3 dsRNA and the protein levels remained unchanged even after 120 hrs. Furthermore, immunofluorescence analysis revealed that chromosome morphology and chromosome segregation appeared normal in the dsRNAi treated cells and CAP-D3 localisation was unaffected (Figure 6.16 D). These results were the same after treatment with the two different dsRNAs, suggesting that CAP-D3 protein is very stable, alternatively it has no mitotic function or, the antibodies recognise another protein.

6.8. Immunoprecipitation with the CAP-D3 antibody

Since CAP-D3 has been proposed to be a member of the condensin complex II along with CAP-G2 (so far not identified in flies) CAP-H2, SMC2 and SMC4, immunoprecipitations were performed with the CAP-D3 antibody in order to confirm that a condensin complex

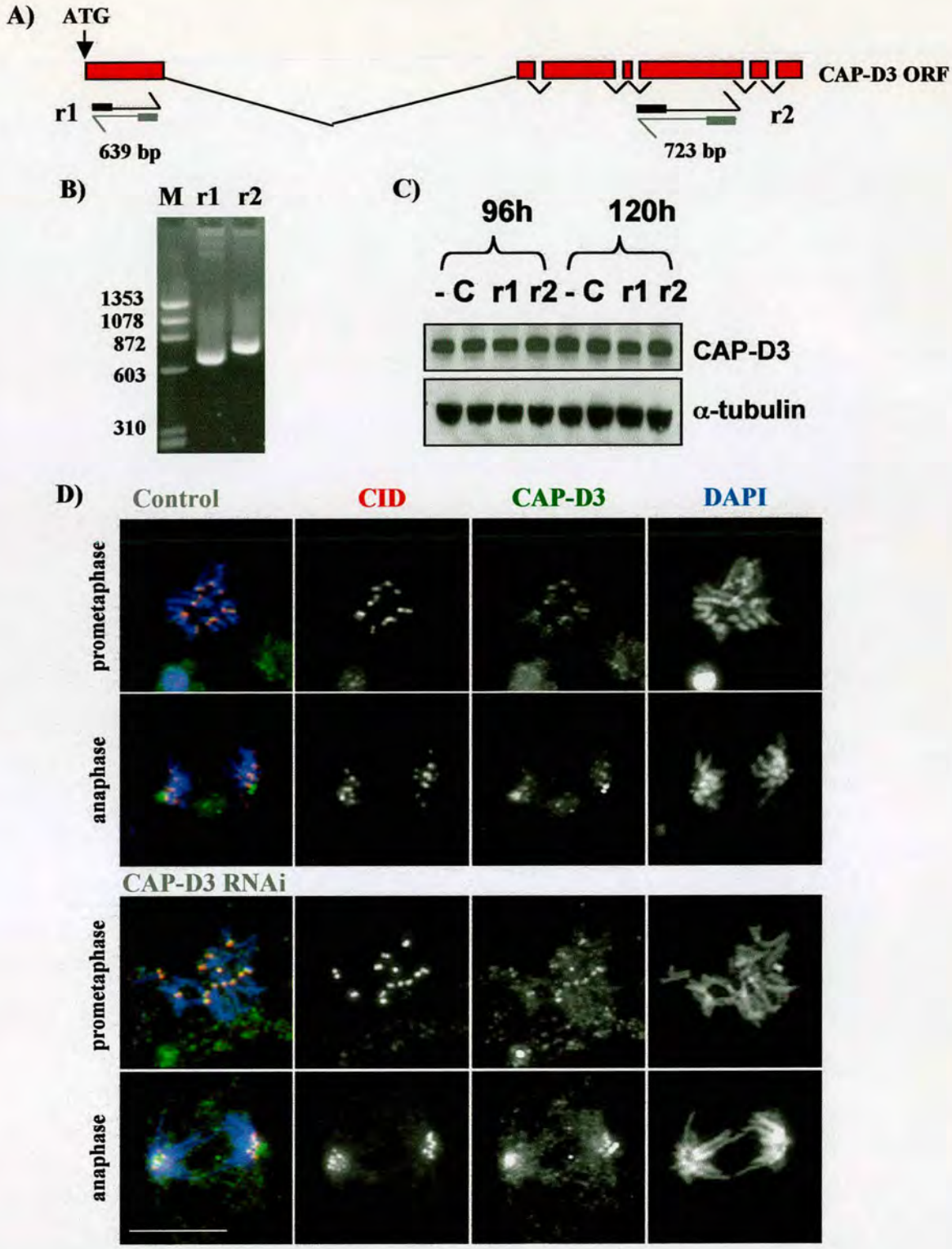

Figure 6.16. A. Diagram showing the position of the two primer pairs (r1 and r2) that were used to amplify products for CAP-D3 dsRNA. The primers are summarised in Tables XII and XIV. **B.** PCR products after amplification of two regions (r1 and r2) of CAP-D3 ORF by using the primer pairs shown in 6.15(A). These products were used as template for dsRNA production. **C.** Immunoblotting of control and CAP-D3 dsRNA treated cell extracts with an antibody to CAP-D3 shows that the protein levels are unaffected after treatment with dsRNA from different regions of the message. α-tubulin was used as a loading control. C (control dsRNA), - (no RNA), r1 and r2 (CAP-D3 dsRNA from two different regions of the message). **D.** CAP-D3 dsRNA treated cells 96 hours after treatment (r2 dsRNAi). Cells were cytospun onto poly-L-lysine slides, extracted during fixation and stained for CAP-D3 (green, A2923), CID (red), and DNA (blue). Chromosome morphology is normal and CAP-D3 protein still localises at the centromeres as in control cells. The scale bar is 10 μm.

II exists in *Drosophila*. For this reason, immunoprecipitations with both *Drosophila* CAP-D3 antibodies were performed independently by using magnetic dynabeads and 0-24 hour embryo extracts. Pre-immune serum was used as a control. Bound proteins were eluted sequentially with 0.25 M NaCl, 0.5 M NaCl and 2% SDS in PBS and the fractions were analysed by immunoblotting with CAP-D3, SMC2 and SMC4 antibodies. However, no protein could be detected with any of the CAP-D3 antibodies (or with pre-immune sera) (data not shown). Similarly, the SMC2 and SMC4 antibodies were not detecting the expected bands in the CAP-D3 immonoprecipitations as were detected with CAP-D2 immunoprecipitations (data not shown). The background banding pattern was similar to the one observed with the pre-immune sera. These results could suggest that either the two antibodies are not recognising the CAP-D3 protein or that CAP-D3 is not present/abundant in embryos. For this reason, extracts from testes should be used in order to test if the CAP-D3 antibody can pull down CAP-D3 protein and the rest of the condensin II complex. The problem with this procedure is that a large amount of testes material is needed which would be difficult to obtain. Furthermore, affinity purification of the CAP-D3 antibody is necessary so as to ensure that the antibody is recognising the appropriate protein.

6.9. CAP-D3 function is independent of CAP-D2

Since CAP-D2 and CAP-D3 are proposed to be subunits of two different complexes, it would be expected that they do not interact with each other. To assess if this is true, the fractions immunoprecipitated using the CAP-D2 antibody (Chapter 3, Figure 3.10) were probed with the CAP-D3 antibody and no interaction was detected between the two proteins (data not shown). In addition to this no difference in the level of CAP-D3 was observed in either the CAP-D2 or Topo II single depletions or CAP-D2/Topo II double depletion, suggesting that CAP-D3 was not affected (Figure 6.17 A). Also, the overall localisation of CAP-D3 was not affected in the CAP-D2 depleted cells. CAP-D3 was present at the centromeres in the CAP-D2 depleted cells and when CID was stretched, CAP-D3 was also stretched (Figure 6.17 B). These results suggest that functions of CAP-D2 and CAP-D3 are probably independent of one another.

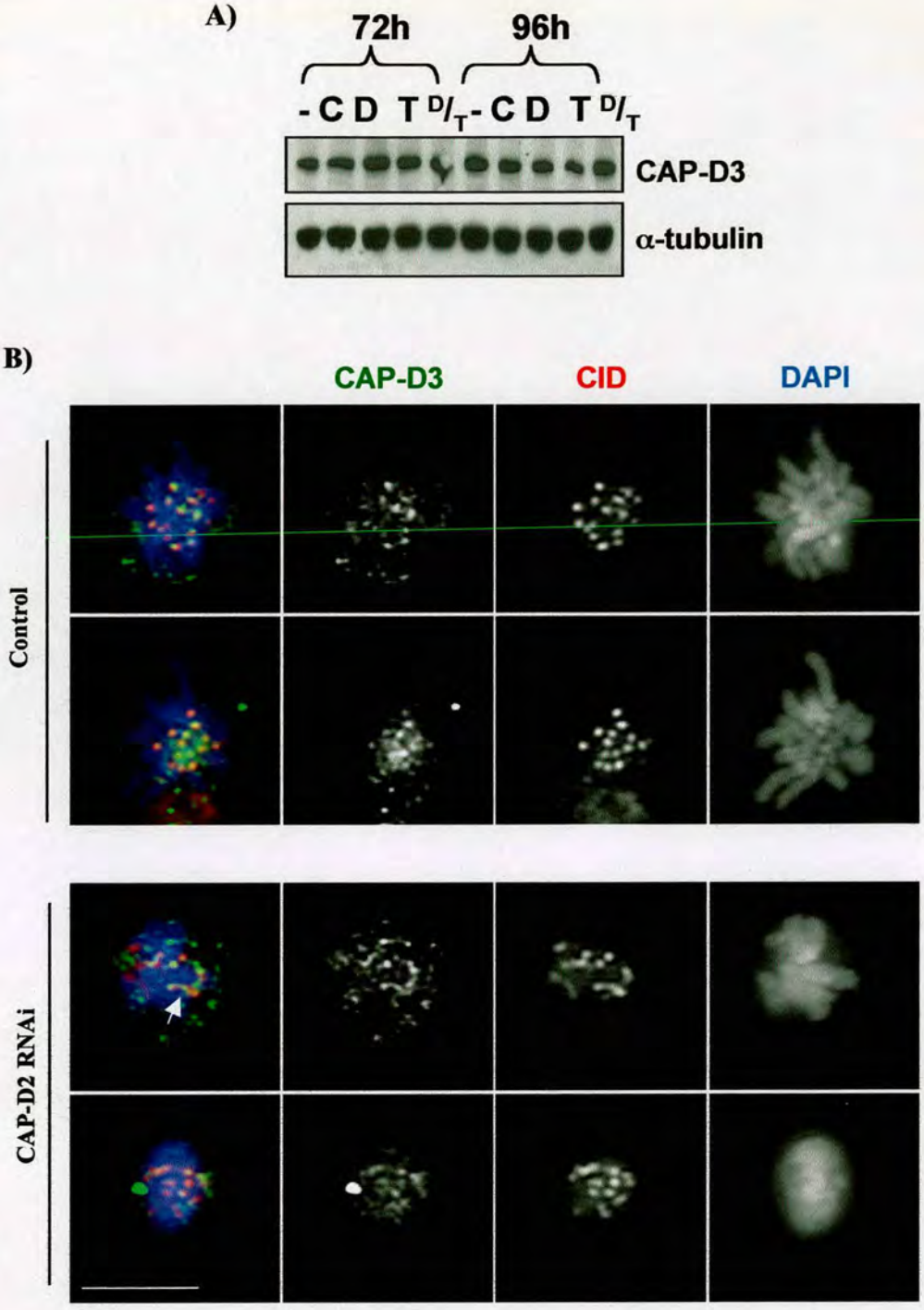

Figure 6.17. A. Immunoblotting of control, CAP-D2 depleted, Topo II depleted and CAP-D2/Topo II doubly depleted cell extracts with the CAP-D3 antibody (A2922). The CAP-D3 levels are unaffected in either the single or the double depletions. α-tubulin was used as a loading control. C (control dsRNA), - (no RNA), D (CAP-D2 dsRNA), T (Topo II dsRNA) and $^{D}/_{T}$ (CAP-D2/Topo II double dsRNA).

B. CAP-D2 dsRNA treated cells 72 hours after treatment. Cells were cytospun onto poly-L-lysine slides, extracted during fixation and stained for CAP-D3 (green, A2923), CID (red), and DNA (blue). CAP-D3 protein still localises at the centromeres in the CAP-D2 depleted cells and is stretched when CID is stretched (white arrow). The scale bar is 10 μm.

6.10. Phenotypic analysis of CAP-D3 mutant testes

The only phenotype observed in the *CAP-D3* mutant was male sterility and thus, phenotypic analysis of homozygous testes for the *CAP-D3* mutation was attempted. Two different avenues were followed to investigate the reason(s) behind male sterility. Firstly, whole testes from late pupae were observed after staining for DNA (Figure 6.18). The morphology of the mutant pupal testes was normal as their width and length appeared similar to control (Figure 6.18 A and B). The only possible defect observed was that the tips of the mutant testes were more pointed suggesting that they may have reduced germ cell content (Figure 6.18 B). This appearance is usually more common in older testes, where germ cells have proceeded into mitosis and meiosis and mature sperm has been produced repeatedly. Bearing in mind that the testes were dissected from late pupae, they would be expected to have a rich germ cell content and thus more rounded tips as observed in control testes. At the base of testes, in both wild type and mutant preparations, mature cysts with elongated sperm were present (Figure 6.18 A and B). When these cysts were more carefully observed, it was obvious that in wild type most of the spermatid nuclei were clustered in cysts while some were scattered (Figure 6.19 A). In the mutant testes, spermatid nuclei were clustered and individual cysts could be recognised but a significantly higher fraction of spermatid nuclei were scattered compared to controls (Figure 6.19 B). While spermatid nuclei were elongated from mutant testes, this was not as extreme as in wild type (compare Figure 6.19 A(1-3) and 6.19 B(1-3)). This could be because the mutant testes were slightly younger compared to wild type (even though wild type and mutant testes were dissected from the same late pupa stage) or that the mutant spermatids differentiate and mature slower compared to control. The second assumption could be more possible bearing in mind that testes from mutant mature adults have a white/transparent colour compared to a yellow colour of wild type testes. The yellow colour is a consequence of spermatid maturation and aging. If none of the above is valid then possibly what appears to be a minor chromosome

A) **Control**

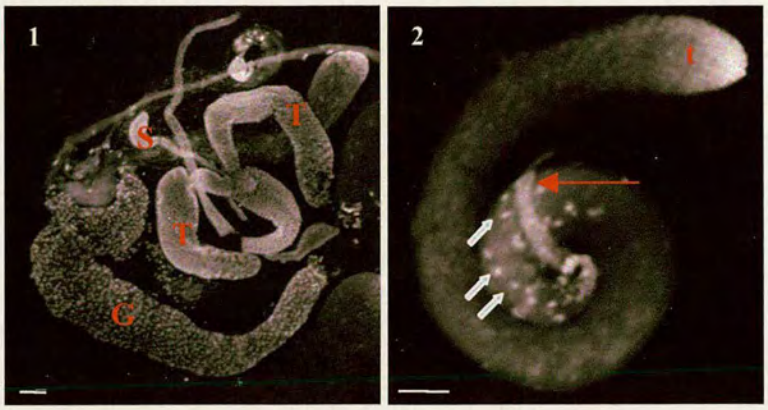

B) ***CAP-D3/CAP-D3***

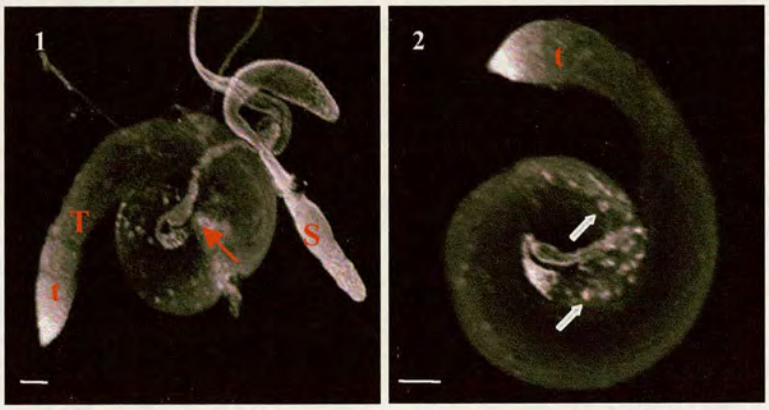

Figure 6.18. A. Testes from wild type pupae. Testes were fixed and stained for DNA (DAPI). Pupal testes (T) with accessory glands (G) are shown in (1) and a single testis is shown in (2). The red arrow (2) at the base of the testis indicates junction between testis and seminal vesicle (S). The tip of the pupal testis (t) is round. Mature spermatid cysts are obvious at the base of the testis (white block arrows).
B. Testes from *CAP-D3* homozygous pupae. Testes were fixed and stained for DNA (DAPI). Pupal testis (T) are shown in (1) and a single testis is shown in (2). The red arrow (1) at the base of the testis indicates junction between testis and seminal vesicle (S). The tip of the pupal testis (t) is pointed in contrast to wild type which is rounded. Mature spermatid cysts are obvious at the base of the testis (white block arrows).
The scale bar is 10μm.

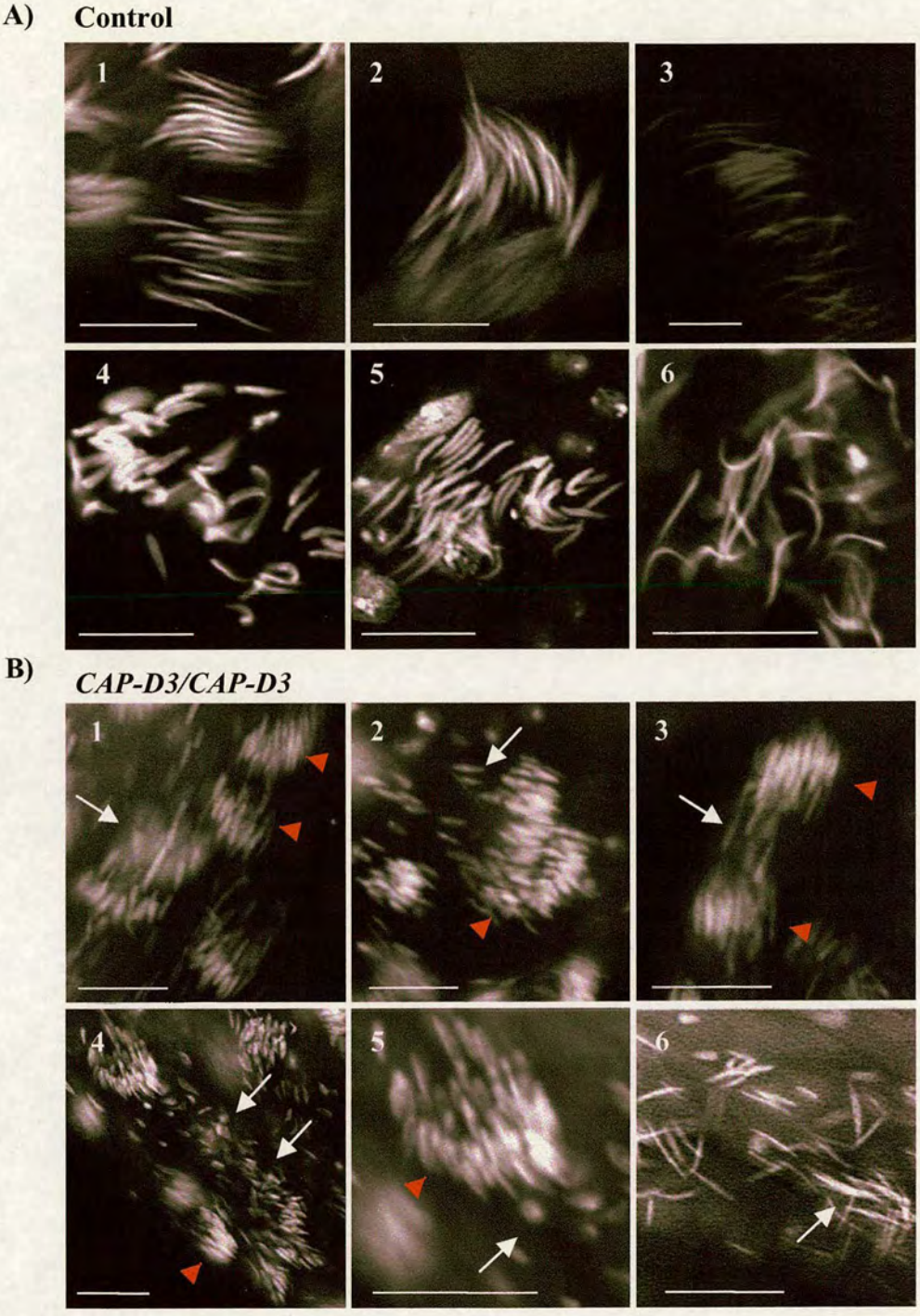

Figure 6.19. A. Elongated spermatid nuclei morphology from wild type pupae. Testes were fixed and stained for DNA (DAPI). Several clusters of threadlike spermatid nuclei are visible. Although most nuclei are clustered into cysts (1, 2 and 3) some are scattered (4, 5 and 6), possibly as a result of testes handling.

B. Elongated spermatid nuclei morphology from *CAP-D3* homozygous pupae. Testes were fixed and stained for DNA (DAPI). Although individual cysts can be recognised (arrowheads) most of the spermatid nuclei are scattered (white arrows). Notice that the spermatid nuclei are elongated but are not fully condensed (wider and shorter) compared to control.

The scale bar is 10μm.

condensation defect, which persists during spermatid differentiation, may impact on final sperm function.

In the second approach, unfixed testes were observed by phase contrast microscopy. In this way it was possible to observe stages that were not visible by DAPI staining such as 'onion-stage' early spermatid cysts. The regular appearance of onion-stage early spermatid cyst serves as a diagnostic for identification of mutants that caused defects during the meiotic divisions. Thus, onion-stage early spermatid cysts were observed by phase contrast microscopy from both wild type and *CAP-D3* homozygous mutant flies (Figure 6.20 and 6.21, respectively). In wild type, each spermatid nucleus appeared as a pale sphere (white) and next to it was a dark, equal in size, spherical "Nebenkern" or mitochondria derivative (Figure 6.20). In the *CAP-D3* mutant, most of the nuclei and Nebenkern appeared normal and equal in size but abnormalities were also observed (Figure 6.21). These defects include onion-stage spermatid cysts with large or variable Nebenkern associated with variable numbers of differently sized nuclei. Particularly, these defects are grouped in several categories such as: one big Nebenkern associated with two smaller nuclei of uniform size (Figure 6.21 A(1)), one small Nebenkern associated with a bigger and a smaller nucleus (Figure 6.21 A(2)), two unequal Nebenkern associated with a smaller nucleus (Figure 6.21 A(3)), two Nebenkern associated with one nucleus (Figure 6.21 A(4)), one big Nebenkern associated with smaller nucleus (Figure 6.21 A(5) and 6.21 B(2)), one Nebenkern associated with a smaller nucleus and a micronucleus (abnormally small nucleus) (Figure 6.21 B(1)) and two big Nebenkern associated with four smaller nuclei of uniform size (Figure 6.21 B(3)). These abnormalities are probably a consequence of abnormal chromosome segregation and cytokinesis. Nevertheless, all these phenotypes should be quantified in order to draw any significant conclusions about the role of CAP-D3 in male meiosis. Despite the defects in chromosome segregation and cytokinesis, spermatid differentiation proceeded nonetheless and elongated cysts were produced in the *CAP-D3* mutant testes, an observation that is also mentioned in the literature for mutations with similar phenotypes (Castrillon et al., 1993; Fuller, 1993). Furthermore,

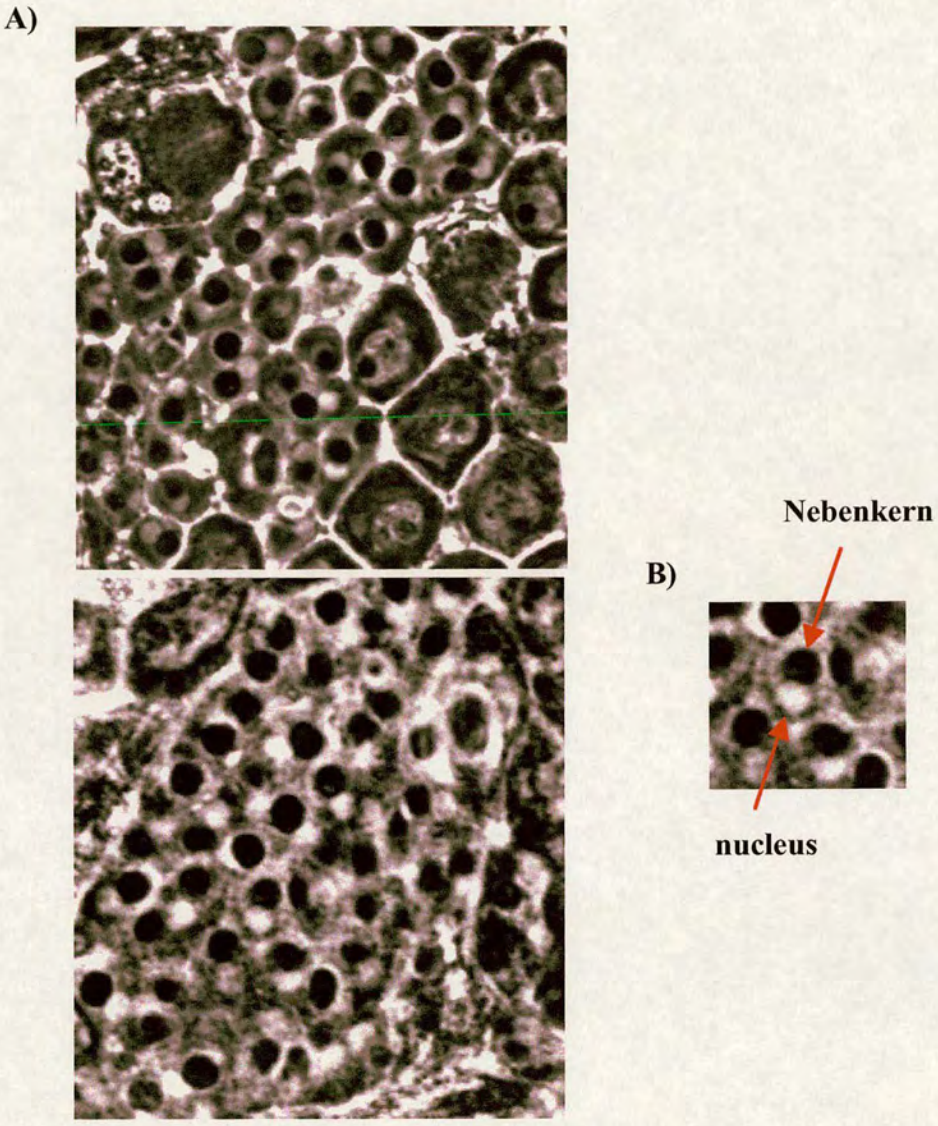

Figure 6.20. A. Morphology of onion-stage early spermatid cysts visualised by phase contrast microscopy of unfixed wild type testes. Each spermatid contains a single nucleus (white circle) and a single Nebenkern (black circle) of uniform size, which can be easily observed in higher magnification (B). One cyst contains 64 spermatids.

A)

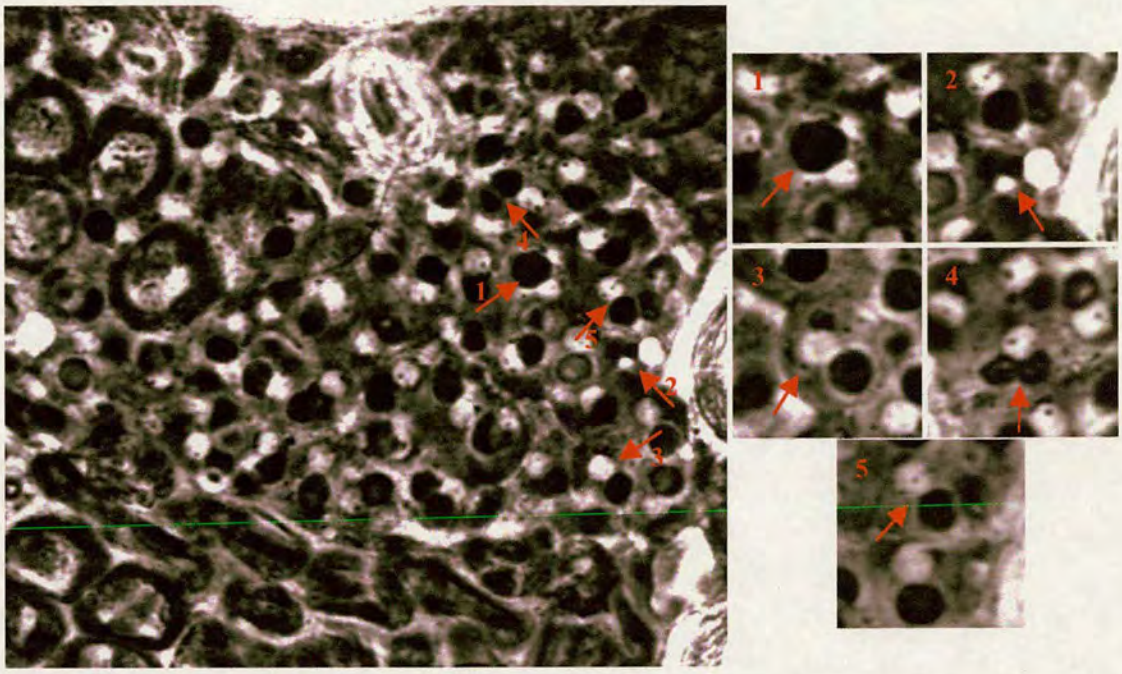

B)

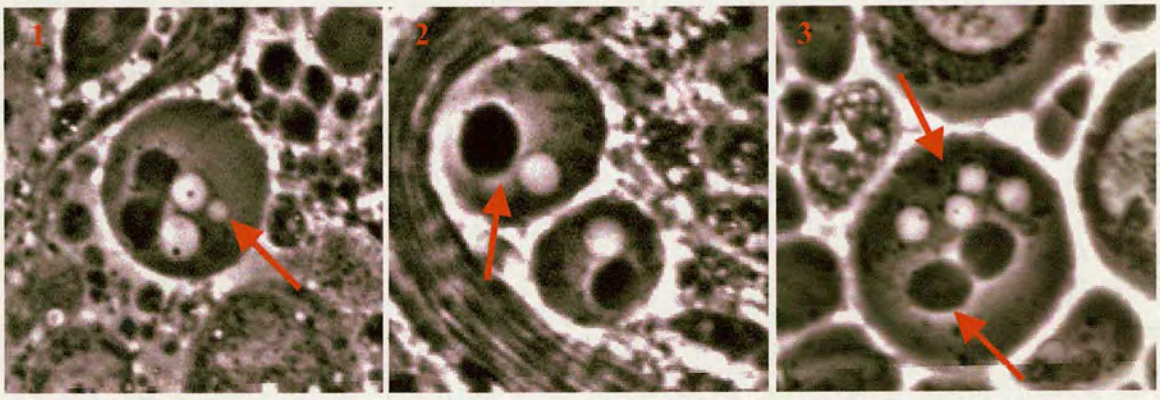

Figure 6.21. A. Morphology of onion-stage early spermatid cysts visualised by phase contrast microscopy of unfixed homozygous *CAP-D3* mutant testes. Most of the spermatids appear normal and they contain a single nucleus (white circle) and a single Nebenkern (black circle) of uniform size. However, meiotic division defects were also observed:(1) one large Nebenkern is associated with two nuclei of smaller size, (2) one small Nebenkern is associated with a bigger and a smaller nucleus, (3) one nucleus is associated with a bigger and a smaller Nebenkern, (4) two equal Nebenkern are associated with one nucleus, (5) one Nebenkern is associated with a nucleus smaller in size.

B. Parts of an onion-stage early spermatid cyst visualised by phase contrast microscopy of unfixed homozygous *CAP-D3* mutant testes. Meiotic division defects can be easily recognised:(1) one Nebenkern and an equal in size nucleus are associated with a micronucleus, (2) a large Nebenkern is associated with a smaller in size nucleus, (3) two large Nebenkern are associated with four smaller but equal in size nuclei.

the mature spermatids of *CAP-D3* homozygous male flies were motile as judged by a motility assay that was performed on sperm from seminal vesicles (Tim Karr, personal communication), suggesting that the male sterility is not a consequence of immotile sperm but probably a result of aneuploidy that occurred during the mitotic and/or meiotic stages.

In conclusion, there are several defects observed in the CAP-D3 homozygous testes. The testes tips are pointed instead of round in late pupae, the colour of the testes is white instead of yellow in mature adults, the spermatid nuclei are more scattered, shorter and wider compared to wild type and a fraction of the onion-stage early spermatids are defective. The most suggestive phenotype of all are the abnormalities observed in the onion-stage early spermatid cysts. As already mentioned, these abnormalities are probably a consequence of defective chromosome segregation and cytokinesis during the meiotic stages. The defects in the colour of the testes, the scattering of spermatid nuclei and the size of spermatid nuclei in mutant preparations could be a secondary consequence from the defects observed in the onion-stage. Nevertheless, a more detailed phenotypic analysis of different developmental stages of the testes, along with quantification of the defects observed is necessary to fully understand the consequences of CAP-D3 loss. In general the defects observed in the *CAP-D3* mutant testes were very mild and possibly analysis of testes from *CAP-D3/Df* (CAP-D3 over the deficiency) flies could be more informative. In this way, one of the two alleles will be completely absent and thus the phenotype could be more severe. Eventually further investigation will highlight the role of CAP-D3 in male meiosis. I was not able to perform this analysis due to lack of time.

6.11. Brief discussion

Preliminary functional analysis of the CAP-D3 protein revealed a putative role in spermatogenesis and most probably in male meiosis. However during this study many of the results could not be interpreted and many questions still need to be answered. The major boundary in this analysis is the quality of the CAP-D3 antibody. In tissue culture cells, the antibody recognises a band that is significantly smaller than the predicted size,

while in the testes, where a full length protein of the estimated size is detected, a protein of similar size is also present in the testes of the homozygous CAP-D3 flies.

Even though several possible explanations have been given in order to justify the presence of the full length protein in the homozygous mutant flies, the fact that 8 base pairs are duplicated in the insertion point of the P-element, definitely excludes the possibility that a full length wild type protein could be produced. The 8 base pair duplication would destroy the ORF downstream of the P-element insertion and even if the P-element is somehow not transcribed along with the rest of the CAP-D3 message, the message downstream of the transposon will not be in frame. Thus no wild type and/or full length protein should be produced. These data strongly support the idea that the CAP-D3 antibody does not recognise the CAP-D3 protein and that probably the antibody detects a non-specific epitope.

Further data that support the non-specificity of the CAP-D3 antibody, is the failure to detect a reduction in the level of CAP-D3 protein after RNAi treatment. However, the attempt to deplete CAP-D3 by RNAi in S2 cells also had no effect on either mitotic chromosome organisation or mitotic progression. The lack of a mitotic phenotype supports the idea that CAP-D3 probably has no mitotic role. An experiment to test if the RNAi disrupts CAP-D3, is to perform an RT-PCR with primers that cover CAP-D3 mRNA. If the level of the CAP-D3 mRNA is reduced after RNAi treatment, two possibilities emerge. Either the CAP-D3 protein is very stable and it can function for a long time after its expression and thus the protein can be still detected (by immunoblotting) and no phenotype can be observed (by immunofluorescence). Alternatively, the CAP-D3 antibody may not recognise the right protein and CAP-D3 has no mitotic role. However, at this point there is no evidence if CAP-D3 protein is expressed in S2 cells.

If we assume that the CAP-D3 antibody does not recognise CAP-D3, then the centromeric staining observed after immunofluorescence would be non-specific. Not infrequently, antibodies unspecifically recognise subcellular structures such as centrosomes - but centromeres are not commonly detected unspecifically. A good way to analyse the subcellular localisation of the CAP-D3 protein during the cell cycle, is to

tag the protein with GFP. This strategy would allow live imaging of the CAP-D3 protein and its localisation during the cell cycle, and it would permit comparison of the localisation of the protein after antibody staining and GFP-tagging. Furthermore, extract from cells that express CAP-D3 protein tagged with GFP could be used for further analysis by immunoblotting (using an anti-GFP antibody), thus allowing the detection of the full length CAP-D3 protein and a shifted size (with CAP-D3 antibody). Furthermore, an antigen competition experiment could be performed as additional control in order to test if the antibody recognises the CAP-D3 protein. In this experiment, the peptide (antigen) that was used for the generation of the CAP-D3 antibody will be incubated with the antibody and this mixture will then be used to detect the CAP-D3 protein on tissue culture or testes extract, by immunoblotting. If the expected protein does not appear or the strength of the signal is significantly reduced, it suggests that the antibody recognises the "right" protein. If no change occurs, it is most probable that the antibody detects a non-specific epitope.

However, a few more assumptions could be made of what the CAP-D3 antibody could be recognising. If alternatively spliced forms of the CAP-D3 gene exist, and the third exon is completely removed in one of these splice variants then the P-element insertion might not affect the expression of the protein. Nevertheless, exclusion of the third exon would imply a change of the protein size (~27 kDa). Alternatively, it could be possible that the CAP-D3 protein is produced by a splice variant lacking the last exon. The CAP-D3 antibody would not recognise this protein, as the CAP-D3 antibody was generated against the predicted final 15 amino acids of the CAP-D3 protein. The last exon is relatively small and the size difference after its removal would not be significant (~10 kDa). Unfortunately, no EST data exist so far to support the existence of the two splice variants proposed above.

In conclusion, generation of several antibodies against different regions of the CAP-D3 protein should be pursued. Also Northern and RT-PCR analysis using different parts of the CAP-D3 gene as probes will indicate if different isoforms of this protein exist.

CHAPTER 7
DISCUSSION

7.1. The role of Drosophila CAP-D2

In my thesis research, I have shown that CAP-D2 is part of a complex containing other condensin subunits (SMC2, SMC4, CAP-H/Barren and CAP-G) in *Drosophila*. Interestingly, the non-SMC subunits, CAP-D2 and Barren, appear to be more tightly associated with each other than they are with the SMC subunits. This finding is reminiscent of studies in the Heck lab of the cohesin complex in *Drosophila* where it was shown that Scc1/Drad21 and Scc3/SA1 appeared to have a higher affinity for one another than for SMC1 and SMC3 (Vass et al., 2003).

The subcellular localisation of CAP-D2 revealed that the protein was nuclear throughout interphase with levels increasing during S phase, and peaking in late G2/early prophase. This result was particularly intriguing as *Drosophila* SMC4 and Barren appear cytoplasmic during interphase and associate with chromatin only during prophase (Steffensen et al., 2001). In human cells the majority of CAP-D2 (and SMC2 and SMC4) localises in the cytoplasm during interphase, finally becoming nuclear during prophase, suggesting that the subcellular distribution of the entire condensin complex in human cells may be regulated in a cell cycle-dependent manner (Ball et al., 2002; Schmiesing et al., 2000). Differential localisation of condensin subunits during interphase in *Drosophila* suggests that CAP-D2 may be sequestered *away* from SMCs to regulate activity or may be utilized for a function other than that required of other condensin subunits during interphase. It has recently been shown in *Xenopus* that CAP-D2 (pEg7) along with SMC2 (XCAP-E) localise in the granular compartment of the nucleolus suggesting that these subunits may be involved in nucleolar organisation and /or ribosome biogenesis (Uzbekov et al., 2003). Furthermore in *S. cerevisiae*, the CAP-D2 homolog *Ycs4* is nuclear during interphase, implicated in suppressing inter-repeat rDNA recombination and believed to be required for silencing at the silent mating loci (Bhalla et al., 2002). Thus, it is possible that *Drosophila* CAP-D2 is responsible for a

non-mitotic function during interphase, possibly during S phase when its level increases. Alternatively, expression during S phase may be important to template the protein appropriately for its mitotic role (Loupart et al., 2000; Shelby et al., 1997). The increase of nuclear CAP-D2 levels during S phase could be either because protein expression is up-regulated or because the protein is imported into the nucleus from the cytoplasm. A potential nuclear bipartite targeting signal between amino acids 1347 and 1363 was identified on the *Drosophila* CAP-D2 protein (this study). Similarly human CAP-D2 (CNAP1) has been shown to have a functional bipartite nuclear localisation signal responsible for the localisation of CAP-D2 to the nucleus (Ball et al., 2002). During mitosis, CAP-D2 localises to the chromatid cores and remains tightly associated with chromosomes until late telophase/cytokinesis, even as chromosomes are decondensing. DmSMC4 and Barren proteins are loaded onto chromosomes in early prophase but they dissociate from chromosomes late in anaphase/telophase when decondensation begins (Steffensen et al., 2001). This distinct timing of dissociation of the different condensin subunits could be because CAP-D2 performs a function beyond that required of condensin, or to regulate activity of condensin. In human cells it has been shown that the C terminal-end of CAP-D2 possesses a mitotic chromosome-targeting domain that does not require the other condensin subunits (Ball et al., 2002). It is possible that a similar regulation occurs in *Drosophila* and that CAP-D2 binds to chromosomes independently of the other subunits. Beyond the axial localisation of CAP-D2 on mitotic chromosomes, a specific accumulation of this protein has been observed at centromeres during mitosis and especially during metaphase. A similar localisation has been also reported for Barren and SMC4 in *Drosophila* (Steffensen et al., 2001), while an interaction between CAP-G and CID has been recently reported suggesting a role for the condensin complex in kinetochore structure (Jager, 2005).

I have shown that depletion of CAP-D2 by RNAi in *Drosophila* cultured cells results in an abnormal mitotic phenotype. The major defect is the loss of sister chromatid (arm and centromere) resolution and the resulting failure of chromosomes to segregate normally during anaphase, a phenotype similar to that observed in *barren, DmSMC4* and *dCAP-G* (*red sea*) mutant alleles (Bhat et al., 1996; Dej et al., 2004;

Steffensen et al., 2001) and DmSMC4 RNAi (Coelho et al., 2003). No complete loss of compaction defect *per se* has been observed, consistent with the existence of additional essential factors in *Drosophila*, as in chicken cells (Hudson et al., 2003). Although loss of Barren in *Drosophila* appears not to have an effect on cell cycle progression (Bhat et al., 1996), loss of SMC4 causes a metaphase delay in embryos (Steffensen et al., 2001) and even more pronounced prometaphase delay (unpublished data), similarly, loss of dCAP-G causes a prometaphase delay in embryos (Dej et al., 2004). Depletion of CAP-D2 in S2 cells results in a temporal prometaphase delay, though cells do eventually undergo aberrant anaphase and cytokinesis.

The delay is possibly a consequence of checkpoint activation, since chromosomes have not aligned properly on the metaphase plate, and exhibit elevated levels of BubR1 labeling (which persists during anaphase and cytokinesis). The mis-alignment of chromosomes in the metaphase plate could be a consequence of the loss of interaction between the condensin complex and chromokinesisn KIF4A. It has been shown recently, that human chromokinesin KIF4A interacts with the condensin I and condensin II complexes, while depletion of this protein by RNAi results in defective prometaphase organisation and chromosome mis-alignment at metaphase (Mazumdar et al., 2004). Thus, the interaction between condensin and chromokinesin KIF4A could be essential for the alignment of chromosomes on the metaphase plate.

Furthermore, centromere organisation seems to be affected by the depletion of CAP-D2 since centromeres appear stretched during anaphase. Similar results have been observed in DmSMC4 RNAi (Coelho et al., 2003) where kinetochores associated with spindle microtubules were stretched polewards, sometimes well beyond the chromatin mass. However, when microtubules were depolymerised by colchicine, centromere stretching was not observed, suggesting that the observed defect was microtubule and tension dependent. In *C. elegans*, the condensin complex is required for the restricted orientation of centromeres towards spindle poles (Hagstrom et al., 2002), while in an *S. cerevisiae* BRN1 mutant, centromere function is defective and centromeres do not segregate normally (Ouspenski et al., 2000). Recently it has been shown that depletion of condensin I or condensin II in vertebrate cells results in structural distortions of the

centromere/kinetochore region which affects the opposing orientation of sister kinetochores and interaction with the mitotic spindle (Ono et al., 2004). Moreover, an interaction between the Drosophila CAP-G and CID, the centromere-specific histone H3 variant CENP-A, has been reported (Jager et al., 2005). CID has been shown to play a role in kinetochore specification and assembly (Blower and Karpen, 2001; Howman et al., 2000; Oegema et al., 2001).

Taken together, these results suggest that the condensin complex may have a role in centromere organization and ensuing kinetochore-spindle interactions. This defect in turn could impact the localization of chromosome passenger proteins as shown in this study. INCENP showed temporal disruption of localisation in the CAP-D2 depleted cells. Very similar defects in INCENP localization were observed when the Scc1/Rad21 cohesin subunit was depleted in cultured cells (Vass et al., 2003). These results argue that proper chromosome organisation is necessary for the correct temporal localisation of at least one chromosome passenger protein.

Different subunits of the condensin complex appear to behave differently following the depletion of CAP-D2. Barren is unstable when CAP-D2 is depleted and any residual protein is cytoplasmic. Similarly, in the DmSMC4 RNAi, Barren localisation was dependent on SMC4 (Coelho et al., 2003). In a *Barren* mutant, CAP-D2 was unstable to a similar level as Barren, corroborating the interdependence of the two proteins on one another for stability. On the other hand, levels of SMC2 and SMC4 were not greatly affected by the CAP-D2 depletion and the two proteins were still localised to chromatin, albeit in a non-axial fashion. This is likely a reflection of compromised structural integrity of mitotic chromosomes as observed in chicken DT40 cells depleted of SMC2 (Hudson et al., 2003). Nevertheless, a number of CAP-D2 RNAi cells have reduced levels of SMC4 and SMC2 on their chromosomes, and are possibly more severely affected by the CAP-D2 RNAi.

In *S. cerevisiae* and *S. pombe,* the condensin SMCs can bind chromatin only when the non-SMC subunits are present (Freeman et al., 2000; Lavoie et al., 2002). The question that arises then is whether the SMCs remaining on chromosomes are in any way functional? Recently, a condensin II complex was found in vertebrate cells which

shares the same two SMC subunits as the 'original' condensin I complex but contains different non-SMC subunits (two of three have been identified in *Drosophila* (Ono et al., 2003)). Should a functional condensin II complex exist, then the remaining chromosomal SMCs (after CAP-D2 depletion) may be members of the condensin II complex. Consistent with this is the observation that SMC2 and SMC4 are similarly reduced in a *Barren* mutant, but not as severely as Barren and CAP-D2. Attempts to deplete the CAP-D3 subunit of the *Drosophila* condensin II complex by RNAi in S2 cells failed to present a mitotic phenotype while mutation by P-element insertion in the CAP-D3 gene caused male sterility. It therefore remains to be determined if the condensin complex II has a meiotic, but not a mitotic role in *Drosophila*. If so, then SMCs remaining on chromosomes after depletion of CAP-D2 and Barren may be involved in yet another complex, distinct from condensin I and II complexes.

In this study, the first disruption in *Drosophila* of two components (condensin and topo II) known to be involved in chromosome organisation was performed. When a double depletion of CAP-D2/Topo II was performed, abnormal chromosome appearance and behaviour similar to that observed in the individual Topo II and CAP-D2 RNAi experiments was seen. Chromosomes were fuzzy and unresolved, inadequately aligned on the metaphase plate, and formed chromosome bridges during anaphase and cytokinesis. Surprisingly, the double depletion phenotype was no more severe than in either of the single depletions. This result suggests not only that topo II and the condensin complex participate in the same pathway required to organise mitotic chromosomes into well-defined structures, but also that factors other than these proteins still remain to be identified for their essential roles in chromosome condensation.

7.2. Characterisation of JSL2 - an SMC2 mutation

A point mutation affecting the *SMC2* gene causes lethality in early pupae. The fact that homozygous individuals for the *JSL2* mutation live up to this point is surprising, bearing in mind the importance of this protein for chromosome dynamics as well as the fact that mutants affecting SMC4 ($gluon^{17C}$ and $gluon^{88\text{-}82}$) and Barren ($barr^{L305}$) condensin subunits die during embryogenesis. The maternal contribution to the embryo

would be expected to maintain the function of the condensin complex up to cellularisation or even until the end of embryogenesis, but possibly no further than this stage. However, this protein and generally the condensin complex are also necessary after embryogenesis, for the development of larval tissues that are mitotically active, such as brains and imaginal discs.

Several hypotheses could be made for the reason that *JSL2* mutant live up to pupation. One possibility is that the SMC2 truncated protein is functional in a way and it can partially rescue the loss of SMC2 protein. The fact that SMCs are dimerised by hinge-hinge interactions (Hirano and Hirano, 2002) and that only the C-terminal region of the SMC2 protein is missing it could be suggested that the truncated SMC2 protein participates in the formation of a "condensin" complex. However, this complex is not expected to function properly since one of the catalytic domains is missing. A second scenario is that the SMC4 subunit forms homodimer in the *JSL2* mutant and thus a substitute "condensin" complex is assembled. The second assumption is supported by the observation that eukaryotic SMCs were able to form homodimers when fusion proteins were highly overexpressed, thereby titrating out the natural SMC partner (Strunnikov et al., 1995). Nevertheless, a condensin complex containing a homodimer of SMCs should not be functional as the *in vitro* activity of the complex depends on the combined presence of both subunits (Kimura and Hirano, 1997; Kimura et al., 1999; Schmiesing et al., 1998; Sutani and Yanagida, 1997) while mutation of only one SMC partner produces defects *in vivo* (Chuang et al., 1994; Dej, 2004; Lieb et al., 1998; Michaelis et al., 1997; Saka et al., 1994; Steffensen et al., 2001; Strunnikov et al., 1995; Strunnikov et al., 1993). Indeed, whatever is responsible for the surprisingly 'long life' of the homozygous animals can not certainly replace the contribution of SMC2 in chromosome organisation.

The absence of a functional SMC2 protein results in abnormal mitotic phenotype. The major defect observed is the loss of sister chromatid resolution and the failure of chromosome segregation during anaphase, defects that were also observed after the depletion of other condensin subunits in *Drosophila* (Bhat et al., 1996; Coelho et al., 2003; Dej, 2004; Savvidou et al., In Press; Steffensen et al., 2001). However, no

complete loss of compaction defect *per se* has been observed. The fact that undercondensed chromosome regions were observed in a minority of mitotic cells in the *JSL2* mutation, could be an indirect effect of accumulated chromosome defects from the failure of previous mitotic divisions. This is supported by the observation that these defects are only observed in a minority of cells in third instar larval brains but not in second instar larvae. Loss of SMC2 results in a slightly higher prometaphase/metaphase index in the mutant compared to control, suggesting that progression through mitosis may be somewhat delayed in mutant larval brains. It has been reported that loss of Barren in *Drosophila* appears not to have an effect on cell cycle progression (Bhat et al., 1996), while loss of SMC4, dCAP-G and CAP-D2 cause metaphase or prometaphase delay (Coelho et al., 2003; Dej et al., 2004; Savvidou et al., In Press; Steffensen et al., 2001).

The protein levels of the rest of the condensin subunits were reduced by the absence of SMC2. This reduction in level was more severe than that observed in the *gluon*^{17C} allele of SMC4. Moreover, INCENP levels, were significantly decreased in homozygous *JSL2* third instar larvae brains. Nevertheless, as INCENP is responsible for the correct targeting of Aurora B during mitosis and that Aurora B phosphorylates histone H3 at the onset of mitosis (Adams et al., 2001a), it would be expected the levels of phosphorylated histone H3 might be affected in mutant *JSL2* cells. Interestingly, H3 was normally phosphorylated in the mitotic cells of the homozygous *JSL2* larval brains as judged by immunofluorescence analysis. Therefore, the reduction observed in the levels of INCENP is possibly a consequence of the low mitotic index of the homozygous *JSL2* third instar larvae brains. However, the levels of Drad21/Scc1 were largely unaffected in the homozygous brain extracts. *Drosophila* Drad21/Scc1 dissociates from chromosomes in prophase and only a small population remains associated with centromeres until the metaphase to anaphase transition (Warren et al., 2000b). I would suggest, the low mitotic index observed in second and even more so in third instar larval brains is a consequence of accumulated chromosome abnormalities or activation of the DNA structure checkpoint. So as to test if the distribution of condensin subunits and INCENP is affected in mitotic cells lacking SMC2, immunofluorescence

for these proteins should be performed on larval brains. However, previous attempts to use these antibodies on neuroblast squashes was unsuccessful.

Strikingly, loss of SMC2 appears to affect the organisation of the mitotic spindle. Interestingly, a recent analysis has shown that the condensin complex is required for mitotic spindle assembly and function in *Xenopus laevis* egg extract (Wignal et al., 2003). In this study, immunodepletion of condensin inhibited microtubule growth and organisation around chromosomes, and eliminated the formation of mitotic spindles. However, in *Drosophila*, depletion of CAP-D2 or SMC4 by RNAi or loss of SMC4 and dCAP-G by mutation, did not display any abnormalities in mitotic spindle formation (Coelho et al., 2003; Dej et al., 2004; Steffensen et al., 2001). Thus, it is possible, that the spindle defects observed in the *JSL2* mutant were specific to this subunit or may be an indirect effect, caused by the overall chromosome abnormalities accumulated in previous cell cycles.

Surprisingly, level of H3 was reduced in *JSL2* homozygous third instar larval brains. This observation does not appear to be a consequence of second site mutations in any of the histone *H3* genes. Whether other histones are affected is unknown. The fact that the mitotic index is significantly reduced, make the analysis of chromosome dynamics very difficult in this mutant. Furthermore, the major part of this analysis has to be performed in second instar larvae, which are extremely difficult to handle, while immunofluorescence using antibodies against condensin subunits and INCENP was not highly successful in larval neuroblasts. For these reasons, further analysis of this mutant was not performed. However, the phenotypic analysis of the *JSL2* mutant confirmed that SMC2 and likely the entire condensin complex is primarily required for sister chromatid resolution and segregation in *Drosophila* and that the stability of the other subunits of the complex is compromised after loss of SMC2.

7.3. Characterisation of CAP-D3, a condensin II subunit

Recently, a condensin II complex was found in vertebrate cells. This complex shares the same two SMC subunits as the 'original' condensin I complex but contains different non-SMC subunits, CAP-D3, CAP-G2 and CAP-H2 (Ono et al., 2003). In *Drosophila*

only two of the three non-SMC subunits have been identified, CAP-H2 and CAP-D3 (not CAP-G2). In this study analysis of the CAP-D3 subunit was performed. CAP-D3 localises to the centromeres and partially colocalises with CID in mitotic *Drosophila* S2 cells. Attempts to coimmunoprecipitate proteins interacting with CAP-D3 were unsuccessful and thus it is not yet clear if this protein interacts with SMC4, SMC2 and CAP-H2 to form a condensin complex II in *Drosophila*. Furthermore, attempts to deplete CAP-D3 by RNAi in S2 cells failed to present a mitotic phenotype, suggesting that either this protein does not have a role in mitotic chromosome dynamics or that the protein is quite stable and it can not be depleted by RNAi. Interestingly, a P-element insertion in the *CAP-D3* gene causes male sterility, indicating a role for this protein in spermatogenesis. Mature spermatids of *CAP-D3* homozygous male flies were motile, suggesting that male sterility was not a consequence of decreased motility. In contrast, several defects were mainly observed in the onion stage spermatids. These abnormalities are probably a consequence of abnormal chromosome segregation and cytokinesis, which occurred in the meiotic stages (Bate and Martinez, 1993; Castrillon et al., 1993). Despite the defects in chromosome segregation and cytokinesis, spermatid differentiation proceeded nonetheless and elongated cysts were produced in the *CAP-D3* mutant testes, an observation that is also mentioned for mutations with similar phenotypes (Castrillon et al., 1993; Fuller, 1993). Nevertheless, further and detailed analysis of this mutation is necessary to draw any significant conclusions about the role of CAP-D3, and possibly for the whole condensin complex II, in male meiosis in *Drosophila*.

7.4. Conclusions and future perspectives

The precise mechanism of chromosome condensation and decondensation remains a mystery, despite progress over the last 25 years aimed at identifying components essential to the compaction of the genome during mitosis. However, modern experimental approaches are now providing novel insights into the old questions. Indeed, recent studies of condensin have resolved one old controversy by showing that

non-histone proteins (and not just the histones) play an essential role in mitotic chromosome structure.

In this study, it has been demonstrated for the first time that a condensin complex exists in *Drosophila* embryos. This complex contains CAP-D2, the anticipated SMC2 and SMC4 proteins, the CAP-H/Barren and CAP-G (non-SMC) subunits. Analysis of the localisation of CAP-D2 showed that this protein is nuclear throughout interphase, increasing in level during S phase, present on chromosome axes in mitosis, and still present on chromosomes as they start to decondense late in mitosis. *In vitro* and *in vivo* analyses of different *Drosophila* condensin subunits, have shown that condensin is required mainly for chromosome resolution rather than chromosome compaction *per se*, in this organism. Particularly, when the consequences of CAP-D2 loss after dsRNA-mediated interference were analysed, it was discovered that the protein was essential for chromosome arm and centromere resolution. The loss of CAP-D2 after RNAi has additional downstream consequences on the stability of CAP-H, the localization of DNA topoisomerase II and other condensin subunits, chromosome segregation, and the dynamics of chromosome passenger proteins. Similarly, loss of SMC2 subunit by mutation, confirmed the requirement of this protein, and probably of the entire condensin complex, in chromosome resolution and segregation. Furthermore, in this mutant, the stability of other condensin subunits and chromosome passenger proteins was compromised. However, while loss of CAP-D2 only affects the stability of the Barren subunit, loss of SMC2 affects the stability of all the examined condensin subunits, suggesting that the strength of the interactions between the four examined members of the condensin complex may vary or that phenotypes in cultured cells may differ from those in the animal.

In contrast to vertebrates, analysis of the *Drosophila* condensin complex II revealed so far that this complex is more likely to be involved in male meiosis rather than mitosis. If this is true, it would then be tempting to suggest that different mechanisms may exist between *Drosophila* and vertebrates, that regulate the organisation of mitotic and meiotic chromosomes. *Drosophila* offers a good system for the analysis of male meiosis and thus detailed analysis of the condensin complex II in

References

Adachi, Y., K s, E., and Laemmli, U. K. (1989). Preferential Cooperative Binding of DNA Topoisomerase II to Scaffold Attachment Regions. EMBO *13*, 3997-4006.

Adachi, Y., Luke, M., and Laemmli, U. K. (1991). Chromosome assembly in vitro: Topoisomerase II is required for condensation. Cell *64*, 137-148.

Adams, R. R., Carmena, M., and Earnshaw, W. C. (2001a). Chromosomal passengers and the (aurora) ABCs of mitosis. Trends Cell Biol *11*, 49-54.

Adams, R. R., Maiato, H., Earnshaw, W. C., and Carmena, M. (2001b). Essential roles of Drosophila inner centromere protein (INCENP) and aurora B in histone H3 phosphorylation, metaphase chromosome alignment, kinetochore disjunction, and chromosome segregation. J Cell Biol *153*, 865-880.

Akhmedov, A. T., Frei, C., Tsai-Pflugfelder, M., Kemper, B., Gasser, S. M., and Jessberger, R. (1998). Structural maintenance of chromosomes protein C-terminal domains bind preferentially to DNA with secondary structure. J Biol Chem *273*, 24088-94.

Anderson, D. E., Losada, A., Erickson, H. P., and Hirano, T. (2002). Condensin and cohesin display different arm conformations with characteristic hinge angles. J Cell Biol *156*, 419-24.

Andrade, M. A., Petosa, C., O'Donoghue, S. I., Muller, C. W., and Bork, P. (2001). Comparison of ARM and HEAT protein repeats. J Mol Biol *309*, 1-18.

Andreassen, P. R., Lacroix, F.B., Margolis, R.L.. (1997). Chromosomes with two intact axial cores are induced by G2 checkpoint override: evidence that DNA decatenation is not required to template the chromosome structure. J Cell Biol *136*, 29-43.

Aono, N., Sutani, T., Tomonaga, T., Mochida, S., and Yanagida, M. (2002). Cnd2 has dual roles in mitotic condensation and interphase. Nature *417*, 197-202.

Arumugam, P., Gruber, S., Tanaka, K., Haering, C. H., Mechtler, K., and Nasmyth, K. (2003). ATP Hydrolysis Is Required for Cohesin's Association with Chromosomes. Curr Biol *13*, 1941-1953.

Bachant, J., Alcasabas, A., Blat, Y., Kleckner, N., and Elledge, S. J. (2002). The SUMO-1 isopeptidase Smt4 is linked to centromeric cohesion through SUMO-1 modification of DNA topoisomerase II. Cell *9*, 1169-1182.

Ball, A. R., Jr., Schmiesing, J. A., Zhou, C., Gregson, H. C., Okada, Y., Doi, T., and Yokomori, K. (2002). Identification of a chromosome-targeting domain in the human condensin subunit CNAP1/hCAP-D2/Eg7. Mol Cell Biol *22*, 5769-81.

Bate, M., Martinez Arias, A.. (1993). Spermatogenesis in Drosophila. In The Development of Drosophila melanogaster, M. Bate, Martinez Arias, A. ed. (USA, Cold Spring Harbor Laboratory Press), pp. 71-147.

Bazett-Jones, D. P., Kimura, K., and Hirano, T. (2002). Efficient supercoiling of DNA by a single condensin complex as revealed by electron spectroscopic imaging. Mol Cell *9*, 1183-90.

Beisel, C., Imhof, A., Greene, J., Kremmer, E., Sauer, F.. (2002). Histone methylation by the Drosophila epigenetic transcriptional regulator Ash1. Nature *419(6909)*, 857-62.

Bellen, H. J., Levis, R.W., Liao, G., He, Y., Carlson, J.W., Tsang, G., Evans-Holm, M., Hiesinger, P.R., Schulze, K.L., Rubin, G.M., Hoskins, R.A., Spradling, A.C.. (2004). The BDGP gene disruption project: single transposon insertions associated with 40% of Drosophila genes. Genetics *167(2)*, 761-81.

Belmont, A. S. (2002). Mitotic chromosome scaffold structure: new approaches to an old controversy. Proc Natl Acad Sci U S A *99*, 15855-7.

Belmont, A. S., and Bruce, K. (1994). Visualization of G1 chromosomes: a folded, twisted, supercoiled chromonema model of interphase chromatid structure. J Cell Biol *127*, 287-302.

Belmont, A. S., Sedat, J. W., and Agard, D. A. (1987). A three-dimensional approach to mitotic chromosome structure: evidence for a complex hierarchical organization. J Cell Biol *105*, 77-92.

Bernard, P., Maure, J. F., Partridge, J. F., Genier, S., Javerzat, J. P., and Allshire, R. C. (2001). Requirement of Heterochromatin for Cohesion at Centromeres. Science *294*, 2539-2542.

Bhalla, N., Biggins, S., and Murray, A. W. (2002). Mutation of YCS4, a budding yeast condensin subunit, affects mitotic and nonmitotic chromosome behavior. Mol Biol Cell *13*, 632-45.

Bhat, M. A., Philp, A. V., Glover, D. M., and Bellen, H. J. (1996). Chromatid segregation at anaphase requires the *barren* product, a novel chromosome-associated protein that interacts with topoisomerase II. Cell *87*, 1103-1114.

Bickmore, W. A., Oghene, K. (1996). Visualizing the spatial relationships between defined DNA sequences and the axial region of extracted metaphase chromosomes. *Cell.* 84(1), 95-104.

Blower, M. D., and Karpen, G. H. (2001). The role of Drosophila CID in kinetochore formation, cell-cycle progression and heterochromatin interactions. Nat Cell Biol *3*, 730-739.

Bomar, J., Moreira, P., Balise, J. J., and P., C. (2002). Differential regulation of maternal and paternal chromosome condensation in mitotic zygotes. J Cell Sci *115*, 2931-40.

Bonaccorsi, S., Giansanti, M. G., and Gatti, M. (2000). Spindle assembly in *Drosophila* neuroblasts and ganglion mother cells. Nature Cell Biology *2*, 54 - 56.

Boy de la Tour, E., and Laemmli, U. K. (1988). The metaphase scaffold is helically folded: sister chromatids have predominantly opposite helical handedness. Cell *55*, 937-944.

Bradbury, E. M. (1992). Reversible Histone Modifications and the Chromosome Cell Cycle. BioEssays *14*, 9-16.

Britton, R. A., Lin, D. C., and Grossman, A. D. (1998). Characterization of a prokaryotic SMC protein involved in chromosome partitioning. Genes Dev *12*, 1254-1259.

Buchenau, P., Saumweber, H., and Arndt-Jovin, D. J. (1993). Consequences of topoisomerase II inhibition in early embryogenesis of *Drosophila* revealed by in vivo confocal laser scanning confocal microscopy. J Cell Sci *104*, 1175-1185.

Buonomo, S. B., Clyne, R. K., Fuchs, J., Loidl, J., Uhlmann, F., and Nasmyth, K. (2000). Disjunction of homologous chromosomes in meiosis I depends on proteolytic cleavage of the meiotic cohesin Rec8 by separin. Cell *103*, 387-398.

Cabello, O. A., Eliseeva, E., He, W., Youssoufian, H., Plon, S. E., Brinkley, B. R., and Belmont, J. W. (2001). Cell cycle-dependent expression and nucleolar localization of hCAP-H. Mol Biol Cell *12*, 3527-3537.

Carpenter, A. J., Porter, A.C. (2004). Construction, characterization, and complementation of a conditional-lethal DNA topoisomerase IIalpha mutant human cell line. *Mol Biol Cell.* 15(12), 5700-11.

Case, R. B., Chang, Y.P., Smith, S.B., Gore, J., Cozzarelli, N.R., Bustamante, C.. (2004). The bacterial condensin MukBEF compacts DNA into a repetitive, stable structure., 101126/science *1098225 (Science Express Research Articles)*.

Casso, D., Ramirez-Weber, F., and Kornberg, T. B. (2000). GFP-tagged balancer chromosomes for *Drosophila melanogaster*. Mech Dev *88*, 229-232.

Castrillon, D. H., Gonczy, P., Alexander, S., Rawson, R., Eberhart, C.G., Viswanathan, S., DiNardo, S., Wasserman, S.A.. (1993). Toward a molecular genetic analysis of spermatogenesis in Drosophila melanogaster: characterization of male-sterile mutants generated by single P element mutagenesis. Genetics *135(2)*, 489-505.

Chaly, N., Chen, X., Dentry, J., Brown, D.L.. (1996). Organisation of DNA topoisomerase II isotypes during the cell cycle of human lymphocytes and HeLa cells. Chromosome Research *4*, 457-466.

Chang, C. J., Goulding, S., Earnshaw, W. C., and Carmena, M. (2003). RNAi analysis reveals an unexpected role for topoisomerase II in chromosome arm congression to a metaphase plate. J Cell Sci *116*, 4715-4726.

Chen, R. H. (2002). BubR1 is essential for kinetochore localization of other spindle checkpoint proteins and its phosphorylation requires Mad1. J Cell Biol *158(3)*, 487-96.

Christensen, M. O., Larsen, M. K., Barthelmes, H. U., Hock, R., Andersen, C. L., Kjeldsen, E., Knudsen, B. R., Westergaard, O., Boege, F., and Mielke, C. (2002). Dynamics of human DNA topoisomerases IIalpha and IIbeta in living cells. J Cell Biol *157*, 31-44.

Christensen, T. W., Tye, B.K.. (2003). Drosophila MCM10 interacts with members of the prereplication complex and is required for proper chromosome condensation. Mol Biol Cell *14(6)*, 2206-15.

Chuang, P.-T., Albertson, D. G., and Meyer, B. J. (1994). DPY-27: A Chromosome Condensation Protein Homolog That Regulates C. elegans Dosage Compensation through Association with the X Chromosome. Cell *79*, 459-474.

Chuang, P. T., Lieb, J. D., and Meyer, B. J. (1996). Sex-specific assembly of a dosage compensation complex on the nematode X chromosome. Science *274*, 1736-1739.

Ciosk, R., Shirayama, M., Shevchenko, A., Tanaka, T., Toth, A., Shevchenko, A., and Nasmyth, K. (2000). Cohesin's binding to chromosomes depends on a separate complex consisting of Scc2 and Scc4 proteins. Mol Cell *5*, 243-254.

Ciosk, R., Zachariae, W., Michaelis, C., Shevchenko, A., Mann, M., and Nasmyth, K. (1998). An ESP1/PDS1 complex regulates loss of sister chromatid cohesion at the metaphase to anaphase transition in yeast. Cell *93*, 1067-1076.

Clemens, J. C., Worby, C. A., Simonson-Leff, N., Muda, M., Maehama, T., Hemmings, B. A., and Dixon, J. E. (2000). Use of double-stranded RNA interference in *Drosophila* cell lines to dissect signal transduction pathways. Proc Nat Acad Sci USA *97*, 6499-6503.

Cleveland, D. W., Mao, Y., Sullivan, K.F. (2003). Centromeres and kinetochores: from epigenetics to mitotic checkpoint signaling. *Cell.* 112(4), 407-21. Review.

Cobb, J., Miyaike, M., Kikuchi, A., and Handel, M. A. (1999). Meiotic events at the centromeric heterochromatin: histone H3 phosphorylation, topoisomerase II alpha localization and chromosome condensation. Chromosoma *108*, 412-425.

Cobbe, N. (2003). Phylogenetic and functional analysis of SMC4 in *Drosophila melanogaster*. PhD.

Cobbe, N., and Heck, M. M. S. (2000). SMCs in the world of chromosome biology: from prokaryotes to eukaryotes. J Struct Biol *129*, 123-143.

Cobbe, N., and Heck, M. M. S. (2004). The Evolution of SMC proteins: Phylogenetic Analysis and Structural Implications (Epub 2003 Dec 05). Mol Biol Evol *21*, 332-47.

Coelho, P. A., Queiroz-Machado, J., and Sunkel, C. E. (2003). Condensin-dependent localisation of topoisomerase II to an axial chromosomal structure is required for sister chromatid resolution during mitosis. J Cell Sci *116*, 4763-76.

Collas, P., Le Guellec, K., and Tasken, K. (1999). The A-kinase-anchoring protein AKAP95 is a multivalent protein with a key role in chromatin condensation at mitosis. J Cell Biol *147*, 1167-1180.

Cosgrove, M. S., Boeke, J.D., Wolberger, C. (2004). Regulated nucleosome mobility and the histone code. *Nat Struct Mol Biol.* 11(11), 1037-43. Review.

Cubizolles, F., Legagneux, V., Le Guellec, R., Chartrain, I., Uzbekov, R., Ford, C., and Le Guellec, K. (1998). pEg7, a new *Xenopus* protein required for mitotic chromosome condensation in egg extracts. J Cell Biol *143*, 1437-1446.

Cuvier, O., and Hirano, T. (2003). A role of topoisomerase II in linking DNA replication to chromosome condensation. J Cell Biol *160*, 645-55.

Darwiche, N., Freeman, L. A., and Strunnikov, A. (1999). Characterization of the components of the putative mammalian sister chromatid cohesion complex. Gene *233*, 39-47.

de la Barre, A. E., Angelov, D., Molla, A., Dimitrov, S.. (2001). The N-terminus of histone H2B, but not that of histone H3 or its phosphorylation, is essential for chromosome condensation. EMBO J *20(22)*, 6383-93.

de La Barre, A. E., Gerson, V., Gout, S., Creaven, M., Allis, C. D., and Dimitrov, S. (2000). Core histone N-termini play an essential role in mitotic chromosome condensation. EMBO J *19*, 379-391.

Dej, K. J., Ahn, C., Orr-Weaver, T.L.. (2004). Mutations in the Drosophila Condensin Subunit dCAP-G: Defining the Role of Condensin for Chromosome Condensation in Mitosis and Gene Expression in Interphase. Genetics *168(2)*, 895-906.

Dietzel, S., Belmont, A.S.. (2001). Reproducible but dynamic positioning of DNA in chromosome during mitosis. Nat Cell Biol *3*, 767-770.

DiNardo, S., Voelkel, K., and Sternglanz, R. (1984). DNA topoisomerase II mutant of *Saccharomyces cerevisiae*: topoisomerase II is required for segregation of daughter molecules at the termination of DNA replication. Proc Natl Acad Sci USA *81*, 2616-2620.

Donjerkovic, D., Scott, D.W. (2000). Regulation of the G1 phase of the mammalian cell cycle. *Cell Res.* 10(1), 1-16. Review.

Doree, M., Hunt, T. (2002). From Cdc2 to Cdk1: when did the cell cycle kinase join its cyclin partner? *J Cell Sci.* 115(Pt 12), 2461-4. Review.

Downes, C. S., Mullinger, A. M., and Johnson, R. T. (1991). Inhibitors of DNA topoisomerase II prevent chromatid separation in mammalian cells but do not prevent exit from mitosis. Proc Nat Acad Sci USA *88*, 8895-8899.

Earnshaw, W. C., Halligan, B., Cooke, C. A., Heck, M. M. S., and Liu, L. F. (1985). Topoisomerase II is a structural component of mitotic chromosome scaffolds. J Cell Biol *100*, 1706-1715.

Earnshaw, W. C., and Heck, M. M. S. (1985). Localization of topoisomerase II in mitotic chromosomes. J Cell Biol *100*, 1716-1725.

Earnshaw, W. C., and Laemmli, U. K. (1983). Architecture of metaphase chromosomes and chromosome scaffolds. J Cell Biol *96*, 84-93.

Eide, T., Carlson, C., Tasken, K. A., Hirano, T., Tasken, K., and Collas, P. (2002). Distinct but overlapping domains of AKAP95 are implicated in chromosome condensation and condensin targeting. EMBO Rep *3*, 426-32.

Ekholm, S. V., Reed, S.I. (2000). Regulation of G(1) cyclin-dependent kinases in the mammalian cell cycle. *Curr Opin Cell Biol.* 12(6), 676-84. Review.

Elledge, S. J. (1996). Cell cycle checkpoints: preventing an identity crisis. *Science.* 274(5293), 1664-72. Review.

Estey, E., Adlakha R.C., Hittelman, W.N., Zwelling, L.A.. (1987). Cell cycle stage dependent variations in drug-induced topoisomerase II mediated DNA cleavage and cytotoxicity. Biochemistry *2*, 4338-4344.

Fousteri, M. I., and Lehmann, A. R. (2000). A novel SMC protein complex in *Schizosaccharomyces pombe* contains the Rad18 DNA repair protein. EMBO J *19*, 1691-1702.

Freeman, L., Aragon-Alcaide, L., and Strunnikov, A. (2000). The condensin complex governs chromosome condensation and mitotic transmission of rDNA. J Cell Biol *149*, 811-824.

Fujioka, Y., Kimata, Y., Nomaguchi, K., Watanabe, K., and Kohno, K. (2002). Identification of a novel non-SMC component of the SMC5/SMC6 complex involved in DNA repair. J Biol Chem *277*, 21585-21591.

Fuller, M. T. (1998). Genetic control of cell proliferation and differentiation in Drosophila spermatogenesis. Semin Cell Dev Biol *9(4)*, 433-44. Review.

Fuller, T. M. (1993). Spermatogenesis in Drosophila. In The development of Drosophila melanogaster, M. Bate, Arias, A.M.. ed. (New York, Cold Spring Harbor Laboratory Press), pp. 71-147.

Gasser, S. M., Laroche, T., Falquet, J., Boy de la Tour, E., and Laemmli, U. K. (1986). Metaphase chromosome structure. Involvement of topoisomerase II. J Mol Biol *188*, 613-629.

Gassmann, R., Carvalho, A., Henzing, A. J., Ruchaud, S., Hudson, D. F., Honda, R., E.A., N., Gerloff, D. L., and Earnshaw, W. C. (2004). Borealin: A novel chromosomal passenger required for stability of the bipolar mitotic spindle. J Cell Biol.

Gerbi, S. A., Strezoska, Z., Waggener, J.M. (2002). Initiation of DNA replication in multicellular eukaryotes. *J Struct Biol.* 140(1-3), 17-30. Review.

Geyer, P. K., Corces, V.G.. (1992). DNA position-specific repression of transcription by a Drosophila zinc finger protein. Genes Dev *6(10)*, 1865-73.

Giet, R., Glover, D.M.. (2001). Drosophila aurora B kinase is required for histone H3 phosphorylation and condensin recruitment during chromosomecondensation and to organize the central spindle during cytokinesis. J Cell Biol *152(4)*, 669-82.

Gimenez-Abian, J. F., Clarke, D. J., Devlin, J., Gimenez-Abian, M. I., De la Torre, C., Johnson, R. T., Mullinger, A. M., and Downes, C. S. (2000). Premitotic chromosome individualization in mammalian cells depends on topoisomerase II activity. Chromosoma *109*, 235-244.

Gimenez-Abian, J. F., Clarke, D. J., Mullinger, A. M., Downes, C. S., and Johnson, R. T. (1995). A postprophase topoisomerase II-dependent chromatid core separation step in the formation of metaphase chromosomes. J Cell Biol *131*, 7-17.

Goldstone, S., Pavey, S., Forrest, A., Sinnamon, J., Gabrielli, B. (2001). Cdc25-dependent activation of cyclin A/cdk2 is blocked in G2 phase arrested cells independently of ATM/ATR. *Oncogene.* 20(8), 921-32.

Gorbsky, G. J. (1994). Cell cycle progression and chromosome segregation in mammalian cells cultured in the presence of the Topoisomerase II inhibitors ICRF-187 [(+)-1,2-bis(3,5-dioxopiperazinyl-1-yl)propane; ADR-529] and ICRF-159 (Razoxane). Cancer Research *54*, 1042-1048.

Goto, H., Tomono, Y., Ajiro, K., Kosako, H., Fujita, M., Sakurai, M., Okawa, K., Iwamatsu, A., Okigaki, T., Takahashi, T., and Inagaki, M. (1999). Identification of a novel phosphorylation site on histone H3 coupled with mitotic chromosome condensation. J Biol Chem *274*, 25543-9.

Goto, H., Yasui, Y., Nigg, E. A., and Inagaki, M. (2002). Aurora-B phosphorylates Histone H3 at serine28 with regard to the mitotic chromosome condensation. Genes Cells *7*, 11-17.

Graumann, P. L. (2000). *Bacillus subtilis* SMC is required for proper arrangement of the chromosome and for efficient segregation of replication termini but not for bipolar movement of newly duplicated origin regions. J Bacteriol *182*, 6463-6471.

Graumann, P. L., Losick, R., and Strunnikov, A. V. (1998). Subcellular localization of *Bacillus subtilis* SMC, a protein involved in chromosome condensation and segregation. J Bacteriol *180*, 5749-5755.

Gruber, S., Haering, C. H., and Nasmyth, K. (2003). Chromosomal cohesin forms a ring. Cell *112*, 765-777.

Grue, P., Gr §er, A., Sehested, M., Jensen, P. B., Uhse, A., Straub, T., Ness, W., and Boege, F. (1998). Essential mitotic functions of DNA topoisomerase IIa are not adopted by topoisomerase IIb in human H69 cells. J Biol Chem *273*, 33660-33666.

Guacci, V., Hogan, E., and Koshland, D. (1994). Chromosome Condensation and Sister Chromatid Pairing in Budding Yeast. J Cell Biol *125*, 517-530.

Guacci, V., Koshland, D., and Strunnikov, A. (1997). A Direct Link Between Sister Chromatid Cohesion and Chromosome Condensation Revealed Through the Analysis of MCD1 in S.cerevisiae. Cell *90*, this issue.

Guo, X. W., Th'ng, J. P., Swank, R. A., Anderson, H. J., Tudan, C., Bradbury, E. M., and Roberge, M. (1995). Chromosome condensation induced by fostriecin does not require $p34^{cdc2}$ kinase activity and histone H1 hyperphosphorylation, but is associated with enhanced histone H2A and H3 phosphorylation. EMBO J *14*, 976—985.

Haering, C. H., Lowe, J., Hochwagen, A., and Nasmyth, K. (2002). Molecular Architecture of SMC Proteins and the Yeast Cohesin Complex. Mol Cell *9*, 773-88.

Haering, C. H., and Nasmyth, K. (2003). Building and breaking bridges between sister chromatids. Bioessays *25*, 1178-1191.

Hagstrom, K. A., Holmes, V. F., Cozzarelli, N. R., and Meyer, B. J. (2002). *C. elegans* condensin promotes mitotic chromosome architecture, centromere organization, and sister chromatid segregation during mitosis and meiosis. Genes Dev *16*, 729-42.

Hagstrom, K. A., and Meyer, B. J. (2003). Condensin and cohesin: more than chromosome compactor and glue. Nat Rev Genet *4*, 520-534.

Hans, F., Dimitrov, S. (2001). Histone H3 phosphorylation and cell division. Oncogene *20*, 3021-3027.

Harlow, E., and Lane, D. (1999). Using antibodies, a laboratory manual. (Cold Spring Harbor, Cold Spring Harbor Laboratory).

Hart, C. M., and Laemmli, U. K. (1998). Facilitation of chromatin dynamics by SARs. Curr Op Gen Dev *8*, 519-525.

Hartman, T., Stead, K., Koshland, D., and Guacci, V. (2000). Pds5p is an essential chromosomal protein required for both sister chromatid cohesion and condensation in *Saccharomyces cerevisiae*. J Cell Biol *151*, 613-626.

Harvey, S. H., Sheedy, D.M., Cuddihy, A.R., O'Connel, M.J.. (2004). Coordination od DNA damage responses via the SMC5/SMC6 complex. Mol Cell Biol *24(2)*, 662-674.

Hauf, S., Waizenegger, I. C., and Peters, J. M. (2001). Cohesin cleavage by separase required for anaphase and cytokinesis in human cells. Science *293*, 1320-1323.

Heck, M. M., Hittelman, W. N., and Earnshaw, W. C. (1988). Differential expression of DNA topoisomerases I and II during the eukaryotic cell cycle. Proc Natl Acad Sci USA *85*, 1086-1090.

Heck, M. M. S. (1997). Condensins, Cohesins, and Chromosome Architecture: How to Make and Break a Mitotic Chromosome. Cell *91*, 5-8.

Hendzel, M. J., Wei, Y., Mancini, M. A., Van Hooser, A., Ranalli, T., Brinkley, B. R., Bazett-Jones, D. P., and Allis, C. D. (1997). Mitosis-specific phosphorylation of histone H3 initiates primarily within pericentromeric heterochromatin during G2 and spreads in an ordered fashion coincident with mitotic chromosome condensation. Chromosoma *106*, 348-360.

Henikoff, S., Ahmad, K., Platero, J.S., van Steensel, B. (2000). Heterochromatic deposition of centromeric histone H3-like proteins. Proc Natl Acad Sci U S A *97(2)*, 716-21.

Hiraga, S. (1992). Chromosome and plasmid partition in Escherichia coli. Annu Rev Biochem *61*, 283-306.

Hiraga, S. (2000). Dynamic localization of bacterial and plasmid chromosomes. Annu Rev Genet *34*, 21-59.

Hirano, M., Anderson, D. E., Erickson, H. P., and Hirano, T. (2001). Bimodal activation of SMC ATPase by intra- and inter-molecular interactions. EMBO J *20*, 3238-3250.

Hirano, M., and Hirano, T. (1998). ATP-dependent aggregation of single-stranded DNA by a bacterial SMC homodimer. EMBO J *17*, 7139-7148.

Hirano, M., and Hirano, T. (2002). Hinge-mediated dimerization of SMC protein is essential for its dynamic interaction with DNA. Embo J *21*, 5733-44.

Hirano, M., Hirano, T.. (2004). Positive and negative regulation of SMC-DNA interactions by ATP and accessory proteins. EMBO *23*, 2264-2673.

Hirano, T. (1999). SMC-mediated chromosome mechanics: a conserved scheme from bacteria to vertebrates? Genes Dev *13*, 11-19.

Hirano, T. (2002). The ABCs of SMC proteins: two-armed ATPases for chromosome condensation, cohesion, and repair. Genes Dev *16*, 399-414.

Hirano, T. (2005). Condensins: organizing and segregating the genome. *Curr Biol.* 15(7), R265-75.

Hirano, T., Kobayashi, R., and Hirano, M. (1997). Condensins, chromosome condensation protein complexes containing XCAP-C, XCAP-E and a *Xenopus* homolog of the *Drosophila* barren protein. Cell *89*, 511-521.

Hirano, T., and Mitchison, T. J. (1991). Cell cycle control of higher-order chromatin assembly around naked DNA in vitro. J Cell Biol *115*, 1479-1489.

Hirano, T., and Mitchison, T. J. (1993). Topoisomerase II Does Not Play a Scaffolding Role in the Organization of Mitotic Chromosomes Assembled in Xenopus Egg Extracts. J Cell Biol *120*, 601-612.

Hirano, T., and Mitchison, T. J. (1994). A heterodimeric coiled-coil protein required for mitotic chromosome condensation in vitro. Cell *79*, 449-458.

Hirota, T., Gerlich, D., Koch, B., Ellenberg, J., Peters, J.M.. (2004). Distinct functions of condensin I and II in mitotic chromosome assembly. J Cell Sci *117(Pt 26)*, 6435-45.

Holm, C., Goto, T., Wang, J. C., and Botstein, D. (1985). DNA topoisomerase II is required at the time of mitosis in yeast. Cell *41*, 553-563.

Houchmandzadeh, B., and Dimitrov, S. (1999). Elasticity measurements show the existence of thin rigid cores inside mitotic chromosomes. J Cell Biol *145*, 215-223.

Houchmandzadeh, B., Marko, J.F., Chatenay, D., Libchaber, A.. (1997). Elasticity and structure of eukaryote chromosomes studied by micromanipulation and micropipette aspiration. J Cell Biol *139(1)*, 1-12.

Howman, E. V., Fowler, K.J., Newson, A.J., Redward, S., MacDonald, A.C., Kalitsis, P., Choo, K.H.. (2000). Early disruption of centromeric chromatin organization in centromere protein A (Cenpa) null mice. Proc Natl Acad Sci U S A *97(3)*, 1148-53.

Hsu, J. Y., Sun, Z.W., Li, X., Reuben, M., Tatchell, K., Bishop, D.K., Grushcow, J.M., Brame, C.J., Caldwell, J.A., Hunt, D.F., Lin, R., Smith, M.M., Allis, C.D.. (2000). Mitotic phosphorylation of histone H3 is governed by Ipl1/aurora kinase and Glc7/PP1 phosphatase in budding yeast and nematodes. Cell *102(3)*, 279-91.

Hu, K. H., Liu, E., Dean, K., Gingras, M., DeGraff, W., Trun, N.J.. (1996). Overproduction of three genes leads to camphor resistance and chromosome condensation in Escherichia coli. Genetics *143(4)*, 1521-32.

Huang, J., Raff, J.W. (1999). The disappearance of cyclin B at the end of mitosis is regulated spatially in Drosophila cells. EMBO J *18(8)*, 2184-95.

Hudson, D. F., Vagnarelli, P., Gassmann, R., and Earnshaw, W. C. (2003). Condensin is required for nonhistone protein assembly and structural integrity of vertebrate mitotic chromosomes. Dev Cell *5*, 323-36.

Inoué, S., and Sato, H. (1964). Deoxyribonucleic acid arrangement in living sperm. In Molecular Architecture and Cell Physiology., T. Hayashi, and A. G. Szent-Gyorgi. eds. (Englewood Cliffs, NJ, Prentice-Hall), pp. 209-248.

Irniger, S. (2002). Cyclin destruction in mitosis: a crucial task of Cdc20. *FEBS Lett.* 532(1-2), 7-11. Review.

Ishida, R., Iwai, M., Marsh, K.L., Austin, C.A., Yano, T., Shibata, M., Nozaki, M., Hara, A.. (1996). Threonine 1342 in human topoisomerase IIalpha is phosphorylated throughout the cell cycle. J Biol Chem *271*, 30077-30082.

Ishida, R., Takashima, R., Koujin, T., Shibata, M., Nozaki, M., Seto, M., Mori, H., Haraguchi, T., Hiraoka, Y.. (2001). Mitotic specific phosphorylation of serine-1212 in human DNA topoisomerase IIalpha. Cell Sructure and Function *26*, 215-226.

Izaurralde, E., K s, E., and Laemmli, U. K. (1989). Highly preferential nucleation of histone H1 assembly on scaffold-associated regions. J Mol Biol *210*, 573-585.

Jablonski, S. A., Chan, G.K., Cooke, C.A., Earnshaw, W.C., Yen, T.J.. (1998). The hBUB1 and hBUBR1 kinases sequentially assemble onto kinetochores during prophase with hBUBR1 concentrating at the kinetochore plates in mitosis. Chromosoma *107(6-7)*, 386-96.

Jackman, M. R., Pines, J.N. (1997). Cyclins and the G2/M transition. *Cancer Surv.* 29, 47-73. Review.

Jager, H., Rauch, M., Heidmann, S.. (2005). The Drosophila melanogaster condensin subunit Cap-G interacts with the centromere-specific histone H3 variant CID. Chromosoma *113(7)*, 350-61.

Jessberger, R., Riwar, B., Baechtold, H., and Akhmedov, A. T. (1996). SMC proteins constitute two subunits of the mammalian recombination complex RC-1. EMBO J *15*, 4061-4068.

Kaitna, S., Pasierbek, P., Jantsch, M., Loidl, J., and Glotzer, M. (2002). The Aurora B Kinase AIR-2 Regulates Kinetochores during Mitosis and Is Required for Separation of Homologous Chromosomes during Meiosis. Curr Biol *12*, 798-812.

Kania, A., Salzberg, A., Bhat, M., D'Evelyn, D., He, Y., Kiss, I., and Bellen, H. J. (1995). P-element mutations affecting embryonic peripheral nervous system development in *Drosophila melanogaster*. Genetics *139*, 1663-1678.

Kaszas, E., and Cande, W. Z. (2000). Phosphorylation of histone H3 is correlated with changes in the maintenance of sister chromatid cohesion during meiosis in maize, rather than the condensation of the chromatin. J Cell Sci *113*, 3217-3226.

Katis, V. L., Galova, M., Rabitsch, K.P., Gregan, J., Nasmyth, K.. (2004). Maintenance of cohesin at centromeres after meiosis I in budding yeast requires a kinetochore-associated protein related to MEI-S332. Curr Biol *14(7)*, 560-72.

Kerrebrock, A. W., Moore, D. P., Wu, J. S., and Orr-Weaver, T. L. (1995). Mei-S332, a Drosophila protein required for sister-chromatid cohesion, can localize to meiotic centromere regions. Cell *83*, 247-256.

Kimura, K., Cuvier, O., Hirano, T. (2001). Chromosome condensation by a human condensin complex in Xenopus egg extracts. J Biol Chem *276(8)*, 5417-20.

Kimura, K., Hirano, M., Kobayashi, R., and Hirano, T. (1998). Phosphorylation and activation of 13S condensin by Cdc2 in vitro. Science *282*, 487-90.

Kimura, K., and Hirano, T. (1997). ATP-Dependent Positive Supercoiling of DNA by 13S Condensin: A Biochemical Implication for Chromosome Condensation. Cell *90*, 625-634.

Kimura, K., and Hirano, T. (2000). Dual roles of the 11S regulatory subcomplex in condensin functions. Proc Natl Acad Sci U S A *97*, 11972-7.

Kimura, K., Rybenkov, V. V., Crisona, N. J., Hirano, T., and Cozzarelli, N. R. (1999). 13S condensin actively reconfigures DNA by introducing global positive writhe: implications for chromosome condensation. Cell *98*, 239-48.

Kimura, K., Saijo, M., Tanaka, M., and Enomoto, T. (1996). Phosphorylation-independent stimulation of DNA topoisomerase IIa activity. J Biol Chem *271*, 10990-10995.

Kireeva, N., Lakonishok, M., Kireev, I., Hirano, T., Belmont, A.S. (2004). Visualization of early chromosome condensation: a hierarchical folding, axial glue model of chromosome structure. *J Cell Biol.* 166(6), 775-85.

Kitajima, T. S., Kawashima, S.A., Watanabe, Y.. (2004). The conserved kinetochore protein shugoshin protects centromeric cohesion during meiosis. Nature *427(6974):*, 510-7.

Kornberg, R. D. (1974). Chromatin structure: a repeating unit of histones and DNA. Science *184*, 868-871.

Koshland, D., and Strunnikov, A. (1996). Mitotic Chromosome Condensation. Ann Rev Cell Dev Biol *12*, 305-333.

Krause, S. A., Loupart, M.-L., Vass, S., Harrison, S., and Heck, M. M. S. (2001). Loss of Cell Cycle Checkpoint Control in *Drosophila* Rfc4 Mutants. Molec Coll Biol *21*, 5156-5168.

Laemmli, U. K., Cheng, S. M., Adolph, K. W., Paulson, J. R., Brown, J. A., and Baumbach, W. R. (1978). Metaphase chromosome structure: the role of nonhistone proteins. Cold Spring Harb Symp Quant Biol *42*, 351-360.

Larionov, V., Karpova, T., Kouprina, N., and Jouravleva, G. (1985). A mutant of *Saccharomyces cerevisiae* with impaired maintenance of centromeric plasmids. Curr Genet *10*, 15-20.

Lavoie, B. D., Hogan, E., and Koshland, D. (2002). In vivo dissection of the chromosome condensation machinery: reversibility of condensation distinguishes contributions of condensin and cohesin. J Cell Biol *156*, 805-15.

Lavoie, B. D., Tuffo, K. M., Oh, S., Koshland, D., and Holm, C. (2000). Mitotic chromosome condensation requires Brn1p, the yeast homologue of Barren. Mol Biol Cell *11*, 1293-1304.

LeBlanc, H. N., Tang, T. T., Wu, J. S., and Orr-Weaver, T. L. (1999). The mitotic centromeric protein MEI-S332 and its role in sister- chromatid cohesion. Chromosoma *108*, 401-11.

Lee, M. H., Yang, H.Y. (2003). Regulators of G1 cyclin-dependent kinases and cancers. *Cancer Metastasis Rev.* 22(4), 435-49. Review.

Lewis, C. D., and Laemmli, U. K. (1982). Higher order metaphase chromosome structure: evidence for metalloprotein interactions. Cell *29*, 171-181.

Li, G., Sudlow, G., and Belmont, A. S. (1998). Interphase cell cycle dynamics of a late-replicating, heterochromatic homogeneously staining region: precise choreography of condensation/decondensation and nuclear positioning. J Cell Biol *140*, 975-989.

Lieb, J. D., Albrecht, M. R., Chuang, P. T., and Meyer, B. J. (1998). MIX-1: an essential component of the *C. elegans* mitotic machinery executes X chromosome dosage compensation. Cell *92*, 265-277.

Lieb, J. D., Capowski, E. E., Meneely, P., and Meyer, B. J. (1996). DPY-26, a link between dosage compensation and meiotic chromosome segregation in the nematode. Science *274*, 1732-1736.

Locher, K. P., Lee, A.T., Rees, D.C.. (2002). The E. coli BtuCD structure: a framework for ABC transporter architecture and mechanism. Science *296(5570)*, 1091-8.

Losada, A., Hirano, M., and Hirano, T. (1998). Identification of *Xenopus* SMC protein complexes required for sister chromatid cohesion. Genes Dev *12*, 1986-1997.

Losada, A., Hirano, M., and Hirano, T. (2002). Cohesin release is required for sister chromatid resolution, but not for condensin-mediated compaction, at the onset of mitosis, *16*, 3004-16.

Losada, A., and Hirano, T. (2001). Shaping the metaphase chromosome: coordination of cohesion and condensation. Bioessays *23*, 924-35.

Losada, A., Yokochi, T., Kobayashi, R., and Hirano, T. (2000). Identification and characterization of SA/Scc3p subunits in the Xenopus and human cohesin complexes. J Cell Biol *150*, 405-16.

Loupart, M.-L., Krause, S. A., and Heck, M. M. S. (2000). Aberrant replication timing induces defective chromosome condensation in *Drosophila* ORC2 mutants. Curr Biol *10*, 1547-1556.

Löwe, J., Cordell, S. C., and van den Ent, F. (2001). Crystal structure of the SMC head domain: an ABC ATPase with 900 residues antiparallel coiled-coil inserted. J Mol Biol *306*, 25-35.

Lukas, J., Lukas, C., Bartek, J. (2004). Mammalian cell cycle checkpoints: signalling pathways and their organization in space and time. *DNA Repair (Amst).* 3(8-9), 997-1007. Review.

Lupas, A., Van Dyke, M., and Stock, J. (1991). Predicting coiled coils from protein sequences. Science *252*, 1162-1164.

Lupo, R., Breiling, A., Bianchi, M. E., and Orlando, V. (2001). *Drosophila* chromosome condensation proteins Topoisomerase II and Barren colocalize with Polycomb and maintain Fab-7 PRE silencing. Mol Cell *7*, 127-136.

MacCallum, D. E., Losada, A., Kobayashi, R., Hirano, T.. (2002). ISWI remodeling complexes in Xenopus egg extracts: identification as major chromosomal components that are regulated by INCENP-aurora B. Mol Biol Cell *13(1)*, 25-39.

Maeshima, K., and Laemmli, U. K. (2003). A two-step scaffolding model for mitotic chromosome assembly. Dev Cell *4*, 467-480.

Manders, E. M., Stap, J., Brakenhoff, G. J., van Driel, R., and Aten, J. A. (1992). Dynamics of three-dimensional replication patterns during the S-phase, analysed by double labelling of DNA and confocal microscopy. J Cell Sci *103*, 857-862.

Maiato, H., DeLuca, J., Salmon, E.D., Earnshaw, W.C. (2004). The dynamic kinetochore-microtubule interface. *J Cell Sci.* 117(Pt 23), 5461-77. Review.

Mailand, N., Podtelejnikov, A.V., Groth, A., Mann, M., Bartek, J., Lukas, J. (2002). Regulation of G(2)/M events by Cdc25A through phosphorylation-dependent modulation of its stability. *EMBO J.* 21(21), 5911-20.

Mao, Y., Abrieu, A., Cleveland, D.W. (2003). Activating and silencing the mitotic checkpoint through CENP-E-dependent activation/inactivation of BubR1. *Cell.* 114(1), 87-98.

Marsden, M. P. F., and Laemmli, U. K. (1979). Metaphase chromosome structure: evidence for a radial loop model. Cell *17*, 849-858.

Marshall, W. F., Marko, J. F., Agard, D. A., and Sedat, J. W. (2001). Chromosome elasticity and mitotic polar ejection force measured in living *Drosophila* embryos by four-dimensional microscopy-based motion analysis. Curr Biol *11*, 569-578.

Marston, A. L., Amon, A.. (2004). Meiosis: cell-cycle controls shuffle and deal., Nat Rev Mol Cell Biol *5(12)*, 983-97. Review.

Mascarenhas, J., Soppa, J., Strunnikov, A. V., and Graumann, P. L. (2002). Cell cycle-dependent localization of two novel prokaryotic chromosome segregation and condensation proteins in *Bacillus subtilis* that interact with SMC protein. EMBO J *21*, 3108-3118.

Mazumdar, M., Sundareshan, S., Misteli, T.. (2004). Human chromokinesin KIF4A functions in chromosome condensation and segregation. J Cell Biol *166(5)*, 613-20.

McHugh, B., Heck, M.M. (2003). Regulation of chromosome condensation and segregation., Curr Opin Genet Dev *13(2)*, 185-90. Review.

McHugh, B., Krause, S. A., Yu, B., Deans, A. M., Heasman, S., McLaughlin, P., and Heck, M. M. (2004). Invadolysin: a novel, conserved metalloprotease links mitotic structural rearrangements with cell migration. J Cell Biol *67(4):*, 673-686.

Melby, T. E., Ciampaglio, C. N., Briscoe, G., and Erickson, H. P. (1998). The symmetrical structure of structural maintenance of chromosomes (SMC) and MukB proteins: long, antiparallel coiled coils, folded at a flexible hinge. J Cell Biol *142*, 1595-1604.

Meraldi, P., Lukas, J., Fry, A.M., Bartek, J., Nigg, E.A. (1999). Centrosome duplication in mammalian somatic cells requires E2F and Cdk2-cyclin A. *Nat Cell Biol.* 1(2), 88-93.

Meyer, B. J. (2000). Sex in the worm: counting and compensating X-chromosome dosage. Trends Genet *16*, 247-253.

Meyer, K. N., Kjeldsen, E., Straub, T., Knudsen, B. R., Hickson, I. D., Kikuchi, A., Kreipe, H., and Boege, F. (1997). Cell cycle-coupled relocation of types I and II topoisomerases and modulation of catalytic enzyme activities. J Cell Biol *136*, 775-788.

Michaelis, C., Ciosk, R., and Nasmyth, K. (1997). Cohesins: Chromosomal Proteins that Prevent Premature Separation of Sister Chromatids. Cell *90*, this issue.

Mikhailov, A., Cole R.W., Rieder, C.L.. (2002). DNA damage during mitosis in human cells delays the metaphase/anaphase transition via the spindle-assembly checkpoint. Curr Biol *12(21)*, 1797-806.

Mirkovitch, J., Gasser, S. M., and Laemmli, U. K. (1987). Relation of chromosome structure and gene expression. Philos Trans R Soc Lond B Biol Sci *317*, 563-574.

Mirkovitch, J., Mirault, M. E., and Laemmli, U. K. (1984). Organization of the higher-order chromatin loop: specific DNA attachment sites on nuclear scaffold. Cell *39*, 223-232.

Moens, P. B., and Earnshaw, W. C. (1989). Anti-topoisomerase II recognizes meiotic chromosome cores. Chromosoma *98*, 317-322.

Moore, D. P., Page, A. W., Tang, T. T., Kerrebrock, A. W., and Orr-Weaver, T. L. (1998). The cohesin protein MEI-S332 localizes to condensed meiotic and mitotic centromeres until sister chromatids separate. J Cell Biol *140*, 1003-1012.

Morgan, D. O. (1997). Cyclin-dependent kinases: engines, clocks, and microprocessors. *Annu Rev Cell Dev Biol.* 13, 261-91.

Moroy, T., Geisen, C. (2004). Cyclin E. *Int J Biochem Cell Biol.* 36(8), 1424-39. Review.

Moriya, S., Tsujikawa, E., Hassan, A. K., Asai, K., Kodama, T., and Ogasawara, N. (1998). A *Bacillus subtilis* gene-encoding protein homologous to eukaryotic SMC motor protein is necessary for chromosome partition. Mol Microbiol *29*, 179-187.

Murnion, M. E., Adams, R. A., Callister, D. M., Allis, C. D., Earnshaw, W. C., and Swedlow, J. R. (2001). Chromatin-associated protein phosphatase 1 regulates aurora-B and histone H3 phosphorylation.w J Biol Chem *276*, 26656-26665.

Murray, A. W. (2004). Recycling the cell cycle: cyclins revisited. *Cell* 116(2), 221-34. Review.

Musacchio, A., Hardwick, K.G. (2002). The spindle checkpoint: structural insights into dynamic signalling. *Nat Rev Mol Cell Biol.* 3(10), 731-41. Review.

Myer, D. L., Bahassi, el. M., Stambrook, P.J. (2005). The Plk3-Cdc25 circuit. *Oncogene.* 24(2), 299-305. Review.

Neuwald, A. F., and Hirano, T. (2000). HEAT repeats associated with condensins, cohesins, and other complexes Involved in chromosome-related functions. Genome Res *10*, 1445-1452.

Newport, J., and Spann, T. (1987). Disassembly of the nucleus in mitotic extracts: membrane vesicularization, lamina disassembly, and chromosome condensation are independent events. Cell *48*, 219-230.

Nicklas, R. B. (1983). Measurements of the force produced by the mitotic spindle in anaphase. J Cell Biol *97(2)*, 542-8.

Niki, H., Jaffe, A., Imamura, R., Ogura, T., and Hiraga, S. (1991). The new gene *mukB* codes for a 177 kd protein with coiled-coil domains involved in chromosome partitioning of *E. coli.* EMBO J *10.*

Nilsson, I., Hoffmann, I. (2000). Cell cycle regulation by the Cdc25 phosphatase family. *Prog Cell Cycle Res.* 4, 107-14. Review.

Null, A. P., Hudson, J., Gorbsky, G.J.. (2002). Both alpha and beta isoforms of mammalian DNA topoisomerase II associate with chromosomes in mitosis. Cell Growth Differ *13*, 325-333.

O'Hare, K., Rubin, G.M.. (1983). Structures of P transposable elements and their sites of insertion and excision in the Drosophila melanogaster genome. Cell Mol Life Sci *4(1)*, 25-35.

Oegema, K., Desai, A., Rybina, S., Kirkham, M., Hyman, A.A.. (2001). Functional analysis of kinetochore assembly in Caenorhabditis elegans. J Cell Biol *153(6)*, 1209-26.

Ohsumi, K., Katagiri, C., and Kishimoto, T. (1993). Chromosome condensation in Xenopus mitotic extracts without histone H1. Science *262*, 2033-2035.

Olins, A. L., Carlson, R. D., Wright, E. B., and Olins, D. E. (1976). Chromatin nu bodies: isolation, subfractionation and physical characterization. Nucleic Acids Res *3*, 3271-3291.

Ono, T., Fang, Y., Spector, D. L., and Hirano, T. (2004). Spatial and Temporal Regulation of Condensins I and II in Mitotic Chromosome Assembly in Human Cells. Mol Biol Cell *15*, 3296-3308.

Ono, T., Losada, A., Hirano, M., Myers, M. P., Neuwald, A. F., and Hirano, T. (2003). Differential contributions of condensin I and condensin II to mitotic chromosome architecture in vertebrate cells. Cell *115*, 109-121.

Ouspenski, I. I., Cabello, O. A., and Brinkley, B. R. (2000). Chromosome condensation factor Brn1p is required for chromatid separation in mitosis. Mol Biol Cell *11*, 1305-1313.

Panizza, S., Tanaka, T., Hochwagen, A., Eisenhaber, F., and Nasmyth, K. (2000). Pds5 cooperates with cohesin in maintaining sister chromatid cohesion. Curr Biol *10*, 1557-64.

Patton, J. S., Gomes, X.V., Geyer, P.K.. (1992). Position-independent germline transformation in Drosophila using a cuticle pigmentation gene as a selectable marker., Nucleic Acids Res *20(21)*, 5859-60.

Paulson, J. R., and Laemmli, U. K. (1977). The Structure of Histone-Depleted Metaphase Chromosomes. Cell *12*, 817-828.

Pflumm, M. F., and Botchan, M. R. (2001). Orc mutants arrest in metaphase with abnormally condensed chromosomes. Development *128*, 1697-707.

Poirier, M., Eroglu, S., Chatenay, D., Marko, J.F.. (2000). Reversible and irreversible unfolding of mitotic newt chromosomes by applied force. Mol Biol Cell *11(1)*, 269-76.

Poirier, M. G., and Marko, J. F. (2002). Mitotic chromosomes are chromatin networks without a mechanically contiguous protein scaffold. Proc Natl Acad Sci U S A *99*, 15393-7.

Pollard, D. T., Earnshaw, C. William. (2002). CELL BIOLOGY (Philadelphia, United States of America, SAUNDERS, An imprint of Elsevier Science).

Porter, A. C. G., Farr, C.J.. (2004a). Topoisomerase II: untangling its contribution at the centromere. Chromosome Research *12*, 569-583.

Porter, I. M., Khoudoli, G.A., Swedlow, J.R.. (2004b). Chromosome condensation: DNA compaction in real time. Curr Biol *14*, 554-556.

Preuss, U. (2003). Nonel mitosis-specific phosphorylation of histone H3 at Thr 11 mediated by Dlk/ZIP kinase. Nuc Acids Res *31*, 878-885.

Rabitsch, K. P., Gregan, J., Schleiffer, A., Javerzat, J.P., Eisenhaber, F., Nasmyth, K.. (2004). Two fission yeast homologs of Drosophila Mei-S332 are required for chromosome segregation during meiosis I and II. Curr Biol *14(4)*, 287-301.

Raff, J. W., Jeffers, K., Huang, J.Y.. (2002). The roles of Fzy/Cdc20 and Fzr/Cdh1 in regulating the destruction of cyclin B in space and time. J Cell Biol *157(7)*, 1139-49.

Rattner, J. B., Hendzel, M. J., Furbee, C. S., Muller, M. T., and Bazett-Jones, D. P. (1996). Topoisomerase II a is associated with the mammalian centromere in a cell cycle- and species-specific manner and is required for proper centromere/kinetochore structure. J Cell Biol *134*, 1097-1107.

Rattner, J. B., and Lin, C. C. (1985). Radial loops and helical coils coexist in metaphase chromosomes. Cell *42*, 291—296.

Reed, S. I. (1997). Control of the G1/S transition. *Cancer Surv.* 29, 29:7-23. Review.

Richmond, T. J., Finch, J. T., Rushton, B., Rhodes, D., and Klug, A. (1984). Structure of the nucleosome core particle at 7 resolution. Nature *311* , 532-537.

Rieder, C. L., Maiato, H. (2004). Stuck in division or passing through: what happens when cells cannot satisfy the spindle assembly checkpoint. *Dev Cell.* 7(5), 637-51. Review.

Riedel, C. G., Gregan, J., Gruber, S., Nasmyth, K.. (2004). Is chromatin remodeling required to build sister-chromatid cohesion?, Trends Biochem Sci *29(8)*, 389-92. Review.

Rogers, E., Bishop, J. D., Waddle, J. A., Schumacher, J. M., and Lin, R. (2002). The aurora kinase AIR-2 functions in the release of chromosome cohesion in Caenorhabditis elegans meiosis. J Cell Biol *157*, 219-29.

Rogers, S. L., Rogers, G.C., Sharp, D.J., Vale, R.D. (2002). Drosophila EB1 is important for proper assembly, dynamics, and positioning of the mitotic spindle. J Cell Biol *158(5)*, 873-84.

Roth, S. Y., Allis, C.D.. (1992). Chromatin condensation: does histone H1 dephosphorylation play a role?. Trends Biochem Sci *17(3)*, 93-8. Review.

Saitoh, N., Goldberg, I. G., Wood, E. R., and Earnshaw, W. C. (1994). ScII: an abundant chromosome scaffold protein is a member of a family of putative ATPases with an unusual predicted tertiary structure. J Cell Biol *127*, 303-318.

Saitoh, Y., and Laemmli, U. K. (1994). Metaphase chromosome structure: bands arise from a differential folding path of the highly AT-rich scaffold. Cell *76*, 609-622.

Saka, Y., Sutani, T., Yamashita, Y., Saithoh, S., Takeuchi, M., Nakaseko, Y., and Yanagida, M. (1994). Fission yeast cut3 and cut14, members of a ubiquitous protein family, are required for chromosome condensation and segregation in mitosis. EMBO J *13*, 4938-4952.

Salic, A., Waters, J.C., Mitchison, T.J.. (2004). Vertebrate shugoshin links sister centromere cohesion and kinetochore microtubule stability in mitosis. Cell *118(5)*, 567-78.

Sampath, S. C., Ohi, R., Leismann, O., Salic, A., Pozniakovski, A., and Funabiki, H. (2004). The chromosomal passenger complex is required for chromatin-induced microtubule stabilization and spindle assembly. Cell *118*, 187-202.

Savvidou, E., Cobbe, N., Steffensen, S., Cotterill, S., Heck, M.M.S. (In Press). Drosophila CAP-D2 is required for condensin complex stability and regulating mitotic chromosomes dynamics. J Cell Sci.

Sclafani, R. A. (2000). Cdc7p-Dbf4p becomes famous in the cell cycle. *J Cell Sci.* 113 (Pt 12), 2111-7.

Schleiffer, A., Kaitna, S., Maurer-Stroh, S., Glotzer, M., Nasmyth, K., and Eisenhaber, F. (2003). Kleisins. A Superfamily of Bacterial and Eukaryotic SMC Protein Partners. Mol Cell *11*, 571-575.

Schmiesing, J. A., Ball, A. R., Jr., Gregson, H. C., Alderton, J. M., Zhou, S., and Yokomori, K. (1998). Identification of two distinct human SMC protein complexes involved in mitotic chromosome dynamics. Proc Natl Acad Sci U S A *95*, 12906-11.

Schmiesing, J. A., Gregson, H. C., Zhou, S., and Yokomori, K. (2000). A human condensin complex containing hCAP-C-hCAP-E and CNAP1, a homolog of Xenopus XCAP-D2, colocalizes with phosphorylated histone H3 during the early stage of mitotic chromosome condensation. Mol Cell Biol *20*, 6996-7006.

Sedat, J., and Manuelidis, L. (1978). A direct approach to the structure of eukaryotic chromosomes. Cold Spring Harb Symp Quant Biol *42*, 331-350.

Shamu, C. E., and Murray, A. W. (1992). Sister chromatid separation in frog egg extracts required DNA topoisomerase II activity during anaphase. J Cell Biol *117*, 921—934.

Sharp, P. A. (2001). RNA interference. Genes Dev *15*, 485-90.

Shelby, R. D., Vafa, O., and Sullivan, K. F. (1997). Assembly of CENP-A into Centromeric Chromatin Requires a Cooperative Array of Nucleosomal DNA Contact Sites. J Cell Biol *136*, 501-513.

Shen, X., Yu, L., Weir, J. W., and Gorovsky, M. A. (1995). Linker histones are not essential and affect chromatin condensation *in vivo*. Cell *82*, 47-56.

Skibbens, R. V., Corson, L. B., Koshland, D., and Hieter, P. (1999). Ctf7p is essential for sister chromatid cohesion and links mitotic chromosome structure to the DNA replication machinery. Genes & Dev *13*, 307-319.

Smits, V. A., Medema, R.H. (2001). Checking out the G(2)/M transition. *Biochim Biophys Acta*. 1519(1-2), 1-12. Review.

Soppa, J., Kobayashi, K., Noirot-Gros, M. F., Oesterhelt, D., Ehrlich, S. D., Dervyn, E., Ogasawara, N., and Moriya, S. (2002). Discovery of two novel families of proteins that are proposed to interact with prokaryotic SMC proteins, and characterization of the *Bacillus subtilis* family members ScpA and ScpB. Mol Microbiol *45*, 59-71.

Speliotes, E. K., Uren, A., Vaux, D., and Horvitz, H. R. (2000). The Survivin-like *C. elegans* BIR-1 Protein Acts with the Aurora-like Kinase AIR-2 to Affect Chromosomes and the Spindle Midzone. Molecular Cell *6*, 211-223.

Stear, J. H., and Roth, M. B. (2002). Characterization of HCP-6, a *C. elegans* protein required to prevent chromosome twisting and merotelic attachment. Genes Dev *16*, 1498-1508.

Steen, R. L., Cubizolles, F., Le Guellec, K., and Collas, P. (2000). A kinase-anchoring protein (AKAP)95 recruits human chromosome- associated protein (hCAP)-D2/Eg7 for chromosome condensation in mitotic extract. J Cell Biol *149*, 531-6.

Steffensen, S. (2001). Identification and characterisation of condensin and cohesin subunits in *Drosophila melanogaster*. PhD.

Steffensen, S., Coelho, P. A., Cobbe, N., Vass, S., Costa, M., Hassan, B., Prokopenko, S. N., Bellen, H., Heck, M. M. S., and Sunkel, C. E. (2001). A role for *Drosophila* SMC4 in the resolution of sister chromatids in mitosis. Curr Biol *11*, 295-307.

Stray, J. E., and Lindsley, J. E. (2003). Biochemical analysis of the yeast condensin Smc2/4 complex: an ATPase that promotes knotting of circular DNA. J Biol Chem *278*, 26238-26248.

Strick, R., and Laemmli, U. K. (1995). SAR's are cis DNA elements of chromosome dynamics: synthesis of a SAR repressor protein. Cell *83*, 1137-1148.

Strick, T. R., Kawaguchi, T., Hirano, T.. (2004). Real time detection of single-molecule DNA compaction by condensin I. Curr Biol *14*, 874-880.

Strukov, Y. G., Wang, Y., Belmont, A.S. (2003). Engineered chromosome regions with altered sequence composition demonstrate hierarchical large-scale folding within metaphase chromosomes. *J Cell Biol.* 162(1), 23-35.

Strunnikov, A. V., Hogan, E., and Koshland, D. (1995). SMC2, a *Saccharomyces cerevisiae* gene essential for chromosome segregation and condensation, defines a subgroup within the SMC family. Genes Dev *9*, 587-599.

Strunnikov, A. V., and Jessberger, R. (1999). Structural maintenance of chromosomes (SMC) proteins: conserved molecular properties for multiple biological functions. Eur J Biochem *263*, 6-13.

Strunnikov, A. V., Larianov, V. L., and Koshland, D. (1993). SMC1: an essential yeast gene encoding a putative head-rod-tail protein is required for nuclear division and defines a new ubiquitous protein family. J Cell Biol *123*, 1635-1648.

Sumara, I., Vorlaufer, E., Gieffers, C., Peters, B. H., and Peters, J. M. (2000). Characterization of vertebrate cohesin complexes and their regulation in prophase. J Cell Biol *151*, 749-62.

Sumara, I., Vorlaufer, E., Stukenberg, P. T., Kelm, O., Redemann, N., Nigg, E. A., and Peters, J. M. (2002). The dissociation of cohesin from chromosomes in prophase is regulated by Polo-like kinase. Mol Cell *9*, 515-525.

Sumner, A. T. (1996). The distribution of topoisomerase II on mammalian chromosomes. Chromosome Res *4*, 5—14.

Sutani, T., and Yanagida, M. (1997). DNA renaturation activity of the SMC complex implicated in chromosome condensation. Nature *388*, 798-801.

Sutani, T., Yuasa, T., Tomonaga, T., Dohmae, N., Takio, K., and Yanagida, M. (1999). Fission yeast condensin complex: essential roles of non-SMC subunits for condensation and Cdc2 phosphorylation of Cut3/SMC4. Genes Dev *13*, 2271-83.

Swank, R. A., Th'ng, J.P., Guo, X.W., Valdez, J., Bradbury, E.M., Gurley, L.R. (1997). Four distinct cyclin-dependent kinases phosphorylate histone H1 at all of its growth-related phosphorylation sites. *Biochemistry.* 36(45), 13761-8.

Swedlow, J. R., and Hirano, T. (2003). The making of the mitotic chromosome: modern insights into classical questions. Mol Cell *11*, 557-569.

Swedlow, J. R., J.W., S., and Agard, D. A. (1993). Multiple Chromosomal Populations of Topoisomerase II Detected In Vivo by Time-Lapse, Three-Dimensional Wide-Field Microscopy. Cell *73*, 97-108.

Taagepera, S., Rao, P. N., Drake, F. H., and Gorbsky, G. J. (1993). DNA topoisomerase IIa is the major chromosome protein recognized by the mitotic phosphoprotein antibody MPM-2. PNAS *90*, 8407-8411.

Takemoto, A., Kimura, K., Yokoyama, S., and Hanaoka, F. (2003). Cell cycle-dependent phosphorylation, nuclear localization, and activation of human condensin. J Biol Chem.

Tanaka, K., Hao, Z., Kai, M., and Okayama, H. (2001). Establishment and maintenance of sister chromatid cohesion in fission yeast by a unique mechanism. EMBO J *20*, 5779-5790.

Tanudji, M., Shoemaker, J., L'Italien, L., Russell, L., Chin, G., Schebye, X.M. (2004). Gene silencing of CENP-E by small interfering RNA in HeLa cells leads to missegregation of chromosomes after a mitotic delay. *Mol Biol Cell.* 15(8), 3771-81.

Tarapore, P., Okuda, M., Fukasawa, K. (2002). A mammalian in vitro centriole duplication system: evidence for involvement of CDK2/cyclin E and nucleophosmin/B23 in centrosome duplication. *Cell Cycle.* 1(1), 75-81.

Tavormina, P. A., Come, M.-G., Hudson, J. R., Mo, Y.-Y., Beck, W. T., and Gorbsky, G. J. (2002). Rapid exchange of mammalian topoisomerase IIa at kinetochores and chromosome arms in mitosis. J Cell Biol *158*, 23-29.

Taylor, S. S., Hussein, D., Wang, Y., Elderkin, S., Morrow, C.J.. (2001). Kinetochore localisation and phosphorylation of the mitotic checkpoint components Bub1 and BubR1 are differentially regulated by spindle events in human cells. J Cell Sci *114(Pt 24)*, 4385-95.

Tomonaga, T., Nagao, K., Kawasaki, Y., Furuya, K., Murakami, A., Morishita, J., Yuasa, T., Sutani, T., Kearsey, S. E., Uhlmann, F., *et al.* (2000). Characterization of fission yeast cohesin: essential anaphase proteolysis of Rad21 phosphorylated in the S phase. Genes Dev *14*, 2757-2770.

Toone, W. M., Aerne, B.L., Morgan, B.A., Johnston, L.H. (1997). Getting started: regulating the initiation of DNA replication in yeast. *Annu Rev Microbiol.* 51, 125-49. Review.

T th, A., Ciosk, R., Uhlmann, F., Galova, M., Schleiffer, A., and Nasmyth, K. (1999). Yeast cohesin complex requires a conserved protein, Eco1p (Ctf7), to establish cohesion between sister chromatids during DNA replication. Genes & Dev *13*, 320-333.

Turner, B. M. (2002). Cellular memory and the histone code. *Cell.* 111(3), 285-91. Review.

Uemura, T., Ohkura, H., Adachi, Y., Morino, K., Shiozaki, K., and Yanagida, M. (1987). DNA topoisomerase II is required for condensation and separation of mitotic chromosomes in *S. pombe*. Cell *50*, 917-925.

Uemura, T., and Yanagida, M. (1984). Isolation of type I and II DNA topoisomerase mutants from fission yeast: single and double mutants show different phenotypes in cell growth and chromatin organization. EMBO J *3*, 1737—1744.

Uhlmann, F. (2003). Chromosome cohesion and separation: from men and molecules. Curr Biol *13*, R104-R114.

Uhlmann, F. (2004). The mechanism of sister chromatid cohesion. Exp Cell Res *296(1)*, 80-5.

Uhlmann, F., Lottspeich, F., and Nasmyth, K. (1999). Sister-chromatid separation at anaphase onset is promoted by cleavage of the cohesin subunit Scc1. Nature *400*, 37-42.

Uhlmann, F., Wernic, D., Poupart, M. A., Koonin, E. V., and Nasmyth, K. (2000). Cleavage of cohesin by the CD clan protease separin triggers anaphase in yeast. Cell *103*, 375-386.

Uzbekov, R., Timirbulatova, E., Watrin, E., Cubizolles, F., Ogereau, D., Gulak, P., Legagneux, V., Polyakov, V. J., Le Guellec, K., and Kireev, I. (2003). Nucleolar association of pEg7 and XCAP-E, two members of *Xenopus laevis* condensin complex in interphase cells. J Cell Sci *116*, 1667-1678.

Valdeolmillos, A., Rufas, J.S., Suja, J.A., Vass, S., Heck, M.M., Martinez-A, C., Barbero, J.L.. (2004). Drosophila cohesins DSA1 and Drad21 persist and colocalize along the centromeric heterochromatin during mitosis. Biol Cell *96(6)*, 457-62.

Van Hooser, A., Goodrich, D. W., Allis, C. D., Brinkley, B. R., and Mancini, M. A. (1998). Histone H3 phosphorylation is required for the initiation, but not maintenance, of mammalian chromosome condensation. J Cell Sci *111*, 3497-3506.

Vass, S., Cotterill, S., Valdeolmillos, A. M., Barbero, J. L., E., L., Warren, W., and Heck, M. M. S. (2003). Depletion of rad21/Scc1 in *Drosophila* cells leads to instability of the cohesin complex and disruption of mitotic progression. Curr Biol *3*, 208-218.

Vernos, I., Raats, J., Hirano, T., Heasman, J., Karsenti, E., and Wylie, C. (1995). Xklp1, a chromosomal *Xenopus* kinesin-like protein essential for spindle organization and chromosome positioning. Cell *81*, 117-127.

Volkov, A., Mascarenhas, J., Andrei-Selmer, C., Ulrich, H. D., and Graumann, P. L. (2003). A prokaryotic condensin/cohesin-like complex can actively compact chromosomes from a single position on the nucleoid and binds to DNA as a ring-like structure. Mol Cell Biol *23*, 5638-5650.

Wake, R. G., Errington, J.. (1995). Chromosome partitioning in bacteria. Annu Rev Genet *29*, 41-67. Review.

Walker, J. E., Saraste, M., Runswick, M. J., and Gay, N. J. (1982). Distantly related sequences in the a- and b-subunits of ATP synthase, myosin, kinases and other ATP-requiring enzymes and a common nucleotide binding fold. EMBO J *1*, 945-951.

Wang, J. C. (2002). Cellular roles of DNA topoisomerases: a molecular perspective. Nat Rev Mol Cell Biol *3*, 430-440.

Warburton, P. E., and Earnshaw, W. C. (1997). Untangling the role of DNA topoisomerase II in mitotic chromosome structure and function. Bioessays *19*, 97-99.

Warren, W. D., Lin, E., Nheu, T. V., Hime, G. R., and McKay, M. J. (2000a). Drad21, a Drosophila rad21 homologue expressed in S-phase cells. Gene *250*, 77-84.

Warren, W. D., Steffensen, S., Lin, E., Coelho, P., Loupart, M.-L., Cobbe, N., Lee, J., McKay, M. J., Orr-Weaver, T., Heck, M. M. S., and Sunkel, C. E. (2000b). The *Drosophila* RAD21 cohesin persists at the centromere region in mitosis. Curr Biol *10*, 1463-1466.

Watrin, E., Legagneux, V. (2005). Contribution of hCAP-D2, a non-SMC subunit of condensin I, to chromosome and chromosomal protein dynamics during mitosis. *Mol Cell Biol.* 25(2), 740-50.

Wei, Y., Yu, L., Bowen, J., Gorovsky, M.A., Allis, C.D.. (1999). Phosphorylation of histone H3 is required for proper chromosome condensation and segregation. Cell *97(1)*, 99-109.

Weitao, T., Dasgupta, S., and Nordstrom, K. (2000). Role of the *mukB* gene in chromosome and plasmid partition in *Escherichia coli*. Mol Microbiol *38*, 392-400.

Weitzer, S., Lehane, C., and Uhlmann, F. (2003). A Model for ATP Hydrolysis-Dependent Binding of Cohesin to DNA. Curr Biol *13*, 1930-1940.

Wells, N. J., Fry, A. M., Guano, F., Norbury, C., and Hickson, I. D. (1995). Cell cycle phase-specific phosphorylation of human topoisomerase IIa. Evidence of a role for protein kinase C. J Biol Chem *270*, 28357-28363.

Wells, N. J., and Hickson, I. D. (1995). Human topoisomerase IIa is phosphorylated in a cell-cycle phase-dependent manner by a proline-directed kinase. Eur J Biochem *231*, 491-497.

Widom, J., Klug, A.. (1985). Structure of the 300A chromatin filament: X-ray diffraction from oriented samples. Cell *43(1)*, 207-13.

Wignal, S. M., Deehan, R., Maresca, T.J., Heald, R.. (2003). The condensin complex is required for proper spindle assembly and chromosome segregation in Xenopus egg extract. J Cell Biol *161(6)*, 1041-1051.

Williams, S. P., Athey, B.D., Muglia, L.J., Schappe, R.S., Gough, A.H., Langmore, J.P.. (1986). Chromatin fibers are left-handed double helices with diameter and mass per unit length that depend on linker length. Biophys J *49(1)*, 233-48.

Winey, M. (1999). Cell cycle: driving the centrosome cycle. *Curr Biol.* 9(12), R449-52. Review.

Wood, E. R., and Earnshaw, W. C. (1990). Mitotic chromatin condensation in vitro using somatic cell extracts and nuclei with variable levels of endogenous topoisomerase II. J Cell Biol *111*, 2839-50.

Woodcock, C. L., Dimitrov, S.. (2001). Higher-order structure of chromatin and chromosomes. Curr Opin Genet Dev *11(2)*, 130-5. Review.

Woodcock, C. L. F., Frado, L.-L.Y., Rattner, J.B.. (1984). The higher-order structure of chromatin: evidence for a helical ribbon arrangement. J Cell Biol *99*, 42-52.

Yamanaka, K., Ogura, T., Niki, H., Hiraga, S.. (1996). Identification of two new genes, mukE and mukF, involved in chromosome partitioning in Escherichia coli. Mol Gen Genet *250(3)*, 1996 Feb 25.

Yeong, F. M., Hombauer, H., Wendt, K.S., Hirota, T., Mudrak, I., Mechtler, K., Loregger, T., Marchler-Bauer, A., Tanaka, K., Peters, J.M., Ogris, E.. (2003). Identification of a subunit of a novel Kleisin-beta/SMC complex as a potential substrate of protein phosphatase 2A. Curr Biol *13(23)*, 2003 Dec 2.

Yoshimura, S. H., Hizume, K., Murakami, A., Sutani, T., Takeyasu, K., and Yanagida, M. (2002). Condensin Architecture and Interaction with DNA. Regulatory Non-SMC Subunits Bind to the Head of SMC Heterodimer. Curr Biol *12*, 508-13.

Yu, J., Fleming, S. L., Williams, B., Williams, E. V., Li, Z., Somma, P., Rieder, C. L., and Goldberg, M. L. (2004). Greatwall kinase: a nuclear protein required for proper chromosome condensation and mitotic progression in Drosophila. J Cell Biol *164*, 487-492.

Zhao, K., Kas, E., Gonzalez, E., Laemmli, U.K.. (1993). SAR-dependent mobilization of histone H1 by HMG-I/Y in vitro: HMG-I/Y is enriched in H1-depleted chromatin. EMBO J *12(8)*, 3237-47.

Appendix

In the Appendix is a copy of a review entitled "Chromosome Condensation", written by me, currently in press in Encyclopedic Reference of Genomics and Proteomics. Also a research paper entitled "Drosophila CAP-D2 is required for condensin complex stability and resolution of sister chromatids", of which I am the first author, is currently in press in the Journal of Cell Science.

CHROMOSOME CONDENSATION

Ellada Savvidou and Margarete M. S. Heck

Wellcome Trust Centre for Cell Biology, University of Edinburgh

INTRODUCTION

Chromosomal DNA, if stretched end-to-end, measures about 2 metres in any one cell of the human body and therefore it must be highly folded to fit into a nucleus of only 5 μm diameter. In addition to this, DNA has to condense even more prior to cell division in order to form the highly compacted metaphase chromosome. Several levels of packing enable DNA to achieve this packaging and a number of structural proteins are involved. The simplest level of packing involves the winding of DNA around octamers of core histones in a structure called the nucleosome. This shortens DNA about 7-fold relative to naked DNA. The folding of regularly spaced nucleosomes forms a shorter, thicker filament, called the 30 nm chromatin fiber, in which the DNA is about 40-fold more compact than when naked. The most highly condensed and least understood stage takes place prior to chromosome segregation when the DNA in metaphase chromosomes of higher eukaryotic cells is compacted nearly 10,000-fold in length. The way that chromatin organizes into this higher-order structure of mitotic chromosomes is not well understood and the different models that have been proposed remain controversial.

FIRST LEVEL OF COMPACTION: THE NUCLEOSOME

Interphase nucleosomal chromatin under low salt conditions appears (by electron microscopy) as beads on a string with a diameter of about 10 nm. This packaging results when 166 bp of DNA winds around an octamer of core histones in a left-handed superhelix following a helical path along the surface of the octamer. The histone octamer consists of an $[H3]_2$:$[H4]_2$ tetramer, flanked on either side by an H2A:H2B heterodimer. Each core histone has a compact domain of 70 to 80 amino acid residues and a flexible N-terminal tail of approximately 30 amino acids outside the nucleosome. These N-terminal tails allow the nucleosomes to pack into a 30 nm fiber, while specific modifications of the tails are crucial for modulation of chromatin structure. Histone H1, or other linker histones, binds to a variable amount of linker DNA that extends between adjacent nucleosomes. The N-terminal tails of the histones are also important for extra-nucleosomal interactions. The variants of linker histone differ from the core histones in that the globular central domain is flanked by unstructured basic domains at both the N- and C-termini. Histone H1 resides at the side of nucleosome where DNA enters and exits the nucleosome. The master cell cycle regulatory kinase, CDK1 (cdc2:cyclinB), phosphorylates serine and threonine residues on the histone H1 tails during mitosis. Hyperphosphorylation of histone H1 was originally thought to be

important for mitotic chromosome condensation but recent studies show that it is not required for this process. Mitosis-specific phosphorylation of histone H3 at serine-10 (by aurora B kinase) is also not necessary for mitotic chromosome condensation. The N-terminal tails of histones may also be acetylated or methylated, resulting in an epigenetic histone code important for gene expression or assembly of heterochromatin.

ABOVE AND BEYOND THE NUCLEOSOME

Chromatin isolated from interphase nuclei has a diameter of 30 nm. This fibre has been variously modelled as either a solenoidal coiling, random or organized folding of the nucleosomal fibre — its actual structure remains undetermined. Fragility of the 30 nm fibre during preparation is likely responsible for the inability to unambiguously ascertain its architecture. However, the 40-fold length compaction within the 30 nm fibre is not nearly enough to account for the compaction of the genome in interphase nuclei or mitotic chromosomes.

MITOTIC CHROMOSOME CONDENSATION

The mechanism for packaging the 30 nm fibre into the highly compact, characteristc rod-shaped mitotic chromosomes remains a fundamental question for modern cell biologists. The shortening of DNA by roughly 10,000-fold is essential for the proper physical separation of sister chromatids to opposite poles, e.g. in order to avoid cleavage of the genome by an ingressing cleavage furrow. In addition, chromosomes must be properly aligned via their kinetochores to ensure that one of each chromatid pair ends up in each new daughter cell. However, early approaches utilizing electron microscopy to examine isolated native mitotic chromosomes only served to confirm that the DNA is indeed very densely packed within chromosomes.

Several approaches have been utilized in an attempt to expose the factors underlying higher order chromosome structure. By depleting core histones from highly purified mitotic chromosomes (either with a high salt concentration or polyanions which compete with histones by charge) under conditions that maintain residual non-histone proteins, some of the first hints about large scale chromatin folding were obtained. Long extended loops of DNA (about 15-100 kb) surrounded a protein core that retained the general size and shape of a native chromosome. These striking images led to a model known as the radial loop model in which the folding of the chromatin fiber into loops is mediated by proteins of an insoluble chromosome scaffold that is essential for the final size and shape of a chromosome. Others though considered the scaffold to be an artifact, a result of inappropriate protein interactions created during preparation of this fraction. Nonetheless, this model was first proposed more than 25 years ago, and there is a significant amount of data

supporting it. A:T-rich DNA sequences (SARs — scaffold attachment regions, or MARS — matrix attachment regions) have been identified as the *cis*-sequences interacting with the proteinaceous component. The DNA intervening between two SAR sequences bound to the scaffold, separated by up to 100 kb of DNA, would form a chromatin loop.

PROTEIN COMPONENTS: TOPOISOMERASE II AND CONDENSINA biochemical analysis of scaffolds showed there were two major components: Sc1 and Sc2, which later were identified as DNA topoisomerase II and SMC2 (a subunit of the condensin complex), respectively. In addition to this, characterization of chromosomes remodelled from sperm chromatin in *Xenopus* egg extracts, resulted in the identification of several protein components of these *in vitro* assembled structures. The mitotic chromosome fraction contained histones and linker histones, topo IIα, chromokinesin, the chromatin remodeling ATPase ISWI, and a complex subsequently named condensin. These studies demonstrated that mitotic chromosomes are rich in ATPases, which are likely important to induce conformational changes of chromosomes and to support microtubule-dependent movement of chromosomes.

Topoisomerase II is an ATP-dependent enzyme that can alter DNA topology by passing one double-strand helix through another via a transient double-strand break, an activity necessary for the resolution of catenated sister DNA strands. Topo II is located both at the centromeres and axially along mitotic chromosome arms at the base of loops. All eukaryotic organisms have at least one topo II. Higher eukaryotes though, have two isoforms (topo IIα and topo IIβ) that have similar catalytic activities *in vitro* but different localization *in vivo*. Topo II activity is required for the resolution of the catenated strands of DNA so that each chromatid of a pair becomes an individual unit, facilitating successful separation during anaphase. Indeed, mutations in topo II in both *Saccharomyces cerevisiae* and *Schizosaccharomyces pombe* were lethal in mitosis, with sister chromatids failing to segregate properly. Further analysis in *S. pombe* revealed that topo II was also required for the final stages of chromosome condensation, possibly in collaboration with the condensin complex, but its exact role in this process is not yet clear. In *Drosophila*, depletion of topo II by RNAi resulted in a 2.5-fold decrease in the level of chromatin compaction but overall chromosome condensation occurred without topo II. In the same study, chromosome morphology was abnormal and one or more chromosome arms frequently stretched out from the metaphase plate, suggesting an unexpected role for topo II in chromosome arm congression to the metaphase plate. Even though topo II seems to be important for the establishment of chromosome condensation in many different organisms, in *Xenopus* egg extracts it seems not to be essential for the maintenance of chromosome condensation, suggesting that topo II might contribute to the early

stages of this process. Interestingly, as chromosomes decondense at the end of mitosis, topo IIα undergoes specific degradation, only to be resynthesized at the start of S phase if cells are actively cycling.

ScII was identified as SMC2, a Structural Maintenance of Chromosomes protein, and a member of the condensin complex. This complex consists of two SMC proteins (SMC2 and SMC4) and three non-SMC subunits (CAP-D2, CAP-G and CAP-H). SMC2 and SMC4 form a heterodimer, and the non-SMC subunits presumably play regulatory roles. The SMCs are present in all species examined and they constitute a family of highly conserved and ubiquitous proteins. All members are large polypeptides with a molecular mass of 115-165 kDa and a similar structural organization. The proteins have two extended coiled-coil domains, which are separated by a central globular hinge region. The N- and C- termini flanking the coiled-coil domains are highly conserved among SMC proteins. The N-terminal domain contains a Walker A box (an ATP-binding motif). The C-terminal domain contains a DA box resembling a Walker B site (ATP hydrolysis motif) and it has been shown to bind DNA. Eukaryotic SMCs comprise at least six distinct subfamilies (SMC1-SMC6), which form 3 different heterodimers: SMC1/SMC3 (chromatid cohesion), SMC2/SMC4 (chromosome condensation), and SMC5/SMC6 (DNA repair). Recent data suggests that each of the SMC subunits of the cohesin and condensin complex folds intramolecularly and their heterodimerisation is mediated by a hinge-hinge interaction. The intramolecular folding of an SMC molecule allows the association of the N- and C- terminal domains and the formation of an ATP catalytic domain at each end of the heterodimer. The non-SMC subunits bind to one or both of the catalytic domains.

Much of the current understanding of condensin activity comes from the biochemical characterization of the complex from *Xenopus* egg extract. In this system it has been shown that all five subunits are necessary for DNA-stimulated ATPase activity, which reconfigures DNA in an ATP-dependent manner. Condensin introduces positive supercoils into relaxed circular DNA in the presence of topoisomerase I and converts nicked circular DNA into positively knotted forms in the presence of topoisomerase II *in vitro*. Recent observations of the condensin complex by spectroscopic imaging, suggest that a single condensin complex organizes two oriented supercoils, thus inducing superhelical tension. A model that emerges from these observations is that each of the two end domains wraps DNA into nearly one superhelical turn allowing a single condensin complex to create two supercoils. Although the way that DNA interacts with the two-armed structure of condensin is unknown, a recent study showed that the region that binds DNA may be in the coiled-coil arms and not in the catalytic domains. A similar model has been recently proposed

for the action of cohesin. Another study suggests that condensin may form a DNA loop by holding two distantly located DNA segments.

Two models have been proposed to explain how condensin may act on chromatin but both models are highly speculative. The first model proposes that local positive supercoiling driven by condensin introduces a compensatory superhelical tension into the neighbouring region of DNA, which in turn acts as a driving force for the compaction of a chromatin fiber. The problem with this model is that there is no evidence for superhelical tension in metaphase chromosomes. The second model is based on the prediction that a single condensin complex introduces two positive supercoils by a trapping mechanism and forms a topological link between the condensin clamp and the trapped DNA strands. If a free translocation of the DNA strands is allowed without disrupting the topological link, a positive loop of DNA would be created. A continuing creation of positive loops by the action of condensin might contribute to mitotic chromosome organization.

Even though condensin was originally thought to be responsible for chromosome condensation (hence the name), recent genetic studies in different organisms suggest that this complex is required for the proper organization and segregation of mitotic chromosomes, and not condensation *per se*. Yeast mutations in the condensin complex increased the average distance between two loci on a mitotic chromosome arm in the same way depletion of condensin from *Xenopus* mitotic egg extracts resulted in less compact chromosomes. Condensin however seems to be more than a simple compactor and is essential for resolution between sister chromatids *in vivo*. In *Drosophila* SMC4 mutants, shortening of the longitudinal axis of the chromosomes was unaffected, but chromosomes failed to resolve into two distinct chromatids at prophase, and then showed chromosome bridging in anaphase. Similarly depletion of SMC4 by RNAi in *Caenorhabditis elegans* caused dramatic abnormalities in chromosome morphology at prometaphase, yet a high degree of compaction still occurred by metaphase. Mutation or RNAi of non-SMC condensin subunits also resulted in aberrant chromosome segregation (but apparently normal condensation). In *Drosophila*, depletion of the condensin subunit SMC4 disrupted the localization of topo II in a central axial structure and furthermore to led a reduction of topoisomerase II-dependent DNA decatenation activity *in vitro*. Condensin appears to be required for proper chromosome organisation, this facilitating the action of topo II in sister chromatid resolution. Recently in an ScII/SMC2 knockout in chicken cells, it was found that chromosome condensation was delayed but it could finally reach its normal levels. In this study, mitotic chromosomes were missing a number of scaffold proteins and they lacked structural integrity indicating that condensin was necessary for the establishment of a robust chromosome structure. One of the most important results to date is

the observation that when both topo II and condensin are disrupted by RNAi, that chromosomes are still able to condense. There are clearly more components essential for mitotic chromosome condensation to be identified.

The supercoiling activity of the condensin complex has been shown in vertebrates to require mitosis specific phosphorylation of the three non-SMC subunits by CDK1, the major mitotic kinase. CAP-D2 is phosphorylated at its C-terminus probably directly by CDK1, while CAP-H is phosphorylated probably by CDK1 or other kinases. The hyperphosphorylation of the non-SMC subunits is proposed to have two dual roles. The first one is to activate the ATPase activity of SMCs and the second to allow the condensin complex to be associated with chromatin in a mitosis-specific manner.

Recently a second condensin (II) complex was identified in vertebrate cells. Both complexes share SMC2/SMC4, but contain different sets of non-SMC subunits. The two complexes may have distinct distributions along chromosome axes, but show a similar distribution at the centromere region. It has been proposed that the two complexes make distinct mechanistic contributions to mitotic chromosome architecture in vertebrate cells. Depletion of condensin I or condensin II produces weaker defect in chromosome morphology, while simultaneous depletion of both complexes causes the severest defect. Furthermore, the centromeric regions were structurally disorganised after the depletion of either condensin I or II subunits suggesting a role for both complexes in centromere organization. Sequence comparisons suggest that condensin II should exist in other organisms, but experimental data will confirm if that is the case.

Along with the phosphorylation of condensin subunits by the master mitotic kinase CDK1, the phosphorylation of histone H3 at the onset of mitosis has been proposed to play a role in condensin recruitment and chromosome condensation. Histone H3 mutations in *Tetrahymena thermophila* show abnormal chromosome condensation and extensive chromosome loss. In *C. elegans*, *Drosophila* and human cells, Aurora B, a chromosome-bound kinase, is targeted to chromosomes along their length during prophase, becomes concentrated at the centromeric regions during metaphase and is transferred to the spindle midzone when sister chromatids are separated in anaphase. This kinase is thought to interact with two other molecules, the inner centromere protein (INCENP) and survivin, which together are referred to as chromosomal passengers. Aurora B has been proposed to be the physiological kinase that phosphorylates histone H3 during mitosis. A model that connects the phosphorylation of histone H3 and chromosome condensation is that the modification of the histone may send a signal to initiate chromosome condensation. The

phosphorylation could function as a receptor for the recruitment of proteins such as the condensin complex. Experiments in several organisms though, suggest that the phosphorylation of histone H3 is not responsible for the direct recruitment of condensin onto chromosomes and chromosome condensation is not affected when histone H3 phosphorylation is diminished by depletion of Aurora B. Future work will clarify the role of H3 phosphorylation in mitotic chromosome dynamics.

DEPENDENCE ON APPROPRIATE DNA REPLICATION AND REPAIR

The final condensation of mitotic chromosomes is dependent not only on mitotic events, but also on appropriate timing of DNA replication and the satisfaction of DNA-structure checkpoints. In *Drosophila*, mutations of ORC2/3/5, subunits of the Origin Recognition Complex, result in the formation of irregularly condensed chromosomes in mitosis. Regions of euchromatin that were replicated abnormally late in these mutations showed a severe condensation defect in contrast to other regions of the chromosome. Mutations in RFC4 (subunit 4 of Replication Factor C) resulted in DNA-structure checkpoint defects, chromosome pulverization (mitotic catastrophe), and also prematurely separated chromosomes in mitosis — as a result of interfering with different functions of RFC. Whether the condensation defect observed in these mutants is a direct effect on topo II or condensin, is currently unknown.

A YIN-YANG BALANCE WITH COHESION?

Sister chromatid cohesion is established between the two replicated sister chromatids during S phase by an evolutionary conserved complex called cohesin. The cohesin complex (a heterodimer of SMC1 and SMC3 and two additional non-SMC subunits — Scc1 and Scc3) is essential for holding sister chromatids together until the onset of anaphase, ensuring the accurate 1:1 partitioning of chromatids. In yeast all cohesin dissociates from chromosomes at the beginning of anaphase when the Scc1 subunits is cleaved. In higher eukaryotes, most of the cohesin complex dissociates from chromosome arms already in prophase after phosphorylation by the polo kinase with only a small amount of cohesin left at centromeric regions. Residual cohesion is lost at the onset of anaphase by the cleavage of the Scc1 non-SMC subunit. The dissociation of cohesin from chromosome arms in prophase could facilitate either the condensation or resolution of chromatids. Alternatively, condensation may help to release cohesion between chromatids. However, loss of Scc1 (and cohesion) by RNAi has no apparent effect on condensation. However it is plausible that a mechanism ensuring the correct balance between cohesin and condensin may exist. A structural and functional link between cohesion and condensation, if it exists, remains to be determined.

We have attempted to highlight some of the most important issues surrounding chromosome organization and condensation throughout the cell cycle. The organization of a scaffold and its association with specific DNA sequences, along with the mechanism by which chromosomes condense prior to mitosis, or decondense after mitosis are poorly understood. Nevertheless, exciting progress is being made through diverse approaches. We also believe there are as yet, uncharacterized factors that play crucial roles in these events, which may even result in the proposal of new models for the dynamics of higher order chromosome architecture.

References:

Belmont, A. S. (2002). Mitotic chromosome scaffold structure: new approaches to an old controversy. Proc Natl Acad Sci U S A **99**: 15855-7.

Cobbe, N. and M. M. S. Heck (2004). The Evolution of SMC proteins : Phylogenetic Analysis and Structural Implications (Epub 2003 Dec 05). Mol Biol Evol **21**: 332-47.

Hagstrom, K. A. and B. J. Meyer (2003). Condensin and cohesin: more than chromosome compactor and glue. Nat. Rev. Genet. **4**(7): 520-534.

Nasmyth, K. (2001). Disseminating the genome: joining, resolving, and separating sister chromatids during mitosis and meiosis. Ann. Rev. Genetics **35**: 673-745.

Pollard, T. D. and W. C. Earnshaw (2002). Cell Biology. Philadelphia, Saunders.

Swedlow, J. R. and T. Hirano (2003). The making of the mitotic chromosome: modern insights into classical questions. Mol. Cell **11**: 557-569.

Glossary

Chromosome: Each chromosome consists of a single, long DNA molecule with a telomere at each end, and a centromere mediating attachment to the mitotic spindle. Every species has a characteristic number of chromosomes that are visualized as separate entities only during mitosis (e.g. humans have 46 chromosomes). After replication, each chromosome is composed of 2 identical chromatids.

Chromosome passengers: Proteins that are associated with chromosomes during the early stages of mitosis, then with the spindle midzone during anaphase and telophase, and finally with the midbody at the exit from mitosis. So far there are 5 known members: INCENP, survivin, Aurora B, TD-60, and borealin.

Cohesin: a multiprotein protein complex that is required to hold together the sister chromatids of replicated chromosomes. It consists of two SMC proteins (SMC1 and SMC3), and two non-SMC subunits(Scc1 and Scc3). In higher eukaryotes, cohesin dissociates from chromosome arms in prophase and from the centromeres at the onset of anaphase, while in yeast, it dissociates from chromosomes at the onset of anaphase.

Condensin: a multiprotein complex that consists of two SMC subunits (SMC2 and SMC4), and three non-SMC subunits (CAP-D2, CAP-G and CAP-H). Condensin is required for chromosome organization and segregation and it only associates with chromosomes at prophase, when chromosomes condense and dissociates in anaphase when chromosomes start to decondense — though individual subunits show different behaviour.

SMC proteins: Abbreviation for Structural Maintenance of Chromosomes. The SMCs are known to be present in species from mycoplasma to mammals and they constitute a family of conserved and ubiquitous proteins, called the SMC family (with 6 subfamilies). The proteins have two extended coiled-coil domains, which are separated by a central globular hinge region. These proteins, when dimerised, have ATPase activity by bringing together the N- (ATP binding) and C- (ATP hydrolysis) termini.

Topoisomerase II (topo II): An ATP-dependent enzyme that can alter DNA topology by passing one double helix strand through another via a transient double helix break, an activity necessary for the resolution of catenated sister DNA strands. It is located both at centromeres and along mitotic chromosome arms at the base of loops.

Drosophila CAP-D2 is required for condensin complex stability and resolution of sister chromatids

Ellada Savvidou, Neville Cobbe, Søren Steffensen [1], Sue Cotterill [2], and Margarete M. S. Heck *

Wellcome Trust Centre for Cell Biology
Institute of Cell and Molecular Biology
University of Edinburgh
Michael Swann Building, King's Buildings
Mayfield Road, Edinburgh EH9 3JR U.K.

[1] Instituto de Histologia
Faculdade de Medicina
Universidade de Lisboa
Av. Prof. Egas Moniz
1649-028 Lisboa Portugal

[2] Sue Cotterill
St Georges Hospital Medical School
Cranmer Terrace
London
SW17 0RE

* Author for correspondence
email: margarete.heck@ed.ac.uk
tel: +44 (0) 131 650 7114
FAX: +44 (0) 131 650 7778

Running title: Functional analysis of condensin subunit CAP-D2

Key words: chromosome, chromatid, mitosis

Word Count: 7,636 (Introduction, Materials and Methods, Results, Discussion)

Summary

The precise mechanism of chromosome condensation and decondensation remains a mystery, despite progress over the last 20 years aimed at identifying components essential to the mitotic compaction of the genome. In this study, we analyze the localization and role of the CAP-D2 non-SMC condensin subunit and its effect on the stability of the condensin complex. We demonstrate that a condensin complex exists in *Drosophila* embryos, containing CAP-D2, the anticipated SMC2 and SMC4 proteins, the CAP-H/Barren and CAP-G (non-SMC) subunits. We show that CAP-D2 is a nuclear protein throughout interphase, increasing in level during S phase, present on chromosome axes in mitosis, and still present on chromosomes as they start to decondense late in mitosis. We analyzed the consequences of CAP-D2 loss after dsRNA-mediated interference, and discovered that the protein is essential for chromosome arm and centromere resolution. The loss of CAP-D2 after RNAi has additional downstream consequences on the stability of CAP-H, the localization of DNA topoisomerase II and other condensin subunits, and chromosome segregation. Finally, we discovered that even after interfering with two components important for chromosome architecture (DNA topoisomerase II and condensin), chromosomes were still able to compact, paving the way for the identification of further components or activities required for this essential process.

Introduction

Chromosomal DNA, if stretched end to end, measures about 2 metres in any one cell of the human body and therefore must be highly folded to fit into a nucleus of only 5 μm diameter. DNA has to condense even further prior to cell division in order to form the highly compact metaphase chromosome comprising two sister chromatids, capable of withstanding anaphase segregation (Heck, 1997; McHugh, 2003; Swedlow and Hirano, 2003). Thus, mitotic chromosome condensation consists of a process in which interphase chromatin is 1) compacted, and 2) resolved into two distinct rod-shaped sister chromatids. Recent studies have contributed to the unraveling of this process. A five subunit "condensin" complex was initially identified biochemically in *Xenopus* (Hirano et al., 1997; Hirano and Mitchison, 1994), and is comprised of two SMC (Structural Maintenance of Chromosomes) proteins (SMC2 and SMC4) and three non-SMC proteins (CAP-D2, CAP-G or CAP-H [Barren in *Drosophila*]). All five subunits have been identified in the eukaryotes examined to date (Cobbe and Heck, 2000). The SMC proteins belong to a superfamily of highly conserved and ubiquitous chromosomal ATPases (Cobbe and Heck, 2004). The non-SMC subunits have been proposed to have dual roles in the regulation of condensin function: one is to activate the SMC ATPases to perform ATP-dependent supercoiling activity, and the other is to allow the holocomplex to associate with chromatin in a mitosis-specific manner (Kimura and Hirano, 2000). Each of the condensin subunits is essential and required for proper organisation and segregation of mitotic chromosomes, but exactly how the complex contributes to these processes is still unclear. Recently a second condensin complex has been identified, with a different complement of non-SMC subunits (Ono et al., 2003).

Studies of condensin function have resulted in conflicting hypotheses as to the role of this complex. Mutants in Cut3 and Cut14 (the SMC4 and SMC2 subunits respectively) of *Schizosaccharomyces pombe* exhibited chromosome condensation defects and displayed a 'cut' phenotype where septation (cell division) occurred with incompletely separated chromosomes (Saka et

al., 1994). Fluorescence in situ hybridization in these mutants demonstrated that the length of mitotic chromosome arms increased while the centromeric DNA could separate and move to the opposite poles normally. In *S. pombe* and *Saccharomyces cerevisiae*, studies have shown that all members of the condensin complex are required for proper chromosome condensation and segregation (Lavoie et al., 2000; Ouspenski et al., 2000; Strunnikov et al., 1995; Sutani et al., 1999). In *Xenopus*, when condensin was depleted from mitotic extracts before or after condensation, unreplicated chromatin failed to assemble into individual chromatids or became completely disorganised, suggesting that the complex was required both for assembly and maintenance of mitotic chromosomes (Hirano et al., 1997; Hirano and Mitchison, 1994). In contrast, genetic studies in *Drosophila* and *Caenorhabditis elegans* showed that resolution between the sister chromatids rather than condensation of the chromosomes was compromised when the condensin complex was disrupted (Bhat et al., 1996; Hagstrom et al., 2002; Steffensen et al., 2001). In both organisms, a high degree of compaction relative to interphase and a bipolar metaphase plate formed. However, severe chromosome segregation defects and chromosome breakage were observed in anaphase and telophase. DmSMC4 RNAi in *Drosophila* cultured cells confirmed the requirement of this protein for chromosome organisation and segregation (Coelho et al., 2003). A common phenotype of the absence of condensin subunits in most organisms is the formation of chromosome bridges due to incomplete resolution and ensuing failure of sister chromatids to separate completely during anaphase (Hagstrom and Meyer, 2003). Particular insight was gleaned when the robustness of chromosome architecture was assessed after SMC2 knock-out in chicken DT40 cells – while chromosomes still reached normal levels of condensation, clear defects in association of other non-histone chromosomal proteins was observed (Hudson et al., 2003).

Recently, a second condensin complex, called condensin II, was identified in vertebrates (Ono et al., 2003). This complex shares the same two SMC subunits as the original complex, now named condensin I, but appears to contain different non-SMC subunits (named CAP-D3, CAP-G2, and CAP-H2). The two complexes appear to alternate along the axis of metaphase chromatids but are both

present at the centromere, albeit in distinct regions (Ono et al., 2004). Depletion of these complexes in *Xenopus* and HeLa cells produced distinct defects in chromosome morphology, suggesting that the complexes may contribute differently to mitotic chromosome architecture (Ono et al., 2003). Furthermore, the centromere/kinetochore regions were structurally disorganised from the depletion of either condensin I or II subunits suggesting a specific role for both complexes in centromere organisation (Ono et al., 2004).

DNA topoisomerase II (topo II) has long been implicated in chromosome structure and dynamics, since its discovery as a chromosome 'scaffold' protein, and its localization at the base of chromatin loops (Earnshaw et al., 1985; Earnshaw and Heck, 1985; Gasser et al., 1986). SMC2 has also been shown to be a component of the chromosome 'scaffold' fraction (Saitoh et al., 1994). Yeast mutants in topo II exhibit segregation defects similar to those observed in condensin mutants (Holm et al., 1985). The decatenation activity of topo II facilitates the resolution of sister chromatids and the complete separation of chromosomes in anaphase. Topo II has also been shown to be required for chromosome condensation but its role in this process has been controversial since disruption of its function resulted in different chromosome morphologies (Swedlow and Hirano, 2003; Warburton and Earnshaw, 1997). Recently, an unexpected role for topo II in chromosome arm congression emerged after RNAi depletion in *Drosophila* cells (Chang et al., 2003). Localisation studies revealed that Topo II was axially distributed in the chromosome arms with some concentration at the centromeres, a distribution that was also observed for condensin subunits (Maeshima and Laemmli, 2003; Steffensen et al., 2001). The localisation pattern and the phenotype after the depletion of either the condensin complex or topo II suggested that these two components of the chromosome scaffold may collaborate to bring about chromosome compaction and organisation. Biochemical and localisation studies in *Drosophila* showed that CAP-H/Barren associated with topo II throughout mitosis, while SMC4 appeared to be responsible for the axial localisation of topo II on the chromosomes and for its decatenation activity (Bhat et al., 1996; Coelho et al., 2003). However, in *S. pombe*, the localisation

but not the activity of topo II was affected in condensin mutants, while topo II localization to well-defined axial structures in *Xenopus* was independent of condensin (Bhalla et al., 2002; Cuvier and Hirano, 2003). Given that chromosomes experience different constraints depending on the cell, organism, or time in development, it is perhaps not surprising that a 'unified' hypothesis regarding these two components has not emerged.

In this study, we demonstrate that a condensin I complex exists in *Drosophila.* We subsequently examined the cell cycle localization and role of the *Drosophila* CAP-D2 subunit in chromosome dynamics during mitosis. We show that depletion of CAP-D2 by RNAi in *Drosophila* cultured cells results in a compromised mitotic chromosome architecture with defective sister chromatid resolution and subsequent chromosome bridges in anaphase. We demonstrate here for the first time, that the fate of other members of the condensin complex and other chromosomal proteins essential for chromosome dynamics during mitosis is altered when a condensin subunit is disrupted either by depletion or mutation. We additionally examine *Drosophila* mutations of condensin subunits to assess the stability of the complex in the context of the organism. We also show that mitotic coordination with regard to chromosome passengers is compromised when condensin function is affected. Finally we demonstrate that when both condensin and topo II are disrupted by RNAi, chromosomes are surprisingly still able to compact, intimating the existence of additional, currently unknown, factors essential to the assembly of mitotic chromosomes.

Materials and Methods

Identification of the Condensin Complex

Extract preparation: 0-5 hr *Drosophila* embryos were homogenised in one volume of buffer A (15 mM NaCl, 60 mM KCl, 2 mM EDTA, 0.34 M sucrose, 15 mM Hepes pH 7.9) and complete protease inhibitors (Roche) using a loose pestle. The homogenate was centrifuged for 5 minutes at 5000 x g at 4°C in a benchtop centrifuge. The middle layer was collected, aliquoted and flash frozen in liquid nitrogen. Dimethyl pimelimidate cross-linking of CAP-D2 antibody to protein A-sepharose was performed according to Harlow and Lane (Harlow and Lane, 1999). For immunoprecipitation from crude extracts, antibody beads were incubated with the extract for 1 hr at 4°C. The beads were washed 10 times with 20 volumes of PBS, and then eluted and washed with PBS containing 250 and 500 mM NaCl. Protein interactions that were resistant to 500 mM NaCl were eluted using 2% SDS in PBS.

Generation of Antigens and Antibodies

Polyhistidine (6His)-tagged fragments of DmSMC2 and DmCAP-D2 were produced using the residues 24-309 and 951-1162 respectively, by cloning a BamH1-HindIII fragment of the cDNA into a pQE30 (QIA*express* system, Qiagen) expression vector. The constructs were expressed in *E. coli* M15[pREP4] cells (Qiagen) and the proteins were purified on Ni-agarose columns (Qiagen) and subjected to SDS-PAGE. Individual gel bands were excised from the gel, ground under LN_2, and injected into rabbits (Scottish Antibody Production Unit, Pentlands Science Park). The same procedure was followed for the generation of topo II antibody. Residues 1079-1333 were used and a BamH1-HindIII fragment of the genomic DNA was cloned into a pET23a (Novagen) expression vector. The construct was transformed into *E.coli* BL21 cells (Novagen) and the protein was purified as described above. For CAP-D3 antibody, a peptide corresponding to the terminal 15 amino acids of the protein (residues 1253-1267, CDMLVTELIFQPPDW) was synthesised and injected into rabbits (Genosphere).

Cell Culture and RNAi

Drosophila embryonic S2 cells were maintained in serum free Schneider's Insect Medium supplemented with 10% Insect qualified Fetal Bovine Serum (FBS). Cells were grown at 27°C in a humidified atmosphere. RNAi was performed in *Drosophila* S2 cells as previously described (Clemens et al., 2000; Vass et al., 2003). Two fragments from the 5' end of CAP-D2 (forward primer at 251-270 bp of ORF and reverse primer at 873-892 bp of ORF) were fused to T7 RNA polymerase promoter and were used as PCR primers. The *Drosophila* EST clone LD40412 was used as a template for the PCR reaction. The PCR product obtained (~642bp) was used as template for RNA synthesis using the Megascript kit (Ambion). A random human intronic sequence was used to generate control dsRNA, which was synthesized in the same way. Topo II dsRNA was obtained as described previously (Chang et al., 2003). For the CAP-D3 dsRNA the EST clone RE18364 was used as a template for the PCR reactions. Two PCR products were obtained from two different regions of the ORF. The first one was obtained with a primer pair that includes the start codon (r1 ~ 639 bp) and the second one with a primer pair further inside the message (r2~723 bp). The two products were used in two independent experiments. For the RNAi experiment, $1x10^6$ cells/ml were diluted in serum free Schneider's Insect Medium. 20-25 μg/ml of dsRNA was added to the cells (30 μg/ml for the CAP-D3 RNAi). 1ml of these cells was placed into each well of a 35mm 6-well plate and incubated for 60 to 90 min. After the incubation 2mls of Schneider's Media supplemented with 10% FBS was added to each well. The cells were placed in the 27°C humidified incubator and samples were processed for immunoblotting or for immunofluorescence at certain time points. For some experiments, cells were grown on sterilized Concanavalin A treated coverslips in a 35mm 6-well plate (Rogers, 2002), but only for the last 24hr before being processed for immunofluorescence. In some cases S2 tissue culture cells (RNAi treated or control cells) were exposed to 30 μM colchicine for 7 hours, 67 hours after the RNAi treatment. Cells were then processed for immunoblotting or immunofluorescence.

Preparation of Cell Extracts

Cells were counted under the microscope with a hematocytometer, centrifuged at 2000 rpm for 2 min and washed with 0.5 ml of PBS (phosphate-buffered saline: 137 mM NaCl, 2.7 mM KCl, 6.46 mM Na_2HPO_4, 1.47 mM KH_2PO_4 pH 7.4). The pellet was resuspended in a certain amount of PBS and warm sample buffer [3X sample buffer: 2% SDS, 10% Glycerol, 0.01% Bromophenol Blue, 2 mM EDTA,, 50 mM trizma base pH 6.8] with 10 mM DTT (1/10 of final volume). The cells were lysed by sonication and the extract was boiled at 100°C for 5 to 10 min. The volume of PBS and sample buffer was calculated so that the final cell concentration was $5x10^4$cells/µl.

Preparation of Embryo Extracts

To identify homozygous embryos for $barr^{L305}$ and glu^{17C} the mutant chromosomes were balanced over *CyO, P {w^{+mc}=GAL4-Kr.C}DC3, P{w^{+mc}=UAS-GFP.S65T}DC7* as described (Casso et al., 2000). One hour collections of embryos were aged for 12 hours, dechorionated with 50% bleach for 1 min and then sorted under a fluorescence dissecting microscope. Homozygous embryos were homogenised with a motorised pestle in EBR lysis buffer [EBR (13 mM NaCl, 0.47 mM KCl, 0.19 mM $CaCl_2$, 1 mM HEPES pH 6.9), 10 mM EDTA, 10 mM DTT, 1:100 dilution of CLAP, PMSF and trasylol] and warm sample buffer with DTT (1/10) was added immediately. The embryo extract was boiled at 100°C for 10 min.

Immunoblotting

Protein extracts were separated by SDS-PAGE and transferred onto nitrocellulose membranes in a Trans-Blot apparatus. Membranes were blocked in PBS+0.1% Tween 20 (PBSTw) and 5% semi-skimmed milk for 1hr at RT and then incubated for 1-1.5 hours with the primary antibody in PBSTw. After washing three times for 5, 15 and 10 min with PBSTw, the membranes were incubated in a

horseradish peroxidase-linked (HRP) secondary antibody for 1 hr in PBSTw at RT. Finally the membranes were washed as above in PBSTw and immunocomplexes were detected by enhanced chemiluminescence (ECL, Amersham Biosciences). For the RNAi experiment, $5x10^5$ cells were loaded per lane while for the analysis of embryos, 5 embryos were loaded per lane for both the wild type (Canton S) and mutant material.

Phosphorimager Analysis

Samples were processed as described for immunoblotting but instead of using an HRP secondary, a Cy5 conjugated secondary antibody (Jackson ImmunoResearch Laboratories) was used in a dilution of 1:200. The intensity of the signal was measured by using the STORM 860 scanning phosphorimager and calculated using the ImageQuant program (Amersham). The intensity was finally normalised by using α-tubulin as a loading control. Values were corrected by substracting the background of the corresponding lane from each band.

Immunofluorescence of *Drosophila* Cultured Cells

$2x10^5$ cells diluted in EBR were centrifuged onto poly-L-lysine-coated slides for 2 min at 2000 rpm in a cytospin column. The cells were immediately fixed for 4 min in 4% PFA in PBS at RT, washed for 5 min in PBS+0.1% Triton-X (PBSTx) and permeabilised in PBS +0.5% Tx for 5 min. After the permeabilisation, cells were blocked for 1 hr at RT in 0.5% Bovine Serum Albumin (BSA, Sigma). Cells were washed in PBSTx for 5 min and incubated for 1 hr in the primary antibody in PBSTx+0.5% BSA. After three 5 min washes in PBSTx, cells were incubated in the secondary antibody (conjugated fluorochromes, Molecular Probes or Jackson ImmunoResearch Laboratories) in PBSTx+0.5% BSA and in 1μg/ml DAPI for DNA staining. Cells were washed four times, 5 min each, in PBSTx and coverslips were mounted onto the slides with Mowiol (Calbiochem) and viewed under the fluorescent microscope. For some antibodies (SMC2, SMC4, guinea pig topo II and CAP-D3), 0.5% Triton-X was

included in the fixative and the incubation in this solution was done for 10 min. A permeabilisation step was performed as well as described above. For hypotonic treatment, cells were diluted in 0.25X EBR at a concentration of $2x10^5$ for 2 min at RT and then centrifuged onto poly-L-lysine slides and processed as described above. Cells that were grown on Concanavalin A coated coverslips for 24hr in a 35mm 6-well plate were then fixed and processed as described above.

BrdU Incorporation in *Drosophila* Cultured Cells

Cells growing in flasks were incubated for 30 min in medium containing 6 μg/ml BrdU (bromodeoxyuridine). $2x10^5$ cells were centrifuged onto poly-L-lysine slides and processed as described for immunofluorescence except that DAPI was omitted. The primary antibody in this case was anti-CAP-D2 and the secondary was Alexa 594 goat anti-rabbit conjugate. After the anti-CAP-D2 immunofluorescence was complete, the cells were post-fixed immediately in 4% PFA in PBS for 1 hr at RT, washed for 5 min in PBSTx and then incubated for 15 min in freshly prepared 2N HCl. After a 5 min wash in PBSTx, cells were blocked for 30 min in PBS+5% BSA and washed for 5 min in PBSTx and then incubated with the rat anti-BrdU antibody (1:2 dilution) in PBSTx+0.5% BSA at 4°C for 16 hrs. After three 5 min washes, the cells were incubated with Alexa 488 goat anti-rat conjugate (1:500 dilution) in PBSTx+0.5% BSA for 1 hr at RT. 1 μg/ml DAPI was added during the last incubation. Finally cells were washed four times for 5 min each with PBSTx and coverslips were mounted onto the slides with Mowiol.

Microscopy

All preparations were examined with an Olympus Provis microscope, equipped with epifluorescence optics. Images were captured with an Orca II CCD camera (Hamamatsu) and Smart Capture 2 software (Digital Scientific). All images were processed with Adobe Photoshop software. For examining the localisation and the presence of several proteins on the chromosomes in the RNAi

experiment, all images were obtained with the same camera settings and the same exposure time was maintained between the controls and the CAP-D2 RNAi experiment.

Antibodies

The primary antibodies were used for immunofluorescence as follows: α-tubulin (mouse monoclonal antibody B5-1-2 used at 1:500, Sigma), γ-tubulin (mouse monoclonal T 6557 used at 1:50, Sigma), P~H3 (mouse monoclonal used at 1:500, 9706L, New England Biolabs), BrdU (rat antibody used at 1:2, Harlan Sera Lab), CID (chicken polyclonal used at 1:200, (Blower and Karpen, 2001)), topo II (rabbit polyclonal used at 1:500, and guinea pig polyclonal used at 1:500), Barren (rabbit polyclonal used at 1:500 (Bhat et al., 1996)), SMC2 (rabbit polyclonal used at 1;500), SMC4 (rabbit and sheep polyclonals used at 1:500 (Steffensen et al., 2001), SCC1 (rabbit polyclonal used at 1:500 (Warren et al., 2000)), DSA1 (rabbit polyclonal used at 1:500 (Valdeolmillos, 2004)), BubR1 (rabbit polyclonal used at 1:1000). Sheep Cyclin B, INCENP (rabbit polyclonal used at 1:500, (Adams et al., 2001b)), CAP-D2 (rabbit polyclonal used at 1:1000 for immunofluorescence and 1:10,000 for immunoblotting), CAP-D3 (rabbit polyclonal used at 1:200 for immunofluorescence and 1:500 for immunoblotting). All fluorescently conjugated secondary antibodies (Molecular Probes, Jackson ImmunoResearch Laboratories and Amersham Biosciences) were used according to the manufacturer's instructions.

Results

Biochemical identification of a condensin complex in *Drosophila*

In this study we demonstrate for the first time that SMC2, SMC4 and the CAP-D2, CAP-G and CAP-H/Barren proteins exist as a complex in *Drosophila*. Immunoprecipitations with an antibody generated to DmCAP-D2 (Supp Figure 1A) were performed using 0-5 hour embryo extracts. Bound proteins were eluted sequentially with 0.5M NaCl and 2% SDS in PBS. The fractions were analysed by immunoblotting with SMC2, SMC4, CAP-D2, and CAP-H/Barren antibodies. All four proteins were present suggesting that they participate in the same complex. SMC2 and SMC4 proteins were eluted with both NaCl and SDS solutions, while CAP-D2 and CAP-H were only eluted with the SDS (Figure 1A). This result suggests two possibilities. First, the CAP-D2 and CAP-H non-SMC subunits may be more tightly associated with each other than they are with the SMC subunits of the condensin complex (we made a similar observation for the cohesin complex (Vass et al., 2003)). Second, the SMCs eluting with NaCl may be participating in another complex, such as condensin II. As no antibody was available to the CAP-G protein, the presence of this protein in the complex could not be assessed by immunoblotting. However, we were able to identify CAP-G by mass spectrometric analysis of proteins interacting with CAP-D2 (data not shown).

Characterisation of CAP-D2 during the cell cycle

To determine the subcellular localization of the CAP-D2 protein during the cell cycle, S2 cultured cells were centrifuged onto poly-L-lysine slides and processed for indirect immunofluorescence using the CAP-D2 antibody. Immunofluorescence revealed that CAP-D2 was mainly nuclear with varying levels during interphase. Several markers were utilized to further characterise these levels. An antibody to γ-tubulin, a centrosomal component, was used to denote cells that were in G1 phase prior to centrosome duplication. G1 cells showed the level of CAP-D2 in the

cytoplasm was nearly the same as in the nucleus (Figure 1B, top). Cells with 2 centrosomes (in S or G2 phase) (Loupart et al., 2000) had much higher levels of nuclear CAP-D2 (Figure 1B, bottom). S phase cells were identified following BrdU (a thymidine analogue) incorporation. All S phase cells showed nuclear staining of CAP-D2 (Figure 1C). While the intensity of the CAP-D2 signal varied among S phase cells, analysis of replication patterns with 2 thymidine analogues, CldU and IdU (Manders et al., 1992), demonstrated that the nuclear level of CAP-D2 increased as cells progressed through S phase (data not shown). Cyclin B, a cofactor for the mitotic CDC2 kinase, moves from the cytoplasm into the nucleus in late G2/early prophase (Huang, 1999). Cells with nuclear Cyclin B showed an intense nuclear staining for CAP-D2 (Figure 1D). These results suggest that *Drosophila* CAP-D2 is nuclear during interphase, with low levels in G1 that increase during S and are highest in late G2/early prophase.

The localisation of CAP-D2 during mitosis was also examined. In prometaphase, the protein localised along the condensed chromosome arms with more intense labelling of the centromeric regions (Figure 2A and B). The accumulation of CAP-D2 at centromeres can be clearly observed when cells are immunostained for both CAP-D2 and CID, the *Drosophila* homologue of CENP-A, a histone H3 isoform (Henikoff, 2000) (Figure 2B). In metaphase and early anaphase, when chromosomes were fully condensed, the CAP-D2 signal was most intense throughout the core of the chromatids. In telophase, even as histone H3 becomes dephosphorylated and chromosomes start to decondense, CAP-D2 was still tightly associated with chromatin (Figure 2A). The CAP-D2 staining was still intense during late telophase and cytokinesis (Figure 2C). Our results suggest that CAP-D2 associates with chromosomes in prophase, distributes axially on the chromosome arms with enrichment at the centromeres during prometaphase, is present throughout anaphase and telophase and even remains tightly associated with chromosomes as decondensation ensues.

SMC4 and Barren proteins are loaded onto chromosomes in early prophase but they dissociate from chromosomes late in anaphase/telophase when decondensation begins (Steffensen et al., 2001).

Since CAP-D2 appears to persist on chromosomes late in mitosis, we performed co-localisation studies with SMC4 in order to observe if the two subunits dissociate independently from chromatin late in mitosis. During anaphase, SMC4 started to dissociate from chromosomes as they start to decondense. Like P~H3, the SMC4 signal was fainter near the centromeric regions but was quite high at the end of chromosome arms, while CAP-D2 was still present throughout the chromatids (Supp Figure 1C). In telophase, while CAP-D2 was still associated with chromatin, SMC4 was diffuse and the chromosomal staining reduced (Supplemental Figure 1C).

CAP-D2 dsRNA-mediated interference in *Drosophila* cultured cells results in abnormal chromosome morphology and behaviour

As no CAP-D2 mutants were available, dsRNA-mediated interference (RNAi) on S2 cells was used to assess CAP-D2 function. S2 cultured cells were incubated with a 642 bp dsRNA fragment of CAP-D2 and samples were subsequently collected at 24 hr time points. Two negative controls were performed at the same time: cells that were incubated with dsRNA synthesized from a human intron (C) and cells with no dsRNA (-). Protein extracts from each time point were analysed by immunoblotting (Figure 3A). A decrease in CAP-D2 level was apparent at 48 hr with the protein greatly depleted by 72 hr and nearly undetectable by 96 hr (lanes labeled D – the final depletion was estimated to be 94% based on titration of signal from known cell numbers). The level of the protein was unaffected in control cells, and chromosomes appeared normal through mitosis (Figure 3B). Immunofluorescence of the CAP-D2 RNAi cells confirmed that these cells had much diminished CAP-D2 chromatin staining. 48 hr after RNAi, CAP-D2 signal was decreased (data not shown) and by 72 hr CAP-D2 protein was hardly detectable on the chromosomes of cells exhibiting abnormal chromosome morphology (Figure 3C). Chromosomes condensed relative to interphase but appeared fuzzy, unresolved and hypercondensed (a possible consequence of prometaphase delay). Dramatic failures in segregation resulted in chromosome bridges forming bi-nucleate or even tri-nucleate cells (Figure

3C4). We also frequently observed daughter nuclei of unequal size, suggesting that chromosomes had not been equally distributed during anaphase.

In order to better examine chromosome morphology, we treated cells with a hypotonic buffer that results in better chromosome spreading and improved observation of individual chromatids. Control cells appeared to have normal chromosome resolution and individual chromatid arms could be easily distinguished (Figure 3D). Individual chromatids were not visible in hypotonically treated CAP-D2 RNAi cells, and chromosomes appeared as condensed balls of chromatin distinct from one another, with usual levels of phospho~histone H3 (Figure 3E).

The quantitation of numerous mitotic parameters is presented in Supplemental Figure 2. CAP-D2 RNAi cells grew more slowly than control cells and cell number plateaued 72 hrs after treatment (Supp Figure 2A). Different time points were assessed for mitotic index, phenotype, and the distribution of mitotic phases. The percentage of mitotic cells (those positive for phospho~histone H3) after CAP-D2 RNAi increased 3-fold between 36 hrs and 72 hrs (Supp Figure 2B). 25% of the CAP-D2 RNAi mitotic cells were abnormal at 24 hrs, while 95-100% were abnormal after 48 hrs (Supp Figure 2C). After staining for cyclin B, it appeared that CAP-D2 RNAi cells were delaying in prometaphase (cyclin B positive) – this was corroborated by scoring the anaphase index (cyclin B negative, Supp Figure 2D and E). While the dsRNAi experiment was repeated several times, quantification of the phenotypes was performed three times with insignificant deviation between the results. Most of the phenotypic analysis was therefore carried out at 65 or 72 hrs after treatment with dsRNA.

As shown in Figure 3, dramatic chromosome defects were observed after treatment with CAP-D2 dsRNA – apparent failures in chromatid resolution, alignment, and segregation. We therefore asked whether centromere resolution was compromised after staining for two centromeric proteins – CID, and Scc3/DSA1, a subunit of the cohesin complex. The levels of DSA1 (and CID, not shown) appeared largely unaffected in the CAP-D2 RNAi cells (Figure 4A). DSA1 was highly concentrated at

centromeres during prometaphase and metaphase, and localized between CID spots (Figure 4B). DSA1 persisted at centromeres until sister chromatid separation at the onset of anaphase, while CID stained centromeres constitutively (Figure 4B, see also Figure 3B). DSA1 also stained the spindle poles and microtubules, especially during anaphase (Valdeolmillos, 2004). Centromeres were often stretched in the CAP-D2 RNAi cells (Figure 4C2-5, see also Figure 3C), while distinct double dots or cleanly separated sets of dots were observed in control metaphases and anaphases, respectively. Daughter nuclei connected by chromosome bridges still had centromeres extending between them (Figure 4C5 and 3C4).

In order to quantitate these results, cells were categorised into different groups. 95% of the cells that displayed CID stretching between sister centromeres had lower levels of centromeric DSA1 and thus were considered to be in anaphase (Figure 4C3-5). 60% of these anaphase figures were in early anaphase, as deduced from the short distance between the centromeres of sister chromatids. The remaining 5% of cells displaying CID stretching were positive for DSA1 and considered to be in prometaphase/metaphase (Figure 4C2). The CID stretching in these cells was not as extreme as in anaphase cells. A prometaphase/metaphase cell with little or no CID stretching between sister centromeres is shown in Figure 4C1. We observed that the distance between paired CID spots (measured in prometaphase/metaphase cells) was more than 2-fold higher in the CAP-D2 RNAi cells compared to control cells (1.625 μm versus 0.75 μm, Figure 4D). This suggests that tension applied upon bipolar attachment accentuates the defect in resolution, and therefore in anaphase, the most extreme stretching of CID stained regions was detected (Figure 4C5). These results suggest that CAP-D2, and likely the entire condensin complex, is primarily required for resolution of sister chromatids (arms and centromeres) rather than chromosome compaction in *Drosophila*.

CAP-H/Barren is unstable in cells depleted of CAP-D2

As CAP-D2 is one subunit of a complex, it is possible that interacting proteins may be affected by its depletion. For this reason, the stability and localisation of the other subunits of the complex were analysed upon depletion of CAP-D2. Immunoblotting RNAi cell extracts for CAP-H/Barren revealed that the level of this protein was decreased when CAP-D2 was depleted (Figure 5A). CAP-H/Barren may be more tightly associated with CAP-D2 compared to the SMC subunits, as suggested earlier. As no sequence similarity exists between the two proteins, the depletion by RNAi should be specifically directed against CAP-D2. In contrast, no substantial change in SMC4 and SMC2 levels was observed (Figure 5A and 6A). To examine the localization of residual CAP-H, cells were cytospun onto poly-L-lysine slides and processed for immunofluorescence. In control cells, CAP-H associated with the axial cores of sister chromatids (Figure 5B). In the CAP-D2 depleted cells, residual CAP-H protein appeared to localise diffusely in the cytoplasm with no CAP-H detected on the chromosomes (Figure 5C).

Immunolocalisation of SMC4, SMC2 and Topoisomerase II in CAP-D2 depleted cells

To examine the localisation of the SMC4 subunit after CAP-D2 RNAi, we performed double staining with CAP-D2 and SMC4 antibodies. In control cells, SMC4 was localised on mitotic chromosomes (Figure 5D). In the CAP-D2 depleted cells, SMC4 still localized to chromatin, even though chromosome morphology was abnormal (Figure 5E). Distribution was however not restricted to an axial core, presumably because of aberrant chromosome organisation. In approximately half of the abnormal cells, the SMC4 signal was more severely reduced (Figure 5E, top) than in other CAP-D2 depleted cells (Figure 5E, bottom). This may be the result of uneven RNAi efficiency across the cell population.

We also examined SMC2 level and localisation. As observed for SMC4, the level of SMC2 appeared largely unaffected when CAP-D2 was depleted (Figure 6A). Because both CAP-D2 and

SMC2 antibodies were raised in rabbits, double immunolabeling was not possible. Therefore, we double-labeled cells for SMC2 and topo II, a marker for the chromosome "scaffold". The overall level of topo II also appeared not to change (Supp Figure 2F). In control cells, both SMC2 and topo II associated with chromosomes in a striking axial pattern (Figure 6B). After CAP-D2 depletion, SMC2 localized to chromatin masses, albeit in an unrestricted localization, similar to SMC4. Variation in the level of SMC2 was also observed in these cells: cells with more reduced levels of SMC2 also had lower levels of topo II (Figure 6C, top vs bottom). Taken together, these results suggest that the axial localisation of SMC4, SMC2, and topo II correlates with proper chromosome resolution which requires CAP-D2, and by inference CAP-H/Barren (as it is also depleted).

Reciprocal dependence on stability: CAP-D2 is unstable in a *barren* mutant

Depletion of the CAP-D2 protein by dsRNAi affected the stability of the CAP-H/Barren protein. To test if reciprocal stability was true (i.e. the level of CAP-D2 protein was dependent on the presence of CAP-H/Barren), a *barren* mutant ($barr^{L305}$) was examined. $barr^{L305}$ is a null mutation which causes lethality late in embryogenesis (Bhat et al., 1996). Analysis of *barr* homozygous embryo extract (~12-13 hours old) showed that when Barren was decreased, CAP-D2 was greatly reduced as well (Figure 6D). Quantitation of protein levels by phosphorimaging revealed that Barren was reduced 8-fold compared to wild type embryos while the level of CAP-D2 was 6-fold lower. The fact that both proteins were decreased to nearly the same extent strongly suggests that the two proteins are very likely interdependent for stability. When the same membrane was reprobed for SMC2 and SMC4, it was apparent that their levels were reduced, albeit not to the same extent (Figure 6D). SMC2 was reduced 4-fold and SMC4 3.5-fold, consistent with a fraction of the two SMC proteins participating in a second complex. Quantitations were repeated twice in independent experiments. The presence and stability of Scc1/Drad21, a member of the cohesin complex (Vass et al., 2003), and α-tubulin were analyzed and found to be unaffected by mutation of CAP-H/Barren (Figure 6D).

The stability of the condensin subunits was also examined in an SMC4 mutant, *gluon*^{17C}. This is an embryonic lethal null mutation for SMC4, that removes 31 kb including the SMC4 gene (accession AJ543652). Analysis of *gluon*^{17C} homozygous embryo extract (~12-13 hours old) showed that the SMC4 protein decreased 5.9-fold relative to wild type embryos (Figure 6E). Residual protein may suggest that the maternal component is quite stable (and may also explain the SMC4 protein in *barr* extract). When the levels of other subunits was assessed, we observed that the SMC2 subunit was decreased to the same extent as SMC4 (5.6-fold), while CAP-D2 and CAP-H/Barren were reduced 4.7-fold (Figure 6E). These results revealed that in the absence of one of the condensin subunits in *Drosophila*, the abundance and stability of the rest were affected. Furthermore, the strength of the interactions between the four examined members of the condensin complex supports the notion that the non-SMC subunits, CAP-D2 and CAP-H/Barren, show tight dependencies on one another for stability both in cultured cells and in the organism.

A condensin II complex has been recently identified in vertebrate cells, consisting of SMC2 and SMC4, and three additional non-SMC subunits: CAP-D3, CAP-H2 and CAP-G2 (Ono et al., 2003). CAP-D3 and CAP-H2, but not CAP-G2, have been found by sequence analysis in *Drosophila*. To assess the role of CAP-D3 in the experiments of this study, we generated an antibody to CAP-D3 (Supp Figure 1B) and examined localization of the protein during mitosis in S2 cultured cells. Immunostaining revealed that the protein localised at the centromeres, partially overlapping with CID at prometaphase, metaphase and anaphase. However, the signal was reduced by telophase and less restricted to the centromeres (Supp Figure 3A). We attempted to deplete the protein with 2 different dsRNAs targeting different regions of the mRNA, but it remained even after 120 hrs, suggesting that CAP-D3 may be very stable. Furthermore, chromosome morphology and chromosome segregation appeared normal (data not shown). When the fractions immunoprecipitated from embryos using the CAP-D2 antibody were probed for CAP-D3, no CAP-D3 was detected (data not shown). In addition, the overall localisation of CAP-D3 was not affected in the CAP-D2 depleted cells. CAP-D3 was

present at the centromeres in the CAP-D2 depleted cells (Supp Figure 3B) and when CID was stretched, CAP-D3 was also stretched (Supp Figure 3B, top panel). These results suggest that functions of CAP-D2 and CAP-D3 are probably independent of one another. Interestingly, flies homozygous for insertion of a P-element in the third exon of the CAP-D3 gene are viable, but male sterile. This strongly suggests a meiotic role for the CAP-D3 protein, and possibly the condensin II complex in *Drosophila*.

Depletion of both CAP-D2 and topo II results in chromosome morphology no more severe than that observed in cells depleted of CAP-D2 alone

Since the resolution of sister chromatids is compromised in the CAP-D2 depleted cells and topo II is important for decatenating DNA strands, it is possible that condensin and topo II collaborate to organise mitotic chromosomes. Furthermore, the phenotype observed in this study after CAP-D2 RNAi, was similar to the phenotype obtained after topo II depletion (Chang et al., 2003). In order to determine if these proteins have similar or distinct roles in organising mitotic chromosomes, CAP-D2/topo II double RNAi was performed. Immunoblotting showed that both proteins were greatly depleted 72 hours after treatment (Figure 7A). The topo II level was not significantly affected after CAP-D2 RNAi, nor was the level of CAP-D2 affected in the topo II-depleted cells (similar to previous observations for Barren (Chang et al., 2003). We observed only a 2-fold increase in mitotic index, using P~H3 as a mitotic marker. Immunofluorescence analysis at 96 hours revealed that cells depleted of both proteins exhibited abnormal chromosome morphology and behaviour no more severe than in either of the single depletions (Figure 7C). Surprisingly, the ability of chromosomes to compact appeared as it did in either single RNAi. Chromosomes in the double RNAi failed to resolve and formed bridges during anaphase. We also noted the unusual phenotype of chromosome arm congression defects observed previously after topo II depletion (Chang et al., 2003) (Figure 7C, top row).

In order to better assess the chromosome phenotypes of the single and double depletions, metaphase chromosome spreads were performed after cells were arrested in metaphase with colchicine. dsRNA treated and control cells were cytospun onto poly-L-lysine slides and stained for CAP-D2, topo II and DNA. Control cells displayed the typical "X" shape indicative of proper sister chromatid resolution. Both CAP-D2 and topo II localised axially along the length of the chromosomes and the two proteins partially co-localised (Figure 8A1-2 and 8B, control). In both single and the double depletions, chromosome morphology was highly abnormal. The structural integrity of these chromosomes was compromised and chromatin appeared torn and stretched. No axial staining could be observed in any of the experiments (Figure 8A3-5). Individual chromosomes, while compacted, were not resolved and appeared fuzzy and diffuse (Figure 8B, RNAi panels). Since no difference in phenotype was observed at this level between the CAP-D2, topo II and CAP-D2/topo II doubly depleted cells, we believe that topo II and the condensin complex participate in the same pathway to resolve sister chromatids. We additionally noted no difference in the level of CAP-D3 in either the single depletions or CAP-D2/topo II double depletion, suggesting that this protein was not affected (Supp Figure 3C). We therefore suggest that additional, as yet unidentified, factors are required to bring about appropriate chromosome condensation during mitosis.

Discussion

In this study we have shown that CAP-D2 is part of a complex containing other condensin subunits (SMC2, SMC4, CAP-H/Barren and CAP-G) in *Drosophila*. Interestingly, the non-SMC subunits, CAP-D2 and Barren, appear to be more tightly associated with each other than they are with SMC2 and SMC4. This finding is reminiscent of our studies of the cohesin complex in *Drosophila* where we showed that Scc1/Drad21 and Scc3/SA1 appeared to have a higher affinity for one another than for SMC1 and SMC3 (Vass et al., 2003).

The subcellular localisation of CAP-D2 revealed that the protein was nuclear throughout interphase with levels increasing during S phase, and peaking in late G2/early prophase. This was intriguing as *Drosophila* SMC4 and Barren are cytoplasmic during interphase and associate with chromatin only during prophase (Steffensen et al., 2001). In human cells, the majority of CAP-D2, SMC2, and SMC4 is cytoplasmic during interphase, finally becoming nuclear during prophase, suggesting that distribution of the holocomplex may be regulated coordinately in human cells (Ball et al., 2002; Schmiesing et al., 2000). Differential localisation of condensin subunits during interphase in *Drosophila* suggests that CAP-D2 may be sequestered *away* from SMCs to regulate activity or may be utilized for a function other than that required of other condensin subunits during interphase. It has recently been shown in *Xenopus* that CAP-D2 (pEg7) along with SMC2 (XCAP-E) localise in the granular compartment of the nucleolus suggesting that these subunits may be involved in nucleolar organisation and/or ribosome biogenesis (Uzbekov et al., 2003). In *S. cerevisiae*, the CAP-D2 orthologue *Ycs4* is nuclear during interphase, implicated in suppressing inter-repeat rDNA recombination and required for silencing at the mating type loci (Bhalla et al., 2002). Thus, *Drosophila* CAP-D2 may be involved in a non-mitotic function – possibly during S phase when its level increases.

Alternatively, expression during S phase may be important to "template" the protein appropriately for a mitotic role (Loupart et al., 2000; Shelby et al., 1997). The increase of nuclear CAP-D2 during S phase could be because protein expression is up-regulated or because the protein is

preferentially imported into the nucleus. A potential nuclear bipartite targeting signal between amino acids 1347 and 1363 was identified in the *Drosophila* CAP-D2 sequence (this study). Human CAP-D2 (CNAP1) has a functional bipartite nuclear localisation signal (Ball et al., 2002). During mitosis, CAP-D2 localises to the chromatid cores and remains tightly associated with chromosomes until late telophase/cytokinesis, even as chromosomes are decondensing. In contrast, while DmSMC4 and Barren proteins are loaded onto chromosomes in early prophase, they dissociate from chromosomes late in anaphase/telophase when decondensation begins (Steffensen et al., 2001) (and this study). This distinct timing of condensin subunit dissociation is again suggestive of a role for CAP-D2 beyond that of condensin. In human cells it has been shown that the C terminal-end of CAP-D2 possesses a mitotic chromosome-targeting domain that does not require the other condensin subunits (Ball et al., 2002). Perhaps a similar regulation occurs in *Drosophila* and CAP-D2 binds to chromosomes independently of the other subunits.

We have shown that depletion of CAP-D2 by RNAi in *Drosophila* results in an abnormal mitotic phenotype. The major defect is the loss of sister chromatid (arm and centromere) resolution and the resulting failure of chromosomes to segregate normally during anaphase, a phenotype similar to that observed in *barren, DmSMC4* and *dCAP-G* mutant alleles (Bhat et al., 1996; Dej KJ, 2004; Steffensen et al., 2001) and DmSMC4 RNAi (Coelho et al., 2003). Chromosome compaction still occurs, as in chicken cultured cells (Hudson et al., 2003), consistent with the existence of additional factors essential for this process. Although loss of Barren in *Drosophila* does not affect cell cycle progression (Bhat et al., 1996), loss of SMC4 causes a metaphase delay in embryos (Steffensen et al., 2001) and even more pronounced prometaphase delay (data not shown). Similarly, loss of dCAP-G causes a prometaphase delay in embryos (Dej KJ, 2004). Depletion of CAP-D2 in S2 cells results in a prometaphase delay, though cells do eventually undergo aberrant anaphase and cytokinesis. The delay is possibly a consequence of kinetochore checkpoint activation, since chromosomes exhibit elevated levels of BubR1 at centromeres persisting into anaphase and cytokinesis (data not shown). This may,

in turn, be a result of altered centromere resolution manifest as stretched centromeres in anaphase. Similar results have been observed after DmSMC4 RNAi where kinetochores associated with spindle microtubules were stretched polewards, sometimes well beyond the chromatin mass (Coelho et al., 2003).

In *C. elegans*, the condensin complex is required for the restricted orientation of centromeres towards spindle poles (Hagstrom et al., 2002), while in an *S. cerevisiae* BRN1 mutant, centromere function is defective and centromeres do not segregate normally (Ouspenski et al., 2000). Recently it has been shown that depletion of condensin I or condensin II in vertebrate cells results in structural distortions of the centromere/kinetochore region which affects the opposing orientation of sister kinetochores and interaction with the mitotic spindle (Ono et al., 2004). Taken together, these results suggest that the condensin complex may have a role in centromere organization and ensuing kinetochore-spindle interactions, which could impact the localization of chromosome passenger proteins. Indeed, we noted a temporal disruption of INCENP localisation following CAP-D2 depletion (date not shwon). We observed similar defects in INCENP localization when the DRad21 cohesin subunit was depleted (Vass et al., 2003). These results argue that proper chromosome organisation is necessary for the correct temporal localisation of at least one chromosome passenger protein.

Behaviour of different condensin subunits varies following depletion of CAP-D2. Barren is unstable when CAP-D2 is depleted and any residual protein is cytoplasmic. Barren localisation was also shown to be dependent on SMC4 (Coelho et al., 2003). In a *Barren* mutant, CAP-D2 was unstable, corroborating the interdependence of the two proteins on one another for stability. On the other hand, levels of SMC2 and SMC4 were not greatly affected by CAP-D2 depletion and the two proteins still localised to chromatin, albeit in a non-axial fashion. This is likely a reflection of compromised structural integrity of mitotic chromosomes as observed in chicken DT40 cells depleted of SMC2 (Hudson et al., 2003). In *S. cerevisiae* and *S. pombe,* the condensin SMCs bind chromatin only in the presence of non-SMC subunits (Freeman et al., 2000; Lavoie et al., 2002). One intriguing

question is whether the SMCs remaining on chromosomes are in any way functional? Should a condensin II complex exist in *Drosophila*, then the chromosomal SMCs remaining after CAP-D2 depletion may be members of this complex. Consistent with this, we observed that SMC2 and SMC4 are similarly reduced in a *Barren* mutant (but not as severely as Barren and CAP-D2). We were unable to deplete the CAP-D3 subunit of the *Drosophila* condensin II complex by RNAi in S2 cells (perhaps due to long half-life), but mutation by P-element insertion in the CAP-D3 gene caused male sterility (data not shown). It remains to be determined what precise role a putative condensin complex II has in meiosis in *Drosophila*.

In this study, we also performed the first disruption in *Drosophila* of two components known to be involved in mitotic chromosome dynamics: condensin and topo II. When a double depletion of CAP-D2/topo II was performed, abnormal chromosome appearance and behaviour similar to that observed in the single topo II and CAP-D2 RNAi was observed. Chromosomes were fuzzy and not resolved, and formed chromosome bridges during anaphase and cytokinesis. Surprisingly, the double depletion phenotype was no more severe than in either of the single depletions. This result suggests not only that topo II and the condensin complex participate in the same pathway required to organise mitotic chromosomes into well-defined structures, but also that factors other than these proteins still remain to be identified for their essential roles in chromosome condensation. These may include proteins involved in DNA replication (Dej KJ, 2004; Loupart et al., 2000) or diverse factors such as kinases (Yu et al., 2004) and proteases (McHugh et al., 2004), demonstrating that much remains to be learnt about the full requirements for chromosome condensation.

Acknowledgements

We would like to thank Hugo Bellen (Barren), Bill Earnshaw (INCENP), Gary Karpen (cid), Neil Osheroff (topoisomerase II), Jordan Raff (Cyclin B), and Claudio Sunkel (BubR1) for generous gifts of antibodies. We are grateful to Mar Carmena and Chih-Jui Chang for collaborating in the CAP-D2/topo II double RNAi. Ellada Savvidou has been supported by a PhD studentship from the Darwin Trust. Margarete Heck and the research in her laboratory is funded by a Wellcome Trust Senior Research Fellowship in the Biomedical Sciences.

References

Adams, R. R., Carmena, M. and Earnshaw, W. C. (2001a). Chromosomal passengers and the (aurora) ABCs of mitosis. *Trends Cell Biol* **11**, 49-54.

Adams, R. R., Maiato, H., Earnshaw, W. C. and Carmena, M. (2001b). Essential roles of Drosophila inner centromere protein (INCENP) and aurora B in histone H3 phosphorylation, metaphase chromosome alignment, kinetochore disjunction, and chromosome segregation. *J Cell Biol* **153**, 865-880.

Ball, A. R., Jr., Schmiesing, J. A., Zhou, C., Gregson, H. C., Okada, Y., Doi, T. and Yokomori, K. (2002). Identification of a chromosome-targeting domain in the human condensin subunit CNAP1/hCAP-D2/Eg7. *Mol Cell Biol* **22**, 5769-81.

Bhalla, N., Biggins, S. and Murray, A. W. (2002). Mutation of YCS4, a budding yeast condensin subunit, affects mitotic and nonmitotic chromosome behavior. *Mol Biol Cell* **13**, 632-45.

Bhat, M. A., Philp, A. V., Glover, D. M. and Bellen, H. J. (1996). Chromatid segregation at anaphase requires the *barren* product, a novel chromosome-associated protein that interacts with topoisomerase II. *Cell* **87**, 1103-1114.

Blower, M. D. and Karpen, G. H. (2001). The role of Drosophila CID in kinetochore formation, cell-cycle progression and heterochromatin interactions. *Nat. Cell Biol.* **3**, 730-739.

Casso, D., Ramirez-Weber, F. and Kornberg, T. B. (2000). GFP-tagged balancer chromosomes for *Drosophila melanogaster*. *Mech. Dev.* **88**, 229-232.

Chang, C. J., Goulding, S., Earnshaw, W. C. and Carmena, M. (2003). RNAi analysis reveals an unexpected role for topoisomerase II in chromosome arm congression to a metaphase plate. *J. Cell Sci.* **116**, 4715-4726.

Clemens, J. C., Worby, C. A., Simonson-Leff, N., Muda, M., Maehama, T., Hemmings, B. A. and Dixon, J. E. (2000). Use of double-stranded RNA interference in *Drosophila* cell lines to dissect signal transduction pathways. *Proc. Nat. Acad. Sci. U.S.A* . **97**, 6499-6503.

Cobbe, N. and Heck, M. M. S. (2000). SMCs in the world of chromosome biology: from prokaryotes to eukaryotes. *J. Struct. Biol.* **129**, 123-143.

Cobbe, N. and Heck, M. M. S. (2004). The Evolution of SMC proteins: Phylogenetic Analysis and Structural Implications (Epub 2003 Dec 05). *Mol Biol Evol* **21**, 332-47.

Coelho, P. A., Queiroz-Machado, J. and Sunkel, C. E. (2003). Condensin-dependent localisation of topoisomerase II to an axial chromosomal structure is required for sister chromatid resolution during mitosis. *J Cell Sci* **116**, 4763-76.

Cuvier, O. and Hirano, T. (2003). A role of topoisomerase II in linking DNA replication to chromosome condensation. *J. Cell Biol.* **160**, 645-55.

Dej KJ, A. C., Orr-Weaver TL. (2004). Mutations in the Drosophila Condensin Subunit dCAP-G: Defining the Role of Condensin for Chromosome Condensation in Mitosis and Gene Expression in Interphase. *Genetics.* **168(2)**, 895-906.

Earnshaw, W. C., Halligan, B., Cooke, C. A., Heck, M. M. S. and Liu, L. F. (1985). Topoisomerase II is a structural component of mitotic chromosome scaffolds. *J. Cell Biol.* **100**, 1706-1715.

Earnshaw, W. C. and Heck, M. M. S. (1985). Localization of topoisomerase II in mitotic chromosomes. *J. Cell Biol.* **100**, 1716-1725.

Freeman, L., Aragon-Alcaide, L. and Strunnikov, A. (2000). The condensin complex governs chromosome condensation and mitotic transmission of rDNA. *J. Cell Biol.* **149**, 811-824.

Gasser, S. M., Laroche, T., Falquet, J., Boy de la Tour, E. and Laemmli, U. K. (1986). Metaphase chromosome structure. Involvement of topoisomerase II. *J. Mol. Biol.* **188**, 613-629.

Gassmann, R., Carvalho, A., Henzing, A. J., Ruchaud, S., Hudson, D. F., Honda, R., E.A., N., Gerloff, D. L. and Earnshaw, W. C. (2004). Borealin: A novel chromosomal passenger required for stability of the bipolar mitotic spindle. *J Cell Biol.*

Hagstrom, K. A., Holmes, V. F., Cozzarelli, N. R. and Meyer, B. J. (2002). *C. elegans*

condensin promotes mitotic chromosome architecture, centromere organization, and sister chromatid segregation during mitosis and meiosis. *Genes Dev* **16**, 729-42.

Hagstrom, K. A. and Meyer, B. J. (2003). Condensin and cohesin: more than chromosome compactor and glue. *Nat. Rev. Genet.* **4**, 520-534.

Harlow, E. and Lane, D. (1999). Using antibodies, a laboratory manual. Cold Spring Harbor: Cold Spring Harbor Laboratory.

Heck, M. M. S. (1997). Condensins, Cohesins, and Chromosome Architecture: How to Make and Break a Mitotic Chromosome. *Cell* **91**, 5-8.

Henikoff, S., Ahmad, K., Platero, J.S., van Steensel, B. (2000). Heterochromatic deposition of centromeric histone H3-like proteins. *Proc Natl Acad Sci U S A.* **97(2)**, 716-21.

Hirano, T., Kobayashi, R. and Hirano, M. (1997). Condensins, chromosome condensation protein complexes containing XCAP-C, XCAP-E and a *Xenopus* homolog of the *Drosophila* barren protein. *Cell* **89**, 511-521.

Hirano, T. and Mitchison, T. J. (1994). A heterodimeric coiled-coil protein required for mitotic chromosome condensation in vitro. *Cell* **79**, 449-458.

Holm, C., Goto, T., Wang, J. C. and Botstein, D. (1985). DNA topoisomerase II is required at the time of mitosis in yeast. *Cell* **41**, 553-563.

Huang, J., Raff, J.W. (1999). The disappearance of cyclin B at the end of mitosis is regulated spatially in Drosophila cells. *EMBO J.* **18(8)**, 2184-95.

Hudson, D. F., Vagnarelli, P., Gassmann, R. and Earnshaw, W. C. (2003). Condensin is required for nonhistone protein assembly and structural integrity of vertebrate mitotic chromosomes. *Dev Cell* **5**, 323-36.

Kimura, K. and Hirano, T. (2000). Dual roles of the 11S regulatory subcomplex in condensin functions. *Proc Natl Acad Sci U S A* **97**, 11972-7.

Lavoie, B. D., Hogan, E. and Koshland, D. (2002). In vivo dissection of the chromosome

condensation machinery: reversibility of condensation distinguishes contributions of condensin and cohesin. *J Cell Biol* **156**, 805-15.

Lavoie, B. D., Tuffo, K. M., Oh, S., Koshland, D. and Holm, C. (2000). Mitotic chromosome condensation requires Brn1p, the yeast homologue of Barren. *Mol. Biol. Cell* **11**, 1293-1304.

Loupart, M.-L., Krause, S. A. and Heck, M. M. S. (2000). Aberrant replication timing induces defective chromosome condensation in *Drosophila* ORC2 mutants. *Curr. Biol.* **10**, 1547-1556.

Maeshima, K. and Laemmli, U. K. (2003). A two-step scaffolding model for mitotic chromosome assembly. *Dev. Cell* **4**, 467-480.

Manders, E. M., Stap, J., Brakenhoff, G. J., van Driel, R. and Aten, J. A. (1992). Dynamics of three-dimensional replication patterns during the S-phase, analysed by double labelling of DNA and confocal microscopy. *J. Cell Sci.* **103**, 857-862.

McHugh, B., Heck, M.M. (2003). Regulation of chromosome condensation and segregation. *Curr Opin Genet Dev.* **13(2)**, 185-90. Review.

McHugh, B., Krause, S. A., Yu, B., Deans, A. M., Heasman, S., McLaughlin, P. and Heck, M. M. (2004). Invadolysin: a novel, conserved metalloprotease links mitotic structural rearrangements with cell migration. *J. Cell Biol.* **67(4):**, 673-686.

Ono, T., Fang, Y., Spector, D. L. and Hirano, T. (2004). Spatial and Temporal Regulation of Condensins I and II in Mitotic Chromosome Assembly in Human Cells. *Mol Biol Cell* **15**, 3296-3308.

Ono, T., Losada, A., Hirano, M., Myers, M. P., Neuwald, A. F. and Hirano, T. (2003). Differential contributions of condensin I and condensin II to mitotic chromosome architecture in vertebrate cells. *Cell* **115**, 109-121.

Ouspenski, I. I., Cabello, O. A. and Brinkley, B. R. (2000). Chromosome condensation factor Brn1p is required for chromatid separation in mitosis. *Mol. Biol. Cell* **11**, 1305-1313.

Rogers, S. L., Rogers, G.C., Sharp, D.J., Vale, R.D. (2002). Drosophila EB1 is important for proper assembly, dynamics, and positioning of the mitotic spindle. *J Cell Biol.* **158(5)**, 873-84.

Saitoh, N., Goldberg, I. G., Wood, E. R. and Earnshaw, W. C. (1994). ScII: an abundant chromosome scaffold protein is a member of a family of putative ATPases with an unusual predicted tertiary structure. *J. Cell Biol.* **127**, 303-318.

Saka, Y., Sutani, T., Yamashita, Y., Saithoh, S., Takeuchi, M., Nakaseko, Y. and Yanagida, M. (1994). Fission yeast cut3 and cut14, members of a ubiquitous protein family, are required for chromosome condensation and segregation in mitosis. *EMBO J.* **13**, 4938-4952.

Sampath, S. C., Ohi, R., Leismann, O., Salic, A., Pozniakovski, A. and Funabiki, H. (2004). The chromosomal passenger complex is required for chromatin-induced microtubule stabilization and spindle assembly. *Cell* **118**, 187-202.

Schmiesing, J. A., Gregson, H. C., Zhou, S. and Yokomori, K. (2000). A human condensin complex containing hCAP-C-hCAP-E and CNAP1, a homolog of Xenopus XCAP-D2, colocalizes with phosphorylated histone H3 during the early stage of mitotic chromosome condensation. *Mol Cell Biol* **20**, 6996-7006.

Shelby, R. D., Vafa, O. and Sullivan, K. F. (1997). Assembly of CENP-A into Centromeric Chromatin Requires a Cooperative Array of Nucleosomal DNA Contact Sites. *J. Cell Biol.* **136**, 501-513.

Steffensen, S., Coelho, P. A., Cobbe, N., Vass, S., Costa, M., Hassan, B., Prokopenko, S. N., Bellen, H., Heck, M. M. S. and Sunkel, C. E. (2001). A role for *Drosophila* SMC4 in the resolution of sister chromatids in mitosis. *Curr. Biol.* **11**, 295-307.

Strunnikov, A. V., Hogan, E. and Koshland, D. (1995). SMC2, a *Saccharomyces cerevisiae* gene essential for chromosome segregation and condensation, defines a subgroup within the SMC family. *Genes Dev.* **9**, 587-599.

Sutani, T., Yuasa, T., Tomonaga, T., Dohmae, N., Takio, K. and Yanagida, M. (1999). Fission yeast condensin complex: essential roles of non-SMC subunits for condensation and Cdc2 phosphorylation of Cut3/SMC4. *Genes Dev* **13**, 2271-83.

Swedlow, J. R. and Hirano, T. (2003). The making of the mitotic chromosome: modern insights into classical questions. *Mol. Cell* **11**, 557-569.

Uzbekov, R., Timirbulatova, E., Watrin, E., Cubizolles, F., Ogereau, D., Gulak, P., Legagneux, V., Polyakov, V. J., Le Guellec, K. and Kireev, I. (2003). Nucleolar association of pEg7 and XCAP-E, two members of *Xenopus laevis* condensin complex in interphase cells. *J. Cell Sci.* **116**, 1667-1678.

Valdeolmillos, A., Rufas, J.S., Suja, J.A., Vass, S., Heck, M.M., Martinez-A, C., Barbero, J.L.. (2004). Drosophila cohesins DSA1 and Drad21 persist and colocalize along the centromeric heterochromatin during mitosis. *Biol Cell.* **96(6)**, 457-62.

Vass, S., Cotterill, S., Valdeolmillos, A. M., Barbero, J. L., E., L., Warren, W. and Heck, M. M. S. (2003). Depletion of rad21/Scc1 in *Drosophila* cells leads to instability of the cohesin complex and disruption of mitotic progression. *Curr. Biol.* **3**, 208-218.

Warburton, P. E. and Earnshaw, W. C. (1997). Untangling the role of DNA topoisomerase II in mitotic chromosome structure and function. *Bioessays* **19**, 97-99.

Warren, W. D., Steffensen, S., Lin, E., Coelho, P., Loupart, M.-L., Cobbe, N., Lee, J., McKay, M. J., Orr-Weaver, T., Heck, M. M. S. et al. (2000). The *Drosophila* RAD21 cohesin persists at the centromere region in mitosis. *Curr. Biol.* **10**, 1463-1466.

Yu, J., Fleming, S. L., Williams, B., Williams, E. V., Li, Z., Somma, P., Rieder, C. L. and Goldberg, M. L. (2004). Greatwall kinase: a nuclear protein required for proper chromosome condensation and mitotic progression in Drosophila. *J. Cell Biol.* **164**, 487-492.

Figure Legends

Figure 1. Identification of a condensin complex in *Drosophila* and characterisation of CAP-D2 during interphase.

A. Identification of a condensin complex in 0-5 hr embryo extracts following immunoprecipitation with an antibody recognizing *Drosophila* CAP-D2. Three 0.5M NaCl washes and three 2% SDS elutions are shown for preimmune and immune precipitations. The samples were analysed by immunoblotting with SMC2, SMC4, CAP-D2 and CAP-H/Barren antibodies. A fraction of SMC2 and SMC4 eluted in the washes, but more so with the elutions, while CAP-D2 and CAP-H/Barren only eluted with 2% SDS. B-D. S2 cultured cells were cytospun onto poly-L-lysine slides, then fixed and stained with various antibodies as described. B. CAP-D2 localises in the nucleus during interphase. G1 cells (using γ-tubulin as a marker) show nuclear staining for CAP-D2 with a diffuse cytoplasmic staining. Cells in G1 phase (single centrosome, arrow in upper panel) have less nuclear CAP-D2 than cells with two centrosomes (cells in S or G2 phase, arrow in lower panel). γ-tubulin (red), CAP-D2 (green), and DNA (blue). C. S phase cells (detected after BrdU incorporation) show strong nuclear staining for CAP-D2, but at differing levels. BrdU (green), CAP-D2 (red), and DNA (blue). D. Cells in late G2/early prophase (arrow) show an intense staining for CAP-D2. Cyclin B (nuclear during late G2/early prophase) was used as a marker for this stage. Cyclin B (green), CAP-D2 (red), and DNA (blue).

Figure 2. Characterisation of CAP-D2 during mitosis.

A. CAP-D2 localises to a central axis in chromatids and shows accumulation at the centromeres from prometaphase until telophase. P~H3 was used as a mitotic marker. During late anaphase and telophase, where chromosomes begin to decondense, CAP-D2 still associates with chromosomes. CAP-D2 (red), P~H3 (green), and DNA (blue). B. CAP-D2 accumulates at centromeres during

metaphase. CID was used as a centromere marker. CAP-D2 (red), CID (green), and DNA (blue). C. CAP-D2 is still strong in the daughter nuclei of a cell undergoing cytokinesis (arrow). CAP-D2 (red), α-tubulin (green), and DNA (blue).

Figure 3. CAP-D2 dsRNA-mediated interference in *Drosophila* S2 cells results in abnormal chromosome morphology and segregation.

A. Immunoblot showing the depletion of CAP-D2 after treatment with dsRNA. $5x10^5$ cells were loaded per lane. CAP-D2 levels start to decrease as early as 48 hours and the protein is undetectable at 96 and 120 hours. α-tubulin was used as a loading control. C (control dsRNA), – (no dsRNA), D (CAP-D2 dsRNA). B and C. Immunofluorescence analysis of control and CAP-D2 RNAi cells. Cells were cytospun onto poly-L-lysine slides 65 hours after treatment and stained for CAP-D2 (green), CID (red), and DNA (blue). C. CAP-D2 depleted cells have no CAP-D2 on condensed chromosomes and exhibit abnormal chromosome morphology. Sister chromatids failed to resolve and segregate properly, and chromosomes were not properly aligned on the metaphase plate. Centromeres appeared stretched. D and E. Hypotonic treatment of control (D) and CAP-D2 depleted (E) cells 65 hours after dsRNA treatment shows that chromatid resolution is defective in the CAP-D2 depleted cells. Cells were hypotonically treated, centrifuged onto poly-L-lysine slides, fixed and stained for CAP-D2 (red), P~H3 (green) and DNA (blue). Note that individual chromatids are not readily apparent after depletion of CAP-D2. The scale bar represents 10μm.

Figure 4. Chromosome arm and centromere resolution are compromised after CAP-D2 depletion.

A. Immunoblotting showing that the levels of DSA1 were not affected 72 hours after CAP-D2 RNAi treatment. C (control dsRNA), – (no dsRNA), D (CAP-D2 dsRNA). α-tubulin was used as a loading control. B and C. Centromere resolution is disrupted in the CAP-D2 depleted cells. Control (B) and

CAP-D2 depleted (C) cells were cytospun onto poly-L-lysine slides 72 hours after dsRNAi treatment, fixed and stained for DSA1 (green), CID (red) and DNA (blue). The majority of prometaphase/metaphase cells had normal CID staining between sister chromatids (C1 and higher magnification), while a small percentage showed a slightly stretching for CID (C2 and higher magnification). Cells in anaphase showed severe centromere stretching on chromosomes (C3-5 and higher magnification). The white boxes indicate the region from where the higher magnifications were taken. The scale bar represents 10μm. D. Graph showing the distance (in μm) between paired CID spots of cells in prometaphase/metaphase after staining for DSA1/CID/DAPI. The distance in CAP-D2 depleted cells is more than 2-fold higher compared to control cells.

Figure 5. Effect on Barren and SMC4 after CAP-D2 depletion.

A. Immunoblotting of control and CAP-D2 depleted extracts with Barren and SMC4 antibodies demonstrates that Barren levels are reduced while SMC4 levels appear largely unaffected after loss of CAP-D2. α-tubulin was used as a loading control. C (control dsRNA), – (no RNA), D (CAP-D2 dsRNA). B and C. Cells from both control (B) and CAP-D2 RNAi (C) experiments were cytospun onto poly-L-lysine slides 72 hours after treatment and stained for Barren (red), Cyclin B (green) and DNA (blue). Barren is absent from mitotic chromosomes and localised diffusely in the cytoplasm after CAP-D2 RNAi. D and E. Control (D) and CAP-D2 RNAi (E) cells were cytospun onto poly-L-lysine slides 65 hours after treatment, extracted during fixation, and stained for SMC4 (red), CAP-D2 (green) and DNA (blue). While cells have varying levels of SMC4 on chromatin, any axial localisation of SMC4 is lost in the CAP-D2 depleted cells. The scale bar is 10 μm.

Figure 6. Effect on SMC2 and DNA topoisomerase II in CAP-D2 depleted cells.

A. Immunoblotting of control and CAP-D2 depleted extracts with an antibody to SMC2 shows that the protein level is largely unaffected by the CAP-D2 depletion. α-tubulin was used as a loading control.

C (control dsRNA), – (no RNA), D (CAP-D2 dsRNA). B and C. Immunolocalisation of SMC2 and topo II in control (B) and CAP-D2 depleted (C) cells after 65 hours of dsRNA treatment. Cells were cytospun onto poly-L-lysine slides, extracted during fixation and stained for SMC2 (green), topo II (red), and DNA (blue). Despite the fact that SMC2 and topo II still localise to chromatin, albeit at varying levels, any axial definition is lost. The scale bar is 10 μm. D and E. Instability of condensin subunits after mutation of CAP-H and SMC4 in *Drosophila*. D. CAP-D2 is unstable when Barren is absent in a $barr^{L305}$ mutant. Immunoblot of 12-13 hour wild type (Canton S) and $barr^{L305}$ homozygous embryo extracts shows that Barren is almost undetectable in mutant embryos. The remaining protein likely represents maternal contribution to the embryos. The membrane was probed for Barren, CAP-D2, SMC2, SMC4 and Scc1. The decrease in protein level was determined using phosphorimaging (5 embryos were loaded per lane). Barren levels decreased 8-fold, CAP-D2 levels decreased 6-fold and SMC2 and SMC4 levels decreased 4-fold and 3.5-fold respectively. α-tubulin was used as a loading control. E. Stability of condensin subunits in an SMC4 ($gluon^{17C}$) mutant. Immunoblot of 12-13 hour wild type (Canton S) and $gluon^{17C}$ homozygous embryo extract with the SMC4, SMC2, CAP-D2 and Barren antibodies. The levels of the four proteins were calculated using phosphorimaging (5 embryos were loaded per lane). SMC4 shows a 5.9-fold decrease in protein levels, SMC2 shows a 5.6-fold decrease, while Barren and CAP-D2 show a 4.7-fold decrease. α-tubulin was used as a loading control.

Figure 7. Depletion of CAP-D2 and DNA topoisomerase II by double RNAi in S2 cells.

A. The depletion of CAP-D2 and topo II after treatment with two dsRNAs was assessed at 72 and 96 hours by immunoblot analysis. Both proteins were similarly depleted and almost undetectable by 96 hrs. α-tubulin was used as a loading control. – (no dsRNA), C (control dsRNA), D (CAP-D2 dsRNA), T (topoII dsRNA), $^{D}/_{T}$ (CAP-D2/topo II dsRNA). B and C. Analysis of chromosome morphology in control (B) and CAP-D2/Topo II doubly-depleted (C) cells. Cells were cytospun onto poly-L-lysine

slides, extracted during fixation and stained for topo II (red), CAP-D2 (green), CID (white) and DNA (blue), 96 hours after dsRNA treatment. Chromosome morphology was abnormal and remarkably similar to that observed after single CAP-D2 RNAi. Centromeres were stretched along the chromatin in anaphase as observed after CAP-D2 depletion alone. The scale bar is 10 μm.

Figure 8. Examination of CAP-D2 and DNA topoisomerase II in metaphase chromosomes after dsRNA treatment.

A and B. Metaphase chromosome spreads of control (1-2), topo II depleted (3), CAP-D2 depleted (4) and CAP-D2/Topo II doubly-depleted (5) cells, after cells were arrested with colchicine. Cells were cytospun onto poly-L-lysine slides, extracted during fixation and stained for topo II (red), CAP-D2 (green) and DNA (blue), 74 hours after dsRNA treatment. A. Control cells displayed the typical X-shape and sister chromatids could be easily distinguished. Both CAP-D2 and topo II localised axially along the length of the chromosomes with partial colocalisation (A1-2 and B, Control). In topo II, CAP-D2 single depletions, and in the CAP-D2/Topo II double depletion, no sister chromatid resolution could be observed and chromosomes appeared fuzzy. The scale bar is 10 μm. B. Individual chromosomes observed in chromosome spreads. The chromosome phenotype was similar between the two single and the double RNAi experiments.

Supplemental Figure 1. Co-immunolocalisation of SMC4 and CAP-D2.

A. Schematic representation of the protein region used to generate the CAP-D2 antibody (amino acids 951 to 1162 amino acid residues). Immunoblot analysis against cell extract with the CAP-D2 antibody revealed that the antibody recognises a band of the expected size (~148 kDa, asterisk) using three different bleeds (1,2 and 3) in a dilution of 1:10,000. The band was absent from the pre-immune lane (1=1:1000, 2=1:5000, and 3=1:10,000 dilutions). B. Schematic representation of the protein region used to generate the CAP-D3 peptide antibody (15 terminal amino acid residues were used).

Immunoblot analysis against cell extract with the CAP-D3 antibody revealed that the antibody recognises a prominent band of about 80 kDa (asterisk). The band was absent from the pre-immune lane. C. Co-immunolocalisation of CAP-D2 and SMC4. Cells were cytospun onto poly-L-lysine slides, extracted during fixation and stained for SMC4 (red), CAP-D2 (green), and DNA (blue). The two proteins co-localise during prometaphase. SMC4 dissociates from chromosomes as they decondense during anaphase, while CAP-D2 persists throughout the chromosomes. In telophase SMC4 is diffuse in the cytoplasm and the nucleus, while CAP-D2 is still tightly associated with chromosomes. The scale bar is 10 μm.

Supplemental Figure 2. Quantitation of effects on cells after CAP-D2 RNAi.

A. Growth curve showing the number of cells at different time points after CAP-D2 dsRNA treatment. Cells grew more slowly, plateaued at 72 hrs, and did not change significantly after that time. B. Histogram showing the percentage of mitotic cells in control and CAP-D2 RNAi cells. The percentage of mitotic cells increased 2-3 fold in the CAP-D2 RNAi between 36 and 72 hours (6.7% versus 2.2% at 48 hrs). C. Histogram showing the percentage of abnormal mitotic cells in control and CAP-D2 RNAi cells. The majority of mitotic cells are abnormal 36 hrs and later after dsRNAi treatment. D. Histogram showing the percentage of cells in prometaphase after staining for Cyclin B/P~H3/α-tubulin in control and CAP-D2 RNAi cells. Cells delay in prometaphase in the CAP-D2 depleted cells. E. Histogram showing the percentage of cells in anaphase after staining for Cyclin B/P~H3/α-tubulin, in control and CAP-D2 RNAi cells. The anaphase index in CAP-D2 RNAi cells is lower than in control cells. F. Immunoblotting of control and CAP-D2 depleted extracts for topo II shows that depletion of CAP-D2 does not affect the level of topo II. α-tubulin was used as a loading control. C (control dsRNA), – (no RNA), D (CAP-D2 dsRNA).

Supplemental Figure 3. CAP-D3 localisation in mitotic control and CAP-D2 depleted cells.

A. Immunolocalisation of CAP-D3 in S2 cells. Cells were cytospun onto poly-L-lysine slides, extracted during fixation and stained for CAP-D3 (green), CID (red), and DNA (blue). In control cells, CAP-D3 localises at the centromeres and partially overlaps with CID at prometaphase, metaphase and anaphase. The antibody gives a non-specific centrosomal staining as well. B. CAP-D2 RNAi cells 72 hours after treatment. Cells were cytospun onto poly-L-lysine slides, extracted during fixation and stained for CAP-D3 (green), CID (red), and DNA (blue). CAP-D3 protein still localises to CID-positive regions in the CAP-D2 depleted cells. The scale bar is 10 μm. C. Immunoblotting of control, CAP-D2 depleted, topo II depleted and CAP-D2/topo II doubly depleted cell extracts with the CAP-D3 antibody. CAP-D3 levels are unaffected in either the single or the double depletions. α-tubulin was used as a loading control. C (control dsRNA), – (no RNA), D (CAP-D2 dsRNA), T (topo II dsRNA) and $^{D}/_{T}$ (CAP-D2/topo II double dsRNA).

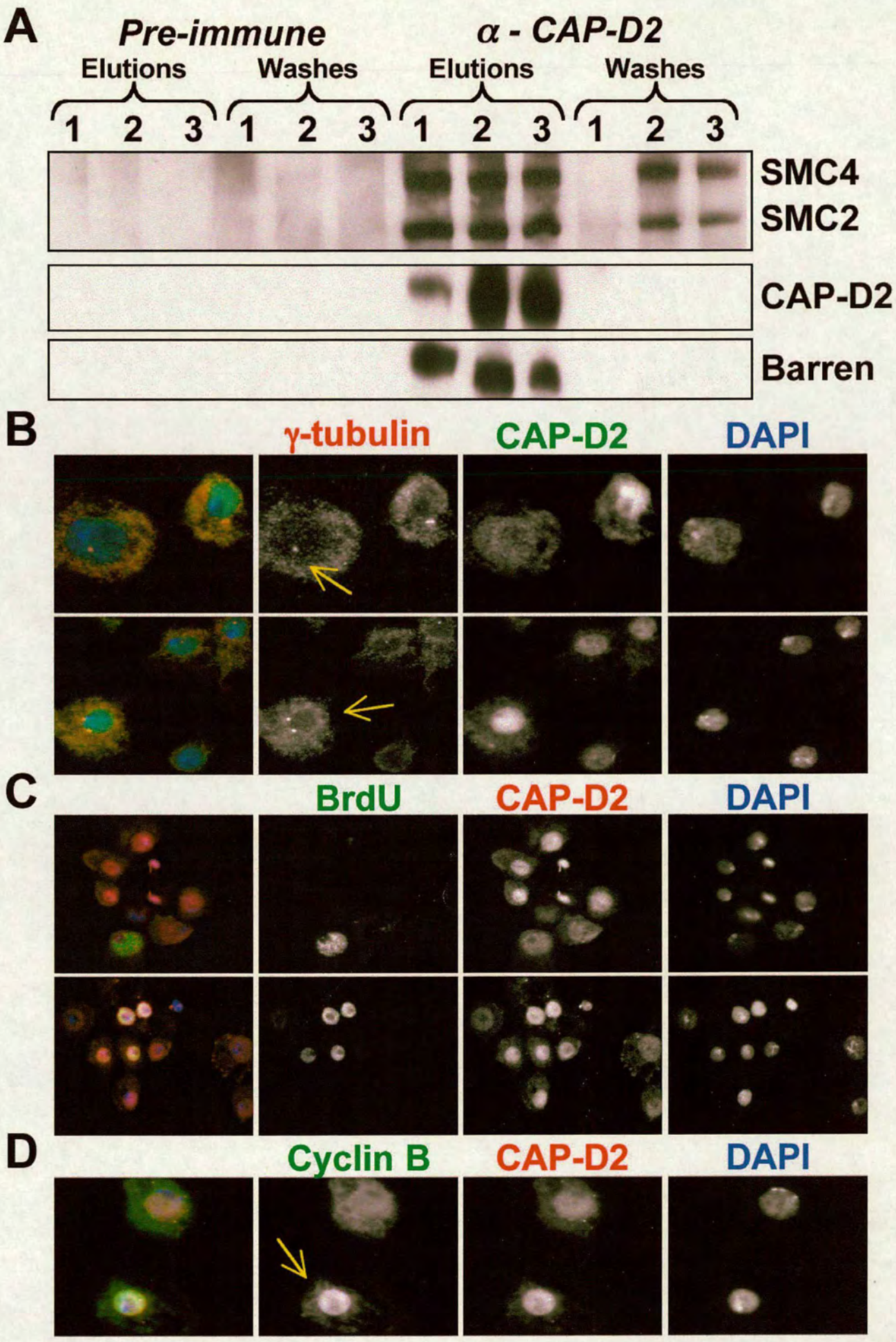

Figure 1.
Savvidou, *et al.*

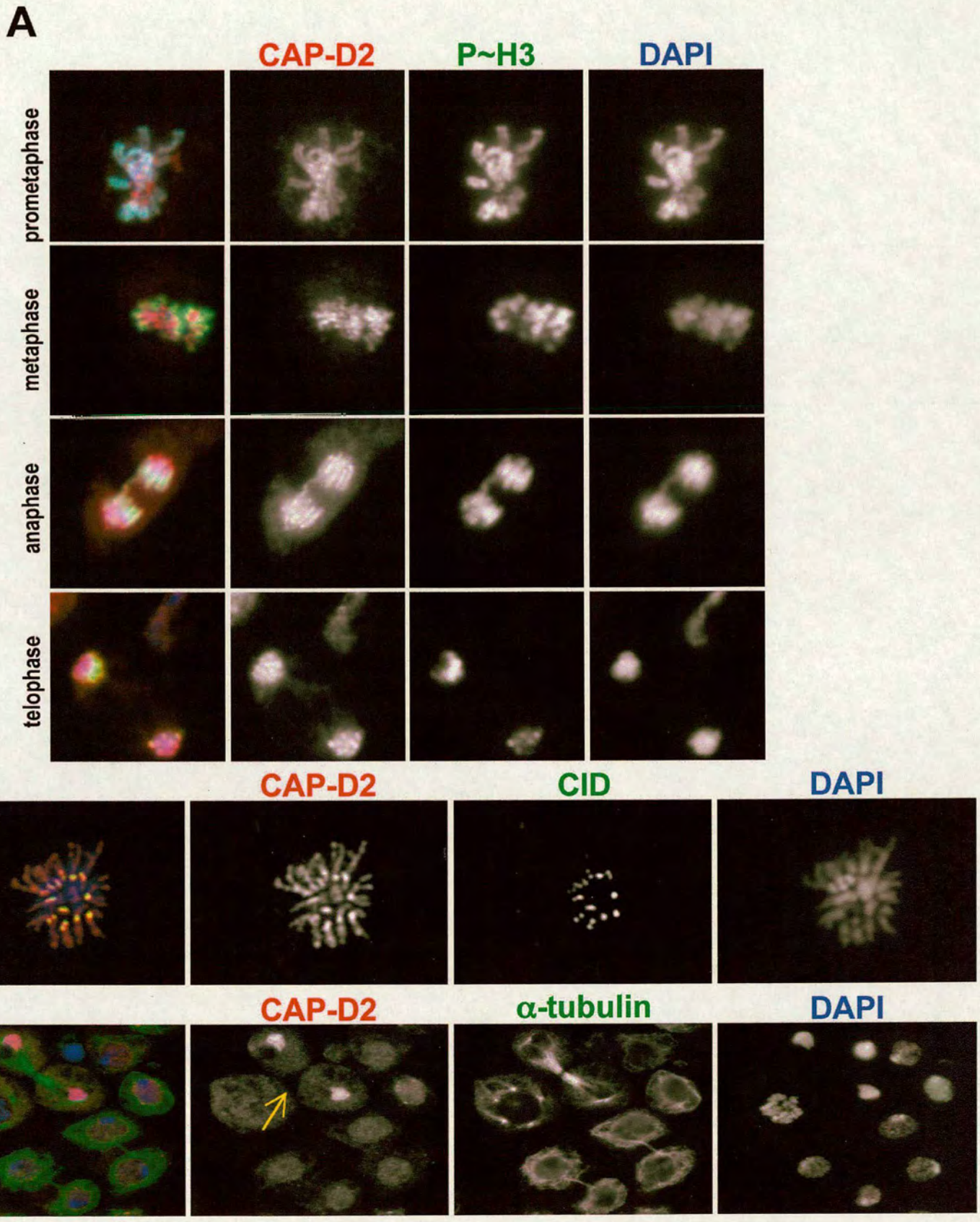

Figure 2.
Savvidou, *et al.*

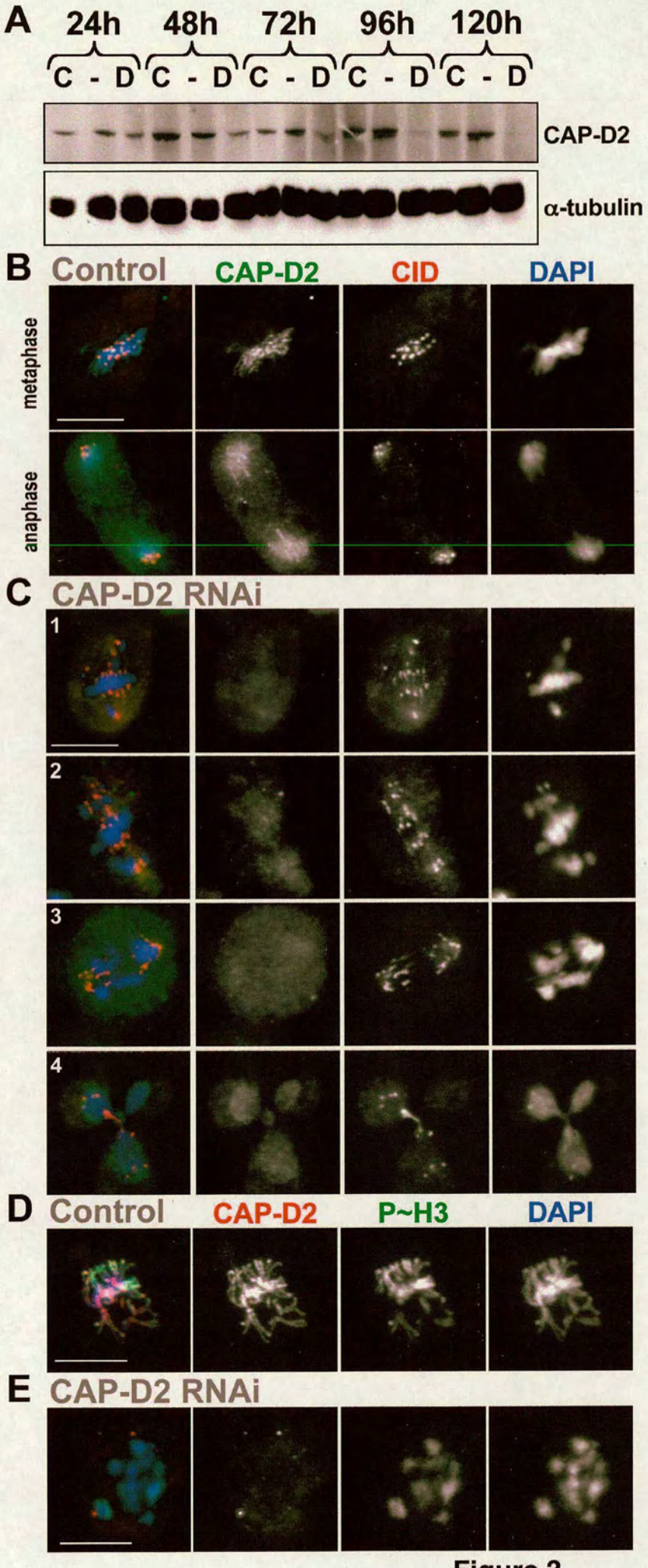

Figure 3.
Savvidou, *et al.*

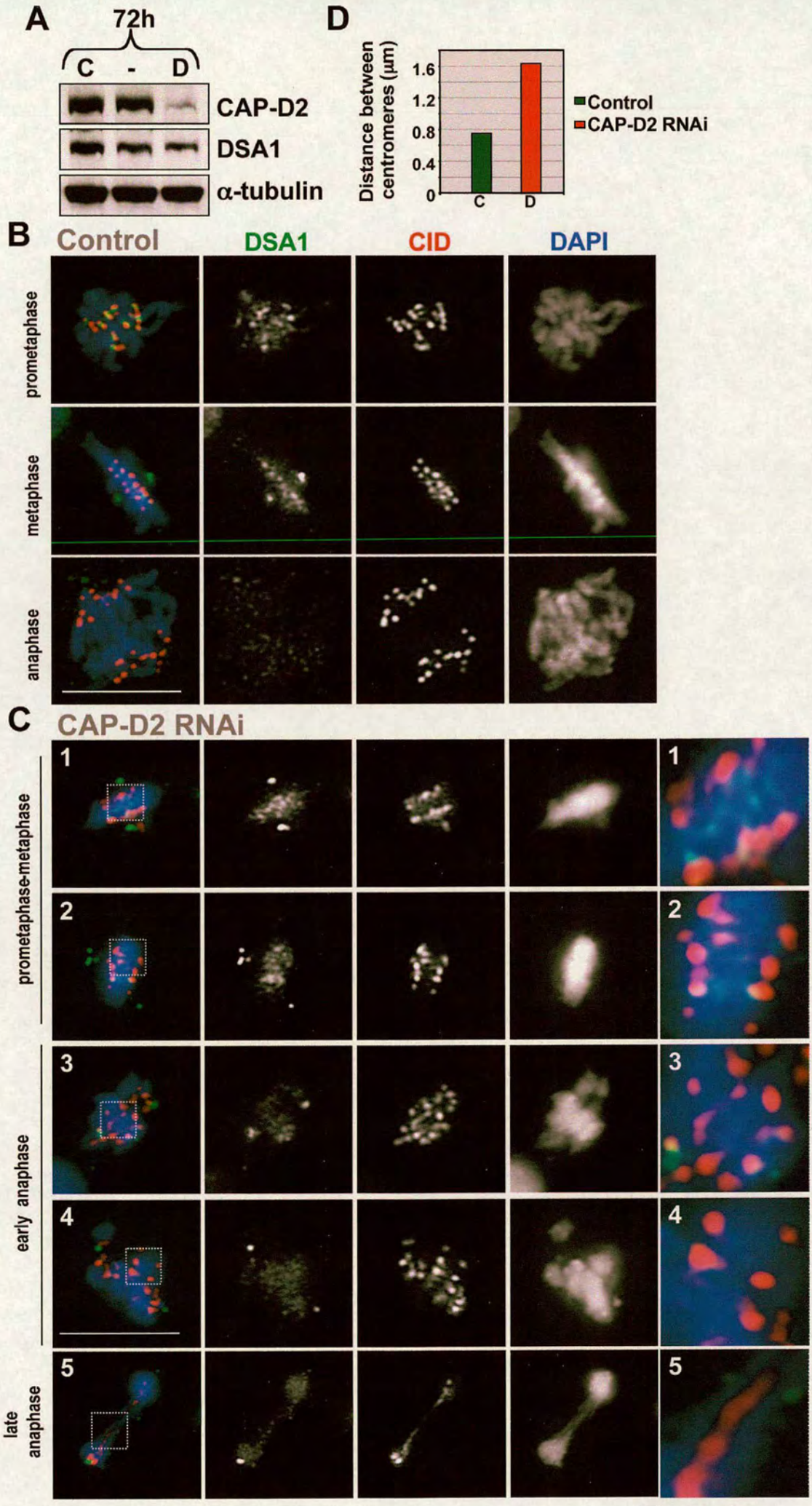

Figure 4.
Savvidou, *et al.*

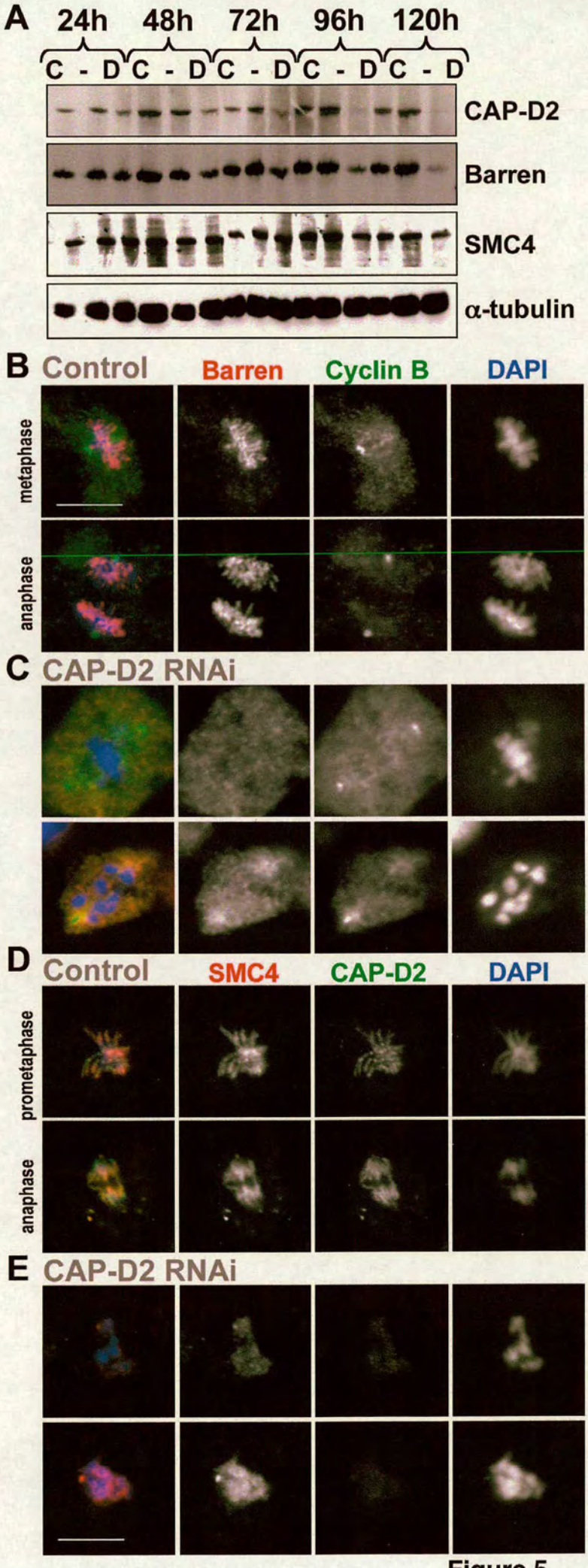

Figure 5.
Savvidou, *et al.*

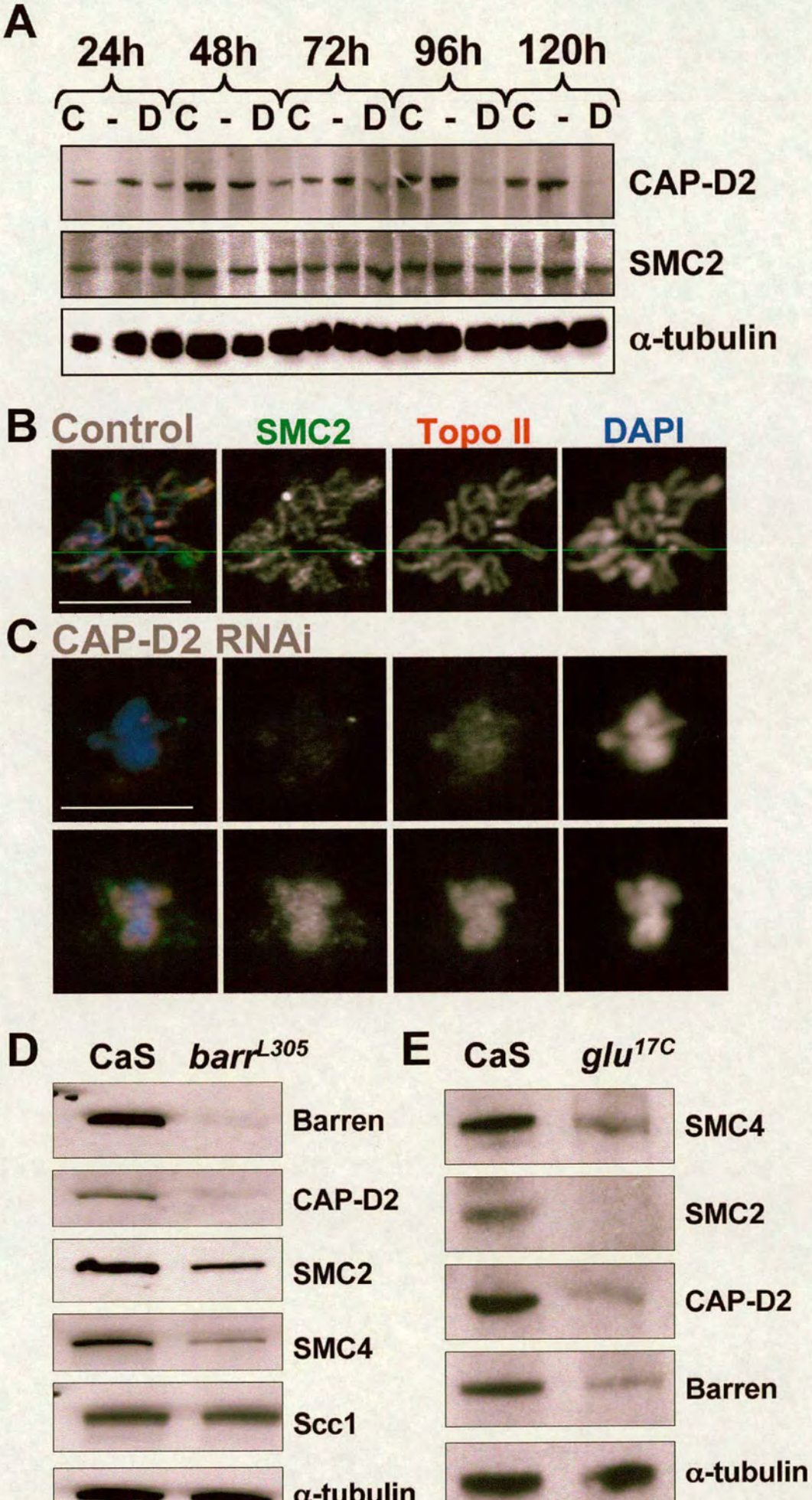

Figure 6.
Savvidou, *et al.*

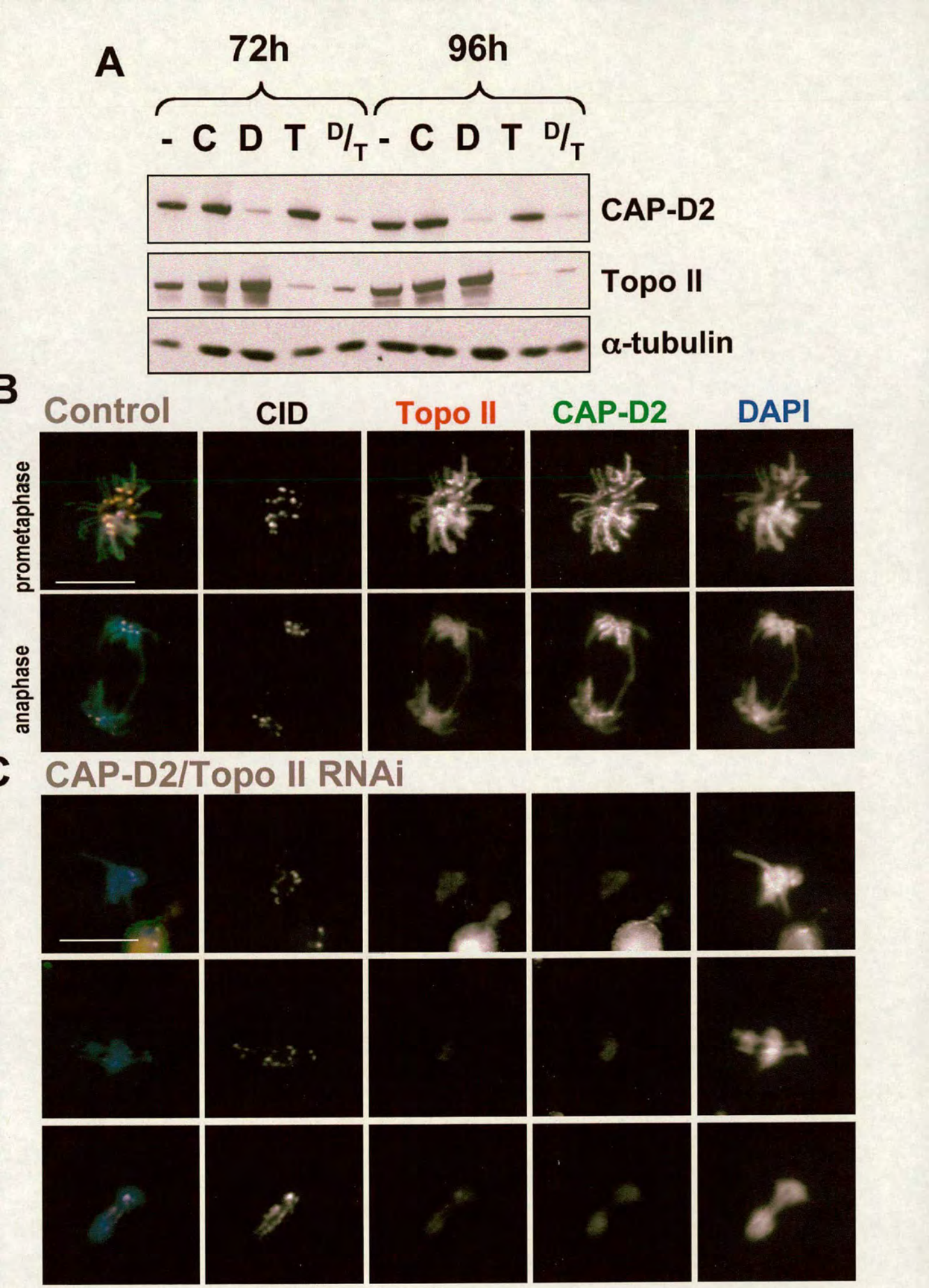

Figure 7.
Savvidou, *et al.*

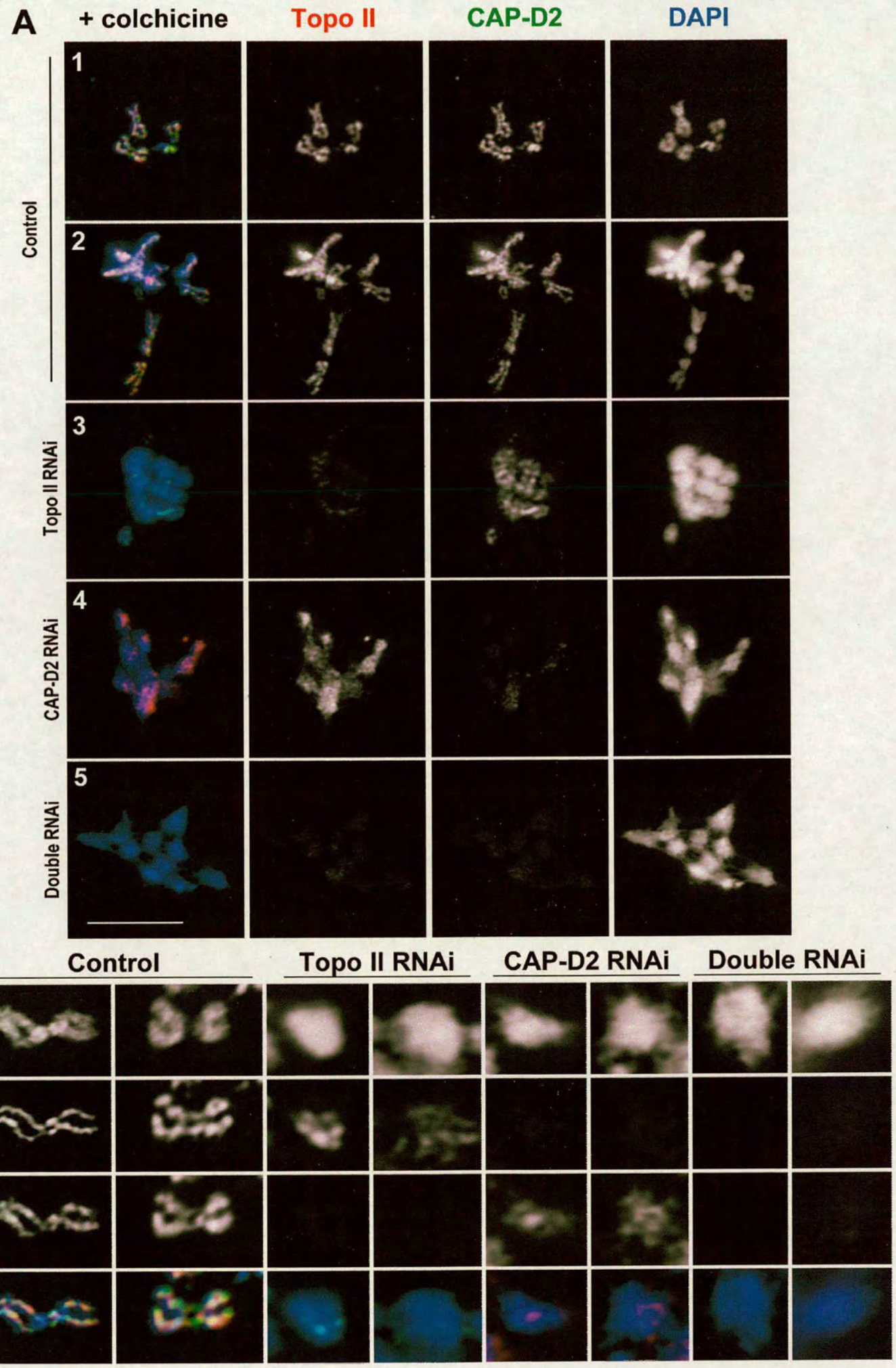

Figure 8.
Savvidou, *et al.*

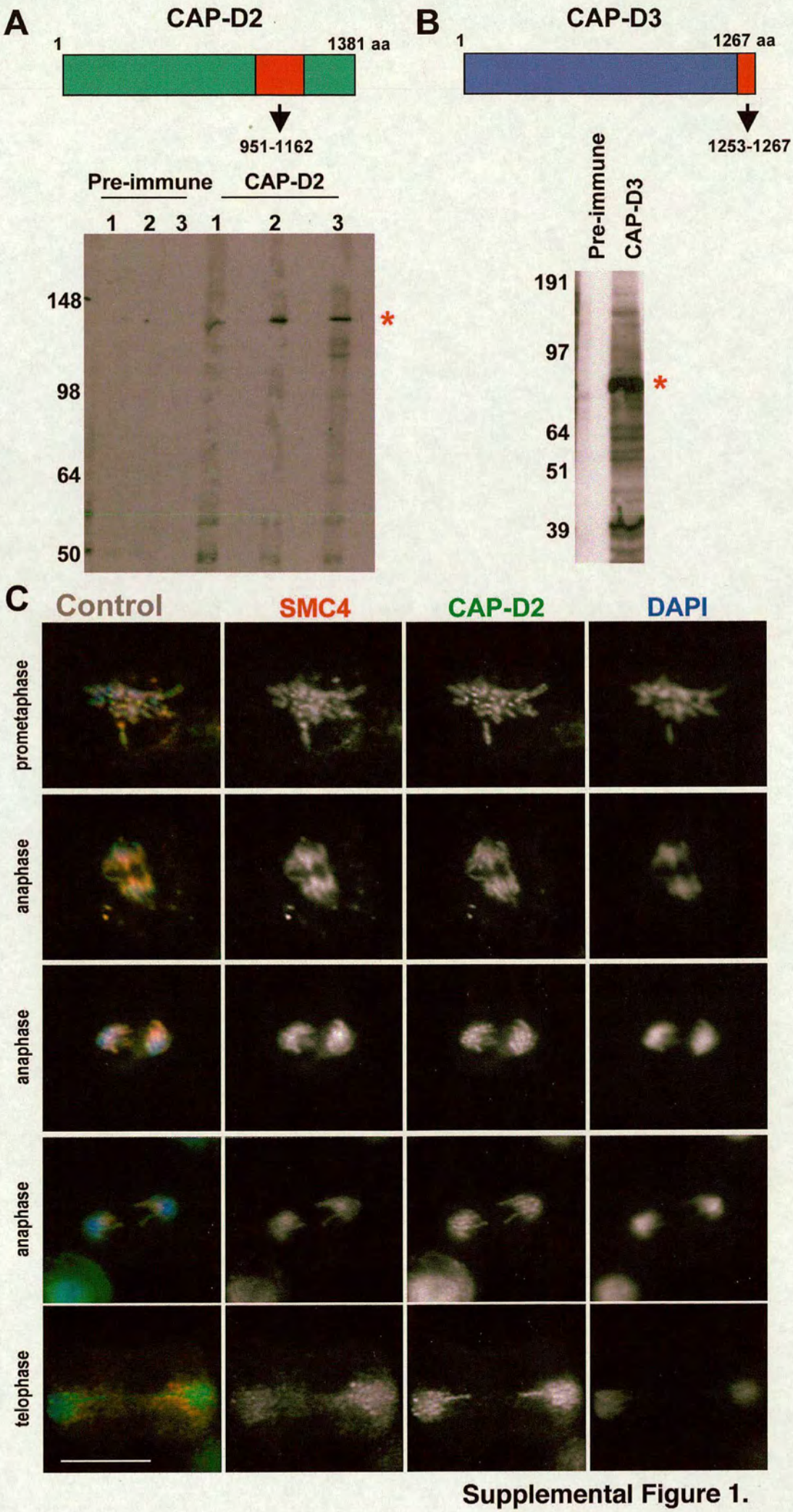

Supplemental Figure 1.
Savvidou, *et al.*

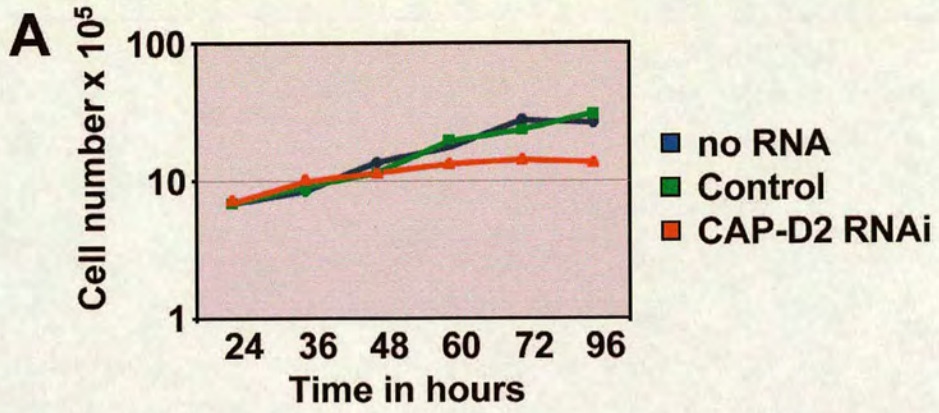

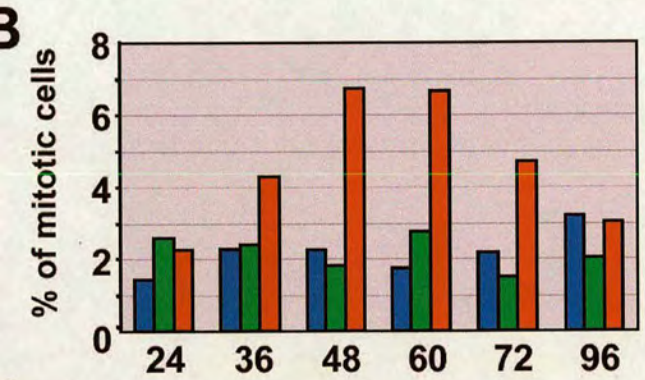

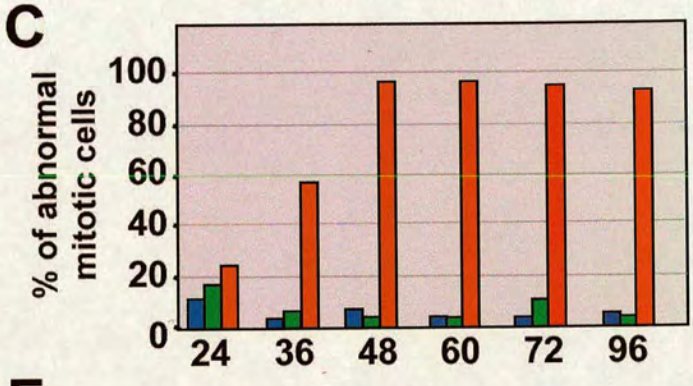

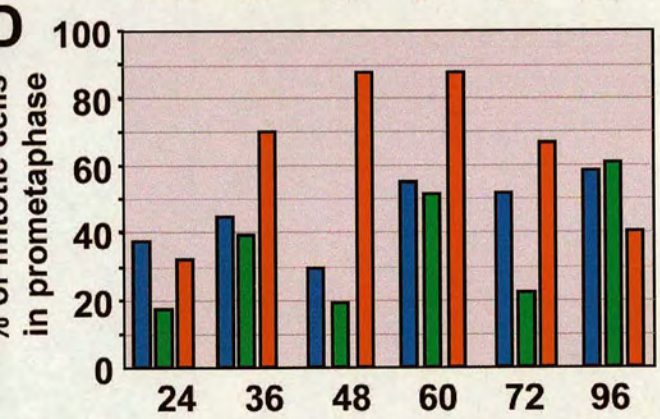

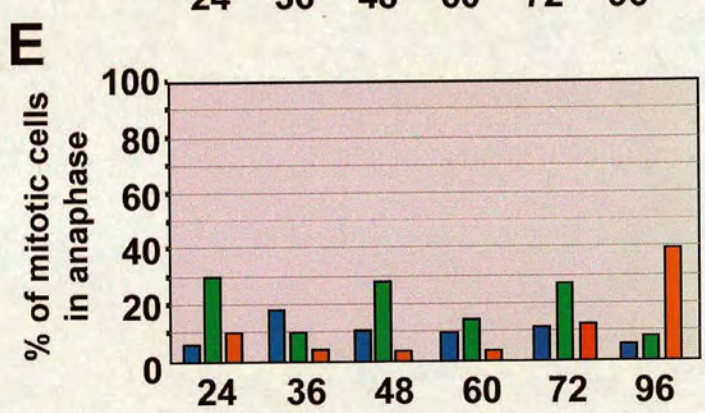

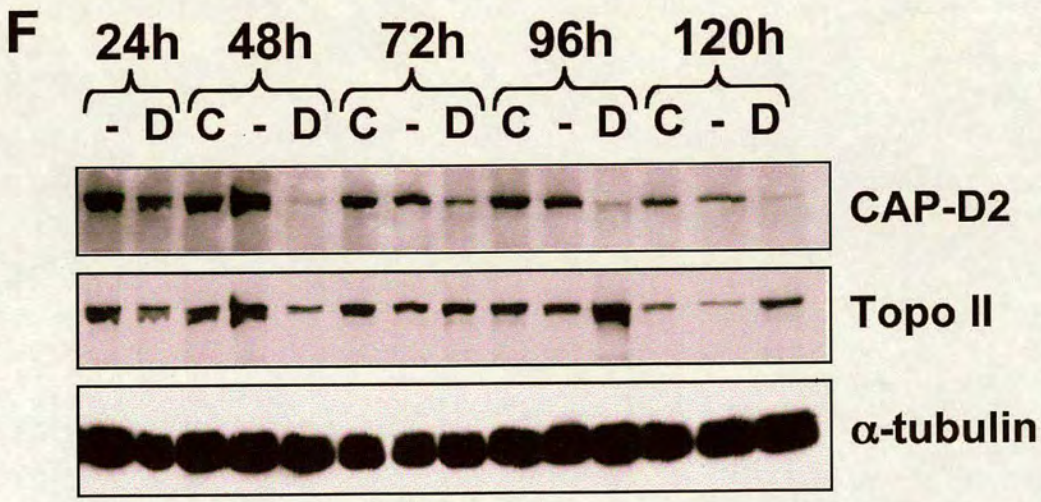

Supplemental Figure 2.
Savvidou, *et al.*

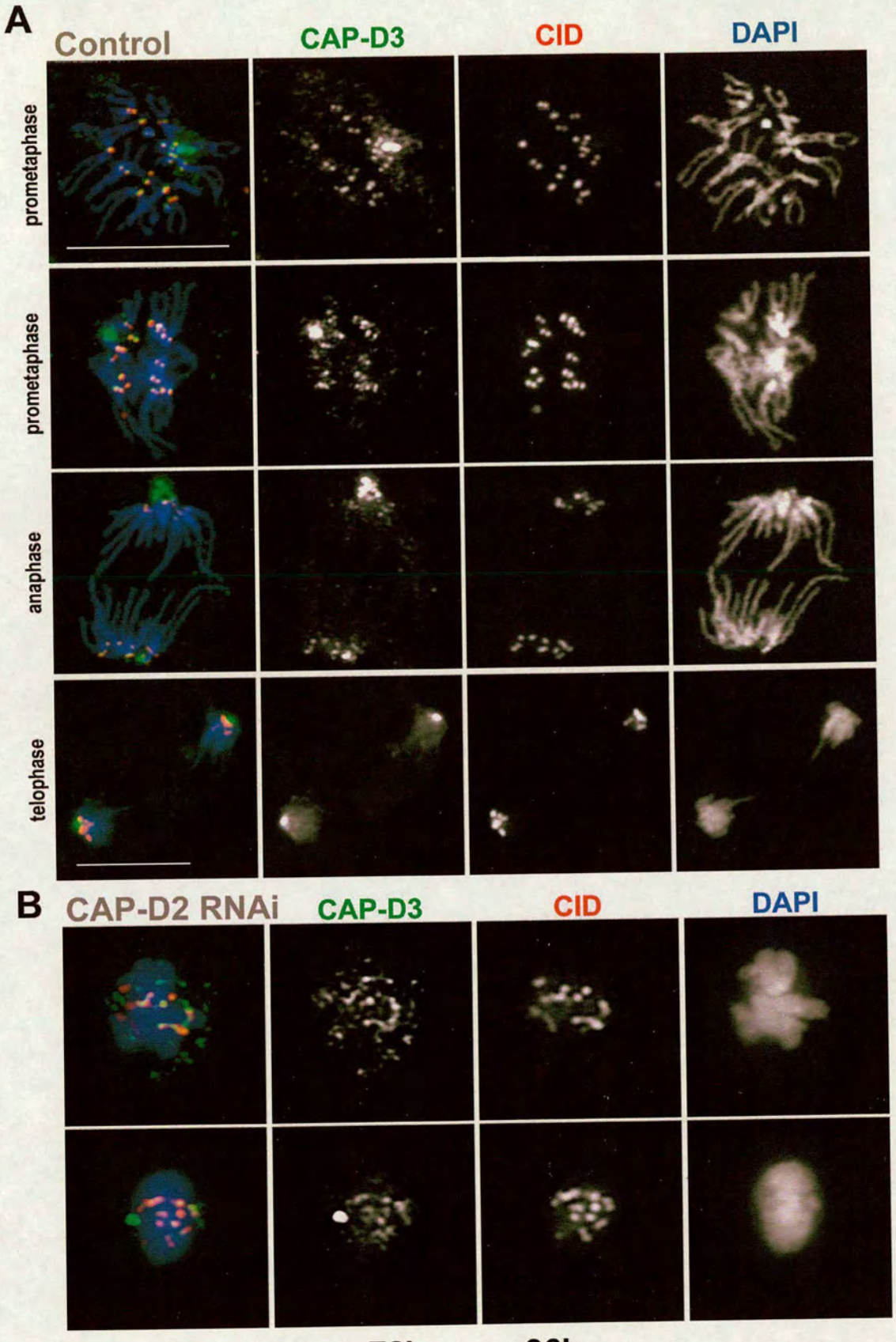

Supplemental Figure 3.
Savvidou, *et al.*